IBIC 2025

# PROCEEDINGS AT A GLANCE

THE FOURTEENTH

# INTERNATIONAL BEAM INSTRUMENTATION CONFERENCE

Liverpool, UK

7 – 11 September 2025

ibic2025.org



Science and Technology Facilities Council

The Cockcroft Institute of Accelerator Science and Technology

John Adams Institute for Accelerator Science

ISBN: 978-3-95450-262-2 ISSN: 2673-5350 doi: 10.18429/JACoW-IBIC2025-MOBC01

# MEASUREMENT OF NANOAMPERE BEAM INTENSITIES AT FAIR*

T. Sieber†, H. Braeuning, M. Schwickert, GSI, Darmstadt, Germany
L. Crescimbeni[1], Friedrich-Schiller-University Jena, Jena, Germany
T. Stoehlker[1,2], V. Tympel[1], Helmholtz Institute Jena, Jena, Germany
R. Stolz[3], V. Zakosarenko[4], Leibniz IPHT, Jena, Germany
G. Khatri, T. Koettig, J. Tan, CERN, Geneva, Switzerland
S. Kolbe, B. Voss, Ernst Abbe Hochschule, Jena, Germany
[1]also at GSI Helmholtz Centre for Heavy Ion Research, Darmstadt, Germany
[2]also at Institute for Optics and Quantum Electronics, Jena, Germany
[3]also at Technical University Ilmenau, Ilmenau, Germany
[4]also at supracon AG, Jena, Germany

*Abstract*

Analog to the working principle of standard beam transformers, the cryogenic current comparator (CCC) measures the intensity of particle beams via their azimuthal magnetic field. The superior performance of the CCC hereby derives from the high sensitivity of a SQUID (Superconducting Quantum Interference Device), which detects the current in the CCC pickup coil. This enables for a current resolution in the nA range, but in return needs extremely careful protection from external influences like stray fields and mechanical vibrations. The CCC therefore requires an elaborated superconducting magnetic shielding and is housed in a specially developed, vibration damped He bath cryostat.

We have recently achieved half a year of non-stop operation in stand-alone (closed Helium circuit) mode. The nA resolution has been demonstrated during several beamtimes, in CRYRING as well as with slow extracted beams from SIS18. Among the CCC types, which have been investigated, the 'Dual Core' (DCCC) version showed the best performance with respect to bandwidth and current resolution. The DCCC and its cryostat therefore mark a provisional closure of CCC development for FAIR.

In this contribution we present the latest results and the system status.

## INTRODUCTION

During the last ten years, the CCC went through a process of steady optimization and redesigning to match the requirements in the storage rings and extraction lines at GSI/FAIR as well as in the CERN AD. The first prototype at GSI (1995) proved the possibility of nA intensity measurement by a CCC in an accelerator environment and was the groundbreaking idea and basis for all later work [1]. Looking back (and facing today's requirements at FAIR), this prototype had a number of severe disadvantages, which made it unsuitable for practical and longterm operation in the HEBT and excluded the operation in storage rings. The necessary development work to match the FAIR requirements covered the full spectrum of cryogenic, vacuum, mechanical properties, as well as external field attenuation, SQUID-electronics, DAQ and signal processing. Investigations performed by a collaboration of institutes specialized on the various subtopics resulted in a variety of CCC types with respect to field-pickup, magnetic shielding, SQUID types and SQUID coupling. Many of them have been tested under laboratory and under beamline conditions, which in total formed a detailed picture of the application possibilities for CCCs in accelerators. The details of this work are described in [2-4]. Latest achievements were spill measurements with a 'classical' radial Niobium CCC as well as with a Pb Dual Core DCCC at GSI SIS18, advanced filtering of periodic disturbance and - last not least - the stand-alone operation of the He bath cryostat for >6 months.

Regarding its basic principle the CCC consists of a superconducting magnetic shielding in combination with a pickup coil, which is connected to a SQUID. The shielding provides an attenuation of non-azimuthal external fields in the range -70 dB to -150 dB (depending on shield geometry). It guides the superconducting Meissner-Current to an internal pickup loop, which is basically a one-winding coil around a high permeability ring core as flux concentrator. The ring core is used in the 'classical' CCC, as shown in Fig. 1, to provide an efficient coupling of the beam magnetic field to the SQUID circuit. In later versions it was omitted (coreless CCC) or replaced by a pair of cores (DCCC).

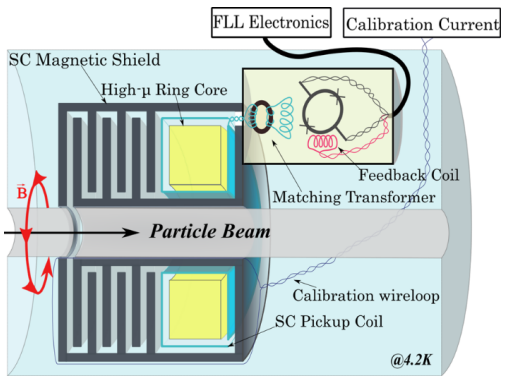



Figure 1: Classical CCC originally developed at the PTB (Physikalisch-Technische Bundesanstalt) [5].

*Supported by BMBF under contracts 05P18RDRB1 and 05P18SJRB1.
†T.Sieber@gsi.de

Content from this work may be used under the terms of the CC BY 4.0 licence (© 2025). Any distribution of this work must maintain attribution to the author(s), title of the work, publisher, and DOI.

ISBN: 978-3-95450-262-2 ISSN: 2673-5350 doi: 10.18429/JACoW-IBIC2025-MOBC02

# PERFORMANCE STUDY OF FAST BEAM CURRENT TRANSFORMER CALIBRATION IN THE LHC

J. Marafuz Gaspar*,[1], T. Levens, D. Alves, M. Gasior, K. Lasocha, CERN, Geneva, Switzerland
[1]also at Instituto Superior Técnico, Lisbon, Portugal

*Abstract*

Fast Beam Current Transformers (FBCTs) are essential devices for measuring bunched beam intensities in the Large Hadron Collider (LHC). A cross-calibration of these devices against DC Beam Current Transformers (DC-BCTs) is used in the LHC ring, but this method relies on assumptions that introduce inaccuracies. FBCTs are also used in the LHC transfer lines, where DC-BCTs are unavailable, making absolute calibration crucial for transmission studies. To allow absolute calibration, the FBCTs are equipped with a pulsed current source to perform a calibration before each fill. However, a systematic underestimation in the calculated scaling factors has been observed when comparing them to the cross-calibration with the DC-BCTs. This work characterizes the calibrator performance, evaluates different algorithms for calculating the scaling factors and reports on issues found linked to processing chain modeling inaccuracies, ghost/satellite bunches, and the FPGA-based digital integration. A revised model of the processing chain improved calibration accuracy by 0.4 %, while an initial test of a batch-by-batch baseline in the digital integration seems to explain the remaining 3 % underestimation.

## INTRODUCTION

Accurate measurement of beam intensity is essential for both accelerator operation and, as it is an input used to calculate luminosity, for physics analysis at the Large Hadron Collider (LHC). Beam intensity corresponds to the number of particles in the beam and is measured by dedicated instruments, with Beam Current Transformers (BCTs) being the standard devices used for this purpose.

DC Beam Current Transformers (DC-BCTs) measure the total circulating charge, including bunched and unbunched particles. Since they can be calibrated using accurate DC current sources, they provide a highly stable reference with a long-term accuracy of about ±0.3 % [1]. Fast Beam Current Transformers (FBCTs), in contrast, can resolve the individual bunch charge. They are periodically cross-calibrated against the DC-BCTs in the LHC ring, and this cross-calibration is designed to achieve ±1 % accuracy [2].

Cross-calibration has important limitations. It can only be performed during/after the energy ramp to ensure that all uncaptured beam particles (invisible to the FBCTs) will have been lost, and therefore cannot be systematically repeated before every fill. Moreover, in the LHC transfer lines where no DC-BCTs are available, the FBCTs cannot be cross-calibrated. These constraints reduce the accuracy of bunch intensity monitoring, especially for transmission studies.

* joao.marafuz.gaspar@tecnico.ulisboa.pt

To overcome these challenges, the LHC FBCTs have been equipped with a precise pulsed current source that enables absolute calibration without relying on DC-BCTs [3] with the aim that the calibration can be executed before every fill. The calibration system has so far only been demonstrated as a proof of principle and requires further development before it can be routinely used in LHC operation [4].

This paper addresses this need by characterizing the calibration unit as well as developing and evaluating algorithms for calculating absolute calibration scaling factors from the measured FBCT data. The observed systematic underestimation of the absolute calibration scaling factors relative to cross-calibration is shown to be linked with the processing chain modeling inaccuracies, ghost and satellite bunches, and FPGA-based baseline removal and digital integration.

## CROSS-CALIBRATION

During the energy ramp, and in particular in the 1 to 6 TeV energy range, the FBCT and the DC-BCT should ideally measure the same beam intensity, as any unbunched particles are rapidly lost. The correction factor $\alpha$ is determined as the mean ratio of the two signals within the 1 to 6 TeV interval. Applying $\alpha$ to the self-calibration scaling factor $C_{\mathrm{CAL}}$ yields the cross-calibration factor $C'_{\mathrm{CAL}} = \alpha C_{\mathrm{CAL}}$, effectively overlapping the two measurements, as shown in Fig. 1. Before the energy ramp, the FBCT signal deviates from the DC-BCT reference due to the presence of uncaptured particles in the beam.

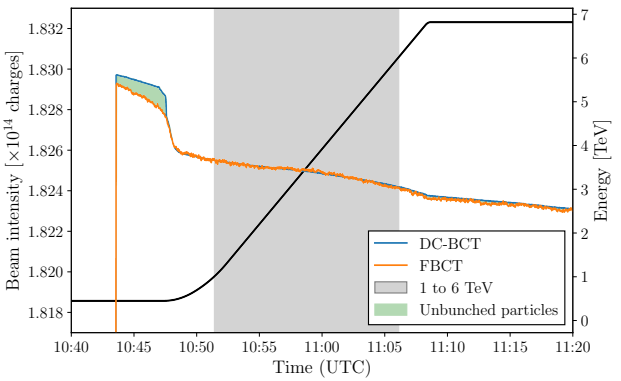



Figure 1: FBCT and DC-BCT beam intensity comparison after cross-calibration for LHC Beam 1 (fill 9523) on 15/04/2025, with the corresponding LHC energy also shown.

## ABSOLUTE CALIBRATION

### *FBCT Processing Chain*

Each LHC FBCT consists of a CERN designed Wall Current Transformer (WCT) [4] and a front-end processing chain

Content from this work may be used under the terms of the CC BY 4.0 licence (© 2025). Any distribution of this work must maintain attribution to the author(s), title of the work, publisher, and DOI.

ISBN: 978-3-95450-262-2 ISSN: 2673-5350 doi: 10.18429/JACoW-IBIC2025-MOBI01

# TRANSVERSE MOMENTUM MEASURING SYSTEMS: THE CRYOGENIC MOMENTATRON AND TESS

G. Adhikari*, T. Vecchione, Stanford Linear Accelerator Center, USA
I-J Shan, W. A. Schroeder, University of Chicago, Illinois, USA
L. B. Jones†, H. M. Churn, UKRI, STFC Daresbury Laboratory, UK

*Abstract*

Photocathode performance optimization is crucial to the operation of X-ray Free Electron Laser (FEL) facilities such as LCLS-II and the future UK XFEL as the initial photoelectron phase-space distribution directly impacts x-ray generation efficiency in the undulator. Key photocathode parameters such as transverse emittance and quantum efficiency are routinely measured to monitor and improve performance, but other metrics are influenced by the photocathode material such as operating temperature, vacuum and RF environmental conditions and the characteristics of laser illumination (e.g., wavelength, and pulse energy, duration, and repetition rate). To better understand these factors, SLAC has developed a laboratory-based Cryogenic Momentatron system to measure the emission properties of photocathodes at temperatures between 30 K and 300 K using 200 – 800 nm wavelength-tunable light. The system's design and initial commissioning performance have been validated through simulations and error analysis, confirming its reliability for photocathode characterization. We present measurements taken at SLAC, along with complementary data for $Cs_2Te$ obtained using the TESS system at Daresbury Laboratory - a similar photocathode characterization tool. These results provide valuable insights into photoemission physics that may be leveraged to optimize photocathode performance and thus that of X-ray FELs.

## ENERGY / MOMENTUM MEASUREMENT

Laser-driven photocathode electron sources are essential components of modern advanced x-ray generation systems, including free-electron lasers (FELs), instruments for ultrafast electron diffraction (UED) and dynamic transmission electron microscopy (DTEM). In all these applications, the ultimate performance is determined and limited by the transverse emittance of the electron beam at the photocathode. The emittance is typically defined as a quantity that remains invariant under acceleration to relativistic energies, referred to as the normalized emittance:

$$\text{So, } \varepsilon_{n,rms} = \frac{1}{mc}\sqrt{\langle x^2\rangle\langle p_x^2\rangle} = \frac{\sigma_x\sqrt{\langle p_x^2\rangle}}{mc}, \qquad (1)$$

where $\sigma_x$ is the rms transverse size of the beam, $p_x$ is the transverse momentum, $m$ is the electron mass and $c$ the speed of light. Eq. (1) suggests that emittance can, in principle, be reduced indefinitely by decreasing the beam size. However, in practice, this reduction is fundamentally limited by space-charge effects. As a result, for practical applications, lowering the transverse momentum is the only effective route to minimizing emittance. For many light source applications, such as FELs, achieving a normalized emittance below 0.5 μm/mm is a critical performance target. Using the three-step framework, Dowell and Schmerge [1] expressed the normalized emittance in terms of the mean transverse energy (MTE) and quantum efficiency (QE) as:

$$MTE(\lambda) = \frac{E_{excess}}{3}, \qquad QE(\lambda) \propto E_{excess}^2, \qquad (2)$$

where $E_{excess} = \hbar\omega - \theta$ with $\hbar\omega$ being the photocathode illumination photon energy and $\phi$ the photocathode work function. This model was later extended by Vecchione [2] to account for the effects of photocathode temperature and further refined by Saha [3] to include the influence of surface disorder (roughness). The temperature dependence of the rms transverse momentum is illustrated in Fig. 1, reproduced from [2]. The figure shows that reducing the photocathode temperature leads to a lower rms transverse momentum. Exploiting near-threshold photoemission at cryogenic temperatures has enabled record-low energy spreads, such as the 5 meV value reported for a copper photocathode [4].

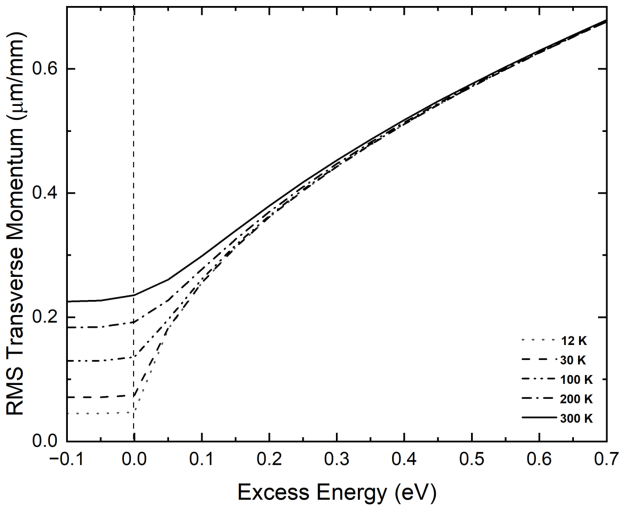



Figure 1: The effect of excess energy and temperature on transverse momentum during photoemission.

The primary motivation for developing these instruments is to identify photocathodes exhibiting low rms transverse

* gowri@slac.stanford.edu
† lee.jones@stfc.ac.uk

Content from this work may be used under the terms of the CC BY 4.0 licence (© 2025). Any distribution of this work must maintain attribution to the author(s), title of the work, publisher, and DOI.

ISBN: 978-3-95450-262-2 ISSN: 2673-5350 doi: 10.18429/JACoW-IBIC2025-MOCC01

# CURRENT ACTIVITIES OF BEAM DIAGNOSTICS IN THE J-PARC LINAC

K. Moriya†,[1], T. Miyao[2], M. Ishikawa[3], M. Chimura[1], H. Takahashi[1], Y. Morohashi[1], K. Takeishi[1], J. Kamiya[1]
[1]Japan Atomic Energy Agency (JAEA), 2-4 Shirakata, Tokai, Ibaraki, Japan
[2]KEK, 2-4 Shirakata, Tokai, Ibaraki, Japan
[3]Nuclear Engineering Ltd. (NECO), 2-4 Shirakata, Tokai, Ibaraki, Japan

Content from this work may be used under the terms of the CC BY 4.0 licence (© 2025). Any distribution of this work must maintain attribution to the author(s), title of the work, publisher, and DOI.

*Abstract*

The J-PARC Linac accelerates a high-intensity beam of 50 mA using RF systems operating at 324 MHz and 972 MHz. To achieve stable acceleration and transport of such high-intensity beams, it is essential to measure the beam's current, centroid, and distribution in order to determine optimal operating conditions. This paper reports on the developments and improvements in linac beam diagnostics since 2015. As a specific example, carbon nanotubes have been implemented in the transverse profile monitor located at the upstream section of the linac, and no unintentional failures have occurred since this replacement. Additionally, this paper presents the current status and operational improvements of the longitudinal profile monitor.

## INTRODUCTION

The Japan Proton Accelerator Research Complex (J-PARC) consists of three accelerators—the Linac, the 3 GeV Rapid Cycling Synchrotron (RCS), and the 50 GeV Main Ring Synchrotron (MR)—and three experimental facilities: the Materials and Life Science Experimental Facility (MLF), the Hadron Experimental Facility, and the Neutrino Experimental Facility [1].

The J-PARC Linac extracts negative hydrogen ions ($H^-$) generated from the ion source at 50 keV and accelerates them to 3 MeV using a Radio Frequency Quadrupole (RFQ) operating at 324 MHz. The beam is further accelerated to 50 MeV with a Drift Tube Linac (DTL), to 191 MeV with a Separated-type DTL (SDTL), and finally to 400 MeV with an Annular Coupled Structure (ACS) linac operating at 972 MHz. It is then injected into the RCS. In the RCS, the beam is accelerated to 3 GeV and subsequently transported to the MLF and the MR.

Figure 1 shows the time structure of the J-PARC Linac beam. To achieve a beam power of 1 MW in the RCS, the Linac delivers $H^-$ beams accelerated to 400 MeV with a pulse width of 500 μs (macropulse) at a repetition rate of 25 Hz. Since the beam is accelerated at 324 MHz and 972 MHz, micropulses are formed at intervals of about 3 ns. In the RCS, which has a circumference of about 350 m, the beam is accelerated using RF at about 1 MHz. For matching with the RCS RF buckets, a portion of the beam is chopped in the Medium Energy Beam Transport 1 (MEBT1) between the RFQ and the DTL, producing an intermediate comb-like bunch structure. Thus, the time structures that must be monitored in the Linac are the microbunches for Linac beam matching and the intermediate bunches for matching to the RCS injection beam.

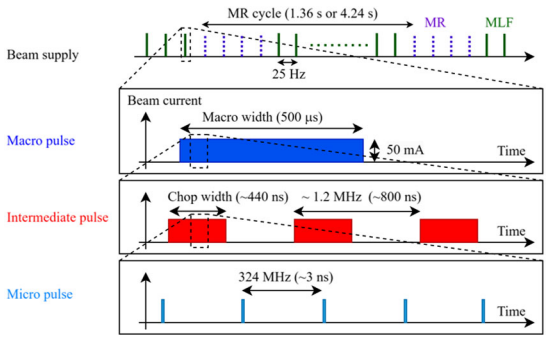



Figure 1: Time structure of J-PARC Linac's beam.

In general, to transport high-intensity beams without beam loss, it is necessary to measure the number of particles per bunch, the beam centroid positions in both transverse and longitudinal planes, and the transverse and longitudinal beam distributions. Here, the number of particles per bunch corresponds to the beam current, the beam centroid is expressed as ($x$, $x'$, $y$, $y'$, $t$, $E$), and the beam distribution as ($\alpha_x$, $\beta_x$, $\varepsilon_x$, $\alpha_y$, $\beta_y$, $\varepsilon_y$, $\alpha_z$, $\beta_z$, $\varepsilon_z$). At the J-PARC Linac, beam tuning is performed using a commissioning software system consisting of JCE and XAL [2,3].

JCE is a development environment for creating beam tuning applications for the J-PARC Linac, based on the SAD scripting language developed at KEK. XAL is a beam dynamics and control software framework developed at the SNS in the U.S. [4]. It uses two configuration files: one describing the accelerator device parameters and another describing the beam properties, enabling beam simulations of the accelerator. The behavior of the beam centroid can be represented by a six-dimensional vector, while the behavior of the beam distribution can be reproduced using a 6×6 sigma matrix. In beam tuning, the optimal accelerator operating conditions are explored based on beam measurement results and beam simulations.

Table 1 summarizes the beam diagnostics employed for beam tuning and anomaly diagnosis in the J-PARC linac. Although several reports on the status of the J-PARC linac beam monitors have been published in the past, they date back more than eight years [5,6]. This paper provides an updated overview of the beam monitors, including recent developments and ongoing activities in the linac. Furthermore, it presents waveforms observed during abnormal

† moriya.katsuhiro@jaea.go.jp

ISBN: 978-3-95450-262-2 ISSN: 2673-5350 doi: 10.18429/JACoW-IBIC2025-MOCC02

# BEAM DIAGNOSTICS FOR IFMIF-DONES: ADDRESSING THE CHALLENGES OF HIGH-POWER IRRADIATION FACILITIES

A.Ortega Moral*, IFMIF-DONES, Granada, Spain
J. Herranz, A. Ibarra, I.Podadera, C. Torregosa-Martin [1], IFMIF-DONES, Granada, Spain
P. Cara, Fusion for Energy, Barcelona, Spain
C. de la Morena, D. Jiménez-Rey, C. Oliver, D. Regidor, A.Rodríguez Páramo, V. Villamayor
CIEMAT, Madrid, Spain
F. Benedetti, J. Marroncle, Université Paris-Saclay, France
D. Cosic, T. Tadic, K. Tomic-Luketic, RBI, Zagreb, Croatia
L. Macia, IREC, Barcelona, Spain
J. F. Valenzuela Valdés, UGR, Granada, Spain

Content from this work may be used under the terms of the CC BY 4.0 licence (© 2025). Any distribution of this work must maintain attribution to the author(s), title of the work, publisher, and DOI.

*Abstract*

The IFMIF-DONES (International Fusion Material Irradiation Facility- DEMO Oriented Neutron Source) facility, currently under construction in Granada (Spain), is dedicated to testing materials under neutron irradiation, as part of advanced materials research for next-generation fusion reactors. The superconducting linear accelerator of the facility is intended to deliver a continuous-wave deuteron beam with an energy of 40 MeV and an unprecedent average deuteron current of 125 mA. The production of neutrons is then achieved by driving the 5 MW beam into a liquid lithium target. Beam diagnostics play a critical role in the IFMIF-DONES accelerator due to several unique challenges. These include the extremely high beam power, the harsh environment due to neutron and gamma radiation, and the required operational availability of the accelerator. Moreover, the accelerator may operate in pulsed and continuous wave for commissioning and standard operation, respectively. This work presents an overview of the main beam diagnostic techniques and strategies needed to address these challenges, the prototyping works that have been already achieved, and those to be still developed.

## INTRODUCTION

The strong global demand for sustainable, low-carbon electricity, particularly from reliable base-load power, has driven extensive research into fusion energy. Fusion is one of the few technologies that has the potential to meet this demand. However, achieving it involves complex, interrelated scientific and engineering challenges. One of the challenges to address is the study of materials that can withstand the extremely high radiation dose in fusion reactors. Within this framework, the IFMIF-DONES [1] project plays a crucial role by providing the material testing infrastructure essential for the development and qualification of fusion reactor components. To achieve this, IFMIF-DONES will generate fusion-reactor-like neutrons (up to $10^{17}$ 55 MeV neutrons per second). This neutron flux is produced by directing a continuous-wave 125 mA deuteron beam accelerated up to 40 MeV onto a lithium target. From a technological point of view, the facility is composed of three main elements, a deuteron accelerator, a liquid lithium target and irradiation modules to host the material samples for irradiation. In the last 20 years, prototypes of these three elements have been developed and operated in the context of the IFMIF EVEDA (Engineering Validation and Engineering Design Activities) project [2]. Notable examples include the Linear IFMIF Prototype Accelerator (LIPAc) in Rokkasho (Japan) [3], the EVEDA lithium test loop in Oarai [4], the Li loop (Lifus6) in Brasimone [5] as well of irradiation prototypes in the Belgian BR2 test reactor [6, 7]. Furthermore, in the last decade, significant integration efforts have been made during the engineering phase of the future facility and its three different parts [8]. These efforts have taken place within the framework of the EUROfusion Consortium (Work Package Early Neutron Source, WPENS) in close collaboration with the Fusion for Energy organization [9]. The IFMIF-DONES infrastructure is currently under construction, with the various systems of the facility also entering their respective construction phases [10, 11]. In the present work, only the former topic—related to the Accelerator System (AS) —is addressed, with a focus on its specific features and the beam diagnostic techniques required to properly tune, characterize, and monitor the accelerated beam.

## DONES ACCELERATOR AND BEAM DIAGNOSTICS STRATEGY

The AS system can be divided into the following components, as shown in a conceptual form in Fig. 1:

- Injector: composed by a source and extraction subsystem for extraction and acceleration of deuteron and protons up to 100 keV and a Low Energy Beam Transport (LEBT) line to guide the low-energy ions to the Radio-Frequency Quadrupole (RFQ).
- RFQ: provides deuteron/proton acceleration from 100 keV to 5 MeV.
- MEBT: Medium Energy Beam Transport Line shaping the beam in both transverse and longitudinal directions for a proper transport and matching of the beam from

* aurora.ortega@ifmif-dones.es

ISBN: 978-3-95450-262-2 ISSN: 2673-5350 doi: 10.18429/JACoW-IBIC2025-MOCI01

# COMMISSIONING AND FIRST OPERATION OF SLS 2.0, THE UPGRADE OF THE SWISS LIGHT SOURCE

B. Keil on behalf of the SLS 2.0 Team
PSI Center for Accelerator Science and Engineering, Villigen, Switzerland

Content from this work may be used under the terms of the CC BY 4.0 licence (© 2025). Any distribution of this work must maintain attribution to the author(s), title of the work, publisher, and DOI.

*Abstract*

After more than 20 years of successful operation, the storage ring of the Swiss Light Source (SLS) has recently been replaced with a new diffraction-limited storage ring (DLSR) called SLS 2.0. After a dark time of 15 months from October 2023 until December 2024, SLS 2.0 now provides more than 40 times higher brilliance for hard X-ray users, thanks to an innovative compact 7-bend achromat magnet lattice with reverse bending magnets that fits into the old SLS 1.0 tunnel. In this contribution, we give an overview of the commissioning of the new storage ring and first user operation experience, highlighting key differences between SLS 1.0 and 2.0, as well as the role and usage of different beam instrumentation systems during the commissioning process from the operations perspective. Moreover, we present the status of beam-based feedback systems, and the resulting beam stability and performance that has been achieve so far during first user operation.

## INTRODUCTION

Table 1 provides an overview of the key parameters of the SLS 1.0 and SLS 2.0 storage ring [1]. In addition to a more than 40 times higher brilliance, SLS 2.0 also has an increased electron energy of 2.7 GeV. Combined with newly designed insertion devices, SLS 2.0 provides a 50 % higher hard X-ray photon energy range.

Table 1: SLS Storage Ring Beam Parameters

| Parameter | Units | SLS 1.0 | SLS 2.0 |
|---|---|---|---|
| Circumference | m | 288 | |
| Beam Current | mA | 400 | |
| Injection Charge | nC | ~0.01-0.4 @ 3 Hz | |
| Beam Energy | GeV | 2.4 | 2.7 |
| Main RF | MHz | 499.637 | 499.654 |
| Harmonic No. | # | 480 | |
| Hor. Emittance | pm | 5030 | 131-158 |
| Vert. Emittance | pm | 5-10 | 10 |
| Hor. Tune | | 20.43 | 39.37 |
| Vert. Tune | | 8.74 | 15.22 |
| Ring BPMs | # | 75 | 136 |

While the SLS storage ring and most of its subsystems required a completely new design to achieve the requested design parameters of the SLS 2.0 project, the original SLS 1.0 linac and full energy booster synchrotron could be re-used, thanks to the low booster emittance of 12 pm.rad that is sufficient for high SLS 2.0 injection efficiency. The few upgrades of linac and booster that were performed during the SLS dark time include a new gun pulser, as well as a replacement of the ageing 1000 A power supply of the combined function booster main dipole magnets. Linac and booster are currently still using the original SLS 1.0 BPM system and magnet power supplies (except for the main dipole circuit). Although these systems meet SLS 2.0 requirements, they are scheduled to be upgraded 2026+ for maintenance reasons, where the BPM and magnet cables have already been replaced.

## INJECTOR RECOMMISSIONING

In order to save time for the storage ring commissioning scheduled for mid-January 2025, the linac was recommissioned already in November 2024, and the booster in December 2024, while the storage ring and its subsystems were still being installed. Both linac and booster reached their design performance within less than one week, including the extraction of the 2.7 GeV booster beam through the newly designed booster-to-ring transfer line up to the storage ring septum [2].

## STORAGE RING COMMISSIONING

### *Getting the First Turn*

On January 14, 2025, the beam commissioning of the new SLS 2.0 storage ring started [3, 4], following careful pre-beam tests of all systems and components. After optics matching of injected beam to stored beam via screen monitors, the first turn in the ring was achieved using only two dipole corrector magnets after the septum, while tuning septum and injection kickers, as well as booster / transfer line energy and trajectory using RF BPMs (see Fig. 1).

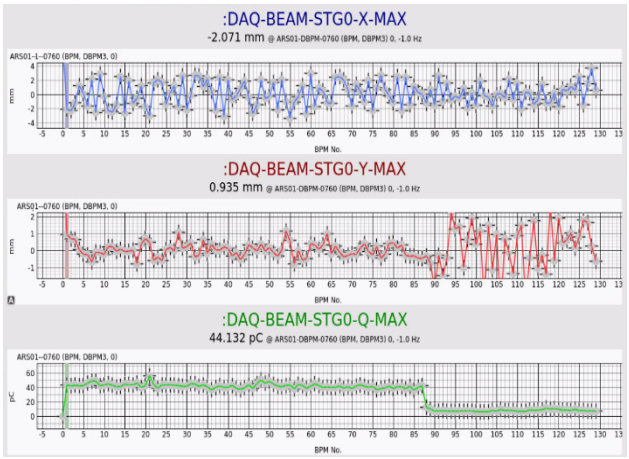



Figure 1: Storage ring horizontal orbit (top, blue), vertical orbit (middle, red), and bunch charge (bottom, green), measured by BPMs in turn-by-turn mode. The beam was intentionally blocked at BPM no. 87 by a closed valve.

ISBN: 978-3-95450-262-2 ISSN: 2673-5350 doi: 10.18429/JACoW-IBIC2025-MODC02

# PERFORMANCE ANALYSIS OF THE LHC BSRL AND POSSIBLE IMPROVEMENTS *

A. N. Jury†,1,2, A. Hill[1], C. P. Welsch[1], H. D. Zhang[1], D. Butti[2], M. Gonzalez-Berges[2], M. Martin Nieto[2], S. Mazzoni[2], A. Schloegelhofer[2]
[1]University of Liverpool, Liverpool, United Kingdom
[2]European Organization for Nuclear Research (CERN), Geneva, Switzerland

*Abstract*

The Beam Synchrotron Radiation Longitudinal density monitor (BSRL) at the LHC leverages time-correlated single-photon counting (TCSPC) to provide high-dynamic-range measurements of the relative charges in each RF bucket with a time resolution of 50 ps. These measurements are needed for the operation of the LHC as well as for the luminosity calibration required by the LHC Experiments. In this work, we identify sources of error for each of the BSRL components. These components are the optics (mirrors, filters and optical fibres), the detector (a hybrid photomultiplier - HPM), the electronics (a Time to Digital Converter - TDC), and some data analysis used for the final results. Knowledge of the errors of the BSRL is crucially important as any errors are passed directly into the luminosity calibration of the LHC experiments. We quantify the errors introduced by each of these parts and for external systems, like the LHC timing. For the largest contributors to the overall error, we propose mitigation strategies that can be deployed in the short term.

## INTRODUCTION

Not every RF bucket in the Large Hadron Collider (LHC) is intended to be filled. The RF at the LHC's operating energy has a period of 2.5 ns, however, the minimum distance between filled buckets is 25 ns. For most purposes only the filled buckets are of interest. We introduce the concept of an RF slot, a set of 10 buckets arranged as can be seen in Fig. 1. Charges in the nine nominally empty buckets surrounding a filled bucket are referred to as "Satellites". In addition, many slots are also left unfilled. Charges within these unfilled slots are referred to as "Ghosts". Satellites are of concern to the experiments as they contribute to the luminosity background [1].

The BSRL monitors the relative longitudinal charge distributions, including ghosts and satellites, for the identification of operational issues and allows for a correction for satellites in the luminosity calibration. There are two BSRL instruments, one for each beam. The Synchrotron Radiation (SR) used by the BSRL is produced as a beam passes through a bending magnet or a purpose-built superconducting undulator. The latter is necessary to generate visible SR at injection energies [2]. The SR is passed through a range of neutral density filters to control the intensity, followed by a band pass filter to limit the effect of dispersion on the arrival time resolution. The light is then extracted from the tunnel through fibre-optic cables before being detected by a Hybrid Photo-Multiplier (HPM), which is capable of detecting individual photons.Photon counts are given timestamps relative to the start of the turn by the Time-to-Digital Converter (TDC), and histogrammed over many turns to increase statistics, see Fig. 2. From this, the relative populations within each RF bucket can be inferred.

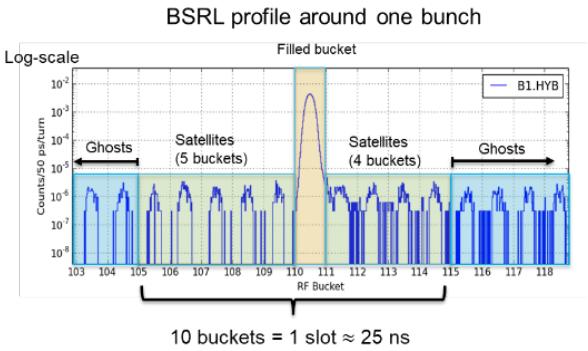



Figure 1: Example of one RF slot, highlighting the definitions of filled, ghost and satellite buckets.

The histogram is built over several minutes. The longer the integration time the larger the dynamic range in counts, and therefore the charges in satellite and ghost buckets are more distinguishable from the background.

## COUNTING ERRORS

Due to physical limitations of the detector and the time-to-digital converter, not every photon present at the detector will result in a count, and therefore, true counts will be lost. Equally, due to phenomena such as dark counting and after-pulsing, it is possible to have counts where there is no photon.

### *Dead Time*

After the arrival of a photon, the detector system, composed of the HPM and TDC, will be unavailable to detect any further photons for a given time.

The availability function $S(t)$ is defined as the probability that the detector system is available at some time $t$ after an initial detection.

Left uncorrected, this would cause a distortion in the histogram, favouring counts from the beginning of buckets. As the intensity of filled buckets is much larger than that of

* This work was supported by CERN doctoral student program and Science and Technology Facilities Council under grant agreement ST/W006766/1.
† alexander.jury@liverpool.ac.uk

Content from this work may be used under the terms of the CC BY 4.0 licence (© 2025). Any distribution of this work must maintain attribution to the author(s), title of the work, publisher, and DOI.

ISBN: 978-3-95450-262-2 ISSN: 2673-5350 doi: 10.18429/JACoW-IBIC2025-MODI01

# THE ROLE OF BEAM DIAGNOSTICS DURING APS-U COMMISSIONING*

W. Cheng†, Argonne National Laboratory, Lemont, IL, USA
on behalf of the APS-U Diagnostics Team

Content from this work may be used under the terms of the CC BY 4.0 licence (© 2025). Any distribution of this work must maintain attribution to the author(s), title of the work, publisher, and DOI.

*Abstract*

The Advanced Photon Source Upgrade (APS-U) represents the latest advancement in ultra-low emittance storage ring light sources. Since its commissioning and the commencement of user operations in 2024, APS-U has successfully reached its design beam current of 200 mA and operates reliably for user experiments. The diagnostic systems have been integral to the successful commissioning and operation of the machine. This paper presents the commissioning results for various diagnostic systems in the APS-U storage ring, with a focus on beam position monitors (BPMs). Additionally, we will discuss various beam measurements, including beam current and lifetime, tune, beam stability, and swap-out injection bunch motion.

## INTRODUCTION

APS-U is an ultimate low emittance storage ring [1] recently constructed and commissioned at Argonne National Laboratory. The new storage ring is an upgraded of the original Advanced Photon Source (APS) ring; the electron beam energy was reduced from 7 GeV to 6 GeV, and the new lattice features a multi-bend achromat design with horizontal emittance of 42 pm rad. A novel swap-out on-axis injection method has been implemented.

Commissioning of the new storage ring started on April 10, 2024, with beam passing through the Booster to Storage ring (BTS) beamline shortly after. After correcting the polarity of several BTS magnets, beam was injected into the storage ring on April 11. The first turn beam was achieved on April 13, and the beam circulated in the ring for more than 10 turns on April 14, as measured by sum signals from the BPMs at turn-by-turn (TBT) rate. Shielding validation then took place intentionally dumping the injected beam at selected locations. Stored beam was achieved on April 20 with RF systems turned on; the DCCT measured less than 500 μA of stored beam on that day. The injection efficiency and stored beam current were gradually improved in the following days. Swap-out injection was demonstrated later that month, with stored beam DCCT and Bunch Current Monitor (BCM) used to measure the beam currents. As one of the Key Performance Parameter (KPP) thresholds, 25 mA stored beam was achieved in mid-May after fixing a septum issue. Beamline commissioning started in June after achieving 50 mA stored beam.

Diagnostic systems have played a pivotal role in the rapid and successful commissioning of the storage ring. Prior to beam commissioning, major diagnostic systems were carefully tested and integrated with other systems. These pre-beam tests were essential for identifying software bugs, verifying cable connections, and rehearsing data acquisition and analysis procedures. BPM offsets were also measured during the period and have been used for day-1 commissioning [2, 3].

The following sections provide an overview of the APS-U diagnostic systems, pre-beam test and checkout results, and commissioning results for the BPM system, current monitors, and other diagnostics. Machine performance has continued to improve over the past year, with many diagnostic systems brought online and optimized. Some of key improvements that have supported machine operation and development are presented.

## APS-U DIAGNOSTICS OVERVIEW

There are 14 RF BPMs installed in a typical APS-U sector, giving a total of 560 BPMs in 40 sectors. Although the BPM feedthroughs share the same design, there are four different types of BPM pickups with different housing dimensions: P0 type, STD type, AP2 type, and BP5 type. The P0 and STD types have circular chambers of 22 mm diameter, and four buttons are symmetrically located at 45-degree angles. The AP2 and BP5 types have photon extraction slots and antechamber; consequently, the button is located at 60-degree angles relative to the horizontal plane. Within a sector, there is one AP2, one BP5, two P0, and ten STD BPMs. The BPM pickup and feedthrough design is described in [4].

Storage ring tunnel side of the BTS transfer line has also been newly constructed, with new button-type BPMs installed. There are 11 such BPMs installed in the new BTS, with the same feedthroughs as the storage ring (SR). The BTS on the booster tunnel side remains the same, so the original stripline-type BPMs are still being used. All the BTS BPMs now use a new type of electronics.

Commercial electronics from Instrumentation Technologies [5] have been selected for the APS-U BPMs, with APS-U specified features. The BTS BPMs are equipped with Spark-EL single-pass electronics, which provide sufficient resolution at 1 nC even with the 8 mm button pickups. External 20 dB attenuators are added for the old stripline BPMs to avoid saturation of the new sensitive electronics at high charge.

The storage ring button BPM signals feed to Libera Brilliance Plus (LB+) electronics via coaxial cables. Each LB+ unit houses four BPM modules, one controller module, one timing module, and one Global Data Transmitter (GDX) module. The BPM modules condition the analog signals, digitize them, and process the data at various bandwidths and precision. The controller module manages the LB+ unit and houses the EPICS IOC; the timing module communicates with the MRF timing

*Work supported by DOE contract No: DE-AC02-06CH11357
† wcheng@anl.gov

ISBN: 978-3-95450-262-2 ISSN: 2673-5350 doi: 10.18429/JACoW-IBIC2025-MOPCO01

# END TO END SIMULATIONS OF A NOVEL OPTICAL FIBRE MONITORING SYSTEM FOR ENERGY RECOVERY LINACs *

A. Jones†,1, J. Wolfenden[1], L. Eley[1,2], C. P. Welsch[1], University of Liverpool, Liverpool, UK
S. Boogert, Cockcroft Institute, Warrington, UK
[1]also at Cockcroft Institute, Warrington, UK
[2]also at Adaptix Ltd., Oxford, UK

*Abstract*

Energy recovery LINACs (ERLs) are a type of novel accelerator, which recycle energy from old beams to new beams to increase machine energy efficiency. However, this can heighten beam instabilities, which limits the maximum beam current and increases beam losses. An optical fibre beam loss monitor (oBLM) can provide rapid and reliable beam loss monitoring, which is important for mitigating these instabilities. It obtains the beam loss location via time-of-flight analysis of Cherenkov radiation (CR) produced in optical fibres by relativistic particle showers from beam loss events. Operational demonstration of the oBLM system has previously been shown at several non-ERL facilities, but the multiple-energy, fast-repeating beams of ERLs present a unique challenge. Successful interpretation of ERL beam loss signals involves distinguishing losses from beams of different energies, which can be investigated through end-to-end Monte Carlo simulations of the radiation environment and its interaction with the oBLM system. This contribution presents Geant4 simulations of the oBLM response to sample sources of beam loss for beam energies of 7-500 MeV and bunch populations of (1-10) × $10^6$ electrons.

## INTRODUCTION

Optical fibre-based beam loss monitors (oBLMs) consist of optical fibres running alongside a beamline, where at least one end of a fibre is monitored by a photodetector. oBLMs were first developed as a low-cost beam loss monitoring solution, with the capability for continuous accelerator coverage and better than 1 m precision in the reconstruction of beam loss locations [1–3].

Beam losses are detected through monitoring secondary particle showers from beam loss events, produced when high-energy beam particles strike an obstacle such as the inner wall of the beam pipe. The particle showers that intersect the optical fibre produce a pulse of Cherenkov radiation inside it [4] (Fig. 1). This radiation travels along the fibre and exits at the ends, where the photodetectors convert it into a voltage signal. The beam loss location can be reconstructed from the arrival time of the Cherenkov pulse [5]. A step-index silica fibre, with core diameter above 200 µm, is one type of optical fibre that is effective for this purpose.

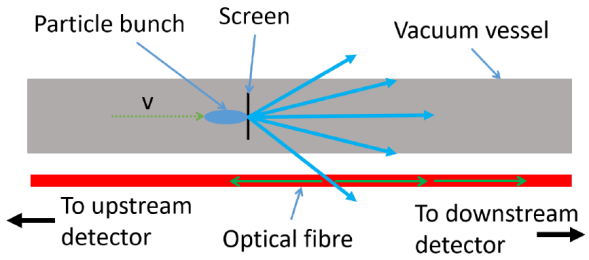



Figure 1: A diagram of the beam loss detection mechanism of the oBLM. Reproduced from [4] with permission.

Energy recovery LINACs (ERLs) are a type of novel accelerator in which the beam is returned to the RF cavities and decelerated after use, returning energy to the RF field and reducing the power consumption of the machine. However, the recirculating configuration necessary for ERLs leaves them at risk of high beam losses due to their unique susceptibilities to destabilising collective effects such as beam break-up [6] and the microbunching instability [7]. A beam loss monitor with continuous machine coverage, such as the oBLM, would provide useful data for diagnosing beam losses and managing collective effects across the whole length of an ERL.

The multiple recirculating beams present in ERLs pose a challenge for beam loss reconstruction with the oBLM.

ERL bunch properties, including their energy, can change significantly as they complete turns in the machine. Bunches that have made more turns (higher turn number) can be more susceptible to beam loss, since the effects of instabilities and slight variations from design specification can build up over time [8]. Therefore, it is important to have a method to determine the turn number of the bunch that produced a detected beam loss, as this can allow the losses of individual ERL bunches to be tracked throughout their full journey in the machine.

One potential method for this is through energy estimation of the bunch based on the recorded number of photons in the Cherenkov pulse. This is possible because the ERL bunch energy changes by a fixed value per turn, set by the energy gain or decrease from a single pass through the LINAC module(s) [9] - hence the bunch energy corresponds to its turn number. Also, the number of Cherenkov photons produced by a particle shower is expected to vary linearly with the energy of the shower-instigating particle [10] - so the bunch energy can, in principle, be estimated from the intensity of the oBLM Cherenkov signal. To aid distinguishing between

* This work is supported by the Enhancing ERL development in the UK Grant (STFC ST/X000540/1) and the Cockcroft Institute Core Grant (STFC ST/V001612/1).
† sgajon11@liverpool.ac.uk

Content from this work may be used under the terms of the CC BY 4.0 licence (© 2025). Any distribution of this work must maintain attribution to the author(s), title of the work, publisher, and DOI.

ISBN: 978-3-95450-262-2 ISSN: 2673-5350 doi: 10.18429/JACoW-IBIC2025-MOPCO02

# PREDICTION OF FEL PERFORMANCE USING BPM MEASUREMENTS AND MACHINE LEARNING

C. Liu, X. Yang, Y. M. Deng, Y. B. Leng†
NSRL, University of Science and Technology of China, Hefei, P. R. China

Content from this work may be used under the terms of the CC BY 4.0 licence (© 2025). Any distribution of this work must maintain attribution to the author(s), title of the work, publisher, and DOI.

*Abstract*

This study developed and validated a machine learning approach to analyze the correlation between beam position monitor (BPM) measurement data and output laser power in the Hefei Infrared Free-Electron Laser (FEL) facility. Using transverse position, charge, and longitudinal phase information from 280 individual bunches collected by BPM probes upstream of the undulator, we successfully constructed a high-precision predictive model, demonstrating that BPM measurements can effectively predict the output laser power of the infrared FEL.

Based on the trained predictive model, we further deconstructed the neural network architecture to accurately identify key bunches and sensitive parameters that most significantly influence laser power output. This provides a clear and targeted optimization basis for subsequent beam tuning experiments. The data-driven strategy employed in this method significantly reduces the workload associated with traditional experience-based tuning, offering an effective technical means to enhance accelerator operational stability.

## INTRODUCTION

Free-electron laser (FEL) facilities, as advanced fourth-generation coherent light sources, play an indispensable role in cutting-edge scientific fields. FELiChEM, a major research infrastructure in China, relies critically on the quality and stability of its radiation for successful user experiments[1, 2]. However, direct diagnostics of FEL radiation often involve destructive methods or lack real-time capability, introducing interference or delays during operation.

The core challenge lies in electron beam quality, which is highly sensitive to accelerator conditions yet poorly quantitatively understood. Traditional tuning approaches depend heavily on operator experience and trial-and-error, resulting in low efficiency and poor reproducibility.

Recent advances in beam position monitor (BPM) systems enable non-invasive, simultaneous measurement of multiple bunch parameters (such as transverse position, longitudinal phase, bunch length, etc.), providing rich diagnostic data [3]. However, the vast data volume exceeds the capabilities of manual analysis.

This study develops a data-driven machine learning approach to address these limitations. Using multi-parameter bunch data from upstream BPMs, we establish a virtual diagnostic model for predicting radiation quality in real-time, without disruption to user experiments. Beyond online monitoring, the trained neural network is interpreted to identify the most influential bunches and physical parameters. This provides explicit optimization guidance—such as which BPM parameters to adjust or which bunch regions to stabilize—enabling precise beam tuning via correctors or RF parameters. Ultimately, this work facilitates a shift from experience-dependent operation to a data-driven intelligent paradigm for accelerator control.

## METHODOLOGY

This chapter details the data-driven modeling approach used to establish the relationship between FEL laser power and BPM measurements. The overall research framework consists of three core components: data preprocessing and feature engineering; construction and training of a neural network prediction model; and model interpretation and feature importance analysis.

### *Data Preprocessing and Feature Construction*

The data used in this study, benefiting from groundbreaking advances in bunch-by-bunch diagnostic techniques, were obtained from the Hefei Infrared Free-Electron Laser facility[4,5]. Specifically, they were collected from six upstream beam position monitor (BPM) probes (numbered 1, 2, 3, 7, 8, 9) and one downstream BPM probe (numbered 10) of the undulator. Each BPM probe measured parameters for 280 individual bunches within a macropulse, including transverse position (X, Y), Sum signal (Sum), and longitudinal phase (Phase)[6,7]. These parameters were calculated by the HOTCAP program[8-10], with one turn of data shown in Fig. 1.

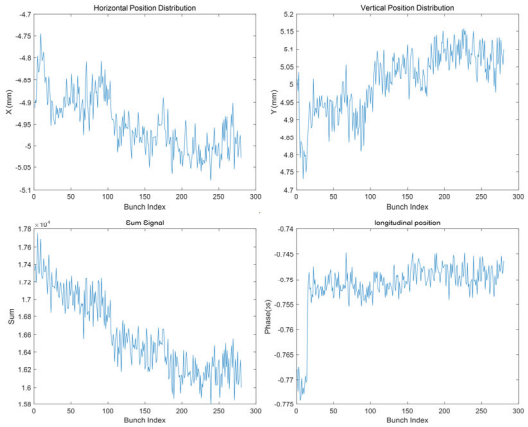



Figure 1: BPM measurement parameters display.

† e-mail address: lengyb@ustc.edu.cn

ISBN: 978-3-95450-262-2 ISSN: 2673-5350 doi: 10.18429/JACoW-IBIC2025-MOPCO03

# BEAM DIAGNOSTICS OF THE NEWGAIN PROJECT

C. Jamet[1,†], S. Leloir[1], P. Salou[1], T. Andre[1], C. Potier de Courcy[1], G. Ledu[1], G. Monier[1], C. Hocini[1], E. Dessay[1], J-C. Foy[1], G. Brunet[1], S. Ferey[1], M. Michel[1], C. Maazouzi[2], T. Adam[2], P. Graehling[2]
[1]GANIL, Caen, France
[2]IPHC, Strasbourg, France

*Abstract*

The aim of the NEWGAIN Project (NEW GAnil INjector), is to build a second injector on the SPIRAL2 accelerator to produce and accelerate heavier beams with A/q up to 7. The NEWGAIN injector is based on 2 ECR ion sources, two LEBT, one RFQ and MEBT lines to send new ion beams in the LINAC and the S3 experimental room.

Diagnostic monitors are planned to measure and control beam intensities, profiles, phases, energies and emittances. A presentation of beam characteristics and a description of the diagnostic monitors are done. Modifications of the beam duty cycle system and the machine protection system are also detailed.

## INTRODUCTION

The NEWGAIN project aims to increase the capabilities of SPIRAL2 LINAC with the build of a second injector designed for A/q = 3 to 7 ions, to produce very intense heavy ion beams up to uranium, exceeding the performance of the existing injector. NEWGAIN will be integrated in the SPIRAL2 facility with these two experimental rooms named NFS (Neutron For Science), S$^3$ (Super Separator Spectrometer) and the low beam experimental room DESIR (Decay, Excitation and Storage of Radioactive Ions) under construction (Fig. 1).

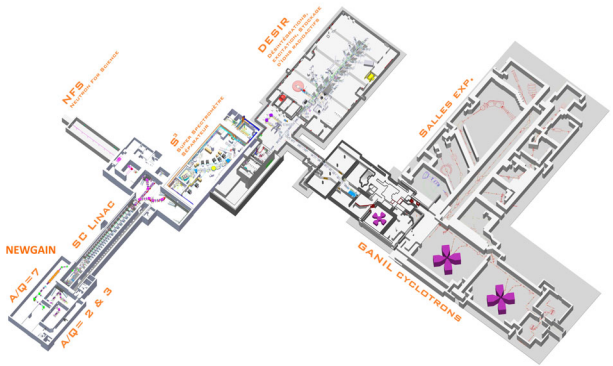



Figure 1: General Layout of GANIL, SPIRAL2 Facilities.

The project includes a new superconducting ion source (ASTERICS), developed to complement the existing sources, two low energy beam transport lines, a second Radio Frequency Quadrupole (RFQ) and medium energy beam lines connecting the SPIRAL2 LINAC with the possibility to send the beam into an experimental area (to be built) in the future (Fig. 2) [1].

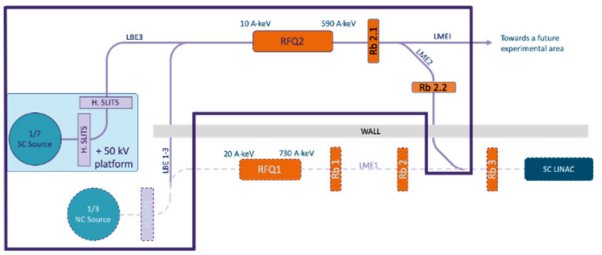



Figure 2: NEWGAIN principle layout (in dotted lines are the existing elements of SPIRAL2).

The injector will be installed in an existing cave in the SPIRAL2 building. The view of the injector inside the existing facility is shown on Fig. 3. Table 1 lists the main injector parameters and Table 2 [2] shows the beam characteristics of the two reference beams considered for the design.

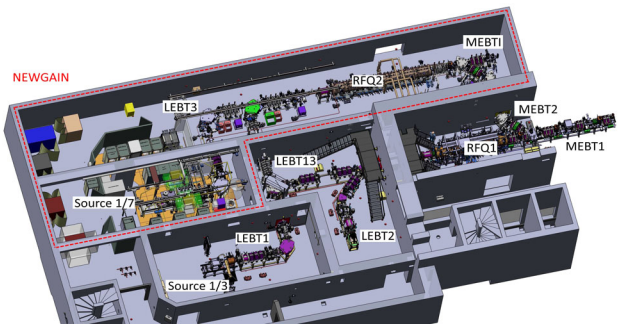



Figure 3: General 3D Layout of the NEWGAIN injector.

Table 1: NEWGAIN Parameters

| **Main Frequency** | **88.0525** | **MHz** |
|---|---|---|
| LEBT Input energy | 10 | A.keV |
| MEBT Input energy | 0.59 | A.MeV |
| HEBT Input energy for A/q = 7 | 7 | A.MeV |

Table 2: Beam Characteristics

| **Reference Beam** | $^{48}Ca^{11+}$ | $^{238}U^{34+}$ | |
|---|---|---|---|
| Normalised RMS emittance | 0.2 | 0.15 | π.mm. mrad |
| Beam intensity | 210 | 340 | µA |
| LEBT beam power | 10 | 24 | W |
| MEBT beam power | 0.54 | 1.4 | kW |
| HEBT beam power | 6.9 | 16.7 | kW |

Content from this work may be used under the terms of the CC BY 4.0 licence (© 2025). Any distribution of this work must maintain attribution to the author(s), title of the work, publisher, and DOI.

ISBN: 978-3-95450-262-2 ISSN: 2673-5350 doi: 10.18429/JACoW-IBIC2025-MOPCO04

# MACHINE LEARNING USING BEAM LOSS MONITORS FOR DIAMOND-II

C. Lehmann*,[1,2], L. Bobb[2], P. N. Burrows[1]
[1]John Adams Institute, University of Oxford, Oxford, UK
[2]Diamond Light Source, Oxfordshire, UK

*Abstract*

The slow losses measured by Beam Loss Monitors (BLMs) at synchrotron light source facilities offer useful but indirect insight into the state of the beam. Patterns arise across the set of BLMs depending on the movement of insertion devices, beam current, temperature, humidity, and other contributors. A variety of neural network models were designed and evaluated to model this behaviour under user beam operation. By applying an anomaly detection algorithm, a set of known disturbances were successfully detected.

## INTRODUCTION

With the upcoming Diamond-II upgrade [1] new BLMs are being installed. The Libera BLMs from Instrumentation Technologies [2] are scintillator-based and capable of measuring losses in both the fast regime (125 MHz, approaching bunch-by-bunch speeds) and slow regimes (5 Hz averaging). The same systems are already in use at several other light sources such as Soleil [3] and ESRF [4]. The data from BLMs is commonly used to identify where and when high loss rates occur for decision making around the Machine Protection Systems (MPS) [5]. However, there is untapped potential to analyse their data to gain diagnostics about the beam itself.

Machine Learning methods are well suited to this problem since a change in the measured loss rate can originate from a variety of sources, often with complex non-linear relationships [6]. Unlike colliders such as the LHC which have quite stable beam conditions, synchrotron light sources such as Diamond have a constantly changing beam state primarily due to beamlines adjusting the gap size or phase of their Insertion Devices (IDs). Beamlines and users adjust these parameters to meet the needs of their experiment sporadically throughout the day, causing subtle changes to the lattice and beam dynamics. Feed-forward tables [7] and feedback systems [8] are heavily used to minimise these effects, but aren't perfect. With sufficient data and appropriate design, a Machine Learning model can predict the effects of these loss rate changes under normal beam conditions, allowing abnormal behaviour to be identified.

Abnormal changes in the losses can come from many sources outside of the knowledge of the model [5]. The difference between the measured beam losses and those predicted by the model can be used to identify these abnormalities. Some abnormalities can have severe consequences for accelerator operations, causing beam degradation or leading to a beam dump. This paper describes the early design and performance of such a BLM anomaly detection system to analyse the slow losses (on the order of seconds) to identify these anomalies and alert an operator to provide corrective action.

## EXPERIMENTAL SETUP

Diamond Light Source is a synchrotron light source facility. Electrons are accelerated to 3 GeV energy and stored in the Storage Ring providing synchrotron radiation for users at the beamlines. The facility is receiving a major upgrade to Diamond-II starting in December 2027 [1], including a new set of Beam Loss Monitors from I-Tech [2].

Diamond-II will have a BLM placed in each of its 24 cells, and more in areas of interest. The term BLM refers to the digitisation and controls box, which each controls and receives data from 4 Beam Loss Detectors - a scintillator with photomultiplier tube [2]. As such, Diamond-II will be able to monitor losses from over 100 detectors simultaneously.

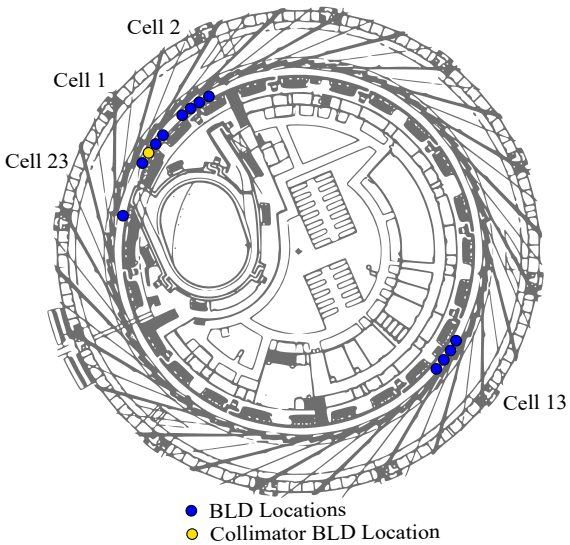



Figure 1: Positions of BLDs for initial testing in the Diamond Light Source storage ring, modified from [9]. The Collimator BLD is shown in yellow.

In preparation for this upgrade, 13 BLDs across 4 BLMs have been deployed in the Diamond storage ring for testing. The locations of these BLDs are shown in Fig. 1, also highlighting the Collimator BLD which has the strongest signal. All BLDs have been calibrated using LED methods similar to those at Soleil [3].

* corey.lehmann@physics.ox.ac.uk

Content from this work may be used under the terms of the CC BY 4.0 licence (© 2025). Any distribution of this work must maintain attribution to the author(s), title of the work, publisher, and DOI.

ISBN: 978-3-95450-262-2 ISSN: 2673-5350 doi: 10.18429/JACoW-IBIC2025-MOPCO05

# LHC BLM SYSTEM AUTOMATIONS FOR FAULT DETECTION, DIAGNOSIS, AND ISSUE TRACKING

D. E. O. Tzamarias*, B. Salvachua, C. Zamantzas
CERN, Geneva, Switzerland

Content from this work may be used under the terms of the CC BY 4.0 licence (© 2025). Any distribution of this work must maintain attribution to the author(s), title of the work, publisher, and DOI.

*Abstract*

One of the principal roles of CERN's Beam Loss Monitoring (BLM) system pertains to the protection of the Large Hadron Collider's (LHC) superconducting magnets against beam-induced quenches. Thus, continuous monitoring of the performance of the BLM system is essential to ensure the high reliability and availability of the LHC BLM protection system. This paper focuses on the architecture of a novel data pipeline with implementations on monitoring the communication status between the 864 acquisition tunnel modules that digitize the analog beam loss measurements and the 432 processing surface modules that determine and act upon the criticality of the beam losses. The discussed pipeline replaces an older batch Extract-Transform-Load (ETL) process, which published daily BLM status reports, in favor of a streaming ETL process. The new pipeline expands beyond the daily publication of static status reports by exploiting real-time data analysis and processing enabling the live assessment of the system's status via online fault detection, web-based dashboards, and automated Jira issue generation enabling issue tracking. Future development on the implemented pipeline envisions online machine learning features permitting fault prognosis.

## INTRODUCTION

The LHC Beam Loss Monitoring (BLM) system plays a pivotal role in guaranteeing the high availability and reliability of the LHC accelerator at CERN from contributing to the optimization of the accelerator to preventing the quenching of superconducting magnets [1]. The BLM system covers, with nearly 4 000 detectors, the 27 km of accelerator elements and comprises thousands of interconnected components ranging from detectors to processing and acquisition electronic units that generate on the order of several Megabytes of data every second. In addition to the system's built-in redundancies and fail-safe design, due to its criticality and large scale, high-level system-wide surveillance is required in order to maintain high dependability. The benefits of such surveillance on the BLM system comprise the anticipation of issues, planning of interventions, and fast fault identification on occasions requiring immediate response.

This paper focuses on a novel high-level surveillance of the BLM system that is accomplished through a streaming Extract-Transform-Load (ETL) pipeline, coined as BL-ARMA an abbreviation for Beam-Loss Analysis, Reporting, and Monitoring Automations. The new data pipeline replaces the original batch ETL design that was limited to providing static insights on the status of the BLM system. BL-ARMA extracts data from various sources, performs streaming transformations, loads the results into databases and, in addition, performs various automations. By harnessing its real-time analytic capabilities, BL-ARMA enhances the surveillance of the BLM system with features including real-time monitoring, daily status reports, automated fault detection and diagnosis, alerts, and issue tracking. The discussed pipeline is part of the Efficient Particle Accelerator project, which aims to incorporate automations, reporting, anomaly detection and real-time analysis on accelerator systems [2].

* dion.efstathios.tzamarias@cern.ch

## BL-ARMA ARCHITECTURE

Prior to implementation, special considerations were given to the design choices of the new streaming data pipeline. The architecture of BL-ARMA aims to exploit on-the-fly data processing and a modular design. In order to accommodate such design features, optimized for CERN's infrastructure, the proposed data pipeline was built upon the Unified Controls Acquisition and Processing (UCAP) framework [3]. UCAP enables the development of event-driven streaming data pipelines through instantiating virtual devices with high throughput processing and pub/sub capabilities.

The modular character of BL-ARMA is accomplished by distributing the pipeline's workload among an ensemble of interconnected virtual devices, each maintaining a designated role. Such a configuration evokes fault-tolerant properties and facilitates the expansion of the pipeline by easily incorporating additional devices. The core processing units of BL-ARMA consist of the Batch-Ingestion, Analysis, Diagnostics, and Reporting devices that are arranged according to Fig. 1.

The role of the Batch-Ingestion device is limited to ingesting data from sources that are updated infrequently such as databases that contain BLM system parameters. The device triggers in a diurnal fashion and consolidates data through merging operations. The resulting information is transmitted to the Analysis device and is stored in buffers for further processing. This acts as a loose coupling connection between the Analysis and Batch-Ingestion devices, increasing BL-ARMA's reliability and robustness against faults localized to individual modules.

Apart from data received from the Batch-Ingestion unit, the Analysis device also ingests measurements from the BLM system at a 1 Hz rate. Its main function consists of performing the core analysis on the raw measurement data to render it amenable to subsequent devices. Most data publications are performed in real-time, however, event-driven publications consisting primarily of data aggregations also

ISBN: 978-3-95450-262-2 ISSN: 2673-5350 doi: 10.18429/JACoW-IBIC2025-MOPCO06

# HIGH-RESOLUTION DIAGNOSTICS OF THE TOP-IMPLART 71 MeV PROTON BEAM USING PHOTOLUMINESCENT COLOR CENTERS IN LiF CRYSTALS *

E. Nichelatti†, ENEA C.R. Casaccia, Rome, Italy
M. Piccinini, A. Ampollini, M. D. Astorino, G. Bazzano, A. Doria, F. Fortini, P. Nenzi, E. Pavoni, G. Picardi, V. Surrenti, E. Trinca, M. A. Vincenti, C. Ronsivalle, ENEA C.R. Frascati, Frascati, Italy

*Abstract*

A LiF crystal plate is irradiated edge-on by the nominal 71 MeV proton beam of the TOP-IMPLART linac, after it has traversed several materials plates and air gaps. The irradiation induces the formation of point defects in the LiF crystal, known as color centers, some of which emit visible radiophotoluminescence when optically excited with blue light. This property is exploited to map the energy deposited by the protons within the LiF crystal, by visualizing the luminescent pattern of the color centers using a fluorescence microscope. Analysis of this pattern, which replicates a superposition of monochromatic proton Bragg curves, enables the estimation of the beam energy spectrum at the LiF crystal position. The corresponding energy spectrum at the linac exit is then inferred by applying a theoretical backpropagation method.

## INTRODUCTION

TOP-IMPLART (Terapia Oncologica con Protoni—Intensity Modulated Proton Linear Accelerator for Radio-Therapy) is a radio frequency (RF) pulsed linear proton accelerator developed at the ENEA Frascati Center laboratories as a prototype for proton therapy, and is now evolving into an irradiation facility for various fields of application [1, 2]. The accelerator consists of a 7 MeV, 425 MHz injector, followed by a 3 GHz booster composed of a series of eight side-coupled drift tube linac (SCDTL) accelerating modules. A scheme of the accelerator is reported in Fig. 1.

The proton beam can be accelerated to 71 MeV or 63 MeV (by switching off the last module) in 2.5 µs pulses, with a typical repetition rate of 25 Hz and a maximum pulse current of 25 µA [3]. Intermediate and lower energies can be obtained by using suitable degraders.

This work employs a recently developed technique for beam energy measurement, which is based on analyzing the spatial distribution of dose deposited in lithium fluoride (LiF) crystals through the detection of radiation-induced luminescent defects. Indeed, upon exposure to various types of ionizing radiation, including accelerated ions, LiF forms stable lattice point defects known as color centers (CCs) [4]. Among them, the $F_2$ and $F_3^+$ centers—consisting of two electrons bound to two and three anion vacancies, respectively—emit visible radiophotoluminescence (RPL) in the red and green regions of the spectrum, respectively, when optically excited within their nearly overlapping absorption bands in the blue region [5]. For the proton energies tested so far, the emitted RPL intensity has been found to vary linearly with the absorbed dose up to approximately $10^5$–$10^6$ Gy [6, 7]. Beyond this threshold, saturation effects begin to appear [8–10].

Under appropriate irradiation geometry, these characteristics can be exploited to map the dose distribution deposited by a proton beam within a LiF crystal plate. As described below, an experimental method combining this mapping with subsequent data analysis is applied to characterize the energy spectrum of the 71 MeV TOP-IMPLART beam.

## ENERGY DIAGNOSTICS METHOD

The method employed to characterize the energy spectrum of a proton beam consists essentially of two experimental phases, illustrated in Fig. 2, followed by the analysis of the resulting data.

In the first experimental step, referred to as the irradiation phase, a thin LiF crystal plate is irradiated in air, with its edge facing the incoming proton beam. This irradiation induces the stable formation of a spatial distribution of CCs, whose local density is directly proportional to the energy deposited by the protons at each point, provided that the dose remains below the previously mentioned threshold of $10^5$–$10^6$ Gy. Consequently, along the beam penetration direction ($z$-axis), the CC density reflects a superposition of Bragg curves corresponding to the monochromatic components that constitute the proton beam energy spectrum. In the subsequent step, the readout phase, the visible RPL emitted by $F_2$ and $F_3^+$ centers is detected from the top face of the crystal using a fluorescence microscope. A two-dimensional map of the RPL emission is then recorded as a high-resolution image for further analysis.

A rectangular region of interest (ROI) is selected within the RPL image (see Fig. 3). By integrating the pixel intensity along the $x$-axis within this ROI, a one-dimensional profile of RPL intensity as a function of proton penetration depth ($z$-axis) is obtained. The RPL intensity profile is then fitted using a weighted superposition of monochromatic Bragg curves, calculated through an analytical model [11] that accounts for fluence reduction due to multiple Coulomb scattering through the faces of the LiF crystal [12]. The weight of each monochromatic Bragg curve is iteratively determined using a localized random search (LRS) algorithm [13]. The resulting distribution of these weights, as a function of the corresponding monochromatic energies, is assumed to rep-

* Work supported by the TOP-IMPLART (Oncological Therapy with Protons – Intensity Modulated Proton Linear Accelerator for Radiotherapy) project, funded by Regione Lazio, Italy.

† enrico.nichelatti@enea.it

Content from this work may be used under the terms of the CC BY 4.0 licence (© 2025). Any distribution of this work must maintain attribution to the author(s), title of the work, publisher, and DOI.

ISBN: 978-3-95450-262-2 ISSN: 2673-5350 doi: 10.18429/JACoW-IBIC2025-MOPCO07

# THE SPS BEAM LOSS MONITORING SYSTEM RENOVATION PLAN

E. Calvo*, E. Effinger, S. Jensen, M. Saccani, B. Salvachua, W. Viganò, C. Zamantzas
European Organization for Nuclear Research, Geneva, Switzerland

Content from this work may be used under the terms of the CC BY 4.0 licence (© 2025). Any distribution of this work must maintain attribution to the author(s), title of the work, publisher, and DOI.

*Abstract*

The Super Proton Synchrotron (SPS) beam loss monitoring (BLM) system at CERN, which has been operational for several decades, will be completely renovated during Long Shutdown 3 (LS3), encompassing detectors, cabling, and acquisition electronics. The upgraded architecture will adopt a design similar to the current Large Hadron Collider (LHC) BLM system, featuring front-end and back-end electronics housed in separate crates and connected via optical links, ensuring compatibility with the LHC upgrade scheduled around LS4. This paper presents an overview of the proposed architecture for the SPS ring and transfer lines, detailing the key components and expected improvements in performance, modularity, and reliability.

## INTRODUCTION

The SPS, the second largest accelerator in the CERN accelerator complex, commissioned in 1976, has a rich and diverse physics programme, providing proton and ion beams to the LHC and to several fixed-target experimental areas such as AWAKE, HiRadMat and the CERN North Area [1, 2].

The BLM system at the SPS, operational for several decades, consists of 286 Ionisation Chambers (IC) distributed around the ring and an additional 144 more located along the various extraction lines (TT20, TT40, TT60) and experimental halls. The ageing and obsolescence of its components compromise maintainability and future operational performance. Consequently, a complete system upgrade is planned for LS3, encompassing detectors, acquisition electronics, and all associated cabling. The proposed architecture has been designed for compatibility with the LHC upgrade planned for LS4 and to optimise BLM system homogeneity across CERN machines. It will deliver substantial improvements over the legacy system, such as shorter acquisition periods, wider dynamic range and sensitivity, reduced beam dump request latency, enhanced remote diagnostics, and improved signal integrity through shorter cables and optimised cabling strategy.

## DETECTOR RENOVATION

The legacy SPS detectors will be replaced by gas ionisation chambers based on the LHC design (Fig. 1). Both designs operate on the same principle but differ in dimensions, gas volume, and operating parameters.

The legacy SPS detectors are 278 mm long and 114 mm diameter cylindrical chambers equipped with 31 circular parallel plates spaced 5 mm apart. They enclose approximately

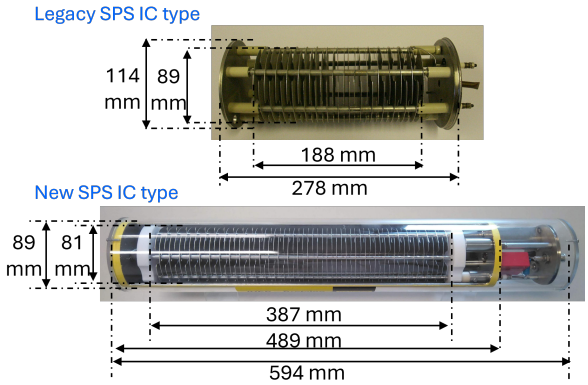



Figure 1: Comparison of legacy and new SPS detectors.

1.1 litres filled with air at room temperature and 1.1 bar pressure and biased at 800 V [3–5].

On the other hand, the new detectors are 489 mm long and 89 mm in diameter, with a sensitive volume of 1.5 litres filled with $N_2$ at 1.1 bar and operated at 1.5 kV. The internal structure consists of 61 parallel aluminium electrodes separated by 5 mm. The respective conversion factors are 36 µC/Gy and 54 µC/Gy [6], thus yielding an approximate 50 % increase in sensitivity, primarily from the larger gas volume.

### *Detector Distribution*

To ensure a smooth migration of one of the SPS's most critical machine safety systems, it is proposed that both systems will operate in parallel until the complete commissioning of the new system. This strategy will enable a systematic comparison of the loss maps evolution, distinguishing between changes due to machine configuration and those attributable to the BLM system upgrade.

To achieve this, the new detectors will be placed on the existing supports using high-density polyethylene insulators to accommodate the detector size differences and enhance the insulation to the machine earth. The old detectors will be mounted on clamp kits, resulting in just a few cm displacement compared to pre-LS3 positions. These clamp kits (Fig. 2) can be easily deployed and removed, accommodate the diversity of existing supports, and do not require any additional drilling in highly activated regions.

However, this arrangement will not be feasible everywhere. In the legacy system, detectors in the arc regions are alternately positioned at beam height in the space between magnets, in front of the defocusing quadrupoles (QD), or beneath the first dipole downstream of the focusing quadrupoles (QF). The new detectors, being longer, will not fit below the dipoles. Moreover, this asymmetric layout causes measurements along the arcs to exhibit a triangular

* eva.calvo.giraldo@cern.ch

ISBN: 978-3-95450-262-2 ISSN: 2673-5350 doi: 10.18429/JACoW-IBIC2025-MOPCO08

# A 3 GHz WALL CURRENT TRANSFORMER FOR VERY HIGH BANDWIDTH BEAM CURRENT MEASUREMENTS

F. Stulle†, H. Bayle, L. Dupuy, E. Touzain, Bergoz Instrumentation, Saint-Genis-Pouilly, France
P. Korysko*, University of Oxford, Oxford, United Kingdom
R. Corsini, W. Farabolini, CERN, Geneva, Switzerland

## *Abstract*

Non-destructive beam current measurements are a crucial aspect of beam instrumentation in any particle accelerator. Often, these measurements must be capable of distinguishing individual beam pulses. In an increasing number of accelerators, pulse repetition rates reach the GHz range. Consequently, beam current measurement bandwidth must exceed a few GHz.

To meet this requirement, a wall current transformer was developed with a bandwidth exceeding 3 GHz. It was tested using a vector network analyser and with an electron beam at CERN's CLEAR facility. Both measurements showed excellent agreement. We introduce the wall current transformer principle and discuss the measurement results. Additionally, we highlight some challenges that must be addressed when measuring high-frequency signals.

## INTRODUCTION

In particle accelerators, beam current measurements are used to evaluate long-term stability, transport efficiency, bunch-to-bunch variations or even bunch length. Each of these applications demands different measurement characteristics, notably bandwidths. To allow the separation of individual bunch signals, current measurement bandwidth must surpass the bunch repetition rate, which can be in the GHz range.

Previous attempts to push bandwidth limits above several GHz showed that Wall Current Monitors (WCM) and Wall Current Transformers (WCT) are principally capable of achieving such a goal [1-3]. However, no device evolved out of these efforts that is as versatile and generally available as a normal current transformer.

At Bergoz Instrumentation a development was carried out aiming to achieve 3 GHz bandwidth with a device that resembles closely a normal UHV-compatible current transformer of 40 mm length.

### *Very Fast Current Transformer*

The Very Fast Current Transformer (VFCT) (Fig. 1) is based on the WCT measurement principle [3-5]. That means, instead of measuring the beam current with a single current transformer that surrounds the entire beam, the vacuum chamber wall is cut into several segments, and small transformers measure the beam-induced currents flowing across each of these segments. Since these transformers are considerably smaller, detrimental resonances are pushed to higher frequencies. Individual transformer signals are combined inside the VFCT.



Figure 1: Very Fast Current Transformer.

As a particularity, the VFCT was designed to provide a differential output signal using two SMA connectors. The difference of these signals gives the measurement result proportional to beam current. Creating a differential output signal was preferred because it reduces signal perturbations inside the VFCT. Using two SMA output connectors allows signal transmission over low-loss coaxial cables.

The VFCT has a bandwidth from below 200 kHz to above 3 GHz and a sensitivity of about 1 V/A. It is intended to measure short single pulses or high-repetition rate pulse trains.

### *CLEAR Facility*

The CERN Linear Electron Accelerator for Research (CLEAR) is a user facility providing electron beams for a varied and large range of experiments [6]. The electron beam is produced by sending a pulsed UV laser to a $Cs_2Te$ photocathode and is then accelerated to 200 MeV with three 3 GHz accelerating structures in a 20 m long linear accelerator. The accelerated beam is then transported to several experimental beamlines, both in air and in vacuum.

A pulse made of 1 to 150 bunches can be sent to all these experimental beamlines. The bunch length is typically around 3 ps and the bunch separation can be either 333 ps (3 GHz bunch repetition rate) or 667 ps (1.5 GHz bunch repetition rate). The pulse repetition rate can range from 0.833 Hz to 10 Hz.

Being able to produce bunches at 3 GHz repetition rate, CLEAR requires high frequency beam instrumentation for successful accelerator tuning and, consequently, high quality beam delivery to the experiments. However, sufficiently fast beam current diagnostics was previously not available for standard operation.

For the measurements performed at CLEAR, the VFCT was installed in air at the end of the CLEAR beamline just in front of the beam dump.

Content from this work may be used under the terms of the CC BY 4.0 licence (© 2025). Any distribution of this work must maintain attribution to the author(s), title of the work, publisher, and DOI.

† stulle@bergoz.com
* pierre.korysko@cern.ch

ISBN: 978-3-95450-262-2 ISSN: 2673-5350 doi: 10.18429/JACoW-IBIC2025-MOPCO09

# EPAC BEAMLINE PROTOTYPE: DEVELOPMENT AND OPTIMISATION OF A HIGH-REPETITION-RATE LWFA SYSTEM

K. Fedorov†,1, O. Finlay[1], D. Symes[1], A. Bennett[1], J. Giles-Friend[1], A. Bhardwaj[1], N. Bourgeois[1], C. D. Armstrong[1], C. Selig[1], A. Thomas[1], C. Spindloe[1], R. Pattathil[1], B. Morkot[1], S. J. D. Dann[1], B. Spiers[1], C. Hernandez-Gomez[1], E. Kiely[2], D. McCartney[3], M. Streeter[3]
[1]Central Laser Facility, STFC Rutherford Appleton Laboratory, Didcot, UK
[2]Warwick Manufacturing Group, University of Warwick, Warwick, UK
[3]Centre for Light-Matter Interactions, Queen's University Belfast, Belfast, UK

*Abstract*

The Extreme Photonics Applications Centre (EPAC) is a next-generation high-power laser facility designed to deliver stable, high-repetition-rate (10 Hz) electron beamline with high quality parameters (~1 nC, ~1 GeV, <5 % energy spread) produced by laser-wakefield acceleration (LWFA). These beams will serve as drivers for compact secondary sources, including high-brilliance betatron and inverse-Compton X-rays, enabling a broad range of scientific and industrial applications. To de-risk the commissioning of EPAC, Target Area 2 (TA2) of the Central Laser Facility (CLF) Gemini laser has been set up as a prototype beamline, allowing development of reliable gas-cell targetry, identifying beam-instability sources, testing of optimisation routines, and electron transport configurations. Results from the new beamline highlight the feasibility and challenges of achieving multi-hour operation, providing a practical route toward reliable EPAC operation.

## INTRODUCTION

Delivering consistent operation of a LWFA beamline in the Extreme Photonics Applications Centre (EPAC) [1] requires stable laser [2] and target behaviour [3] over many hours. Even small variations in plasma density, laser pointing, or optical aberrations can strongly influence beam charge, energy and stability, making it essential to combine durable hardware solutions with advanced optimisation methods. In this work we use the Gemini TA2 prototype beamline as a development platform to investigate gas-cell design and aperture survivability, assess the origins of electron beam fluctuations, and implement Bayesian optimisation routines capable of efficiently tuning multi-parameter control spaces. The TA2 laser system can provide 5 Hz, 400 mJ, 40 fs laser pulses focused to a 20 µm spot (Fig. 1). The laser pulse interacts with the 2-3 mm gas-cell target filled with 98 % He with 2 % $N_2$.

## TARGETRY DEVELOPMENT

To control the plasma density and profile we have designed a custom gas-cell, maintaining the flexibility of the design in Ref. [4]. The aim was to ensure easy maintenance of the cell, since laser jitter can cause significant damage to the entrance/exit apertures of the cell and blackening of the probe beam windows from debris, especially operating at 5 Hz repetition rate. The main components of the new design are highlighted in Fig. 2.

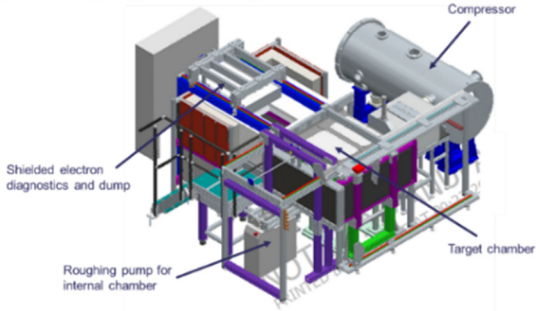



Figure 1: Compact LWFA system in Gemini Target Area 2.

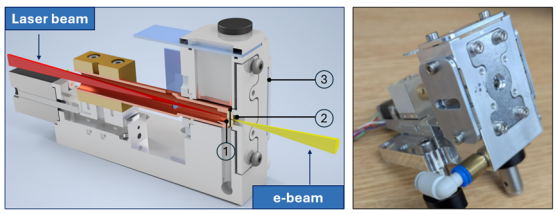



Figure 2: Left: Gas-cell assembly design: 1: replaceable entrance aperture (variable position); 2: replaceable exit aperture; 3: probe beam windows. Right: Assembly with motorised stage to control gas-cell length.

The investigation of both aperture disk thickness and aperture hole diameter, and their influence on the gas density profile, is important for optimising LWFA performance. The aperture hole diameter (e.g., 200 µm entrance, 400 µm exit) determines gas leakage rate, shaping the density across the cell and influencing gas load in the target chamber. At the same time, aperture thickness determines the density ramp length impacting electron injection efficiency and beam stability. A well-optimized combination of these parameters reduces electron energy spread and improves charge [5]. We performed a set of simulations in OpenFOAM software [6] to demonstrate how thicker apertures (up to 1 mm) produce a longer density profile slope, potentially smoothing injection but reducing efficiency, whereas a thinner (down to 300 µm) apertures maintain a sharper gradient (Fig. 3 Left). At the same time, increasing entrance/exit hole sizes decrease overall density due to increased leakage (Fig. 3 Right). The dependence of the gas density profile on gas cell configuration, particularly aperture diameters, highlights the importance of studying aperture durability, as they are critically exposed to high-power

† Kirill.fedorov@stfc.ac.uk

Content from this work may be used under the terms of the CC BY 4.0 licence (© 2025). Any distribution of this work must maintain attribution to the author(s), title of the work, publisher, and DOI.

ISBN: 978-3-95450-262-2 ISSN: 2673-5350 doi: 10.18429/JACoW-IBIC2025-MOPCO10

# THE IMPACT OF POSITIONAL INACCURACY ON 3D X-RAY IMAGE QUALITY *

L. Eley†,[1], C. P. Welsch[1], University of Liverpool, Liverpool, UK
A. Mavalankar, S.Wells, Adaptix Ltd, Oxford, UK
[1]also at Cockcroft Institute, Warrington, UK

*Abstract*

X-ray imaging of both material and biological samples is a key application of synchrotrons and laser wakefield accelerators. However, it is possible that undiagnosed beam location offsets can impact the quality of the image created. This is particularly the case in 3D imaging, for which the 3D reconstructions require precise knowledge of the location at which each x-ray projection was taken. This study uses a low-energy x-ray imaging device designed to perform mobile digital tomosynthesis (DT), a modality of 3D x-ray imaging, for veterinary scanning to investigate the impact of this. An intentional offset is randomly applied of size 0.5 mm and 1 mm from the expected x-ray source position, and the quality of the reconstructed image is assessed for both the case where this offset is accounted for, and where it is not. From this, it is concluded that x-ray beams used for 3D imaging applications can have up to a 1 mm error without seeing large degradation in reconstructed image quality.

## INTRODUCTION

The ability of synchrotrons and laser-wakefield accelerators to create x-ray beams to be used for imaging of both biological and material samples is an application of interest for this technology [1–5]. For biological samples, studies have found that the monochromaticity of such sources helps constrain patient dosage without the need of extra filtration layers [2], while for NDE studies, the ability to reach very high x-ray energies mean samples with high density can be quickly imaged. These findings apply to both 2D imaging, in which only a single image is taken, and 3D imaging, in which multiple projections of an x-ray source are required in order to for a 3D image to be mathematically reconstructed.

The most common mathematical approach to 3D image reconstruction is filtered backprojection [6, 7]. For each position of the source, a raytracing approach between the source and individual projection is used in order to average and transform the signal per pixel at different object heights. Therefore, with precise knowledge of where the source is for each image collected, a quasi-3D model can be mathematically created. This has the benefit over 2D images of being able to distinguish overlapping features more clearly.

Digital tomosynthesis (DT) is an example of a 3D imaging modality. Multiple projections of an X-ray source are used to create data that can be reconstructed using filtered backprojection, or similar techniques, into a 3D image. Adaptix Ltd have developed a mobile DT device that uses a planar two-axis grid of x-ray emitters to create data that can be 3D reconstructed [8, 9].

The overlap of the reconstruction techniques for both this small DT device and that used for imaging from accelerators means that this study, performed on Adaptix Ltd's veterinary scanner [10] in Fig. 1, can be used to infer the importance of knowing the exact location of the x-ray beam output from accelerator x-ray sources.

## METHOD

As stated, this study was performed using a veterinary scanner produced by Adaptix Ltd, as seen in Fig. 1 [9]. This device uses a transmission-type X-ray tube moved by mechanical stages to collect multiple projections at a voltage of 70 kV. The exact positions of the tube can be externally set, so for this investigation, a 6 x 6 grid of projections spaced by 10 mm was used. An image set was taken with no offset introduced. A second set was taken with a random positional offset of 0.5 mm introduced, and a third with a 1 mm offset randomly applied. To test the impact of these offsets in a way that could be quantified, 5 mm thick layer of PMMA with a grid of 25 equally spaced 1 mm aluminium spheres embedded within it from the Leeds Test objects TOMO IQ set [11] was imaged. Figure 1 displays both the veterinary scanner and the TOMO IQ phantom described above, which is placed on the detector.

To reduce error and improve image quality, all datasets taken had two frames per projection: one in which the phantom was present, and another where it was not. The image without the phantom present was subtracted from the one where it was to remove the effect of any features of the system from the images to be analysed. The images subtracted are known as 'air' frames, or for the sake of brevity, simply 'airs'.

The datasets containing offset projections were reconstructed four times. In the first, the images taken with the offset applied use the same air data and reconstruction positions, or 'keys', as if there were no offset. In the second, the offset keys are applied to the mathematical reconstruction, but the incorrect air data is subtracted. In the third, the correct air data is subtracted, but the uncorrected keys applied. Finally, both correct keys are used in the reconstruction and the correct air data for the position is applied. This approach was chosen under the assumption that a system where positional inaccuracies are present, it is likely both the airs and keys will be incorrect in the reconstruction, so the aim

* This work was jointly supported by Adaptix Ltd and the Science and Technology Facilities Council (STFC) under grant agreement ST/W006766/1.
† lauryn.eley@liverpool.ac.uk

Content from this work may be used under the terms of the CC BY 4.0 licence (© 2025). Any distribution of this work must maintain attribution to the author(s), title of the work, publisher, and DOI.

ISBN: 978-3-95450-262-2 ISSN: 2673-5350 doi: 10.18429/JACoW-IBIC2025-MOPCO11

# OPTICAL BEAM LOSS MONITOR INSTALLED AT THE SPS SLOW EXTRACTION REGION

M. King*[1], S. Benitez Berrocal, E. Effinger, J. Esteban, J. Kearney, J. M. Meyer, B. Salvachua
CERN, Geneva, Switzerland
C. P. Welsch[1], J. Wolfenden[1], Cockcroft Institute, Daresbury, United Kingdom
[1]also at University of Liverpool, Liverpool, United Kingdom

*Abstract*

An optical beam loss monitor (oBLM) has recently been installed at the slow extraction region of the Super Proton Synchrotron (SPS) at CERN. The oBLM offers a new method for detecting beam losses at the SPS by utilizing the Cherenkov radiation emitted during beam loss interactions with an optical fibre. This setup should allow to measure losses continuously over a large section of the accelerator, thus minimising the non-linearities caused by the finite coverage of the currently installed ionisation chambers. Due to the high radiation levels and low expected signals at this location, special care was taken during the procurement process to maximise the signal levels while at the same time extending the lifetime of the system as much as possible. The rationale behind the choice of specific components is discussed, highlighting their advantages compared to other options. Furthermore, initial measurements of beam loss during extraction are presented, and the system's ability to provide real-time diagnostics for machine protection and beam optimization investigated.

## INTRODUCTION

The Super Proton Synchrotron (SPS) at CERN not only delivers high-intensity proton beams to the LHC, but also to a variety of other experiments, including fixed target experiments in the North Area. The beams toward the North Area are extracted over several seconds using a slow extraction technique based on a third-order resonance, a method that is inherently lossy [1, 2].

To monitor these losses and support safe and efficient operation, the SPS operators rely on a number of ionisation chamber (IC) beam loss monitors (BLMs) installed in this region. However, conventional IC-BLMs provide limited spatial coverage. Therefore, when using the beam loss signals to optimize the machine, it cannot be distinguished between a local reduction of beam losses or a shift of beam losses to an area that is not covered by the IC-BLMs system.

The need for a longitudinal BLM has been expressed as a solution to improve the longitudinal coverage of the beam loss monitoring during the slow extraction [3]. It was chosen to pursue optical BLMs (oBLMs) as the primary option for this region. oBLMs have been investigated at multiple facilities around the world [4–9] and recently at CERN at the CERN linear electron accelerator for research (CLEAR) [10, 11]. oBLMs are based on Cherenkov light being emitted when charged loss particles traverse optical fibres at a high speed. The optical fibre not only detects the loss particles but can also transport the emitted Cherenkov photons to either end of the fibre at which photodetectors are located. This enables position-resolved monitoring over long distances. Previous installations have typically been at accelerators with low beam repetition rates and clear bunch structures. This allows to use the timing information of the loss signals to reconstruct the loss position.

However, using oBLMs to cover the SPS slow extraction region presents a unique combination of challenges not encountered in earlier test campaigns at CLEAR or other installations. These include high radiation levels, the absence of time structure within the unbunched beam, a lack of shielding for the photodetectors, and the relatively large distance between the fibre duct and the beam due to integration restrictions.

In the following, decisions taken during the procurement process to minimise the impact of these issues will be discussed and preliminary results will be shown.

## INSTALLATION

For this installation, three main choices had to be made. What type of optical fibre to use, which photodetectors are best suited to these conditions and how to readout the data.

### *Optical Fibre*

Through simulations and a previous prototype [12], it quickly became clear that it would be vital to increase the signal capture as much as possible. Therefore, instead of the 200 µm, 0.22 numerical aperture (NA) fibre previously installed, it was decided to install a 600 µm, 0.5 NA, high hydroxyl group (OH) concentration optical fibre, FP600URT from "Thorlabs, Inc.". By choosing a thicker fibre, both the area covered by the oBLM and the mean path length of particles hitting the fibre is increased. This leads to a noticeable increase in captured signal. Simulations indicate that signal levels increase with the thickness of the fibre to the power of 2.5 [12]. This results in an increase of a factor of 15.6 when comparing between these two fibres.

Increasing the NA increases the angular range in which photons are captured and transported along the fibre, as visualised in Fig. 1. The curves were calculated based on formula (22) in [13]. This comes at the cost of higher dispersion [6]. Going from a NA of 0.22 to a NA of 0.5 increases the overall captured signal by a factor of 5.42, assuming a uniform angular distribution of loss particles. This is calculated by

* m.king@cern.ch

Content from this work may be used under the terms of the CC BY 4.0 licence (© 2025). Any distribution of this work must maintain attribution to the author(s), title of the work, publisher, and DOI.

ISBN: 978-3-95450-262-2 ISSN: 2673-5350 doi: 10.18429/JACoW-IBIC2025-MOPCO12

# FIRST BEAM COMMISSIONING EXPERIENCE WITH RF SYSTEM-ON-CHIP-BASED BUNCH-BY-BUNCH SIGNAL PROCESSING SYSTEM AT SLS 2.0

P. Baeta, B. Keil, G. Marinkovic, Paul-Scherrer-Institut, Villigen, Switzerland

Content from this work may be used under the terms of the CC BY 4.0 licence (© 2025). Any distribution of this work must maintain attribution to the author(s), title of the work, publisher, and DOI.

*Abstract*

After a dark time of 15 months, the new diffraction limited storage ring SLS 2.0 had first beam in January 2025. In April 2025, the nominal beam current of 400 mA was reached. In this contribution, we present the status and first beam commissioning experience with the RF System-on-Chip (RFSoC) based signal processing systems of the new SLS 2.0 ring. RFSoCs integrate several fast multi-GSample/s ADCs and DACs, FPGA (programmable logic) fabric and multi-core CPUs all on the same chip. During SLS 2.0 commissioning, the integrated EPICS IOC of the RFSoCs provided bunch-by-bunch diagnostics of dedicated BPM position and charge readings. Integrated DACs are driving newly developed transverse and longitudinal kicker magnets, enabling bunch-by-bunch excitation and damping. Bidirectional multi-Gigabit fiber optic links connect the RFSoC to the event system master, thus enabling both synchronisation of the RFSoC to the event system, as well as real-time control of the event system master by the RFSoCs, e.g. for control of beam injection timing and filling pattern.

## INTRODUCTION

The Swiss Light Source (SLS), the 3rd generation light source at Paul Scherrer Institut (PSI), began user operation in 2001. After more than two decades of successful operation, SLS was decommissioned in September 2023. Between September 2023 and December 2024 (the "dark time"), the storage ring was replaced by the new diffraction-limited storage ring of the SLS 2.0 upgrade project. The new ring features a lower emittance and an increased beam energy of 2.7 GeV, providing up to 60-fold higher brightness for hard X-ray users to ensure competitiveness with other state-of-the-art facilities. Commissioning of SLS 2.0 started in January 2025. By mid-2025, the main performance goals of the storage ring had been achieved [1], paving the way for the first pilot user experiments in July 2025. As part of the SLS 2.0 upgrade, RFSoC-based signal processing systems were introduced, replacing ageing VME-based electronics and providing feedback systems: The multi-bunch feedback (MBFB), the filling pattern feedback (FPFB), as well as diagnostics tools such as coupled-bunch mode (CBM) instability monitoring, bunch-by-bunch beam arrival-time measurement, and charge monitoring. The feasibility and development of these systems with the RFSoC were previously demonstrated in [2, 3] and they have now been deployed in the upgraded storage ring. This contribution reports on the status of the RFSoC-based systems in the upgraded machine and presents results from the first six months of commissioning.

## RFSOC-BASED SYSTEMS

The hardware set-up of the RFSoC-based processing systems at the SLS 2.0 storage ring is built around the AMD ZCU111 evaluation board, which we packaged in a 19″ enclosure together with two in-house developed add-on cards and referred to as the RFSoC-box. One add-on card provides control of a separate RF front-end (RFFE) and a fast beam-dump controller (BDC), while the other breaks out the 8 ADC and 8 DAC channels of the RFSoC via SMA connectors. The ZCU111 incorporates a first-generation Xilinx Zynq UltraScale+ RFSoC, integrating multi-GS/s ADCs and DACs, FPGA programmable logic, and two multi-core ARM CPUs: A quad-core 64-bit application processing unit (APU) and a dual-core real-time 32-bit processing unit (RPU). In this configuration the device offers eight 12-bit ADCs at 4.096 GS/s and eight 14-bit DACs at 6.5 GS/s. In the present setup, three RFSoC-boxes are deployed: one dedicated to the FPFB (including bunch arrival-time and bunch charge measurement), one to the transverse MBFB, and one to CBM diagnostics. This modular approach was chosen for initial operation to simplify development, where integration of MBFB and advanced diagnostics on a single RFSoC is planned [2]. Signals from four capacitive BPM buttons are conditioned in an RF hybrid network, generating a sum signal (S), proportional to bunch charge, and a difference signals (X, Y), proportional to horizontal and vertical bunch offsets times bunch charge. These signals are connected to an external RFSoC RFFE box that provides digital step attenuators (DSAs) and RF amplifiers. With ~1 GHz bandwidth, three analogue conditioning paths enables on-line user-controllable gain/attenuation adjustments, providing overvoltage protection for the RFSoC data converters, and allowing independent channel on/off switching. For the FPFB, the sum signal S is directly sampled at approximately 4 GS/s and processed in real-time by the RFSoC's RPU, enabling bunch-charge and arrival-time diagnostics as well as execution of the feedback algorithm. A dedicated bidirectional 2.5 Gbit/s optical fiber link between the FPFB and the event system master (EVM) closes the FPFB loop, with the RFSoC transmitting and receiving information to control beam injection timing and thus the filling pattern. In addition, the FPFB is connected to a second optical link from the EVM carrying event codes. These are decoded by an embedded event receiver (EEVR) in the programable logic (PL), synchronizing both the FPFB and the MBFB system with the SLS 2.0 event system. In contrast to the FPFB, which directly samples the BPM sum signal, the MBFB still relies on analogue down-conversion at the current stage of commissioning, while direct sampling is foreseen for future operation. Before digitization in the RFSoC, the

ISBN: 978-3-95450-262-2 ISSN: 2673-5350 doi: 10.18429/JACoW-IBIC2025-MOPCO13

# SIMULATION AND FEASIBILITY ANALYSIS OF A NON-INVASIVE CAVITY BUNCH CHARGE MONITOR FOR LOW-ENERGY ANTIPROTON BEAMS

S. Chandran[1,2,*], N. Kumar[1,2], B. Rienacker[1], B. S. Rawat[1,2], C. P. Welsch[1,2]
[1]University of Liverpool, Liverpool, United Kingdom
[2]Cockcroft Institute, Warrington, United Kingdom

*Abstract*

For high-precision experiments involving low-energy antiprotons, accurate non-invasive beam charge measurements are essential. This work presents a simulation study of a cavity-based Bunch Charge Monitor (BCM) as an alternative to invasive methods such as Faraday Cups and Microchannel Plate (MCP) detectors, which suffer from charge loss. The challenge is particularly significant for low-energy antimatter beams, where accounting for such losses is difficult. Motivated by the needs of antimatter experiments like AEgIS at CERN, the study explore the feasibility of a compact re-entrant cavity design for non-relativistic beams. Preliminary simulations are presented along with identified limitations, highlighting the potential of this BCM and its prospects for further development.

## INTRODUCTION

Non-invasive charge measurement of low-energy particle beams remains a challenge in precision physics experiments. As noted in [1], beams with long bunch lengths, low repetition rates, or non-relativistic energies are especially difficult to diagnose with conventional non-invasive techniques since detector sensitivity drops at long timescales and the induced image currents become weaker and broadened. Invasive devices such as Faraday Cups or MCPs can provide charge information, but they suffer from charge loss and cannot detect neutral secondaries (photons, pions, neutrons) generated during beam-matter interactions [2, 3]. This limitation is substantial for low-energy antimatter, where annihilation and complex interactions with matter make charge loss difficult to quantify. On the other hand, established non-invasive approaches such as current transformers or wall current monitors require integration over multiple bunches, which is not feasible in facilities with long bunch delivery intervals.

The Antimatter Experiment: Gravity, Interferometry, Spectroscopy (AEgIS) at CERN [4] exemplifies these challenges. It produces antihydrogen from antiprotons delivered by the Extra Low ENergy Antiproton (ELENA) ring, where bunches arrive only once every two minutes [5]. Precise single-bunch charge measurements are essential for optimizing the experimental setup and accurately interpreting results, but remain difficult to achieve. AEgIS currently employs invasive detectors alongside scintillator-based non-invasive diagnostics. However, the former cannot account for neutral secondaries [3], while the latter suffers from systematic uncertainties at the level of 50 % [6]. ELENA also operates a Cryogenic Current Comparator (CCC) [7], which provides excellent sensitivity but requires cryogenic cooling and magnetic shielding, limiting its applicability in environments such as AEgIS, where strong magnetic fields and tight spatial constraints are present.

These limitations motivate the search for an alternative diagnostic method. A promising approach is a cavity-based Bunch Charge Monitor (BCM), which exploits the resonant response of an RF cavity to a passing beam. While cavity monitors are widely used for high-frequency, relativistic beams [8–11], their extension to the low-frequency, large-bunch-spread regime relevant to antimatter experiments has not yet been explored. This work presents a simulation-based feasibility study of a compact re-entrant cavity BCM designed to measure the charge of a single non-relativistic beam pulse of antiprotons. The study investigates how geometric modifications and material loading can reduce cavity size while maintaining sensitivity, and discusses the challenges involved. The results provide a first step toward future experimental implementation and highlight prospects for broader application in low-energy antimatter beam diagnostics.

## CONCEPT OF A CAVITY BUNCH CHARGE MONITOR

The principle of a cavity BCM is well established; a closed metallic cavity supports discrete electromagnetic modes. A passing charged particle bunch excites modes whose frequencies overlap with its bunch spectrum components. This stored energy is extracted as a signal proportional to bunch charge [12]. Such devices have been successfully implemented at facilities including PSI, Switzerland and the TOP-IMPLART facility at INFN Frascati, Italy [8, 9].

Among the available modes, the $TM_{010}$ mode is commonly used, as its longitudinal electric field couples efficiently to the beam. In most applications, the cavity frequency is chosen to match the bunch repetition frequency, enabling multi-bunch integration for high sensitivity. At very low repetition rates, like ELENA, matching frequency to repetition rate is impractical. Instead, it is more effective to tune the cavity to the bunch spectral width. In this study, a gaussian bunch of $\sigma_t \approx 75$ ns, corresponding to the ELENA beam, was chosen as the design target.

The fundamental frequency $f_0$ scales with cavity size. In the 1–100 MHz range, dimensions of a pillbox cavity span

* sruthy.chandran@liverpool.ac.uk

Content from this work may be used under the terms of the CC BY 4.0 licence (© 2025). Any distribution of this work must maintain attribution to the author(s), title of the work, publisher, and DOI.

ISBN: 978-3-95450-262-2 ISSN: 2673-5350 doi: 10.18429/JACoW-IBIC2025-MOPCO14

# COMMISSIONING OF THE CLARA FACILITY: STATUS UPDATE AND DIAGNOSTICS PERFORMANCE

T. H. Pacey*,[1], T. Hall[1], V. Malconi[1], S. Mathisen[1], T. Overton[1], Y. M. Saveliev[1], E. Shackleton[1], R.J. Smith[1], E.W. Snedden[1], D.A. Walsh[1]
ASTeC, STFC Daresbury Laboratory, Warrington, UK
G. Cox, L. McNicholl, M. Shaw, J. Wilson
Technology Department, STFC Daresbury Laboratory, Warrington, UK
[1]also at Cockcroft Institute, Sci-Tech Daresbury, Warrington, UK

*Abstract*

The Compact Linear Accelerator for Research and Applications (CLARA) is STFC Daresbury Laboratory's flagship accelerator facility. We present the latest data from the commissioning of the CLARA facility at Daresbury Laboratory. This will include initial beam measurements and diagnostic performance for the 250 MeV high brightness, highly compressed electron bunches. An overview of the diagnostic requirements and anticipated challenges for these high impact user experiments will be provided. The future direction of diagnostics at CLARA, including potential system upgrades and plans for virtual diagnostics, is also discussed.

## INTRODUCTION

The Compact Linear Accelerator for Research and Applications (CLARA) is a high-brightness electron beam facility at Daresbury Laboratory [1]. Following an upgrade and commissioning period, the accelerator reached the final design energy of 250 MeV in April 2025. Bunches at CLARA are generated at 100 Hz from a 1.5 cell S-Band photoinjector gun and then accelerated with 4 S-band linacs (one 2 m long and three 4 m long). The Full Energy Beam Exploitation (FEBE) beamline, which includes a shielded user experiment hutch, has been installed [2]. A 120 TW laser system has been installed (2.8 J, 23 fs at 5 Hz), which can be brought to a focus within the FEBE experimental chambers for interaction with the CLARA electron beam. A schematic of the CLARA facility is shown in Fig. 1, the total length is ≈ 80 m. The target beam parameters to be delivered to the FEBE hutch for first experiments are shown in Table 1, alongside future research and development targets following a periods of machine development.

## BEAM DIAGNOSTICS AT CLARA

The CLARA lattice is highly instrumented with 94 diagnostic systems; utilising both commercial off-the-shelf and in-house developed bespoke systems. A breakdown of these systems is given in Table 2. Further experimental systems are utilised to verify the parameters in Table 1 [3]. A S-Band transverse deflecting cavity is installed at CLARA, providing bunch profile and longitudinal phase space measurements before the FEBE arc (see Fig. 1).

Table 1: Specification for CLARA Beam parameters delivered to FEBE hutch. All beam parameters are specified for 250 MeV, with $Q$: bunch charge, $\sigma_i$: RMS value, $\epsilon_{N,i}$: normalised projected RMS emittance.

| | Target | | R&D | |
|---|---|---|---|---|
| **Parameter** | **High $Q$** | **Low $Q$** | **High $Q$** | **Low $Q$** |
| $Q$ (pC) | 250 | 5 | 250 | 5 |
| $\sigma_t$ (fs) | 100 | 50 | ≤ 50 | ≪ 50 |
| $\sigma_{x,y}$ (µm) | 100 | 20 | 50 | ~ 1 |
| $\sigma_E$ (%) | < 5 | < 1 | 1 | 0.1 |
| $\epsilon_{N,x}$ (µm-rad) | 5 | 2 | < 5 | < 1 |
| $\epsilon_{N,y}$ (µm-rad) | 5 | 2 | < 1 | < 1 |

Table 2: System Breakdown of the 94 Electron Beam Diagnostic Systems Installed in the CLARA Beamline

| **System** | **No. of devices** |
|---|---|
| Charge Measurement | 10 |
| Scintillator Screens | 35 |
| Beam Position Monitors | 44 |
| Beam Arrival Monitors | 3 |

### *Charge Measurement*

The ten charge measurement devices on CLARA break down as follows: 1 wall-current monitor (WCM), 5 Faraday cups and 4 integrating current transformers (ICT).

The WCM is a non-interceptive diagnostic located between the photoinjector gun and first linac. The WCM signal is processed using a variable sensitivity front-end. This allows for absolute measurement of the dark-current from the gun and simultaneous relative measurement of the primary bunch charge. The WCM bunch charge is cross-calibrated against the readings from a Faraday cup.

The Faraday cups are interceptive diagnostics integrated into the 3 energy spectrometers and 2 final beam dumps. Each dump consists of a 300 mm diameter stainless steel core, with a length of 300 mm to dissipate the electron beam. A 20 mm aluminum insert is used to reduce backscattering. Each core is suspended in HDPE and encased in a concrete and lead clamshell to manage radiation from activation. They are instrumented using the same variable sensitivity front-ends as the WCM, which have a dynamic range from

* thomas.pacey@stfc.ac.uk

Content from this work may be used under the terms of the CC BY 4.0 licence (© 2025). Any distribution of this work must maintain attribution to the author(s), title of the work, publisher, and DOI.

ISBN: 978-3-95450-262-2 ISSN: 2673-5350 doi: 10.18429/JACoW-IBIC2025-MOPCO15

# PHYSICS-GUIDED DATA EXPANSION FOR PHOTOCATHODES USING TESS TRANSVERSE MOMENTUM MEASUREMENTS

S. Malhotra*,[1,2], L. B. Jones[2,3], N. Kumar[1,2], C. P. Welsch[1,2]
[1]Department of Physics, University of Liverpool, Liverpool, United Kingdom
[2]The Cockcroft Institute, Warrington, United Kingdom
[3]ASTeC, Daresbury Laboratory, STFC, Warrington, United Kingdom

*Abstract*

Precise characterisation of photocathode mean transverse energy is critical for optimising electron beam quality. This paper presents a physics-informed image processing pipeline using Transverse Energy Spread Spectrometer data (231–291nm), incorporating Gaussian Point Spread Function fitting, Wiener deconvolution, resolution equalisation via reblurring, and physics informed noise-aware augmentation. A high-fidelity dataset of 6500 synthetic images was generated, achieving average SSIM = 0.997 and $R^2 \approx 0.98$, enabling robust MTE prediction and supporting future ML-based diagnostics for next-generation photoinjectors.

## INTRODUCTION

In electron accelerators, beam emittance governs brightness. This is fundamentally limited by the electron transverse momenta at the photocathode, $p_x$ and $p_y$ as follows:

$$\varepsilon_{nx,\mathrm{rms}} = \frac{\sigma_x\sqrt{\langle p_x^2\rangle}}{mc} \quad \text{and} \quad \varepsilon_{ny,\mathrm{rms}} = \frac{\sigma_y\sqrt{\langle p_y^2\rangle}}{mc}. \quad (1)$$

Reducing $\langle p_{x,y}^2\rangle$ is essential to achieve sub-0.5 $\mu$m/mm emittance from photocathodes [1]. Both the mean transverse energy (MTE) and mean longitudinal energy (MLE) originate from the intrinsic emittance of the photocathode, which is mainly governed by the material's surface morphology and the excess energy imparted to each electron at the instant of photoemission. This is the difference between the incident photon energy and the material work function [2, 3].

The ability to measure the transverse component of the excess energy of emitted electrons facilitates research to characterise existing and new photocathode materials, and to reduce intrinsic emittance.

The Transverse Energy Spread Spectrometer (TESS) developed by the ASTeC at STFC Daresbury Laboratory is specifically designed to measure the MTE by acquiring the transverse energy distribution curve (TEDC) from photocathode materials. TESS illuminates the photocathode with a low-intensity beam (<10 pW) to ensure single-electron emission at femtoampere currents, tracking each electron's radial displacement on a phosphor screen. Electrons travel 35 mm in 8–25 ns, depending on the source–detector potential, producing footprints up to 8 mm radius. The transverse energy $\varepsilon_{tr}$ is then extracted from the radial position using:

$$\varepsilon_{\mathrm{tr}} = \frac{m_e}{2}\left(\frac{r}{\tau}\right)^2, \quad (2)$$

where $m_e$ is the electron mass, $r$ is the measured footprint radius, and $\tau$ is the electron time of flight.

$$N_e(\varepsilon_{\mathrm{tr}}) = \frac{dN}{d\varepsilon_{\mathrm{tr}}} = \frac{2\pi\tau^2}{m_e} I_c(r). \quad (3)$$

In Eq. (3) $I_c(r)$ is footprint function and $N_e(\varepsilon_{\mathrm{tr}})$ is TEDC as function of emittance. This work follows the methodology described in Ref. [2], where careful calibration and negligible space-charge effects allow TESS to achieve 1–2 meV resolution, enabling precise photocathode R&D and beam-brightness optimisation.

## METHODOLOGY

Accurate MTE measurement is vital for optimising photocathodes. Our pipeline (Fig. 1) from data processing to physics-informed augmentation enables real-time MTE prediction and ML-based beam diagnostics.

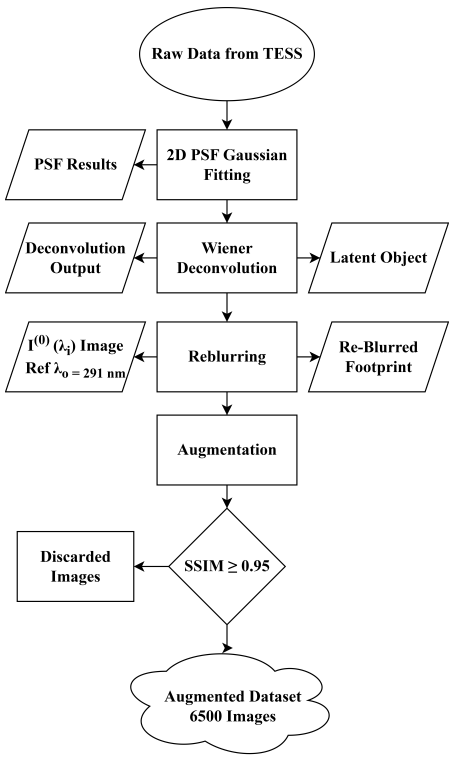



Figure 1: Flowchart summarising the complete TESS data processing and augmentation pipeline.

Single photoelectrons fall onto a microchannel plate (MCP) that generates a 'beamlet' which falls onto a phosphor

* saransh.malhotra@liverpool.ac.uk

Content from this work may be used under the terms of the CC BY 4.0 licence (© 2025). Any distribution of this work must maintain attribution to the author(s), title of the work, publisher, and DOI.

ISBN: 978-3-95450-262-2 ISSN: 2673-5350 doi: 10.18429/JACoW-IBIC2025-MOPCO17

# DESIGN STATUS OF THE ELECTRON-ION COLLIDER BEAM INSTRUMENTATION*

D. M. Gassner†, B. Bacha, G. Bassi, J. Bellon, A. Blednykh, L. Flader, R. Hulsart, C. Hetzel, K. Matsushima, C. Liu, R. Michnoff, F. Micolon, M. Oh, M. Paniccia, I. Pinayev, A. Pramberger, J. Pomaro, M. Sangroula, E. Skordis, M. Wendt
Brookhaven National Laboratory, Upton, NY, USA

*Abstract*

The Electron Ion Collider (EIC) is being built at Brookhaven National Laboratory (BNL). The system design phase efforts are underway. In addition to upgrading the existing RHIC instrumentation for the EIC hadron storage ring, new electron accelerator subsystems will include a 750 MeV Linac, accumulator ring, rapid-cycling synchrotron, electron storage ring, and a hadron cooling facility. The scope of the instrumentation includes devices to measure beam position, loss, current, charge, tune, transverse and longitudinal profiles, emittance, and crabbing angles. A description of the planned instruments and the present design status will be presented.

## INTRODUCTION

The Electron-Ion Collider, designed in a partnership between BNL and TJNAF, aims at delivering an electron-proton luminosity of $10^{34}$ $cm^{-1}s^{-1}$. The facility is based on the existing RHIC complex at BNL, taking advantage of the hadron injector complex and infrastructure. An Electron Storage Ring (ESR) will be added in the RHIC tunnel. An electron injector facility, that includes a Rapid-Cycling Synchrotron (RCS) that serves as a polarized electron injector for the ESR will be built adjacent to the RHIC tunnel. Electrons and hadrons will be brought into collision in a dedicated interaction region in the IR6 straight section [1]. The EIC project has been separated into subprojects, the first subproject covers the Hadron Storage Ring and Electron Storage Ring. The plan is to begin the construction phase of the first subproject next year. Subsequent subproject construction start dates will happen later.

## EIC BEAM INSTRUMENTATION ELECTRONICS HARDWARE

The existing Collider-Accelerator Department (C-AD) hadron injector facility will be utilized as the hadron injector for the EIC Hadron Storage Ring (HSR). Progress has been made designing upgraded beam instrumentation electronics for use at C-AD which will also be used for all the future EIC beam instrumentation systems. The new BNL designed custom architecture will utilize a general-purpose carrier board based on the Xilinx Zynq Ultrascale+ System-on-Chip (SoC) that will interface with a family of application specific daughter cards to satisfy the requirements for each system [2].

* Work supported by Brookhaven Science Associates, LLC under Contract No. DE-SC0012704 with the U.S. Department of Energy

## ELECTRON INJECTOR FACILITY INSTRUMENTATION

The electron injector facility design includes a 310 kV polarized gun feeding a 750 MeV S-Band Linac, followed by a 51 m accumulator ring, which feeds a 1.4 km rapid cycling synchrotron that can accelerate the polarized electrons to 5, 10, and 18 GeV for injection into the ESR. The beam diagnostics systems will provide measurements to ensure bunch charges up to 28 nC, with 23 ps bunch lengths with 85 % polarization and normalized H/V emittance of 196/18 microns, and an energy spread of $0.68\times10^{-3}$ dp/p can be delivered to the ESR. The electron injector facility EIC subproject is presently in a conceptual design phase, along with the beam diagnostics [3].

The electron pre-injector diagnostics systems are designed to provide a complete characterization of the beam, this includes bunch position, trajectory, orbit, beam energy, energy spread, transverse beam size, emittance, longitudinal bunch size, and beam polarization. The diagnostics must accommodate bunch intensities <1 nC during beam commissioning.

### *Electron Pre-Injector Diagnostics*

The 65 m long pre-injector section includes a 310 kV DC polarized gun, Wein filters (spin rotators), a 197 MHz buncher, two 1.3 GHz NCRF cavities, fourteen 3 m long S-band cavity Linac modules to accelerate up to 750 MeV, a Mott polarimeter, and three diagnostics beamlines. The beam parameters include accelerating bunches up to 1 nC with an energy spread of <0.5 %, polarization of >88 %, transverse normalized emittance of <75 mm-mrad, and with a repetition rate up to 30 Hz. The planned beam diagnostics planned are shown in Table 1.

Table 1: Electron Pre-Injector Diagnostics

| Monitor | Beam Parameter | Qty |
|---|---|---|
| BPM | Beam position | 21 |
| BLM | Beam losses | 5 |
| FCT, WCM, ICT | Bunch charge | 6 |
| YAG Screens | Transverse profile | 11 |
| Bunch length | Longitudinal profile | 1 |
| Polarimeter | Polarization (Mott) | 1 |

Content from this work may be used under the terms of the CC BY 4.0 licence (© 2025). Any distribution of this work must maintain attribution to the author(s), title of the work, publisher, and DOI.

ISBN: 978-3-95450-262-2 ISSN: 2673-5350 doi: 10.18429/JACoW-IBIC2025-MOPCO18

# SOFTWARE UPGRADE OF BEAM DIAGNOSTICS READOUT SYSTEM BASED ON PXIe HARDWARE*

Z. H. Xu[1,2], F. Li[1,2], W. L. Huang[1,2], L. Zeng[1,2], R. Qiu[1,2],
M. A. Rehman[1,2], B. Zhang[1,2], R. J. Yang†,[1,2]
[1]Institute of High Energy Physics, Chinese Academy of Sciences (CAS), Beijing, China
[2]China Neutron Spallation Source, Dongguan, China

*Abstract*

In the beam diagnostics system of the China Spallation Neutron Source accelerator, multiple National Instruments PXIe multifunction DAQ modules were utilized for readout system development. The original software architecture, implemented with LabVIEW and DSC modules on the Windows system, introduced substantial challenges in EPICS integration, including closed-source limitations, high licensing costs, and suboptimal real-time performance. This paper details a comprehensive software upgrade methodology that preserves the existing NI PXIe hardware infrastructure. The upgraded system implements standard EPICS Input/Output Controllers developed in C language under the Linux system, integrating signal acquisition and front-end electronics control functionalities within EPICS IOC. By developing a Linux kernel-level driver, and implementing real-time optimizations, the new architecture achieves significant performance improvements, including reduced latency and higher sampling rates. This re-engineering approach enhances the readout system's stability, reliability, and flexibility of EPICS data interaction, providing a viable open-source alternative to the traditional LabVIEW/Windows stack for accelerator instrumentation systems.

## INTRODUCTION

The beam diagnostics system at CSNS relies heavily on NI PXIe hardware for precise signal acquisition and processing. The original readout software was built on the LabVIEW and Windows platform, utilizing NI-DSC modules for limited EPICS integration. While LabVIEW offers rapid graphical development, its closed nature, coupled with the Windows operating system's limitations in real-time and distributed control scenarios, posed challenges for long-term maintenance, scalability, and integration within the broader EPICS-based control system framework at CSNS and future projects like CSNS-II. These challenges necessitated a software upgrade that retained the proven PXIe hardware investment while migrating to a more open, robust, and performant software ecosystem based on Linux and native EPICS.

*Work Supported by National Natural Science Foundation of China (NO. 12305166) and the Natural Science Foundation of Guangdong Province, China, (NO. 2024A1515010016)
†yangrenjun@ihep.ac.cn

## OLD SOFTWARE ARCHITECTURE

In the Beam Diagnostics System of the China Spallation Neutron Source [1], there are over a dozen PXI-based data acquisition hardware systems, including those for beam current measurement, beam position measurement, and beam profile measurement, among others.

The specific distribution is shown in Fig. 1.

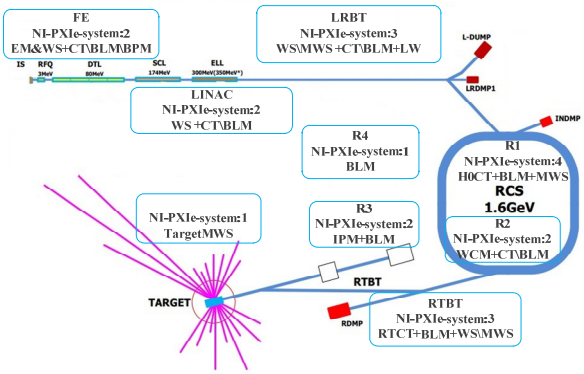



Figure 1: Distribution of PXI beam diagnostics equipment.

Software architecture is based on the PXI platform and operating on the Windows system, the data acquisition software architecture is developed using LabVIEW. The system performs functions such as analog input signal reading and digital I/O control. After data acquisition is completed, data sharing and Process Variable publishing are achieved through the NI-DSC (Data Acquisition and Control) module integrated with EPICS functionality [2]. The Control System Studio Operator Interface serves as the client for monitoring and operation.The software architecture diagram is shown in the Fig. 2.

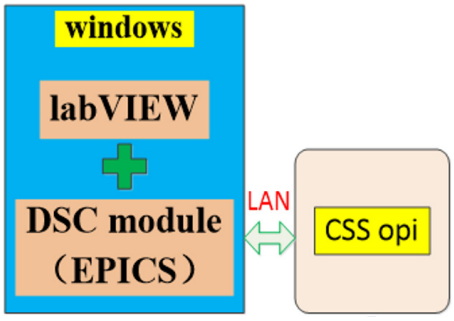



Figure 2: Software architecture.

Content from this work may be used under the terms of the CC BY 4.0 licence (© 2025). Any distribution of this work must maintain attribution to the author(s), title of the work, publisher, and DOI.

ISBN: 978-3-95450-262-2 ISSN: 2673-5350 doi: 10.18429/JACoW-IBIC2025-MOPCO19

# LARGE DYNAMIC RANGE BEAM INTENSITY MEASUREMENT FOR BOTH $H^0$ AND PROTON BEAMS IN INJECTION UPGRADE OF CSNS-II*

W. L. Huang†, R. Y. Qiu, X. J. Nie, F. Li, L. Zeng, R. J. Yang, Z. H. Xu
Institute of High Energy Physics, Chinese Academy of Sciences, Beijing, China
Spallation Neutron Source Science Center, Dongguan, China

*Abstract*

China Spallation Neutron Source (CSNS) upgrade project (CSNS-II) started in 2024. As the first important task, the injection section will be redesigned and a lot of beam instruments will be installed along the injection to I-Dump beam line. The $H^0$ beam intensity at the downstream of the stripping foils is several microampere during the normal operation, while the proton beam intensity at the I-dump may be over 80 mA during the commissioning of linac and RCS. A corresponding design of the ACCT sensor and electronics is introduced in this paper. There are two nanocrystalline cores in H0CT, providing two different turns ratio for the large dynamic range beam intensity measurement. The gain of the electronics is switchable in two ranges. The INDCT is equipped with only one core and the electronics design is aiming to a high SNR for the injected proton beam power evaluation. Tests in the lab showed a good linearity of the H0CT and INDCT sensors with the electronics. Beam commissioning of the injection section is planned in October of 2025.

## INTRODUCTION

As explained in Ref. [1], the H- charge exchange injection technique is adopted to overcome the intensity limitation of the beam emittance increase with the number of injected turns and high losses at the septum. Thus, the multi-turn charge-exchange injection in spallation neutron sources is very common and proved to be effective. In CSNS-II, the injection energy of $H^-$ beam changes from 80 MeV to 300 MeV, beam intensity from 15 mA to 50 mA (or 80 mA) and the maximum pulse width from 550 μs to 650 μs [2]. Thus the injection instruments layout has been redesigned last year [3], including the new chicane and many beam instruments for diagnostics, which consists of two current transformers (H0CT and INDCT), a fluorescent screen (INDVS), 3 multiwire profile monitors (INMWS01, INMWS02 and INDMWS01), an electron collector (INCOL), 8 beam loss monitors and two beam position monitors, as shown in Fig. 1.

The new H0CT has larger inner diameter (120 mm) and aims to evaluate the stripping efficiency and the foil aging, the same as that in CSNS [4]. It measures the ultra-low intensity of $H^0$, which are not stripped completely by the 1st foil but totally stripped charge changing to $H^+$ and delivered to the IN-DUMP. While the INDCT has an inner diameter of 160 mm, aiming to measure the proton beam intensity to the INDUMP during the commissioning of the injection zone and the linac. Meanwhile the proton beam passes through the H0CT too, because the two CTs is only 1.2 m away. So the BCT in H0CT is a dual-function low noise current monitor and a new two-range electronics was designed for both H0CT and INDCT. Crosscheck is very convenient between the readouts of the two current monitors.

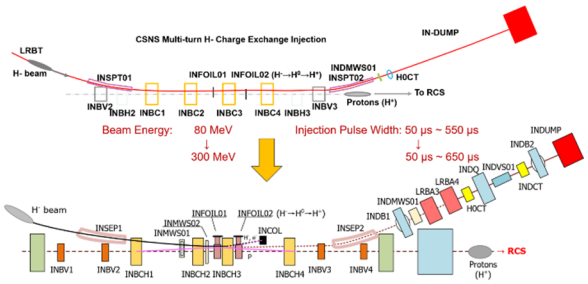



Figure 1: Different layout of the injection zone in CSNS and CSNS-II.

## SENSOR DESIGN AND FABRICATION

As in Ref. [5], the classical transformer circuit is depicted in Fig. 2. Current in any $N$ turn winding $k$ produces magnetic flux in the core of magnitude $\Phi_k = L_k \cdot i_k / N_k$ . The voltage appearing across each winding is proportional to the time rate change of the total flux $\Phi_T$. The beam is seen as 1 turn wire, then we find

$$\frac{i_s}{i_{beam}} = \frac{1}{N_s} \cdot \left(1 + \frac{R_s}{N_s^2 \cdot R_{beam}}\right)^{-1}. \quad (1)$$

For $R_{beam} \gg R_s$, the familiar approximate result, $i_s = i_{beam}/N_s$, is obtained. The secondary current is very closely equal to $1 / N_s$ times the beam current. The sensor response to a bunch pulse is characterized with a risetime and droop. The droop time is figured as $L_s / R$, indicating that a large $L_s$ and a small $R$ will lead to a slow droop.

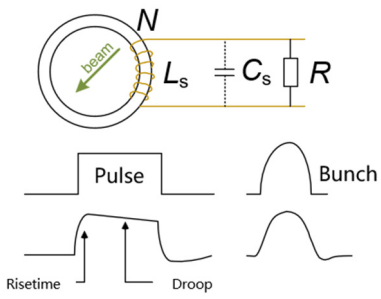



Figure 2: Equivalent circuit and pulse response of a classical current transformer [6].

* This work is supported in part by National Key R&D Program of China under Contracts No. 2023YFE0105700, and National Natural Science Fund (No. 12275294).
† huangwei@ihep.ac.cn

Content from this work may be used under the terms of the CC BY 4.0 licence (© 2025). Any distribution of this work must maintain attribution to the author(s), title of the work, publisher, and DOI.

ISBN: 978-3-95450-262-2 ISSN: 2673-5350 doi: 10.18429/JACoW-IBIC2025-MOPCO22

# HEPS BEAM CHARGE MEASUREMENT SYSTEM

Y. Zhao†, Y. Sui, Y. Du, J. He, L. Wang, T. Xu, J. Yue, J. Cao
Institute of High Energy Physics, CAS, Beijing, China

*Abstract*

HEPS beam charge measurement includes bunch charge measurement system and average current measurement system. The injection scheme of HEPS requires charge monitor with high precision, stability, and a large dynamic range at each phase. This paper introduces the design and commissioning status of HEPS charge measurement system Signal reconstruction method applied in bunch charge measurement is also described in the paper.

## INTRODUCTION

The High Energy Photon Source (HEPS) is a fourth generation synchrotron light source based on a 6 GeV diffraction-limited storage ring (SR) [1]. The injector system of HEPS consists of a LINAC a low-energy transport line (LTB), a booster (BST), and two high-energy transport lines (RTB).

Integrated Current Transformer (ICT) is used in LINAC, LTB and RTB for bunch charge measurement. Six ICT sensors are positioned separately at the output of the electron gun and each accelerating section in LINAC, extra two are in the LTB. Additionally, two ICT sensors are positioned at each end of the BTR respectively, and the same sensor arrangement is implemented for RTB. Two DCCTs are used in SR, with one unit serving as a backup for the other. BST follows the same redundancy consideration. All sensors are in-flange type from Bergoz Instrumentation [2]. The details of charge measurement sensor in HEPS are list in Table 1.

Table 1: Charge Sensors in HEPS

| Location | Type | Quantities |
|---|---|---|
| LINAC | ICT | 6 |
| LTB | ICT | 2 |
| BST | DCCT | 2 |
| RTB | ICT | 2 |
| BTR | ICT | 2 |
| SR | DCCT | 2 |

## SYSTEM DESIGN

### *LINAC/BTR/RTB Charge*

ICT is chosen for LINAC and transport line according to the beam pulse length, for monitoring the bunch charge and injection efficiency. All sensors are 5 V.C/s sensitivity (manufactured), and the diameters are 34.9 mm.

The electronics of ICT (ICT-E) is developed with commercial open-source hardware. The bandwidth of the ICT-E input channel is DC-65 MHz which cover the ICT signal spectrum.The sample rate is 125 MHz, each ICT-E could process 2 channel signals as show in Fig. 1. As the on-axis injection scheme for the booster at 500 MeV, the LINAC must provide an electron pulse with a charge of not less than 6.25 nC [3]. The ICT-E dynamic range of linac and LTB should be 0-10 nC. For RTB and BTR , the dynamic range is 0-5 nC. Trigger from timing system is used to signal synchronous. The ICT-E are in the equipment hall, LMR400 cable is used to transmit ICT output signal. An extra cable connected calibration wire input of the sensor is used to do the calibration and check the sensor function.

The electronic complete the algorithm and integration for each ICT. A self-starting IOC is run on each board to post charge data. The system setting interface is developed by Phoebus, running in the BI station.




Figure 1: HEPS ICT-E.

### *Signal Reconstruction Algorithm for ICT*

ICT signals are susceptible to interference from high-power devices. The bandwidth and sampling rate of ICT-E could suppress most high-frequency noise, but for integral calculations, a sufficient number of data points is still required to ensure accuracy. Therefore, the signal reconstruction method is adopted in ICT-E. The primary objectives are maintaining time-domain smoothness to avoid artifactual oscillation, ensuring accurate waveform representation, and enabling computationally efficient real-time operation.

For choosing a proper function to complete the signal reconstruction, an experiment has been carried out for comparing two regular method: Sinc and Cubic Spline interpolation method. Balance between processing speed and reconstruction accuracy are considered.

In the experiment, original ICT signal was acquired by a high-sampling-rate oscilloscope, then we decimated the original ICT signal with the equivalent sampling rate as ICT-E, applied interpolation algorithms separately to the decimated signal, then compare the results [4]. The basic function is list below in Eqs. (1) and (2). $f_{recon_sinc/spline}(x)$ is data after interpolation. $f(x_n)$ is the data that being interpolated, $T$ is the sample rate of $f(x_n)$, $N$ is the points of $f(x_n)$. $a_i$, $b_i$, $c_i$, $d_i$ are spline interpolation coefficients need to be solved for each interval.

† zhaoying@ihep.ac.cn

Content from this work may be used under the terms of the CC BY 4.0 licence (© 2025). Any distribution of this work must maintain attribution to the author(s), title of the work, publisher, and DOI.

ISBN: 978-3-95450-262-2 ISSN: 2673-5350 doi: 10.18429/JACoW-IBIC2025-MOPCO23

# COMMISSIONING OF THE 71 MeV BEAM DELIVERY LINE OF THE TOP-IMPLART ACCELERATOR*

P. Nenzi[1,†], A. Ampollini[1], M. D. Astorino[1], G. Bazzano[1], A. Doria[1], F. Fortini[1], E. Pavoni[1], G. Picardi[1], M. Piccinini[1], C. Ronsivalle[1], V. Surrenti[1], E. Trinca[1], E. Nichelatti[2]
[1]ENEA C.R. Frascati, Frascati, Italy
[2]ENEA C.R. Casaccia, Roma, Italy

Content from this work may be used under the terms of the CC BY 4.0 licence (© 2025). Any distribution of this work must maintain attribution to the author(s), title of the work, publisher, and DOI.

*Abstract*

TOP-IMPLART is a pulsed RF proton linear accelerator in operation at the ENEA Frascati Research Center originally built as a technological demonstrator for a full linear solution to proton therapy, it is currently evolving towards a facility available to research and industrial users in different fields, ranging from biomedical to aerospace applications. It consists of a commercial AccSys PL7 model 425 MHz injector followed by eight SCDTL accelerating modules operating at 3 GHz. Proton beams in the range 1-6 MeV are available from a vertical delivery line placed at the exit of the injector, and at 63 MeV or 71 MeV (intermediate and lower energies are achieved by degraders) from a horizontal delivery line at the exit of the accelerator, where a pulse current variable up to 25 μA is provided in pulses 2.5 μs long at a typical repetition rate of 25 Hz. Our contribution presents the first experimental results from the commissioning of the high-energy line. It is a multi-purpose in-house designed line featuring a magnetic scanning system and a set of instrumentation, diagnostics, and target positioning frames placed on motorized platforms allowing for customizable irradiation setups.

## INTRODUCTION

TOP-IMPLART linac is a pulsed proton linear accelerator in operation at the ENEA Frascati Research Center. It was developed as part of the TOP-IMPLART Project [1], funded by Regione Lazio, in collaboration with the Italian Institute of Health (ISS) and the Regina Elena-IFO oncological hospital in Rome to become a technological demonstrator for the full linear approach to proton therapy.

The accelerator is composed of a 425 MHz injector linac, followed by eight SCDTL modules operating at 2998 MHz. The maximum energy available at the output window is 71 MeV. However, it is possible to achieve a secondary energy level of 63 MeV by turning off the radiofrequency in the last accelerating module. Intermediate and lower energies can be obtained using passives degraders. The beam is delivered in pulses with 2.4 μs FWHM (Full width Half Maximum), at a typical repetition rate of 25 Hz.

The proton beam is used in radiobiology experiments—with output energies corresponding to a water-equivalent range of 30 to 40 mm—as well as in radiation hardness testing of electronic devices and assemblies. The beam at the accelerator exit window has a diameter of approximately 3 mm FWHM. Irradiation of larger samples can be accomplished either by using a passive scatterer (lead foil), which enlarges the irradiated area at the expense of fluence and dose rate, or through a magnetic scanning system integrated into the delivery line.

The line, designed at ENEA [2] specifically for the TOP-IMPLART beam, has been fully installed, and has undergone preliminary commissioning tests.

## 71 MEV BEAM DELIVERY LINE

The delivery line, illustrated in Fig. 1, begins with an extraction section located at the accelerator's output, which includes two permanent magnet quadrupoles (PMQs) and non-interceptive diagnostic devices.

The primary function of the extraction section is to shape the beam into a circular profile with a 3 mm FWHM diameter at the accelerator's exit and to measure its intensity. Beam intensity is monitored using a low-noise, dual-core current transformer (model ACCT-CF1"1/3-7-20-UHV-2CORE by BERGOZ) and a passive cavity detector [3].

The beam exits the extraction section through a 25 μm-thick titanium window and travels approximately 13 cm through air. In this region, a custom-built integral ionization chamber (IC) monitors the pulse charge, enabling dose-controlled irradiation.

After the IC, the beam reaches a remotely operated platform equipped with different diagnostics and control components: a Faraday collector [4], a scattering foil holder, an optical spot measurement system (telescope), and an open slot that allows the beam to continue to the end of the delivery line. The Faraday collector functions as a beam shutter, blocking the beam from reaching the target and enabling verification of the machine setup. Positioned in front of the collector, a 19 mm-thick aluminum block stops protons with energies below 70 MeV, allowing only higher-energy protons to be collected. By comparing the total beam current measured by the energy-insensitive current transformer with the current detected by the Faraday collector, the fraction of protons with energies above 70 MeV can be estimated [5]. Agreement between both measurements confirms that all protons in the pulse have the correct energy and that the accelerator is properly set (the aluminum block is replaceable with a 16 mm one for the 63 MeV beam). Once the beam exits the platform, it enters an X-Y

*Work supported by the TOP-IMPLART (Oncological Therapy with Protons – Intensity Modulated Proton Linear Accelerator for Radiotherapy) project, funded by Regione Lazio, Italy.
† paolo.nenzi@enea.it

ISBN: 978-3-95450-262-2 ISSN: 2673-5350 doi: 10.18429/JACoW-IBIC2025-MOPCO24

# ADVANCEMENTS IN A CHERENKOV FIBER-BASED MACHINE PROTECTION SYSTEM AT TRIUMF'S E-LINAC*

R. Hermann†, M. Alcorta Moreno, H.W. Koay, F. Ames
TRIUMF, Vancouver BC, Canada

*Abstract*

A Cherenkov fiber-based shut-off system is being developed for TRIUMF's ARIEL e-Linac to provide a scalable, cost-effective solution for monitoring beam losses in high-radiation environments. The system uses a single 100 m long thin silica fiber with photomultiplier tubes at both ends, allowing sensitive electronics to be located outside the radiation area. This design is favorable over bulky ionization chambers and more expensive scintillation-based detectors, as it improves and simplifies deployment in complex environments, particularly the ARIEL beamline tunnel. The prototype demonstrates sub-10 µs response times and position-sensitive detection via the time delay between upstream and downstream signals. Ongoing work focuses on the achievable spatial resolution, the integration into ARIEL's operations control environment and the systematic evaluation of reliability and sensitivity. Compared to conventional long ionization chambers (LIC) and BGO-based detectors, the fibre-based system promises improved deployment flexibility and faster response times.

## INTRODUCTION

### *TRIUMF e-Linac and ARIEL Tunnel*

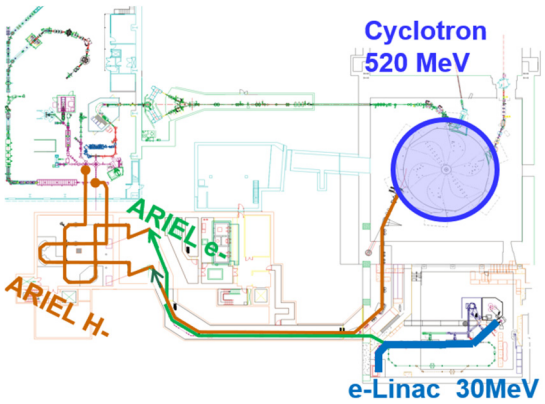



Figure 1: Outline of a part of the TRIUMF facility, highlighting the cyclotron, the e-Linac and the under-construction beamline tunnel to ARIEL.

TRIUMF, Canada's particle accelerator center, is at its core a 520 MeV cyclotron proton accelerator [1] for the production of secondary particles in particular radioactive isotopes. This will be complemented by the isotope production via photo fission induced by bremsstrahlung from high energy electrons. For this purpose a 30 MeV superconducting electron linear accelerator, the e-Linac, was installed. Most rare isotope production experiments can be adequately served by a 30 MeV, 3 mA electron beam [2].

* Work supported by the National Research Council of Canada.
† rhermann2@triumf.ca

As shown in Fig. 1, the new ARIEL facility will have two target stations: one for the isotope production driven by the proton beam and one driven by the electron beam. Both accelerators shall deliver beam through the same tunnel. This under-construction beamline will be equipped with beam protection systems based on reliable beam loss monitors (BLMs), explained below. In addition to the ionization chambers and bismuth germanate (BGO) detectors already used at the e-Linac a Cherenkov fiber-based prototype system is planned for the tunnel with the potential to replace the current BLM system on the long run.

### *Current Beam Loss Monitors (BLMs)*

As part of the Machine Protection System (MPS), which is the sum of all diagnostics in place to control the beam, the BLMs are two types of detectors:

- Long ionization chambers (LICs) placed along the beamline in roughly one meter distance.
- BGO scintillator-based detectors (shaped like microphones) with photomultiplier tube (PMT) readouts, placed a few centimeters away from the beamline and close to bending magnets for higher precision at these crucial points.

These two detector types combined and spread out in the described way provide reliable protection. Full and redundant protection is necessary as a 10 mA electron beam deviating from its intended path can damage the beamline. Such accidents are very expensive and a set back to any experiment timeframe. To prevent damage like this any malfunction must be detected and the beam shut down within a maximum of 10 µs.

## CHERENKOV-FIBER BASED MPS

In addition to the existing BLMs a detector prototype has been installed at the beam line close to the e-Linac, which is, instead of ionization or scintillation, based on the Cherenkov process.

### *Cherenkov Principle*

Cherenkov radiation occurs when charged particles exceed the speed of light in a medium. Therefore, the condition to be fulfilled would be $v_{\text{particle}} > c/n$ and hence the threshold Lorentz factor is $\gamma_{th} = 1/\sqrt{1-1/n^2}$. The refractive index $n$ for quartz fibers is about 1.5. The minimal necessary kinetic energy can be derived from:

$$E_{\text{kin,th}} = (\gamma_{th} - 1)mc^2, \qquad (1)$$

which results in 0.18 MeV for electrons and 321 MeV for protons. For protons, even lower energies can still be detected through secondary particle showers, whereas

Content from this work may be used under the terms of the CC BY 4.0 licence (© 2025). Any distribution of this work must maintain attribution to the author(s), title of the work, publisher, and DOI.

ISBN: 978-3-95450-262-2 ISSN: 2673-5350 doi: 10.18429/JACoW-IBIC2025-MOPCO26

# DESIGN AND SIMULATION OF MINIATURIZED PERMANENT MAGNET ARRAYS FOR COMPACT DIAGNOSTIC APPLICATIONS*

D. Aflyatunova†[1], C. Welsch[1], The University of Liverpool, Liverpool, UK
G. Gao, G. Travish, ViBo Health, Los Alamos, USA
[1]also at Cockroft Institute, Daresbury, UK

*Abstract*

This paper presents the design and simulation of miniaturized permanent magnet configurations for Nuclear Magnetic Resonance (NMR) applications where compactness and field quality are critical. Traditional NMR systems require large and costly equipment to achieve high magnetic field uniformity, which limits portability and broader diagnostic use. We investigate compact magnet geometries, including H-type and Halbach arrays, evaluating their field strength and homogeneity. Special attention is given to the trade-off between device miniaturization and achievable field uniformity, a key factor in measurement sensitivity. Through computational modelling, we establish a framework for quantifying and optimizing magnetic field homogeneity, providing design strategies relevant for portable diagnostic instrumentation and potential applications where in-situ, non-invasive measurements are required.

## INTRODUCTION

The development of compact and precise diagnostic instrumentation often depends critically on the design of strong, homogeneous magnetic fields. Compact permanent magnet assemblies could support portable NMR-based field probes [1] or calibration devices for accelerators [2], where diagnostic magnets must be small, stable and cost-effective.

Nuclear Magnetic Resonance (NMR) techniques, in particular, require high field strength and uniformity to achieve accurate and reproducible measurements. Conventional high-field NMR magnets are heavy, bulky, expensive, [3] and hence limited to fixed laboratory installations, which restricts their applicability in portable diagnostic devices.

In order to overcome these limitations recently there have been efforts [4] to design miniaturized NMR systems that reduce magnet size while maintaining adequate field quality. Achieving this balance is challenging: strong and homogeneous magnetic fields typically require larger magnet volumes, which runs counter to portability.

As a result, compact NMR devices must adopt innovative magnet geometries and optimization techniques to deliver both sufficient field strength and uniformity to perform reliable diagnostics.

The aim of this paper is to introduce a simulation and analysis methodology to compare and assess different magnet assembly designs based on magnetic field strength and uniformity within manufacturing constraints.

## MODEL

Two types of permanent magnet configurations were considered in this study: H-shaped magnet and Halbach Cylinder shown in Fig. 1.

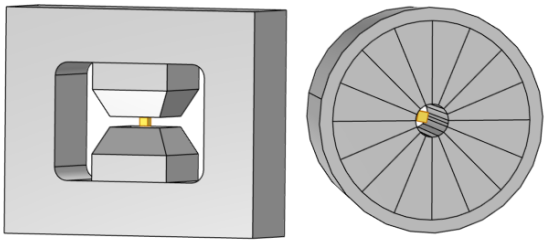


Figure 1: Magnets configurations: H-shaped magnet (left) and Halbach cylinder (right). ROI is highlighed by yellow color.

Magnetic field calculations have been performed using COMSOL software Magnetic Fields, No Currents (mfnc) physics interface [5], where following set of magnetostatic Maxwell equations [6] have been solved under the assumption of no free currents ($\mathbf{J} = 0$) using Finite Element Method stationary study:

Gauss's law for magnetism:

$$\nabla \cdot \mathbf{B} = 0. \tag{1}$$

Constitutive relation between the magnetic flux density and magnetic field:

$$\mathbf{B} = \mu_0 \mu_r \mathbf{H} + \mathbf{B}_r, \tag{2}$$

where $\mathbf{B}_r$ is the remanent flux density;

Ampère's law:

$$\nabla \times \mathbf{H} = \mathbf{J}. \tag{3}$$

Since $\nabla \times \mathbf{H} = 0$, the magnetic field $\mathbf{H}$ can be expressed as the gradient of a scalar potential $V_m$:

$$\mathbf{H} = -\nabla V_m. \tag{4}$$

Equations are completed by magnetic insulation as boundary condition which enforces that the normal component of the magnetic flux density vanishes at the boundary:

$$\mathbf{n} \cdot \mathbf{B} = 0. \tag{5}$$

* Work supported by STFC Impact Acceleration Award
† daliya@liverpool.ac.uk

Content from this work may be used under the terms of the CC BY 4.0 licence (© 2025). Any distribution of this work must maintain attribution to the author(s), title of the work, publisher, and DOI.

ISBN: 978-3-95450-262-2 ISSN: 2673-5350 doi: 10.18429/JACoW-IBIC2025-MOPCO28

# WEB STREAMING INTEGRATION FOR THE TLS BEAM SIZE MONITORING BROADCAST SYSTEM

L. P. Hsu, C.Y. Liao, C.Y. Wu, J. K. Liao, Z. Q. Wu
National Synchrotron Radiation Research Center, Hsinchu, Taiwan, R.O.C.

Content from this work may be used under the terms of the CC BY 4.0 licence (© 2025). Any distribution of this work must maintain attribution to the author(s), title of the work, publisher, and DOI.

*Abstract*

The beam size monitor (BSM) broadcast system at the Taiwan Light Source (TLS) has traditionally used analog coaxial cables and modulators to transmit measurement images and data to control rooms and beamline stations via televisions and tuners. While simple and network-independent, this setup suffers from low resolution, frequent interference, and aging hardware with no ongoing maintenance. This paper presents a lightweight, non-intrusive upgrade that replaces the original system with a web-based real-time streaming solution. By capturing the existing output from the measurement system and streaming it using standard web technologies, users can access beam size visuals on any browser-enabled device, gaining better image quality and improved stability while eliminating traditional broadcast maintenance. With plans underway to retire TLS in the near future, this solution offers a fast, low-risk, and cost-effective modernization path without altering existing instruments or computing environments. The system is currently under testing, and this paper describes its architecture, implementation, and preliminary results.

## INTRODUCTION

The Taiwan Light Source (TLS) is a third-generation synchrotron radiation facility operating at a beam energy of 1.5 GeV. Reliable beam diagnostics are essential to ensure optimal machine performance. Beam size monitoring is a critical role in beam tuning, stability assessment, routine operations, and various beam physics studies. Traditionally, beam size images at TLS have been transmitted through analog video modulators to multiple monitoring stations via coaxial cables. These stations are equipped with analog televisions or signal receivers. However, the original analog broadcasting system presents several limitations. The image resolution is constrained by analog standards, restricting the ability to present detailed information. In addition, long-distance analog signal transmission is susceptible to noise and attenuation, degrading data quality. Aging hardware further complicates maintenance and increases the risk of unexpected failures, posing challenges to continuous operation. This work proposes a lightweight, non-intrusive web-based streaming solution aimed at enhancing the quality of beam size images while minimizing interference with the existing instrumentation system. The upgrade targets improvements in image resolution and system stability, reduction in maintenance overhead, and greater accessibility to beam monitoring data through standard web browsers.

## SYSTEM ARCHITECTURE

The synchrotron radiation monitor system [1,2] consists of image forming optics, a CCD digital camera, and image processing tools. A local Windows-based server hosts a LabVIEW network server environment, which is responsible for camera operation and system management. This environment integrates multiple functionalities such as the camera driver interface, neutral density (ND) filter adjustment through a serial bus, image acquisition, preliminary data pre-processing, and subsequent image analysis and display. The system also employed traditional analog television display as a means of real-time monitoring, allowing operators to directly observe the beam profile without the need for computational post-processing. The traditional analog broadcast system is illustrated in Fig. 1.

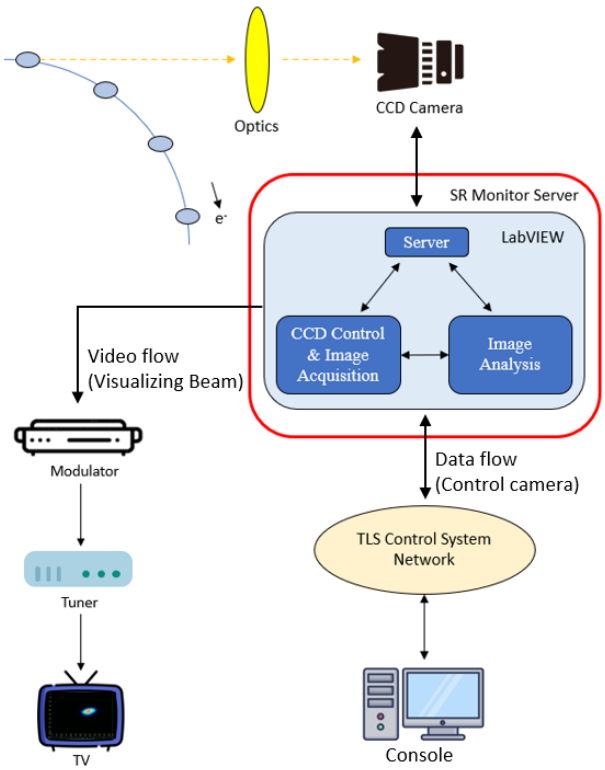



Figure 1: The traditional analog broadcast system architecture of the Synchrotron radiation monitor system.

In the upgraded beam size monitor (BSM) broadcast system, web-based real-time streaming was achieved without modifying the existing diagnostic instrumentation or computational infrastructure. To accomplish this, the video signal was directly captured from the DVI-I output of the original SR monitor server. In conventional analog transmission systems, long-distance signal delivery often

ISBN: 978-3-95450-262-2 ISSN: 2673-5350 doi: 10.18429/JACoW-IBIC2025-MOPCO29

# EXPLORING BEAM DIAGNOSTIC PERFORMANCES OF cSTART USING THE KARA BOOSTER SYNCHROTRON

D. El Khechen*, E. Blomley, M. Fuchs, E. Huttel, K. Kaljic, A. Mochihashi, R. Ruprecht, P. Schreiber, M. Schuh, J. L. Steinmann, Anke-Susanne Müller
Karlsruhe Institute of Technology, Eggenstein-Leopoldshafen, Germany

*Abstract*

cSTART is a future storage ring currently under development at KIT with the purpose of investigating various non-equilibrium beam conditions and the injection and storage of laser plasma accelerator (LPA) beams. To understand and control the non-equilibrium beam dynamics at cSTART, various beam diagnostics with demanding specifications are required.

First and foremost, suitable diagnostics are necessary in order to be able to operate the cSTART storage ring even under non-equilibrium conditions with ultra-short electron bunches. The KARA booster has been used as an important tool to explore diagnostics for cSTART due to similarities in parameters, in particular the low electron beam energy (53 MeV) and the relatively high revolution frequency. Several beam diagnostics installed in the booster will be also installed in cSTART, i.e. the BPM readout electronics, the beam loss detection system, etc. In this context, dedicated beam time was used to test the performances of the different beam diagnostics systems, and to prepare for workaround solutions in case of limitations if any. In this paper, we will describe the different experiments, emphasizing the procedures, and highlighting the applied analysis. Moreover, we will discuss the results obtained and elaborate on their indications for the cSTART performance.

## INTRODUCTION

The main beam diagnostic systems for the operation of the cSTART storage ring [1] were ordered, and a few were already delivered. Meanwhile, some instrumentation such as the Libera ERXR [2] modified for TBT (turn-by-turn) beam position measurements has been characterized [3]. Moreover, the Libera Digit 500 digitizer [4] for TBT charge measurements in the the VLA-cSR (Very Large Acceptance compact Storage Ring) was also characterized with signal generators such as an AWG (Arbitrary Wave Generator) and with electron beams at FLUTE. In addition to beam position and charge measurements, tune measurements are crucial for understanding and optimizing the beam behavior. These measurements help to determine the stability of the beam and ensure optimal operating conditions. For tune measurements at cSTART, we will use a stripline kicker to be placed at one of the straight sections of the VLA-cSR. To define the specifications of such a stripline, we tried to perform some tests with the stripline electrodes in the KARA booster using different setups.

## KARA BOOSTER

The KARA booster synchrotron shares a few parameters with the VLA-cSR, such as beam energy and fast revolution frequencies (see Table 1). In the booster (see Fig. 1), the electron beam is injected from the microtron once a second and ramped up from 53 MeV to 500 MeV in 0.6 seconds corresponding to the booster cycle. To study the cSTART case, we tried to get the beam conditions in the booster as close as possible to that of cSTART. We store the beam at 53 MeV and clean all but one bunch to store only a single bunch.

Table 1: Parameters of the KARA Booster and the VLA-cSR

| | Booster | VLA-cSR |
|---|---|---|
| Energy (MeV) | 53 to 500 w/ ramp | 50 to 90 MeV w/o ramp |
| Harmonic number | 44 | single bunch |
| Revolution frequency (MHz) | 11.36 | 6.94 |
| Bunch charge (pC) | 10 | 1 to 200 |
| Bunch length | 30 ps | 10 fs to 10 ps |
| Partial tunes ($\nu_h$,$\nu_v$) | (0.18, 0.74 ) | (0.16, 0.65) |

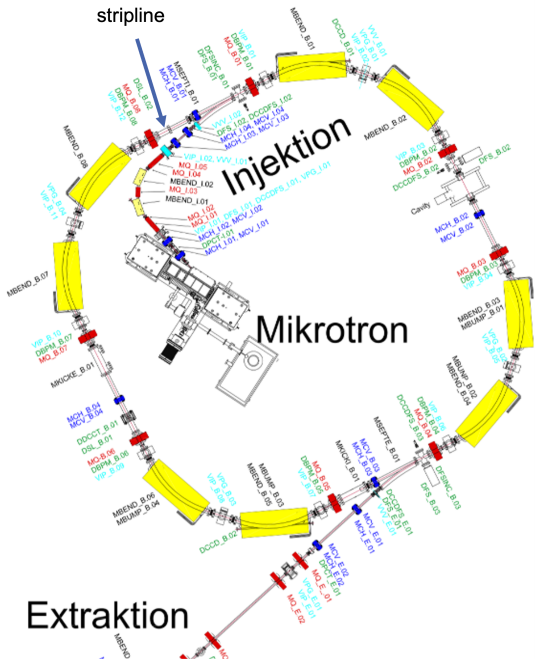



Figure 1: The schematic of the booster synchrotron including all diagnostics and the stripline kicker.

* dima.khechen@kit.edu

Content from this work may be used under the terms of the CC BY 4.0 licence (© 2025). Any distribution of this work must maintain attribution to the author(s), title of the work, publisher, and DOI.

ISBN: 978-3-95450-262-2 ISSN: 2673-5350 doi: 10.18429/JACoW-IBIC2025-MOPCO31

# DEVELOPMENT OF BPM ELECTRONICS FOR PIP-II AT FERMILAB*

S. Liu†, N. Eddy, A. Semenov, B. Fellenz
Fermilab, Batavia, IL, USA

*Abstract*

This paper presents the uTCA4.0-based BPM electronics for PIP-II, featuring four 250 MSPS ADCs and a Xilinx UltraScale+ MPSoC FPGA with 10 GbE uplink. Design elements include signal conditioning, clock, and thermal management. The FPGA performs signal processing, time tagging, digital down-conversion, and phase drift compensation. Position and phase resolution, and thermal stability is validated through dedicated testing.

## INTRODUCTION

PIP-II (Proton Improvement Plan-II) is Fermilab's next-generation high-intensity superconducting proton LINAC, replacing the aging 400 MeV linac with an 800 MeV $H^-$ beam injected into the Booster [1]. As shown in Fig. 1, the beamline includes the warm front-end (WFE) - comprising the ion source, LEBT, RFQ, and MEBT - and operates at three RF frequencies: 162.5 MHz (RFQ and early SC sections), 325 MHz, and 650 MHz. The $H^-$ beam is bunched at 162.5 MHz, chopped into pulses up to 0.55 ms (with future CW capability), and operates at up to 20 Hz repetition.

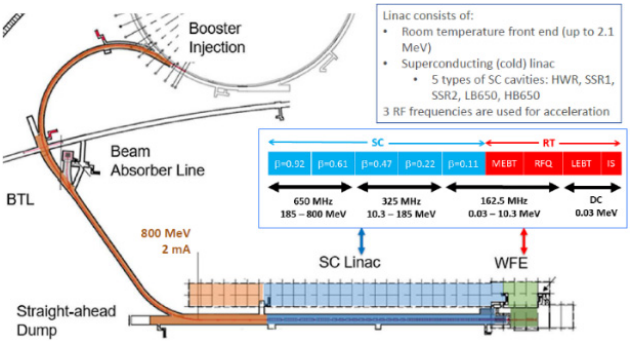



Figure 1: Beamline layout of the PIP-II SC Linac and BTL.

PIP-II will deploy 126 BPMs across the WFE, SC LINAC, and BTL. Warm and cold BPMs measure horizontal/vertical position, beam phase relative to the RF, and relative intensity, with performance requirements of: 10 µm position resolution, 0.1 mm accuracy, 1 % intensity resolution, 0.3° phase resolution, and 1° phase stability. The 56 BTL BPMs measure a single transverse coordinate, totalling 392 BPM signals for processing.

## BPM DATA ACQUISITION SYSTEM

The latest uTCA.4 platform offers cutting-edge technologies, including high-speed Ethernet for data transfer, hot-swappable modules for high availability, and IPMI-based platform management. The PIP-II BPM data acquisition system is built on this platform and consists of a uTCA Carrier Hub (MCH), up to 12 Advanced Mezzanine Cards (AMCs), and 12 Rear Transition Modules (RTMs), as shown in Fig. 2.

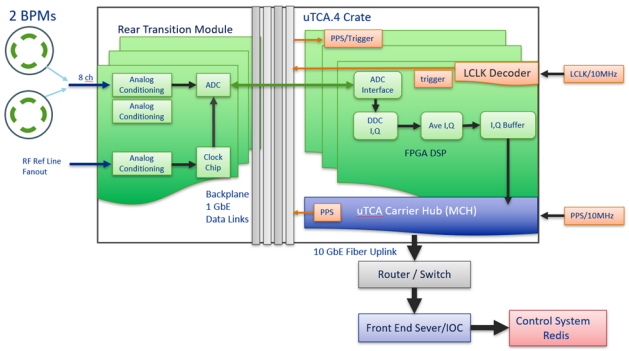



Figure 2: PIP-II's uTCA BPM system architecture.

Each AMC/RTM pair accepts 8 analog inputs, enabling a 12-slot chassis to process up to 96 signals. The analog and digital sections are connected via the zone-3 connector, eliminating the need for extensive front-panel RF cabling typical in VME systems. Each RTM receives a 162.5 MHz RF reference signal distributed via a low-drift RF line in the beam tunnel.

A 10 MHz clock and an encoded clock (LCLK) are input through one AMC front panel and distributed over MLVDS buses (ports 17–20) on the backplane. LCLK is decoded on each AMC to extract trigger and other event signals. The White Rabbit LEN module supplies a 10 MHz and PPS signal via the MCH which distributes these clocks through TCLKA and TCLKB lines in a star topology. Together this provides single 162.5 MHz bucket resolution.

Each AMC sends processed BPM data through backplane port 0 via 1 GbE to the MCH, which aggregates and forwards via 10 Gbps uplink to a front-end (FE) server - a 1U industrial Linux computer. The FE server further processes and publishes BPM data to PIP-II's control system using the REDIS distributed database.

## RTM: ANALOG SIGNAL, CLOCK, AND ADC

As seen the Fig. 3, the RTM's Analog Front-End (AFE) channel includes a high-isolation RF switch, a SAW bandpass filter, and a fixed 20 dB RF amplifier. The clock channel uses the same AFE as the BPM signal path to ensure shared thermal drift characteristics, preserving phase stability. However, the drift of the PLL needs an active self-calibration to be performed.

The RTM integrates TI's 250 MSPS ADS42JB69 ADC with a JESD204B interface, necessitating the use of TI's JESD204B-compliant LMK04832 clock chip to meet

* This manuscript has been authored by FermiForward Discovery Group, LLC under Contract No. 89243024CSC000002 with the U.S. Department of Energy, Office of Science, Office of High Energy Physics
† sliu@fnal.gov

Content from this work may be used under the terms of the CC BY 4.0 licence (© 2025). Any distribution of this work must maintain attribution to the author(s), title of the work, publisher, and DOI.

ISBN: 978-3-95450-262-2 ISSN: 2673-5350 doi: 10.18429/JACoW-IBIC2025-MOPCO32

# DEVELOPMENT OF A FAST EXTRACTION METHOD FOR SHORT HIGH INTENSITY PULSES AT ELSA

L. Thome*, K. Desch, D. Proft, M. Switka, Physics Institute, University of Bonn, Bonn, Germany

*Abstract*

Studies concerning the FLASH effect for radiation therapy are currently performed at ELSA. The booster synchrotron is used in a preliminary mode of operation to deliver electron beam pulses of 1.2 GeV energy with fixed length of 250 ns to irradiate cell samples. To enable different spill durations ranging from nanoseconds up to several ms in an energy range of 0.8 GeV to 3.2 GeV a fast extraction from the stretcher ring is developed. Therefore a repurposing of the existing injection kickers for extraction is under study to achieve single turn extraction, up to extraction within a few turns. While the effect on the beam dynamics is observed with a streak camera, the measurement of the extracted beam is performed via current and chromox monitors. For longer spill durations, reaching up to ms, the feasibility of multiple concepts for a quicker resonant extraction at ELSA is investigated.

## FLASH@ELSA

The electron accelerator facility ELSA at the University of Bonn is a three stage accelerator. First a linear accelerator (linac) accelerates electrons up to 26 MeV, provided by either a thermal or a polarized source. Afterwards the electrons are injected into the booster synchrotron and accelerated up to 1.2 GeV. The electrons are then injected with a rate of up to 50 Hz into the stretcher ring, where they can be further accelerated up to 3.2 GeV.

### *Current FLASH Operation Mode*

For current irradiation studies [1] a direct extraction of electron pulses with a pulse length of 250 ns and charges of up to 2.5 nC from the booster synchrotron to an experimental area is used. The extracted electrons are therefore guided via the stretcher ring used as transfer beam line towards the extraction site.

### *Extraction Site*

Before irradiating a target placed inside a water phantom, the electron pulses pass several detectors (Fig. 1). First traversing an integrating current transformer (ICT) right after the beamline exit, for a measurement of the pulse charge. The transverse beam profile and position is measured with a luminescence screen (chromox) camera setup. It is analyzed by an in-house developed image analysis software package [2]. This setup provides precise information on the beam profile, position and spill charge.

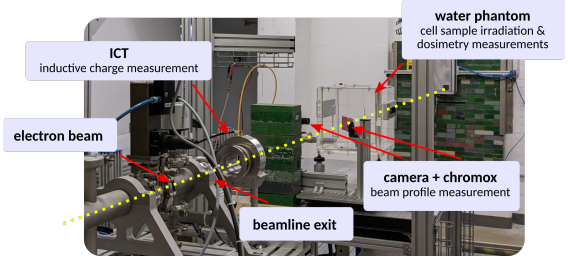



Figure 1: Experimental setup for cell sample irradiation and dosimetry measurements.

## SINGLE TURN EXTRACTION

Three fast kicker magnets dedicated for the injection process are located in the stretcher ring. Their location is marked in Fig. 2. The usage of those kickers for single turn extraction is investigated.

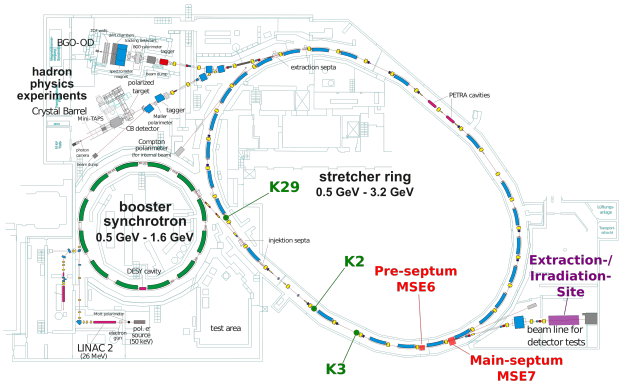



Figure 2: Accelerator facility ELSA with the marked location of the injection kickers in green, pre- and main-septum in red and the extraction site in purple.

Investigation of the beam optics for single turn extractions shows that a combination of kicks must be used. Thus producing a large offset from the design orbit at the position of the pre-septum to cross the septum blade for extraction. To achieve this offset, large beta functions at the location of the injection kickers and the pre-septum as well as a suitable phase advance between kicker and septum are essential. Following [3] one obtains for the displacement at the pre-septum:

$$\Delta x_{\text{sep.}} = \Delta x'_{\text{kicker}} \sqrt{\beta_{\text{kicker}} \beta_{\text{sep.}}} \sin\left(\mu_{\text{kicker}\rightarrow\text{sep.}}\right), \quad (1)$$

where the influence of a kick $\Delta x'_{\text{kicker}}$ to the beam displacement $\Delta x_{\text{sep.}}$ at the septum is described, with the beta functions $\beta_i$ and the phase advance $\mu_{\text{kicker}\rightarrow\text{sep.}}$. Those quantities are simulated with the simulation toolkit `ELEGANT` [4] and given in Table 1, stating the usability of the kickers for single turn extraction. Since linear beam optics are assumed for Eq. (1), further simulations including sextupole field contributions from dipoles and chromaticity correcting sextupoles were conducted. These simulations lead to a suitable kicker setting for single turn extraction with extraction efficiencies

* l.thome@uni-bonn.de

Content from this work may be used under the terms of the CC BY 4.0 licence (© 2025). Any distribution of this work must maintain attribution to the author(s), title of the work, publisher, and DOI.

ISBN: 978-3-95450-262-2 ISSN: 2673-5350 doi: 10.18429/JACoW-IBIC2025-MOPCO33

# STATUS OF THE SOURCE OF POLARIZED ELECTRONS AT ELSA WITH IMPROVED LASER AND ELECTRON BEAM DIAGNOSTICS

M. Switka*, K. Desch, D. Proft, A. Spreitzer, Physics Institute, University of Bonn, Bonn, Germany

*Abstract*

The ELSA facility at the University of Bonn uses a storage ring to accelerate polarized electrons up to 3.2 GeV. The photoinjector source is driven by a Ti:Sa laser beam to obtain a high polarization degree (~86 %) from a GaAsP strained-layer superlattice crystal photocathode. After a prolonged shutdown of the source we restored its status to *fully operational* and fine-tuned the laser system, the crystal storage and cleaning apparatus as well as the Linac transfer beamline. The in-house developed diagnostic software FGrabbit has been employed for the analysis of laser and electron beam camera images, providing increased precision and dynamic range in the optimization process. The impact of the crystal cleaning process was studied with spatially resolved quantum efficiency mapping of the photocathode surface.

## INTRODUCTION

The source of polarized electrons at the ELSA facility [1] had not been in use since 2017 due to minor defects in the subsystems and subordinate demand from the experimental program. However, upcoming experiments [2] favor photoproduction with polarized electrons, having lead to a reactivation effort of the required source. After repairs of water cooling and electrical infrastructure the source initially showed poor performance, demanding extensive analysis and fine-adjustment of all involved subsystems: The Ti:Sa laser pulse energy had to be increased from 2 mJ to 20 mJ by optimizing resonator and subsequent laser beamline, the quantum efficiencies of the available photocathodes had to be increased by an order of magnitude as well as the electron transfer beamline efficiency to the Linac.

## DESIGN OF THE POLARIZED ELECTRON SOURCE

The 50 kV source of polarized electrons at ELSA has been developed by W. Hillert [3] and extended by D. Heiliger [4] with crystal storage and hydrogen cleaning chambers (see Fig. 1). Up to six crystals can be stored and activated by heat- and atomic hydrogen cleaning procedures with subsequent deposition of caesium oxide on the crystal surface, to restore their quantum efficiency. A 4 mJ laser pulse (at 780 nm for GaAs/GaAsP crystals) is required to generate a 200 mA electron pulse for 1 µs duration, which is transferred to the 26 MeV Linac.

### *Titanium Sapphire Laser and Photon Beamline*

A free running 50 Hz flashlamp-pumped Ti:Sa laser generates laser pulses of up to 200 mJ and 10 µs length. To

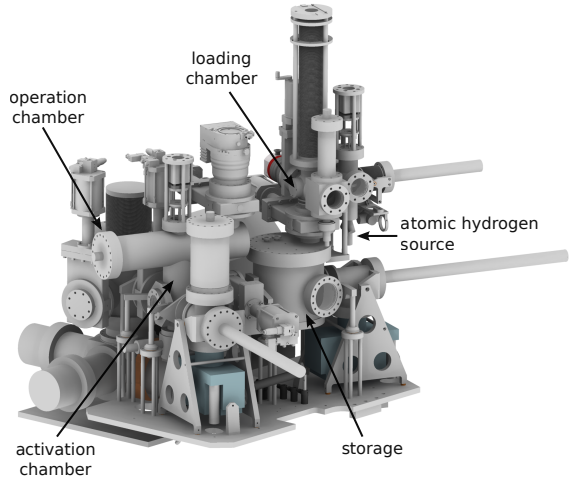



Figure 1: Overview of the source assembly with operation chamber, crystal activation-, storage- and loading chambers [4]. The latter includes a source for atomic hydrogen cleaning.

synchronize the useful part of the laser pulse precicely with the Linac RF timing, a pulse picker setup is used consisting of a triggered Pockels cell and polarizing beam splitter (see Fig. 2). It transmits 20 mJ towards a ~ 80 m long optical fiber, transporting the laser beam to the source assembly [5]. The multimode fiber defines the beam profile and leads to full polarization loss, requiring repolarization with a combined polarizing beam splitter and switchable $\lambda/4$ Pockels cell. The transfer efficiency of approximately 20 % provides 4 mJ circularly polarized laser pulses with alternating helicity, fully illuminating the GaAs-based photocathode crystals in the operation chamber.

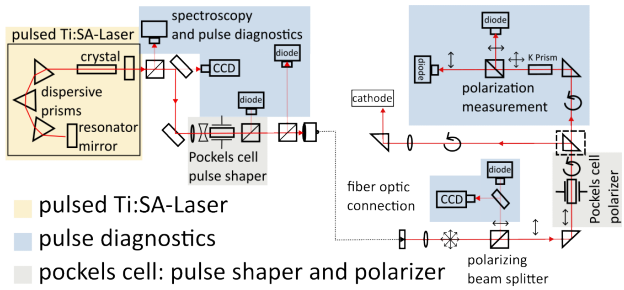



Figure 2: Sketch of the Ti:Sa laser photon beamline with pulse shaper and polarizer [5] with improved diagnostics.

### *Photocathode*

The GaAs/GaAsP strained-layer superlattice crystal photocathode [6] diameter amounts 8.9 mm and is illuminated

* switka@physik.uni-bonn.de

Content from this work may be used under the terms of the CC BY 4.0 licence (© 2025). Any distribution of this work must maintain attribution to the author(s), title of the work, publisher, and DOI.

ISBN: 978-3-95450-262-2 ISSN: 2673-5350 doi: 10.18429/JACoW-IBIC2025-MOPCO34

# DEVELOPMENT OF BPM ELECTRONICS FOR KOREA 4TH GENERATION STORAGE RING

Siwon Jang*, Dongcheol Shin, Pohang Accelerator Laboratory, Pohang, South Korea

*Abstract*

New BPM electronics have been developed for installation in the storage ring of the 4th Generation Synchrotron Radiation Facility (4GSR) in Ochang, Korea. Based on the first prototype, two different platforms were implemented for the second prototype: an RFSoC-based system optimized for high-performance and broadband data acquisition, and a uTCA-based system designed for long-term maintainability. This paper describes the design, hardware implementation, and test results of both prototypes, including resolution, stability, and compensation methods using crossbar switching. Beam test results at PLS-II are presented and compared with the requirements for the Korea-4GSR storage ring.

## INTRODUCTION

The Korea 4th Generation Storage Ring (4GSR) [1], under construction in Ochang, is designed as a diffraction-limited facility with a target emittance nearly 100 times smaller than the existing third-generation PLS-II. This drastic reduction enables ultra-high brilliance photon beams for advanced research in materials science, biology, and industry. Achieving nanometre-level orbit stability under such conditions requires the development of high-performance beam position monitor (BPM) electronics.

The BPM electronics must deliver high-resolution beam position data at multiple acquisition rates—Turn-by-Turn (TbT), Fast Acquisition (FA), and Slow Acquisition (SA)—for orbit feedback, interlock, and closed-orbit determination. To meet long-term stability requirements, two complementary platforms are being developed: an RFSoC-based system for broadband acquisition and future bunch-by-bunch (BbB) capability [2, 3], and a uTCA-based system optimized for integration and maintainability. The design specifications of the BPM electronics are summarised in Table 1.

## KOREA 4GSR BPM ELECTRONICS

The system architecture is shown in Fig. 1. Pickup signals are digitised and processed in the BPM electronics, with machine clock and trigger distributed via the event system. Beam position data are transmitted over SFP/SFP+ links to the FOFB, interlock, event system, and fast DAQ, ensuring support for both fast and slow control loops.

The internal data flow is illustrated in Fig. 2. Buffered ADC data are separated into TbT, FA, and SA streams: TbT supports feedback and interlock, FA feeds the fast DAQ, and SA is decimated to 10 Hz for EPICS-based closed-orbit determination.

* siwon@postech.ac.kr

Table 1: Design Specifications of 4GSR BPM Electronics

| Quantity | Requirement |
|---|---|
| TbT position | 375 kHz, ≤1 μm |
| FA position | 15.6 kHz, ≤200 nm |
| SA position | 10 Hz, ≤20 nm |
| Long-term stability | ≤±0.2 μm within ±0.5 °C |
| Data streaming | SFP to FOFB/FOI/Fast DAQ |
| Future option | BbB monitoring (RFSoC version) |

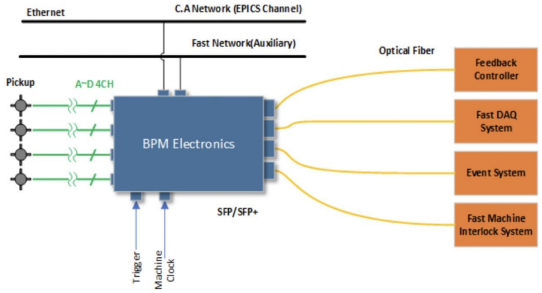



Figure 1: System overview of the BPM electronics.

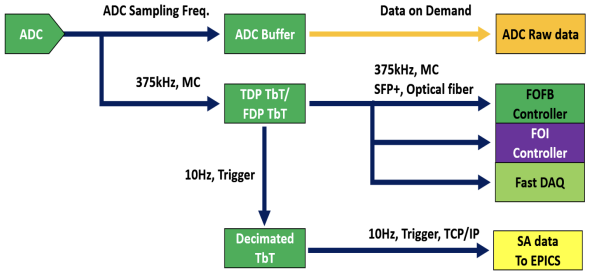



Figure 2: Data flow inside the BPM electronics. ADC raw data are processed into TbT, FA, and SA streams.

### *RFSoC BPM Electronics*

The RFSoC BPM electronics employ interchangeable AFEs (500 MHz narrowband and 2 GHz wideband) with a 2.5 GS/s ADC and FPGA-based processing. A key feature is the integrated crossbar, which removes offset errors from gain and phase mismatches, thereby ensuring the SA 20 nm specification and enhancing long-term stability.

The prototype (Fig. 3) integrates all required I/O, including SMA inputs, SFP+ streaming, Ethernet, and timing interfaces on the front panel. The rear panel provides AC power with EMI filtering, cooling fans, debug, and auxiliary network access. This prototype has passed factory acceptance tests (FAT) and will be evaluated with beam at PLS-II prior to 4GSR installation [3, 4].

### *Performance of RFSoC BPM Electronics*

The performance of the RFSoC BPM electronics was evaluated through measurement and simulation. Figure 4

Content from this work may be used under the terms of the CC BY 4.0 licence (© 2025). Any distribution of this work must maintain attribution to the author(s), title of the work, publisher, and DOI.

ISBN: 978-3-95450-262-2 ISSN: 2673-5350 doi: 10.18429/JACoW-IBIC2025-MOPCO36

# APPLICATION OF CONVOLUTIONAL NEURAL NETWORKS FOR PILE UP CORRECTION IN SINGLE PARTICLE COUNTING

T. Habermann*,[1], M. Kumm[1], R. Singh[2]
[1]Fulda University of Applied Sciences, Fulda, Germany
[2]GSI Helmholtzzentrum fuer Schwerionenforschung, Darmstadt, Germany

Content from this work may be used under the terms of the CC BY 4.0 licence (© 2025). Any distribution of this work must maintain attribution to the author(s), title of the work, publisher, and DOI.

*Abstract*

An exploration into the application of machine learning (ML) approaches for real time identification and correction of pile-ups in single particle counters at the GSI Helmholtz Centre for Heavy Ion Research is presented. About 26,000 particle pulse data were manually labelled and a convolutional neural network (CNN) was developed to accurately locate the particles without domain-specific knowledge. This contribution represents proof-of-work for a fast error-free automated particle counting system. The identified algorithm was developed with a perspective of implementation into FPGA.

## INTRODUCTION

Accurate particle counting along with their arrival time determination is fundamental to experimental nuclear and particle physics. Similarly in accelerator beam diagnostics, real-time and precise measurements of particle fluxes and their temporal distribution is critical for providing usable particle beams (spill) to the user experiments. Scintillator-type single particle counters face significant challenges from pile-up events [1], e.g., where multiple particles arrive within a short time interval causing superimposed pulse shapes at the output of the sensor. Typically the number of pile-ups in extracted beams from particle accelerators is much more than one expects from a random discrete process or Poisson process [2,3]. Figure 1 shows examples where pulses pile-up in the time series data.

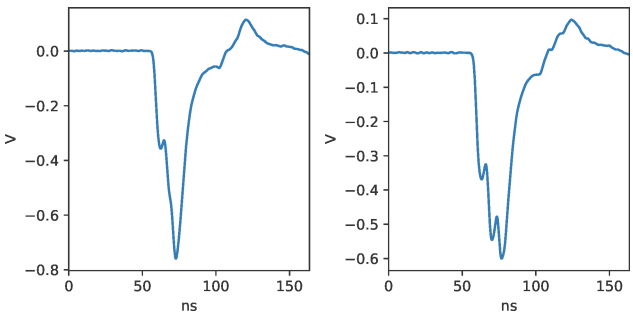



Figure 1: Examples of pile-ups of multiple particles where pulses overlap in the time series data of the scintillator sensor.

Traditional real-time methods struggle to decompose this complex composite signals. This can lead to significant undercounting which can impact precision experiments. Most traditional methods rely on analytical models and expert-designed algorithms that require extensive calibration and often fail with complex pile-up scenarios involving multiple overlapping particles [4]. The most used algorithm for high rate real-time particle counting is still single or double threshold crossing algorithms. Other post-processing algorithms relying on analytical models or heuristics like template matching with deconvolution, or peak property–based detection have also been used [5–7].

Recent advances in machine learning, particularly convolutional neural networks (CNNs), have demonstrated remarkable success in pattern recognition tasks involving complex time series data [8, 9]. CNNs can automatically learn hierarchical representations without requiring explicit domain knowledge, making them well-suited for pile-up identification where relevant features may be subtle and difficult to capture analytically.

In this work, we present a CNN-based approach for particle counting and pile-up identification in scintillator counters. We trained our network on approximately 26,000 manually labeled particle pulse events, treating the time series data as one-dimensional signals suitable for CNN analysis. Our approach achieves accurate particle counting without relying on detailed analytical models, with the CNN model developed specifically for their real-time implementation on field programmable gate arrays (FPGAs).

## DATA

Single particle induced pulse data was collected at the HTP beamline at GSI Helmholtz Centre for Heavy Ion Research. Average beam extraction rate from synchrotron SIS-18 is controlled with the spill optimization system [10]. A plastic (BC400) scintillator coupled with a photo multiplier tube via a light guide was used to collect the single particle pulse data. The scintillator is irradiated with Carbon ($C^{6+}$) ion beam with an extraction kinetic energy of 300 MeV/u.

### *Pulse Characteristics*

All single pulses are caused by production of many photons (100-10000s depending on energy deposition) per ion incidence in the scintillation medium which results in a linearly scaled number of charges at the PMT output. Therefore, ions within the same spill (which are of the same energy and charge state) induce PMT pulses which share the same characteristics. Since the area under all pulses is comparable, the integral can be used to estimate the number of pulses present in any user defined time window. The integral-indicator is a

* tobias.habermann@informatik.hs-fulda.de

ISBN: 978-3-95450-262-2 ISSN: 2673-5350 doi: 10.18429/JACoW-IBIC2025-MOPCO40

# DESIGN OF DIGITAL ACQUISITION FOR BEAM CURRENT MONITOR*

R. T. White†, J. R. Berlioz
Fermi National Accelerator Laboratory, Batavia, IL, USA

Content from this work may be used under the terms of the CC BY 4.0 licence (© 2025). Any distribution of this work must maintain attribution to the author(s), title of the work, publisher, and DOI.

*Abstract*

As a part of the Proton Improvement Plan – II (PIP-II) at Fermilab, instrumentation systems are being modernized to take advantage of the higher speeds and ease of use offered by standardized embedded systems like MicroTCA. A rear-transition module (RTM) is being designed to interface with said embedded systems. In each of the four identical channels on the RTM, the differential signal from an alternating-current current transformer (ACCT) transimpedance amplifier will again be amplified by a differential operation-amplifier, then filtered by a low-pass topology. The conditioned signal is then digitized at a maximum of 10 MS/s by an analog to digital converter (ADC) integrated circuit. After digitization, the ADC passes the data to an off the shelf AdvancedMC (AMC) Xilinx FPGA module using low voltage differential signals. This paper will describe the simulation of analog circuitry for signal conditioning, simulation of digital signal integrity based on physical design as well as verification of design characteristics critical to signal integrity. This work aims to create a methodology that can be applied to future RTMs requiring application of high-speed digital design principles.

## INTRODUCTION

Historically, instrumentation infrastructure at Fermilab utilized VME architecture to achieve modularity [1]. Over time, there became an increasing need for higher bandwidth signal processing and data transfer to facilitate research and development. MicroTCA was selected as the replacement to meet these needs and others, including flexibility in processing power through the selection of the AMC and better maintainability via the integrated management systems and hot-swappable RTMs (see Fig. 1).

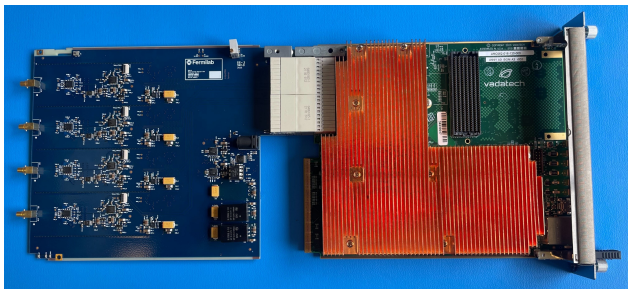


Figure 1: RTM and AMC outside of MicroTCA chassis.

In order to incorporate beam current monitor measurements into the MicroTCA update effort, a prototype ACCT RTM was designed. The raw signal is created by a Bergoz ACCT with a maximum cutoff frequency of 5.0121 MHz. The raw signal then passes through a shielded twisted pair to interface with the Bergoz ACCT-E-RM-3R transimpedance amplifier. To reduce the risk of failure due to radiation degradation, the transimpedance amplifier will be placed just outside the enclosure, necessitating a cable length longer than the Bergoz specified 20 m. Three outputs exist on the ACCT-E-RM-3R, a 50 Ω single ended BNC, 1 MΩ BNC, and a 100 Ω differential BNO output. The 1 MΩ output was not used because the high impedance increases the risk of coupled electro-magnetic interference generating electrical noise. The 50 Ω single ended connection was already in use, leaving the differential output. The generated differential output voltage can vary depending on the termination of the signal at the ACCT RTM. Again, the low impedance termination was selected for the ACCT RTM and, per specification, the differential output voltage has a range of ±2 V.

## HARDWARE DESIGN

To ensure compatibility with the AMC562 and MicroTCA system, the ACCT RTM was designed with the intention to meet specifications laid out in conjunction with Vadatech. The specifications defined requirements such as: the dimensional envelope the ACCT RTM printed circuit board (PCB) must fit in, the location and functional pinout of the high-speed backplane connectors, and a required set of circuitry referred to as Zone 3 circuitry (Fig. 2). Several RTMs are being designed concurrently at the laboratory, so the Zone 3 components and topology were selected to be common.

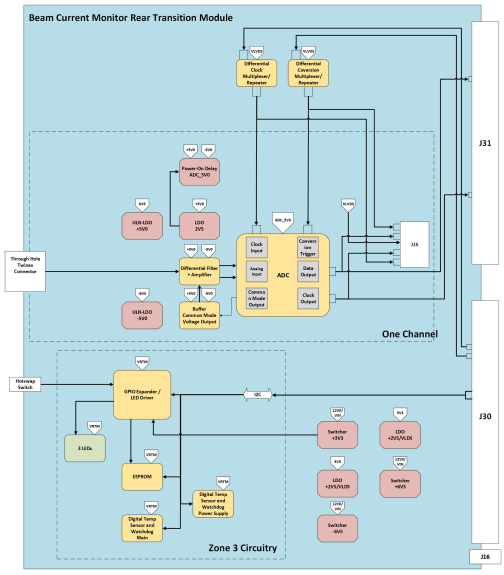



Figure 2: ACCT RTM block diagram.

* This manuscript has been authored by FermiForward Discovery Group, LLC under Contract No. 89243024CSC000002 with the U.S. Department of Energy, Office of Science, Office of High Energy Physics.

† twhite1@fnal.gov

ISBN: 978-3-95450-262-2 ISSN: 2673-5350 doi: 10.18429/JACoW-IBIC2025-MOPMO01

# BUNCH-BY-BUNCH BEAM CURRENT AND LIFETIME MEASUREMENT WITH INTERLEAVED SAMPLING AT HLS*

An Wang[1], Xing Yang[1], Youming Deng[1], Jianhui Chen[2], Yongbin Leng†,[1]
[1]NSRL, University of Science and Technology of China, Hefei, P. R. China
[2]Suzhou Laboratory, Suzhou, P. R. China

*Abstract*

To achieve high-precision, bunch-by-bunch beam current and lifetime measurements at the Hefei Light Source (HLS), we developed a beam diagnostics system based on interleaved sampling technology, achieving an equivalent sampling rate of 6.5 GHz. In single-bunch mode, amplitude extraction via cross-correlation with a single response function yields a turn-by-turn current relative resolution of 0.12 %. By averaging over 200 turns, the resolution is improved to 0.04 % at a 23 kHz data refresh rate, enabling fast and accurate lifetime calculations. However, in multi-bunch high-current mode, large longitudinal oscillations degrade the accuracy of amplitude extraction when using a fixed-response function. We propose an integration method to mitigate the effects of bunch length and phase oscillations on beam current measurements. The method and experimental results provide a practical solution for machines exhibiting large longitudinal oscillations, such as HLS.

## INTRODUCTION

HLS is a dedicated second-generation VUV light source. It employs a top-up injection mode, with a typical beam current of 420 mA, a lifetime of 10 hours, and an RF frequency of 204 MHz. The existing bunch-by-bunch current measurement system uses a 4 GHz oscilloscope to sample the sum signal from the beam position monitor (BPM). The relative measurement error is 0.2 % [1].

High-precision, fast-response bunch-by-bunch beam current and lifetime measurements allow comprehensive analysis of single-bunch and bunch-to-bunch dynamics [2, 3]. To achieve this goal, a beam measurement system based on interleaved sampling has been developed, and its current measurement accuracy has been evaluated.

Significant longitudinal oscillations in the HLS beam cause continuous variations in bunch length and phase on a turn-by-turn basis, leading to changes in the response waveform of individual bunches. Currently, bunch-by-bunch current information is primarily obtained by measuring the amplitude of the BPM signal [4]. However, under dynamic variations in the response waveform, the signal amplitude no longer solely reflects the relative charge quantity but also incorporates information about changes in bunch length , phase, etc [5]. To mitigate the interference caused by large longitudinal oscillations on current measurement, this paper proposes a current extraction algorithm based on an integration method.

*Work supported by Large-Scale Scientific Facility Renovation and Upgrade Project of the Chinese Academy of Sciences -"Universal Signal-Processing Platform for Accelerator Beam Measurement and Control"
†email address: lengyb@ustc.edu.cn

## MEASUREMENT SYSTEM SETUP

The structure of the phase-sampling-based bunch-by-bunch measurement system is illustrated in the Fig. 1. When measuring beam current, the system first combines the four electrode signals from the BPM into a single sum signal using a power combiner. This sum signal is then equally split into eight channels via phase shifters and fed into an eight-channel processor for synchronous acquisition. The phase-locked sampling clock is derived from a quadrupled-frequency signal of the RF system. A single bunch can be sampled at 32 points, corresponding to an equivalent sampling rate of 6.5 GHz. This architecture enables the system to measure bunch-by-bunch parameters such as bunch length, phase, and current. This paper focuses on evaluating its bunch current measurement capability. To assess the system's accuracy in this regard, we conducted experimental analysis of bunch-by-bunch current under single-bunch operation mode

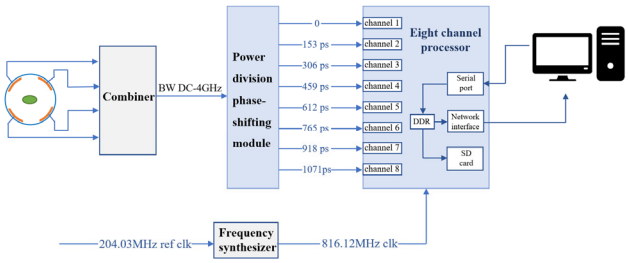



Figure 1: Architecture of the measurement system.

### *Single-bunch Mode*

When a bunch with an current of 7.6 mA is injected, the signal waveform acquired through the eight-channel processor is shown in the Fig. 2.

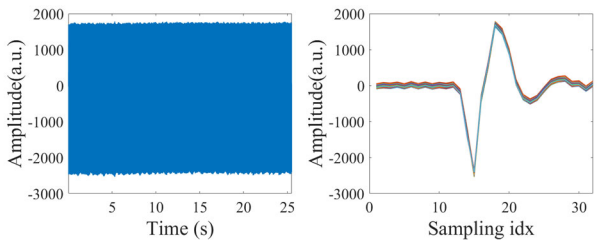



Figure 2: Single-bunch beam acquired signal.

Figure 2 displays the signals corresponding to 5200 consecutive turns of this single bunch. Under single-bunch operation mode, the influence of longitudinal bunch oscillations on the measurement is negligible. The relative variation in charge is characterized by extracting the signal amplitude at a fixed phase. Taking the peak value as an example, the resulting data is presented in the Fig. 3.

Content from this work may be used under the terms of the CC BY 4.0 licence (© 2025). Any distribution of this work must maintain attribution to the author(s), title of the work, publisher, and DOI.

ISBN: 978-3-95450-262-2 ISSN: 2673-5350 doi: 10.18429/JACoW-IBIC2025-MOPMO02

# DESIGN STUDIES OF A RETARDING POTENTIAL ENERGY ANALYSER (RPEA) FOR LOW ENERGY ANTIMATTER EXPERIMENTS

B. S. Rawat*[,1,2], N. Kumar[1,2], S. Chandran[1,2], B. Rienacker[1], C. P. Welsch[1,2]
[1] Department of Physics, University of Liverpool, Liverpool, UK
[2] Cockcroft Institute, Sci-Tech Daresbury, Warrington, UK

*Abstract*

Retarding Potential Energy Analysers (RPEAs) are widely used diagnostic instruments for measuring the energy distribution of charged particle beams. In this work, we will discuss the conceptual design studies of a RPEA for low energy antimatter beams (antiprotons/positrons). Simulation tools such as CST Studio and G4Beamline were used to study the prototype RPEA and for different geometries to consider effects parameters such as beam properties, collector geometry, the losses occurring due to secondary electrons and annihilations, etc. The proposed diagnostic can offer the potential to measure the energy and current of low energy (1–10 keV) antiproton/positron bunches in experiments such as AE$\bar{g}$IS, with promising energy resolution. In addition, detailed studies are required to assess its viability and improve its accuracy for implementation in a practical experimental setup.

## INTRODUCTION

Retarding Potential Energy Analyzers (RPEAs) are beam diagnostic instruments that are used to measure the energy distribution function of an incoming charged particle beam [1]. They typically consist of a series of grids that serve different purposes, such as energy discrimination and suppressing secondary electrons. However, gridless (without meshed grids) RPEAs have also been demonstrated [2,3], where no mesh grid is used for particle energy discrimination. In antimatter detection, annihilation at the collector surface generates secondary particles (photons, pions, neutrons) leading to signal loss. To quantify and minimize these losses, we use G4Beamline simulations [4] to evaluate collector materials behavior and CST Studio [5] to simulate the Discriminator Electrode (D.E.) for particle filtering and determining the Energy Distribution Function (E.D.F).

## G4Beamline MODEL

G4Beamline, a Geant4-based toolkit for beamline design and optimization, was used to simulate secondary particles from antiproton/positron interactions with various collector materials. Figure 1 shows the typical RPEA simulation setup. The system includes a main collector and a Discriminator Electrode (D.E.) located near the entrance. Although the collector material is varied across simulations, the D.E. modeled using stainless steel. In the current study, initially a gridless D.E model was used for the G4Beamline simulations to minimize the computational load due to the secondaries formed due to the antiproton / positron interaction, whereas later for the filtering simulation, a meshed D.E was used in the CST simulation. Two cylindrical scoring volumes ( labeled side and forward detectors, shown in green) register secondary particles that escape the interaction region, with dimensions shown in Fig. 1. The dimensions are not optimal, but were chosen to ensure efficient scoring of the secondary particles. A 10 keV antiproton beam with 100,000 events was simulated, using typical beam properties from the literature [6], with widths of 0.5 – 2.5 mm depending on the collector geometry. Secondary particles escaping back toward the RPEA entrance were not considered.

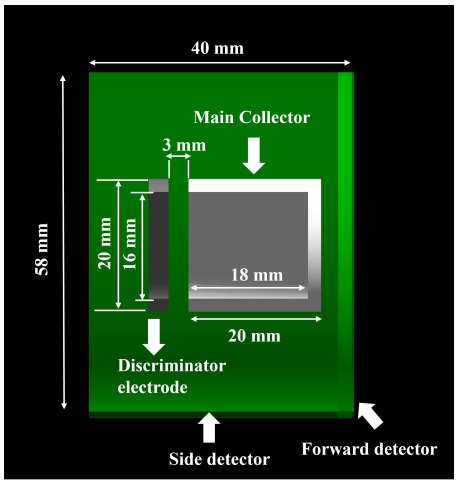



Figure 1: G4Beamline simulation setup of the RPEA with the collector and the Discriminator Electrode (D.E.).

## SECONDARY PARTICLE DISTRIBUTIONS

To investigate the effect of secondary particle production on various collector materials, G4Beamline particle tracking simulations were performed for the collector geometry using different materials. An example of the energy distribution of secondary particles formed by the interaction of a 10 keV antiproton beam on a copper collector is shown in Fig. 2. The x-axis corresponds to the particle energy in MeV, and the y-axis represents the number of particles (N). Unlike normal particles, antiprotons annihilate upon interacting with the collector material, producing a variety of secondary particles, including electrons, pions, photons, and others. As shown in Fig. 2, charge loss is mainly due to high energy gamma rays (magenta) and neutrons (cyan). In normal matter beams, secondary electrons are the main issue and are suppressed electrostatically or magnetostatically. For

* bharat26@liverpool.ac.uk

Content from this work may be used under the terms of the CC BY 4.0 licence (© 2025). Any distribution of this work must maintain attribution to the author(s), title of the work, publisher, and DOI.

ISBN: 978-3-95450-262-2 ISSN: 2673-5350 doi: 10.18429/JACoW-IBIC2025-MOPMO03

# DEVELOPMENT OF A NOVEL DC CURRENT MONITOR DEVICE, BASED ON TUNNELLING MAGNETORESISTIVE SENSORS, FOR ION BEAM CURRENT MEASUREMENT

C. Manna*, Laboratori Nazionali del Sud - Istituto Nazionale di Fisica Nucleare, Catania, Italy

*Abstract*

In this work, the development of a non-invasive DC Current Monitor device (DCCM), based on Tunnelling MagnetoResistive (TMR) sensors, is presented. The device is primarily intended for measuring the current intensity of an ion beam without the need of intercepting it (therefore not altering its characteristics), making it suitable for online current monitoring. Details are given about the design of the device and its performance assessment, namely the linearity of its static response and its frequency-domain behavior.

## INTRODUCTION

The first concept of a non-invasive device for measuring ion beam currents appeared in 1969 thanks to the work of Unser at CERN [1]. The device, known in the literature as DC Current Transformer (DCCT), was based on the use of a pair of "twin" ferromagnetic cores driven by a modulating current $I_{modulation}$ at a given frequency $f$ which, without ion beam, would induce, inside the cores, magnetic fluxes of equal amplitudes but opposite phases, thanks to a proper connection of the two coils (see Fig. 1).

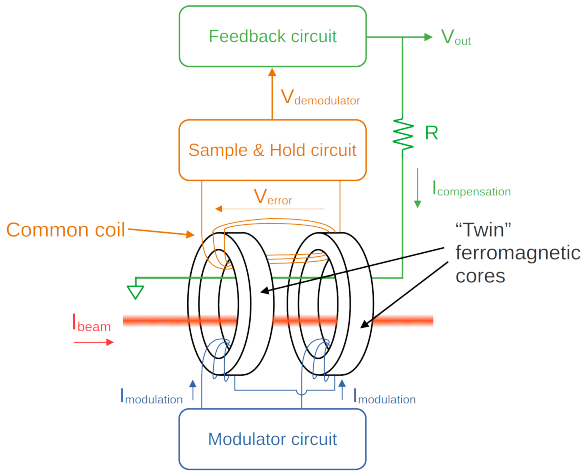



Figure 1: Classical DCCT scheme.

In the presence of an ion beam current passing through the cores, a small asymmetry in the magnetic fluxes arises, generating a $V_{error}$ signal on the common coil, having a dominant frequency component equal to $2f$. This signal is then used to derive a DC voltage signal $V_{demodulator}$ by means, e.g., of a synchronized Sample & Hold circuit, referred in [1] as "demodulator". $V_{demodulator}$ is then used, by means of a feedback circuit, to produce a DC current $I_{compensation}$ which, passing through the cores in opposite direction to the ion beam, cancels out the asymmetry in the fluxes introduced by the ion beam current, bringing $V_{error}$ to zero and thus creating a zero-flux condition. The amplitude of $V_{out}$ is $V_{out} = R \cdot I_{compensation}$ and it is then used as an indirect measure of the ion beam current. The design of such a device is ingenious but quite complicated, since it requires the use of different modules (modulator, magnetic flux detector coil, demodulator, feedback circuit) and, mostly critical, the use of perfectly matched "twin" ferromagnetic cores (see also [2, 3]).

Recently, a new class of magnetic sensing devices, based on the Tunnelling MagnetoResistive (TMR) effect, have been introduced in the market and extensively studied in [4–8]; these sensors have a sensitivity in the order of mV/Gs and a noise figure in the order of 250 pT/$\sqrt{\text{Hz}}$ [9]. These sensors, in addition, have a low magnetic saturation level, in the order of few Gauss, and, hence, are well-suited for all those applications where the magnetic field to be measured is very close to zero.

The aim of the work here presented is to explore the use of such sensors for a non-invasive ion beam DC Current Monitor (DCCM) based on zero-flux detection, in view of the characteristics previously discussed. In the following section of this article, the design of a DCCM based on TMR sensors is presented; the main drawbacks related to the use of TMR technology are also discussed. The results of a linearity test and of a frequency-domain characterization on a prototype are included in the last section.

## DESIGN OF THE DCCM SYSTEM

### *Working Principle*

The block diagram of the DCCM device here described is shown in Fig. 2.

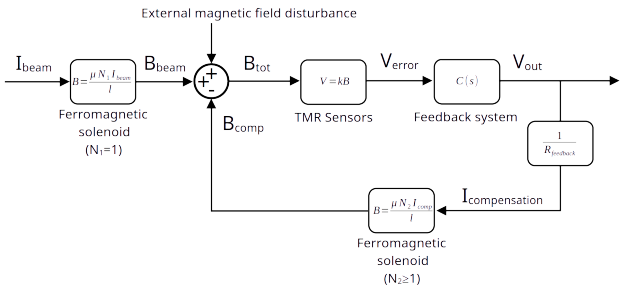



Figure 2: DCCM block diagram.

The current to be measured (referred in the block as $I_{beam}$) induces a magnetic field $B_{beam}$ inside a ferromagnetic core

* carmelo.manna@lns.infn.it

Content from this work may be used under the terms of the CC BY 4.0 licence (© 2025). Any distribution of this work must maintain attribution to the author(s), title of the work, publisher, and DOI.

ISBN: 978-3-95450-262-2 ISSN: 2673-5350 doi: 10.18429/JACoW-IBIC2025-MOPMO04

# DIAGNOSTIC CONTRIBUTIONS TO THE COMMISSIONING OF SLS 2.0

C. Ozkan Loch†, M. Aiba, F. Armborst, M. Rey Barrera, J. Vila-Comamala,
A. Citterio, M. Dehler, A. Fazan, A. Foskolos, R. Ischebeck, J. Kallestrup, B. Keil
Paul Scherrer Institute, Villigen, Switzerland

*Abstract*

In January 2025, beam was first stored in the SLS 2.0, and by April 2025, the milestone of 400 mA stored beam current was reached. A variety of diagnostics were utilized to reach these milestones; for example, charge, current and loss monitors for minimizing losses and optimizing transmission and injection efficiency, polarized visible light for vertical beam size measurement, and more. This paper will highlight the contributions of the various diagnostics to the machine commissioning process.

## INTRODUCTION

The Linac and Booster from the original SLS have largely been retained, except for the electron source pulser, the power supply for the booster dipole magnets [1], machine protection system [2], and some controls systems upgrades. The Booster-to-Ring Transfer Line (BRTL) and the Storage Ring (SR) injection system were completely redesigned. Several of the BRTL components and the four-kicker bump from the storage ring were inherited from the SLS.

The SLS 2.0 Storage Ring consists of 12 identical arcs with short, medium, and long straights arranged in a three-fold symmetry. There are three long straight sections. The first long straight section is dedicated to beam injection. In this injection straight, four kickers create a bump that brings the stored beam within 3 mm of the injected beam [1, 2]. The injected beam is first deflected by a permanent magnet thick septum in the BRTL, followed by a pulsed thin septum. A dedicated kicker magnet has been installed to dump the beam in a controlled manner onto a copper block upstream of the thin septum [3]. Four new 500 MHz RF cavities with Higher-Order Mode (HOM) dampers [4] are installed in sequence in a long straight section followed by horizontal and vertical collimators, while the SLS superconducting third-harmonic cavity (3HC) [5] is located in the last long straight followed by another pair of collimators.

From the Linac down to the BRTL, the existing SLS diagnostics were used. To improve injection into the Booster, beam loss monitors were added at the entrance of the Booster.

Several of the diagnostics for the BRTL and the SR were designed anew and installed at strategic locations to help commission and effectively characterize the beam parameters.

Two beamlines are dedicated to beam diagnostics, and specially developed BPM and feedback systems continuously monitor and stabilize the beam [6].

† cigdem.ozkan@psi.ch

## PRINCIPLE DIAGNOSTICS

### *Linac to Booster Diagnostics*

The available integrated current transformers from the SLS (ICTs, Bergoz instrumentation [7]) were used to measure the beam charge within the range of 100 - 500 pC, and transmission in the Linac and the Linac-to-Booster transfer line (LBTL).

The beam transmission into the Booster of 90 - 95 % was measured at 10 - 50 pC, and at high(er) charges the transmission was ~80 %.

To tune injection into the Booster and correct the beam in the first turns, turn-by-turn losses were detected using RF BPM turn-by-turn intensity readings as well as the Libera BLM system [8] to help minimize the losses. These systems were key to getting the beam into the Booster and establishing the first 100 odd turns for the RF and the ramp take over.

The injected and extracted charges at beginning and end of ramp are measured with the original SLS current monitor (MPCT). As far as upgrades to the diagnostics are concerned, the following activities were carried out: the readout of the charge monitors and current monitor in these sectors was changed to the SLS 2.0 compatible CPSI DAQ system [9], the screen monitor controls have been upgraded to the SLS 2.0 compatible motion control system, and the camera servers over Gbit links are new.

### *Booster to Ring Transfer Line Diagnostics*

The BRTL provides the possibility for nominal injection into the SLS 2.0 SR. The purpose of the BRTL diagnostics is to support machine development with invasive screen monitors for determination of beam profiles, transverse emittance, beta-functions, dispersion and energy spread, as well as charge and loss monitors for non-invasive monitoring of transmission and injection efficiency into the SR during operation.

The ICT in the BRTL measures the transmission from the Booster to the BRTL. During the initial commissioning, the injection into the ring was established very quickly but the Booster to SR injection efficiency was limited to ~40 %.

### *Beam Loss Monitoring*

For the commissioning and daily operation of the storage ring, loss monitors are used in the SR and the entrance of the Booster, that can detect “fast” losses from faults or beam perturbation from injection (single or turn-by-turn) and “slow” losses that influence lifetime during standard operation.

Content from this work may be used under the terms of the CC BY 4.0 licence (© 2025). Any distribution of this work must maintain attribution to the author(s), title of the work, publisher, and DOI.

ISBN: 978-3-95450-262-2 ISSN: 2673-5350 doi: 10.18429/JACoW-IBIC2025-MOPMO05

# DEVELOPMENT OF A WIDE DYNAMIC RANGE AND HIGH-PRECISION AMMETER FOR BEAMLINE INSTRUMENTATION AT SIRIUS

V. S. Oliveira*, P. H. Nallin, F. H. Cardoso, Brazilian Synchrotron Light Laboratory, Campinas, Brazil
B. G. Oliveira, Brazilian Center for Research in Energy and Materials, Campinas, Brazil

*Abstract*

SIRIUS beamlines require specialized electronic devices to monitor key parameters of the photon beam, such as position and flux, through the detection of extremely low-level electrical currents. Furthermore, experiments conducted in on-the-fly scan mode usually demand fast, high-precision low-level current measurements. To address these requirements, the development of a wide dynamic range ammeter (from 1 pA to 10 mA) has been addressed, based on a logarithmic transimpedance amplifier, eliminating the need for scale switching and featuring high precision and fast response. The proposed device converts the input current into a logarithmic output voltage and offers two operation modes: the logarithmic ammeter and the logarithmic ratiometer, both of which are particularly useful in X-ray spectroscopy experiments. This paper considers an overview of the device as well as its preliminary characterization and results, including logarithmic conformity, bandwidth, and noise.

## INTRODUCTION

X-ray beam diagnostics often rely on measuring the photocurrents generated by photodiodes or ionization chamber [1]. During commissioning or experiment preparation, such as beam alignment and focusing, the photocurrent may vary over several orders of magnitude. Conventional ammeters are limited in these conditions, as range switching slows data acquisition and degrades the signal-to-noise ratio [2]. Similarly, synchrotron-based techniques such as X-ray absorption spectroscopy require instrumentation with fast response, wide dynamic range and the capability to compute logarithmic ratios [3]. This work aims to describe a compact logarithmic transimpedance amplifier(Log-TIA) developed to address challenges in experiments and diagnostics on the SIRIUS beamlines.

## LOGARITHMIC TRANSIMPEDANCE AMPLIFIER

The proposed device is based on the ADL5304 [4], the State Of The Art Logarithmic Transimpedance Amplifier from Analog Devices, chosen for its capability of producing a logarithmic voltage response to input currents from 1 pA to 10 mA. Moreover, the ADL5304 features high-speed operation, adaptive biasing for photodiode inputs, two current inputs, enabling logarithmic ratio measurements, and a high-precision 100 nA current source for operation as a logarithmic ammeter.

* vinicius.silva@lnls.br

Building upon these features, a logarithmic ammeter/ratiometer was developed, where the operating mode is selected via high-insulation relays controlled by external digital inputs. Furthermore, an auxiliary circuit was implemented to enable current inversion in one of the input channels, thereby extending the measurement capability to negative currents and overcoming a common limitation of conventional logarithmic amplifier.

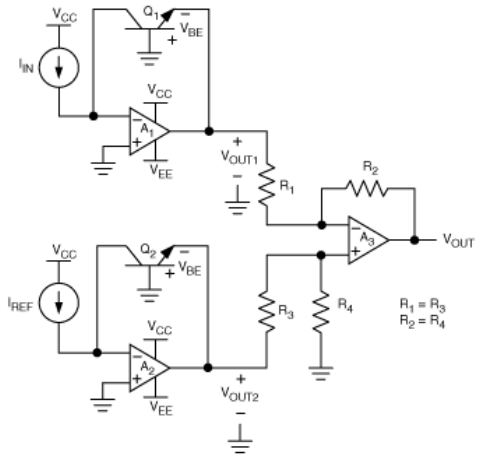



Figure 1: Conventional topology of Log-TIA [5].

### *Working Principle*

The conventional implementation of logarithmic amplifier relies on inserting a bipolar junction transistor into the feedback loop of an operational amplifier [6] as shown in Fig. 1. This circuit exploits the exponential relationship of $V_{BE}$ and $I_C$ shown in Eq. (1).

$$V_{BE} = V_T \log\left(\frac{I_C}{I_S}\right), \tag{1}$$

where $V_T$ is the thermal voltage, equal to 26 mV at $T = 25\,^{\circ}\mathrm{C}$ and increasing with temperature. The saturation current $I_S$ is highly sensitive to temperature and also depends on fabrication processes.

To mitigate these variations in the circuit response, a robust approach is to add a second logarithmic amplifier, where both transistors are matched and kept in thermal equilibrium. The output voltages of the two amplifiers are then subtracted, effectively canceling the influence of $I_S$, resulting in the fundamental relationship of logarithmic ammeter as shown in Eq. (2).

$$\Delta V_{BE} = V_T \log\left(\frac{I_{C_1}}{I_{C_2}}\right). \tag{2}$$

Content from this work may be used under the terms of the CC BY 4.0 licence (© 2025). Any distribution of this work must maintain attribution to the author(s), title of the work, publisher, and DOI.

ISBN: 978-3-95450-262-2 ISSN: 2673-5350 doi: 10.18429/JACoW-IBIC2025-MOPMO06

# CHALLENGES WITH THE BEAM DESTINATIONS FOR THE ESS LINAC

E. Donegani*, A. Gevorgyan, A. Olsson, L. Page, European Spallation Source (ESS) Lund, Sweden
V. Bertrand, Pantechnik, Bayeux, France
I. Bustinduy, ESS Bilbao, Zamudio, Spain
J. Herranz, Proactive R&D, Sabadell, Spain
M. Peli, Allectra Ltd, Sheffield Park, East Sussex, UK
T. Hodgetts, M. Ruelas, RadiaBeam Technologies, Santa Monica, CA, USA
P. Brooker, TWI Limited, UK

*Abstract*

For the ESS linac commissioning, twelve compact beam destinations were designed in place of bulky beam dumps, in order to dump [0.075, 250] MeV protons. The beam destinations were either Faraday Cups (FC) for the NCL commissioning or Insertable Beam Stops (IBS) for the SCL commissioning. Both FC and IBS are beam-intercepting devices installed in the ESS proton linac, operated under vacuum, water cooled and movable by means of a pneumatic actuator. The FC and IBS manufacturing relied on high-precision machining. The limited installation space and vacuum requirements required strict tolerances, complex welding of small components and vacuum brazing of compact cooling pipes. The installation of the devices themselves, their radiation shielding and portable cleanrooms were particularly challenging due to the limited space not only outside but also inside the beamline. The main challenge during the operation was posed by the beam power density. Radiation transport calculations allowed to minimize residual dose rates. Thermo-mechanical simulations allowed to define the operational limits thus avoiding damage to the beam destinations themselves and linac components nearby. This paper addresses some FAQs about the ESS beam destinations.

## WHAT IS A BEAM DESTINATION?

The high-power proton accelerator of the ESS [1] has been incrementally commissioned since 2018 [2]. The beam destinations have been essential to safely dump the beam at the end of each section under commissioning. Twelve compact beam destinations were tailored to the ESS linac, in place of bulky beam dumps. The most demanding beam modes are: slow tuning (62.5 mA, 50 µs, 1 Hz) and fast tuning (62.5 mA, 5 µs and 14 Hz). Each beam destination is operated under vacuum, water-cooled and movable in/out of the beam pipe by means of a pneumatic actuator. In the ESS Normal Conducting Linac (NCL), the beam destinations are Faraday cups measuring the proton beam current and pulse length. In the ESS SuperConducting Linac (SCL), the beam destinations are movable beam stops for protons up to the nominal energy of either 100 or 250 MeV.

The design, fabrication, cleaning, assembly, handling and installation phases are subject to the vacuum requirements.

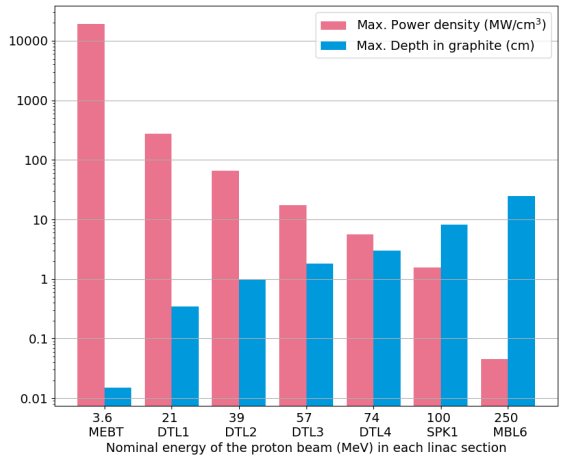



Figure 1: Maximum beam power density and beam's penetration depth in the graphite core of each ESS beam destination (assuming the ESS nominal proton current of 62.5 mA).

The closest beam destination to the ESS proton source [3] relies on a copper collector for stopping 75 keV protons up to 14 kW/cm$^2$, whereas graphite is the only suitable material for the core of all the other destinations, given the thermo-mechanical and radiation protection aspects. Details about the design and initial performance of the beam destinations can be found in [4–7]; this short paper summarizes the main challenges in the manufacturing, installation and operation of the ESS beam destinations. All challenges stem from the demanding beam power density to be dissipated within the limited space inside as well outside the vacuum beam line. Figure 1 points out that the higher the proton energy, the less the beam power density, but more space along the beam path is needed to fully stop the proton beam.

## WHY IS MANUFACTURING TAKING SO LONG?

Manufacturing a beam destination for the ESS linac has never taken less than seven months. There exists no company that can perform all the manufacturing steps between the detailed design and the final acceptance tests. Therefore, global sourcing and compliance with international regulations are unavoidable. On top of this, the materials, assembly procedures and rigorous tests have to be customized for the ESS accelerator environment. Four manufacturing steps are

* elena.donegani@ess.eu

Content from this work may be used under the terms of the CC BY 4.0 licence (© 2025). Any distribution of this work must maintain attribution to the author(s), title of the work, publisher, and DOI.

ISBN: 978-3-95450-262-2 ISSN: 2673-5350 doi: 10.18429/JACoW-IBIC2025-MOPMO07

# FIRST Attila4MC SIMULATIONS FOR THE HIGH-POWER PROTON ACCELERATOR OF THE EUROPEAN SPALLATION SOURCE

E. Donegani*, European Spallation Source (ESS) Lund, Sweden

*Abstract*

Radiation transport simulations allow the design and operation of entire facilities such as the European Spallation Source (ESS) in Lund, Sweden. This paper summarizes three of the first applications of Attila4MC simulations to the high-power proton accelerator of ESS and its beam instrumentation. Entire linac sections and beam-interceptive instrumentation were modelled by implementing existing CAD models, relying on unstructured tetrahedral meshes and zeroing out the time spent in manually crafting MCNP6 models. As a result, it was possible to accurately quantify the beam power density within beam-interceptive devices and in turn their operational limits. Activation and 3D dose maps were computed and swiftly visualized in 3D, on top of the actual linac model. This work paves the way for e.g. advanced instrumentation design, linac operation, safe maintenance, categorization of radiation waste and future dismantling.

## INTRODUCTION

The European Spallation Source (ESS) [1] in Lund (Sweden) will be the world's most powerful accelerator-based neutron source for groundbreaking science. The ESS accelerator will deliver 2.86 ms long proton pulses, at a repetition rate of 14 Hz with a proton current of 62.5 mA. The high current of protons in the [0.075, 2000] MeV range poses two main challenges: the beam power density and the radiation induced activation. Therefore, radiation transport simulations are necessary to compute the operational limits (for avoiding structural failures, melted components and quenches of superconducting sections), to map residual dose rates and to provide radionuclide inventories. In the past, radiation transport simulations of the ESS accelerator were performed with MCNPX [2], PHITS [3] and FLUKA [4]. In all cases, an extensive amount of time had to be invested to simplify CAD models and manually implement complex linac models. This paper presents for the first time the simulations of the ESS linac with Attila4MC [5], demonstrating the efficiency, versatility and accuracy of Attila4MC to speed up the simulation workflow, simulate linac components as-built and swiftly visualize computational meshes as well as the results directly on top of complex CAD models.

## Attila4MC TO DEFINE THE OPERATIONAL LIMITS OF BEAM-INTERCEPTIVE DEVICES

Beam-interceptive devices in the ESS linac have to safely absorb and dissipate the high power of the ESS proton beam [6]. For example, the ESS MEBT Faraday cup [7] has to stop 3.6 MeV protons and measure the proton current (up to 62.5 mA). The most demanding beam modes are: the Fast Tuning (5 µs, 14 Hz) and the Slow Tuning (50 µs, 1 Hz). Besides the shallow Bragg peak of 3.6 MeV protons, the beam is typically Gaussian with $\sigma_x$ and $\sigma_y$ usually smaller than 5 mm. The key component of the ESS MEBT Faraday cup is its graphite collector that fully stops the proton beam.

No temperature sensor was integrated, because it would not quickly provide protection capabilities nor temperature measurements within the pulse duration. In addition, during the linac commissioning it was not possible to measure the actual size of the proton beam. Therefore, MCNP simulations coupled with thermomechanical calculations in ANSYS [8] were performed to foresee the operational limits. Attila4MC was the only software capable of computing the beam power density within the actual indented geometry, which could not be defined by means of the standard MCNP surfaces and macrobodies.

The Attila4MC results are swiftly visualized in 3D (see Fig. 1), with Tecplot [9], without the need to develop dedicated scripts for each different beam-interceptive device. The Attila4MC workflow for quantifying the beam power density starts by importing the CAD model in the Parasolid format (.x_t) into Attila4MC via ANSYS SpaceClaim [10]. The Unstructured Mesh (UM) is defined on top of the actual geometry of the ESS MEBT Faraday cup. The mesh is composed of first order tetrahedral elements, including 157589 node points and 736542 cells. The MCNP6.2 [11] input file (including materials, cross-sections, region attributes, MCNP controls and importances) is prepared via the GUI of Attila4MC. Protons, neutrons, electrons and photons are

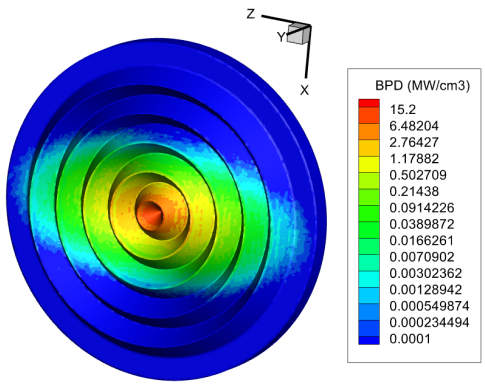



Figure 1: Beam Power Density (BPD) computed with Attila4MC within the graphite collector of the ESS MEBT Faraday cup. The collector has a radius of 29 mm and thickness of 8 mm. The 3.6 MeV protons beam is Gaussian with $\sigma_x$ = 3 mm and $\sigma_z$ = 5 mm; the proton current is 62.5 mA.

* elena.donegani@ess.eu

Content from this work may be used under the terms of the CC BY 4.0 licence (© 2025). Any distribution of this work must maintain attribution to the author(s), title of the work, publisher, and DOI.

ISBN: 978-3-95450-262-2 ISSN: 2673-5350 doi: 10.18429/JACoW-IBIC2025-MOPMO08

# DEVELOPMENT AND CHARACTERIZATION OF A RADIATION-TOLERANT POWER SUPPLY FOR BEAM INSTRUMENTATION

W. Viganò*, E. Effinger, J. M. Meyer, S. Michelis, C. Zamantzas,
CERN, Geneva, Switzerland

*Abstract*

CERN's Beam Instrumentation Group is developing a mini-crate to host the future Beam Loss Monitor (BLM) and Beam Positioning Monitor (BPM) systems acquisition electronics at HL-LHC and SPS accelerators. For this purpose, a new power supply has been designed to meet the low noise requirements, high reliability, and availability standards for these harsh radioactive environments. This design makes use of CERN-developed ASICs and radiation-tolerant qualified COTS and follows a modular architecture for quick interventions and safe handling. The paper presents the design, prototype characterisation results, identified issues, and mitigation methods to achieve the required radiation tolerance.

## INTRODUCTION

CERN's Large Hadron Collider (LHC) Beam Loss Monitoring system [1-3] is a critical system for the protection of the particle accelerator and is extensively used to optimise and crosscheck several other instruments and beam processes. An upgrade of the electronics stack is planned for the Hi-Lumi project's changes in the Inner Triplet areas of IP1 & 5 and at the complete SPS ring during the Long Shutdown (LS3). Once the performance of the new electronics is validated at those regions, the same system will be installed also in the LHC accelerator during LS4 for monitoring a total of about 4000 ionisation chamber type detectors.

Given the system's scale in terms of electronics and detectors, it is essential to design a tunnel acquisition mini-crate capable of withstanding radiation doses up to 1 kGy. The crate must reliably supply low-noise power to the sensitive front-end analogue circuits while remaining resilient to short circuits and robust to enable all types of interventions.

## MINI-CRATE DESIGN

To meet the requirements mentioned before, it was decided to choose an architecture in which the voltage conversion takes place by means of two independent modules: Input Power Unit (BLEIPU) and Power Supply Unit (BLEPSU). The BLEIPU is used to transform the 230 VAC input into different AC voltage buses that are filtered, monitored, protected, and finally sent to the BLEPSU via a passive backplane. Then the BLEPSU is used to produce different DC voltages needed by the acquisition electronics. The voltage buses provided are as follows: +5 VDC; -5 VDC; +2.5 VDC and +1.2 VDC, where the +5 VDC; -5 VDC are dedicated to supplying the "analogue" circuitry, while the +2.5 VDC and +1.2 VDC supply the "digital" circuitry of the acquisition board. In addition, the BLEPSU also includes the 1500 VDC detector bias voltage conversion function, supplied by the surface rack to the whole detectors chain, to adapt such voltage to a level compatible with the monitoring function, which is mandatory to ensure the reliability of the entire detector installation.

All voltages present on the backplane are monitored by a control unit (BLEACCM) which offers the possibility of remotely restarting both the 'analogue' and 'digital' power buses. Also available through a front panel connector is the possibility to plug a diagnostic tool module.

The architecture maintains full backwards compatibility with the current LHC system electronics, so parts could be swapped, which is the preferred approach to upgrade an existing system classified with Safety and Integrity Level 3 (SIL3), and to provide high flexibility during the development and testing phases.

Figure 1 shows the prototype of the mini-crate where the BLEIPU and BLEPSU modules are tested with the current BLM electronics installed at the LHC.



Figure 1: Mini-crate overview.

### *Input Power Unit (BLEIPU)*

The BLEIPU core component is a custom toroidal transformer, with a diameter of 83 mm and a height of 50 mm which delivers a global output power of about 90 Watts. The output stage consists of three independent windings (WDG) which are distributed as summarised in Table 1.

Table 1: Winding Outputs

| WDG | Output Voltage | Output Current |
|---|---|---|
| 1 | 8.0 V | 7.87 A |
| 2 | 8.0 V | 2.00 A |
| 3 | 9.3 V | 1.39 A |

Materials chosen for radiation resistance and compatibility with the CERN facility installations are Steel Tape for the core, PET film (mylar A) for the insulation layers, and braided fiberglass coated with a modified polyvinyl chloride resin for the sleeve.

*William.vigano@cern.ch

Content from this work may be used under the terms of the CC BY 4.0 licence (© 2025). Any distribution of this work must maintain attribution to the author(s), title of the work, publisher, and DOI.

ISBN: 978-3-95450-262-2 ISSN: 2673-5350 doi: 10.18429/JACoW-IBIC2025-MOPMO09

# ROBOTIC SOLUTION FOR BLM DETECTOR MAINTENANCE IN HIGH RADIATION AREAS

W. Viganò*, M. Di Castro, S. Di Giovannantonio, E. Effinger, F. Sanda, J. Piehl, M. Sta, C. Zamantzas, CERN, Geneva, Switzerland

*Abstract*

CERN's Beam Loss Monitoring (BLM) system is essential for the protection of machine elements against energy deposition due to beam losses. The protection function relies on approximately 5000 ionisation chamber type detectors installed along all of CERN's accelerators. Some of the areas where the detectors are installed have a high background dose (above 2 mSv/h). Installation and maintenance times must be minimised to ensure personnel safety. For this reason, a new solution was designed that allows the manipulation of detectors and their supports by robotic action. Every aspect of the solution has been designed to reduce intervention time, using a rapid locking mechanism and the possibility of transporting the material by robot. The paper presents the design, prototype characterisation results, identified issues, and mitigation methods developed for the automated manipulation of these detectors.

## INTRODUCTION

At the CERN Accelerator Complex, machine protection and optimization are critically dependent on the Beam Loss Monitoring (BLM) systems [1]. These systems are essential for providing continuous and highly reliable loss measurement histories, capturing data with a dynamic range spanning up to ten orders of magnitude at microsecond-level resolution [2, 3]. This capability is vital for ensuring the safe and efficient operation of the accelerator. The standard BLM detectors, which are based on ionisation chambers, are connected using coaxial bayonet connectors. While effective, the manual connection and disconnection of these components expose personnel to significant risks. The time required for tasks like installation, testing, and maintenance directly increases personnel radiation exposure. To mitigate this occupational hazard, a more efficient and safer solution is needed for a rapid installation system for the stand itself, as well as the detector and interconnections.

CERN has developed an extensive robotic service to support maintenance and inspection tasks in hazardous environments across its accelerator complex [4, 5]. Over the past decade, several robotic platforms, such as the CERN-Bot, the Train Inspection Monorail, and various robotic tool changers, have been developed to serve operational needs. The present work builds upon this experience by creating a dedicated mechanical interface compatible with robotic manipulation for BLM detector interventions.

The BLM support and detector, designed for robotic transport and installation, must also allow manual installation in at least ten times less time, i.e. in a couple of minutes, compared to the traditional solution in which detectors, equipped with bayonet connectors, fixed to a pole and anchored to the floor require. To design the new solution to be compatible with both robotic and manual handling, several key requirements were defined such as: the support must fix to an independent ground-anchored base installed during long shutdowns; the support pole must be lightweight, i.e. < 5 kg, to allow use of a smaller and more accessible robot; the interconnection between the detector and the harness must be simple and reliable; and the system must use high radiation resistant material, including those for connector isolation.

## DESIGN OF THE BLM SUPPORT AND THE DETECTOR ASSEMBLY

The elements that make up the BLM support and the detector assembly are shown in Fig. 1 (left). Once the ground-anchored base is in place, the robot can transport the support pole together with the sliding cylinder, the electrical insulator, the detector guide and the electromechanical interconnection cup with the interconnection cables. The latter consist of special high-radiation resistant coaxial cables designed for use in highly radiative areas of CERN. The total weight of the holder assembly with everything needed for the interconnection of the BLM detector is less than 5 kg. The BLM detector, highlighted in yellow in Fig. 1, also complies with the under 5 kg rule. The solution presented consists of three independent assemblies: a base anchored to the ground, a complete stand, and a detector.

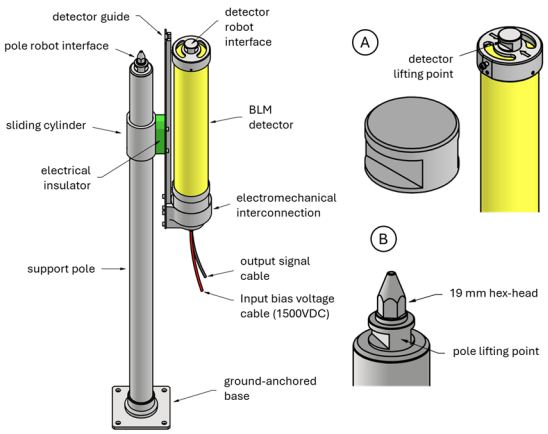



Figure 1: BLM support (left), Lifting points for the detector assembly and support pole (right).

* william.vigano@cern.ch

Content from this work may be used under the terms of the CC BY 4.0 licence (© 2025). Any distribution of this work must maintain attribution to the author(s), title of the work, publisher, and DOI.

ISBN: 978-3-95450-262-2 ISSN: 2673-5350 doi: 10.18429/JACoW-IBIC2025-MOPMO10

# PERFORMANCE OF THE CRYOGENIC BEAM LOSS MONITORS DEVELOPED AT THE LHC

E. Effinger*, J. M. Meyer, S. Morales Vigo, B. Salvachua, J. Storey, C. Zamantzas
CERN, Geneva, Switzerland
E. Griesmayer, CIVIDEC, Vienna, Austria

*Abstract*

Several systems protect the superconducting magnets of the Large Hadron Collider (LHC), which operate at −271.3 °C. The Beam Loss Monitoring (BLM) system is critical for detecting lost particles around the machine and reacting on their quantity and associated energy. It protects the machine from quenching and irreversible damage. To measure these losses, various detectors are used, primarily Ionisation Chambers (IC), but also other types of monitor depending on the intensity loss or time structure that needs to be detected. As an example, in injection and extraction areas, fast poly-crystalline Chemical Vapour Deposition (pCVD) diamond detectors measure time structured losses. To increase sensitivity, a new detector, the Cryogenic Beam Loss Monitor (CryoBLM), based on single-crystalline diamond (sCVD), was developed. It is mounted inside the cryostat between two superconducting magnets in the vicinity of the beam pipes and operates at cryogenic temperatures. Two CryoBLM locations in the LHC target different loss scenarios: betatron halo cleaning and luminosity losses from the CMS physics debris. This contribution presents the CryoBLM performance and comparisons with the ionisation chambers.

## DETECTOR TYPES AND DESCRIPTION

Beam losses along the CERN accelerator complex are monitored with a distributed system with close to 4 500 ionisation chambers (IC) connected and read out by different electronics depending on the accelerator. The most widely used detector is the LHC-type IC [1] shown in Fig. 1. It is a 60 cm-long ionisation chamber filled with $N_2$ gas at 1.1 bar with 61 electrodes spaced every 5 mm.

Despite the differences, all the readout electronics have common design choices; they are based on the usage of integrator input circuits [2–4] with high dynamic range of around 120 dB. The time resolution of the different systems depends on the integration window of the used electronics, which is typically 2 µs, 10 µs or 40 µs.

However, in some areas and applications, it is necessary to measure losses with either higher time resolution down to the order of tens of nanoseconds or higher sensitivity. In this case, pCVD and sCVD diamond detectors (see Fig. 2) are used. They are read out with fast Analog-to-Digital Converters (ADCs) with a sampling rate up to 650 MHz. This is the configuration used in the LHC injection and collimation regions. However, in other areas, such as the LHC dispersion suppressor region, there is the need to measure very small losses. For this purpose, the CryoBLM system was developed. The system operates at cryogenic temperatures and can be installed inside the magnet cryostats, closer to the beam pipe, thereby enhancing sensitivity. The CryoBLM is based on the sCVD diamond which provides superior energy resolution and charge collection efficiency compared to the pCVD [6].

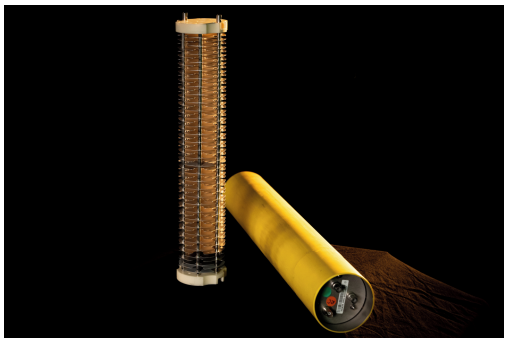


Figure 1: LHC type IC [5].

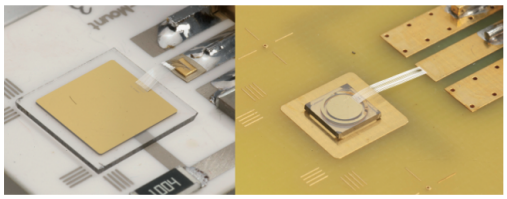


Figure 2: pCVD and sCVD Diamond Detector [7].

## CryoBLM DESIGN AND INSTALLATION

The installation of these detectors inside the magnet cryostat restricts the choice of used materials, since they operate at a cryogenic temperature of around −271.3 °C in vacuum. The carrier Printed Circuit Board (PCB), made of ceramic ($Al_2O_3$), connects and encloses the sCVD substrate. The detectors themselves are fixed with a support on the cryostat between two superconducting magnets, see Fig. 3. Two CryoBLM prototypes were installed in the LHC Cell 9L5 in IP5, colliding point of the Compact Muon Solenoid (CMS) detector, and in Cell 9R7 in IP7, main betatron collimation region. These detectors are read out with standard LHC BLM front-end electronics, publishing data at 1 Hz for 12 different integration windows, so-called running sums (RS). More details about the complete installation can be found in [8].

In order to validate the performance and calibration of the diamond-type detectors, a sCVD and a pCVD diamond

* ewald.effinger@cern.ch

Content from this work may be used under the terms of the CC BY 4.0 licence (© 2025). Any distribution of this work must maintain attribution to the author(s), title of the work, publisher, and DOI.

ISBN: 978-3-95450-262-2 ISSN: 2673-5350 doi: 10.18429/JACoW-IBIC2025-MOPMO11

# MACHINE VISION CAMERAS FOR BEAM SPOT ANALYSIS

M. A. Bree*, T. D. Batten, W. Javed
Canadian Light Source, Saskatoon, Canada

*Abstract*

In 2020, the Canadian Light Source (CLS) began a project to replace all beam diagnostic analogue cameras with digital ones. Over time, this project has expanded to include beam analysis capabilities. We present an EPICS-based imaging system that uses inexpensive Machine Vision (MV) cameras. The system computes beam parameters including intensity, centroid, ellipticity, eccentricity, orientation, and more.

## INTRODUCTION

The Canadian Light Source is a third generation synchrotron that supports 22 operational beamlines [1]. When the CLS was commissioned in 2005, analogue video cameras were used for beam diagnostics and analysis at various locations. The limitations of these cameras include:

- no (or minimal) remote control,
- no external triggering (they are free running),
- poor image quality (the analogue images need to be digitized to perform any kind of quantitative analysis).

Advances in digital sensor technology have rendered analogue cameras obsolete. Digital cameras now dominate all areas of imaging, including consumer, military, scientific, and industrial applications. In particular, Machine Vision (MV) cameras are a class of camera tailored for industrial applications [2].

The CLS has invested in commercial solutions, such as those from BeamGage [3], for beam spot analysis at select locations. However, these systems are expensive and require integration into our EPICS [4] control system.

In 2020 a project was initiated at the CLS to add inexpensive MV cameras to our instrumentation toolkit. The goals of this project have expanded to include:

- creation of a scalable infrastructure to support an arbitrary number of MV cameras,
- replacing obsolete analogue cameras and associated infrastructure (cables, CRTs, etc.) with MV ones,
- adding cameras to previously unmonitored locations,
- adding quantitative beam spot analysis capabilities (similar to those provided by BeamGage), and
- replacing expensive commercial systems such as BeamGage.

### *Machine Vision Cameras*

Machine Vision is a general term used to describe cameras designed for industrial and automation applications. MV camera features include:

- small and robust construction; fanless,
- simple cabling requirements,
- external triggering,
- access to raw data (i.e., no lossy compression),
- standardized Application Programming Interface (API) support,
- global shutter across all pixels.

The CLS has chosen the **BFS-PGE-16S2M-CS** (`1440 X 1080`, 78 FPS) from Teledyne FLIR [5] for the majority of the cameras in the MV system. This camera is GigE Power over Ethernet (PoE), which means that a single Ethernet cable to a 1 Gigabit/s switch port that supports PoE provides both data and power. The cameras use monochrome CMOS sensors and ADCs that support 8, 10 or 12 bits per pixel. In addition, the cameras support the **GigE Vision 1.2** and **GenICam** standards [6, 7]. Therefore, with the available vendor-supplied software development kit (SDK), these cameras are supported by EPICS **areaDetector** [8].

## SYSTEM ARCHITECTURE

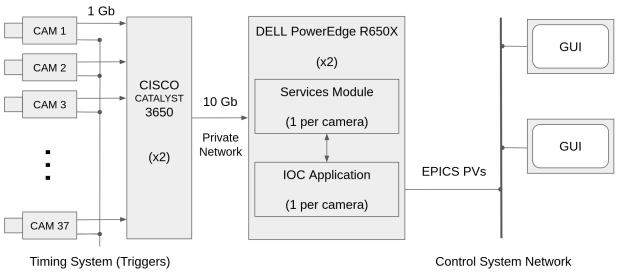



Figure 1: MV camera system architecture.

The system architecture, illustrated in Fig. 1, is very simple. The cameras are connected to the CLS timing system [9] for external triggering. They are connected to 1 Gb ports on two Cisco Catalyst 3650 switches for data and power. The switches are connected via 10 Gb copper links to two Dell EMC PowerEdge R650XS servers running the Debian 12 operating system. The servers are equipped with Intel 82599 10 Gb Ethernet Controller cards, single Xeon 4309Y CPUs, and 32 Gb of memory.

### *Data Rates and Hardware Requirements*

Consider the **BFS-PGE-16S2M-CS** 1440 x 1080 pixel camera. At 12 bits per pixel, 2,332,800 bytes are generated per image (the data is transmitted using 3 bytes per 2 pixels) and the maximum acquisition rate is 43 images per second.

A system with one 10 Gb switch has been stress tested at approximately 600 Mb/s (i.e., 60% capacity) which corresponds to approximately 260 images[1] per second. Above

* michael.bree@lightsource.ca

[1] 1440 x 1080 pixels, 12 bits per pixel, 2,332,800 bytes per image.

Content from this work may be used under the terms of the CC BY 4.0 licence (© 2025). Any distribution of this work must maintain attribution to the author(s), title of the work, publisher, and DOI.

ISBN: 978-3-95450-262-2 ISSN: 2673-5350 doi: 10.18429/JACoW-IBIC2025-MOPMO12

# OPTIMIZATION OF BEAM INTENSITY MEASUREMENT SYSTEM OF HIPA AT PSI

J. L. Sun†, P. Huber, W. Koprek, P. A. Duperrex, Paul Scherrer Institut, Villigen PSI, Switzerland

*Abstract*

Beam intensity measurement of High Intensity Proton Accelerator (HIPA) at PSI mainly consists of several passive cavity type monitors and corresponding electronics. New VME electronics were designed to replace the old CAMAC ones. The VME system is suffering significant temperature-dependent drift, leading to an inaccurate measurement. Many compensation schemes were considered to address this issue and eventually achieving a temperature coefficient 166 ppm/degree for RF test signal. Furthermore, the new electronics incorporate a phase measurement of the 50.6 MHz proton bunches for beam energy monitoring, which greatly facilitates the commissioning and status monitoring of the accelerator.

## INTRODUCTION

The HIPA can generate up to 1.4 MW continuous proton beam. The proton beam is accelerated from a Cockcroft-Walton source followed by two cyclotrons: the so-called Injector 2 cyclotron accelerating the beam from 870 keV to 72 MeV and the so-called Ring cyclotron further accelerating to 590 MeV [1].

The beam intensity measurement system of HIPA consists of many beam current monitors mounted on the different beam transport line for beam current measurement and transmission calculation, the overall layout can be found in Fig. 1.

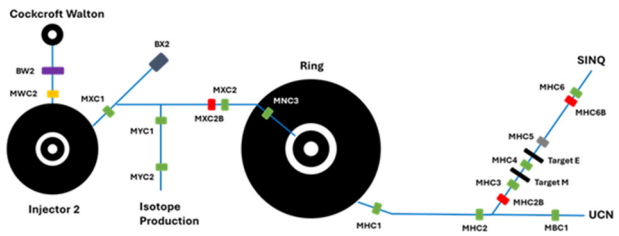



Figure 1: Layout of the beam current monitors of HIPA.

MWC2 located in front of Injector2 is measuring the DC 870 keV proton beam coming from the Cockcroft Walton ion source. MXC1/2 and MNC3 are located in the beam line from Injector2 to Ring and MYC1/2 in the Isotope Production line for the 72 MeV/50.63 MHz CW beam current measurement. MHC1-6 and MBC1 are mounted after the Ring for high energy (590 MeV) beam current measurement.

There are also 3 Bergoz current monitors, which measure the current in absolute way, running as a reference for the other beam current monitors. Beside the Bergoz monitor, beam dump e.g., BX2 can also provide the absolute beam intensity value for calibration.

† jilei.sun@psi.ch

For most beam intensity monitors of HIPA (Green icon). The measurement principle is based on the use of a coaxial resonator (reentrant cavity) [2], which can be tuned to a specific resonance frequency by modifying the dimension of the capacitance gap and the inductance wall, see Fig. 2 (left). A wall current with the same time structure as the beam will be induced when the proton beam passing through the cavity. The amplitude of the magnetic field, shown in Fig. 2 (right), in the resonator is directly proportional to the beam current, a measurement of this field provides a measure of the proton beam current.

The resonator is tuned to the 2nd harmonic (101.26 MHz) of the proton beam pulse frequency. This frequency is used because of the better signal-to-noise ratio, the RF disturbance components being mainly at the odd harmonics.

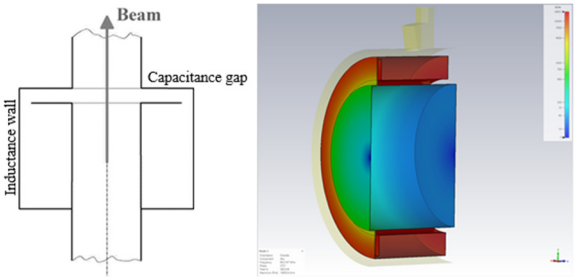



Figure 2: Measurement principle of the cavity type monitor (left); Magnetic field distribution in the cavity (right).

The signal from the monitor is brought to the electronics by using low-loss 50 Ohm cables, with lengths between 50 and 250 m. The output is further used for the transmission calculation and interlock generation when the current value is above a given limit.

## DIGITAL SYSTEM DESIGN

The old CAMAC based electronics have been served for decades. A new VME based version has been developed to replace the CAMAC. The core of the new system is digital electronics based on a VME card IFC1210 from Ioxos company as presented in Fig. 3.

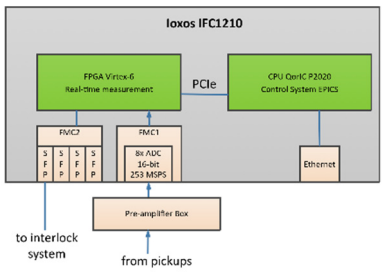



Figure 3: Block diagram of the digital electronics.

Content from this work may be used under the terms of the CC BY 4.0 licence (© 2025). Any distribution of this work must maintain attribution to the author(s), title of the work, publisher, and DOI.

ISBN: 978-3-95450-262-2 ISSN: 2673-5350 doi: 10.18429/JACoW-IBIC2025-MOPMO13

# INTELLIGENT RETRIEVAL SYSTEMS FOR ACCELERATOR PHYSICS: MATCHING RETRIEVAL APPROACHES TO USE CASES

R. Ischebeck*, M. Sapinski, L. Stuhlmann,
PSI Center for Accelerator Science and Engineering, Villigen, Switzerland
Q. Dai, University of Zurich, Zurich, Switzerland

*Abstract*

Accelerator facilities generate diverse documentation, from technical reports to structured wikis and semi-structured logbooks, which complicates efficient knowledge access. While Retrieval-Augmented Generation (RAG) offers a path toward intelligent operator assistants, no single method is universally optimal. We present three use cases from PSI: for technical documentation, naive dense retrieval with summarization provides fast and interpretable access; for the AcceleratorWiki, a graph-augmented approach improves reasoning over hierarchies and cross-references; and for ELOG, an agentic pipeline with specialized agents supports multimodal interpretation, temporal reasoning, and iterative refinement. Together, these case studies illustrate how matching retrieval paradigms to data types enables reliable, context-aware assistance in accelerator operations.

## INTRODUCTION

Large Language Models (LLMs) have demonstrated impressive performance across a broad array of tasks, including question answering, code generation and debugging, multilingual translation or summarization. Yet, they often suffer from factual errors, limited domain coverage, and poor verifiability. A key issue is hallucination [1], where models generate plausible but incorrect statements due to their probabilistic nature. In scientific and technical contexts, such errors are particularly problematic, as they can result in misleading or harmful conclusions. To address these challenges, Retrieval-Augmented Generation (RAG), proposed by [2], enhances LLM outputs by incorporating external knowledge at inference time, retrieving relevant documents from trusted sources to improve accuracy, reliability, and transparency.

In a standard RAG system, as shown in Fig. 1, a retriever first selects relevant passages from a document collection, which are then provided to the LLM to ground its response. This mechanism reduces hallucinations, allows answers to be verified against the source material, and enables integration of continuously updated information.

Recent surveys highlight the rapid evolution of RAG, open challenges such as retrieval efficiency, hybrid retrievers, and multimodal integration, and the importance of tailoring the pipeline to the target domain [3]. In this work, we extend these ideas to accelerator physics, showing that different documentation sources—technical reports, internal wikis, and logbooks—require distinct retrieval paradigms. Through three case studies, we illustrate when naive dense retrieval suffices, when lightweight knowledge graphs add value, and when agentic RAG pipelines become necessary for complex scenarios. Furthermore, all systems described in this work are powered by locally deployed LLMs, ensuring data privacy, reducing latency, and avoiding reliance on external APIs.

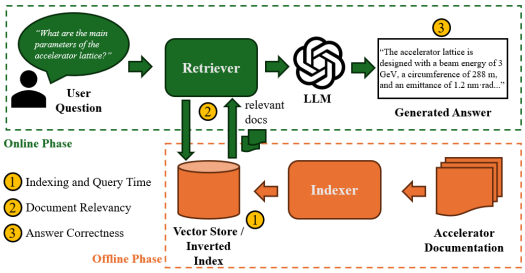



Figure 1: Example naive RAG pipeline [4].

## RELATED WORK

Efficient access to accelerator documentation and electronic logbooks (eLogs) has long been a challenge due to their heterogeneous and often unstructured content. Recent work has explored AI-driven solutions to enhance information retrieval in these contexts. Sulc et al. proposed AI pipelines for accelerator logbooks, highlighting opportunities for hybrid retrieval and multimodal analysis across facilities such as Fermilab, Jefferson Lab, and SLAC [5, 6]. Complementary approaches have introduced general AI assistants for accelerator operations, combining RAG with reasoning and action frameworks to interface directly with control systems [7].

Together, these studies underline the importance of tailoring retrieval pipelines to accelerator-specific contexts. Building on these insights, our work investigates when naive dense retrieval suffices, when knowledge-graph-enhanced pipelines are advantageous, and when agentic multimodal RAG becomes necessary.

## USE CASES AT PSI

### *Technical Documentations*

The High Intensity Proton Accelerator (HIPA) at PSI was built over 50 years ago, at a time when digital documentation was largely absent [8]. Over decades of experiments and continuous development, the facility has grown significantly, but without a consistent long-term record. As a result, any new specialist taking over a system typically requires several years to reach expert-level performance. To address this

* rasmus.ischebeck@psi.ch

Content from this work may be used under the terms of the CC BY 4.0 licence (© 2025). Any distribution of this work must maintain attribution to the author(s), title of the work, publisher, and DOI.

ISBN: 978-3-95450-262-2 ISSN: 2673-5350 doi: 10.18429/JACoW-IBIC2025-MOPMO14

# DEVELOPMENT OF A FARADAY CUP FOR THE FETS-FFA

S. Sapkota*, University of Portsmouth, Portsmouth, UK
D. W. Posthuma de Boer†, E. Yamakawa, ISIS Neutron and Muon Source, RAL, Harwell, UK

Content from this work may be used under the terms of the CC BY 4.0 licence (© 2025). Any distribution of this work must maintain attribution to the author(s), title of the work, publisher, and DOI.

*Abstract*

The proposed FETS-FFA would exhibit high-intensity operation of a Fixed-Field Alternating Gradient (FFA) accelerator, as a demonstrator for a spallation neutron source driver. Faraday cups are planned to be installed in the injection straight to investigate injection efficiency and infer beam-position during early commissioning stages; and in the extraction line to inspect extraction efficiency. The chosen Faraday cup design must be suitable for the 3 - 12 MeV proton energy range, the average beam power of the FETS Linac and the FETS-FFA's extracted beam.

Thermal aspects of this design will be introduced, including cooling water flow-rate calculations and an approximate method of simulating this flow with equivalent convective cooling. The 3D tracking for a secondary electron suppressor will also be presented, as well as calculations to estimate the required suppression voltage.

## INTRODUCTION

ISIS-II is a proposed MW-class pulsed neutron and muon source currently in the design phase, with three options being considered for its driving accelerator: a Rapid Cycling Synchrotron (RCS), a high-energy linear accelerator with an accumulator ring (AR), and a Fixed-Field Alternating Gradient (FFA) accelerator [1]. RCS and AR machines have already demonstrated MW operations [2, 3], but the FFA option has not. The FETS-FFA (Front End Test Stand - FFA), has therefore been proposed to demonstrate aspects of high-intensity operation of an FFA, using its beams of 3-12 MeV protons [4].

As with the RCS and AR options, charge-exchange injection will be used to inject a beam of $H^-$ ions into the FFA ring through a stripper foil. A Faraday cup (FC) has been proposed to measure injection efficiency and align the beam during commissioning. A second FC in the extraction line has also been proposed to measure extraction efficiency. The feasibility of producing a FC that is suitable for both the injected and extracted beams will be studied in this paper.

This study has focused on two challenging aspects of FC design: managing the heat load imparted by the incident proton beam, and emission of low-energy secondary electrons which can cause systematic measurement errors.

## MATERIAL AND GEOMETRY

Copper has been chosen for the FETS-FFA FC, because of its good thermal and electrical properties (see Table 1), as well as its relatively low secondary electron yield (SEY) [5]. A schematic of the cross-sectional view of the FC's geometry is shown in Fig. 1. A conical cutout has been adopted to reduce secondary electron emission (SEE) [7] and to spread heat load over a larger volume. The copper will have a minimum thickness of 5 mm, which was found from SRIM simulations [8] to prevent almost all 12 MeV protons from penetrating through the cup.

Table 1: Copper Properties Close to Room Temperature [6]

| | |
|---|---|
| Thermal Conductivity [W/cm/K] | 4.01 |
| Electrical Resistivity [$10^{-8}$ Ωm] | 1.725 |
| Specific heat capacity [J/g/K] | 0.385 |
| Melting point [°C] | 1084.62 |

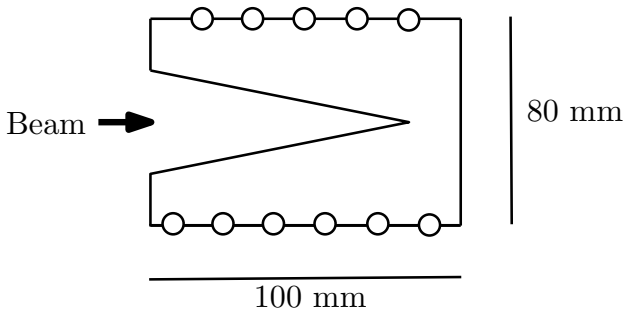



Figure 1: Schematic cross-section of the FC model, with the beam directed into a conical cutout. Circles represent pipes for cooling water wrapped around the outer cylinder.

## THERMAL ANALYSIS

The maximum instantaneous temperature rise of the FC due to thermal load imparted by the beam was calculated, as well as its steady-state temperature. The latter of these was found using the steady-state thermal simulation of ANSYS Mechanical (2024 R2 version) [9].

### *Instantaneous Temperature Rise*

The real-space transverse distribution of the FETS beam was assumed to be a round, 2D Gaussian with $\sigma_x = \sigma_y$ = 1.5 mm. The peak energy density was estimated using the product of maximum protons density for a single injected pulse (i.e. $2.12 \times 10^{10}$ protons/mm$^2$) and peak stopping power per ion (dE/dx/ion) obtained from SRIM. The temperature rise due to a single injected pulse inside the FC was calculated using

$$\Delta T = \frac{E'}{\rho c}, \tag{1}$$

with $E'$ as highest energy density, $\rho$ being material density and $c$ as the specific heat capacity. The calculated temperature rises, listed in Table 2, suggest that if the diffusion

* up2134915@myport.ac.uk
† david.posthuma-de-boer@stfc.ac.uk

ISBN: 978-3-95450-262-2 ISSN: 2673-5350 doi: 10.18429/JACoW-IBIC2025-MOPMO15

# BEAM INSTRUMENTATION FOR THE NEW LINEAR ACCELERATOR AT THE CANADIAN LIGHT SOURCE

T. D. Batten*, M. A. Bree, I. Kolmakov, E. Nebot del Busto, C. L. Randall, S. Saadat
Canadian Light Source, Saskatoon, Canada

*Abstract*

The linear accelerator (LINAC) at the Canadian Light Source (CLS) serves as the injector for the 2.9 GeV synchrotron. The original 2856 MHz LINAC, which made use of components installed in the 1960s, was replaced in 2024 with a new 3000.24 MHz LINAC which was designed and built by RI Research Instruments GmbH. This upgrade has reinforced the importance of having the right diagnostic equipment in place to support visualization and analysis.

## OVERVIEW

The new LINAC is made up of a 90 kV-thermionic-source, a 500.04 MHz sub harmonic prebunching cavity (SPB), a 3 GHz single cell cavity acting as a Pre Buncher (PBU), a 3 GHz 14 cell traveling wave structure acting as the Final Buncher (FBU), three 3000.24 MHz 158 cell, 5 m long accelerating structures (ACC1/2/3) and a SLED pulse compression system to accelerate electrons up to 250 MeV.

Early in the project, diagnostic equipment was sacrificed as a result of budgetary constraints. The destructive diagnostic equipment incorporated in the final design included one faraday cup (FC) and five optical monitors (OM). The non-destructive diagnostic equipment included one beam position monitor (BPM), one wall current monitor (WCM) and one integrating current transformer (ICT). Shortly before installation additional non-destructive diagnostic equipment from the original CLS LINAC, was integrated into the new RI LINAC by the CLS, as shown in Fig. 1.

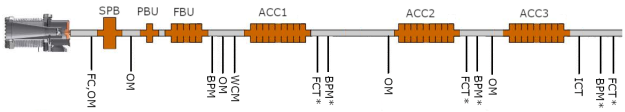



Figure 1: LINAC diagnostic equipment (where * identifies equipment integrated into the design by the CLS).

During RF conditioning additional directional couplers and microphones were added to provide insight into the location of RF breakdowns.

## BEAM INSTRUMENTATION

### *Faraday Cup*

A faraday cup was installed on a linear feed through with an optical monitor at the exit of the electron source. The FC is connected to an oscilloscope, has a bandwidth of 3.5 GHz, and is used to measure beam properties like bunch charge and time structure. It was also used to perform dark current scans to ensure proper operation of the electron source.

* tonia.batten@lightsource.ca

### *Optical Monitors*

The optical monitors consist of a YAG:Ce crystal plate, 30 mm in diameter, installed on a black plate engraved with cross hairs, mounted on a linear feed through. When intercepting the beam the YAG fluoresces and the image produced is digitized using a FLIR GigE machine vision camera. This system supports visualization of the transverse profile of the beam at various locations, the camera system also analyzes the image to compute beam parameters [1], including intensity, centroid, ellipticity, eccentricity, orientation, and more. The camera system has also been used for stability and emittance measurements.

### *Wall Current Monitor*

A wall current monitor was installed before the first accelerating section. It has a bandwidth of 2 GHz which allows analysis of the time structure of the 500 MHz bunched beam. This equipment was calibrated against the ICT, to support non-destructive beam current measurements.

### *Beam Position Monitors*

One button BPM was incorporated in the original RI LINAC design. This BPM was installed right after the bunchers. Three cavity BPMs were installed by the CLS, one downstream of each accelerating section, with the intention of eventually using this equipment to automate LINAC setup and steering. The BPMs are monitored using Instrumentation Technology Libera Spark EL units [2]. Instrumentation Technologies DWP-SP down-converters with a 2.5 GHz local oscillator [3], have also been installed, because the Libera Spark EL units are sensitive to the 500 MHz component of the BPM signals.

### *Fast Current Transformers*

Fast current transformers (FCT) were integrated into the new LINAC by the CLS. One FCT was installed downstream of each accelerating section, this equipment does not have enough bandwidth to fully resolve the 3 GHz RF structure of the beam, but does enable additional non-destructive current and charge measurements. The signals are being monitored by Pico Technology oscilloscopes [4]. The 500 MHz bunching of the beam can clearly be resolved on an oscilloscope and the 3 GHz RF structure appears as ripples on the 500 MHz bunches.

### *Integrating Current Transformer*

A Bergoz in-flange integrating current transformer [5] was installed downstream of ACC3. This signal is digitized using a struck SIS3316 Channel VME Digitizer [6]. The

Content from this work may be used under the terms of the CC BY 4.0 licence (© 2025). Any distribution of this work must maintain attribution to the author(s), title of the work, publisher, and DOI.

ISBN: 978-3-95450-262-2 ISSN: 2673-5350 doi: 10.18429/JACoW-IBIC2025-MOPMO16

# JOINT ANALYSIS OF BEAM LOSS AND BEAM POSITION DURING THE INJECTION PROCESS AT HEFEI LIGHT SOURCE

Y. Z. Xiao[1], Y. H. Liu[1], Y. B. Leng[†,1,2]
[1]SNST, University of Science and Technology of China, Hefei, P. R. China
[2]NSRL, University of Science and Technology of China, Hefei, P. R. China

*Abstract*

The Hefei Light Source is a synchrotron radiation facility operating in the vacuum ultraviolet and soft X-ray regions. If the evolution of beam parameters and beam loss during the injection transient process can be observed synchronously, analyzing their correlation can provide more quantitative guidance for further optimizing the injection process. To achieve this goal, a monitoring system capable of synchronously capturing the 3D position of each bunch and rapid beam loss has been established at the Hefei Light Source. Experiments investigated both TOP-UP injection and empty-ring injection processes. Thanks to the unique multi-parameter synchronous diagnosis capability of this system, some previously unnoticed special phenomena have been captured, and a deeper analysis of the correlation between bunch parameters can be conducted. TOP-UP mode exhibited maximum beam loss in the injected bunch, with secondary losses at the 14th subsequent bunch. Peak beam loss occurred immediately after injection in both modes, followed by rapid attenuation within several turns. Loss resurgence appeared after ~85 turns (TOP-UP) or 180 turns (empty ring), followed by oscillatory decay.

## INTRODUCTION

Hefei Light Source (HLS), completed and operational in April 1989, is a dedicated vacuum ultraviolet (VUV) and soft X-ray synchrotron radiation source. The basic parameters of its storage ring are as follows: energy 800 MeV, circumference 66.13 m, RF frequency 204 MHz, harmonic number 45, revolution period 220.59 ns, beam lifetime exceeding 10 hours, and average beam current 300 mA [1].

For an electron storage ring, beam loss is inevitable during the running period. It reduces the beam current and shortens the beam lifetime. Therefore, a beam loss monitoring (BLM) system is needed to evaluate the condition of beam loss and help researchers to optimize the parameters of the ring.

The optimization of the injection process is of great importance for synchrotron radiation facilities [2]. The injection system of HLS using a nonlinear kicker (NLK) which the injected off-axis beam passes through and receives a kick to achieve the injection [3]. The nonlinear kicker should be designed to bring the injected beam to the acceptance of the storage ring without considerable disturbance to the stored beam. Throughout the entire process from injection to stable storage operation, multiple beam loss mechanisms exist. First, during injection, the electron beam may strike the septum magnet and vacuum chamber wall, leading to beam loss. Second, a mismatch between the Twiss parameters of the freshly injected bunch and those at the injection point of the storage ring may cause particle loss. Additionally, the pulsed electromagnetic fields of injection elements could perturb the stored beam, triggering transverse or longitudinal beam instabilities and consequently resulting in beam loss. If beam loss consistently exceeds acceptable levels during the injection process, it will severely limit the improvement of beam injection efficiency and beam lifetime. Therefore, it is essential to study beam dynamics and beam loss during injection.

The nanosecond-level time response of scintillators enables bunch-by-bunch beam loss monitoring. In recent years, scintillator-based beam loss monitors have been employed at facilities such as J-PARC [4], the European Synchrotron Radiation Facility (ESRF) [5], and SOLEIL [6].

In this paper, we report a bunch-by-bunch beam loss measurement system based on a plastic scintillator, PMT, and high-speed oscilloscope. Combined with the already installed bunch-by-bunch beam position measurement system, it forms a synchronized monitoring system with nanosecond-level high time resolution for beam loss and bunch position. This system is used to monitor and analyse beam loss during steady-state operation and injection processes at the Hefei Light Source.

## BEAM LOSS MONITORING SYSTEM

### *Measurement Principle*

When a lost high-energy electron hits the storage ring's vacuum chamber, it initiates a secondary particle shower (or cascade). This shower consists of a multitude of secondary particles, including photons (gamma-rays), electrons, positrons, and sometimes neutrons. A particle from the shower enters the scintillator material. It deposits its energy within the material and the deposited energy excites the molecules/atoms of the scintillator. As these excited states return to their ground state, they emit flashes of light. The light pulses travel to a Photomultiplier Tube (PMT), which is optically coupled to the scintillator. The PMT's photocathode absorbs the photons and, via the photoelectric effect, releases photoelectrons. These few photoelectrons are accelerated and multiplied through a series of dynodes within the PMT. This cascade effect creates a large, measurable electrical pulse which is captured by a high-speed oscilloscope.

### *Design of the BLM System at the HLS*

The high temporal resolution beam loss monitoring system consists of a scintillator-based radiation detector, a beam position monitor, and a high-speed oscilloscope. The

† Email address: lengyb@ustc.edu.cn

Content from this work may be used under the terms of the CC BY 4.0 licence (© 2025). Any distribution of this work must maintain attribution to the author(s), title of the work, publisher, and DOI.

ISBN: 978-3-95450-262-2 ISSN: 2673-5350 doi: 10.18429/JACoW-IBIC2025-MOPMO19

# THE NEW SLS 2.0 BOOSTER-TO-RING TRANSFER LINE – DESIGN CRITERIA, DIAGNOSTICS LAYOUT AND FIRST BEAM RESULTS

V. Schlott†, F. Armborst, J. Kallestrup, B. Keil, C. Ozkan-Loch
PSI Center for Accelerator Science and Engineering, Villigen, Switzerland

*Abstract*

Due to the limited transverse acceptance of fourth generation light sources, the characterization and control of the incoming beam from the booster to the storage ring is an important asset to achieve highly efficient and reproducible injection. For the upgraded Swiss Light Source (SLS 2.0) storage ring, a new booster-to-ring transfer line (BRTL) has been designed with a non-dispersive section for beam parameter measurements and a double-BPM-corrector configuration for position and angle feedback of the injected beam.

Based on the BRTL design criteria, first beam results during SLS 2.0 commissioning are presented, including experience with quadrupole scans to document emittance exchange at the end of the booster ramp and steering-stabilization of the beam at the injection point, resulting in a stepwise optimization of transmission into the storage ring.

## INTRODUCTION

After 22 years of successful user operation with about 5000 h/year beam time for 18 user stations at excellent availability of 98.5 % and <1 µm rms photon beam stability in the front ends, the Swiss Light Source was upgraded to a modern diffraction limited light source. A regular 7-bend achromat lattice has been chosen for the new SLS 2.0 storage ring providing low horizontal emittance of 150 pm·rad, beam lifetime of ≈9 h at 400 mA and a sufficiently large transverse dynamic aperture to allow off-axis injection [1]. Together with the additional beam energy increase from 2.4 to 2.7 GeV, it results in a 60 times higher hard X-ray brightness (>10 keV), which will further be enhanced by new insertion devices with shorter periods and improved beamline optics. The variety of radiation sources ranging from period elliptic undulators to superconducting super-bends of up to 5 T peak field provides photon energy ranges from 6 eV to 80 keV for the users [2]. The 15 months "dark period" for storage ring exchange, beamline reconfiguration and infrastructure upgrades started in September 2023. By December 2024 the re-commissioning of the mostly unchanged injector consisting of the 100 MeV pre-injector LINAC and the 2.7 GeV booster synchrotron was accomplished without problems, allowing the start of storage ring commissioning in January 2025. All design parameters were achieved, by April 2025, so that beamline commissioning at full beam current could follow with first expert user operation for selected beamlines in July 2025.

## BRTL DESIGN CRITERIA

For the limited dynamic apertures of fourth generation storage rings, the knowledge of beam parameters from the injector can be advantageous for achieving and keeping good injection efficiency, especially if manipulations like emittance exchange by coupling resonance crossing [3] are applied at the end of the booster ramp.

While the SLS injector remained so far unchanged (LINAC and linac-to-booster transfer line upgrades are foreseen during the shut-down periods in 2026), the geometric layout of the SLS 2.0 storage ring with a slightly moved injection point and the newly developed injection scheme consisting of a permanent magnet thick and a pulsed thin septum required a redesign of the BRTL. This remodeling presented the unique opportunity to integrate extended diagnostics capabilities for beam characterization and to implement full trajectory control (beam positions and angles) through the injection path.

In case of synchrotron light source upgrade projects, the disassembly of storage ring components offers a unique and cost-effective opportunity to re-use well proven and well characterized accelerator equipment (hardware and electronics) for the BRTL design. At SLS 2.0, we additionally benefited from the availability of spare parts from the former SwissFEL Injector Test Facility (SITF) [4] and integrated compact, high-gradient quadrupole magnets and combined diagnostics monitors, consisting of resonant stripline BPMs and screen monitors in the BRTL. Figure 1 shows a CAD overview with beam diagnostics, the main measurement locations and the steering capabilities indicated along the beam path. The insert provides a representation of the BRTL optical functions with a schematic illustration of magnets and diagnostics stations.

Since quadrupole scans for emittance measurements in dispersive regions turned out to be complicated and unreliable [5], a dispersion-free section was designed between the first and the second BRTL dipoles for a more accurate determination of beam emittance and Twiss parameters. The emittance scans are performed by four pairs of SITF quadrupoles (two each connected in series) and the related beam profiles are recorded at the location of screen monitor SCRM-1 (see Fig.1). This arrangement allows for the usual single-quadrupole scans, or a scan of multiple quadruples simultaneously to restrict beam size changes in both directions while varying the phase advance over an adequate range. The latter method is our preferred option, since it has proven to provide more robust results, due to better fitting of Gaussian distributed beam profiles. The SCRM-2 screen monitor has been placed at the location of maximum dispersion to determine the energy distribution of the beam from the booster synchrotron. At the same location, BPM-4 (as part of the combined diagnostics station) is used for online monitoring of the beam energy stability. Full trajectory control of the injected beam into the storage ring has been obtained by placement of two beam position monitors

† volker.schlott@psi.ch

Content from this work may be used under the terms of the CC BY 4.0 licence (© 2025). Any distribution of this work must maintain attribution to the author(s), title of the work, publisher, and DOI.

ISBN: 978-3-95450-262-2 ISSN: 2673-5350 doi: 10.18429/JACoW-IBIC2025-MOPMO20

# BEAM LOSS MONITORING SYSTEM AT SOLARIS

K. Dudek*, R. Panaś, P. Andryszczak, A. I. Wawrzyniak
SOLARIS National Synchrotron Radiation Centre, Kraków, Poland

*Abstract*

The SOLARIS storage ring is equipped with a set of twelve Beam Loss Detectors, operated via Libera Beam Loss Monitors. This system significantly enhances the facility's ability to monitor and analyze beam losses, contributing to improved operational efficiency and machine protection. The detectors are strategically positioned around the storage ring and along the transfer line, enabling optimization of injection losses and precise localization of beam loss events.

Real-time monitoring allows for rapid identification and mitigation of abnormal loss patterns, thereby improving overall beam stability and reliability. The data collected by the system support beam lifetime studies and offer valuable insights for future performance diagnostics and machine optimization.

## INTRODUCTION

SOLARIS National Synchrotron Radiation Centre located in Kraków, Poland, is a third-generation synchrotron radiation light source, where ensuring high operational reliability is a key priority [1]. In early 2025, the facility commissioned a new beam loss monitoring system based on Libera Beam Loss Monitors (BLM), developed by Instrumentation Technologies [2]. The system is designed to precisely detect and quantify beam loss events, contributing to improved machine protection and performance optimization.

Effective beam loss monitoring is essential for safeguarding accelerator components and maintaining stable operation. The integration of the Libera BLM system into the SOLARIS control environment represents a significant enhancement of the facility's diagnostic infrastructure. It enables real-time detection of loss patterns, supports beam lifetime studies, and provides valuable data for future performance analysis and machine tuning.

## HARDWARE

The beam loss monitoring system at SOLARIS consists of twelve Libera Beam Loss Detectors (BLDs) connected to three Libera BLM units. Each BLD incorporates an EJ-200 plastic scintillator coupled to a photomultiplier tube (PMT), which converts the detected radiation into an electrical pulse proportional to its intensity [3]. To minimize background noise from low-energy radiation, each scintillator is enclosed in a 2 mm thick lead housing, ensuring sensitivity to beam loss events while suppressing unwanted signals.

Signals from the PMTs are transmitted to the Libera BLM units, which serve as central data acquisition and processing modules. Each BLM is equipped with a high-speed, four-channel analog-to-digital converter (ADC) operating at 125 MHz, enabling precise digitization of the detector signals. The system is synchronized with the machine's revolution clock, allowing accurate correlation of beam loss events with the longitudinal position in the accelerator and other operational parameters.

Through real-time signal processing, the BLM system provides essential feedback for beam tuning, loss mitigation, and machine protection. It plays a key role in improving operational reliability and supports advanced diagnostics, including beam lifetime studies and performance optimization. Similar systems were implemented in other facilities like ESRF [4] with later upgrade [5], SOLEIL [6] or SPEAR3 [7].

## DEPLOYMENT

The Beam Loss Detector units were strategically deployed at locations identified as most sensitive to potential beam instabilities and loss events. Within the storage ring, detectors were installed near critical components such as the RF accelerating cavities, Landau cavities, and selected insertion devices. Additionally, two BLDs were positioned along the transfer line—one near the end of the LINAC and the other immediately after the injection section (Fig. 1).

The majority of detectors were placed on the outer side of the storage ring, specifically at the entrances to the bending sections, where beam losses are expected to be most pronounced due to increased dispersion and reduced dynamic aperture. This configuration ensures comprehensive coverage of both routine operational conditions and non-standard loss scenarios.

Such a distribution enables precise localization of beam loss events and facilitates correlation with beam dynamics simulations and other diagnostic systems. It also supports optimization of injection efficiency and contributes to improved machine protection and operational reliability.

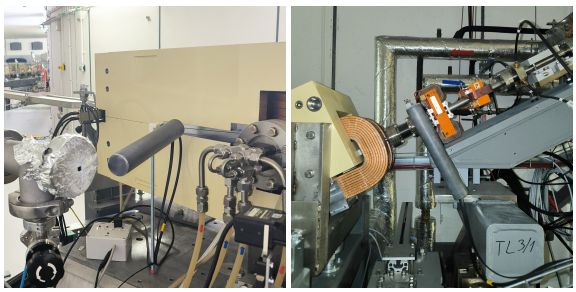



Figure 1: Beam Loss Detector enclosed in lead shielding, installed in the storage ring (left) and along the transfer line (right).

* klaudiusz.dudek@uj.edu.pl

Content from this work may be used under the terms of the CC BY 4.0 licence (© 2025). Any distribution of this work must maintain attribution to the author(s), title of the work, publisher, and DOI.

ISBN: 978-3-95450-262-2 ISSN: 2673-5350 doi: 10.18429/JACoW-IBIC2025-MOPMO21

# BEAM DIAGNOSTIC SIGNAL PROCESSOR FOR SHINE*

Y. X. Han[1,2], L. W. Lai[†,3], Y. M. Zhou[3], S. L. Wang[4], J. L. Pan[1,2], C. L. Wang[1,2], S. S. Cao[3], J. Chen[3], R. X. Yuan[3], X. Q. Liu[3], L. F. Hua[3]
[1] Shanghai Institute of Applied Physics, Chinese Academy of Sciences, Shanghai, China
[2] University of Chinese Academy of Sciences, Beijing, China
[3] Shanghai Advanced Research Institute, Chinese Academy of Sciences, Shanghai, China
[4] School of Information Engineering, Nanchang University, Nanchang, China

*Abstract*

SHINE has developed different signal processors for beam diagnostics, including processors for cold button beam position monitor (BPM), stripline BPM, chicane BPM, cavity BPM, cavity bunch arrival-time monitor (BAM), electro-optic BAM, CSR bunch length monitor (BLM), beam charge loss monitoring, and fast orbit feedback system (FOFB). The processors employ a common SoC-FPGA-based digital motherboard and accommodate diverse applications by hosting various daughterboards. This paper presents the design of these processors and the applications on SHINE.

## INTRODUCTION

The Shanghai HIgh repetitioN rate XFEL and Extreme light facility (SHINE) is China's first hard X-ray FEL, scheduled for completion in 2027 [1]. The 3.1 km facility, located 30 m underground in Zhangjiang, comprises an injector, superconducting LINAC, three undulator lines, three photon beamlines, and ten experimental stations.

Beam diagnostics are essential for stable accelerator operation. Over 500 devices will be installed, including button BPMs, stripline BPMs, chicane BPMs, cavity BPMs, bunch arrival-time monitors (BAMs), electro-optic BAMs, CSR bunch length monitors, beam charge loss monitors, and the fast orbit feedback (FOFB) system [2].

To meet the requirements of high-performance diagnostics, SHINE has developed a series of signal processors supporting real-time operation at 1 MHz. All processors are based on a common SoC-FPGA motherboard, adapted to specific applications with dedicated daughterboards. Table 1 summarizes the processors, and the following sections present the platform design and implementations.

## COMMON FPGA PLATFORM

A generic FPGA motherboard was developed as the core of the common platform (Fig. 1). It is based on a SoC FPGA integrating a quad-core ARM processor and programmable logic. An FMC LPC interface allows mounting a White Rabbit timing card to provide bunch ID and trigger signals, enabling synchronous data acquisition.

* Work supported by The National Science Foundation of China (Grant No.12175239). Youth Innovation Promotion Association, CAS (Grant No.2019290). Outstanding member of the Youth Innovation Promotion Association, CAS (Gant No.Y2023079).
† lailw@sari.ac.cn

The motherboard connects to ADC daughterboards via the FMC HPC interface. Different ADC boards can be used to implement multiple processors, reducing cost and design effort. Table 1 summarizes the diagnostic monitors and requirements that define each processor specification. This flexible architecture makes the platform suitable for a wide range of diagnostics at SHINE.

Table 1: SHINE Beam Diagnostic Processors

| Monitors | Number | Daughterboard specification |
|---|---|---|
| Cold button BPM | 80 | 1 GSPS, 14-bit |
| SBPM | 90 | 1 GSPS, 14-bit |
| Chicane BPM | 3 | 8-channel 1 GSPS, 14-bit |
| CBAM | 6 | 1 GSPS, 14-bit |
| LTU CBPM | 80 | 1 GSPS, 14-bit |
| Undulator CBPM | 100 | 2.6 GSPS, 14-bit |
| EO-BAM | 4 | 250 MSPS, 16-bit |
| CSR-BLM | 2 | 250 MSPS, 16-bit |
| FOFB | 12 | 8 × SFP, 8 × FL |
| Charge interlock | 11 | 8 × SFP, 5 × interlock |

On the software side, all processors share a common IOC framework based on Debian and EPICS. The system supports automatic startup, remote access, time synchronization, and save / restore of IOC status. The IOC monitors ADC waveforms, beam position, bunch ID, and interlock signals. User interfaces, developed with PyDM, display process variables and system status on control room screens. Figure 2 shows the SHINE signal processor PyDM main interface.



Figure 1: FPGA motherboard.

Content from this work may be used under the terms of the CC BY 4.0 licence (© 2025). Any distribution of this work must maintain attribution to the author(s), title of the work, publisher, and DOI.

ISBN: 978-3-95450-262-2 ISSN: 2673-5350 doi: 10.18429/JACoW-IBIC2025-MOPMO22

# UPGRADE OF THE BPM PROCESSOR FOR SXFEL*

S. L. Wang[1,2], L. W. Lai[†,1], H. Jiang[1,2], Y. M. Zhou[1], Q. R. Yan[†,2], W. W. Xie[1,2], C. L. Wang[3]
[1]Shanghai Advanced Research Institute, Chinese Academy of Sciences, Shanghai, China
[2]School of Information Engineering, Nanchang University, Nanchang, China
[3]Shanghai Institute of Applied Physics, Chinese Academy of Sciences, Shanghai, China

*Abstract*

The Shanghai Soft X-ray Free Electron Laser (SXFEL) is scheduled for a digital and intelligent upgrade over the next two years, aiming to achieve fully autonomous operation. This upgrade requires timestamping the BPM measurement results in the beam diagnostics system to enable synchronous acquisition of all measurement data at SXFEL. A new prototype of the digital BPM signal processor (DBPM) has been developed based on a Zynq UltraScale+ MPSoC FPGA. In addition to high-speed data connectors for the ADC board, the design features an FMC slot to accommodate a White Rabbit timing board for receiving bunch ID and trigger signals as timestamps. It also includes 10 GB SFP ports to support high-speed data transmission between processors. In this paper, the design of the hardware, firmware, and software of the upgraded BPM signal processor is presented.

## INTRODUCTION

SXFEL, located on the campus of the Shanghai Synchrotron Radiation Facility, has an overall length of 532 m, comprising a linear accelerator tunnel of approximately 250 m, a 40 m beam distribution hall, a 160 m undulator hall, and an 80 m section housing the beamlines and experimental stations [1]. The electron beam energy reaches up to 1.5 GeV, with a maximum bunch charge of 0.5 nC. The photon energy can reach 620 eV, and the beam repetition rate is adjustable between 10 and 50 Hz [2].

At SXFEL, more than one hundred beam position monitors (BPMs) are distributed along the facility, including stripline BPMs and cavity BPMs. The stripline BPMs achieve a resolution better than 10 μm, while the cavity BPMs reach a resolution of 1 μm [3]. The processors and racks currently in operation are shown in Fig. 1 and Fig. 2, respectively.

In the currently operating BPM processors, the absence of timestamps for individual bunches prevents synchronous data acquisition, making machine-learning-related studies impossible. In the processors at SHINE, White Rabbit timing signals have been integrated, enabling synchronized acquisition of measurement results [4] and supporting high-repetition-rate hard X-ray free-electron laser output [5]. The White Rabbit card is shown in Fig. 3. The WR system provides sub-nanosecond time synchronization while simultaneously distributing trigger signals and bunch identification (Bunch ID) information required for accelerator operation. Using these timing references, multiple BPM processors can acquire data under a unified time base and accurately associate measurements with the corresponding bunches, thereby enabling high-precision alignment among different processors.

SXFEL is undergoing a digital and intelligent upgrade. According to project requirements, the SXFEL processors are to be upgraded, with completion targeted within two years. The proposed solution employs the same system-on-chip FPGA while maintaining compatibility with the existing ADCs and front-end boards. It also supports the integration of a White Rabbit timing mezzanine card and provides high-speed SFP interfaces for data transmission. Furthermore, associated FPGA logic, signal processing algorithms, and EPICS IOC control software will be developed. The prototype hardware has been successfully constructed, incorporating both the stripline BPM signal processing algorithm and the EPICS IOC. In addition, White Rabbit timing data can now be acquired.



Figure 1: Current BPM processor.



Figure 2: BPM processor rack.



Figure 3: White Rabbit card.

* Work supported by The National Science Foundation of China (Grant No.12175239). Youth Innovation Promotion Association, CAS (Gant No.2019290). Outstanding member of the Youth Innovation Promotion Association, CAS(Gant No.Y2023079).
† Corresponding author: lailw@sari.ac.cn, yanqiurong@ncu.edu.cn

Content from this work may be used under the terms of the CC BY 4.0 licence (© 2025). Any distribution of this work must maintain attribution to the author(s), title of the work, publisher, and DOI.

ISBN: 978-3-95450-262-2 ISSN: 2673-5350 doi: 10.18429/JACoW-IBIC2025-MOPMO24

# OVERVIEW OF DIAGNOSTIC AND INSTRUMENTATION FOR SIAM PHOTON SOURCE-II

P. Sudmuang†, S. Naeosuphap, T. Pulampong, S. Jummunt, S. Kongtawong, W. Promdee, T. Chanwattana, T. Phimsen, P. Klysubun
Synchrotron Light Research Institute, Nakhon Ratchasima, Thailand

*Abstract*

Siam Photon Source II (SPS-II) is a 4th-generation synchrotron light source to be constructed in Thailand, envisioned as a major synchrotron facility for Southeast Asia. It is designed with a 3 GeV low-emittance electron storage ring based on a Double Triple Bend Achromat (DTBA) lattice, with a circumference of 327.6 meters and a natural emittance of 0.97 nm·rad. The design and machine parameters have recently been carefully revised to enhance beam stability and operational reliability. In parallel, key prototypes are being developed to support smooth construction and ensure long-term performance. This paper presents the detailed specifications and a comprehensive overview of the planned beam diagnostics and instrumentation systems, along with initial results from their ongoing R&D and testing.

## INTRODUCTION

The SPS-II accelerator complex comprises four main components: a 3.0 GeV low-emittance storage ring, a 0.25–3.0 GeV ramping booster, a 150–270 MeV S-band linac, and low- and high-energy transfer lines [1-3]. The storage ring is based on 14 Double Triple Bend Achromat (DTBA) cells with a natural emittance of 0.97 nm·rad, accommodating insertion devices in both standard and middle straight sections. The linac and booster will operate in single-bunch mode, while the storage ring will run at a high beam current of 300 mA with strict requirements to maintain 1 % beam stability during top-up injection.

To satisfy these demands, a comprehensive diagnostic system has been developed to monitor all major subsystems. It delivers detailed measurements of beam position, intensity, shape, and filling pattern, thereby supporting machine commissioning, beam physics studies, and long-term stable operation.

## STORAGE RING DIAGNOSTIC

### *Beam Position Monitor*

A four-button beam position monitor (BPM) was developed to provide high-precision position data in closed-orbit, low to fast feedback, and turn-by-turn modes. The storage ring will employ 140 BPMs, with ten installed per achromatic cell as shown in Fig. 1. Each BPM is designed as a removable flange type, comprising top and bottom flanges mounted on the elliptical chamber [4].

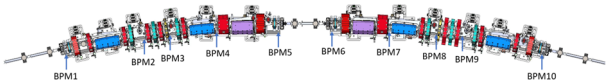



Figure 1: Location of BPMs in the SPS-II storage ring.

The button geometry, as shown in Fig. 2 was optimized for a resolution of ~100 nm at 100 mA with 2 kHz bandwidth. Each button has a 6 mm diameter, 4 mm thickness, and a 0.3 mm electrode housing gap, chosen to maximize capacitance and shift HOM resonances. A horizontal separation of 10.5 mm yields horizontal and vertical sensitivities of ~0.134. Buttons and central conductors are fabricated from molybdenum and integrated with reverse-polarity SMA connectors, while alumina ($Al_2O_3$) insulators provide electrical isolation and vacuum sealing.

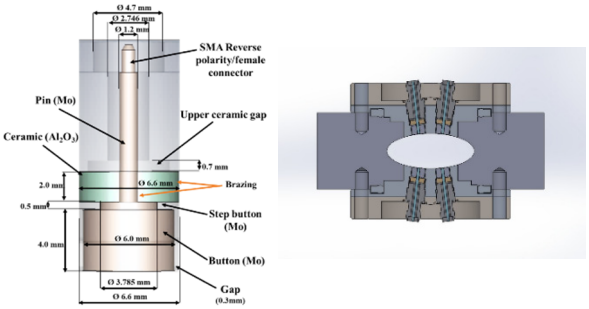



Figure 2: BPM button (left), engineering design of BPM flange installed on the BPM chamber (middle and right).

### *Current Monitor*

The average beam current in the storage ring will be measured using Bergoz's New Parametric Current Transformer (NPCT) [5], which provides a large dynamic range and high bandwidth with a 1 µA/√Hz resolution option. The system consists of a flange-type sensor head, a 19″ 3U RF-shielded chassis with dual power supplies and auto-range AC input, and two NPCT electronic cassettes. The sensors are equipped with radiation-tolerant features and a bake-out option rated for operation below 100 °C.

### *Beam Loss Monitor*

Two complementary systems will be used for beam loss detection and localization. Scintillator–PMT monitors provide fast, localized detection with 8 ns resolution and MHz-level acquisition rates, making them well suited for identifying rapid injection losses. Each unit comprises an EJ-200 scintillator, a Hamamatsu H10721-110 photomultiplier tube, an aluminum housing with lead shielding, and a data acquisition system. In parallel, a fiber-based BLM system using Cherenkov light in long optical fibers will offer simple, cost-effective, distributed detection. Each unit comprises an optical fiber, PMT, and a data acquisition system. The fibers (Thorlabs pure silica, 100 µm core with hard polymer cladding) provide high sensitivity, with about seven 45 m fibers installed around the ring. A prototype has already been set up in the existing machine [6].

† porntip@slri.or.th

Content from this work may be used under the terms of the CC BY 4.0 licence (© 2025). Any distribution of this work must maintain attribution to the author(s), title of the work, publisher, and DOI.

ISBN: 978-3-95450-262-2 ISSN: 2673-5350 doi: 10.18429/JACoW-IBIC2025-MOPMO25

# OPERATIONAL EXPERIENCE WITH MACHINE PROTECTION SYSTEM FOR HIGH CURRENT, HIGH BRIGHTNESS ACCELERATOR *

S. Seletskiy†, A. Fedotov, D. M. Gassner, X. Gu, R. Hulsart, P. Inacker, D. Kayran, J. Kewisch, K. Mernick, R. Michnoff, P. Oddo, M. Paniccia, W. Pekrul, L. Smart
Brookhaven National Laboratory, Upton, NY, USA

Content from this work may be used under the terms of the CC BY 4.0 licence (© 2025). Any distribution of this work must maintain attribution to the author(s), title of the work, publisher, and DOI.

*Abstract*

The Low Energy RHIC Electron Cooler (LEReC), the world's first electron cooler utilizing an RF electron accelerator, was designed to operate with 1.6 - 2.6 MeV electron beams of up to 140 kW beam power. The LEReC successfully worked through RHIC Runs 2019 - 2021, substantially increasing RHIC luminosity, and has been routinely used for various studies since then. A dedicated, highly configurable Machine Protection System (MPS) is a critical part of the LEReC. This paper summarizes our experience with operating the LEReC MPS.

## INTRODUCTION

The Low Energy RHIC Electron Cooler [1-4] is the first electron cooler based on RF acceleration of electron bunches. LEReC utilizes a non-magnetized electron beam and provides the cooling of colliding ions with the same e-beam in both RHIC rings. LEReC was commissioned in 2019, was successfully used in RHIC operations in 2020 (at $\gamma = 4.9$) and in 2021 (at $\gamma = 4.1$), and has been routinely used for various studies since then.

Electron bunches in LEReC are produced by a 375 keV photo-gun. In operations the CW electron beam consists of 9 MHz macrobunches, each containing 30-36 704 MHz electron bunches. Each ion bunch passing through the LEReC cooling section (CS) is overlapped with one electron macrobunch. In studies LEReC is also operated with uninterrupted 704 MHz CW beam.

The LEReC gun is followed by the SRF Booster, which accelerates the beam to 1.6-2 MeV. The transport beamline and the merger bring the beam to the cooling section in the Yellow RHIC ring, and then through the 180° bending magnet to the CS in the Blue RHIC ring, where electrons and $Au^{79}$ ions are co-traveling with the same velocity. Finally, the extraction beamline sends electrons to the high-power beam dump.

Besides the high-power dump, there are two additional destinations for the beam. One is a gun diagnostic beamline, equipped with 25 kW beam dump. The other destination is a RF-diagnostic beamline equipped with a deflecting cavity, a mirrorless profile monitor and a mini dump accepting up to 10 W of beam power. This beamline is used for optimizing the e-bunch parameters in a longitudinal phase space and for fine-tuning of the LEReC RF system.

The LEReC layout is schematically shown in Fig. 1.

* Work supported by Brookhaven Science Associates, LLC under Contract No. DE-SC0012704 with the U.S. Department of Energy
† seletskiy@bnl.gov

By design LEReC can produce up to 85 mA current of electron beam with <2 μm emittance, and can operate at a maximum power of 140 kW. A robust, highly configurable Machine Protection System (MPS) with fast reaction time is a critically important part of LEReC.

## MPS OVERVIEW

The LEReC MPS [5-7] is designed to protect the machine from damage caused by the loss of electron beam. The MPS parameters were derived from considering tolerable beam losses under various failure scenarios.

### *LEReC Beam Modes and MPS Levels*

We devised four MPS levels. Each level defines what beam operations are allowed, what beam destinations are permitted, and what signals are monitored. The relations of MPS levels to various modes of LEReC beam operation are listed below:

- The MPS Level 1 corresponds to LEReC pulsed beam mode, in which trains of electron macrobunches are emitted with 1 Hz rate. The maximum allowed current in that mode is 40 nA. The beam can be sent to any LEReC beamline. It is allowed to intercept beam with profile monitors and emittance measurement slits in this mode.
- The Level 2 was designed to deliver long trains of macrobunches to the RF-diagnostic beamline. While the beam is allowed to be sent to any destination, the beam intercepting devices can not be operated in this mode.
- In Level 3 the LEReC is operating in CW mode, which corresponds to either 9 MHz, 704 MHz or 75 kHz current (75 kHz is RHIC revolution frequency, this mode was used for initial cooling setup). In Level 3 the beam power must be below 25 kW and the two possible destinations for the beam are the injection beamline dump or the high-power dump.
- The Level 4 is reserved for sending beam with average power of up to 140 kW to the high-power dump.

There is an additional Level/Mode, called the "Laser Alignment Mode", which is used to align the high-power laser on the gun cathode with the gun power supply being turned off.

### *MPS Signals*

The MPS relies on numerous diagnostic systems [8].

The MPS utilizes the fast current transformer (FCT) located at the gun exit to measure the beam current and to determine the MPS Level.

ISBN: 978-3-95450-262-2 ISSN: 2673-5350 doi: 10.18429/JACoW-IBIC2025-MOPMO26

# PERFORMANCE EVALUATION OF TAILORED SHIELDING FOR ENERGY-SELECTIVE NEUTRON DETECTION IN REACTOR ENVIRONMENTS

A. Jones*, A. Detkina, School of Engineering, University of Liverpool, Liverpool, UK
B. Merk, C.P. Welsch[1], Department of Physics, University of Liverpool, Liverpool, UK
[1]also at Cockcroft Institute, Sci-Tech Daresbury, Warrington, UK

Content from this work may be used under the terms of the CC BY 4.0 licence (© 2025). Any distribution of this work must maintain attribution to the author(s), title of the work, publisher, and DOI.

*Abstract*

With nuclear reactor technology rapidly advancing and the plan to raise the nuclear energy production by a factor of 4, the need for advanced detectors, geometries and shields has become apparent.To support this development there is a strong need for advanced instrumentation, as precise and reliable measurement of the neutron flux is not only relevant for the safe operation of nuclear reactors, but also for future reactor experiments essential for progressing the technology. In the presented work, simulations were performed using MCNP-6.3 to investigate the effects of various common reactor materials in different shield geometries on the performance of benchmark detectors. This was performed using a validated simulation of a 1 Ci Am/Be neutron source located at the University of Liverpool for a detailed experiment to simulation evaluation, followed by simulations of the detector in use near a zero power molten salt reactor. The use of a conical shield/reflector material around a thermal neutron detector showed an increase in efficiency for the detection of thermal neutrons when compared to the results for no additional material. The tailored measurement of neutrons of specific energies is highly relevant not only for reactor experiments on innovative technologies, but also has applications in neutron beam monitoring.

## INTRODUCTION

The transition to a low-carbon, stable energy system is one of the major challenges of our time. Nuclear power is expected to be at the forefront of this transition, offering a stable source of very low-carbon electricity that is complementary to the intermittency of current renewables.

The International Energy Agency (IEA) has pointed out that nuclear energy is today the world's second-largest source of low-carbon electricity and has already avoided over 60 gigatonnes of $CO_2$ emissions over the last half-century [1]. Most recently, more than 20 nations pledged at COP28 to tripling global nuclear capacity by 2050, recognising its contribution to reaching net-zero goals and improving energy security [2].

Yet fulfilling these hopes will require more than simply enlarging existing reactor designs. Many of the world's older nuclear fleet, particularly in OECD countries, is ageing, meanwhile new large-scale projects, are often beset by delays and escalating costs. A central part to overcoming this challenge is the development of zero-power reactors (ZPR). ZPRs have historically provided the essential experimental data required to validate reactor physics models, qualify design codes, and demonstrate system behaviour in a safe, controlled low-power environment. They also serve as training facilities, such as AKR-2 at TU Dresden, for example, for students, reactor operators, scientists, and regulators, building the technical expertise required for eventual implementation.

It is obvious that this massive expansion of nuclear power capacities should go hand in hand with an improvement of the sustainability indices, increased fuel use and reduced waste production. To provide answers to this challenges, the iMAGINE concept has been developed [3].

One of the many opportunities provided by such a facility is the ability to operate reactors and design and implement new reactor instruments, using Monte-Carlo methods, and then experimentally test and validate them. New detector materials, along with new ways of placing detectors and shielding them all offer the opportunity to create a tailored detector system for each type of reactor.

In this paper, the design and simulation of a new conical reflector will be discussed, in two settings: firstly, in a neutron facility, using a 1 Ci Am/Be source, to validate the model, and secondly, once the model is validated, in a reduced reactor model of a zero power NaCl-UCl based molten salt reactor.

## MODELLING

Simulations were carried out using MCNP-6.3, and started with the modelling and validation of the facility and detector used at the University of Liverpool (UoL). For this, a model was created as shown in Fig. 1 including the source, water tank, moderating materials present in the room and the structure of the room itself.

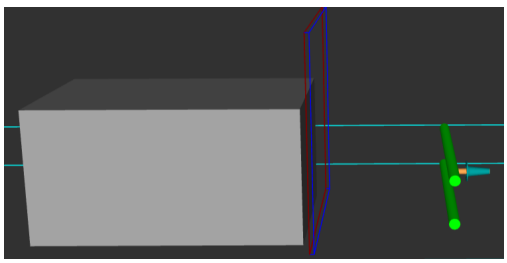


Figure 1: Wireframe view inside neutron tank facility at UoL, with $He^3$ detectors alongside test detector with reflector cone.

* psajone2@liverpool.ac.uk

ISBN: 978-3-95450-262-2 ISSN: 2673-5350 doi: 10.18429/JACoW-IBIC2025-MOPMO27

# THE BEAM TEST FACILITY OF THE NATIONAL LABORATORIES OF FRASCATI

B. Buonomo, F. Cardelli, D. Di Giovenale, C. Di Giulio, E. Diociaiuti*, L. G. Foggetta, C. Taruggi
Laboratori Nazionali di Frascati dell'INFN, Frascati (RM), Italy

*Abstract*

The Beam Test Facility (BTF) at the National Laboratories of Frascati (LNF) provides highly configurable positron/electron beams for different type of experiments. Extracted from the DAΦNE LINAC, the beam delivers up to 49 bunches/s, with 1 to $10^{10}$ particles/bunch. Secondary beams span 25–780 MeV (electrons) and up to 550 MeV (positrons). BTF includes two experimental halls: BTFEH1, suited for high-intensity and long-term experiments, and BTFEH2, optimized for lower intensities (up to $10^6$ particles/s). Both halls feature remote-controlled movable tables, beam diagnostics, and essential services like laser alignment, networking, high-voltage support, and gas pipelines, ensuring comprehensive experimental capabilities and 24/7 user support. A notable strength of BTF lies in its user-friendly approach. Beam can easily be manipulated to meet users' specific needs, even during ongoing data collection. In this paper the upgrades concerning the development of a new control system based on Epik8s (EPICS on Kubernates) will be reported as well as the new improvement in beam dimension and energy loss concerning the substitution of the 500 µm BeO exit window with 120 µm Anticorodal one.

## EXPERIMENTAL HALLS, BEAMS, AND USER

As a component of the DAΦNE accelerator complex [1], the INFN Laboratori Nazionali di Frascati (INFN-LNF) houses the Beam Test Facility [2] (BTF), a system of beam transfer lines and two experimental halls designed to transport electron or positron, primary or secondary beams to various hit points with the aid of beam diagnostics and High Energy Physics (HEP) experiment-focused services.

The LINAC [3] can operate at repetition rates up to 50 Hz and is capable of continuous 24/7 operation, delivering beams to the experimental halls. BTFEH1, offering over 30 $m^2$ of experimental area, typically receives conditioned, fixed-energy primary electron and positron beams. These beams have nominal energies of 510 MeV, with operational ranges from 160 (200) MeV to 780 (530) MeV for electrons (positrons), and an energy spread of approximately 0.5 % (depending on the selected energy). The pulse duration is typically 10 ns, extendable up to 320 ns, with emittance values of 1 (10) mm·mrad [4]. Beam intensities at the DUT point can reach up to $10^{10}$ particles/s, subject to radioprotection constraints.

Secondary beams are produced by directing the LINAC primary beam onto a variable-depth copper target (1.7–2.3 $X_0$), generating a continuous momentum distribution. These quasi-neutral, highly chromatic secondary beams are momentum and particle-type-selected using a 45-degree bending dipole and beam scrapers. The resulting beam intensity is energy dependent and significantly reduced compared to the primary beam. By adjusting the scraper positions, the beam multiplicity can be tuned down to the single-particle level across the full secondary energy range.

A summary of these different operational modes [5] and beam characteristics is reported in Fig. 1.

| Parameters | BTF1 Time sharing | | BTF1 Dedicated | | BTF2 Time sharing | BTF2 Dedicated |
|---|---|---|---|---|---|---|
| | With Cu target | Without Cu target | With Cu target | Without Cu target | With Cu target | With Cu target |
| Particle Type (Dependance) | $e^+$ / $e^-$ (User ) | $e^+$ / $e^-$ (DAΦNE status) | $e^+$ / $e^-$ (User ) | | $e^+$ / $e^-$ (User ) | |
| Energy (MeV) | 25–500 | 510 | 25–700 ($e^-$/$e^+$) | 167–700 ($e^-$) 250–550 ($e^+$) | 25–500 | 25–700 |
| Best Energy Resolution at the experiment | 0.5% at 500 MeV | 0.5%/1% | 0.5% | Energy dependent | 1% at 500 MeV | |
| Repetition rate (Hz) | Variable from 1 to 49 (DAΦNE status) | | 1–49 (User) | | Variable from 1 to 49 (DAΦNE status) | 1–49 (User) |
| Pulse length (ns) | 10 | | 1.5–320 (User) | | 10 | Expected 10-100 |
| Intensity (particle/bunch) | $1–10^5$ (Energy dependent) | 1 to $10^7$ / $1x10^{10}$ | $1–10^5$ (Energy dependent) | 1 to $10^{10}$ | $1–10^4$ (Energy dependent) | |
| Max int flux | $1x10^{10}$ part./s | | | | $1x10^6$ part./s | |
| Beam waist size(mm) | 0.5–55 X / 0.35–25 Y (vacuum window dependent) | | | | 1x1 | |
| Divergence (mrad) | Down to 0.5 | | | | Down to 0.5 | |

Figure 1: BTF beam characteristics.

Both experimental halls can receive secondary beams with minimal configuration differences. The beam spot size can be tuned to as small as $0.4 \times 0.4\,mm^2$ using the final quadrupole doublet or easily reaching the desired users dimension. BTFEH2, with over 10 $m^2$ of experimental space, is primarily used for weekly-based user shifts and has operated without major faults during recent user calls. Although limited to beam currents of $10^6$ particles/s, BTFEH2 has supported beam performance optimization, low-energy beam prototype development for FCC-related projects, and the testing of BTF-developed detectors such as the Pulsed Ionization Chamber and calorimeters [6]. In Fig. 2 the setup of the BTF experimental halls is reported.

The facility maintained a high level of beam availability, with approximately 240 operational days dedicated to both external and internal users. More than 200 users accessed the beamlines, receiving continuous support from beamline scientists. 2025 has been dedicated to the data taking of the PADME/X-17 experiment [7], and three weeks of external user activities are planned for December 2025. The BTF hosted a significant number of users and activities over the years (see Fig. 3). In 2024, the typical user team had an average shift duration of 6.5 days and involved around 7 participants per team.

BTF hall activities in 2024 are categorized as follows: low-multiplicity external users (43 %), internal (LNF) projects and commissioning beam time (~20 %), dedicated PADME

* eleonora.diociaiuti@lnf.infn.it

Content from this work may be used under the terms of the CC BY 4.0 licence (© 2025). Any distribution of this work must maintain attribution to the author(s), title of the work, publisher, and DOI.

ISBN: 978-3-95450-262-2 ISSN: 2673-5350 doi: 10.18429/JACoW-IBIC2025-MOPMO28

# UV–VIS EMISSIONS FROM HIGH ENERGY HEAVY IONS: MECHANISMS AND APPLICATIONS TO SINGLE-ION DETECTION

R. Ghagi*,[1], R. Singh, P. Boutachkov, B. Walasek-Hoehne, GSI, Darmstadt, Germany
H. Zhang, C. Welsch, University of Liverpool, Liverpool, UK
[1] also at University of Liverpool, Liverpool, UK

*Abstract*

We investigate two well known ultraviolet–visible (UV–VIS) photon emission processes from highly charged uranium ions with energies of 300- 700 MeV/u. By combining theoretical models with estimates from the literature, we evaluate fluorescence yields from air and transition radiation from surfaces. Experimental studies with slow-extracted $U^{73+}$ beam at the high-energy beam transport line at GSI–FAIR confirm the feasibility of single-ion detection, with prototype detectors achieving up to 99.5 % efficiency. These findings suggest UV–VIS emission as a robust method for fast, radiation-hard single-particle counting.

## INTRODUCTION

High-energy, high-intensity heavy-ion beams are essential tools for exploring new physics and probing fundamental interactions at facilities such as GSI–FAIR [1]. Reliable, fast, and radiation-hard diagnostics, capable of sustained performance over extended periods, are essential prerequisites for their successful operation. In this paper, we summarize the primary mechanisms of UV–VIS emission from relativistic heavy ions in air and on metallic targets, and highlight the development and testing of a prototype detector that harnesses this emission for efficient, radiation-hard particle counting.

## BEAM-INDUCED FLUORESCENCE

Beam-induced fluorescence (BIF) in pure gases is a well-established phenomenon [2] with wide applications in beam diagnostics [3, 4]. Air fluorescence studies with electrons over a wide energy range of 500 keV to 50 GeV [5–8], with protons at 120 GeV [9], and with 0.3–5.1 MeV $\alpha$-particles in radioluminescence studies [10], reports a yield of $\approx$ 20 photons per MeV of energy deposited in air in the 300–420 nm band under conditions close to normal temperature and pressure (NTP).

Air fluorescence at atmospheric pressure (1013.25 hPa) is dominated by the second positive (2P) system[1] of $N_2$, with only a small contribution from the first negative (1N) system of $N_2^+$. Within the 2P system, the 2P(0,0) band at 337.1 nm is the strongest single feature, accounting for $\approx$ 25 % of the yield, while many other 2P bands together contribute far more than the 1N(0,0) band at 391.4 nm [5, 12].

Collisional quenching, i.e. non-radiative de-excitation of excited molecules by collisions, reduces both the fluorescence yield and the radiative lifetime. In air, the fluorescence yield increases with pressure due to higher molecular density, but this is counteracted by quenching. For a given gas composition, the pressure dependence of the yield for a $v \to v'$ transition, $Y_{vv'}(P)$, and of the corresponding excited-state lifetime $\tau_v(P)$, is described by the Stern–Volmer equation [11, 13]:

$$\frac{Y_{vv'}(P)}{Y^0_{vv'}} = \frac{\tau_v(P)}{\tau^0_v} = \frac{1}{1+P/P^0_v}, \quad (1)$$

where $Y^0_{vv'}$ and $\tau^0_v$ are the radiative yield and lifetime of the $v \to v'$ transition in the absence of quenching. The parameter $P^0_v$ is the characteristic Stern–Volmer pressure of state $v$, defined as the pressure at which collisional quenching and radiative decay occur with equal probability. For the $2P(0, v'')$ and $1N(0, v'')$ transitions in air, the values are $P^0 = 15.3$ hPa and $P^0 = 1.2$ hPa, respectively. At atmospheric pressure (1013.25 hPa), the corresponding quenching factors, $1 + P/P^0_v$, are 67.2 and 845.4. Thus, quenching reduces the lifetime of the 337.1 nm band from 38.9 ns to 0.57 ns, and that of the 391.4 nm band from 65.2 ns to 77 ps. These values have been experimentally confirmed for the 2P system, whereas the very low yield of the 391.4 nm band and the presence of neighboring 2P bands (e.g. 380.5 nm and 399.8 nm) present practical challenges for accurate lifetime measurements of the 1N system [13].

Apart from collisional quenching, the dominance of the 2P system in atmospheric air is further reinforced by a significant fraction of $N_2^+$ converting to excited 2P states of $N_2$ rather than emitting via the 1N system [2, 14]. The dominant pathway for this re-population of $N_2(C^3\Pi_u)$ in the 2P system proceeds via the formation of $N_4^+$, followed by dissociative recombination with an electron [15].

As fluorescence is driven mainly by cascades of low-energy secondary electrons generated during ionization by the primary charge, precise calculation of their energy deposition is essential for reliable estimates of the photon yield in any experimental geometry [14]. For the present study, we estimate the number of photons for the experimental ion beams (Table 1) by calculating the energy lost by primary ions using the Bethe–Bloch formula and assuming a geometry in which all of this energy loss is deposited in the medium.

* r.ghagi@liverpool.ac.uk

[1] The second positive (2P) system refers to electronic transitions in neutral nitrogen, $N_2(C^3\Pi_u \to B^3\Pi_g)$, while the first negative (1N) system corresponds to transitions in the nitrogen ion, $N_2^+(B^2\Sigma_u^+ \to X^2\Sigma_g^+)$ [11]. Individual bands are denoted as $2P(v, v')$ or $1N(v, v')$, where $v$ and $v'$ are the vibrational quantum numbers of the upper and lower states, respectively. For example, the 2P(0,0) band at 337.1 nm arises from the $v = 0 \to v' = 0$ transition of neutral $N_2$, while the 1N(0,0) band at 391.4 nm corresponds to the analogous transition in $N_2^+$.

Content from this work may be used under the terms of the CC BY 4.0 licence (© 2025). Any distribution of this work must maintain attribution to the author(s), title of the work, publisher, and DOI.

ISBN: 978-3-95450-262-2 ISSN: 2673-5350 doi: 10.18429/JACoW-IBIC2025-MOPMO31

# QUANTUM EFFICIENCY MEASUREMENTS AND BEAM DIAGNOSTICS TEST STAND DESIGN FOR A DUAL-MODE ELECTRON GUN AT ELSA

S. Kronenberg*, K. Desch, B.Gatzsche, P. Hänisch, D. Proft, Y. Schober, M. Switka
Physikalisches Institut, University of Bonn, Germany

*Abstract*

To support both routine operation and accelerator research at ELSA, a dual-mode dispenser-cathode based electron gun capable of thermionic emission and thermally assisted photoemission (TAPE) is being developed. A dedicated gun test stand is being designed to measure beam properties and quality, as well as quantum efficiency in the TAPE mode under operational conditions. Instrumentation will include a pepper pot emittance stage, quadrupole scan capabilities, profile measurements using screens and wire-scans or SEM grids, and bunch charge and energy spread determination. In a basic test environment, experiments were carried out at low accelerating voltages using a setup consisting of the dispenser cathode, a pickup anode, and a simple laser system with an optical shutter. The shutter enables alternating measurements of photocurrent and dark current at the anode, allowing first estimations of quantum efficiency. The influence of different cathode heating cycles on both the absolute quantum efficiency and its temporal stability was investigated with this setup. Quantum efficiency measurements under different conditions and simulations of the test beamline are presented.

## INTRODUCTION

The injector at ELSA (Electron Stretcher Accelerator, operated by the University of Bonn), requires modernization due to aging infrastructure and limited diagnostic capabilities. A new dual-mode electron gun is being manufactured to maintain current operational capabilities while enabling single-bunch operation for machine studies in the stretcher ring. This mode should offer such short electron pulses, that only one bucket in the stretcher ring is filled, this will be assured by only filling one bucket in the Linac and the booster synchrotron. The design of this new gun has been previously presented in detail [1].

### *Existing Injector Infrastructure*

The ELSA facility (shown in Fig. 1) employs a 3 GHz travelling wave LINAC2 with both spin-polarised (GaAs photocathode) and non-polarised (thermionic cathode) electron sources, the latter delivers up to 0.5 A current. The aging beamline connecting the thermionic gun to the linac has resulted in loss of diagnostic capabilities in favor of additional vacuum pumps. Spatial constraints in the injector area complicate replacement planning.

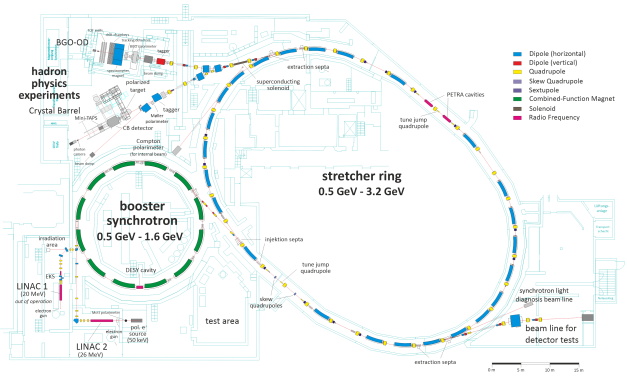



Figure 1: Overview of the ELSA facility.

### *Electron Gun Upgrade*

The thermionic gun design is chosen for reliability and durability. Due to spatial constraints, a hybrid design has been chosen, combining thermionic emission and thermal-assisted photoemission within a single assembly. This ensures that the space constraints are met whilst enabling short-pulse generation via laser pulsing. The gun follows an inverted triode geometry based on the Pierce design.

The upgrade extends the operational range and enhances maintenance ease while addressing age-related issues. This involves increasing the electron current to 2 A, offering the possibility to increase the current in the Linac and reducing required injections into the stretcher ring. Beam quality equal to the current setup with transverse emittance of 8.3 mm mrad or lower is targeted.

## THERMALLY ASSISTED PHOTOEMISSION

The TAPE effect enables dispenser cathodes to function as photocathodes. Heating shifts the electron energy distribution, increasing the population of electrons with sufficient energy for photoemission at longer wavelengths including the visible range [2, 3]. This is more convenient than UV wavelengths required for metal cathodes.

For caesium dispenser cathodes, thermal operation causes caesium emission that reduces the surface work function. This effect is expected to further enhance quantum efficiency (QE) even with reduced caesium deposition in TAPE mode. The specific cathode (EIMAC Y845) planned for this application is not yet characterized under TAPE conditions.

* s.kronenberg@uni-bonn.de

Content from this work may be used under the terms of the CC BY 4.0 licence (© 2025). Any distribution of this work must maintain attribution to the author(s), title of the work, publisher, and DOI.

ISBN: 978-3-95450-262-2 ISSN: 2673-5350 doi: 10.18429/JACoW-IBIC2025-MOPMO32

# CHARACTERIZATION OF THE RADIATION ENVIRONMENT IN THE FCC-ee TUNNEL

A. Frasca[1,*], G. Broggi, R. Bruce, B. Humann, A. Lechner, G. Lerner, CERN, Geneva, Switzerland
M. Boscolo, A. Ciarma, INFN, Frascati, Italy
C. Welsch[1], N. Kumar[1], Cockcroft Institute, Sci-Tech Daresbury, Warrington, UK
[1]also at Department of Physics, University of Liverpool, Liverpool, UK

*Abstract*

The Future Circular $e^+e^-$ Collider (FCC-ee) at CERN will provide collisions at four interaction points along a 91 km long ring, with beam energies ranging from 45.6 GeV (Z pole) to 182.5 GeV ($t\bar{t}$ threshold). The radiation environment along the accelerator varies significantly, with different dominant sources depending on location and operational mode. Accurate characterization of this environment is essential for the design and placement of machine equipment, particularly electronic systems and beam instrumentation. In this study, the Monte Carlo code FLUKA is used to characterize tunnel radiation levels from the main sources, including radiative Bhabha scattering, synchrotron radiation, and beam-gas interactions. The results at the Z pole and $t\bar{t}$ threshold for both the interaction regions and arcs are presented to guide early-stage design considerations and to quantify exposure risks for electronics at potential installation locations.

## INTRODUCTION

The first stage of the Future Circular Collider (FCC) at CERN foresees a high-luminosity lepton collider, FCC-ee [1]. The FCC-ee will serve as an electroweak, Higgs and top quark factory by providing $e^+e^-$ collisions at four interaction points (IPs) along a 91 km long ring. It will cover beam energies from 45.6 GeV (Z pole) to 182.5 GeV ($t\bar{t}$ threshold). The power radiated as synchrotron radiation (SR) is by design limited to 50 MW/beam across all the operational modes by adjusting the beam current according to the energy. At the Z pole, the beam current reaches 1294 mA with a luminosity per IP of $145 \times 10^{34}\,\mathrm{cm^{-2}\,s^{-1}}$, while at the $t\bar{t}$ threshold the current is reduced to 5.1 mA, with a corresponding luminosity of $1.41 \times 10^{34}\,\mathrm{cm^{-2}\,s^{-1}}$.

Characterizing the tunnel radiation environment is essential for the safe operation of machine equipment and electronics and directly influences the design of beam instrumentation systems, such as beam loss monitors (BLMs) and beam position monitors (BPMs). This task is particularly challenging at FCC-ee, where variations in beam parameters across operational modes lead to significant shifts in the dominant radiation sources and, consequently, in the environment throughout the accelerator.

In circular lepton machines, SR is a major source of radiation, as the energy loss per turn scales with $\frac{E^4}{m_e^4 \rho}$, where $E$ is the beam energy, $m_e$ the electron mass, and $\rho$ the bending radius. Although the SR power loss is kept constant by design for all FCC-ee operating points, the tunnel radiation levels strongly depend on the photon energy spectrum, defined by the critical energy $E_c \propto \frac{E^3}{\rho}$. This value is 0.02 MeV at the Z pole, where photons have a short attenuation length and are mostly absorbed in the vacuum chamber, making tunnel leakage negligible. At the $t\bar{t}$ threshold, the harder photon spectrum ($E_c = 1.3$ MeV) produces radiation showers beyond the chamber, making SR a dominant concern for the tunnel environment. On the other hand, the Z pole mode is more affected by beam loss mechanisms that scale with beam intensity, such as beam-gas (BG) interactions, and by collision-induced losses driven by luminosity. As a result, while the most severe radiation environment in the FCC-ee arcs occurs at the $t\bar{t}$ mode due to SR, the interaction regions (IRs) around the IPs present a critical scenario even at the Z mode, with contributions from radiative Bhabha (RB) scattering, beamstrahlung (BS) and secondary particles from collimators upstream of the experiment.

In this work, the Monte Carlo code FLUKA [2–4] is used to simulate radiation showers from the main sources and to estimate dose levels in FCC-ee tunnel. The aim is to provide an early characterization of the expected radiation environment and support the development of design strategies. The study does not quantify the beam loss sources for which BLMs must be designed, but rather highlights the radiation conditions in which different systems will have to operate. Results are presented for a representative arc section at the $t\bar{t}$ mode, and for a generic IR at both Z and $t\bar{t}$ modes, allowing comparison across operational scenarios.

## SIMULATION SETUP

Geometries representative of a FCC-ee arc section and IR for V24.4 of the Global Hybrid Correction lattice [5–7] were implemented in FLUKA, including the main beamline elements and tunnel infrastructure relevant to radiation transport. Magnet and tunnel models are based on Refs. [1, 8]. A 2 mm-thick copper beam pipe with a radius of 30 mm and horizontal winglets is assumed. The horizontal winglets of the dipole vacuum chambers embed 37 cm long discrete photon stoppers made of a copper alloy (CuCrZr), designed to intercept SR photons [9–12]. The arc model features a $t\bar{t}$ FODO cell, with a length of about 52 m. Previous studies have highlighted the need for additional shielding around the photon stoppers, as well as the effectiveness of preliminary shielding concepts [13, 14]. The present arc shielding layout builds upon the configuration presented in [15], now featuring a bulkier photon stopper and a simplified shield-

* alessandro.frasca@cern.ch

Content from this work may be used under the terms of the CC BY 4.0 licence (© 2025). Any distribution of this work must maintain attribution to the author(s), title of the work, publisher, and DOI.

ISBN: 978-3-95450-262-2 ISSN: 2673-5350 doi: 10.18429/JACoW-IBIC2025-MOPMO34

# PERFORMANCE VALIDATION OF HIGH-GRADIENT X-BAND STRUCTURES AT THE UNIVERSITY OF MELBOURNE'S X-LAB

M. Volpi*, P. J. Giansiracusa[1], R. P. Rassool, P. Pushkarna, S. L. Sheehy [1],
J. Valerian, G. Taylor, The University of Melbourne, Melbourne, Australia
Y. R. E. Tan, R. Dowd, AS - ANSTO, Clayton, Australia
[1] also at ANSTO, Clayton, Australia

*Abstract*

The X-band Laboratory for Accelerators and Beams (X-LAB) at the University of Melbourne enables high-power testing of X-band accelerator technologies, including components for CERN's Compact Linear Collider (CLIC). At its core is Mel-BOX, a high-gradient test stand rebuilt from CERN's XBOX3. Two TD24 structures, previously conditioned at CERN, have been successfully re-tested, along with RF windows, SLED-I pulse compressors, and 1-meter-long loads. Beam instrumentation at X-LAB includes Faraday cups with high-resolution digitizers to measure dark current and breakdown emissions. Fast time-domain measurements along the waveguide using GHz-bandwidth oscilloscopes allow localization of breakdown events. Optical fibers detect Cherenkov light near the structures, providing complementary pulse-resolved signals. These are cross-referenced with Faraday cup data to study early-stage field emission. X-LAB integrates RF testing and diagnostics to support the development of compact, high-gradient accelerator systems.

## INTRODUCTION

To maintain luminosity with losses of less than 1 % the maximum allowable breakdown rate for the normal conducting accelerating structures operating at 100 MV/m in the final 3 TeV version of CLIC [1] is $3 \times 10^{-7}$ per pulse per meter.

To reach a gradient of 100 MV/m is require approximately 40 MW depending on the design of the structure. An extensive research program is underway to test and characterise over tens prototype CLIC accelerating structures, with a key objective being to understand and control the RF breakdown rate.

The Mel-BOX [2–5], instead of using a single high peak power klystron of ~50 MW, combines the power of two low peak power klystrons and longer pulse lengths 4.5 µs and higher repetition rates 400 Hz. High repetition rates significantly reduce conditioning time by increasing the number of pulses.

The required peak power is maintained by combining the output power of the two klystrons (~6 MW) and through SLED-Type I pulse compression [6].

Ultimately, this process allows for the production of 200 – 300 ns 50 MW pulses with a repetition rate of 400 Hz, higher than would be possible with a single klystron.

The maximum accelerating gradient in normal-conducting structures is limited by electrical breakdown, i.e. vacuum arc formation under high electric fields. The breakdown probability increases with field strength, and during conditioning the RF power is gradually increased while keeping the breakdown rate below a defined threshold, typically $5 \times 10^{-5}$ per pulse. Applying the CLIC design breakdown rate would be impractical, as conditioning a structure to maximum power would require excessive time.

A detailed understanding of breakdown dynamics is therefore essential for operating structures at high gradients. To advance this understanding, accurate time-resolved measurements of breakdown phenomena are required.

In this paper, we present an overview of the Mel-BOX layout and the results from conditioning a high-gradient TD24-N2 structure. We also report preliminary studies of an alternative method that digitizes input power and reflection/transmission signals using an oscilloscope. This approach enables localization of breakdown positions and identification of reflections along the waveguide system without breaking the vacuum.

## TEST STAND LAYOUT

A layout of the final RF network of Mel-BOX configuration is shown in Fig. 1.

The RF power from a klystron is divided by a hybrid coupler into two high-$Q$ resonant cavities, which store energy during the first few µs of the RF pulse. Near the end of the pulse, the klystron phase is reversed by 180°, releasing the stored energy as a compressed pulse with up to four to five times higher peak power but shorter duration.

Both lines are terminated with a 1 m stainless-steel RF load, with directional couplers, pumping ports, and vacuum gates completing the network. Newly designed RF windows (E42170, Canon Electron Tubes & Devices) have been installed between the klystrons and the waveguide network [7], as shown in Fig. 1, providing additional protection for the klystrons, which have long replacement lead times, particularly in Australia.

The high-gradient test stand is equipped with a comprehensive suite of diagnostics, including RF directional couplers (DC), Faraday cups (FCs), Cherenkov fibres, and radiation monitors. Among these, the FCs provide the primary measurement of charge released during both dark current emission and breakdown events as shown in Fig. 2.

Locating the position of RF breakdowns within the structure is crucial for understanding accelerator performance. The most common method relies on measuring the time dif-

* m.volpi@unimelb.edu.au

Content from this work may be used under the terms of the CC BY 4.0 licence (© 2025). Any distribution of this work must maintain attribution to the author(s), title of the work, publisher, and DOI.

ISBN: 978-3-95450-262-2 ISSN: 2673-5350 doi: 10.18429/JACoW-IBIC2025-MOPMO35

# MEASUREMENTS OF DARK CURRENT AND BREAKDOWN PROCESSES USING FARADAY CUPS AND FAST DIGITISERS AT THE XBAND LABORATORY FOR ACCELERATORS AND BEAMS (XLAB)

P. J. Giansiracusa*,[1], M. Volpi, P. Pushkarna, J. Valerian, R. P. Rassool, S. L. Sheehy[1], G. Taylor
The University of Melbourne, Melbourne, Victoria, Australia
R. Dowd, Y. E. Tan, ANSTO, Clayton, Australia
[1]also at ANSTO, Clayton, Australia

*Abstract*

CLIC TD24 accelerating structures, manufactured by CERN, are undergoing high-power testing on the 12 GHz RF test stand, MelBOX, at the x-Band Laboratory for Accelerators and Beams (XLAB). Installed in late 2024, these are the first devices tested at the facility. The goal is to condition the structures for stable operation at gradients of 100 MV/m. The maximum gradient is limited by electrical breakdown, vacuum arc formation under high electric fields, which interrupts RF transmission and can damage the structure. To study breakdown dynamics and validate models of their initiation, detailed, time-resolved charge measurements are needed. Faraday cups upstream and downstream, combined with high-performance 5 GS/s, 12-bit, 3 GHz FEB digitisers, enable precise characterisation of both dark and breakdown current emissions. Fast digitiser readout allows continuous acquisition at the 400 Hz repetition rate, capturing breakdown events and several hundred preceding pulses. This dataset supports in-depth analysis of precursors. We present initial results from structure conditioning, including breakdown statistics, dark current trends, and preliminary analysis of breakdown behaviour.

## INTRODUCTION

The Experimental Laboratory for Accelerators and Beams (XLAB) at the University of Melbourne (UoM) is now fully commissioned and operational [1]. The XLAB is the result of a long term long term collaboration between the UoM, CERN and the Australian Nuclear Science and Technology Organisation (ANSTO). The primary goal of XLAB is the testing of Compact Linear Collider (CLIC) accelerating structures and technology for the CLIC collaboration; while providing local researchers and students with opportunities to develop and refine experimental accelerator physics research skills.

The first of two CLIC TD24 accelerating structures, manufactured by CERN, is currently installed and undergoing high power high gradient testing at 12 GHz radio frequency (RF), on the test stand now known as Melbox, with the aim to verify that accelerating gradients of 100 $\mathrm{MVm}^{-1}$ are achievable and maintainable. Maximum achievable accelerating gradients are ultimately limited by the phenomenon of electrical breakdown, vacuum arc formation within the accelerating structure. The likelihood of a breakdown occurring is dependent on the applied electric field. During conditioning the RF power level is slowly increased such that the breakdown rate (breakdowns per pulse) is below the set point, nominally $5 \times 10^{-6}$ $\mathrm{pulse}^{-1}$. Ultimately, for the final stage CLIC 3 TeV design to ensure luminosity losses of less than 1 %, the maximum allowable breakdown rate at 100 $\mathrm{MVm}^{-1}$ is $3 \times 10^{-7}$ $\mathrm{pulse}^{-1}\mathrm{m}^{-1}$ [2].

Understanding the breakdown process is critical to operating accelerating structures at increasingly higher powers. To improve the understanding and further develop the theories of breakdown formation accurate measurements of breakdown phenomena are required. A range of diagnostic devices are installed on the high gradient test stand to monitor the accelerating structures during conditioning. These devices include; RF directional couplers, Faraday cups (FCs), Cherenkov fibres and radiation monitors. The FCs are the key diagnostics for measuring the current released by the structure during both normal operation (dark current) and breakdowns. As such the FC readout system was recently upgraded to include a new high-speed digitiser from Spectrum, operating at 5 GS/s, 12-bit, 3 GHz bandwidth, with the aim of better measuring temporal and transient phenomena. Preliminary results from this system are presented here.

## MELBOX - HIGH GRADIENT TEST STAND

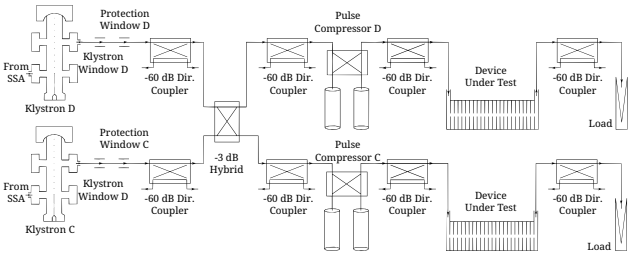



Figure 1: The MelBOX high power RF network. -60 dB directional couplers installed throughout the network are readout by NI-PXI DAQ and are the key diagnostic for monitoring and measuring RF power.

MelBOX at XLAB is half of XBOX3 that was previously installed and operated at CERN, provided to the University of Melbourne as a long term loan through the CLIC collaboration [3–6].

A National Instruments (NI) PXI crate and associated digitisers and vector signal generators form the backbone of

* gpaul@unimelb.edu.au

Content from this work may be used under the terms of the CC BY 4.0 licence (© 2025). Any distribution of this work must maintain attribution to the author(s), title of the work, publisher, and DOI.

ISBN: 978-3-95450-262-2 ISSN: 2673-5350 doi: 10.18429/JACoW-IBIC2025-MOPMO36

# REALIZATION OF A FARADAY CUP FOR THE GUN OF PERLE

M. B. Abdillah†,[1], R. Roux[1], D. Reynet[1], A. Bechtold[2]
[1]IJCLab, University Paris Saclay, Orsay, France
[2]NTG, Gelnhausen, Germany

*Abstract*

Faraday Cups (FC) have been used as diagnostic tools to measure the charged particle beam current directly. Up to now, different designs have been introduced for this purpose. In this work, a new design of Faraday cup has been performed for the gun of PERLE, a Powerful Energy Recovery Linac to be installed at IJCLab Orsay. FC's dimensions and desirable material have been considered based on PERLE Gun beam characteristics (maximum energy of 350 KeV and maximum current of 20 mA). Appropriate specifications were written for this FC. In addition, the heat power generated by electron collision with FC material has been calculated and the required cooling system has been specified. The Faraday cup is realized and tests should be run early next year to measure the electron beam current out of PERLE gun.

## INTRODUCTION

The PERLE facility represents a new generation of energy recovery machines. It operates in the 10 MW power regime, handling a beam current of 20 mA. The nominal beam energy reaches 500 MeV, marking a significant milestone in ERL development.

PERLE is designed as a compact, multi-pass energy recovery linac. Its architecture relies on superconducting radio-frequency (SRF) technology. The primary goal is to serve as a testbed for accelerator physics studies. It also provides a platform for validating technical choices for future projects.

A schematic overview of the machine is presented in Fig. 1. On the far right is the photocathode gun, which generates the electron beam. This is directly followed by the injector section, feeding the main accelerator.

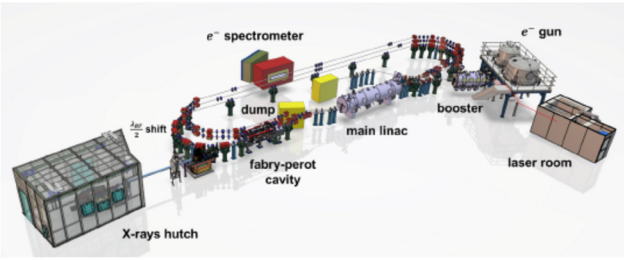



Figure 1: An overview of PERLE.

In the initial setup, the maximum beam energy is limited to 250 MeV. This energy is achieved through three successive passes in a single SRF cryomodule. The injector delivers the beam with a starting energy of 7 MeV.

The first phase, scheduled for late 2028, focuses on commissioning the injector. This includes testing the high current electron gun.

Standard diagnostics are installed, two BPMs with integrated steerers will monitor the orbit of the beam. The beam transverse profile is monitored thanks to a view screen. Finally, a Faraday cup (FC) will measure the beam current profile.

The scope of this document is to detail the specifications, the design and the realization of the Faraday cup mentioned above.

With each pass, the beam gains approximately 82.2 MeV. The intermediate energies obtained are 89 MeV, then 171 MeV. Finally, after the third recirculation, the beam reaches 250 MeV. At this point, the beam path is shifted by half an RF period. This precise phase adjustment enables the deceleration process to begin. The beam then re-enters the same linac structure in a decelerating mode.

During this stage, the previously gained energy is gradually returned to the RF system. As a result, the beam is slowed back down to 7 MeV, its injection energy. It is then directed to the beam dump, where it is safely absorbed. This operation demonstrates the principle of multi-pass energy recovery. It also validates operation at high beam current with efficient energy reuse.

Looking towards the future, a second project phase is already under consideration. This upgrade would add a second SRF cryomodule in the opposite straight section. Such an extension was anticipated in the conceptual design report [1]. The additional module would significantly enhance machine performance. In doing so, PERLE will remain a key facility for advancing accelerator research.

## FARADAY CUP SPECIFICATIONS

During the start-up and commissioning phases of PERLE gun and injector, the beam current is measured either with non-interceptive or interceptive devices. The Faraday cup is included in the latter category. It serves as beam destination and measures the beam current. Faraday cup should withstand the nominal beam pulses with a charge up to 500 pC and a repetition rate up to 40 MHz, which corresponds to a beam mean current up to 20 mA. The gun would deliver an electron beam with an energy set to 350 keV.

The Faraday cup would operate under two configurations:

- Configuration 1: a beam current up to 20 mA with a repetition rate of 40 MHz and a beam transverse size down to 3 mm RMS.
- Configuration 2: a beam current up to 5 mA with a repetition rate of 10 MHz and a beam transverse size down to 1 mm RMS.

† sidi-mohammed.ben-abdillah@ijclab.in2p3.fr

Content from this work may be used under the terms of the CC BY 4.0 licence (© 2025). Any distribution of this work must maintain attribution to the author(s), title of the work, publisher, and DOI.

ISBN: 978-3-95450-262-2 ISSN: 2673-5350 doi: 10.18429/JACoW-IBIC2025-MOPMO37

# DEVELOPMENT OF CMOS BEAM LOSS MONITOR FOR KOREA-4GSR

Bokkyun Shin[†,1], Garam Hahn[1], Dong Cheol Shin[1], Donghyun Song[1], Dotae Kim[1], Gyujin Kim[1], Seohyeon An[1], Siwon Jang[1], Changbum Kim[1], Jung Yun Huang[1], Woojin Song[2]
[1]Pohang Accelerator Laboratory, Pohang, Korea
[2]Postech, Pohang, Korea

*Abstract*

The beam loss monitor (BLM) is a diagnostic system designed to protect accelerator components from unexpected high-energy radiation. We have developed a cost-effective BLM system for the next-generation synchrotron light source, Korea-4GSR. The system utilizes plastic scintillators, optical fibers, and a CMOS camera to localize beam losses with a time resolution of 10 ms. Scintillators placed along the beam-line and emit blue light proportional to the energy deposited by loss particle. This light is transmitted through optical fibers, bundled into a 2D array, and imaged by a CMOS sensor operating at 100 Hz. The prototype, consisting of 10 BLM detectors, was calibrated using a 2.3 MBq Co-60 gamma-ray source. The end-to-end calibration results were consistent with analytical estimates. Energy deposition was simulated using Geant4, and the photon-to-ADC count conversion was characterized using a calibrated LED source. This presentation outlines the system design, calibration methodology, and performance evaluation of the prototype system.

## INTRODUCTION

Beam loss monitoring is a critical component of accelerator operations, designed to detect unexpected beam losses, protect the machine, and diagnose the causes of losses. This system was designed based on the CMOS-based beam loss monitor developed for the SLS [1]. While slower in response compared to photomultiplier tube (PMT)-based systems, the CMOS-based BLM is significantly more cost-efficient, costing approximately one-tenth of a PMT-based system.

For the Korea 4GSR accelerator, the CMOS-based BLM will be used in conjunction with PMT-based systems. The CMOS-based BLM is primarily positioned for spatial monitoring, while the PMT-based BLM focuses on timing-critical applications.

## BEAM LOSS MONITOR SYSTEM

The CMOS BLM system consists of detector and DAQ. The detector consists of a scintillator, a wavelength-shifting (WLS) fiber, and DAQ consists of a CMOS camera for optical signal readout. Figure 1 shows configuration of detector and DAQ.

The detector design evolved through two primary configurations. The first version employed a 15-meter-long scintillating fiber with a 1 mm core diameter, optimized for a large interaction volume. However, the long winding fiber introduced challenges in light collection efficiency and signal uniformity. In the second and current version, shown in Fig. 2, a flat scintillator plate (EJ-200, 100 mm × 100 mm × 10 mm) was adopted. The plate is coated with a highly reflective blue light material (EJ-510), which provides a reflectivity of 98 %. The WLS fiber was embedded in a groove along the perimeter of the plate.

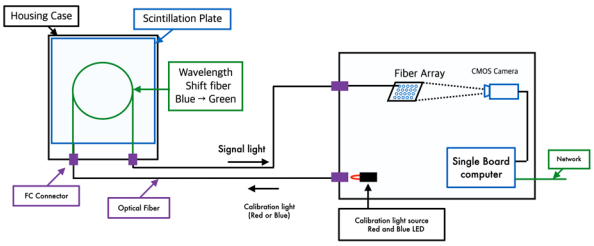



Figure 1: Configuration of the BLM System.

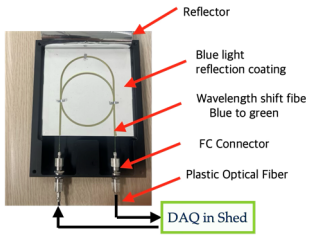



Figure 2: Configuration of Detector.

The scintillator emits photons within the 400–500 nm wavelength range, with a peak emission at 420 nm. These photons are absorbed by the wavelength-shifting (WLS) fiber, which has an absorption peak at 460 nm and re-emits green light centered at 520 nm. The re-emitted light is transmitted to the CMOS camera through a plastic optical fiber (POF; Mitsubishi GH-4001, 1 mm core diameter), which exhibits a measured attenuation of approximately 0.12 dB/m at 520 nm. The optical transmission path includes FC-type connectors to ensure modularity and ease of maintenance. The detector incorporates a dual-port configuration, enabling both signal acquisition and external light injection for calibration purposes.

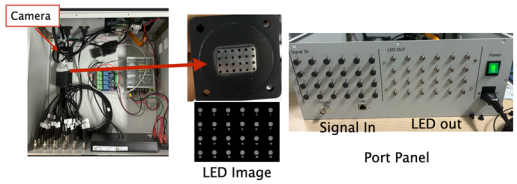



Figure 3: Configuration of the DAQ.

The data acquisition system shown in Fig. 3 employs a CMOS camera (acA720-520um, Basler) with a 10 mm lens (MCA-10, VS-Tech) to capture scintillation light. Standard

† bkshin@postech.ac.kr

Content from this work may be used under the terms of the CC BY 4.0 licence (© 2025). Any distribution of this work must maintain attribution to the author(s), title of the work, publisher, and DOI.

ISBN: 978-3-95450-262-2 ISSN: 2673-5350 doi: 10.18429/JACoW-IBIC2025-MOPMO38

# DEVELOPMENT OF CURRENT MONITOR FOR STACKING BEAM IN FETS-FFA TEST RING

E. Yamakawa*, J. FitzGibbon, Science and Technology Facilities Council, Didcot, UK
Y. Iwashita, Osaka University, Osaka, Japan

*Abstract*

Design studies of the FETS-FFA demonstration ring have been conducted as part of the ISIS-II proposal for a new high-power spallation neutron source. Beam stacking has been proposed to overcome space-charge limits in an FFA, and the feasibility of this will be evaluated in the FETS-FFA test ring by stacking up to four pulses at 50 Hz. To monitor the long-pulsed current of the coasting stacked beams over around 80 ms, the demonstration monitor of large-aperture Current Transformer (CT) with a Negative Impedance Converter (NIC) amplifier is being developed. NIC amplifier compensates the decay constant of the CT signal by cancelling the resistance of the wound coil. In addition to measuring long-pulsed coasting beam currents, the feedforward system is also added in NIC amplifier to boost the frequency band up to a few MHz to enable to measure accelerating bunch currents. This paper presents a design study of a CT monitor using a NIC amplifier and a feasibility test of a demonstration monitor detects long-pulsed signals (1 s).

## INTRODUCTION

A small-scaled prototype machine of Fixed Field Alternating gradient (FFA) accelerator, called Front End Test Stand (FETS) [1] FFA (FETS-FFA) ring [2], has been designed to demonstrate its feasibility and reliability suitable for the high-power hadron ring in the ISIS-II facility at the Rutherford Appleton Laboratory. The beam parameters are summarised in Table 1. A beam stacking is one of the unique features that allows multiple bunches to be accumulated within the ring, minimizing the effects of space charge while increasing the overall beam intensity, as demonstrated in the KURNS FFA ring [3]. As illustrated in Fig. 1, the FETS-FFA is designed to stack up to four bunches over a duration of 80 ms, operating at a frequency of 50 Hz. Conventional beam diagnostic devices for measuring coasting beam currents are direct current transformers (DCCTs) that use two identical toroidal cores. However, achieving the cores with identical properties is significant challenges for the FETS-FFA due to its large horizontal aperture to accommodate the orbit excursion from injection to extraction. As an alternative solution, a single core combined with a Negative Impedance Converter amplifier (pseudo-DCCT) [4–6] has been proposed to measure a coasting beam current for the FETS-FFA [7]. This report presents feasibility studies of pseudo-DCCT involving NIC amplifier for measuring long-pulsed beam currents. The beam position dependence of pseudo-DCCT sensitivity using NIC amplifiers will be also explained, which has not been discussed in [7] to date. A new scheme of NIC amplifier designed to enable monitoring of short pulse beam currents will be introduced.

Table 1: Beam Parameters in the FETS-FFA

| | |
|---|---|
| Beam energy range | 3 MeV-12 MeV |
| Revolution frequency range | 1 MHz-1.8 MHz |
| Harmonic number | 2 |
| Maximum beam Intensity | $3 \times 10^{11}$ppp |

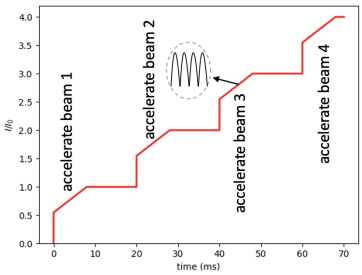



Figure 1: Time structure of beam stacking operation in the FETS-FFA.

## PSEUDO-DCCT

To investigate a feasibility and a reliability of the CT monitor for the FETS-FFA, a demonstration monitor (pseudo-DCCT) was constructed using the racetrack-shaped high-inductive core of FT3M [8] designed with a horizontal aperture of 762 mm and a vertical aperture of 122 mm, along with NIC amplifier (Fig. 2), which is larger than the tentative design of the vacuum chamber for the FETS-FFA. Four sets of 100-turns coils are wound around the core using 0.4 mm (26 gauge) Kynar wires. The RF shield box enclosing the core provides not only to mitigate RF noise but also functions as a primary coil by applying a current signal to the solid wire with a 1 kΩ resistor in series, situated between the lid of the box and the inner protrusion. In Fig. 2, to reduce the effect of parasitic resonance, the laminated cross-section side (upper and lower surfaces) of the core was covered with aluminium foils on top of the coil winding. Two input BNC ports, named port1 (edge of the monitor aperture) and port2 (centre of the monitor aperture), were positioned on the center line of the protruding copper structure.

### *NIC Amplifier*

Figure 3 illustrates a diagram of the demonstration Negative Impedance Converter (demo-NIC), a transimpedance amplifier designed for the FETS-FFA. By satisfying the condition of resistors $R_{s-}R_{f+} = R_{s+}R_{f-}$ in the input impedance of $Z$ given by

$$Z = \frac{R_{s-}R_{f+} - R_{s+}R_{f-}}{R_{f+}}, \quad (1)$$

* emi.yamakawa@stfc.ac.uk

Content from this work may be used under the terms of the CC BY 4.0 licence (© 2025). Any distribution of this work must maintain attribution to the author(s), title of the work, publisher, and DOI.

ISBN: 978-3-95450-262-2 ISSN: 2673-5350 doi: 10.18429/JACoW-IBIC2025-MOPMO39

# DEVELOPMENT OF WALL CURRENT MONITOR ON FETS-FFA TEST RING

E. Yamakawa*, I. Gardner, K. Fazlee, Science and Technology Facilities Council, Didcot, UK

*Abstract*

Conceptual design studies of the FETS-FFA demonstration ring have been actively performed to confirm the reliability of a Fixed Field Alternating gradient (FFA) accelerator for a future high-power spallation neutron source, called ISIS-II. A wall Current Monitor (WCM) is a choice of non-destructive intensity monitor to evaluate the circulating proton beams from 3 MeV (about 1 MHz in revolution frequency) to 12 MeV (about 2 MHz in revolution frequency) in the FETS-FFA test ring. As the beam orbit shifts radially with beam energy in FFAs, the aperture of FETS-FFA WCM will be about 700 mm horizontally. The maximum mean circulating beam current is about 100 mA and tomographic and Schottky measurements require a bandwidth of 370 MHz (100 harmonics). This is a challenge for such a large monitor. A half-width demonstration WCM (demo-WCM) was designed and manufactured to benchmark numerical simulations and to understand monitor responses. Whilst measured frequency band was shorter than expected, 1% intensity resolution was achieved in demo-WCM. In this paper, the detail design study as well as the signal response of the demo-WCM will be presented.

## INTRODUCTION

The FETS-FFA test ring is a small-scaled demonstration FFA accelerator to confirm its reliability and suitability for high-power operation in ISIS-II facility [1]. The frequency bandwidth required for a beam current monitor is from the fundamental frequency (a few MHz) up to 100 harmonics of the RF frequency at 3.74 MHz. This range is sufficient for tomographic measurements and is adequate for Schottky measurements for the FETS-FFA. To meet the requirements, a WCM has been chosen as the bunched beam intensity monitor for the FETS-FFA. The challenge in designing the FETS-FFA WCM is to achieve the physics requirements while accommodating a large horizontal aperture that covers the excursion from injection to extraction (~700 mm). The propagation patterns of the image current across the resistance will also vary with beam positions, leading to different time responses on each resistor and affecting the frequency characteristics of the monitor. To better understand the signal response from a large aperture of WCM, a half-scale demo-WCM was designed and tested at Rutherford Appleton Laboratory.

## DESIGN OF DEMO-WCM

While the tentative design of vacuum chamber for the FETS-FFA features a racetrack shape with an internal aperture of 700 mm×80 mm, the chamber size of demo-WCM was constructed by 344.5 mm×50 mm to handle and test the monitor more easily, allowing for efficient evaluation of its performance characteristics. The vacuum gap was filled by alumina ceramics ($\epsilon$=9.4) owing to its good strength and thermal stability. According to the stress analysis conducted on a similar ceramic spacer for the RF cavity, the minimum thickness of the ceramic gap was determined to be 22 mm in the FETS-FFA. This will need to be tested under vacuum in the future. The characteristic impedance of ceramic gap ($Z_c$) can be computed by $Z_c = 377 \cdot d/W/\sqrt{\epsilon_r}$ where $d$ is the gap length and $W$ is the mean circumference of the ceramic gap with the dielectric constant of $\epsilon_r$. By adopting the gap length of 22 mm and thickness of 22 mm in the demo-WCM, the characteristic impedance of the ceramic gap is estimated to be 2.96 Ω ($R_g$), providing a higher cutoff frequency of about 710 MHz along with an estimated capacitance of 76.2 pF for the ceramic gap. The ceramic spacer was covered by a flexible PCB where chip resistors were attached in parallel to the beam direction. Two different cores: FT3M [2] and FR68 [3] were prepared for testing, similar to the WCM used in Fermilab [4]. These cores aim to achieve a bandwidth of several GHz by employing different cores. The interior size of the racetrack shape of the core is 414.5 mm×75 mm with thickness of 25 mm and the length of 25 mm. The monitor components were fastened to the chamber flanges using bolts and enclosed within a shield box made by 1.2 mm copper sheets. Three input ports were positioned at the centre of the monitor aperture with resistors of 1 kΩ, allowing for the measurement of monitor responses at different input positions within the aperture. Six solid wires were placed along the PCB board, both in the middle and at the edges of the aperture, to read out the output signals as shown in Fig. 1.

## FREQUENCY RESPONSE

Analytical formulae of the equivalent circuit of the monitor show the expected frequency bandwidth in Table 1 with the expected capacitance ($\epsilon_0\epsilon_r S/d$) of the ceramic gap ($d$) of 76.2 pF, the measured resistance of 3.12 Ω across the ceramic gap and measured inductance of 17.0 μH in FT3M, 0.98 μH in FR68 and 17.1 μH in combined FT3M and FR68 respectively.

Table 1: Expected Bandwidth for Different Cores with the Inductance of Cores at 10 kHz for FT3M and at 1 MHz for FR68 Measured by the LCR Meter

| Cores | Lower [kHz] | Higher [MHz] |
|---|---|---|
| FT3M | 31 ($\mu_r$ at 10 kHz) | 670 |
| FR68 | 22 ($\mu_r$ at1 MHz) | 670 |

* emi.yamakawa@stfc.ac.uk

Content from this work may be used under the terms of the CC BY 4.0 licence (© 2025). Any distribution of this work must maintain attribution to the author(s), title of the work, publisher, and DOI.

ISBN: 978-3-95450-262-2 ISSN: 2673-5350 doi: 10.18429/JACoW-IBIC2025-MOPMO40

# DEVELOPMENT OF AN IMAGING PROTOCOL FOR LASER DRIVEN X-RAY SOURCES

E. Kiely*,[1], M. A. Williams, J. M. Warnett, WMG, University of Warwick, Coventry, UK
K. Fedorov, O. Finlay, A. Bhardwaj, C.D. Armstrong, D. R. Symes, STFC, Oxford, UK
J. Giles-Friend[1], Swansea University, Swansea, UK
A. Bennett[1], University of Nottingham, Nottingham, UK
[1]also at Central Laser Facility, STFC, Oxford, UK

*Abstract*

The Extreme Photonics Applications Centre (EPAC) being built at the Central Laser Facility in the UK will utilise a 10 Hz Laser Wakefield Accelerator (LWFA) to produce a directional, tuneable X-ray source, with energies ranging from 3 keV up to 10s of MeV while maintaining a micron-scale source size and ultra-short pulse duration. A combination of such characteristics opens an opportunity for cutting-edge high-resolution industrial imaging of dense materials: battery packs, historical artefacts and dynamic processes: fluid flows, motor engines running. The primary challenge for imaging with LWFA X-ray sources stems from shot-to-shot instabilities of flux, energies and pointing. Using simulations and real-world data these effects are shown, with different methods for accounting for each demonstrated and discussed.

## INTRODUCTION

Diagnostic X-ray imaging is a powerful multi-disciplinary tool for non-destructive inspection of objects that require internal viewing without disassembly. Current X-ray sources (X-ray tubes, synchrotrons, and linear accelerators (LINACS)) used in computed tomography provide the range of energies and X-ray characteristics that are needed to image objects with a range of sizes and for objects requiring low keV up to multi-MeV X-rays to penetrate. Each has its own limitations, and the brightest and most powerful among them such as LINACs and synchrotrons are not readily available to most users. Laser wakefield accelerators (LWFA) are capable of overcoming some of the challenges seen with conventional sources, producing both monochromatic and polychromatic X-rays from a few keV up to 10s of MeV with a micron-scale source size. LWFAs can also be designed for lab-scale use making it possible to have a synchrotron-like light source readily available at multiple facilities. As the technology for using LWFA is relatively new, there are characteristic effects of LWFA that need to be addressed to make these sources commercially viable for industrial imaging. This includes instabilities in the X-ray flux, the position of the X-ray source jittering shot-to-shot, and the X-ray source having a 3D structure.

The Central Laser Facility has a dedicated experimental area (Gemini TA2) for developing a high repetition LWFA where the facility can test the diagnostics, protocols and equipment that will be used at the Extreme Photonics Applications Centre (EPAC), which is due to open to users in 2027. Currently the experimental area has focused on characterising the stability of the accelerator and the factors that affect electron acceleration. With the addition of an X-ray camera suitable for the energies generated and frame rates that meet the 5 Hz repetition rate of the laser, the focus can shift towards characterising and developing protocols for X-ray imaging.

This paper aims to outline the effect that the characteristics of LWFA sources have on their imaging capabilities and to propose methods to limit their influence.

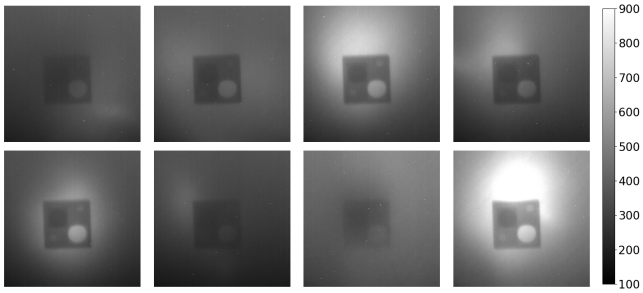



Figure 1: Images taken using MeV X-rays generated by inverse Compton scattering at the GEMINI TA3 target area. The images shown demonstrate the flux instabilities seen using LWFA for generating X-rays.

## X-RAY FLUX INSTABILITIES

While the brightness of LWFA x-ray sources is extremely high, their average flux is limited by the laser repetition rate, typically producing a total flux of $10^7$-$10^{11}$ photon/s [1, 2] depending on the generation mechanism. This is low compared to conventional sources that have a flux ranging from $10^{13}$-$10^{16}$ photons/s [2–4]. This means that for imaging at very high resolution, or with strong absorption, multiple shots might be needed to obtain high-contrast, low-noise radiographs. This can be trivial for some applications as only the acquisition time per radiograph is affected, but the flux shot-to-shot from LWFA is also unstable, as seen in Fig. 1. To address these issues two approaches are being tested. First is to attempt to stabilise the flux between shots and the second is to optimise the X-ray flux from the LWFA.

Shot-to-shot fluctuations are difficult to correct for without changing the structure of the laser being used, which can

* evan.kiely@warwick.ac.uk

Content from this work may be used under the terms of the CC BY 4.0 licence (© 2025). Any distribution of this work must maintain attribution to the author(s), title of the work, publisher, and DOI.

ISBN: 978-3-95450-262-2 ISSN: 2673-5350 doi: 10.18429/JACoW-IBIC2025-MOPMO42

# MEASURING THE EFFECTS OF FAST BEAM LOSS ON THE ADVANCED PHOTON SOURCE UPGRADE STORAGE RING COLLIMATORS*

J. C. Dooling†, A. J. Dick, M. Borland, R. Lindberg, G. Navrotski, W. Cheng
Argonne National Laboratory, Lemont, IL, USA
D. Lee, S. Riedel, University of California Santa Cruz, Santa Cruz, CA, USA
N. Cook, RadiaSoft, LLC, Boulder CO, USA

*Abstract*

The Advanced Photon Source Upgrade (APS-U) storage-ring (SR) is equipped with five horizontal collimators used to intercept 6-GeV electrons during fast whole-beam aborts and protect the rest of the SR. The collimators are located in sectors 37, 38, 39, 40, and 1. A fan-out kicker (FOK) system has been installed to reduce damage to the collimators during whole-beam loss events. Since APS-U began commissioning in April 2024, dozen of these events have taken place; in most, but not all cases, the FOK system has worked properly. Turn-by-turn beam position monitors provide beam dynamics data during the loss events. However, limited diagnostics prevent in situ evaluation of the collimator beam-facing jaw surfaces. During August 2024 and January 2025 maintenance periods, some of the collimators were extracted from the vacuum chamber and examined. Faint beam strike damage was observed on the S01 collimator jaw, but more significant effects were seen on the S38 jaw. Additional examinations were conducted in May and August 2025. Measurements of beam motion during fast aborts are presented as well as microscopy images of the S38 damage. Coupled simulations results are compared with observations.

## INTRODUCTION

Horizontal aluminum collimators have been placed in sectors 37, 38, 39, 40 and 01 (S37-S01) of the Advanced Photon Source Upgrade (APS-U) storage ring (SR) to intercept electrons lost via Touschek scattering, injection halo, and fast beam aborts; here we focus on the effects from fast aborts. The collimators are located in the high-dispersion region between the A:S1 sextupole and A:Q4 reversed-bend magnets in all five sectors [1, 2]. A plan view of the collimator assembly is presented in Fig. 1. The collimators play a vital role in protecting beam-facing surfaces from direct strikes during fast whole-beam loss events.

The APS-U machine protection system (MPS) receives a number of inputs employed to assess the status of the circulating 6-GeV electron beam. These inputs come from many sources including beam position limit detectors (BPLDs) beam position monitors (BPMs), rf system status indicators, and radiation monitors. Earlier experiments conducted in the former APS SR showed damage occurring in test pieces struck by beams meant to evaluate possible collimator material and geometry [2].

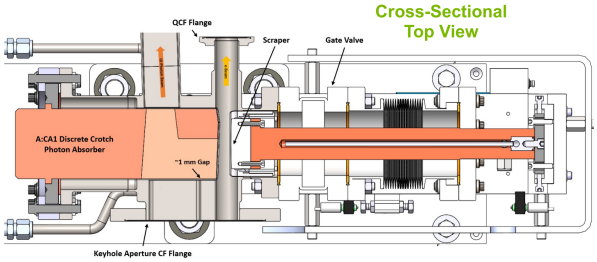



Figure 1: Plan view of the horizontal collimator assembly.

## OBSERVATIONS AND MEASUREMENTS

A vertically-deflecting fan-out kicker (FOK) is designed to protect the five horizontal collimators in the APS-U storage ring (SR) during a fast beam abort [3]. The FOK does this by providing a vertical kick to the beam after a triggering event. The vertical kick lowers the power density by both "painting" the beam vertically on the surface of the collimators as well as decohering or expanding the transverse cross section, in this sense its function is similar to that of the decoherence kicker [4]. To be effective, the FOK must be triggered concurrently with the command given to mute the rf to allow sufficient time for decoherence. Measurements indicate the FOK typically triggers $\approx 7$ μs after rf muting; this is considered an acceptable delay.

Recent data collected by the data acquisition (daq) turn-by-turn (TBT) postmortem (POMO) system have shown that this sequence is not always followed. In the following section, examples are given for when the FOK is triggered properly as well as triggered late during beam loss events.

### *Turn-by-Turn Data*

TBT BPMs provide approximately 1-second of data around fast beam loss events triggered by the MPS. The machine timing event system, designated by the initial MRF provides triggering events for many accelerator systems including the TBT BPMs as well as the FOK. The MPS sends a signal to the MRF when conditions require the stored beam to be dumped. The MRF then issues an event (104) which triggers the FOK thyratron; the resulting magnetic field bumps the bunch train vertically. The rf drive to the cavities is also muted at this time which causes the beam to spiral inboard.

* Work supported by the U.S. D.O.E.,Office of Science, Office of Basic Energy Sciences, under contract number DE-AC02- 06CH11357.
† dooling@anl.gov

Content from this work may be used under the terms of the CC BY 4.0 licence (© 2025). Any distribution of this work must maintain attribution to the author(s), title of the work, publisher, and DOI.

ISBN: 978-3-95450-262-2 ISSN: 2673-5350 doi: 10.18429/JACoW-IBIC2025-MOPMO43

# BEAM LOSS MEASUREMENTS DURING INJECTION INTO THE ADVANCED PHOTON SOURCE UPGRADE STORAGE RING*

J. Dooling†, A. Brill, J. Calvey, W. Cheng, V. Sajaev, Argonne National Laboratory, Lemont, USA

*Abstract*

A fiber-optic (FO) beam loss monitor (BLM) system, installed along the booster to storage ring (BTS) transport line has been useful in identifying loss locations employing time-of-flight (TOF) analysis. The BTS BLM TOF system is comprised of a pair of rad-hard, fused-silica FO cables running along either side of the BTS line at beam elevation. In the initial configuration, we measured losses at both the upstream (US) and downstream (DS) ends of the FO cable pair. However, losses further DS along the septum and injection kicker set are also of interest. We therefore added a 20-m-length, multi-strand fused-silica FO cable bundle, replacing the DS outer FO radiator input. Thus, three of the detectors are configured at the US end of their respective FO radiators. The US detector location provides lower signal but improved spatial resolution over the DS. Loss location identification has been accomplished by inserting YAG screen flags at different positions along the BTS. We present results from studies and operations.

## INTRODUCTION

We previously described a fiber-optic (FO) time-of-flight (TOF) fast beam loss monitor (BLM) system installed in the booster-to-storage ring (BTS) transport line at the Advanced Photon Source (APS) [1]. This system was recently modified to allow a 20-m length of fiber radiator to extend from the downstream (DS) photomultiplier tube (PMT) detector location further downstream to just beyond the S40 horizontal collimator. The DS detectors are located under the DQ2 magnet (Fig. 1). The upstream (US) detectors are located under the AQ1 magnet just after the booster extraction kickers (Fig. 1, top). Both detector locations are Pb-shielded. The installation of the new FO cable was done during the January 2025 maintenance period. Initially, the downstream end of this fiber bundle was pulled just past the swap-out dump in the S40 A:M1 dipole magnet. This arrangement left approximately 2 meters of slack at the US end of the cable. During the May 2025 maintenance period, the slack was removed and the FO cable end was pulled an additional 2-m further downstream. This FO cable now extends downstream of the injection septum and kickers as well as past the swap-out dump and the S40 horizontal collimator locations.

## ANALYSIS

Several challenges must be overcome in order to determine loss position. First, beam loss will shower downstream from its strike location. Second, the speed at which light travels

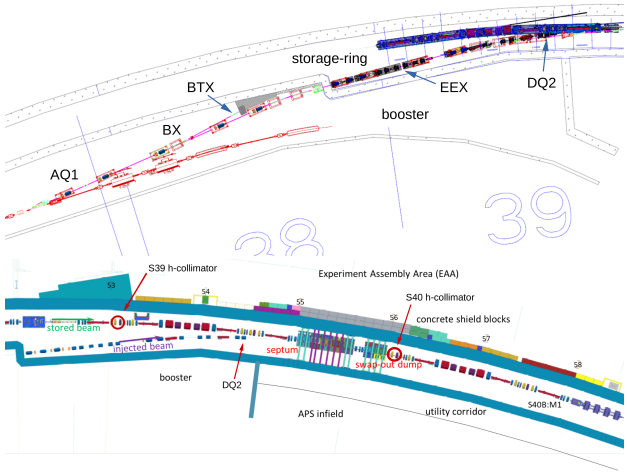



Figure 1: The booster to storage-ring (BTS) transport line. Top: The US PMT detectors are located under the AQ1 magnet, and the downstream detectors under the DQ2 magnet. Both are locations are Pb-shielded. Bottom: The added FO cable radiator now extends downstream past the S40 h-collimator location.

in the fused silica fiber used here is wavelength dependent. The fiber index of refraction, $n_f$ can be determined using Malitson's expression [2] for a given wavelength between 210 and 3710 nm. Čerenkov radiation is relatively broadband; however it does favor the blue end of the spectrum. The Hamamatsu R7400U-06 subminiature photomultiplier tube (PMT) employed here to convert light to electrical signals has an extended UV range [3]. The cathode radiant sensitivity is near 20 mA/W at 200 nm, rising to 34 mA/W at 260 nm.

Prior to saturation, gain as a function of bias voltage, $V$ for this PMT family is expressed as [4],

$$G(V) = G_o \left(\frac{V}{V_o}\right)^{N_d - 1}, \quad (1)$$

where $G_o = 5 \times 10^5$ at $V_o = 800$ V and $N_d$ is the number of dynodes; here $N_d = 8$.

The PMT signals from each of the four channels are recorded on a 2.5-GHz bandwidth Teledyne-Lecroy Model 9254M oscilloscope. The time signals can be mapped into spatial positions, $s_u$ and $s_d$ along the BTS line using a simple model presented in Eqs. (2) and (3), respectively [5].

$$s_u(t) = \frac{c(t - t_{ref,u})}{n_f + 1}, \quad (2)$$

$$s_d(t) = -\frac{c(t - t_{ref,d})}{n_f - 1}, \quad (3)$$

* Work supported by the U.S. D.O.E.,Office of Science, Office of Basic Energy Sciences, under contract number DE-AC02- 06CH11357.

† dooling@anl.gov

Content from this work may be used under the terms of the CC BY 4.0 licence (© 2025). Any distribution of this work must maintain attribution to the author(s), title of the work, publisher, and DOI.

ISBN: 978-3-95450-262-2 ISSN: 2673-5350 doi: 10.18429/JACoW-IBIC2025-MOPMO45

# FERMILAB PIP-II MACHINE PROTECTION SYSTEM DIGITIZED DATA NOISE ELIMINATION SCHEME AND ITS FPGA IMPLEMENTATION*

J. Wu†, A. Warner, Fermi National Accelerator Laboratory, Batavia, IL, USA

Content from this work may be used under the terms of the CC BY 4.0 licence (© 2025). Any distribution of this work must maintain attribution to the author(s), title of the work, publisher, and DOI.

*Abstract*

In Fermilab's PIP-II machine protection system, beam loss signals from various detectors are digitized at 125 MS/s. Noise from both high-frequency sources and low-frequency 60 Hz AC power equipment can contaminate the data. To suppress noise across these ranges—especially 60 Hz and its harmonics, which overlap with beam loss signal frequencies—advanced digital processing beyond standard filtering is required. Several real-time functional blocks were simulated and tested on an FPGA: (1) a dual time-constant discharging integrator filter, (2) a de-ripple baseline extraction and storage block, and (3) a fast-recovery discharging integrator. The nonlinear IIR integrator filter removes high-frequency noise and feeds into the baseline extractor. Upon detecting abrupt beam loss, it switches to a longer time constant to prevent baseline distortion. The de-ripple block calculates a valid baseline by averaging over multiple 60 Hz periods, storing results in a 4096-word FPGA RAM. This baseline is subtracted from raw data before integration by the fast-recovery block, which resets quickly after use. All blocks achieved the expected performance.

## INTRODUCTION

Fermilab's PIP-II [1] features a brand-new, 800 MeV leading-edge Linear Accelerator (Linac) that will enable the Fermilab complex to deliver more than a megawatt of beam power to the Long Base-line Neutrino Facility (LBNF). The system includes a Warm Front-end (WFE) and a 300-meter beam transfer line to the Fermilab Booster. The WFE generates a 30 keV H- beam, defines the beam parameters and accelerates the beam to an energy of 2.1 MeV with its RFQ and provides require bunch patterns. Capitalizing on advances in superconducting radio-frequency technology, five types of superconducting cavities will accelerate the H- ions to 800 MeV for injection into the Booster. Upgrades to the Booster, Main Injector and Recycler rings will enable them to operate at a 20 Hz repetition rate and will provide 1.2 MW proton beam for the Long Baseline Neutrino Facility (LBNF). Figure 1 shows the layout of the complex.

The entire accelerator complex will be protected with a machine protection system (MPS) [2]. Beam current impinging on scrapers and other invasive devices and noninvasive beam current signals from ACCTs and Ring Pickups primarily in the WFE are used to determine loss thresholds and transmission losses at strategics locations in the accelerator. In the scheme for Linac protection system, the beam loss signals from these various detectors are digitized at 125 MS/s. The digitized signals are processed to extract instantaneous and differential beam loss information in the WFE along with critical operating status that ensures the accelerator complex is operating in a safe region that avoids beam and radiation damage from excessive losses. In the digitized data, noise from both high-frequency sources and low-frequency 60 Hz AC power equipment can contaminate the data, and the noise must be carefully measured and eliminated before reliable processing can be performed.

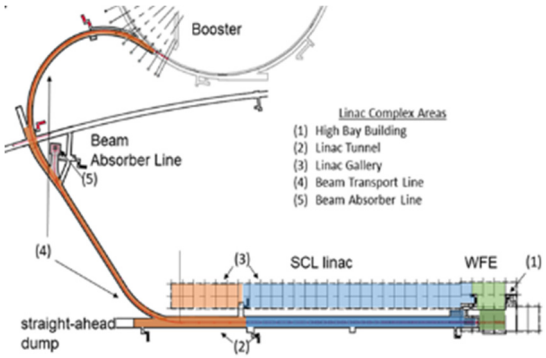



Figure 1: The layout of the PIP-II complex.

To suppress noise across these ranges—especially 60 Hz and its harmonics, which overlap with beam loss signal frequencies—advanced digital processing beyond standard filtering is required.

The block diagram of the ADC and noise elimination functional block is shown in Fig. 2.

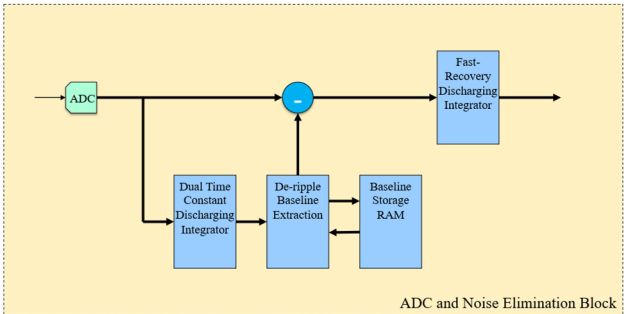



Figure 2: The diagram of the noise elimination functional blocks.

The noise elimination block consists of several real-time functional blocks implemented in an FPGA serving the ADC: (1) a dual time-constant discharging integrator filter, (2) a de-ripple baseline extraction and storage block, and (3) a fast-recovery discharging integrator.

* This manuscript has been authored by FermiForward Discovery Group, LLC under Contract No. 89243024CSC000002 with the U.S. Department of Energy, Office of Science, Office of High Energy Physics.

† email: jywu168@fnal.gov

ISBN: 978-3-95450-262-2 ISSN: 2673-5350 doi: 10.18429/JACoW-IBIC2025-TUAI01

# HIGH-THROUGHPUT DPDK-BASED FRAMEWORK FOR REAL-TIME APPLICATIONS IN ELETTRA 2.0

G. Gaio†, A. Bogani, G. Brajnik, R. De Monte, G. Scalamera, I. Trovarelli
Elettra-Sincrotrone Trieste S.C.p.A., Trieste, Italy

*Abstract*

The Data Plane Development Kit (DPDK) is a framework that enhances real-time communications by providing direct, high-speed access to network interfaces. This architecture centralizes acquisition and control in an HPC cluster, ensuring ultra-fast in-memory updates of all critical data, making it a viable choice for real-time feedback and machine control in particle accelerators.

This approach was chosen for Elettra 2.0 to enable premortem beam dump mitigation, more detailed post-mortem inspection, advanced correlation analysis and the implementation of complex control schemes. Time-sensitive applications implemented in C code interact with Beam Position Monitors (BPM), Low-Level RF (LLRF), Beam Loss Monitors (BLM) and Magnetic Power Supplies (PS) through simple memory read and write operations at megahertz rates, making the system competitive with high-level processing applications based on FPGA architectures.

This paper presents the system under test before the decommissioning of Elettra, highlighting its architecture, performance, and integration, while demonstrating the successful implementation of Fast Orbit Feedback in parallel with Turn-by-Turn (TbT) data acquisition from 7 BPM electronics and one LLRF system.

## INTRODUCTION

Particle accelerators such as synchrotrons require precise real-time control to ensure beam stability, optimize performance, and avoid costly disruptions. Elettra, a third-generation light source in Trieste, is being upgraded to Elettra 2.0, a fourth-generation diffraction-limited storage ring aimed at higher brightness, coherence, and stability, demanding real-time systems capable of handling data at MHz rates.

The gradual adoption of DPDK at both FERMI and Elettra has replaced legacy real-time stacks such as Xenomai and RTAI, while building expertise in using DPDK as a scalable platform whose performance grows with CPU core counts and NIC bandwidths. At the same time, demand for online, high-frequency data has increased, exposing the complexity and rigidity of traditional schemes based on hardware triggers, local buffers, and offline processing.

With DPDK, TbT (1.15 MHz) and other high-rate signals can instead be handled as streaming data, processed in-memory in real-time for filtering, decimation, and analysis. This reduces latency, removes ad hoc buffering and heavy post-processing, and allows diagnostics and control loops to scale naturally on commodity server hardware.

## DATA PLANE DEVELOPMENT KIT

The Data Plane Development Kit (DPDK) is an open-source project under the Linux Foundation, governed by a Governing Board and a Technical Board, with members as chipmakers market leaders such as Intel, AMD, Arm, NVIDIA, Marvell and Broadcom, telecommunications vendors such as Ericsson, Huawei and ZTE and cloud and software providers as Microsoft and Red Hat.

The DPDK community has over 200 contributors, with recent releases featuring around a thousand commits from approximately 150 authors each.

DPDK operates on principles of kernel bypass through poll-mode drivers (PMDs), core isolation to dedicate CPU cores for packet processing, user-space programming to avoid kernel overhead, and minimizing system calls for high performance. It is widely used in User Plane Functions (UPF) for 5G telephony and by hyper-scalers like AWS, Azure, and Google Cloud, where it is offered as an option for high-performance networking in virtual machines.

## ROUND TRIP TIME

The well-established Round-Trip Time methodology (RTT) has been adopted to validate DPDK performance, testing it as a minimal model of a control system cell. In this configuration, two ports on the same host are connected through a loopback cable, with transmission and reception handled by separate processes pinned to dedicated CPU cores (Fig. 1). This arrangement abstracts the essential structure of a feedback loop, where the RTT provides a direct measure of end-to-end latency. In time-critical applications, one-way latency is conventionally taken as half of RTT, serving as a metric for system suitability in real-time control.

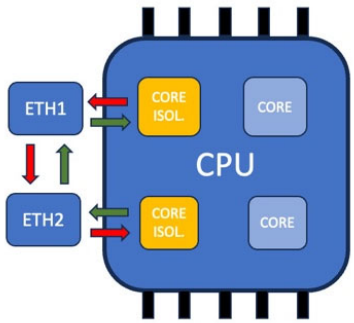



Figure 1: Round Trip Test setup on a single machine using two Ethernet ports.

Content from this work may be used under the terms of the CC BY 4.0 licence (© 2025). Any distribution of this work must maintain attribution to the author(s), title of the work, publisher, and DOI.

ISBN: 978-3-95450-262-2 ISSN: 2673-5350 doi: 10.18429/JACoW-IBIC2025-TUAI02

# TOWARDS CONTINUAL MACHINE LEARNING FOR PARTICLE ACCELERATORS*

K. Rajput†, [1, 2], M. Schram[1], W. Blokland[3], A. Zhukov[3], S. Lin[2]
[1]Thomas Jefferson National Accelerator Facility, Newport News, VA, USA
[2]Department of Computer Science, University of Houston, Houston, TX, USA
[3]Oak Ridge National Laboratory, Oak Ridge, TN, USA

*Abstract*

Machine Learning (ML) has become an essential tool in modern scientific and engineering applications, enabling predictive modeling for complex systems. Many particle accelerator facilities are adopting ML-based solutions to accelerate time-consuming optimization tasks through fast inference, and to enable low-latency anomaly prediction. However, ML models assume stationary data distribution, as such, when data distribution drifts away from the training data, ML models' performance degrade. In particle accelerators, data drift is inevitable. These drifts can originate from either changes in the machine settings or non-measured factors such as equipment degradation. In this paper, we present an application of rehearsal based continual learning method to maintain model performance on drifting data. We present an ML surrogate to reconstruct beam current data from Spallation Neutron Source accelerator that can be used for downstream tasks such as anomaly detection. We use the data from different beam settings that demonstrate systematic known shift in the data. We demonstrate that a model trained incrementally on new data lose performance on previous data distributions due to catastrophic forgetting. In contrast, integrating rehearsal based continual learning can maintain model performance in such scenarios and limit forgetting on previous data distributions.

## INTRODUCTION

Particle accelerators are among the most complex and fast paced scientific instruments in the world, supporting a wide range of applications from high-energy physics to medical diagnostics and material science. The efficient operation and optimization of these facilities require continuous monitoring, calibration, and adaptation in response to changing machine conditions, environmental factors, and evolving experimental requirements. Traditional diagnostics and control strategies, while effective, are often limited by their static nature and inability to generalize across varying operational regimes.

In recent years, machine learning (ML) methods have emerged as powerful tools for diagnostics and control applications within particle accelerators [1]. These approaches are shown to be very good at learning complex, nonlinear dynamics directly from data, enabling more flexible and adaptive modeling schemes. However, a significant limitation of ML techniques, particularly Deep Neural Networks (DNN) is their reliance on fixed training datasets and their tendency to degrade in performance when exposed to new or non-stationary data—a phenomenon known as catastrophic forgetting.

At the Spallation Neutron Source (SNS) accelerator, efforts are underway to develop ML based solutions for preemptive anomaly prediction, optimization of beam losses and anomaly detection in target system. The ML models perform well in short time scales and offline data, however faces significant performance degradation in deployment due to data drifts. Previous studies have adopted conditional models [2] to mitigate the effects of data drifts due to changes in beam settings. However, it is not feasible to train the conditional models on all the possible conditions expected during operation. In addition, conditional models alone can not address drifts caused by non-measured factors such as equipment degradation. As such, we have steered towards developing a self-sustained adaptive ML framework that integrates advance techniques to continuously update ML models to account for data drifts.

Continual learning [3], also referred to as lifelong learning, addresses this challenge by enabling models to learn from a stream of data over time without forgetting previously acquired knowledge. This paradigm is particularly well-suited for particle accelerator environments, where operational conditions can vary significantly across time scales, and where retaining knowledge of past configurations is critical for stable and efficient performance. By integrating continual learning into accelerator diagnostics and control systems, we can build models that not only adapt to new regimes but also retain robustness and generalization across diverse conditions.

In this paper, we present current progress on errant beam prognostication use case at SNS accelerator. The study integrates continual learning techniques, particularly, memory-based methods, to maintain performance of a Conditional Auto-Encoder (CAE) when switching among different beam settings. We demonstrate that integration of continual learning stabilizes model performance even when underlying data drifts. This shows that continual learning holds promises to bridge the significant gap between ML development and long term deployment in particle accelerators.

* This work was supported by the DOE Office of Science, United States under Grant No. DE-SC0009915 (Office of Basic Energy Sciences, Scientific User Facilities Program). This manuscript has been authored by UT-Battelle, LLC, under Contract DE-AC05-00OR22725 with the US Department of Energy (DOE). The Jefferson Science Associates (JSA) operates the Thomas Jefferson National Accelerator Facility for the U.S. Department of Energy under Contract No. DE-AC05-06OR23177.
† kishan@jlab.org

Content from this work may be used under the terms of the CC BY 4.0 licence (© 2025). Any distribution of this work must maintain attribution to the author(s), title of the work, publisher, and DOI.

ISBN: 978-3-95450-262-2 ISSN: 2673-5350 doi: 10.18429/JACoW-IBIC2025-TUBC01

# ISOLATING THE LIGHT OF A SINGLE BUNCH: DETERMINING THE VIABILITY OF OPERATING VERTICAL-PLANE PULSE PICKING BY RESONANT EXCITATION AT DIAMOND-II TO SERVE TIMING MODE USERS

S. Wilkes*, P. N. Burrows, John Adams Institute, Oxford, United Kingdom
L. Bobb, B. A. Coulson, G. Karras, A. F. D. Morgan, M. R. Warren
Diamond Light Source, Didcot, United Kingdom

Content from this work may be used under the terms of the CC BY 4.0 licence (© 2025). Any distribution of this work must maintain attribution to the author(s), title of the work, publisher, and DOI.

*Abstract*

Pulse Picking by Resonant Excitation (PPRE) enables synchrotron facilities to provide single-bunch light for timing users without interrupting multi-bunch operation. We report the first vertical-plane PPRE tests at Diamond using the Multi-Bunch Feedback system, achieving vertical bunch-size growth and measurable X-ray enlargement. A simple novel optimisation improved PPRE purity by reducing the baseline emittance. Beyond readily-available diagnostics, we demonstrate how crystallographic diffraction can be used as a user-relevant method to characterise PPRE with statistically significant evidence of isolating a single excited bunch. Together, these methods provide a practical and user-orientated framework for synchrotron facilities considering similar timing-mode capabilities.

## INTRODUCTION

Whilst most scientific users of a synchrotron facility require maximal brilliance, the "flux users", some scientific users instead prioritise temporal resolution – the "timing users". Example experiments may include pump-probe measurements [1], or studying the dynamics of a chemical process [2]. Diamond currently offers timing users a hybrid fill-pattern, which ensures the target X-ray pulse has an unlit gap either side of it [3]. For Diamond-II, there are additional constraints on fill patterns, beam lifetime, and instability thresholds [4] that may result in the hybrid fill not being offered. A back-up approach is sought.

PPRE is a method, first developed at BESSY, to simultaneously cater to timing users and regular ('flux') users [5]. Conceptually, PPRE works by isolating the light from a single bunch, such that the beamline effectively only sees a single bunch (thus X-ray pulse) in the ring. The two key ingredients for PPRE are the deliberate increase in the size of the X-ray beam and the amount by which the unwanted bunch light is blocked by the beamline optical-apertures. The unwanted bunches are known as the 'train'; for PPRE, any light from the train that reaches the experimental area constitutes background. A schematic of PPRE is shown in Fig. 1. To increase the vertical X-ray beam size requires to first increase the electron bunch size. At Diamond this can be done with the Multi-Bunch Feedback (MBF) system (for details, see [6]). Owing to its flexibility, users would have the option to select arbitrary bunches to excite, allowing for experiment-tailored X-ray pulse structures.

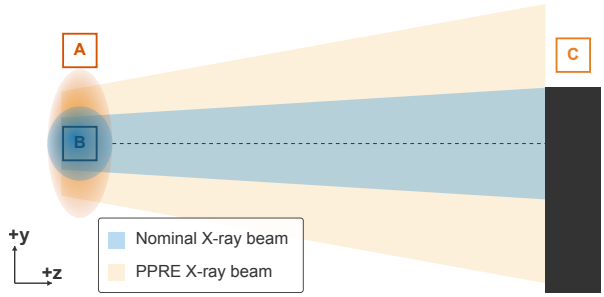



Figure 1: A schematic of the vertical PPRE procedure. As each bunch emits synchrotron radiation, the optical apertures at the beamline (C) must be positioned such that the light from the train (B) is blocked, whilst ensuring that the light from the excited electron bunch (A) is able to pass through.

Some samples used in timing experiments can degrade if exposed to continuous levels of synchrotron radiation, thus requiring illumination from only a single X-ray pulse. Due to blocking of the background radiation, PPRE degrades samples used by timing users more slowly than hybrid-fill. The main trade-off for PPRE is that the amount of flux delivered to the timing user is at least a couple of orders of magnitude smaller than a pure single bunch [5]. Whilst these conditions are sufficient for a subset of timing users, some other timing users may still prefer to seek out other options. Nonetheless, the clear advantage of methods like PPRE is that flux users are unaffected [5, 7].

This paper reports on investigations at Diamond on how to offer PPRE in the vertical plane as an alternative to hybrid fill for Diamond-II. In particular, we highlight both the methods for driving PPRE and its practical assessment at a beamline for its suitability to serve timing users.

## EXPERIMENT SET UP

The storage ring was set up for user-beam operation: 900 bunch train (300 mA) and fast-orbit feedback on. In addition to bunch-by-bunch feedback, the MBF system served a dual role: utilising its excitation capability to increase the equilibrium vertical size of each selected bunch. This approach is similar to [8]. The MBF kick power is specified in decibels, but for simplicity we report its amplitude. The conversion, which takes kicks from a logarithmic to a linear scale, is

* juan.martinezwilkes@physics.ox.ac.uk

ISBN: 978-3-95450-262-2 ISSN: 2673-5350 doi: 10.18429/JACoW-IBIC2025-TUBC02

# BEAM DIAGNOSTICS, DATA ACQUISITION SYSTEM, AND APPLICATIONS OF MACHINE LEARNING AT THE KEK e-/e+ LINAC

F. Miyahara[†,1,2], K. Kinoshita[3], M. Kurata[1,2], M. Iwasaki[3], T. Natsui[1,2], Y. Okayasu[1,2], I. Satake[1], M. Satoh[1,2], K. Uemura[3], Di Wang[1,2]
[1]High Energy Accelerator Research Organization (KEK), Tsukuba, Japan
[2]The Graduate University for Advanced Studies, SOKENDAI, Hayama, Japan
[3]Osaka Metropolitan University, Osaka, Japan

Content from this work may be used under the terms of the CC BY 4.0 licence (© 2025). Any distribution of this work must maintain attribution to the author(s), title of the work, publisher, and DOI.

*Abstract*

The KEK e-/e+ LINAC supplies electron beams to SuperKEKB HER, PF and PF-AR, and positron beams to SuperKEKB LER. In addition to conventional manual tuning based on beam physics and operational experience, we also employ machine learning for beam tuning. In this paper, we report on beam diagnostics, data acquisition and analysis, and beam tuning using machine learning.

Beam tuning using machine learning has proven to be highly effective for increasing positron beam charge and reducing beam emittance. The parameters for these tunings are determined based on beam physics and operational experience, enabling efficient and rapid adjustments. However, it is not always possible to determine the optimal parameters. In beam tuning using machine learning, the choice of parameters to be optimized is critically important. While it is possible to infer key parameters that contribute to beam tuning and beam stability from beam physics models, it is not straightforward to examine all accelerator parameters or to evaluate the magnitude of their influence. Furthermore, identifying the factors that compromise beam stability remains a significant challenge.

To address this issue, we are attempting to analyze the data using explainable AI (XAI) techniques in order to extract the most important parameters affecting the beam. In this paper, we report an example of extracting beam-tuning parameters from large datasets.

## KEK E-/E+ LINAC

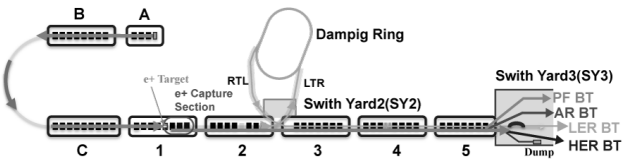



Figure 1: Layout of the KEK e-/e+ LINAC.

The KEK e-/e+ LINAC (the LINAC) serves as the common injector for four accelerators, with beam modes prepared according to the receiving accelerator. The beam repetition rate is 50 Hz, and the allocation of beam modes is adjusted in response to requests from the downstream accelerators. By utilizing the event timing system [1] for pulse-by-pulse control, the beam charge, energy, and optics are adjusted.

*Work supported by JSPS Grant-in-Aid for Transformative Research Areas A JP22H05113 and International Leading Research JP22K21347.
† fusashi.miyahara@kek.jp

Figure 1 shows a schematic layout of the LINAC. The LINAC is equipped with two electron guns (a thermionic gun and a photocathode RF gun [2]) and 226 accelerating structures, with 61 klystrons used to supply RF to these components. The beam energy is adjusted according to the target accelerator; for HER injection the beam is accelerated up to 7 GeV. At the klystron and SLED (pulse compressor) outputs and at the entrances of the accelerating structures, the phase and amplitude of the forward (input) and reflected RF are measured by RF monitors [3]; in total, 65 RF monitors are installed across the injector.

In the LINAC, a total of about 450 DC quadrupole magnets, DC steering magnets, and bending magnets are installed. Since the beam energy varies depending on the beam mode, 46 pulsed quadrupole magnets, 73 pulsed steering magnets [4], and 4 pulsed bending magnets for beam switching are also installed to provide the optimal optics for each mode.

The LINAC is equipped with approximately 100 stripline-type beam position monitors (BPMs), which can be read out with a resolution better than 7 mm [5], and all BPM data are synchronized with the beam. In addition, about 20 high-precision beam profile monitors capable of beam-synchronized measurements [6] and about 60 older monitors for visual inspection are installed. Furthermore, a synchrotron radiation monitor is installed in the J-ARC, enabling non-destructive measurement of the energy spread.

## DATA ARCHIVING SYSTEM

Almost all the equipment in the injector is controlled via EPICS [7]. Data archiving is carried out in two ways: (1) raw data saved for every beam shot, and (2) sampled data stored through the ArchiverAppliance [8] either periodically or when device settings are changed.

The shot-by-shot data consist of BPMs, RF monitors, and pulsed magnets, with raw data saved in text format by each EPICS IOC. These data are synchronized with the beam because, since both the event codes corresponding to the beam modes distributed through the event timing system and the shot IDs assigned to each beam shot are simultaneously recorded. These data are synchronized with the beam, as they are simultaneously recorded with the event codes corresponding to the beam mode distributed via the event timing system and the shot IDs assigned to each beam shot. Such data can be extracted as beam-synchronized datasets for any monitor, beam mode, and specified time. Since there are about 2000 parameters in the synchronized data, outputting long-term (several days or

ISBN: 978-3-95450-262-2 ISSN: 2673-5350 doi: 10.18429/JACoW-IBIC2025-TUBI01

# EXPERIMENTAL INVESTIGATION OF BEAM INSTABILITY IN BEPCII*

Yudong Liu†,1, Jinliu Su[1], Zhi Liu[1], Di Yin[1], Huizhou Ma[1], Huiping Geng[1], Dechong Zhu[1], Junhui Yue[1], Wan Zhang[1], Cunyang Que[2]
[1]Institute of High Energy Physics, Beijing, China
[2]Wuhan University, Wuhan, China

*Abstract*

With the physical operations of the Upgraded Beijing Electron-Positron Collider (BEPCII), thresholds on collision luminosity and beam current have been presented due to various factors such as collision background, noise, and equipment stability and so on. One of the most serious influences on beam dynamics was beam instability which has been exhibited. The comprehensive experimental investigation on beam instabilities in BEPCII is necessary on beam dynamics but also referential to future machine upgrade. Over the past two years, the experimental investigation on beam instability has been carried on, which are source from the various couple impedances, including broadband and narrowband impedances. The measured impedance values are compared with its design.

## INTRODUCTION

BEPCII, the Upgraded project of Beijing Electron-Positron Collider, is the only machine operating in $\tau$-charm energy range of 1.0 to 2.1 GeV, and peak luminosity of $1.0 \times 10^{33}$ cm$^{-2}$s$^{-1}$ at the optimized beam energy of 1.89 GeV [1]. The peak luminosity, $1.096 \times 10^{33}$ cm$^{-2}$s$^{-1}$, was achieved during the physical run in January 2023. Under such high beam current, 849 mA × 852 mA, the serious beam instabilities have been displayed, such as bunch lengthening, coupled-bunch instability and so on, which lead to the beam quality deterioration, luminosity decline, and threshold of the beam current. These instabilities may be critical bottleneck for pushing the beam current and collision luminosity to higher level. A comprehensive investigation on instabilities in BEPCII is critical for high luminosity stable operation. The main parameters of BEPCII rings are listed in Table 1 [2]. The BPR and BER mean for the Positron Ring and Electron Ring of BEPCII, respectively.

Table 1: Main Parameters of BEPCII

| Parameters | BPR | BER |
|---|---|---|
| Circumference (m) | 237.53 | |
| Beam energy (GeV) | 1.89 | |
| RF frequency (MHz) | 499.8 | |
| Harmonic number | 396 | |
| Bunch number | 118 | |
| Horizontal tune | 7.505/5.568 | 7.506/5.572 |
| Synchrotron tune | 0.0299 | 0.0296 |
| Pipe radius (mm) | 54/26 | |

*Work supported by National Foundation of Natural Sciences (U1832132 and12175249)
† liuyd@ihep.ac.cn

## BUNCH LENGTHENING & BROADBAND IMPEDANCE

The longitudinal microwave instability, caused by the longitudinal broadband impedance, can induce bunch lengthening. The classical formula for bunch lengthening would be written as [3],

$$\left(\frac{\sigma_l}{\sigma_{l0}}\right)^3 - \left(\frac{\sigma_l}{\sigma_{l0}}\right) + I_b \frac{\alpha_p Im\left(\frac{Z^{\parallel}}{n}\right)_{eff}}{\sqrt{2\pi}\nu_{s0}^2 (E_0/e)} \left(\frac{R}{\sigma_{l0}}\right)^3 = 0, \quad (1)$$

where $Im\left(\frac{Z^{\parallel}}{n}\right)_{eff}$ is the longitudinal broadband impedance, $I_b$ is the bunch current, $E_0$ is the beam energy, $\alpha_p$ is the momentum compaction factor, $\nu_{s0}$ is the synchrotron oscillation tune, $R$ is the ring radius, and $\sigma_{l0}$ is the natural bunch length. In the experimental measurements, a streak camera was used to measure the bunch lengths of single bunch in BPR and BER with bunch current ranging from 1.0 mA to 19.0 mA, as shown in Fig. 1. Fitting the experimental data of bunch lengths at different currents for the impedance values and bunch natural length of BPR and BER can be obtained as, 0.176 Ω, 0.153 Ω, 13.05mm and 12.91mm, respectively. The longitudinal broadband impedance of BPR is slightly greater than that of BER, and both of them are below the design impedance value of 0.27 Ω for BEPCII [2].

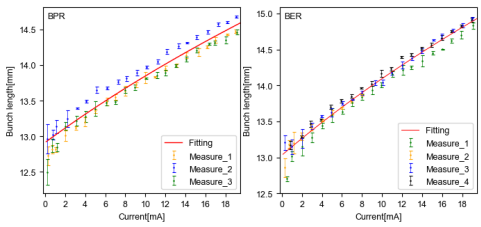



Figure 1: Bunch length vs current.

## TRANSVERSE MODE COUPLING INSTABILITY & BROADBAND IMPEDANCE

The transverse mode coupling instability, caused by the transverse broadband impedance, can induce the tune shift of modes. The relationship between the betatron tune shift and bunch current can be written as [4]

$$\frac{d\nu_\beta}{dI} = \frac{1}{4\sqrt{\pi}} \frac{c^2}{(E_0/e)\nu_\beta \omega_0^2 \sigma_l} i(Z_1^{\perp})_{eff}, \quad (2)$$

where $\nu_\beta$ is the transverse betatron tune, $I$ is the bunch current, $c$ is the light speed, $(Z_1^{\perp})_{eff}$ is the transverse broadband impedance, $E_0$ is the beam energy, $\omega_0$ is the revolution frequency, and $\sigma_l$ is the bunch length.

During the experiments, single bunch oscillations were excited by injection kicker and feedback kicker separately,

Content from this work may be used under the terms of the CC BY 4.0 licence (© 2025). Any distribution of this work must maintain attribution to the author(s), title of the work, publisher, and DOI.

ISBN: 978-3-95450-262-2 ISSN: 2673-5350 doi: 10.18429/JACoW-IBIC2025-TUDC01

# STUDY OF SUPER-RESOLUTION RECONSTRUCTION IN TRANSVERSE PHASE SPACE MEASURED VIA SLIT-SCANNING METHOD

H. Hu*, B. Zhou*, Y. Xia, D. Lu, Y. Zeng, Y. Wang, K. Liu, T. Hu†
Huazhong University of Science and Technology, Wuhan, China

*Abstract*

Electron beam injectors, critical to advanced light sources and ultrafast diffraction systems, require precise transverse phase space diagnostics to optimize beam quality. Conventional slit-scanning combined with computed tomography (CT) enables non-presumptive phase space reconstruction but faces resolution limitations under sparse sampling. This study introduces a deep learning framework to achieve super-resolution reconstruction from minimal scan data. By integrating beam transport physics with neural networks, the method overcomes resolution degradation in low-data regimes. The proposed algorithm, coupled with beam dynamics simulations, forms a systematic engineering solution for high-fidelity diagnostics. This approach enhances phase space characterization efficiency, supporting accelerator commissioning with reduced experimental overhead.

## INTRODUCTION

Accurate transverse phase space diagnostics are essential for optimizing beam quality in electron beam injectors, which are critical components of advanced light sources and ultrafast electron diffraction systems. The slit-scanning method combined with computed tomography [1,2] (CT) enables non-presumptive phase space reconstruction, allowing full distribution characterization without assuming a prior beam model. However, achieving high resolution requires dense angular sampling, which increases measurement time and demands high mechanical and beam stability.

In practical commissioning and tuning, constraints on beam time and stability often force operation in sparse sampling regimes, leading to severe resolution degradation in conventional algebraic reconstruction techniques. This limits the ability to resolve fine phase space features and accurately determine beam parameters such as emittance, thus impacting both diagnostic reliability and accelerator optimization efficiency.

To overcome these limitations, we propose a physics-informed deep learning framework [3] for super-resolution [4] phase space reconstruction from minimal slit-scan data. Trained on synthetic datasets from beam dynamics simulations, the network learns to recover high-frequency details lost in undersampled measurements while ensuring physical consistency. Numerical studies on a low-energy injector test platform demonstrate significant resolution gains and robustness over traditional methods, offering a promising approach for efficient, high-fidelity beam diagnostics.

* equal contribution
† TongningHu@hust.edu.cn

## PRINCIPLE OF SLIT-SCANNING PHASE SPACE MEASUREMENT

### *Principle*

As defined in Eq. (1), the transverse geometric emittance characterizes the phase space area of an electron bunch. However, in practical measurements the particle angles cannot be directly accessed. Instead, the slit-scanning method is commonly employed as an indirect diagnostic of beam emittance [5].

$$\varepsilon \equiv \sqrt{\langle x^2\rangle\langle x'^2\rangle - \langle xx'\rangle^2}. \tag{1}$$

The principle of this method is illustrated in Fig. 1. A typical slit-scan system consists of a transversely movable slit, a downstream fluorescent screen, and a drift section in between. By sampling the beam with a sufficiently narrow slit, a fraction of the bunch is transmitted through and subsequently drifts to the screen. The transverse position of the transmitted beamlet on the screen, together with the drift length, allows the reconstruction of its divergence angle. Repeating this process while incrementally shifting the slit provides a series of beamlets with measured positions and divergences [6]. From these scanning data, the transverse geometric emittance of the main bunch can be approximated. The statistic in Eq. (1) can be derived from Eqs. (2)-(4) [7].

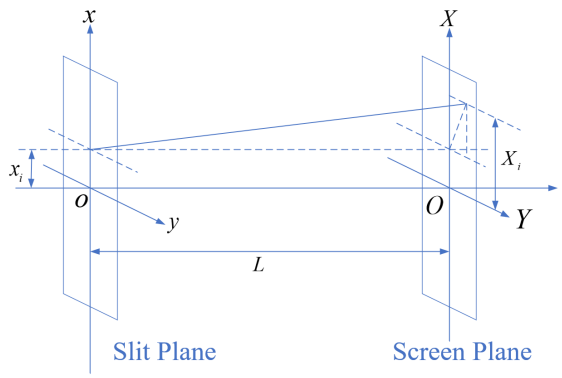



Figure 1: Principle of Slit-Scanning phase space measurement.

$$\langle x^2\rangle = \frac{1}{N}\sum_{i=1}^{N}(x_i - \bar{x})^2 \approx \frac{1}{N}\sum_{j=1}^{p} n_j (x_{sj} - \bar{x})^2, \tag{2}$$

$$\left\langle x'^2\right\rangle = \frac{1}{N}\sum_{i=1}^{N}(x'_i - \bar{x'})^2 \tag{3}$$

Content from this work may be used under the terms of the CC BY 4.0 licence (© 2025). Any distribution of this work must maintain attribution to the author(s), title of the work, publisher, and DOI.

ISBN: 978-3-95450-262-2 ISSN: 2673-5350 doi: 10.18429/JACoW-IBIC2025-TUDI01

# A REVIEW OF SPACE CHARGE COMPENSATION DIAGNOSTICS

E. L. Flannigan*, O. Tarvainen, R. Abel, D. Faircloth, A. Garcia Sosa, D. Morris
STFC ISIS Neutron and Muon Source, Harwell, UK
D. R. Emerson, B. John, K. Jonathan, STFC Scientific Computing Department, Warrington, UK

Content from this work may be used under the terms of the CC BY 4.0 licence (© 2025). Any distribution of this work must maintain attribution to the author(s), title of the work, publisher, and DOI.

*Abstract*

The space charge of high-intensity ion beams makes it challenging to transport the beam through the Low Energy Beam Transport (LEBT) and inject it into the subsequent accelerator. Space charge compensation (SCC) is a process that lowers the space charge of an ion beam by trapping either positive ions or electrons, created by interaction of the beam with residual gas. The compensating secondary particles reduce the beam potential and the space charge-induced divergence of the beam. Significant beam losses during SCC build-up necessitate minimising the SCC time of pulsed high-current ion beams. To address this, diagnostic techniques are used to measure the SCC degree or time or optimise the background gas pressure. These techniques include emittance meters, beam profile monitors, wire scanners, retarding field analysers, Langmuir probes and optical sensors. Such diagnostics are applicable to positive and negative ion beams, with unique challenges based on the specific ion beam and residual gas used. We review common SCC diagnostic techniques to measure various beam characteristics. The diagnostic techniques are often invasive, stopping the beam, changing its characteristics and affecting the local SCC degree. It is therefore important to develop non-invasive diagnostic techniques and to complement diagnostic measurements with particle-in-cell simulations.

## INTRODUCTION

Space charge forces in high-intensity ion beams defocus the beam, leading to beam losses and emittance growth. Space charge compensation (SCC) reduces or eliminates these effects. SCC occurs when an ion beam propagating through a residual or injected gas ionises it through the reaction:

$$A^q + B \rightarrow A^q + B^+ + e^-,$$

where A is the ion beam species, q is the ion beam charge state and B is the gas species. The secondary particles produced by this ionisation reaction (electrons and positive ions) are either repelled or trapped by the beam potential depending on their polarity. The trapped particles reduce the beam potential to a steady state determined by the ionisation rate of the background gas and loss of compensating (and uncompensating) particles. The SCC degree, $\eta$(r,z), is given by [1]:

$$\eta = 1 - \frac{\phi_c(r,z)}{\phi_u(r,z)}, \quad (1)$$

where $\phi_c$(r,z) is the beam potential of the compensated beam and $\phi_u$(r,z) is the potential of the uncompensated beam. Due to the increased mobility of electrons, the steady-state compensation degree of positive ion beams can be limited. However, in addition to electrons created from ionisation of the residual gas, secondary electrons are created when the beam hits surfaces within the beamline and provide an additional source of compensating particles. In contrast, at some gas pressures and with certain beam parameters, negative ion beams can undergo overcompensation due to the heavier positive compensating particles.

The time it takes to build up to this steady-state compensation degree, or SCC time, can be estimated by:

$$\tau = \frac{\eta}{n_g \sigma(E_b) v_b}, \quad (2)$$

where $n_g$ is the gas number density and $v_b$ is the speed of the beam. The ionisation cross section of the reaction, $\sigma(E_b)$, depends on ion beam species, species of the background gas and the energy of the beam. For an $H^+$ beam the compensating reaction $H^+ + H_2 \rightarrow H^+ + H_2^+ + e^-$ has an ionisation cross section of 2.11 x $10^{-20}$ $m^2$ [2]. At a background gas pressure of 1 x $10^{-5}$ mbar and an often-assumed SCC degree of 0.9, the SCC time for a 65 keV $H^+$ is 50 µs. This estimation assumes that all compensating particles are trapped by the beam potential and its validity is dependent on the loss rate of the compensating particles. When the beam potential is the only trapping potential, Eq. (2) is a better approximation for negative beams, where the mobility of the compensating particles is lower.

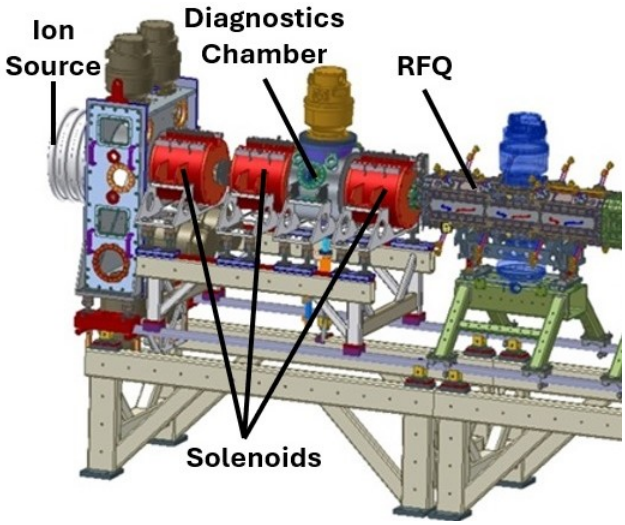



Figure 1: A schematic of the magnetostatic LEBT of the Front-End Test Stand at ISIS Muon and Neutron Source. It consists of three solenoids for focusing into the RFQ.

For a continuous beam, compensation is reached after the transient build-up time. Once a steady state is reached, the

* erin.flannigan@stfc.ac.uk

ISBN: 978-3-95450-262-2 ISSN: 2673-5350 doi: 10.18429/JACoW-IBIC2025-TUPCO01

# DESIGN AND PROTOTYPING FOR DIAMOND-II STRIPLINE KICKERS

A. F. D. Morgan*, A. Amiri, L. Bobb, I. P. S. Martin, V. Zhiltsov, Diamond Light Source, UK

Content from this work may be used under the terms of the CC BY 4.0 licence (© 2025). Any distribution of this work must maintain attribution to the author(s), title of the work, publisher, and DOI.

*Abstract*

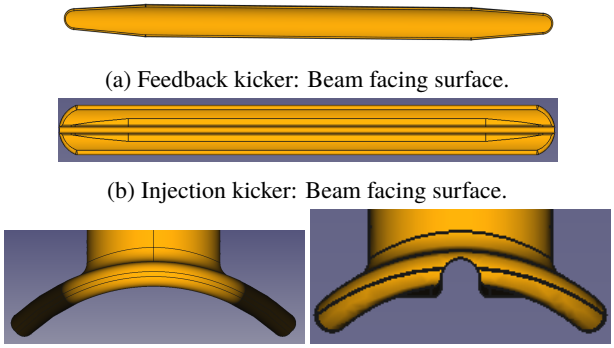
Diamond-II will require two types of stripline kickers during normal operation: the kicker actuators for the transverse multi bunch feedback system; and the injection stripline kickers which enable transparent injection. Both are very similar in design as they need to kick individual bunches without disturbing the following bunches. The main difference is the voltage requirements. The feedback kicker is expected to be driven with a maximum peak voltage of 100 V using a broadband power amplifier, whereas the injection stripline kicker is driven with a trapezoid voltage signal with a maximum peak voltage of 20 kV using a dedicated power supply with 1.6 ns rise and 1.2 ns fall times. This paper will describe the design and prototyping for both stripline kickers along with discussion of the required steps to get to final designs for each type.

## BASIC DESIGN CONSIDERATIONS

As with all Diamond-II [1] vacuum components, there is a desire to improve or at least match the performance and beam impedance of the design used in the current Diamond machine [2]. Higher impedance can reduce instability thresholds and generate localised heating as well as increasing the load on the RF system [3]. Reducing the beam impedance is particularly important as the injection kickers are additional components, and the existing feedback kickers are thought to be a significant contributor to the overall impedance budget of the existing Diamond machine.

Both stripline designs are similar in that they comprise of two copper parallel plates running either side of the electron beam [4]. These are inside a steel vessel shaped to minimise the beam impedance and form a 50 Ω transmission line with the blades. Short counter-propagating pulses are sent along these plates as a single electron bunch passes between them and the field interactions have the effect of giving the electron beam a transverse kick [5–7]. In both cases simulations indicate the beam induces 300-900 V depending on operational mode so protection of the driving circuits needs to be considered.

All the electromagnetic (EM) design work was done using GdfidL [8]. For the initial theoretical designs, where considerations such as buildability are ignored, the main differences are the blade design. The starting point is to have the beam facing surface of the blades match the inner surface of the circular beam pipe which would be in place otherwise (see Fig. 1). This reduces the geometric impedance. The different locations of the striplines in the storage ring lattice define different beam stay clear and shadowing from synchrotron radiation. Therefore the injection stripline blades needed to have notches running down their length to remove the risk of heating due to direct impingement of synchrotron radiation.



(a) Feedback kicker: Beam facing surface.

(b) Injection kicker: Beam facing surface.

(c) Feedback kicker: end view. (d) Injection kicker: end view.

Figure 1: Geometry of the kicker blades.

For the injection kicker there was also a focus on the field flatness near the centre of the pipe aperture. This lead to the addition of a flat running down the length either side of the notch (shown in Figs. 1b and 1d). The high voltage of operation for the injection kicker required consideration of arcing thus care had to be taken that there were no sharp edges and that there was certain minimum distance between surfaces.

## DEVELOPING BUILDABLE DESIGNS

Moving from theoretical designs to full mechanical designs meant we had to care about manufacturability, assembly, adding additional supports due to assembly forces or gravity. For most things the required changes were benign in terms of the impedance as one can see in Figs. 2 and 3 for the feedback and injection kickers respectively. The beam impedance has some changes between the simpler theoretical models and the more detailed mechanical models notably a reduction between 4 and 6 GHz and some frequency shifting in the 7-9 GHz region but is broadly the same.

### *Feedback Kicker*

In the case of the feedback kicker a significant reduction in beam impedance over the existing Diamond design can be seen across the entire frequency range up to the waveguide cut off frequency of 10 GHz (see Fig. 2).

Supporting the stripline blades caused significant design challenges. The addition of flanges which are needed for assembly create a small cavity. The support design was prone to RF heating due to the support screws acting as antennae and coupling power from the main chamber into these small cavities. Over several design iterations we were able to bring this unwanted coupling down to 0.5 W which only generated a few degrees of temperature rise.

* alun.morgan@diamond.ac.uk

ISBN: 978-3-95450-262-2 ISSN: 2673-5350 doi: 10.18429/JACoW-IBIC2025-TUPCO02

# COMMISSIONING OF A LASER WIRE PROFILE MONITOR PROTOTYPE AT CSNS*

B. Zhang, C. Chen, S. Yan, Z. Xu, R. Liu, J. Wei, P. Zhu, R. Yang†, X. Li, S. Wang
Institute of High Energy Physics, Beijing, China
also at China Spallation Neutron Source, Dongguan, China
P. Ding, School of Nuclear Science and Technology, Lanzhou University, Lanzhou, China

*Abstract*

China Spallation Neutron Source (CSNS) accelerator complex will employ a new superconducting accelerating section to achieve high beam power. To protect the superconducting cavity from contamination, the CSNS superconducting linac section will adopt laser stripping technology for transverse distribution measurements of the negative hydrogen beam at nine stations. Recently, a laser wire (LW) prototype was installed to measure the profile of the 80 MeV $H^-$ beam in a non-invasive manner. This paper presents the design and commissioning of this LW prototype.

## INTRODUCTION

The China Spallation Neutron Source (CSNS) linear accelerator (linac) will be upgraded with a superconducting section, boosting the beam energy from 80 MeV to 300 MeV and increasing the Rapid Cycling Synchrotron (RCS) beam power from 100 kW to 500 kW [1, 2]. To prevent contamination of the superconducting cavities from broken physical wires, a non-destructive diagnostic method was developed [3, 4]. This method uses a 1064 nm laser to ionize $H^-$ ions (binding energy 0.75 eV), with the resulting electrons, proportional to the local ion density, collected to reconstruct the beam profile as the laser scans the beam [5–9]. A laser wire profile measurement device was installed at CSNS in 2024 to test this approach, and this paper details its design and commissioning results.

## LASER WIRE SYSTEM

Figure 1 provides a schematic overview of the entire laser wire system. The CSNS linac comprises a radio-frequency quadrupole (RFQ) that accelerates the negative hydrogen beam to 3 MeV and four drift tube linacs (DTLs) that further accelerate the beam to 80 MeV. For the upgrade of the emittance monitor [10, 11], the laser wire station is allocated in the linac transport beam line (about 150 m downstream of the DTL), where the beam energy is 80 MeV. The time structure of the pulsed beam in the linac, shaped by an RF chopper cavity for RCS injection, is depicted in Fig. 2. The beam pulse consists of 324 MHz micro-bunches, 550 ns intermediate bunches, and a 750 µs (max.) macro-pulse with a repetition rate of 25 Hz. A high-power Q-switched Nd:YAG laser, operating at 1064 nm, serves as the light source for efficient photo-detachment. This laser has a full width at half maximum (FWHM) of approximately 10 ns and a repetition rate of 1-10 Hz. By synchronizing the timing between the beam and the laser, the laser can precisely interact with a specific intermediate bunch, detaching approximately six micro-bunches per laser pulse. The demonstrated synchronization timing jitter is about 1 ns.

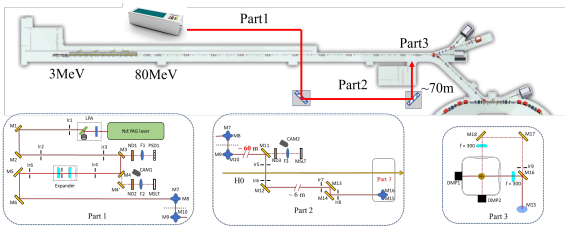



Figure 1: Outline of the laser wire system installed in the CSNS linac.

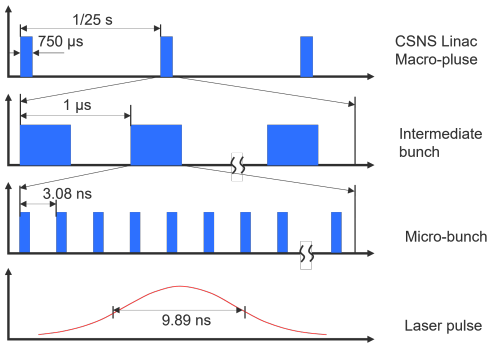



Figure 2: Time structure of the pulses beam in the CSNS linac.

The number of stripped electrons is related to the laser energy and is assessed by

$$-\mathrm{d}n = \sigma(E_{\mathrm{cm}}) \times \Phi(x, y, z, t) \times n(t)dt, \qquad (1)$$

where $n(t)$ is the number of negative hydrogen beam in an elementary volume element, $\sigma(E_{\mathrm{cm}})$ is the photodetachment cross-section [12], and $\Phi$ is the photo flux. For an averaged $H^-$ beam current of 10 mA and a laser pulse energy of more than 100 mJ, there are approximately $10^4 - 10^7$ electrons are detached. These photodetached electrons are deflected by a C-shaped magnet and strike the Faraday cup in the vertical

* Work supported by National Natural Science Foundation of China (No. 12305166), the Natural Science Foundation of Guangdong Province, China (No. 2024A1515010016) and National Key R&D Program of China under Contracts No. 2023YFE0105700.

† yangrenjun@ihep.ac.cn

Content from this work may be used under the terms of the CC BY 4.0 licence (© 2025). Any distribution of this work must maintain attribution to the author(s), title of the work, publisher, and DOI.

ISBN: 978-3-95450-262-2 ISSN: 2673-5350 doi: 10.18429/JACoW-IBIC2025-TUPCO03

# STATUS OF THE SYNCHROTRON RADIATION TELESCOPE AT THE LARGE HADRON COLLIDER

D. Butti*, E. Bravin, S. Burger, A. Guerrero, F. Roncarolo, G. Trad, CERN, Geneva, Switzerland

*Abstract*

Accurate and continuous measurement of the transverse beam profile is essential for optimizing machine performance and ensuring beam quality in particle accelerators. At the Large Hadron Collider (LHC), this task is performed non-invasively and in real time by the Synchrotron Radiation Telescope (BSRT).

Operational since 2015, the BSRT has undergone significant consolidation and a series of upgrades, enhancing its reliability and performance. It operates under conditions that pose specific challenges not commonly encountered in synchrotron radiation diagnostics at electron facilities. These include the complexity of the radiation source, consisting of multiple magnetic elements that evolve during the machine cycle, operation near the diffraction limit in the shortwave Ultra Violet (UV), and the requirement for full remote control, as the setup is inaccessible during regular machine operation.

This contribution presents the current status of the BSRT system, reviewing its key capabilities, operational limitations, and its role in both routine machine operations and dedicated beam physics studies. Finally, an outlook is provided on future upgrades currently under study, aimed at extending the instrument's performance and ensuring its readiness for the upcoming High-Luminosity LHC era.

## INTRODUCTION

At the Large Hadron Collider (LHC), non-invasive emittance monitoring is performed using beam synchrotron radiation telescopes (BSRTs) [1]. The instrument version installed at the LHC startup was based on the Large Electron-Positron collider (LEP) design [2–4]. While online relative measurements proved valuable during the early stages of machine commissioning [5–7], the overall performance was limited by the complexity of the system, based on reflective optics. Moreover, the synchrotron radiation (SR) extraction system, consisting of a metallic mirror protruding into the beam chamber, suffered severe damage due to beam coupling impedance and related RF heating issues [8]. During the Long Shutdown 2 (2018-2021), the 8-element reflective optics was replaced with a simpler double-lens refractor [9] designed to shift the working wavelength to the shortwave Ultra Violet (UV) in order to push the diffraction limit at high beam energy [10]. The light extraction system was also redesigned to provide a low-impedance solution based on a fully dielectric in-vacuum mirror [11].

Since this major redesign, the BSRT has been continuously upgraded to improve the reliability of both the hardware and the control system.

* daniele.butti@cern.ch

## HARDWARE AND CONTROLS

Two SR systems, one per beam, are installed on opposite sides of LHC Point 4, as shown in Fig. 1. The extracted optical SR is used by a variety of operational and R&D diagnostics, both longitudinal and transverse, with the BSRT serving as the main instrument for transverse beam size measurements.

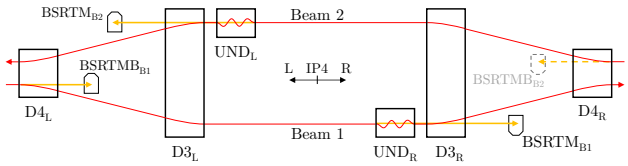



Figure 1: Layout of LHC Point 4 with the operational (BSRTM) and planned (BSRTMB) SR extraction systems.

Since multiple magnetic elements contribute to the emitted radiation, the spatial and spectral characteristics of the light depend significantly on the beam energy [12]. At the injection energy of 450 GeV, superconducting two-period undulators provide visible SR with a spectrum peaking at 600 nm and a spectral width of about 300 nm. As the energy ramp begins, the undulators are turned off, since their spectra drift into the soft X-ray range, which is not used for diagnostics and harmful to the extraction mirror. From 2 TeV, the D3 dipoles become the dominant source of visible SR. The critical wavelength of these dipoles lies in the visible domain at around 3 TeV, and decreases to 60 nm at the flat-top energy of 6.8 TeV, leaving the long-wavelength tail of the broad dipole spectrum in the optical region. SR is intercepted approximately 15 m downstream of the source by an in-vacuum mirror (BSRTM), which deflects it downward and sends it through a viewport into a hutch beneath the beam pipe. The hutch is light-tight and radiation-shielded, allowing the use of off-the-shelf electronics [13]. Inside the hutch, the light is distributed on an optical table to the various SR monitors, as shown in Fig. 2.

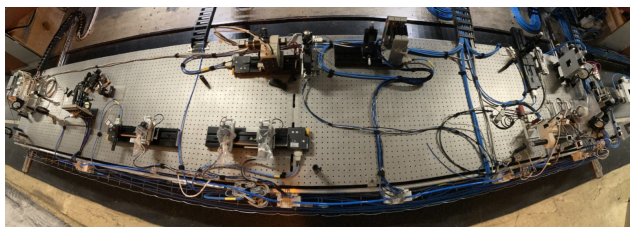


Figure 2: LHC Beam1 SR optical table, before its positioning into the light-tight and radiation-shielded hutch.

The current optical design of the BSRT is based on a Keplerian-type refractor. A main objective lens with $f$ =

Content from this work may be used under the terms of the CC BY 4.0 licence (© 2025). Any distribution of this work must maintain attribution to the author(s), title of the work, publisher, and DOI.

ISBN: 978-3-95450-262-2 ISSN: 2673-5350 doi: 10.18429/JACoW-IBIC2025-TUPCO04

# PERFORMANCE OF THE BEAM GAS CURTAIN AS EMITTANCE MONITOR AT THE LARGE HADRON COLLIDER

D. Butti*, L. Cantu, T. Lefevre, S. Mazzoni, C. Pasquino, G. Schneider,
C. Vazquez Pelaez, R. Veness, CERN, Geneva, Switzerland
O. Sedlacek, O. Stringer, C.P. Welsch, H. D. Zhang, University of Liverpool, Liverpool, UK
P. Forck, S. Udrea, GSI, Darmstadt, Germany

Content from this work may be used under the terms of the CC BY 4.0 licence (© 2025). Any distribution of this work must maintain attribution to the author(s), title of the work, publisher, and DOI.

*Abstract*

The Beam Gas Curtain (BGC) is an instrument for transverse diagnostics in operation at the Large Hadron Collider (LHC). The transverse beam profile is obtained by imaging the fluorescence light resulting from the interaction between the beam and a thin supersonic neon gas jet. This technique can provide minimally invasive and absolute measurements of LHC high-intensity beams, throughout the full machine cycle. It is therefore a potential candidate to complement the limitations of existing LHC transverse diagnostic systems. This contribution highlights the results obtained during the ongoing LHC Run 3. The instrument configuration has been optimized for best performance by combining observations in two spectral ranges of the fluorescence signal: a yellow range, originating from the fluorescence of neutral neon atoms, and a UV range, emitted by ionic neon species. The measurements show good agreement with other profile monitors and enable real-time tracking of the average beam emittance during LHC physics fills. Finally, an overview of planned upgrades is presented, aimed at further improving system performance and progressing towards a fully operational instrument.

## INTRODUCTION

Accurate monitoring of the transverse emittance of circulating particle beams is a key requirement for the operation of accelerators. At the Large Hadron Collider (LHC), transverse diagnostics are provided by two operational devices: wire scanners (BWSs) and synchrotron radiation telescopes (BSRTs). The BWSs serve as the reference instruments for absolute beam size measurements; however, being interceptive devices, their use is restricted to low-intensity beams [1]. The BSRTs offer non-invasive diagnostics and are employed for continuous emittance monitoring in regular operation. However, BSRT performance is constrained by its diffraction-limited regime, and regular calibrations against the BWSs are necessary to preserve its accuracy [2]. Moreover, BSRT measurements are not reliable during the energy ramp, due to characteristics of its synchrotron radiation source. In addition to the diagnostics provided by beam instrumentation, luminosity scans performed at the two main LHC Interaction Points, IP1 (ATLAS) and IP5 (CMS), are also available to estimate the transverse beam distribution and offer an independent reference for the average emittance of the two colliding beams [3]. However, since luminosity scans interrupt regular data-taking, they are performed only occasionally.

An instrument capable of providing a reliable, real-time, and absolute measurement of the average beam emittance during high-intensity operation would be valuable for overcoming the limitations of existing diagnostics. The Beam Gas Curtain (BGC) is a Beam Induced Fluorescence (BIF) monitor that is currently under investigation for this purpose [4]. The instrument generates a thin supersonic jet of neon that intercepts the particle beam. The beam–jet interaction produces fluorescence light, which is collected by an imaging system to assess the transverse beam distribution.

## BEAM IMAGE FORMATION

The operating principle of the BGC is illustrated in Fig. 1. A gas jet, rotated by 45°, intercepts the beam, and the resulting BIF photons generated in the interaction region (highlighted in yellow) are focused by a lens and detected with an intensified camera.

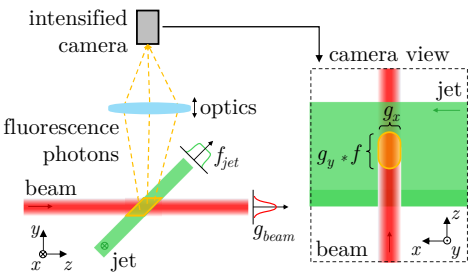



Figure 1: Schematic of beam-image formation in the BGC.

Assuming a Gaussian horizontal beam distribution $g_x$, the horizontal beam emittance can be immediately obtained from the measured image size $\sigma_{\text{meas}}$ by accounting for the magnification $M$ and an optical resolution term $\sigma_{\text{res}}$

$$\varepsilon = \frac{\gamma}{\beta}\sigma^2 = \frac{\gamma}{\beta}\left(\frac{\sigma_{\text{meas}}^2}{M^2} - \sigma_{\text{res}}^2\right), \tag{1}$$

where $\gamma$ is the beam relativistic factor, $\beta$ the betatron function, and the dispersion contribution is neglected.

In the vertical direction, the jet density profile $f_{\text{jet}}$ must be taken into account, since the profile of the interaction region is given by the convolution $g_y * f_{\text{jet}}$, being $g_y$ the vertical beam distribution. The jet profile can be approximated by an almost constant plateau with Gaussian-decaying edges. The plateau width is a design parameter, determined by the

* daniele.butti@cern.ch

ISBN: 978-3-95450-262-2 ISSN: 2673-5350 doi: 10.18429/JACoW-IBIC2025-TUPCO05

# RESEARCH AND DEVELOPMENT OF A RADIATION HARD BEAM PROFILE MONITOR FOR USE IN THE CERN NORTH AREA SECONDARY BEAMLINES

I. Ortega*[,1], H. Danielsson[1], A. Gerbershagen[2], R. Larsen[1,2], M. McLean[1], B. Moser[1], M. Zamkovsky[1]
[1]CERN, Geneva, Switzerland
[2]PARTREC, UMCG, University of Groningen, Groningen, The Netherlands

*Abstract*

The CERN Beam Instrumentation group is currently investigating a radiation-hard beam profile monitor for the CERN North Area. Our main efforts are now focused on straw tubes, a type of wire chamber detector that offers the advantage of being vacuum-compatible and easily equipped with in/out motorisation. We have launched an extensive testing campaign across several CERN accelerators to demonstrate that straw detectors can cover the same dynamic range as traditional wire chambers, from individual particles up to intensities of around $10^{11}$ particles per second, and to prove that they can perform reliably with beams of both protons and heavy ions.

## INTRODUCTION

Multi-Wire Proportional Chambers (MWPCs) are the most widely used beam profile monitors in the CERN North Area beamlines [1]. However, most of these detectors were commissioned in the early 1970s, at the same time as the North Area itself. Their performance has since been severely degraded by ageing and radiation damage, and they no longer meet the requirements of current physics programs. As part of a major renovation of the North Area, the majority of the beam instrumentation will be consolidated. For beams with intensities below $10^8$ particles/s, a scintillating fibre detector, the eXperimental Beam Profile Fibre monitor (XBPF), will replace the old monitors [2]. For higher-intensity beams, up to $10^{11}$ particles/s, the XBPF lacks sufficient radiation tolerance. A new radiation-hard profile monitor is therefore being researched and developed by the CERN Beam Instrumentation Group. Ideally, the new detector should remain highly compatible with the XBPF to optimise long-term maintenance and resource use.

### *Detector requirements*

The new monitor must satisfy the following requirements: active areas of $10 \times 10$ cm$^2$ and $20 \times 20$ cm$^2$, spatial resolution of a few millimeters, operation over beam intensities from $10^5$ to $10^{11}$ particles/s and momenta between 0.5 and 450 GeV/$c$, a material budget below $0.3\,x/X_0$, compatibility with both vacuum and air environments, and integration with a motorised in/out system. To ensure long-term operational reliability over several decades, the active component must withstand radiation doses on the order of MGy, while the mechanical structures and local electronics must remain fully functional in radiation environments up to 1 kGy.

To meet these requirements, different detection concepts are being explored. Two approaches have been investigated for the new beam monitor: light-emitting optical fibres and straw tubes. Three types of light-emitting fibres have been studied: quartz rods, crystal capillaries filled with liquid scintillator, and hollow-core fibres filled with scintillating gas. The results for quartz rods and crystal capillaries were presented at IBIC 2023 [3], while the findings on hollow-core fibres—a novel detection technique showing promising results for medical accelerators—are presented at the IBIC 2025 conference [4].

## STRAW TUBES

Straw tubes are gaseous detectors widely used for tracking and beam monitoring in particle physics [5–7]. They consist of thin cylindrical tubes, typically a few millimetres in diameter, with a central anode wire held at high voltage and the tube wall acting as the cathode. The tubes are filled with a suitable gas mixture, often based on argon, which provides both ionisation and amplification properties.

When a charged particle traverses the straw, it ionises the gas along its path. The liberated electrons drift towards the anode wire under the influence of the electric field, initiating an avalanche multiplication close to the wire. This process produces a detectable electrical signal proportional to the deposited charge. Thanks to their small diameter and low material budget, straw tubes are able to provide good spatial resolution, fast signal collection, and minimal perturbation of the particle beam. They have also been successfully operated in vacuum, as demonstrated by the NA62 experiment at CERN [6]. Moreover, the modular design of straw tubes enables the construction of monitors that are mechanically compatible with the XBPF, allowing the use of the same vacuum tank and thereby improving efficiency in terms of compatibility and long-term maintenance.

### *Detector Design*

The concept of the new monitor is based on an array of straw tubes traversed by the beam, allowing reconstruction of the beam profile and position from the signals induced in the individual straws. Figures 1 and 2 show a prototype detector with an active area of $10 \times 10$ cm$^2$. The straws remain under vacuum, while their electrical readout is located outside at atmospheric pressure. Each straw is 35 cm long in order to carry the signal out of the vacuum, achieved through the

* inaki.ortega@cern.ch

Content from this work may be used under the terms of the CC BY 4.0 licence (© 2025). Any distribution of this work must maintain attribution to the author(s), title of the work, publisher, and DOI.

ISBN: 978-3-95450-262-2 ISSN: 2673-5350 doi: 10.18429/JACoW-IBIC2025-TUPCO06

# STUDY OF PULSED JET OPERATION FOR BEAM GAS CURTAIN MONITORS

S. P. Sethi, H. D. Zhang*, O. Stringer, C. P. Welsch
University of Liverpool / Cockcroft Institute, Daresbury, Warrington, UK

Content from this work may be used under the terms of the CC BY 4.0 licence (© 2025). Any distribution of this work must maintain attribution to the author(s), title of the work, publisher, and DOI.

*Abstract*

A beam gas curtain (BGC) monitor was installed in the LHC for continuous transverse beam profile and emittance measurement. A molecular gas curtain was injected into the LHC continuously. In this work, a pulsed gas jet operation was proposed to minimize the introduction of gas molecules to the beam line and optimize the background pressure. The study was conducted on a gas curtain beam profile monitoring system using nitrogen gas. In this case, the pulse gas jet mechanism enables controlled gas injection into the multiple skimmer chamber to generate a supersonic pulse gas curtain. To achieve maximum current intensity and minimum chamber pressure, key parameters were optimized, such as pulse duration or duty cycle of gas jet, nozzle-skimmer distance, and inlet gas pressure. The results demonstrate a well-tuned pulse jet system can significantly reduce background and enhance the signal-to-noise ratio to monitor a pulse beam. The proposed study exhibits potential applications for beam diagnosis, especially for medical accelerators and laser-based linear accelerators.

## INTRODUCTION

A beam profile monitoring system is a crucial instrumentation setup for emittance measurement and beam profile monitoring of the Large Hadron Collider (LHC) [1]. For non-invasive measurements of particle beams, Beam Gas Curtain (BGC) monitors are preferred over other beam diagnostics instruments. Gas curtain-based Beam-induced fluorescent (BIFs) monitors [2,3] and ionization profile monitors (IPMs) [4,5] are the two important monitoring systems developed based on the beam gas curtain (BGC) monitors.

In this study, gas curtain-based BIF monitors are the only focus. The BIF operational mechanism is solely driven by the phenomena of gas and beam interaction. In this technique, a supersonic gas jet, which is shaped to a 'curtain', interacts with the beam, and the interaction byproducts are collected in the form of fluorescence photons. The generated fluorescence photons are detected using a stand-alone optical system that provides a one-dimensional distribution of the primary beams, from which the beam profile is reconstructed. The developed process is a non-invasive technique, and can measure the beam profile for both lead ion and proton beams for all the stages of LHC operation [6]. The application of BGC can also be extended to other beam diagnostics, in particular for medical accelerators. In radiotherapy, the radiation sources are usually pulsatile rather than continuous. Most clinical linear accelerators (linac) or medical accelerators typically have a pulse duration from 3 ms to 300 ms based on the type of proton or electron beams [7]. Also, a pulsed molecular beam could be defined as a spatially and temporally discrete molecular beam when the beam is traveling through a vacuum under collision-free conditions. Although for designing medical accelerators, other parameters are taken into consideration such as dose rate, pulse repetition rate but they are primarily designed for pulsating beam sources. The proposed method aims to extend the application of the BGC monitors beyond profile monitoring in the LHC. It highlights the outcomes of pulse jet operation of the BGC monitors, and also outlines the key parameters to achieve optimum background pressure and maximum current density.

* haozhang@liverpool.ac.uk

## EXPERIMENTAL SETUP

### *BGC Setup Description*

To conduct a pulse jet injection study, nitrogen gas was injected into the beam profile monitoring system to generate a supersonic gas jet as shown in Fig. 1. Previously, a beam profile monitoring setup was developed by the QUASAR group at the Cockcroft Institute (CI) and commissioned at CERN for beam profile monitoring of the LHC. It's the only monitoring system that can be utilised for the profile monitoring of both proton and lead ion beams of the LHC. The setup operates based on the principle of beam-induced fluorescence, where generated ions due to fluorescence are used to reconstruct the profile of the LHC non-invasively. The setup is made of five vacuum chambers: those are nozzle chamber, the skimmer chambers I and II, the interaction chamber, and the dump chamber. The pumping operation of each chamber is performed by individual turbo-molecular pumps backed by scroll pumps to achieve the required ultra-high vacuum environment.

To mitigate the effect of diffused gas molecules and preserve an ultra-high vacuum environment in the interaction chamber, differential pumping stages separated by skimmers were designed. The sizes of the first skimmer are conical shape, 0.4 mm diameter, the second skimmer is a circular shape with 2 mm diameter, the third skimmer is a rectangular shape with 0.4 × 30 mm size, and the fourth skimmer is a rectangular geometry with 4 × 60 mm size. A supersonic gas jet is injected through a 0.1 mm diameter pulsed nozzle by Parker-Hannifin at varied inlet pressures. It travels mono-directionally through multi-stage skimmers of different geometries to generate a supersonic gas jet curtain, which we refer to as a beam gas curtain.

ISBN: 978-3-95450-262-2 ISSN: 2673-5350 doi: 10.18429/JACoW-IBIC2025-TUPCO07

# RECONSTRUCT TRANSVERSE INITIAL CONDITIONS OF HIGH INTENSITY BEAMS USING MACHINE LEARNING

H. D. Zhang*,[1,2], Q. Xu[1,2,3], C. P. Welsch[1,2]
[1]University of Liverpool, Liverpool, UK
[2]Cockcroft Institute, Warrington, UK
[3]CERN, Geneva, Switzerland

*Abstract*

Space charge effect was considered a driving force for emittance growth in high-intensity beams. To understand it, the emittance needs to be measured. In the past, the quadrupole scan was one of the simple and efficient methods to measure beam emittance, but it is difficult to apply to high-intensity beams where the space charge plays a dominant role due to the deviation from the quadratic fitting. The tomography method was used before for this case to reconstruct phase space and then obtain the emittance, but the scan was time-consuming, and the post-analysis is very complex. One of the solutions is to use the genetic algorithm and treat this as an optimisation problem where the emittance needs to be optimised for the beam to match the quadrupole scans. This method also involves heavy post-analysis, which limits its online application.

In this contribution, machine learning methods will be used to reconstruct the transverse initial conditions based on PIC simulations of space charge-dominated beams. The effectiveness of the machine learning method against the space charge level will be studied.

## INTRODUCTION

Transverse emittance is a key quality factor for particle beams in accelerators. Knowing it precisely will help control the machine and avoid beam loss. Traditionally, it was measured by methods such as a quadrupole scan, a multi-slit, and a pepper pot. Other novel methods [1] have also been applied. Due to its simplicity, the quadrupole scan method was widely used in many accelerator facilities. It utilizes one quadrupole and a beam profile monitor, which can be invasive, such as scintillating screens, optical transition screens, or secondary emission monitors, or non-invasive, such as synchrotron radiation monitors, gas-based ionization, or beam-induced fluorescent monitors. The method relies on varying the quadrupole field and recording the beam sizes. Based on the linear transfer matrix, the measured beam size square can be fitted in a quadratic form associated with the varying quadrupole strength, where initial conditions such as beam size, beam slope, and emittance can be obtained from the coefficients of the quadratic function.

However, in high-intensity beams, space charge plays an important, if not dominant, role, and the transfer matrix cannot be decoupled from the beam sizes and even becomes nonlinear in extreme cases, thus the fitting from the quadrupole scan will overestimate the emittance compared with the measurement by a more precise method, such as multi-slits and simulations [2]. Previously, optimization methods were used to resolve the emittance for space-charge-dominated beams, including particle swarm [3] and genetic algorithms [4]. Those methods tried to solve the initial condition by optimizing them to fit the quadrupole scan data using a linear space charge model when describing the envelope evolution over time. Those methods are effective, but the post-process is very time-consuming.

In this paper, a machine learning method, specifically the regression model, is proposed to obtain the emittance from the quadrupole scan data for high-intensity beams. The space charge level, as well as the effective measurement range of emittance, will be discussed using the quadrupole scan data from particle-in-cell simulations.

## METHOD

### *Dataset Generation*

The beam envelope equation in Eqs. (1) and (2) describes beams with linear space charge force in a non-accelerating environment.

$$X'' + k_x X - \frac{2K}{X+Y} - \frac{{\epsilon_x}^2}{X^3} = 0, \tag{1}$$

$$Y'' + k_y Y - \frac{2K}{X+Y} - \frac{{\epsilon_y}^2}{Y^3} = 0, \tag{2}$$

where $X, Y$ are the horizontal and vertical envelopes of the beam (two times of the rms size), $k_x$, $k_y$ are the external force strength in the x and y direction separately, $K$ is the dimensionless generalized perveance, indicates a space charge level, and $\epsilon_x$, $\epsilon_y$ are the effective emittances in the x and y direction separately. These equations are derived from the single-particle trajectory equation, considering the linear space charge force from a K-V distribution. Still, they can be extended to other distributions in terms of the RMS value. When $K \lesssim 10^{-6}$, the space charge can be ignored; when $10^{-6} \lesssim K \lesssim 10^{-4}$, the space charge is moderate; when $K \gtrsim 10^{-4}$, the beam can be considered as space-charge dominant.

To use the quadrupole scan data for emittance or initial condition reconstruction, a simple case was considered, as shown in Fig. 1. High-intensity beam with initial conditions including beam sizes ($X_0$, $Y_0$), beam slopes ($Xp_0$, $Yp_0$), and beam emittances ($\epsilon_{x0}$, $\epsilon_{y0}$) propagates through the quadrupole scan system, which includes a drift with

* haozhang@liverpool.ac.uk

Content from this work may be used under the terms of the CC BY 4.0 licence (© 2025). Any distribution of this work must maintain attribution to the author(s), title of the work, publisher, and DOI.

ISBN: 978-3-95450-262-2 ISSN: 2673-5350 doi: 10.18429/JACoW-IBIC2025-TUPCO08

# STATUS OF LONGITUDINAL INSTABILITY SUPPRESSION AT NanoTerasu

K. Ueshima*, A. Agui, T. Asaka, Y. Hosaka, K. Inaba, K. Kan, N. Nishimori, S. Obara, C. Saji
NanoTerasu Center, QST, Sendai, Miyagi, Japan
R. Saida, S. Takahashi, K. Moriya, T. Tsuchiyama, R. Yoshioka
NAT Corporation, Hitachinaka, Ibaraki, Japan

Content from this work may be used under the terms of the CC BY 4.0 licence (© 2025). Any distribution of this work must maintain attribution to the author(s), title of the work, publisher, and DOI.

*Abstract*

NanoTerasu is a 3 GeV light source newly constructed in Sendai, Japan. The circumference is 349 m and the natural emittance is 1.14 nm rad, which is realized by a double-double-bend achromat lattice. The commissioning of the storage ring started in June 2023. The longitudinal instability was observed when the stored beam current reached 150 mA in August 2023. The temperature of SR RF cavity was adjusted to suppress the instability. The user operation was started on schedule in April 2024 with a stored beam current of 160 mA. The stored beam current was reached 200 mA without the beam instability in July 2024. The stored beam current at user operation period was limited to 200 mA due to the longitudinal instability. We tried to suppress the longitudinal instability using several methods. We developed the waveguide-overloaded kicker cavity and longitudinal bunch-by-bunch feedback (LBBF) system to suppress the instability. The LBBF system commissioning was carried out in July 2025. We achieved the 400 mA stable beam accumulation using LBBF system. The longitudinal instability suppression at NanoTerasu was reported.

## INTRODUCTION

The NanoTerasu is a compact 3 GeV light source newly constructed in Sendai, Japan [1, 2]. The designed stored beam current is 400 mA. The commissioning of the storage ring started in June 2023 [3]. In August 2023, the longitudinal instability was observed when the stored beam current reached 150 mA. The user operation was started on schedule in April 2024 with a stored beam current of 160 mA. To suppress the longitudinal instability, the temperature of SR RF cavity was adjusted. However, the stored beam current was limited to 200 mA due to the longitudinal instability in 2024. To increase the stored beam current, we started to develop the waveguide-overloaded kicker cavity and LBBF system in January 2024. The kicker cavity was installed in the storage ring in May 2025. The commissioning of LBBF system was carried out in July 2025. The status of longitudinal instability suppression at NanoTerasu was reported.

## LONGITUDINAL INSTABILITY

The accelerating cavity of the NanoTerasu storage ring adopts the world's first compact cavity that accelerates the stored beam in the TM020 mode [4]. The slot is placed at the magnetic field node of the axially symmetric TM020 mode. The ferrite-based RF absorbers are installed inside the slot. This structure is designed to attenuate higher order mode (HOM) components that can induce coupled bunch beam instabilities. During the commissioning of the storage ring, longitudinal instability was observed when the stored beam current exceeded 150 mA. As a result of investigating the accelerating cavity, this instability was attributed to the growth of a 1.9 GHz component of HOM. Figure 1 shows the spectrum of the 1.9 GHz HOM from the pickup of the accelerating cavity, as well as the frequency spectrum of the beam position monitor (BPM), during the occurrence of longitudinal beam instability. The sideband frequency components shifted by approximately 134 MHz from 508.76 MHz appeared in the BPM signal spectrum, indicating that the coupled-bunch mode number of the longitudinal instability was 156. Considering the temporal evolution of the spectrum intensity due to the longitudinal instability and the effect of the radiation damping, the growth rate of the 1.9 GHz HOM was estimated to be approximately 5.8 msec in 2023.

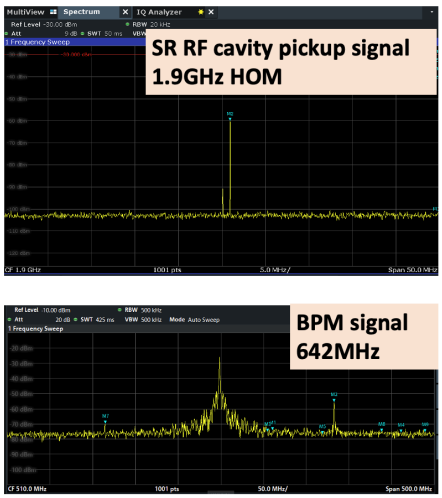



Figure 1: 1.9 GHz HOM signal from the pickup of the accelerating cavity (top) and spectrum of BPM signal (bottom).

At the energy dispersive section the X-ray pinhole camera (XPC) was installed to monitor the stored beam profile [5]. When the longitudinal beam instability increases the energy spread, the horizontal beam size also increases as shown in Fig. 2. The bunch phase is also monitored using the high speed digitizer ADQ7, which also measure the bunch current. The horizontal beam size and bunch phase are continuously monitored to detect the occurrence of the longitudinal instability.

To suppress the growth of the 1.9 GHz HOM, the cooling water condition of the accelerating cavity was adjusted, and

* ueshima.kouta@qst.go.jp

ISBN: 978-3-95450-262-2 ISSN: 2673-5350 doi: 10.18429/JACoW-IBIC2025-TUPCO09

# SIDE EFFECTS OF BUNCH-BY-BUNCH FEEDBACK SYSTEM ON SuperKEKB COLLIDER

M. Tobiyama[†,1], T. Ishida, KEK Accelerator Laboratory, 1-1 Oho, Tsukuba, Japan
[1]also at Department of Accelerator Science, SOKENDAI, Tsukuba, Japan

*Abstract*

The bunch-by-bunch feedback system is now a key function in high-current, multi-bunch storage rings, suppressing coupled-bunch instability and/or reducing the effects of injection vibration. In high-luminosity $e^+$ $e^-$ colliders, such as SuperKEKB, strong beam-beam interactions occur due to collisions, which typically introduce an extensive frequency response to the transverse bunch motion far off the betatron tune. In the vertical plane it may cause an increase of the beam size, which has a significant impact on the luminosity. In this paper, we will present the principles and configuration of our bunch feedback system, the causes of its side effects, and several trials aimed at overcoming them.

## INTRODUCTION

On recent high-luminosity colliders, such as the SuperKEKB collider, it is almost indispensable to use robust transverse bunch-by-bunch feedback systems to suppress fast coupled-bunch instabilities (CBI) arising from strong and wide-band impedance sources, including electron cloud instability or fast ion instability. The feedback gain of the systems tends to be rather large, at least to keep the beam in single beam condition. In the case of SuperKEKB-LER, we usually have set the gain of the system to have the feedback damping time of around 0.5-1 ms, which corresponds to 50 to 100 turns of the revolution of the rings.

During the operation of the KEKB collider, we have unexpectedly observed a degradation of the luminosity related to the excess feedback gain of the LER [1]. Through our detailed study of how the transverse feedback gain relates to the luminosity, we discovered that the vertical feedback gain influences both luminosity and vertical beam size. In contrast, other transverse feedback gains did not show a clear correlation with luminosity or beam size. We have also examined the effect of the vertical feedback gain on vertical beam size observed with the interferometer on both the collision and on the single-beam condition of KEKB-LER. Though the vertical beam size slowly increased (~10 %) with the feedback gain during the single beam condition, it jumped up more than 40 % with a slight change in the feedback gain during the collision. The resulting luminosity decreased by around 10 to 20 % with the blowup of the vertical beam size.

Numerical simulations have shown that the significant beam-beam effect enhances small oscillations induced by the broadband noise of the bunch feedback systems [2]. This effect is thought to be more pronounced in colliders with a small vertical beam emittance, so sufficient consideration was given to the design of the bunch feedback systems from the SuperKEKB accelerator. Unfortunately, we have still observed the effects on luminosity due to the bunch feedback gain.

In this report, we will at first give an overview of the effects of the injected feedback noise observed in the KEKB collider. Secondly, the bunch feedback system for the SuperKEKB will be presented, with a focus on the bunch position detector circuit, where it has the most significant influence on the system's noise figure. The experimental results from the 2024c runs, which began after summer break and continued until the end of 2024, along with the plans, will be presented. The main parameters of SuperKEKB rings in 2024c runs are listed in Table 1.

Table 1: Machine Parameters Achieved at SuperKEKB

| Parameters | LER | HER |
|---|---|---|
| Energy (GeV) | 4 | 7 |
| Circumference (m) | 3016 | |
| Beam current (A) | 1.632 | 1.259 |
| $n_b$ | 2346 | |
| $I_b$ (mA) | 0.696 | 0.537 |
| $\beta^*_x$ (mm) | 60 | 60 |
| $\beta^*_y$ (mm) | 1.0 | 1.0 |
| $\xi_y$ | 0.036 | 0.027 |
| H. size $\sigma_x$* | 15.5 | |
| V. size $\sigma_y$*(μm) | 0.265 | |
| βx/βy at FB monitors (m) | 19.4/20.0<br>19.4/20.0 | 13.4/29.7<br>5.5/6.2 |
| βx/βy at FB T kickers (m) | 23.4/9.9<br>21.9/15.9 | 13.4/29.7<br>5.5/6.2 |
| T. rad D-time (ms) | 43 | 58 |
| CW ratio | 80 % | 60 % |
| $L_{peak}$ ($cm^{-2}s^{-1}$) | $5.1 \times 10^{34}$ | |

## OVERVIEW OF NOISE EFFECT OBSERVED AT KEKB

It is not easy to excite a beam in the transverse plane at a frequency other than the betatron frequency unless it is an extremely low frequency. Therefore, even if the broadband noise injected by the bunch feedback system is quite large, it will not affect the beam. However, if the beam-beam effect due to collision is significant, this situation changes, and the response of the beam is thought to be wide over a range from the betatron frequency to the beam-beam tune shift value. As the beam-beam effect is quite nonlinear, this effect will behave nonlinearly in both the frequency range and the amplitude.

† makoto.tobiyama@kek.jp

Content from this work may be used under the terms of the CC BY 4.0 licence (© 2025). Any distribution of this work must maintain attribution to the author(s), title of the work, publisher, and DOI.

ISBN: 978-3-95450-262-2 ISSN: 2673-5350 doi: 10.18429/JACoW-IBIC2025-TUPCO10

# OVERVIEW OF THE PINHOLE CAMERA DESIGN FOR THE DIAMOND-II UPGRADE

N. Vitoratou*, L. Bobb, Diamond Light Source, Didcot, UK

*Abstract*

Pinhole cameras serve as the primary diagnostic for emittance and energy spread measurements in the storage ring of Diamond Light Source. Similar pinhole cameras will be employed for the Diamond-II upgrade, to enable direct imaging of the stored beam while also allowing for the monitoring of skew, profile, position, and instabilities. The emittance and energy spread are calculated from the acquired beam size measurement, combined with the lattice parameters. In this paper, an overview of the new system for Diamond-II is presented. The changes and upgrades made to the existing setup, the challenges and the choice of the different components are described. Additionally, future work that could improve the performance of the system is explored.

## INTRODUCTION

The Diamond-II upgrade aims to transform the existing Double Bend Achromat lattice into a Multi Bend Achromat, reducing the natural horizontal emittance of the electron beam from 2700 pm.rad to 163 pm.rad, thus enhancing the brightness and the coherence of the synchrotron radiation [1].

X-ray pinhole cameras (XPCs) are deployed for transverse profiling of the electron beam in the storage ring as they offer direct 2D imaging of the stored beam, reliability and sufficient spatial resolution to measure the expected nominal beam sizes in Diamond-II [2, 3]. For a squeezed beam following optics correction, the estimated vertical emittance is 1 pm.rad, resulting in a beam size of 4 µm at the source points [1]. For this range of beam size that are below the pinhole cameras resolution, X-ray diffractometry has been tested in Diamond and can be used as a complementary technique [4]. Although, the design of the XPC system for Diamond-II will be based on the existing design, new challenges have arisen and need to be addressed. In parallel, improvements of the system will be accounted in the design.

## SOURCE POINT SELECTION

Using two transverse beam size monitors located at different positions in the storage ring with different lattice parameters, the emittance and the energy spread in the ring can be calculated in the horizontal and the vertical plane. Two source points have been selected: dipole D1, a longitudinal-gradient bend supplying the X-ray beam to Pinhole Camera 1, and dipole D4, a constant-gradient bend supplying the X-ray beam to Pinhole Camera 2 [1]. The X-ray beam is extracted at 4 mrad and 7.2 mrad into the magnet bend respectively, ensuring clearance from the fringe-field region. The beamline configuration has been verified to prevent any background radiation from upstream components. The corresponding source and lattice parameters for these bending magnets are summarised in Table 1.

Table 1: Parameters of D1 and D4 Bending Magnets and Nominal Beam Conditions

| Parameter | D1 | D4 |
|---|---|---|
| Magnetic field | 0.83 T | 0.7 T |
| Critical energy | 6818 eV | 6103 eV |
| Total power per mrad | 44.9 Watts | 40.6 Watt |
| Horiz beta function | 1.613 m | 0.708 m |
| Vert beta function | 19.858 m | 10.306 m |
| Horiz dispersion | 2.21 mm | 10.04 mm |
| Horiz emittance | 160 pm rad | |
| Vert emittance | 8 pm rad | |
| Energy spread | 0.00094 | |
| Horiz beam size | 16.3 µm | 14.2 µm |
| Vert beam size | 12.6 µm | 9.1 µm |

## PINHOLE CAMERA SETUP

The X-ray pinhole camera setup consists of a bending magnet source, the pinhole aperture at distance $d_0$ from the source and a scintillating screen at distance $d_i$ downstream of the pinhole, which forms the image of the source. The visible light image from the scintillator screen is then relayed through an optical lens onto the camera sensor (see Fig. 1).

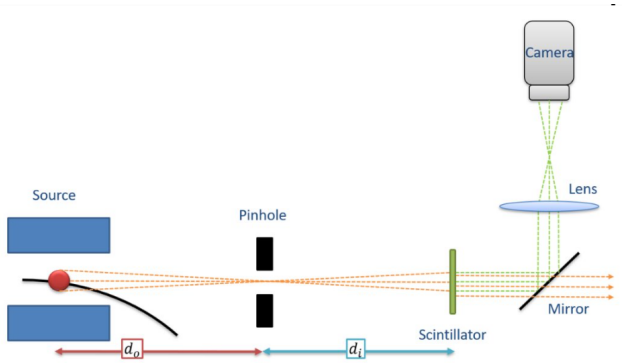



Figure 1: X-ray pinhole camera layout, including source, pinhole aperture, scintillator, mirror, lens, and camera.

The distances for the two pinhole cameras systems and the corresponding magnification $M = d_i/d_0$ are given in the Table 2. To achieve the highest possible magnification, pinhole apertures will be placed as close as possible to the

* niki.vitoratou@diamond.ac.uk

Content from this work may be used under the terms of the CC BY 4.0 licence (© 2025). Any distribution of this work must maintain attribution to the author(s), title of the work, publisher, and DOI.

ISBN: 978-3-95450-262-2 ISSN: 2673-5350 doi: 10.18429/JACoW-IBIC2025-TUPCO11

# EVALUATING MACHINE LEARNING MODELS FOR MULTIMODE-FIBER-BASED TRANSVERSE BEAM PROFILE RECONSTRUCTION

Q. Xu*[,1,2,3], A. Hill[1,2], H. D. Zhang[1,2], F. Roncarolo[3], G. Trad[3], S. Burger[3], W. Farabolini[3], P. Korysko[4], D. Metin[3], C. P. Welsch[1,2]
[1] University of Liverpool, Liverpool, UK
[2] Cockcroft Institute, Daresbury, UK
[3] CERN, Geneva, Switzerland
[4] University of Oxford, Oxford, UK

*Abstract*

Transverse beam profile monitoring is essential for safe and efficient accelerator operation. In high-radiation environments such as beam dumps, cameras degrade rapidly. To address this, a single multimode fiber (MMF) transmission system was previously tested to transport scintillation light from a screen to a remote camera. Because multiple guided modes are excited and coupled during propagation, the fiber output does not preserve the image and requires reconstruction. This contribution evaluates seven machine-learning reconstruction models for recovering the original transverse beam distribution from MMF output. Using data from the MMF-relayed Chromox screen campaign at CERN's CLEAR facility, the study compares models in terms of reconstruction error, convergence speed, and run-to-run stability, with particular attention to the use of incoherent light. The results indicate robust options for radiation-tolerant, MMF-based transverse diagnostics.

## INTRODUCTION

CERN is investigating radiation-resistant approaches for beam imaging to reduce damage to cameras and peripheral electronics [1]. In previous work, a single large-core multimode fiber (MMF) relay was developed to transport light from a Chromox scintillating screen in the beam pipe to a CMOS camera located in a low-dose area [2]. The main difficulty is that propagation modes inside the MMF experience coupling, scattering, and dispersion, which alter the input power distribution [3]. The output intensity is therefore a scrambled mixture rather than an image directly usable for transverse beam parameter extraction. Although fiber-based image reconstruction has been studied, the optimal approach for incoherent, screen-based light remains open. This paper evaluates seven representative reconstruction models—covering image-to-image, generative, and image-to-parameter formulations—using paired data from an MMF-relayed screen campaign. To address practical deployment, we also report model size, training time, and convergence speed, relevant for periodic fine-tuning under drifting MMF conditions (temperature, vibration).

* qiyuan.xu@liverpool.ac.uk

During the campaign, light from a 30 mm × 30 mm Chromox scintillating screen was transmitted through a multimode fiber (FP1500ERT, Ø1.5 mm). Lenses coupled light into and out of the fiber, with a beam splitter sending a fraction to a reference camera for direct screen images. Each dataset entry therefore consists of a paired image (reference screen, MMF output), stored as 256 × 256 single-channel arrays. In total, 6257 pairs were acquired using a triplet scan technique; the main parameters are listed in Table 1.

Table 1: Transverse Beam Image Dataset Collected at CERN

| Dataset Configuration | Specifications |
|---|---|
| Facility | CLEAR |
| Particle source | $e^-$ |
| Energy | ~ 150 MeV |
| Screen type | Chromox ($Al_2O_3$:$CrO_2$) |
| Central $\lambda$ | 693 nm |
| Number of samples | 6257 |

## MACHINE LEARNING MODELS AND TRAINING

Four model families are considered for MMF image reconstruction. First, the vectorized models, such as the transmission matrix (TM) [4] and a single-hidden-layer dense neural network (SHL-DNN) [5], operate on flattened input and output images. Their model parameter count scales as $\mathcal{O}((HW)^2)$, where $H$ and $W$ denote the image height and width, so for these models we restrict the resolution: the SHL-DNN input is reshaped to $64 \times 64$, and both SHL-DNN and TM outputs are constrained to $32 \times 32$.

The convolutional image-to-image models include U-Net [6], a convolutional autoencoder (CAE), and the conditional generative adversarial network Pix2Pix [7], all operating on native 256 × 256 input and output images. These models share an encoder–decoder structure, where the input is progressively compressed into abstract feature representations and then decoded back to an image. U-Net preserves fine detail through skip connections; CAE removes all skip connections and pooling layers, instead using stride-2 convolutions for improved generalization; Pix2Pix extends the U-Net by adding an adversarial discriminator to enhance reconstruction of fine structures.

Content from this work may be used under the terms of the CC BY 4.0 licence (© 2025). Any distribution of this work must maintain attribution to the author(s), title of the work, publisher, and DOI.

ISBN: 978-3-95450-262-2 ISSN: 2673-5350 doi: 10.18429/JACoW-IBIC2025-TUPCO12

# MEASUREMENT OF TRANSVERSE PROFILE IN ELECTRON LINACS: RECENT ADVANCES IN SwissFEL

Rasmus Ischebeck*, F. Addesa, A. Adelmann, V. Guzenko,
P. Juranić, G. L. Orlandi, E. Prat, S. Reiche, T. Schietinger
PSI Center for Accelerator Science and Engineering,
Jonas Schlör, Güney Tekin, ETH Zürich, Switzerland

*Abstract*

The measurement of transverse profiles of the electron beam is key to measuring and optimizing the emittance of a linear accelerator. Also, transverse profile monitors are used in conjunction with an RF transverse deflecting structure (TDS) to measure bunch length and slice emittance. An RF deflector and a profile monitor behind the undulator can furthermore be used to reconstruct the FEL pulse profile. Here, we give an overview on recent advances in beam profile measurements at SwissFEL, including scintillating screens as well as wire scanners. The goal of these advances is the improvement of the resolution in both screens and wire scanners, both by improving the optics, and by improved data processing. Furthermore, we are exploring the possibility to do non-invasive wire scans with micrometer-size wires.

## INTRODUCTION

When setting up and operating an accelerator, one needs to measure and optimize the phase space distribution of the electron beam. No tool exists to directly measure the 6-dimensional $(x, x', y, y', E, t)$ phase space distribution of the particles. Instead, we use beamline elements to rotate the phase space and subsequently make projections on one-dimensional or two-dimensional subspaces. Examples for such beamline elements are:

- A dipole magnet to map the the energy axis onto a transverse dimension.
- Quadrupoles and skew quadrupoles for transverse phase space transformations.
- An RF transverse deflecting structure or a corrugated wakefield structure to map the time axis onto a transverse dimension.

We use transverse profile monitors, for example, wire scanners, or screen monitors, to measure the distribution in the $x$, $y$, or $(x, y)$ sub-spaces. The performance of these monitors is therefore at the core of phase space measurements, and the present manuscript will focus on accurate transverse measurements. For emittance-measurement methodologies at SwissFEL, see Prat et al., [1] and Prat and Aiba, [2]; for TDS-based longitudinal diagnostics, see Craievich et al., [3]; for wakefield-based longitudinal diagnostics, see [4] and [5]. We have established 5-dimensional phase space reconstruction at SwissFEL, following a method demonstrated at DESY [6], and we are working on the full 6-dimensional reconstruction.

## CONTINUED DEVELOPMENT OF BEAM PROFILE MONITORS IN SwissFEL

The instrumentation developed for the commissioning of SwissFEL was continuously improved during its operation in recent years. The goal is to improve resolution, reliability, and to make progress towards minimally invasive measurements.

### *Wire Scanners*

Wire scanners at SwissFEL were designed as high-resolution, quasi-non-destructive beam diagnostics. These systems employ a beam-synchronous data acquisition system to mitigate the effects of shot-to-shot jitter by correlating the scattered particle signal with the wire position, as determined by an encoder, and the beam charge and root-mean-square (rms) position measured by beam position monitors (BPMs) [7].

Improved resolution and reduced beam impact can be achieved through the use of wires fabricated via electron beam lithography and photolithography [8]. By combining measurements from wires positioned at multiple angles, a reconstruction of the four-dimensional $(x, x', y, y')$ phase space distribution is possible [9].

### *Screen Monitors*

Screen monitors in SwissFEL utilize a cerium-doped yttrium aluminum garnet (Ce:YAG) crystal imaged onto a CMOS image sensor via an objective lens. An angled screen insertion minimizes depth-of-field blur and avoids contamination from coherent optical transition radiation [10].

The sensitivity of these monitors is adjusted by inserting neutral density filters into the optical path. Initially, gelatin filters were used. These were found to unnecessarily degrade optical resolution. This degradation was most severe when the beams were most dense and therefore smallest. The gelatin filters of the screen monitors at the most relevant locations in SwissFEL have thus been replaced with glass filters. These filters do require re-focusing after each filter change, but they result in an improved resolution of 14.3 µm [11].

* rasmus.ischebeck@psi.ch

Content from this work may be used under the terms of the CC BY 4.0 licence (© 2025). Any distribution of this work must maintain attribution to the author(s), title of the work, publisher, and DOI.

ISBN: 978-3-95450-262-2 ISSN: 2673-5350 doi: 10.18429/JACoW-IBIC2025-TUPCO13

# DEVELOPMENT OF A CHERENKOV RADIATION-BASED BEAM PROFILE MONITOR FOR A MUON LINEAR ACCELERATOR*

R. Nakagawa†,1, F. Miyahara[1,2], M. Otani[1,2], Y. Hashimoto[2]
[1]The Graduate University for Advanced Studies, Tsukuba, Japan
[2]High Energy Accelerator Research Organization, Tsukuba, Japan

*Abstract*

In order to test the Standard Model through a precision muon g−2 measurement, the J-PARC muon g−2/EDM experiment is constructing a 212 MeV muon accelerator. In the early stages of commissioning, the number of muons per bunch is expected to be as low as only a few tens, and furthermore, since dark current electrons are mixed into the muon beam, the conventional beam diagnostic methods used in accelerators cannot be applied. We are developing a Cherenkov-type beam monitor that utilizes Cherenkov radiation to selectively measure only muons from a muon beam mixed with dark current. The resolution of the profile was evaluated under ideal conditions without errors, based on the optical design of the detector. We are also investigating radiation hardness of the radiators to be used in the measurements.

## INTRODUCTION

To test the Standard Model through precision measurements of the muon anomalous magnetic moment and electric dipole moment, the J-PARC muon g-2/EDM experiment is developing a 212 MeV muon linear accelerator [1]. So far, muons cooled to 25 MeV have been successfully accelerated to 90 keV [2].

In this experiment, since a low-emittance muon beam is required, high-precision position and profile monitors are necessary. In the early commissioning stage, fewer than 40 muons per pulse are expected, with additional background electrons from dark current, making measurements with commonly used types of monitors difficult. To address this, we have developed a novel beam profile monitor utilizing Cherenkov radiation.

This paper reports on the monitors for the 40 MeV and 212 MeV accelerator sections.

## BEAM PROFILE MONITOR

Figure 1 shows a schematic of the muon linear accelerator. We are developing beam profile monitors at the entrance and exit of the Disk-Loaded Structure (DLS) section, which accelerates muons from 40 MeV to 212 MeV, corresponding to 70–94 % of the speed of light, with an accelerating gradient of 20 MV/m [3]. We are currently designing the monitors to be used at the entrance and exit. Unlike electron or proton linacs, the muon beam charge is extremely small; during early commissioning, the charge per pulse is only about 4 fC, several orders of magnitude lower than typical electron linacs. This requires high-precision diagnostics capable of operating with very low beam intensities.

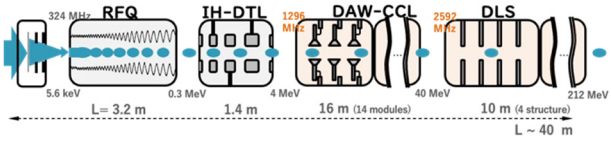



Figure 1: Layout of muon LINAC.

A major challenge is the dark current generated by field emission in the accelerating cavity, with electron energies up to ~14 MeV. Since muons and electrons carry the same charge, electrical measurements cannot distinguish them. When radiators with refractive indices of 1.46 and 1.08 are used in the monitors at 40 MeV and 212 MeV, respectively, the Cherenkov angles become 5.7° and 10.9°. The Cherenkov light emitted from relativistic-energy electrons is more than 4° larger than these angles. In the case of low-energy electrons, Cherenkov light is emitted at the same angle as that of muons; however, such electrons are strongly focused or defocused by the quadrupole magnets located after the accelerating cavity and thus cannot reach the detector. Therefore, only Cherenkov light originating from muons can be collected.

Figure 2 shows the monitor design. The optical system has astigmatism but no chromatic aberration because it uses only mirrors [4, 5]. Although the wavelength dependence of the radiator's refractive index must be taken into account, the entire wavelength range to which the detector is sensitive can be utilized. The Cherenkov light is guided through a vacuum window to an external CMOS sensor, which is shielded with lead and mounted on a motorized stage to allow focus adjustment.

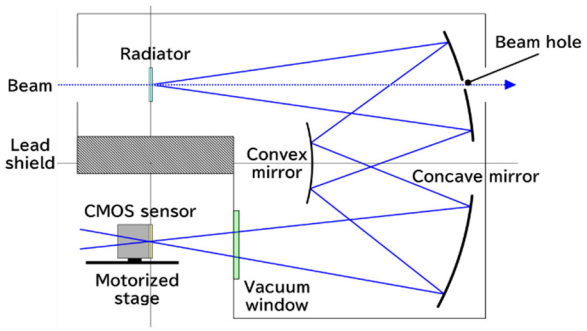



Figure 2: Layout of the beam profile monitor.

* Work supported by JSPS KAKENHI Grant Numbers 22H00141, 21H05088, 25H00401, 25H01295, the JST FOREST Program (Grant Number JPMJFR212O), the Toray Science and Technology Award and Research Grant, and the natural science grant of the Mitsubishi Foundation, Support for academic and research activities from Sumitomo Electric Group CSR Foundation, and Support for academic and research activities from CASIO SCIENCE PROMOTION FOUNDATION.
† nrisa@post.kek.jp

Content from this work may be used under the terms of the CC BY 4.0 licence (© 2025). Any distribution of this work must maintain attribution to the author(s), title of the work, publisher, and DOI.

ISBN: 978-3-95450-262-2 ISSN: 2673-5350 doi: 10.18429/JACoW-IBIC2025-TUPCO14

# STATUS OF OSCILLATING ARM WIRE MONITOR DEVELOPMENT

R. Dölling†,1, A. Sandström, M. Rohrer, S. Warren, D. Befus, S. Jaroslawzew, X. Wang, S. Bugmann, M. Mähr, R. Nicolini, M. Sapinski, S. Lindner, R. Baldinger
PSI Center for Accelerator Science and Engineering, Villigen, Switzerland, [1] Retired

*Abstract*

We present the development of a high-speed oscillating-arm wire monitor (OAWM). Similar devices are in use at PSI's HIPA facility since the 1970s [1-3], however they are significantly slower. The new design maintains the compact longitudinal footprint of the original instrument; a property rarely found among fast wire monitors [4]. First performance tests demonstrated wire velocities of 4 m/s using a stepper motor and 8 m/s with a servo motor. This advancement will allow to use wire scanners to measure the beam profile in the most challenging of the HIPA beamlines, with beam current exceeding 10 mA.

## MECHANICAL SETUP

The present OAWM use a 20:1 worm gear reduction and reach an on-axis wire speed of 0.75 m/s. This is not sufficient to operate at full beam current in the 0.87 MeV injection line. Lower gear reductions allow higher speeds [5]. The new prototype uses a 1:1 direct drive from the motor to the con-rod (Figs. 1-2). To allow for a smaller bellow, the bearings at the arms axis of rotation are now outside the bellow. Bearings with low play are used throughout. The inertia of the monitor arm (MA) is dominated from the material far from the axis of rotation. It consists of two half-shells, fluid formed from 0.1 mm titanium or 0.075 mm 1.4404 stainless steel sheets [6]. Gauges hold the half-shells in place while laser-welded at the outer contour and spot-welded at the elongated corrugations [7]. 6 ceramic beads are clamped in recesses; these guide the signal wire.

Tests were performed with the titanium variant of MA; either a 2-phase stepper motor PKP245D23B2 without brake [8], or a servo motor AM8113-0F01 with brake and resolver [9] were used. The stepper motor was rotated in its holder so that the starting position coincidences with a full step position. The arm position is measured with a potentiometer TEX-0025-415-002-101 [10, 4] and, only for testing in the lab, a laser triangulation sensor ILD2300-50 [11].

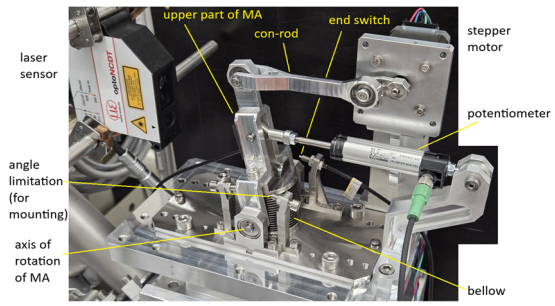



Figure 2: Setup with stepper motor in parking position.

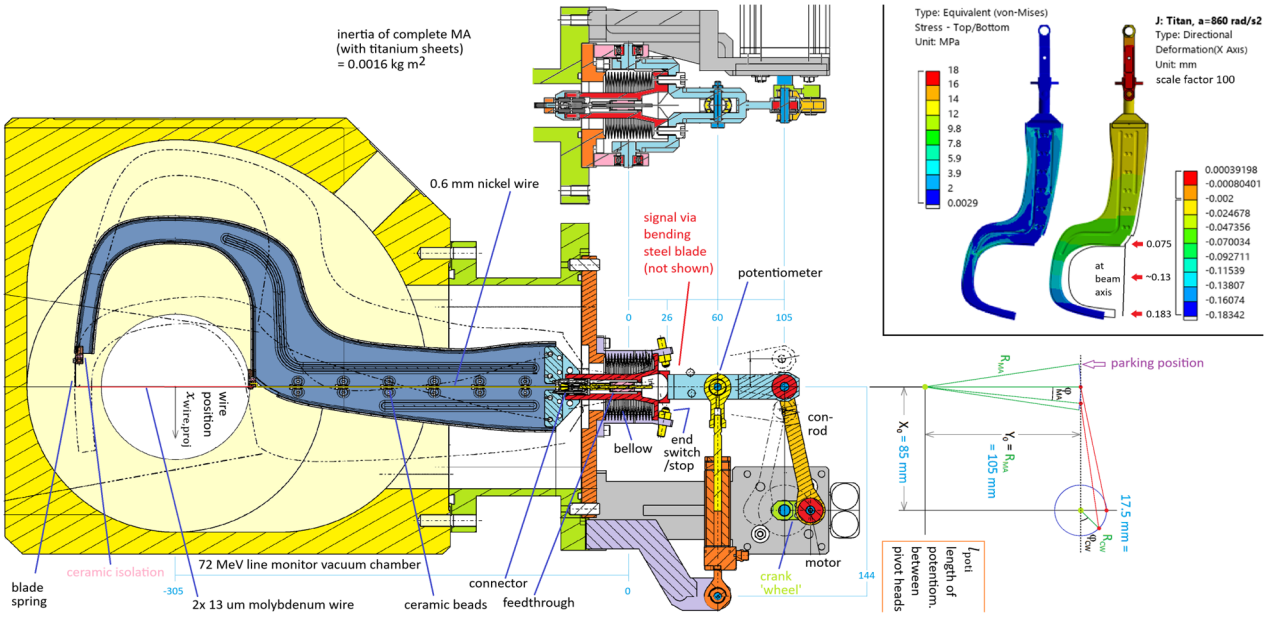



Figure 1: Setup of prototype (horizontal MA). Insert: ANSYS calculation [12] of deformation and stress of MA at constant angular acceleration equal to the maximum acceleration of the below discussed preset trajectory at an on-axis wire speed of 3.9 m/s. Maximum load on the relevant load-bearing areas of the shells is ~10 MPa, much less than the yield strength of 203 MPa for titanium grade 1 (which corresponds to ~17.4 m/s). With the stainless-steel variant, the numbers are ~15 MPa, 596 MPa, ~24.7 m/s at similar deformation and 15 % increased inertia of the MA.

† doelling@protonmail.com

Content from this work may be used under the terms of the CC BY 4.0 licence (© 2025). Any distribution of this work must maintain attribution to the author(s), title of the work, publisher, and DOI.

ISBN: 978-3-95450-262-2 ISSN: 2673-5350 doi: 10.18429/JACoW-IBIC2025-TUPCO15

# FAST CORRECTOR VESSEL SELECTION FOR HIGH BANDWIDTH FAST ORBIT FEEDBACK

S. Banerjee*, F. Malinowski, L. Bobb, Diamond Light Source, Didcot, United Kingdom

*Abstract*

The DiamonDiamond-II upgrade will enhance the performance of the Diamond Light Source synchrotron, including improved beam stability by the Fast Orbit Feedback system. Achieving the targeted closed-loop bandwidth of 1 kHz necessitates an open-loop actuator bandwidth of approximately 10 kHz, which presents significant design challenges for the corrector magnet vacuum vessel. Additionally, subsystems such as the corrector magnet power supplies and Beam Position Monitors must comply with a stringent closed-loop latency of less than 100 µs. Initially, a 1 mm stainless steel vessel was deemed viable; however, experimental findings indicated that the combination of stainless steel and neighbouring copper vessels resulted in a decrease in both integrated magnetic field strength and system bandwidth. This prompted a reassessment of the material selection for the fast corrector vessels to optimise orbit feedback performance. This paper investigates these challenges, analyses experimental data, and explores solutions to achieve the necessary bandwidth for the DiamonDiamond-II upgrade.

## INTRODUCTION

The Diamond-II upgrade project significantly enhances Diamond Light Source (DLS) synchrotron performance through a Fast Orbit Feedback (FOFB) system targeting 1 kHz closed-loop bandwidth. The FOFB controller manages 252 slow correctors (SCs) and 138 fast correctors (FCs) using generalised singular value decomposition (GSVD)-based dual-rate Internal Model Control (IMC) for efficient handling of two-input-single-output (TISO) and single-input-single-output (SISO) subsystems [1].

The system architecture requires 10 kHz open-loop bandwidth for FCs and 150 Hz for SCs [1], creating substantial challenges for FC magnet vacuum vessel material selection. Additionally, the FOFB subsystem requirements include FC magnet power supply units (PSUs) and Beam Position Monitors (BPMs) with Analogue Front-End (AFE), Digital Signal Processing (DSP) filters, and Digital-to-Analogue Converters (DACs) meeting <100 µs closed-loop latency specifications [1–3].

Initial analysis using the Podobedov model [4] indicated 1 mm thick stainless steel (SS) vessels could theoretically achieve the required bandwidth. However, experimental findings revealed unexpected complications when combining SS vessels with neighbouring copper (Cu) vessels, reducing integrated magnetic field strength and overall open-loop bandwidth [5]. This discovery necessitated material selection re-evaluation for Diamond-II FOFB FC vessels.

Given the permanent vessel installation and impracticality of post-installation replacement, optimal material selection is critical for the success of Diamond-II. This paper explores vessel material selection challenges, analyses experimental results, and proposes solutions to achieve desired bandwidth performance.

## VESSEL TRANSFER FUNCTION

To evaluate the transfer function ($TF$) of FC vessels, several assumptions were made:

- All vessels will have a length of 85 mm with a thickness of 1 mm, combined with neighbouring Cu vessels.
- The magnetic field is symmetric across the vessel on both sides of the FC magnet.
- The behaviour in the vertical and horizontal directions is identical.

These assumptions provide a consistent basis for comparing different vessel materials and their effects on the FOFB system performance.

### *Experimental Data*

The Magnet Group at DLS carried out experimental studies using a prototype FC magnet with three 85 mm-long and 1 mm thick vessels. The three configurations were stainless steel (SS) joined to Cu, Inconel joined to Cu, and titanium (Ti) joined to Cu, as shown in Fig. 1(a). For consistency, the Cu sections were manufactured to the same diameter and thickness as the SS vessel. The vessel components were friction-fitted rather than permanently joined; this had only a minor effect on the measured bandwidths, which also showed good agreement with OPERA 3D simulations.

A sinusoidal signal from 10 Hz to 30 kHz was generated and applied to a narrow, long multi-turn search coil as shown in Fig. 1(b), placed at the geometric centre of the vessel shown in Fig. 1(c). All measurements were done using a Zurich Instruments MFLI lock-in amplifier. Its output drove the magnet coil, creating an oscillating magnetic field. A search coil detected the induced voltage, which was fed back into the lock-in input. By sweeping the frequency, repeatable measurements were achieved with minimal noise.

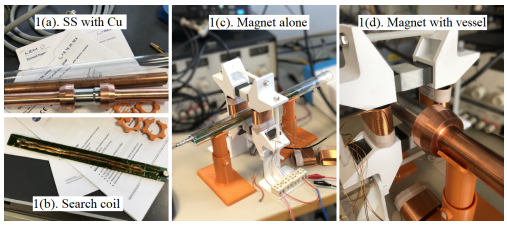



Figure 1: Experimental setup of prototype FC.

* shohan.banerjee@diamond.ac.uk

Content from this work may be used under the terms of the CC BY 4.0 licence (© 2025). Any distribution of this work must maintain attribution to the author(s), title of the work, publisher, and DOI.

ISBN: 978-3-95450-262-2 ISSN: 2673-5350 doi: 10.18429/JACoW-IBIC2025-TUPCO16

# IRRADIATION TESTS OF A DIGITAL RADIATION-TOLERANT CAMERA FOR CERN'S PARTICLE ACCELERATOR INSTRUMENTATION

S. Burger*, F. Roncarolo, E. Bravin, CERN, Geneva, Switzerland
S. Beauvivre, Q. Bouille, D. Kraehenbuehl
MicroCameras and Space Exploration, Neuchatel, Switerland

*Abstract*

Beam imaging systems are integral parts of beam instrumentation at CERN, measuring the shape, size, and position of particle beams in accelerators. Following the worldwide phasing out of analogue cameras and vidicon tubes (which the system was initially based on and still partially uses), part of the ongoing consolidation program involves developing a new camera system based on digital technology for use in CERN's medium radiation environments up to few 100 Gy total dose.

For this purpose, the CERN Beam Instrumentation group initiated the development of a digital camera system in collaboration with MCSE, a Swiss company specializing in space instrumentation. The new camera's performance under radiation was evaluated at CERN's CHARM test facility, with promising results in terms of radiation immunity while maintaining sufficient sensitivity and resolution—which will be the focus of this contribution. Following this prototyping phase, an industrial version is now in development and is expected to undergo testing in 2025.

## INTRODUCTION

The CERN Beam Instrumentation group (SY-BI) uses cameras in over 200 beam imaging systems to monitor beam presence, position, size, and occasionally for remote equipment inspection. Most systems use interceptive screens emitting light via scintillation or Optical Transition Radiation (OTR), captured by cameras through optical setups [1]. These instruments cover CERN's accelerator complex, including ISOLDE, HIRADMAT, AWAKE, and CLEAR. Historically based on analog cameras, they are now transitioning to digital models due to the phase-out of analog devices. Figure 1 illustrates the principle of such a system as deployed across the accelerator chain.

The consolidation program first focused on identifying reliable digital camera suppliers and evaluating the intrinsic radiation tolerance of their products. Dedicated tests [2] established safe operational limits for commercial off-the-shelf (COTS) cameras, beyond which radiation-hardened solutions are needed.

To address varying radiation environments, programs were launched for both radiation-tolerant cameras—withstanding a few hundred gray (Gy)—and radiation-hardened cameras, designed for several megagray (MGy). A key challenge is not only reaching these dose thresholds but also ensuring resilience against single event effects (SEEs), which can disrupt electronics. Unlike analog systems, where damage appears as degraded image quality, digital cameras are especially vulnerable to SEEs, particularly single event upsets (SEUs), which cause temporary bit-flips in memory or logic, often leading to loss of communication.

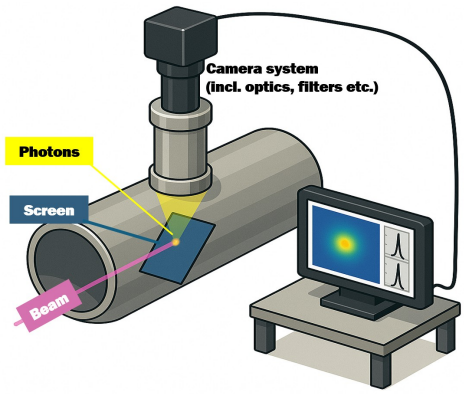



Figure 1: Principle of a camera and screen based instrumentation for beam observation/measurement.

In this paper, we report on the irradiation tests and results for the radiation-tolerant camera "BeamCam", carried out at CERN's CHARM facility [3]. This camera is the result of a collaborative development between MCSE [4] and CERN.

## RADIATION TOLERANT CAMERA DESIGN: 'BEAMCAM'

The design is based on an existing MCSE camera originally developed for space applications. It has been adapted for CERN by removing components unnecessary for operation in particle accelerators—such as specialized (and costly) cosmic ray shielding and systems built to withstand extreme conditions (e.g., wide temperature ranges, strong vibrations, and magnetic fields).

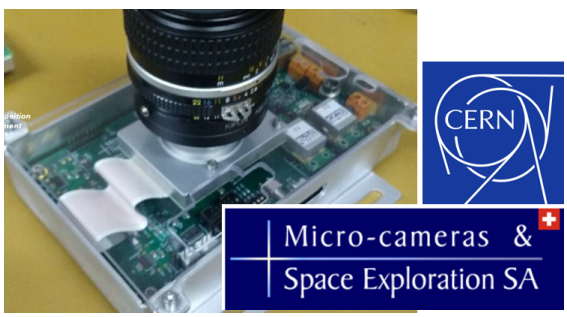



Figure 2: Picture of the 'BeamCam' camera prototype ready for the irradiation test.

* stephane.burger@cern.ch

Content from this work may be used under the terms of the CC BY 4.0 licence (© 2025). Any distribution of this work must maintain attribution to the author(s), title of the work, publisher, and DOI.

ISBN: 978-3-95450-262-2 ISSN: 2673-5350 doi: 10.18429/JACoW-IBIC2025-TUPCO17

# UPGRADE AND EVOLUTION OF THE AD TARGET BEAM IMAGING SYSTEM AT CERN: A TWO-YEAR PERFORMANCE ANALYSIS

S. Burger*, F. Roncarolo, J. Martínez Samblas, M. Gonzalez-Berges, CERN, Switzerland

*Abstract*

During CERN's Long Shutdown 2 (LS2) in 2021, the Anti-Proton Decelerator (AD) target area underwent major renovations, including a significant upgrade to its beam imaging system. The previous tube-based camera, used in a high-radiation environment, had limitations in sensitivity and resolution for continuous measurements. The upgraded design uses an innovative in-air light-emitting screen mechanically coupled to the AD target, monitored by a digital camera through a 20-meter optical line from a radiation-safe zone. This setup improves accessibility during beam operation and enhances measurement capabilities. Over two years of operation, several crucial modifications were made. A key change was transitioning from a scintillation material screen to an Optical Transition Radiation (OTR) screen, though this created new challenges with background interference. To address temperature-dependent calibration variations, an automated calibration mechanism was developed, utilizing advanced image analysis algorithms for real-time adjustments.

## INTRODUCTION

The AD target area required major consolidation [1,2] due to aging and obsolete equipment—including the target, magnetic horn, and support infrastructure—in order to mitigate significant safety risks and ensure long-term operational reliability beyond 2030. The upgrade also aimed to improve the reliability and efficiency of antiproton production. As part of this effort, new instrumentation was requested to measure the beam size and position in front of the AD target for all extracted beams, with a resolution better than 250 µm. This capability enables online verification of the target setup's integrity and helps ensure optimal antiproton yield for physics experiments. Table 1 lists the beam parameters delivered to the new AD target station from the Proton Synchrotron (PS).

Table 1: Nominal Parameters of the Beam Delivered to the AD Target

| Parameter | Value |
|---|---|
| Type | Protons |
| Energy | 26 GeV |
| Intensity | $1.5 \times 10^{13}$ ppp |
| Annual intensity | $2.0 \times 10^{18}$ POT |
| Length | 450 ns |
| Repetition Rate | 0.01 Hz |
| Size at target | $\sigma_x = \sigma_y = 1$ mm |

A critical factor is the intense radiation generated during antiproton production, which results in significant activation of the surrounding area. To achieve 100 % measurement availability while minimizing maintenance, the system employs a fixed scintillating screen, with the emitted photons relayed over a 20 m optical path to a camera located in a radiation-free area. The optical line (see Fig. 1) consists solely of flat mirrors, with no intermediate focusing elements; all image formation, magnification, and focusing are performed by a large-aperture final camera lens (Fig. 2). This configuration preserves image quality, minimizes aberrations, and maintains the required depth of field over the entire optical path.

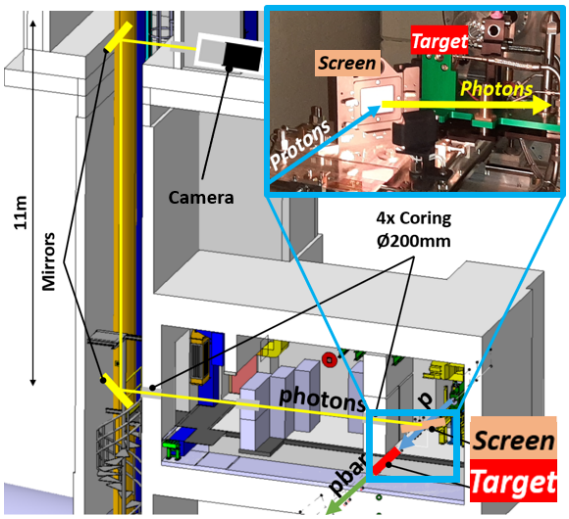



Figure 1: Optical layout of the AD target beam imaging system, highlighting the target/screen station.

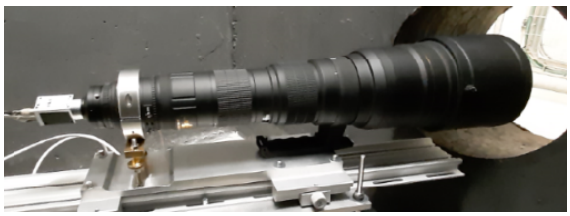


Figure 2: Large-focal-length camera lens with digital camera, installed in a dedicated blackened, radiation-free room.

## DESIGN EVOLUTION

The system is based on a screen mounted on a frame designed for quick installation and can be removed via a fast connection system. This design follows the "As Low As

* stephane.burger@cern.ch

Content from this work may be used under the terms of the CC BY 4.0 licence (© 2025). Any distribution of this work must maintain attribution to the author(s), title of the work, publisher, and DOI.

ISBN: 978-3-95450-262-2 ISSN: 2673-5350 doi: 10.18429/JACoW-IBIC2025-TUPCO18

# EXPERIMENTAL INVESTIGATION INTO SUPERSONIC GAS JET INDUCED BEAM PERTURBATION

W. Butcher[1,2,*], N. Kumar[1,2], M. Patel[1,2], O. Stringer[1,2], F. Thesni[1,2], H. Zhang[1,2], B. S. Rawat[1,2], C. P. Welsch[1,2]
[1]Department of Physics, University of Liverpool, Liverpool, UK
[2]Cockcroft Institute, Sci-Tech Daresbury, Warrington, UK

*Abstract*

In radiotherapy, treatment beams require precise margins to ensure the preservation of surrounding healthy tissue. Clinical studies have shown that to mitigate range deviations of the Bragg peak, safety margins of typically less than 5% around the target volume are employed. Consequently, real-time or online diagnostic techniques should be designed to minimize beam perturbation to the greatest extent possible. A minimally-invasive gas jet beam profile monitor for medical treatment facilities is being developed at the Cockcroft Institute (UK) to provide online monitoring. The monitor operates a thin, low-density, gas jet curtain, transecting with the beam. A proof-of-concept experimental study was carried out to quantify the degree of perturbation the gas jet has on a beam, using a 10 keV electron gun with a maximum current of 100 µA. Any changes in beam profile and current were measured via a scintillator screen and Faraday cup respectively in path of the beam after the gas curtain. In the future, a simulation study will also be carried out using BDSIM, a Beam Delivery Simulation program built on GEANT4, with the experimental beam parameters along with medical hadron beams. This contribution provides the details of an experimental study into the perturbation experienced by an electron beam from a gas jet monitor.

## INTRODUCTION

The QUASAR group, based at the Cockcroft Institute (UK) is developing a minimally invasive gas jet in-vivo profile monitor for the purpose of online beam diagnostics for medical accelerator beams. The key aims of this gas jet monitor is to deliver real time profile monitoring to possibly reduce frequent calibration to progress treatment efficiency [1]. The gas jet monitor has undergone 15+ years of development from original conception to continuing optimization and improvements [1-5]. The monitor was first created and has now been tested for the High Luminosity upgrade of the Large Hadron Collider (HL-LHC) [6,7]. In order to be installed in medical LINACs in the future, the treatment beam must be negligibly affected by the gas jet monitor. This experimental research is vital as the dosage levels transferred to the patient and beam parameters are not compromised. This contribution endeavours to quantify the level of perturbation or "invasiveness" a gas jet may have on a particle beam. The study examines the effects of nitrogen and argon gas jets have on several beam parameters for a low energy, low momentum electron beam (4.9 keV – 5.3 keV).

## GAS JET SYSTEM

Existing invasive monitors such as wire scanners experience from short lifetimes and continual maintenance. Minimally-invasive monitors like residual gas monitors suffer from beam profile distortions. Diagnostics like the residual gas monitors experience distortion because the yield of the ionization will undergo momentum spread initially and the primary beam can cause space charge effects [3]. Hence, there is a requirement present for the development of minimally- or non-invasive beam profile monitors that offer both high resolution, non-distorted beam profiles, and real-time feedback. This potential solution comes in the form of a minimally-invasive supersonic gas jet beam profile monitor. This monitor operates by having a thin, supersonic, low density, gas jet curtain of neutral gas molecules, tilted at 45°, intersecting with the charged particle beam in order to provide a 2D transverse beam profile via ionization [1-6]. Figure 1 below shows a schematic of the extraction system and the gas jet intersecting the beam perpendicularly. Thus far, extensive research and development has been completed by the Gas Jet group, within the QUASAR group, into the design and optimisation of a gas jet beam profile monitor. The key advantage of this system is its minimally-invasive nature and it can provide the 2D transverse beam profile. A schematic of the gas jet monitor can be found in Fig. 2.

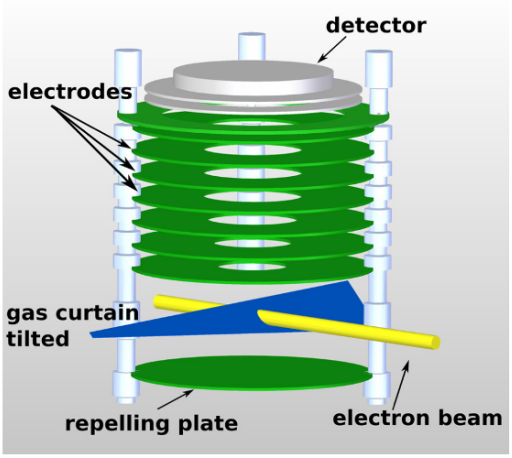



Figure 1: Visualization of the extraction system and gas jet-particle beam interaction [2].

* W.Butcher@liverpool.ac.uk

Content from this work may be used under the terms of the CC BY 4.0 licence (© 2025). Any distribution of this work must maintain attribution to the author(s), title of the work, publisher, and DOI.

ISBN: 978-3-95450-262-2 ISSN: 2673-5350 doi: 10.18429/JACoW-IBIC2025-TUPCO20

# DESIGN AND IMPLEMENTATION OF ALLISON SCANNER AT THE KOMAC LEBT *

S.H. Moon †, D.-H Kim, S. Lee, S.-P Yun, S.-Y Cho, H.-S Kim, H.-J Kwon
Korea Atomic Energy Research Institute, Gyeongju, Republic of Korea

*Abstract*

This study presents the design, specifications, and experimental result of the Allison scanner installed at the injector of the 100 MeV proton accelerator operated at Korea Multi-purpose Accelerator Complex (KOMAC). The Allison scanner was developed to enable precise characterization of the proton beam's phase space at the injector stage. Detailed design parameters and operational principles of the system are described. Experimental measurements were conducted under various operating conditions to assess the performance and reliability of the scanner. Furthermore, the daily measurement data collected by the Allison scanner were analyzed to evaluate the long-term stability of the ion source.

## ALLISON SCANNER

### *Principle of Allison Scanner*

The Allison scanner is a widely known method for measuring beam emittance and it consists of two slits, two deflecting electrodes, and a Faraday cup. At a given position, the scanner sweeps the voltage applied to the deflecting electrode while measuring the beam current collected by the Faraday cup. By repeating this process at multiple positions, a two-dimensional phase space distribution of the beam can be measured.

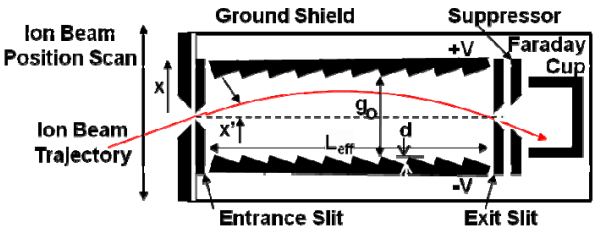



Figure 1: Schematic drawing of Allison scanner [1].

Figure 1 shows a schematic of the Allison scanner designed at the Spallation Neutron Source (SNS) in the United States. After the beam is collimated by the first entrance slit, it receives an angular kick due to the electric field applied to the deflecting plates. Only those particles whose initial angular components are exactly canceled by the electric field can pass through the second exit slit and are subsequently measured by the Faraday cup.

* Work supported by KOMAC operation fund of KAERI by MSIT (Ministry of Science and ICT)
† msh3069@kaeri.re.kr

### *Design of Allison Scanner at KOMAC LEBT*

The Allison scanner installed at the KOMAC LEBT operates based on the same measurement principle as previously described. Its design is shown in Fig. 2. The KOMAC LEBT Allison scanner also consists of an entrance slit, deflecting plates, an exit slit, and a Faraday cup. In addition, a suppression plate is installed in front of the Faraday cup to suppress secondary electrons. Detailed design parameters such as the size of the entrance slit, the length of the deflecting plates, and the gap between the plates were carefully determined to ensure accurate measurements. These specific values are summarized in Table 1.

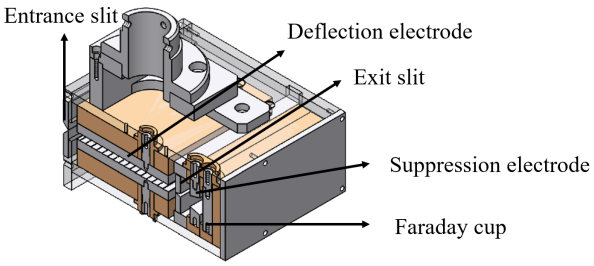



Figure 2: Drawing of Allison scanner at KOMAC LEBT.

Table 1: Design Parameter of Allison Scanner at KOMAC LEBT

| Design Parameter | Value |
|---|---|
| Size of Entrance Slit | 0.1 mm |
| Size of Exit Slit | 0.1 mm |
| Maximum voltage for deflection electrode | 1000 V |
| Maximum voltage for suppression electrode | 1000 V |
| Length of deflection electrode | 57 mm |
| Gap between deflection electrode | 3.5 mm |

### *System Configuration*

Although the hardware of the Allison scanner was fabricated based on the specifications listed in Table 1, system integration with components such as the control box, control software, and power supply is essential for actual beam measurements. To enable this, a complete system was developed, and its configuration is shown in the following diagram.

Figure 3 illustrates the system configuration of the Allison scanner measurement system. The control box consists of an ADC, a DAC, and a motor controller. The motor controller drives the stepper motor mounted on the Allison scanner

Content from this work may be used under the terms of the CC BY 4.0 licence (© 2025). Any distribution of this work must maintain attribution to the author(s), title of the work, publisher, and DOI.

ISBN: 978-3-95450-262-2 ISSN: 2673-5350 doi: 10.18429/JACoW-IBIC2025-TUPCO21

# LOW ENERGY EXPERIMENTAL BENCH (LEEx-B) AND EMITTANCE-METER DEVELOPMENTS AT IPHC

E. Bouquerel†, E. Traykov, C. Maazouzi, T. Adam, P. Graehling, C. Mathieu
Université de Strasbourg, CNRS-IN2P3, Strasbourg, France

*Abstract*

A low-energy experimental bench called LEEx-B is being developed at IPHC-CNRS of Strasbourg, France. The bench is composed of a $Cs^+$ ion gun mounted on a HV platform providing beams up to 25 keV. The main objective of this bench is to support the advancement of beam diagnostics, including the ongoing development of the Allison-type emittance-meter. This paper presents the progress of the construction of the LEEx-B and of the beam diagnostics.

## INTRODUCTION

Beam diagnostics are key for commissioning, tuning and operating particle accelerators, transfer lines and other beam manipulation systems, providing measurements of beam intensity, energy, position and distribution.

Over the past two decades, major accelerator projects (e.g. LHC, ESS) have pushed technologies to deliver extreme beams for fundamental research, while others, notably in the medical sector, focus on lower energies with highly specific requirements. These advances demand diagnostics of higher precision and reliability, often non-invasive, yet existing tools face clear limitations.

At IPHC-CNRS Strasbourg, the Accelerator Instrumentation Team (EIA) has concentrated its efforts on low-energy accelerators and their applications. With nearly 20 years of expertise in beam diagnostics and control systems, the team develops new-generation instruments and upgrades existing ones. A major achievement is the Allison-type emittance meter [1], first proposed in 1983, of which several versions were realized within projects such as SPIRAL2, MYRRHA, FAIR and soon NEWGAIN [2-4].

To gain autonomy and efficiency in validating its developments - previously dependent on external facilities with strong time and location constraints - the team is now building its own dedicated experimental bench.

## THE LOW ENERGY EXPERIMENTAL BENCH

To support the development of beam diagnostics, the EIA team designed a dedicated low-energy experimental bench (LEEx-B). Such a platform enables tests with minimal energy consumption and operating costs, while providing the autonomy needed for systematic validation of new instruments.

### *Specifications and Equipment*

The LEEx-B is intended to validate key aspects of beam diagnostics systems (BDS): accuracy, precision, calibration, sensitivity, compatibility with beam properties, and long-term reliability. These tests ensure robust and trustworthy measurements.

The bench consists of a modular support with a high-voltage platform, a low-energy ion gun based on a surface ionization source, and a beamline section including optics, diagnostics, and a vacuum chamber adaptable for future developments or ion beam experiments (Fig. 1).

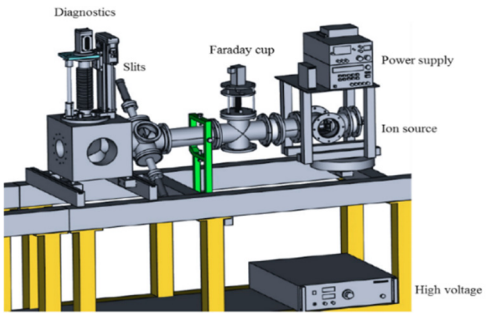



Figure 1: 3D view of the experimental bench.

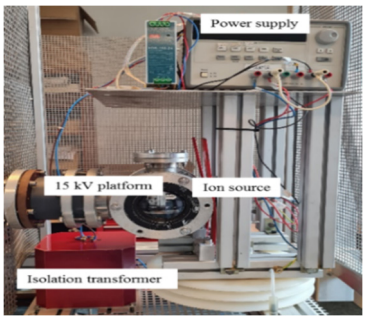



Figure 2: Photograph of the high voltage platform.

The ion source, a HeatWave HWIG-250 [5], can generate a 1 µA, 10 keV $Cs^+$ beam. It operates under ultra-high vacuum ($10^{-6}$ -$10^{-7}$ mbar) maintained by scroll and turbo-molecular pumps, with pressure monitoring by Pirani and Penning gauges. Beam formation relies on a heated Cesium compound pellet, extraction electrode, and focusing optics. The HV platform, powered by a FUG HCN 35 supply and insulated via a dedicated transformer, reaches up to 25 kV (Fig. 2). Safety is ensured through interlocks, light beacons, and secured access to the HV zone. Optical simulations using SIMION [6] were performed to optimize ion transport along the beamline.

### *Control System*

The bench integrates three main components - source, optics, and diagnostics - each with dedicated control. Source: four power channels (heater, source, extraction, focus) are controlled via optical fiber to withstand the HV

† elian.bouquerel@iphc.cnrs.fr

Content from this work may be used under the terms of the CC BY 4.0 licence (© 2025). Any distribution of this work must maintain attribution to the author(s), title of the work, publisher, and DOI.

ISBN: 978-3-95450-262-2 ISSN: 2673-5350 doi: 10.18429/JACoW-IBIC2025-TUPCO22

# CHERENKOV RADIATION SPECTRAL AND RESOLUTION PROPERTIES STUDIES AT SINBAD ARES

A. Novokshonov*, G. Kube, W. Kuropka, B. Stacey, M. Kellermeier, T. Vinatier
Deutsches Elektronen-Synchrotron (DESY), Hamburg, Germany
A. P. Potylitsyn, Institute of Applied Problems of Physics of the National Academy of Sciences of the Republic of Armenia (IAPP NAS RA), Erevan, Armenia

*Abstract*

Optical Cherenkov Radiation (ChR) is a well-known type of radiation, which is utilized in different fields of physics such as charged particle detection or generation of intense THz radiation. It is also widely used in beam diagnostics, for instance, in beam loss monitors or for bunch length measurements. In addition, it is of potential interest for transverse beam profile diagnostics as an alternative for standard techniques as scintillating screens and optical transition radiation. In this work, spectral and resolution properties of optical ChR were studied at the SINBAD ARES accelerator with an electron beam energy of 150 MeV. Several fused silica crystals of different thicknesses were used as radiators. They could be rotated relative to the beam, which allowed to investigate the angular dependency of the ChR spectrum which is quasi-monochromatic. The monochromatization effect arises from the frequency-dependent nature of the fused silica permittivity. In addition, the beam size dependency on the target angle was investigated in view of differences for various crystal thicknesses.

## INTRODUCTION

Cherenkov radiation (ChR) [1,2] is widely used across various fields of physics, including the design and construction of detectors [3], beam diagnostics in modern accelerators [4], and as a radiation source [5]. ChR exhibits three main characteristics: directional emission, a velocity threshold for particle excitation, and a continuous spectrum extending from approximately 100 nm to centimeter wavelengths. The first of these features, directional emission, is described by the following formula:

$$\theta_{ch} = \arccos\left(\frac{1}{\beta\, n(\lambda)}\right), \tag{1}$$

where $\theta_c h$ is ChR opening angle, $\beta = v/c$ is the reduced velocity of the moving charged particle and $n(\lambda)$ is the wavelength dependent refractive index of the media. Consequently the threshold condition is as follows:

$$\beta\, n(\lambda) > 1. \tag{2}$$

The threshold defines the radiation spectral range for constant particle velocity.

Interest in studying ChR has increased in recent years. Advances in the design of artificial structures have enabled the fabrication of materials with unusual electromagnetic properties such as metamaterials, photonic crystals, and metastructures at the nanoscale. These materials can serve as ChR targets and significantly modify its emission characteristics. In beam diagnostics, ChR is already widely used in beam loss monitors (BLMs), and Cherenkov diffraction radiation (ChDR) can be employed for beam profile monitoring or beam position measurements [6]. Possibly, ChR has the potential to serve as an alternative to standard techniques such as optical transition radiation (OTR) [7] and scintillating screens [8], both of which have inherent limitations.

## EXPERIMENTAL SETUP

A series of measurements was carried out using the 150 MeV electron beam of the SINBAD ARES linac. The experimental setup is shown in Fig. 1. Several quartz plates of different thicknesses (0.2, 0.4, 0.6, 1, and 2 mm) were investigated, along with a 0.2 mm thick GAGG:Ce scintillator used as a reference. The samples were placed 60 mm downstream of the accelerator's exit window, which was made of 50 µm thick titanium. Each crystal could be rotated around its vertical axis. Two types of detectors were employed: a CMOS camera and a spectrometer. The camera was a Basler acA2440-20gm equipped with a Schneider-Kreuznach Makro-Symmar 5.6/80 objective, while the spectrometer was a Hamamatsu C10082CA mini-spectrometer. Light was coupled into the spectrometer using a 1 m long Hamamatsu A15262-01 fiber with a 0.6 mm pure quartz core. A $MgF_2$ lens with a 100 mm focal length collimated the light into the fiber. Both images and spectra were recorded at a 45° observation angle.

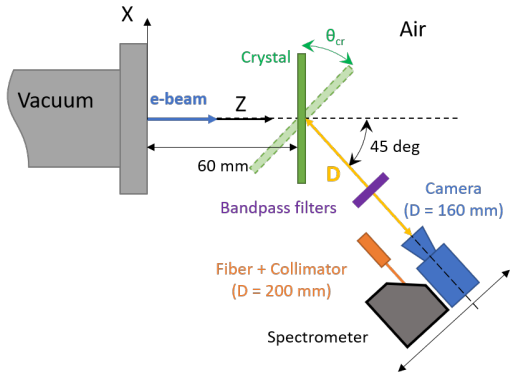



Figure 1: Scheme of the experiment.

* artem.novokshonov@desy.de

Content from this work may be used under the terms of the CC BY 4.0 licence (© 2025). Any distribution of this work must maintain attribution to the author(s), title of the work, publisher, and DOI.

ISBN: 978-3-95450-262-2 ISSN: 2673-5350 doi: 10.18429/JACoW-IBIC2025-TUPCO24

# DESIGN AND PROGRAMMING OF A MULTIFUNCTIONAL DEVICE FOR ACCELERATOR BEAM PROFILE MEASUREMENT AND BEAM STOP*

F. Li†, L. Zeng, R. J. Yang, Z. Xu, J. Y. Lv, R. Yang, W. L. Huang, M. A. Rehman, R. Y. Qiu, A. H. Li
Institute of High Energy Physics, Chinese Academy of Sciences (CAS), Beijing, China
China Spallation Neutron Source, Dongguan, China

*Abstract*

During the pre-research phase of China Spallation Neutron Source (CSNS) upgrade project (CSNS-II), in order to conduct beam commissioning of the Radio Frequency Quadrupole (RFQ) under high-intensity beam conditions, the structure of the last-stage wire scanner of the Medium Energy Beam Transport (MEBT) was innovatively modified. This modification not only added a Beam Stop but also significantly enhanced the efficiency of wire scanner. This paper presents the architecture and operational programming of a novel multifunctional device designed for accelerator beam diagnostics and beam termination: beam profile measurement via advanced sensing mechanisms and Beam Stop using a braided carbon fiber plate as the primary beam stop.

## INTRUDUCTION

The China Spallation Neutron Source (CSNS) [1] is a large-scale scientific facility in China and stands as a vital platform for advancing scientific research and industrial innovation. Its primary mission is to generate intense pulsed neutron beams, which serve as a "super microscope" enabling researchers to explore the microscopic structure and dynamic processes of materials across diverse fields.

The accelerator system of CSNS complex consists of a 50 keV H- ion source, a 3 MeV radio frequency quadrupole (RFQ), an 80 MeV drift tube linac (DTL), a 1.6 GeV rapid-cycling synchrotron (RCS) and several beam lines. The Medium Energy Beam Transport (MEBT) [2] section of CSNS plays a vital role in beam transport and parameter adjustment. As depicted in Fig. 1, which show cases the structure of the MEBT section equipment, the traditional MEBTWS04 has shortcomings in function, Carbon nanotubes are applied as a new wire material and studied in comparison with carbon fiber wires.

Before the upgrade, the CSNS had a designed beam power of 100 kW. However, through continuous efforts and recent upgrades, the beam power had already reached 170 kW. With the Phase II upgrade, the proton beam power is expected to 500 kW. This significant increase in power means that the CSNS will be able to generate a far more intense pulsed neutron beam. The goal is concretely realized through a significant leap in beam current specifically, increasing the beam current from the pre-upgrade 15 mA to the target 50 mA with a repetition frequency of 25 Hz with a pulse width of 560 μs. The beam parameter is described in Table 1.

Table 1: Main Parameters of CSNS

| Project Phase | I | II |
|---|---|---|
| Beam Power | 100kW | 500kW |
| Energy | 1.6GeV | 1.6GeV |
| Beam Current | 15-20 m | 50mA |
| Pulse Length | A | 560us |
| RF Frequency | 560us | 324MHz |
| Repetition Frequency | 324MHz | 25Hz |
| | 25Hz | |

During the pre-research phase of CSNS-II, it is intended to conduct a series of experiments on the ion source and RFQ. However, the beam quality of the accelerator remains relatively poor at this stage. If such a low-quality beam directly enters the DTL cavity, it will cause certain damage to the cavity. Notably, the DTL cavity is a delicate component with high maintenance costs. To protect the DTL cavity, a baffle is proposed to be installed at the end of the Medium Energy Beam Transport (MEBT) section. This baffle will block the beam from entering the DTL during the beam commissioning process of the ion source and RFQ. Nevertheless, the current MEBT section features a compact structure, leaving no extra space for installing an additional Faraday cup. Therefore, a decision has been made to modify the MEBTWS04 device located at the end of the MEBT section. The modified MEBTWS04 is expected to not only retain its original function of beam profile measurement but also serve as a beam baffle.

Additionally, in depth research on the impact of new materials on the beam is necessary. This paper concentrates on the transformation of the WS in the MEBT section [3] of CSNS into a multifunctional device featuring double wires and a baffle. Carbon nanotubes are utilized as the wire material, and carbon fiber is employed for the baffle. A crossed double-wire structure, which enables simultaneous measurement of horizontal and vertical beam profiles, has replaced the original three-wire structure that only supported unidirectional measurement. The wire oriented at the 45° direction—with a relatively low utilization rate—has been removed. With the new structure, measurements for both horizontal and vertical positions can be acquired by moving the structure to one single position, thereby improving the scanning efficiency. The influence of the high

* Work supported in part by National Key R&D Program of China under Contracts No. 2023YFE0105700 and in part by the Open Fund of the China Spallation Neutron Source Songshan Lake Science City , DG24313511
† lifang@ihep.ac.cn

Content from this work may be used under the terms of the CC BY 4.0 licence (© 2025). Any distribution of this work must maintain attribution to the author(s), title of the work, publisher, and DOI.

ISBN: 978-3-95450-262-2 ISSN: 2673-5350 doi: 10.18429/JACoW-IBIC2025-TUPCO25

# DIRECT X-RAY IMAGING FOR THE NEW PINHOLE DIAGNOSTICS AT BESSY II

M. Marongiu*, V. Dürr, C. Kalus, G. Rehm, M. Ries, A. Schälicke, HZB, Berlin, Germany

*Abstract*

In order to improve our transverse diagnostic tools, two new pinhole beamlines will be designed. The pinhole arrays will be in air for easier maintenance: this will result in a significant loss of X-Ray photons when passing through the vacuum window. To overcome this issue, the option to directly illuminate a CCD/CMOS camera with X-Ray radiation without prior conversion into visible light is under study. Tests in the existing beamline both with a conventional CMOS camera and with a dedicated X-Ray camera are foreseen. This report describes our findings regarding the current status regarding the use of X-Ray cameras as a "high flux" diagnostic tool, as well as our preliminary experimental results.

## MOTIVATION

The present BESSY II electron-storage ring of Helmholtz-Zentrum Berlin (HZB) is operated at an electron energy of 1.7 GeV with an RF cavity frequency of 500 MHz [1]. The typical beam current is 300 mA in top-up operation; in Table 1 the more relevant parameters are shown.

Table 1: Main Parameters of BESSY II in Standard Mode Operation

| TopUp | Value |
|---|---|
| Beam Energy (GeV) | 1.7 |
| Rel. Energy Spread (%) | $7 \times 10^{-4}$ |
| Beam Current (mA) | 300 |
| Beam emittance (nm) | 5 |
| Coupling (%) | 2 |
| RMS Bunch-length (ps) | 20 |
| Bending Magnet Field (T) | 1.3 |
| Critical Energy (keV) | 2.5 |
| Lin. Pow. Density (Wmrad$^{-1}$) | 8.1 |
| Circumference (m) | 240 |

Pinhole camera are used as main X-Ray transverse diagnostic at BESSY [2]; two new beamlines will be installed to indirectly measure both emittance and momentum spread. This possibility is not currently available at the current beamline locations.

Furthermore, in order to allow easier and faster maintenance, the new beamlines will be realized in air, rather than in vacuum; this, however, causes a loss of radiation at the vacuum window that needs to be studied and addressed. One possibility is to directly image the X-Ray radiation, rather than previously converted it into visible light with a scintillator screen as it is usually done in synchrotron light sources. Some test using conventional visible light camera to directly image the X-Ray are ongoing: in Fig. 1, an example is shown.

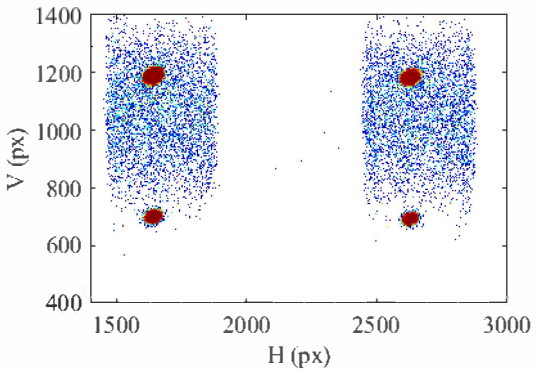



Figure 1: After 3 weeks of operation, an image has been captured by the CMOS camera: the amount of trapped electrons is dominant with respect to the incoming photons. Four beam spots from the pinhole array are visible, and also the radiation fan in the background. The white strip in the middle is due to the cooling grid of the pinhole target [3] (2 mm thick CuBe).

## PINHOLE LOCATIONS

In order to be able to measure emittance and momentum spread, a direct measurement of the transverse beam size in two location with significantly different Twiss parameters is needed. A proper evaluation of the optimal locations requires to estimate the propagation of uncertainties of the indirect measure (momentum spread and emittance) as a function of the Twiss parameters and of the directly measured beam sizes. It can be easily proved that the relative uncertainty of the momentum spread, assuming equal relative uncertainties of the beam sizes and negligible uncertainties of the Twiss parameters, is as follow:

$$\frac{U_{\Delta E}}{\Delta E} \propto \frac{\sqrt{1+x^2}}{1-x}\frac{U_\sigma}{\sigma}, \tag{1}$$

with $x = \frac{\sigma_2^2\beta_1}{\sigma_1^2\beta_2}$. A similar relation can be find for the emittance; in this case there is also a factor 2, and $x = \frac{\sigma_2^2 D_1^2}{\sigma_1^2 D_2^2}$ where $D$ is the dispersion.

It is therefore possible to check all the possible combination of available location and sort them with respect to the uncertainties.

* marco.marongiu@helmholtz-berlin.de

Content from this work may be used under the terms of the CC BY 4.0 licence (© 2025). Any distribution of this work must maintain attribution to the author(s), title of the work, publisher, and DOI.

ISBN: 978-3-95450-262-2 ISSN: 2673-5350 doi: 10.18429/JACoW-IBIC2025-TUPCO26

# REQUIREMENTS FOR EQUIPMENT IN COOLING SECTION OF EIC LOW ENERGY COOLER *

S. Seletskiy†, A. Fedotov, D. Kayran
Brookhaven National Laboratory, Upton, NY, USA

*Abstract*

The Electron Ion Collider (EIC) requires an electron cooler operating at the EIC injection energy to obtain the design proton beam emittances. A non-magnetized RF-based electron cooler, the EIC Low Energy Cooler (LEC), is currently under design. It will be operating at γ-factor 25.4 and will be delivering 70 mA electron current to a 170 m long cooling section (CS). To obtain required cooling an input from electron-proton relative trajectory misalignment into an overall angle in the cooling section must be kept below 15 μrad. In this paper we give comprehensive consideration of the factors affecting the trajectory angles and set the resulting requirements to various CS subsystems.

## INTRODUCTION

The Electron Ion Collider (EIC) Low Energy Cooler (LEC) [1] is designed to pre-cool proton bunches at the injection energy ($\gamma = 25.4$) to $\varepsilon_{np} = 0.3$ μm of normalized vertical emittance.

The LEC is a non-magnetized, RF-based electron cooler. It utilises an approach to the cooling established by LEReC [2-5]. The LEC includes a 170 m long cooling section – a straight section of the Hadron Storage Ring where the overlapping bunches of protons and electrons co-travel with the same velocity.

The LEC electrons are produced in a DC gun by illuminating a photocathode with a high frequency laser. The electrons are accelerated to 13 MeV, transported to the cooling section and dumped after a single pass through the cooling section (CS).

The LEC layout is schematically shown in Fig. 1.

The exact formulas for the cooling rates in non-magnetized RF-based electron coolers are given in [6]. For the purpose of the following discussion, we give an approximate scaling relations between the rate and beam parameters:

$$\lambda \propto \frac{N_e L_{\mathrm{CS}}}{\left(\sigma_{\theta e}^2+\sigma_{\theta p}^2\right)\left(\sigma_{\perp e}^2+\sigma_{\perp p}^2\right)\sqrt{\sigma_{\delta e}^2+\sigma_{\delta p}^2}\sqrt{\sigma_{ze}^2+\sigma_{zp}^2}}, \qquad (1)$$

where $N_e$ is number of electrons, $L_{\mathrm{CS}}$ is a length of the cooling section, $\sigma_{\theta e}$ and $\sigma_{\theta p}$ are respectively electron and proton bunches effective rms angular spreads, $\sigma_{\perp e}$ and $\sigma_{\perp p}$ are respective rms transverse sizes of the bunches, $\sigma_{\delta e}$ and $\sigma_{\delta p}$ are rms energy spreads, and $\sigma_{ze}$ and $\sigma_{zp}$ are rms lengths of the electron and proton bunches respectively.

To maximize the cooling rate while avoiding overcooling of the bunch core we require that the effective overall angular spread of electrons is $\sigma_{\theta e} \approx 25$ μrad, which is close to the protons angular spread in the CS.

The electron angles include the angles due to a "thermal" emittance $\sqrt{\frac{\varepsilon_{ne}}{\gamma\beta_{e\mathrm{CS}}}}$ (here $\beta_{e\mathrm{CS}}$ is electrons average $\beta$-function in the CS), angles ($\Theta_{\mathrm{SC}}$) driven by both the "self space charge" of the electron bunch and the proton-electron focusing in the CS [7], and average angle $\langle\theta\rangle$ caused by relative misalignment of electron and proton trajectories through the CS [8]:

$$\sigma_{\theta e}^2 = \frac{\varepsilon_{ne}}{\gamma\beta_{e\mathrm{CS}}} + \Theta_{SC}^2 + \langle\theta\rangle^2. \qquad (2)$$

Assuming that the combined emittance and space charge driven angular spread is about 20 μrad, we can afford $\langle\theta\rangle = 15$ μrad of average misalignment of trajectories in the cooling section.

## LEC COOLING SECTION

The LEC cooling section consists of fourteen 12 m long modules. Each module contains a short solenoid combined with horizontal and vertical dipole correctors, a drift shielded by two layers of $\mu$-metal, and a BPM. Main parameters of the CS module are listed in Table 1.

Table 1: Design Parameters of CS Module

| Parameter | Value |
|---|---|
| Solenoid length [cm] | 18.9 |
| Maximum solenoid field [G] | 180 |
| Maximum corrector field [G] | 1.1 |
| Solenoid-BPM distance [m] | 12 |
| $\mu$-shielding attenuation | 1000 |

A schematic representation of the LEC cooling section can be seen in Fig. 1.

## TRAJECTORY ALIGNMENT

The electron trajectory through the cooling section will be defined by the CS proton trajectory. In the ideal case, one wants to have zero angle and displacement of electrons trajectory with respect to protons through the whole CS. In reality, there are multiple factors causing relative misalignment of electrons and protons. The electron beam trajectory can get misaligned with respect to the protons because of inclination or transverse displacement of a solenoid. A resulting trajectory angle and displacement at the solenoid's exit, cannot be ideally compensated by the dipole correctors.

* Work supported by Brookhaven Science Associates, LLC under Contract No. DE-SC0012704 with the U.S. Department of Energy
† seletskiy@bnl.gov

Content from this work may be used under the terms of the CC BY 4.0 licence (© 2025). Any distribution of this work must maintain attribution to the author(s), title of the work, publisher, and DOI.

ISBN: 978-3-95450-262-2 ISSN: 2673-5350 doi: 10.18429/JACoW-IBIC2025-TUPCO28

# IMPLEMENTATION AND INITIAL OPERATION OF THE BUNCH-BY-BUNCH FEEDBACK SYSTEM AT SOLARIS

M. Szczepaniak *, K. Dudek, R. Panas, W. Wiatrowska, A.I. Wawrzyniak
NSRC SOLARIS, Cracow, Poland
D. Teytelman, Dimtel Inc., San Jose, CA, USA

*Abstract*

The SOLARIS synchrotron light source has commissioned a transverse bunch-by-bunch feedback system designed to suppress coupled-bunch instabilities and serve as a diagnostic tool for accelerator studies. The system was successfully installed and integrated with the existing infrastructure, including timing and control systems. After a series of commissioning steps, it was brought into operation and tested under standard user conditions. Although routine instability suppression is not currently needed during regular operation, the system has been effectively used in dedicated machine studies. It enabled detailed observation of transverse bunch motion, instability spectra, and individual bunch tune measurements. The system also played a crucial role in advanced measurements such as LOCO experiments with selectively emptied buckets and tune shift studies under varying machine conditions. The bunch-by-bunch feedback system significantly enhances the diagnostic and research capabilities at SOLARIS and provides a solid foundation for potential future applications in active beam stabilization.

## INTRODUCTION

The Solaris synchrotron, located in Kraków, Poland, is a national research facility providing high-quality synchrotron radiation for a wide range of scientific applications [1]. In line with ongoing development, the implementation of a transverse bunch-by-bunch feedback (BBFB) system marks a significant milestone in enhancing beam stability and control. This paper presents the process of system integration, initial operational results, and the impact of the BBFB system on beam dynamics. The results demonstrate its effectiveness in improving machine performance and its potential for supporting future upgrades, including the installation of new insertion devices planned for 2026 and 2027.

## FEEDBACK OVERVIEW

The first transverse bunch-by-bunch feedback tests at the Solaris synchrotron were conducted in May 2023, in collaboration with Dimtel Inc. [2]. Following successful trials, the system was installed, commissioned, and integrated into routine user operation in December 2024. The setup includes a dedicated BPM and a stripline kicker, a Dimtel analog front-end, and wideband high-power amplifiers. The commissioning of the bunch-by-bunch feedback system marked a significant milestone, occurring nearly a decade after Solaris began operation and reached its design parameters, including the nominal beam current of 500 mA.

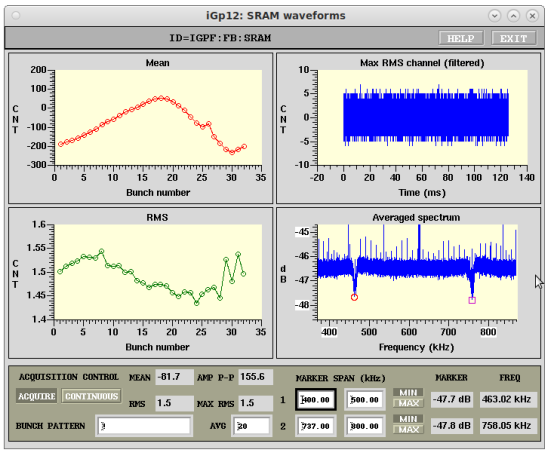



Figure 1: SRAM waveforms recorded during standard operation with closed feedback loop, full filling pattern, and a beam current of 400 mA.

Table 1: The Operating Parameters of the SOLARIS Storage Ring

| Parameter | Value |
|---|---|
| Beam energy | 1.5 GeV |
| Filling pattern | 29 bunches with 10 ns spacing + 3 empty buckets |
| Chromaticity | +1 / +1 |
| Nominal beam current | 500 mA |
| Beam current during operation | 420 mA decaying to ~220 mA/ 12 h |
| Average vacuum pressure | $\sim 1 \times 10^{-9}$ mbar |

Figure 1 presents SRAM waveforms recorded during standard operation of the Solaris storage ring, with the bunch-by-bunch feedback loop closed, a full filling pattern, and a beam current of 400 mA. The signals confirm stable beam conditions and proper synchronization of the feedback system. These waveforms serve as a reference for evaluating system performance and are routinely used for diagnostic purposes, particularly when tuning feedback parameters or investigating beam instabilities.Beyond its primary role in

* mateusz.szczepaniak@uj.edu.pl

Content from this work may be used under the terms of the CC BY 4.0 licence (© 2025). Any distribution of this work must maintain attribution to the author(s), title of the work, publisher, and DOI.

ISBN: 978-3-95450-262-2 ISSN: 2673-5350 doi: 10.18429/JACoW-IBIC2025-TUPCO29

# REAL-TIME EMBEDDED FEEDFORWARD CORRECTION FOR SIRIUS UNDULATORS

P. H. Nallin*, J. P. Burle Ishida, G. Rodrigues de Lima, D. O. Tavares
Brazilian Synchrotron Light Laboratory, LNLS CNPEM, Campinas, Brazil

Content from this work may be used under the terms of the CC BY 4.0 licence (© 2025). Any distribution of this work must maintain attribution to the author(s), title of the work, publisher, and DOI.

*Abstract*

SIRIUS, the Brazilian 4th generation synchrotron light source, has been in operation since 2020. Over time, insertion devices (IDs) are expected to populate its straight sections. To supress edge effects from undulators and support overall beam stability, a feedforward correction system is currently available through EPICS layer for the first installed ID. However, performance could be improved by adopting a lower-level solution with higher actuation rates and reduced jitter. To address this, a new approach has been developed using hardware technology already available: control system nodes based on BeagleBone Black platform, which integrates both embedded linux and dedicated real-time processors within the same SoC. This setup is able to update current setpoints up to 1 kHz and aiming to be scalable. This paper presents an overview of the system's architecture and objectives, first results with IVU and VPU undulators as well as future developments and improvements.

## INTRODUCTION

SIRIUS has been opened to external users since March 2023 and has 10 beamlines fully operational and 4 under commissioning or construction [1, 2]. Several subsystems contribute to beam stability, providing a set of important parameters that must be achieved and maintained to ensure photon beam and experimental viability. Among those subsystems, orbit stability relies on slow orbit feedback (SOFB) and fast orbit feedback (FOFB), this one operating at 48 kHz update rate with 1 kHz cross-over frequency [3].

Commissioning and titular insertion devices (IDs) have been added to SIRIUS storage ring along these years, as listed on Table 1, and some more are expected to be installed in the future. The beam dynamics in an insertion device must be handled in order to minimize the impact on the overall beam stability. The correction system responsible to compensate IDs disturbances are known as feedforward correction, this kind of devices are being employed to improve stability in other synchrotron facilities as well [4, 5]. To cancel the first and second undulator field integrals, operation with feedforward correctors mitigates angular and offset disturbances/perturbations.

Both in-vacuum (IVU) and vertical polarizing (VPU) undulators consider vertical and horizontal correctors, therefore requiring four independent current power supplies. Delta undulator operates with two additional skew quadrupoles, which adds two additional channels.

Table 1: Undulator Beamlines Currently Operating at SIRIUS With Feedforward Correction

| Beamlines | Undulator type |
|---|---|
| SABIA | Delta |
| EMA | In-vacuum (IVU) |
| PAINEIRA | In-vacuum (IVU) |
| CARNAUBA | Vertical Polarizing (VPU) |
| CATERETE | Vertical Polarizing (VPU) |

## FEEDFORWARD CORRECTION TOPOLOGY

Different system architectures have been evaluated considering a standalone solution, independent of EPICS and network layers. In addition, a platform already in use in accelerators' subsystem would be preferable, optimizing spare parts and technical know-how sharing. Fast orbit feedback (FOFB) system integration for further studies is also a valuable requirement, yet optional.

Concerning the controller, both control system node controller (Beaglebone Black, with embedded Linux and real-time cores) [6] and microTCA AFC board (FPGA-based) [7], either shared with FOFB or a dedicated one, were considered. For the actuators, fast correctors FOFB power supply [8] (LAMP, up to ±1 A, in-house developed) could be a candidate as well as SIRIUS standard low-power power supplies [9] (FBP, up to ±10 A, in-house developed) largely used for other accelerators' magnets such as slow correctors and trims.

The proposed modular topology is defined by the BeagleBone Black single board computer and SIRIUS' low-power power supplies, as shown in Fig. 1, which leads to system decoupling, resource and development efforts optimization.

Each module interfaces with up to four current channels, grouped together by construction in one single crate with a RS-485 channel as control interface, making it possible to adjust all current setpoints independently and synchronously at once.

Motion control loops for recent IVU and VPU undulators run on dedicated Beckhoff PLCs and data streaming for feedforward application has been internally developed. Delta undulator is controlled by a Rockwell PLC and has its feedforward loop currently running on high level applications. Incorporate Delta correction in this topology will be addressed in the future to improve its performance.

Also, a secondary input from FOFB subsystem has been considered in hardware requirements, machine studies are

* patricia.nallin@lnls.br

ISBN: 978-3-95450-262-2 ISSN: 2673-5350 doi: 10.18429/JACoW-IBIC2025-TUPCO30

# DEPENDENCE OF TUNE-SWEEP WAVEFORMS IN DIAMOND ON MODE NUMBER

D. Rabusov*, A.F.D. Morgan, I.P.S. Martin, Diamond Light Source, Oxfordshire, UK

Content from this work may be used under the terms of the CC BY 4.0 licence (© 2025). Any distribution of this work must maintain attribution to the author(s), title of the work, publisher, and DOI.

*Abstract*

At Diamond, it was previously observed that the response of the beam changes with mode number when excited by the transverse multi-bunch feedback. This study presents the results of various experimental campaigns carried out to investigate the behaviour of tune-sweep waveforms for a variety of stored beam conditions and TMBF settings. This study identified that not only does the mode dependence appear at a moderate-high beam current but also with a single-bunch only and without the beam. Therefore, there are intensity-independent sources distorting the TMBF output when excitation is applied on different modes. Investigations to explain what is causing the mode-dependent behaviour are ongoing.

## INTRODUCTION

It was observed in Diamond that the response of the beam to excitations on the mode 0 differs from the response on the mode 80 [1]. Normally, the excitation is provided by the transverse multi-bunch feedback (TMBF) [2] system performing a tune sweep on all bunches in the frequency range close to betatron tunes, and the excitation mode is 80. Although it was not investigated in a systematic way, long-range wakefields were suggested to cause the discrepancy between the beam responses on modes 0 and 80. If this hypothesis is correct, the beam response must change with beam current and fill patterns. This work summarises the results of various experimental campaigns that have been conducted to validate or disprove the hypothesis.

## CURRENT-DEPENDENT MEASUREMENTS

This section presents the results of measurements obtained with the beam. The beam intensity has been varied, and the results are compared when the long-range wakes are the strongest (uniform fill pattern) and when the long-range wakes are negligible (single-bunch measurements).

### *Uniform Fill Pattern*

First, the beam response, also referred to as TMBF output tune waveforms, was measured using the uniform fill pattern at 20 mA, 100 mA and 200 mA. When the gaps in the fill pattern are absent, the coupling between the bunches increases, i.e. the effects related to the long-range wakefields are expected to be stronger. In addition, the beam in this configuration is typically unstable at 70-80 mA. Therefore, transverse multi-bunch feedback was turned on to accumulate up to 100 mA and 200 mA.

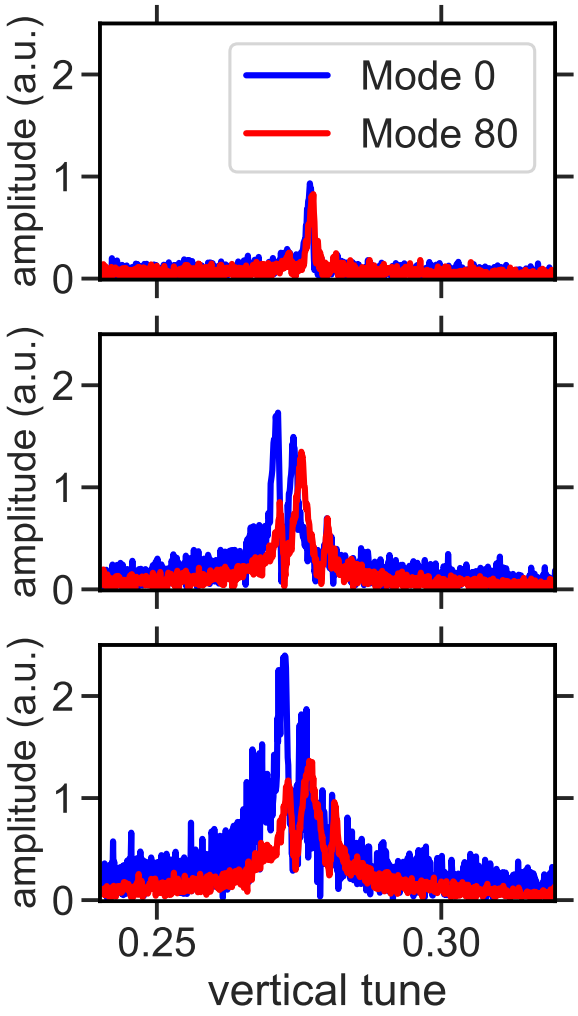



Figure 1: Beam-response waveforms obtained at different beam currents (top 20 mA, middle 100 mA, bottom 200 mA) with the tune excitation set to the modes 0 and 80.

Figure 1 shows the output signals of the TMBF detector recording all bunches. The excitation is applied to all bunches. The blue and red curves correspond to the TMBF excitation applied at modes 0 and 80. The top panel (20 mA) shows a narrow peak which has almost no shift and distortion with the mode number. The middle panel corresponds to a moderate beam intensity of 100 mA, where the blue curve has a stronger amplitude than the red curve. The blue and red curves in the bottom panel (moderate-high intensity, 200 mA) have an even larger difference in their amplitude.

Note that the output signal of the bunch-by-bunch TMBF detectors is proportional at the same time to the bunch offset and the bunch charge. Therefore, the waveforms in Fig. 1

* dmitrii.rabusov@diamond.ac.uk

ISBN: 978-3-95450-262-2 ISSN: 2673-5350 doi: 10.18429/JACoW-IBIC2025-TUPCO31

# R&D OF AN ULTRAFAST X-RAY BEAM SIZE MONITOR FOR SuperKEKB

R. Nomaru[†,1,2], G. Mitsuka[2], M. Andrew[3], K. Yoshihara[3], C. Driver[3], L. Ruckman[4]
[1]The University of Tokyo, Tokyo, Japan
[2]High Energy Accelerator Research Organization, Ibaraki, Japan
[3]University of Hawaii, Honolulu, HI, USA
[4]SLAC National Accelerator Laboratory, Menlo Park, CA, USA

*Abstract*

At SuperKEKB, sudden beam loss (SBL)—a beam instability that develops within several tens of microseconds—has become a major obstacle to higher luminosity. Observations have indicated that the beam size can expand abruptly during SBL, highlighting the need for ultrafast diagnostics. To address this, we are developing a bunch-by-bunch beam size monitor using synchrotron X-rays and a 128-channel silicon strip detector. Initial tests with a pulsed laser confirmed proper detector and readout operation, and gain calibration is underway. The monitor will be installed for beam measurements in the next SuperKEKB operation beginning November 2025.

## INTRODUCTION

The SuperKEKB accelerator [1] is a high-luminosity electron–positron collider employing 4 GeV positrons and 7 GeV electrons. In December 2024, it achieved a world-record peak luminosity of $5.1\times10^{34}$ cm$^{-2}$s$^{-1}$. The ultimate goal is to exceed this record by more than an order of magnitude, and accelerator operations are ongoing toward this achievement. However, a phenomenon known as Sudden Beam Loss (SBL) has emerged as one of the critical obstacles to further luminosity upgrades [2]. SBL refers to a beam instability that rapidly develops over an extremely short timescale of several tens of microseconds, causing severe beam losses and ultimately leading to beam aborts. These aborts not only damage accelerator components and detectors, but also hinder increases in beam current and reduce the effective collision operation time.

Understanding the mechanism of SBL is essential for realizing higher luminosity at SuperKEKB. Previous observations suggest that the beam size can increase abruptly during SBL events [3], indicating the necessity of accurately capturing beam-size variations on such short timescales. Although SuperKEKB is equipped with a beam size monitor capable of turn-by-turn measurements, no existing system provides the faster time resolution required for SBL studies.

To address this limitation, we are developing and testing a novel beam size monitor capable of bunch-by-bunch measurements. In addition to enabling detailed investigations of SBL, this monitor is also expected to serve as a valuable tool for studying other beam instabilities, such as electron cloud effects, which have long been recognized as issues in collider operation.

† nomaru@post.kek.jp

## BEAM SIZE MEASUREMENT METHOD

In the SuperKEKB main ring, the beam size is measured using synchrotron X-rays emitted when the beam is deflected by a bending magnet. The X-rays pass through a coded-aperture slit, and the resulting image is recorded. By fitting the obtained pattern, the beam size is extracted [4]. A schematic view of this method is shown in Fig. 1.

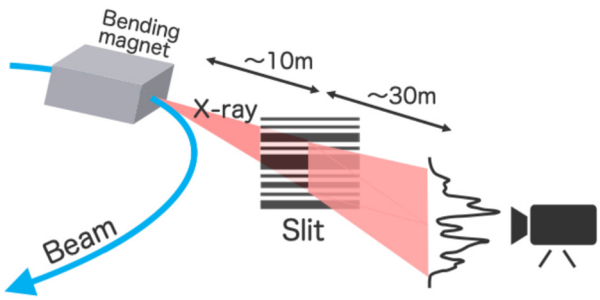



Figure 1: Concept of the X-ray beam size monitor.

The fastest imaging device employed at SuperKEKB has been a CMOS camera, which enables turn-by-turn measurements with a sampling rate of approximately 100 kHz. In this study, we introduce a silicon strip detector as a new imaging device. By sampling synchrotron X-ray images at 2.7 GSa/s, the system achieves bunch-by-bunch beam size measurements, corresponding to a minimum bunch spacing of 4 ns.

## CONFIGURATION OF THE ULTRAFAST BEAM SIZE MONITOR

We are currently conducting performance tests of the ultrafast beam size monitor jointly developed by KEK, the University of Hawaii and SLAC. A photograph of the monitor is shown in Fig. 2. The system consists of three main components: a sensor board equipped with a 128-channel silicon strip sensor, a preamplifier board for signal amplification, and a DAQ board responsible for digitization and data transfer. Each DAQ board can process signals from 32 channels, and by stacking four layers, the system records all 128 channels at a sampling rate of 2.7 GSa/s. The DAQ board employs the same readout circuit developed by the University of Hawaii for the Belle II TOP detector [5].

An enlarged view of the silicon strip sensor is presented in Fig. 3. The sensor was fabricated at the Stanford Nanofabrication Facility and contains 128 cathode strips with a pitch of 50 µm. The depletion layer depth is 75 µm,

Content from this work may be used under the terms of the CC BY 4.0 licence (© 2025). Any distribution of this work must maintain attribution to the author(s), title of the work, publisher, and DOI.

ISBN: 978-3-95450-262-2 ISSN: 2673-5350 doi: 10.18429/JACoW-IBIC2025-TUPCO34

# DESIGN AND DEVELOPMENT OF A FOC ALGORITHM BASED ON MACHINE LEARNING FOR THE HEPS

Yilin Li, Guodong Gao, Daiquan Zhou, Shujun Wei, Jianshe Cao, Xiyang Huang, Hong Zhang*, Junhui Yue,Yanfeng Sui ,Ying Zhao, Jun He, Dechong Zhu
Institute of High Energy Physics, Beijing, China

*Abstract*

The High Energy Photon Source (HEPS) is a fourth-generation synchrotron light source with 6 GeV beam energy developed by the Institute of High Energy Physics. The Fast Orbit Feedback (FOFB) system maintains beam orbit stability for optimal performance. This work presents a neural network-based algorithm to replace traditional PID control in FOFB systems. A Multi-Layer Perceptron (MLP) neural network was designed and trained using simulated data from HEPS, with hyperparameter optimization to enhance performance. The trained model was quantized for FPGA deployment and validated in a laboratory test environment. The system achieved mean error at the 1 mA level, demonstrating the feasibility of neural networks as an effective alternative to PID control in FOFB applications.

## INTRODUCTION

The High Energy Photon Source (HEPS) is a fourth-generation synchrotron radiation facility under construction by IHEP, operating at 6 GeV with brightness of $1 \times 10^{22}$ phs $\cdot$ s$^{-1} \cdot$ mm$^{-2} \cdot$ mrad$^{-2} \cdot$ (0.1 % bw)$^{-1}$ and emittance <60 pm·rad [1].

Fast Orbit Feedback (FOFB) systems are critical for maintaining beam stability. Traditional PID-based FOFB relies on response matrices requiring online measurement, consuming commissioning time. Neural network approaches offer data-driven alternatives with implicit physical encoding, eliminating explicit matrix calculations during operation [2–5].

This work presents an MLP-based FOFB implementation using FPGA technology. The model correlates beam orbit with corrector mappings using HEPS simulation data, with systematic evaluation of latency optimization and BPM malfunction robustness [5, 6].

## SYSTEM ARCHITECTURE

### *FOFB System Overview*

The FOFB system involves coordinated operation of multiple subsystems, including accelerator physics, control systems, power supplies, magnets, and timing. It comprises three main subsystems: the beam position monitor (BPM) system, the FOFB controller system, and the fast corrector subsystem including fast corrector power supplies, magnets, and vacuum boxes.

In each control cycle, the Orbit Feedback Controller (FOC) receives beam position data from all BPMs in the storage ring, applies the orbit feedback algorithm to determine appropriate setpoints for fast corrector power supplies, and transmits results to backend fast corrector power supply controllers (PSC) which convert the data into corresponding currents applied to fast correctors, ultimately adjusting the beam position.

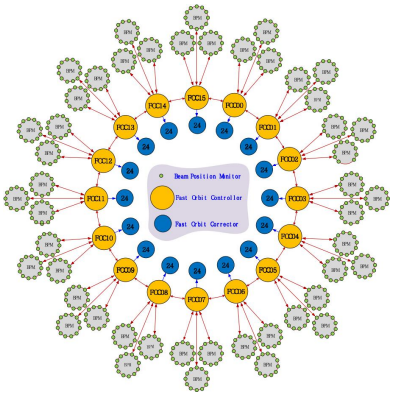



Figure 1: FOFB system topology.

The FOFB system topology, shown in Fig. 1, adopts a 7BA (Seven-Bend Achromat) lattice structure with 48 units. The storage ring is equipped with 576 BPMs, 384 fast correctors, 48 BPM sub-stations, and 16 FOFB sub-stations. Each BPM sub-station contains 12 sets of BPM electronics, while each FOFB sub-station is equipped with one FOC directly controlling 24 correctors across three 7BA cells [4, 7].

### *MLP Neural Network Architecture*

Multi-Layer Perceptron (MLP), also known as a fully connected neural network (FCNN), consists of neurons connected in parallel with multiple hidden layers between input and output layers. The model structure is shown in Fig. 2. MLP is capable of modeling interaction responses and is primarily used for solving classification and regression problems [8].

The designed neural network comprises two hidden layers with 16 and 64 neurons respectively. The input consists of 576 sets totaling 1,152 position data points, while the output yields 384 correction values. These correction values are represented as signed fixed-point numbers with 21-bit data width in amperes, including a 4-bit integer part, a 16-bit fractional part, and a sign bit as the most significant bit.

### *FPGA Implementation Strategy*

FPGA-based implementations provide low-latency, deterministic execution for real-time mapping from 576 BPM

* hongzhang@ihep.ac.cn

Content from this work may be used under the terms of the CC BY 4.0 licence (© 2025). Any distribution of this work must maintain attribution to the author(s), title of the work, publisher, and DOI.

ISBN: 978-3-95450-262-2 ISSN: 2673-5350 doi: 10.18429/JACoW-IBIC2025-TUPCO38

# LASER TRANSPORT AND STABILIZATION FOR THE CSNS LASER WIRE PROFILE MONITOR PROTOTYPE*

C. Chen, B. Zhang, S. Yan, Z. Xu, R. Liu, R. Yang†
Institute of High Energy Physics, Beijing, China
also at China Spallation Neutron Source, Dongguan, China
P. Ding, School of Nuclear Science and Technology, Lanzhou University, Lanzhou, China

*Abstract*

A laser wire monitor prototype has bean developed at the China Spallation Neutron Source (CSNS).The monitor utilizes a 1064 nm laser source to measure the horizontal and vertical profiles of a negative hydrogen ion ($H^-$) beam with an energy of 80 MeV in the injection zone. This paper describes the design of the laser optical path layout and the laser transmission performance of the system. The experiment focuses on the laser system's quality factor $M^2$ of the laser after more than 60 meters of transmission as well as the beam pointing stability. In this experiment, the laser quality factor $M^2$ after transmission is better than 4, and the beam pointing stability after focus is less than $\pm$ 2.5 $\mu$m, which is able to satisfy the required specifications for the first CSNS laser wire monitor.

## INTRODUCTION

The China Spallation Neutron Source (CSNS) complex is designed as a multidisciplinary platform to support scientific research and applications for national institutions, universities, and industries [1]. The CSNS accelerator complex consists of a low-energy linear accelerator (linac), a Rapid Cycling Synchrotron (RCS), and two beam transport lines. For the CSNS-II upgrade, the beam power will be increased to 500 kW, maintaining a beam energy of 1.6 GeV. This upgrade involves increasing the linac beam energy from 80 MeV to 300 MeV by incorporating a new superconducting accelerating section [2]. Consequently, the use of physical wire scanners for beam profile monitoring is impractical in much of the linac due to the risk of wire breakage, which could contaminate the superconducting (SC) cavities. Therefore, a laser wire system has been adopted as a non-invasive alternative [3–5]. Given the challenging tunnel environment, this paper details the commissioning of the laser optical path layout and presents experimental results on laser transmission performance and beam spot stability monitoring.

## LASER OPTICAL PATH SETUP

Figure 1 illustrates the schematic of the complete laser optical path. To mitigate the radiation environment, the laser source and expander system (Part 1) are situated in a subtunnel. A Q-switched Nd:YAG laser, operating at a wavelength of 1064 nm, serves as the light source [6]. The laser operates at a repetition rate of 1 Hz with a pulse width of 9 ns. Synchronization between the laser and the beam is achieved by precisely controlling the trigger timing of the laser flash lamp. Additionally, the laser energy can be adjusted by varying the timing between the Q-switch and the flash lamp. However, this method may compromise laser stability. To address this, the laser pulse energy is regulated using a set of polarization optics. The maximum laser output energy is approximately 800 mJ, sufficient to detach an adequate number of electrons [7]. To ensure high transmission efficiency and maintain beam quality, the laser spot size is expanded from approximately 9 mm to 27 mm using a threefold beam expander. A photodiode (PD) is positioned adjacent to the laser source to monitor the laser emission timing.

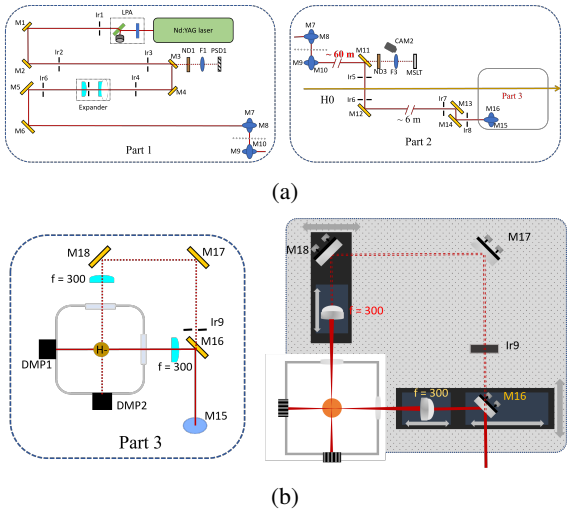



Figure 1: Outline of the laser optical path installed in the CSNS linac.

The laser beam is guided from the sub-tunnel to the main tunnel using mirrors and then propagates along the beam direction toward the laser wire station. Mirrors 7 and 8 are employed to adjust for variations in laser beam height during transmission. A laser position monitor, located 60 m downstream from the laser source, is used to track jitter and drift in the laser position caused by temperature, humidity, and mechanical instabilities. To ensure precise horizontal and vertical alignment of the incident light at the laser station, two additional mirrors (13 and 14) have been incorporated to enable fine adjustments. Additionally, for safety considerations, fire-resistant materials were employed for the laser beam tubes along the transmission path.

* Work supported by National Natural Science Foundation of China (No. 12305166) and the Natural Science Foundation of Guangdong Province, China (No. 2024A1515010016)

† yangrenjun@ihep.ac.cn

Content from this work may be used under the terms of the CC BY 4.0 licence (© 2025). Any distribution of this work must maintain attribution to the author(s), title of the work, publisher, and DOI.

ISBN: 978-3-95450-262-2 ISSN: 2673-5350 doi: 10.18429/JACoW-IBIC2025-TUPCO39

# DEVELOPMENT OF WIRE SCANNER PROFILE MONITOR IN FETS-FFA TEST RING

E. Yamakawa*, A. Chamberlain, Science and Technology Facilities Council, Didcot, UK
A. Pertica, RAL Space, Didcot, UK

*Abstract*

A wire Scanner profile Monitor (WSM) has been developed for the demonstration ring of Fixed Field Alternating gradient (FFA) accelerator, called FETS-FFA. From previous studies, Carbon Nano Tube (CNT) wire is selected for the FETS-FFA WSM, durable for the heat damage of low-energy proton beams on the FETS-FFA test ring (3–12 MeV). A bias voltage, applied to the measuring wires, is required to prevent secondary electrons from returning to the wire due to the stray magnetic fields of the FFA main magnets. The endurance tests of bias voltages on different sizes of CNTs were performed prior to the beam tests on the Front-End Test-Stand (FETS) beam line and the FFA ring at KURNS. The beam tests with bias voltages on FETS and numerical simulations revealed secondary electrons from adjacent wires degraded the reading sensitivity, hence profile accuracy, explaining why the peak of the beam profile was not proportional to the wire size in previous studies. This paper will focus on the endurance test of bias voltages on CNTs as well as beam profile measurements with bias voltages on the FETS beam line. The mechanical design of the rig to install a thin CNT wire (diameter of 10 µm) on the frame head of FETS-FFA WSM will also be presented.

## INTRODUCTION

A wire Scanner profile Monitor (WSM) has been developed to identify the transverse beam profile and position of proton beam for the FETS-FFA [1]. A WSM can also provide a horizontal beam profile of accelerating beams through the interception of the beam with the wire. The challenge is to select an appropriate material of signal wire, durable for heat damage due to interception of low-energy proton beams and its energy depositions on the wire. In previous studies [2], profile measurements of accelerating beams in the FFA ring using carbon nanotube wire (CNT) were successfully performed at KURNS [3] with a 13.5 MeV proton beam. This energy was chosen as it was the minimum required to mitigate the influences of secondary electrons generated at the charge stripping foil during the injection process at KURNS. Additionally, the measurements conducted with 3 MeV H- beam on Front End Test Stand (FETS) [4] at RAL evaluated the durability of wires against the impact of low-energy beams as well as evaluating beam profiles. However, the tests revealed the peak signals of measured profile were not proportional to the cross-section of the wires. To investigate the reason behind, additional experiments with bias voltages applied to the wires in the FETS will be presented. The development of a mounting frame designed for the installation of a thin CNT wire in the frame head of the FETS-FFA WSM will be also discussed.

## BIAS VOLTAGES ON WIRES

The wire signal for the FETS-FFA WSM will be a positive charge as secondary electrons impinged by the proton beam will escape from the wire. To maintain optimal monitor sensitivity, it is crucial the secondary electrons generated from the wire do not return to the wire. When low-energy secondary electrons (~25 eV) are experienced stray magnetic fields from the FETS-FFA magnets, expected to be within 40 Gauss on the median plane, their trajectories will spiral around the magnetic field lines, returning to the wire. This can be avoided by applying negative bias voltages to the wire. The model simulations were performed using CST electromagnetic solver with bias voltages along with the static magnetic fields of 40 Gauss. The simulations revealed that applying negative bias voltages to the wire increased the Larmor radius of electrons, reducing the number of returning electrons to the wire. The ideal bias voltage will be established once the geometry of the FFA vacuum chamber has been determined. Contrary to the FETS-FFA WSM, the wire signals for the FETS H- beam will be a negative charge generated by stopped electrons (~2 keV) of H- ion at the wires. The profile measurements previously made [2] without bias voltages indicated additional electrons were entering the wire from the surrounding space. A likely source of these incoming electrons is the secondary electrons emitted from adjacent wires when the FETS beam strikes the wires. A Monte Carlo simulation using PHITS [5], based on the configuration of the ISIS Single Wire Injector Profile Monitor (SWIPM) [6] (Fig. 1), indicates that low-energy electrons, within a few tenths of eV generated at the wire by the protons, can entre the adjacent wires as shown in Fig. 2. The secondary electron interference can potentially be minimised by applying positive bias voltages on the wires.

### *Durability Tests of Bias Voltage*

Before profile measurements with bias voltages, durability tests of bias voltages were conducted in different sizes of CNT wires: $\phi$10 µm, $\phi$20 µm, $\phi$30 µm and $\phi$40 µm, all installed on the test frame (Fig. 3). The wires underwent various baking conditions prior to endurance tests, ranging from −300 V to 0 V applied on the wires twice. Other conditions were placing the wire in a baking chamber at 250 °C for three days or heating the wires by DC currents at 100 mA for six hours. The leakage currents from the CNT wires were monitored by ramping up the bias voltages as shown in Fig. 4. In the case of CNTs heated in a baking chamber at 250 °C, the increase in leakage currents was observed

* emi.yamakawa@stfc.ac.uk

Content from this work may be used under the terms of the CC BY 4.0 licence (© 2025). Any distribution of this work must maintain attribution to the author(s), title of the work, publisher, and DOI.

ISBN: 978-3-95450-262-2 ISSN: 2673-5350 doi: 10.18429/JACoW-IBIC2025-TUPMO01

# DEVELOPMENT OF A HIGH-GAIN RESIDUAL GAS IONIZATION PROFILE MONITOR (HGRGIPM) FOR THE SLOW EXTRACTION PROTON BEAMLINE AT THE J-PARC HADRON EXPERIMENTAL FACILITY*

A. Toyoda[1,2,†], H. Akiyama[1], K. Agari[1], K. Aoki[1], E. Hirose[1], M. Ieiri[1], T. Itaba[1], R. Kurasaki[1], M. Minakawa[1], Y. Morino[1,2], F. Muto[1], Y. Sato[1,2], S. Sawada[1,2], Y. Shirakabe[1], H. Takahashi[1,2], T. Takahashi[1,2], K. Tanaka[1], H. Watanabe[1,2], T. Yamaga[1,2], Y. Yamanoi[1]
[1]High Energy Accelerator Research Organization, KEK, Tsukuba, Ibaraki, Japan
[2]The Graduate University for Advanced Studies, SOKENDAI, Hayama, Kanagawa, Japan

*Abstract*

We have developed a highly sensitive beam profile monitor, the High-Gain Residual Gas Ionization Profile Monitor (HGRGIPM). The HGRGIPM detects electrons ionized by the proton beam in residual gas, which are guided by electric fields to a phosphor screen. The fluorescence is collected by an optical system. RGIPMs have proven to be powerful diagnostic tools for high-intensity beams because they have non-destructive nature. They have been used as the main profile monitors in the primary beam line, A-line (30 GeV, 92 kW, 8.1x10$^{13}$ protons/spill, 4.24 s cycle, vacuum ~0.3 Pa). However, the newly constructed B-line (30 GeV, 11 W, 1.0x10$^{10}$ protons/spill, 4.24 s cycle) presents a significant challenge, as its beam intensity is four orders lower than that of the A-line. To overcome this issue, several improvements were made in the design of the HGRGIPM. These include the use of a thin phosphor screen to enhance the signal-to-noise ratio, optimizing electrode geometry for higher acceleration voltages and improved sensitivity, and incorporating a high-efficiency optical system. These innovations allow profile monitoring even in the low-intensity B line. In this paper, we report on the HGRGIPM's design and performance, beam response measurements, and future prospect.

## INTRODUCTION

The A-line, the primary beam line of the J-PARC Hadron Experimental Facility, delivers a high-intensity proton beam (30 GeV, 92 kW, 8.1x10$^{13}$ protons/spill, 4.24 s cycle) to a variety of particle and nuclear physics experiments [1, 2]. For safe and stable operation of such a high-intensity beam, continuous monitoring of the beam profile is essential. Moreover, the beam profile monitor must be non-invasive to avoid any beam loss. In this facility, the vacuum level inside the beam line is maintained at approximately 0.3 Pa, and a non-destructive beam profile monitor, the RGIPM (Residual Gas Ionization Profile Monitor) that collects electrons generated by ionization of residual gas in the beam duct was successfully developed [3] and is currently in use.

Meanwhile, a new branch beam line, the B-line, has recently been constructed off the A-line. The B-line operates at a lower beam power (30 GeV, 11 W, 1.0x10$^{10}$ protons/spill, 4.24 s cycle) and is located in close proximity to the A-line, resulting in a high background environment and a low signal yield. To address these challenges, we have developed a high-sensitivity beam profile monitor, the HGRGIPM (High-Gain Residual-Gas Ionization Profile Monitor).

## LAYOUT AND INSTALLATION

Figure 1 shows the layout of the HGRGIPM. Electrons ionized by the beam are collected upward by internal electrodes. A magnetic field (up to 400 Gauss), provided by Helmholtz coils, is applied parallel to the electric field in the measurement region. This magnetic field helps suppress the diffusion of electrons due to scattering with residual gas. Outside the internal electrodes, a thin phosphor screen ($Gd_2O_2S$, 20 μm thick) is installed and biased with a high voltage (up to 4 kV). By accelerating the ionized electrons with this electric field, the signal intensity is increased. The thin phosphor layer also helps reduce background light, primarily from upstream of the beam line. The scintillation light generated by the phosphor is transmitted through a fused silica optical window and detected by an optical system and a radiation-resistant CID camera (Thermo Fisher Scientific inc.) housed in a light-tight enclosure.

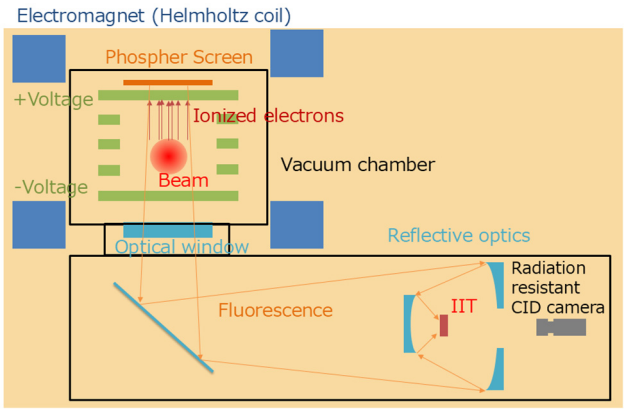



Figure 1: HGRGIPM layout.

Figure 2 shows the HGRGIPM installed in the B-line. The optical system is mounted below the beam line. The relay lens, made of BK7 glass and relatively vulnerable to radiation, is positioned approximately 1500 mm away from the beam line, reducing the frequency of replacement.

* Work supported by JSPS KAKENHI Grant Number 18H01238.
† email address: akihisa.toyoda@j-parc.jp

Content from this work may be used under the terms of the CC BY 4.0 licence (© 2025). Any distribution of this work must maintain attribution to the author(s), title of the work, publisher, and DOI.

ISBN: 978-3-95450-262-2 ISSN: 2673-5350 doi: 10.18429/JACoW-IBIC2025-TUPMO03

# PERFORMANCE OF TITANIUM, TUNGSTEN, AND CARBON AS BEAM PROFILE MONITOR MATERIALS

D. Z. Metin*, A. N. Goldblatt, M. Duraffourg, M. Hamani, C. Vuitton, F. Roncarolo
CERN, Geneva, Switzerland

*Abstract*

This paper investigates the signal characteristics of titanium, tungsten, and carbon materials used in a secondary electron emission grid setup at CERN's North Area. Periodic scans were conducted to reconstruct beam profiles and assess the performance of these materials, configured as wires and bands, under slow-extracted 400 GeV protons. The study aims to inform the design and optimization of new secondary electron emission monitor systems for the NA consolidation project and future installations.

## INTRODUCTION

At the CERN SPS, Secondary Emission Monitors (SEMs) in the form of titanium bands are key instruments for monitoring the transverse structure of high-energy proton and ion beams. Their working principle relies on the release of low-energy secondary electrons from the bands intercepting the beam, which are then collected and converted into spatially resolved signals [1]. These bands have demonstrated reliable performance across many years. They offer a high signal-to-noise ratio, and their minimal thickness helps reduce beam-induced heating while minimizing perturbations and particle losses due to scattering. However, titanium bands also present limitations. Their ultimate spatial resolution is constrained by the minimum manufacturable band width, approximately 300 µm for the devices used at CERN, which restricts achievable pitch to around 400 µm. In addition, the expertise required for their assembly may be more difficult to maintain compared to more conventional CERN wire grid systems.

In particular, carbon and tungsten wire detectors—currently standard across most of the CERN machines, are being considered as a viable alternative to titanium bands for monitoring the position and profile of the slow-extracted beam from the SPS to the North Area (NA) lines.

Thin wires, offering a well-controlled fabrication process, provide higher spatial resolution than bands. Their main limitation is signal strength, due to a smaller filling factor.

Considering both current and future operational scenarios for the SPS North Area, transverse profile monitors are required to operate reliably under a wide range of proton beam conditions †, as summarized in Table 1.

Table 1: Summary of Typical Beam Parameters for the SPS North Area

| | |
|---|---|
| **Beam Type** | Unbunched proton beams |
| **Beam Size (Gaussian $\sigma$)** | From sub-mm to 3 mm |
| **Spill Duration** | 1 s to 10 s‡ |
| **Total Protons per Spill** | ~ $10^{11}$ to a few $10^{13}$ |

‡ 4.8 s during present normal operation, including during the experiments discussed in this paper.

## TEST SETUP

One of the vacuum tanks hosting SEMs in the SPS beam transfer to the North Area (TT20 line), historically reserved for beam instrumentation tests, was modified to study the response of wire samples in comparison to that of titanium bands [2]. The tank was equipped with a detector head movable in steps across the beam pipe. The samples were mounted on a ceramic Printed Circuit Board (PCB)—shown in Fig. 1— installed on the detector head.

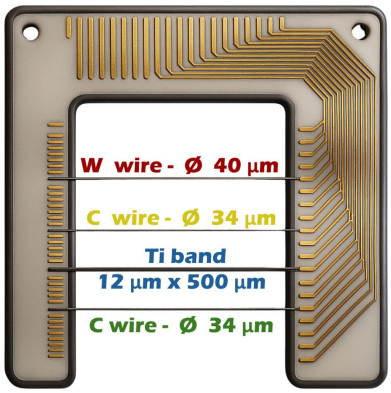



Figure 1: Design of the ceramic PCB used to test the 4 samples.

The setup consists of a titanium band, a tungsten wire and two carbon wires, as summarized in Table 2. The tungsten wire is coated with a thick layer of gold. As in the other CERN systems equipped with this wire type, the coating is required to facilitate the soldering of the wires on the PCB. The coating affects wire cooling because radiation cooling is a surface effect that dominates in vacuum and differs between tungsten and gold [3]. However, it has little impact on the signal, as both materials have very similar expected Secondary Emission Yield (SEY). The two carbon wires only differ in how they were mounted on the detector head: one is glued and the other soldered. In this case, soldering is facilitated by copper coatings deposited only on the extremities of the wire, which are never hit by the beam.

The titanium band, 12 µm thick, 0.5 mm wide is exactly as one of the types routinely used in the SPS NA.

* dani.metin@cern.ch

† The system should also be capable of detecting ion beams with a comparable total number of charges (proton-equivalent).

Content from this work may be used under the terms of the CC BY 4.0 licence (© 2025). Any distribution of this work must maintain attribution to the author(s), title of the work, publisher, and DOI.

ISBN: 978-3-95450-262-2 ISSN: 2673-5350 doi: 10.18429/JACoW-IBIC2025-TUPMO04

# OPTICAL SYNCHROTRON RADIATION AS A NON-INVASIVE TOOL FOR EMITTANCE DIAGNOSTICS

D. Ghosal[1,2,*], J. Wolfenden[1,2], C. P. Welsch[1,2]
[1]Department of Physics, University of Liverpool, Liverpool, UK
[2]Cockcroft Institute, Warrington, UK

Content from this work may be used under the terms of the CC BY 4.0 licence (© 2025). Any distribution of this work must maintain attribution to the author(s), title of the work, publisher, and DOI.

*Abstract*

As next-generation accelerators target higher brightness and lower emittance, conventional diagnostics may fall short. Optical Synchrotron Radiation (OSR), coupled with an optimized optical transport system, offers a scalable, high-resolution alternative. We apply a robust simulation framework for using OSR as a non-invasive tool to extract the transverse emittance of relativistic electron beams aiming for advanced accelerator facilities. The integrated simulation work of Synchrotron Radiation Workshop code and Zemax Opticstudio successfully handles modelling OSR emission and propagation through realistic optics, incorporating detector and transport effects. The feasibility of this emittance measurement study was assessed using a microlens array (MLA) system to capture angular beam distributions from the radiation. The method is benchmarked using beam conditions from the CLEAR facility at CERN, while also providing a base for extending OSR-based emittance diagnostics to other facilities.

## INTRODUCTION AND MOTIVATION

The pursuit of higher beam quality in next-generation particle accelerators, including reduced emittance and enhanced brightness, imposes new demands on diagnostic tools. Emittance, a key parameter for beam quality, quantifies the spread of particle positions and angles in phase space, effectively determining how tightly a beam can be focused or transported. Precise, non-invasive diagnostics are essential for beam monitoring, not only for the calibration and tuning of the machines but also for preserving beam quality in advanced accelerator experiments.

Traditional invasive diagnostics [1, 2] require a stable and consistent beam profile (because they need multiple measurements) and are often insufficient at high repetition rates. As an alternative to multi-shot techniques, single-shot methods such as pepper-pot or slit-scan diagnostics can be used to reconstruct the transverse phase space and extract emittance value. However, these methods are typically limited to low-energy beams and remain inherently invasive. To overcome these limitations, researchers have explored optical radiation-based techniques that are non- or minimally invasive in nature. Among these, Optical Transition Radiation (OTR) [3], has been used to measure transverse beam profiles and angular distributions. But, OTR diagnostics are limited by the invasive nature [2], therefore Optical Synchrotron Radiation (OSR) has emerged as a superior option for non-invasiveness [4, 5]. While carrying valuable information about the transverse properties of the beam, such as divergence, size, and emittance, if properly captured and analyzed, OSR can provide detailed insight into beam phase space without interfering with beam propagation.

In this work, we present a robust simulation framework that combines electromagnetic field calculations with physical optics propagation (POP) to evaluate the viability of OSR as a diagnostic tool for emittance reconstruction. The methodology, described later in this paper, accounts for both the underlying radiation physics and the practical influence of beamline optics.

To benchmark and validate the method, beamline parameters from the CERN Linear Electron Accelerator for Research (CLEAR) facility [6] have been used. In particular, we evaluate the feasibility of using a microlens array (MLA) to sample the angular distribution of OSR and reconstruct the beam emittance from the resulting image. The simulation framework is not only adaptable to existing setups like CLEAR but is also extendable to more advanced and novel acceleration facilities [7], where single-shot, non-invasive emittance measurements is expected in a intense proton-driven plasma wakefield environment.

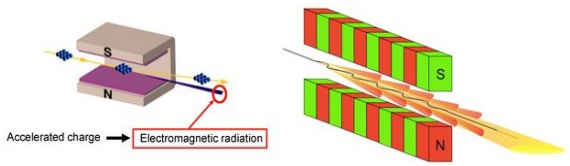



Figure 1: SR generated from a dipole (left), and a wiggler magnet (right) [8].

## OSR AND EMITTANCE MEASUREMENT

When charged particles (e.g. electrons) are accelerated at relativistic speeds, they are deflected in the presence of a magnetic field, and emit synchrotron radiation (refer to Fig. 1). Due to relativistic beam effects, the radiation is highly collimated in the forward direction (a narrow cone of opening angle $\theta \approx 1/\gamma$) [9] and spans a broad spectral range. OSR refers to the specific portion of this radiation that falls within the optical range of the electromagnetic spectrum, encompassing the visible and ultraviolet ranges. The radiation field can be decomposed into two orthogonal polarization components: the $\pi$-polarization, lying in the propagation plane, which exhibits a strong, sharply forward-peaked distribution; and the $\sigma$-polarization, perpendicular to the plane, which shows a broader angular spread with a

* dghosal@liverpool.ac.uk

ISBN: 978-3-95450-262-2 ISSN: 2673-5350 doi: 10.18429/JACoW-IBIC2025-TUPMO05

# GAS-JET BASED IONIZATION PROFILE MONITOR FOR PROTON FLASH THERAPY

F. Thesni[1,2,*], N. Kumar[1,2], M. Patel[1,2], B. S. Rawat[1,2], W. Butcher[1,2], C. P. Welsch[1,2]
[1]Department of Physics, University of Liverpool, Liverpool, United Kingdom
[2]Cockcroft Institute, Sci-Tech Daresbury, Warrington, United Kingdom

Content from this work may be used under the terms of the CC BY 4.0 licence (© 2025). Any distribution of this work must maintain attribution to the author(s), title of the work, publisher, and DOI.

*Abstract*

In proton FLASH therapy, the beam monitoring is crucial to ensure the targetted dose delivery to the tumor and effective Organ at Risk (OAR) sparing. A non- invasive real time beam monitoring gives more control over the beam as the dose is delivered in shorter time scales. To achieve this, the gas-jet based Ionization Profile Monitor (IPM) is currently being developed with potential capability towards real time beam monitoring. It detects ions produced by the interaction of primary beam using a thin (<1 mm) gas-curtain without perturbing the beam. This work presents the simulation of IPM to study the ion extraction under different design configurations to identify parameters affecting the reconstruction of the beam shape. The effect of the IPM electric field on ion trajectory and energy distribution inhomogeneity, which affects the beam profile, are studied. The study also investigates the effect of beam misalignment and the gas-curtain density distribution. Future work will address configuration required to accommodate broader range of beam relevant to clinical application.

## INTRODUCTION

Proton therapy has emerged as a highly precise form of radiation therapy, offering superior tumour control and reduced dose to surrounding healthy tissues compared to conventional photon therapy [1]. The recent development of FLASH proton therapy, where ultra-high dose rates are delivered within milliseconds, has shown additional promise by further sparing surrounding normal tissues while maintaining the tumor control. However, the success of this technique strongly depends on accurate monitoring of the beam to ensure conformal dose delivery and to prevent unintended irradiation of critical OARs [2].

Conventional beam diagnostics face significant challenges when applied to high-intensity proton beams. These FLASH beams often require monitoring at very short timescales. Traditional interceptive diagnostics are not suitable for routine use in a clinical environment, as they can perturb the beam and limit treatment accuracy. Therefore, there is a requirement for non-invasive, real-time monitoring techniques capable of providing reliable beam profiles under FLASH therapy conditions [3].

Gas-jet based Ionization Profile Monitors (IPMs) represent a promising solution. This system introduces a thin curtain of gas into the beam path, the primary protons ionize the gas molecules, and the resulting ions can be extracted and detected without significantly disturbing the beam while keeping the projection of the beam same [4]. This technique, with appropriate optimization, can be adapted for medical accelerators and proton therapy facilities.

In this work, we present initial simulations of a gas-jet based IPM, focusing on ion extraction process and the inhomogeneity in the ion energy distribution at the Micro Channel Plate (MCP) due to the 45 degree tilt of the thin gas curtain and the electric field configuration. Particular attention is given to how these factors influence the reconstruction of the beam profile. The effects of beam position fluctuations and the gas-curtain density distribution, which is considered uniform, are investigated. The probability of generating different ionization states was negligible and therefore omitted from the simulation [5]. The study supports the development of compact gas-jet based IPMs optimized for FLASH proton therapy applications.

## SIMULATION SETUP

The compact configuration of the IPM [6] was modeled in the CST studio suite, with respective bias potentials applied to each electrodes of the system, the schematic of the same is given in Fig. 1, in comparison with the older version of the system. The lateral and vertical sizes were reduced by about 40 %. The potentials were calculated by setting the voltage of MCP at -2 kV and of the interaction point as 0 V. The ionization cross sections are calculated by extrapolating the available experimental cross sections upto 100 MeV using Rudd model [7]. The particle distribution was created considering each incident Gaussian beam of different radii for a 100 MeV proton beam with 600 nA beam current. The density of the gas particles along the thickness of 1 mm of the curtain was assumed uniform, and this was also incorporated when defining the distribution, along with the tilt of 45 degree of the gas curtain. The obtained ion distribution for a beam radius of 2.5 mm, with $\sigma_x$ and $\sigma_y$ of 1.14 mm and 1.08 mm respectively, is shown in Figs. 2(a) and (b).

The particle distribution, simulated using Matlab, was loaded into the CST and the particle trajectory and profile information were obtained. Each ion in the distribution were assigned a constant velocity of 580 m/s, which is due to the supersonic nature of the Argon gas jet. This velocity was calculated considering room temperature of gas jet at 20 °C. These ions are allowed to drift through the electric field created by the electrodes and their distribution on the MCP is recorded to get the beam profile and energy distribution of these ions. A position shift of 1 mm applied in both left/right and up/down directions and again the beam profiles

* f.t.mada-parambil@liverpool.ac.uk

ISBN: 978-3-95450-262-2 ISSN: 2673-5350 doi: 10.18429/JACoW-IBIC2025-TUPMO06

# MECHANICAL DESIGN AND TESTING OF A MAGNETICALLY COUPLED MOTION SYSTEM FOR LHC WIRE SCANNERS

H. Sullivan*, J. Emery†, W. Andreazza, N. El-Kassem, M. R. J. Faure, M. Hamani, L. Hanson, C. Pasquino, M. T. Ramos Garcia, F. Roncarolo, R. Veness
CERN, Geneva, Switzerland

*Abstract*

Linear wire scanners are essential instruments for beam profile measurements in the Large Hadron Collider (LHC) at CERN. The current scanners installed in the machine have shown reliability and performance limitations in recent years. This work presents the development and validation of a bespoke motion system for the next-generation LHC wire scanners. The design replaces vacuum bellows with a planar magnetically coupled linear drive, coupled to a custom ceramic in-vacuum linear guide capable of high-velocity operation in ultra-high vacuum. A dedicated test rig has demonstrated the system's positional accuracy, rigidity, and long-term durability, with over 80,000 cycles completed without degradation. This motion technology will be integrated into the first prototype scanner for impedance verification during the 2025 year end technical stop (YETS) and offers potential for wider application in demanding vacuum environments.

## INTRODUCTION

In the Large Hadron Collider (LHC), Linear Beam Wire Scanners (BWS) play a key role as the reference instrument for machine developments and are used to calibrate other profile measurement devices which provide precise bunch-by-bunch measurements at all energy levels [1].

In November 2023, as part of the Wire Scanner Consolidation Project, work began on a new generation of LHC Linear BWS. The objective of the new design is to address mechanical limitations and reliability issues of the existing scanners, for which the design predates the Large Electron–Positron (LEP) collider installation in the 1980s [2]. The long interval since the legacy design offers the opportunity to integrate modern materials and motion-system technology.

A new scanner design has now been finalised, with the first prototype scheduled for installation in the LHC during the 2025 year-end technical stop (YETS). The new design, shown in Fig. 1, differs significantly from the legacy system, largely to accommodate a new magnetically coupled driving system that eliminates the need for vacuum bellows — a frequent failure mode in current scanners [2]. This paper describes the design and development of this bespoke driving system, and the testing performed to validate its suitability for use in the LHC.

* harry.sullivan@cern.ch
† jonathan.emery@cern.ch

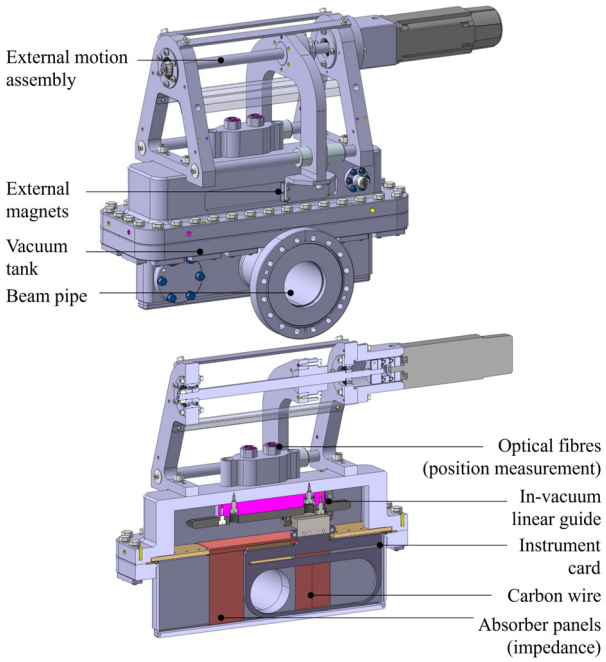



Figure 1: New LHC wire scanner prototype design.

## ENGINEERING DEVELOPMENT

Commercially available magnetically coupled drive products have previously been tested at CERN for their suitability in BWS applications, with positive results [3]. These systems typically operate via a concentric magnet pairing through a thin-walled cylindrical vacuum chamber [4].

Although integration of such an off the shelf system into the new scanner was considered, it was ultimately rejected in favour of a custom-engineered solution. A cylindrical system would require a large space envelope, as the entire drive length must be mounted to the side of the chamber [2]. In addition, a key mechanical limitation of the legacy scanner would remain — the long, unsupported cantilever between the drive fixation point and the wire-measurement point, inside of vacuum, which can cause vibrations and positional uncertainty.

The drive system developed for the new scanner implements a permanent magnet (PM) based planar linear magnetic coupling (PLMC) [2]. A pair of externally driven planar magnet arrays are coupled with a second pair inside the vacuum chamber. The inner arrays are mounted on an in-vacuum linear guide, to which a card supporting the scanning wire is directly attached. Both the coupling and the linear guide have been designed specifically for this application, with the aim of providing repeatable and reliable scans. This new drive system is shown in Fig. 2.

Content from this work may be used under the terms of the CC BY 4.0 licence (© 2025). Any distribution of this work must maintain attribution to the author(s), title of the work, publisher, and DOI.

ISBN: 978-3-95450-262-2 ISSN: 2673-5350 doi: 10.18429/JACoW-IBIC2025-TUPMO07

# BEAM SIZE MEASUREMENT AT SBL IN SuperKEKB

H. Ikeda, H. Fukuma, T. Mitsuhashi, G. Mitsuka, M. Tobiyama
High Energy Accelerator Research Organization (KEK), Tsukuba, Japan
also at The Graduate University for Advanced Studies (SOKENDAI), Tsukuba, Japan

*Abstract*

Sudden beam loss (SBL) is one of the obstacles to improving the luminosity of SuperKEKB. SBL cause damage to collimators and other accelerator components, QCS quench, and large background to the Belle II detector. It also causes beam abort and prevents the accumulation of high currents. Therefore, it is an important issue to investigate and resolve the causes of SBL events. In order to investigate the causes of SBL events, we measured the beam profile at the moment of abort due to SBL using three different cameras and found that the beam size at SBL events was larger than at the moment of abort due to other causes. This paper summarizes the results of the size profile measurements made as part of the investigation into the cause of the SBL.

## INTRODUCTION

The SuperKEKB accelerator is a collider of 7 GeV electrons (HER) and 4 GeV positrons (LER) with a circumference of 3 km. In 2024 operation, we achieved $5.1 \times 10^{34}$ cm$^{-2}$s$^{-1}$ at lower beam current than KEKB [1]. One of the obstacles that must be overcome to increase the luminosity is sudden beam loss (SBL) [2-4]. SBL causes damage to accelerator components, final focusing super conducting magnets (QCS) [5] quenches, and large backgrounds to Belle-II detector. In particular, SBL has caused damage to the collimator head more than 10 times [6]. After various tests, it was found that the most likely candidate to cause SBL is dusts interacting with the beam, and that the dust was thought to come from the vacuum sealant used to prevent vacuum leaks. When the SBL occurred, measurements were characterized by a vacuum burst and an increase in the beam size.

## SUDDEN BEAM LOSS

SBL is a type of beam loss where the circulating beam suddenly loses several tens of percent of its charge during two or three turns, as shown in Fig. 1. Just before the beam loss begins, the orbit appears to move, but the displacement is the order of 0.1 mm. The orbit displacement becomes order of 1 mm after the start of the beam loss. Beam loss occurs in the narrow aperture (collimator, IR) and the starting point of beam loss depends on the collimator setting. SBLs have occurred in both LER and HER, but the damage is more severe in LER because of the greater number of SBLs in LERs and the smaller number of collimators that protect interaction point in LER. Therefore, observations and countermeasure related to SBL in SuperKEKB are mainly made in LER. The measurements in this paper were also performed at LER. SuperKEKB is equipped with a fast beam abort system to dump the beam as soon as possible in an abnormal situation [7-9]. After aborting the beam, it is necessary to accumulate it again from 0 mA, so a large number of beam aborts hinder the gain in integral luminosity. Aborts caused by SBL are 16 % in LER and 1.4 % in HER, indicating that the impact is huge in LER. SBL can occur with both single beam and collision beam. SBL occurs both at β*=1 mm, 3 mm and detuned optics. SBLs occurred with different filling patterns of bunches which were combinations of 2 or 3-bucket spacing, but did not occur when the patterns were significantly different from them. For example, no SBLs were observed when the number of bunches was small though the machine was not operated for long periods of time in these patterns.

Furthermore, a notable feature is that the SBL frequency depends on beam current, and vacuum bursts were observed with the SBL mainly at the wiggler magnet section.

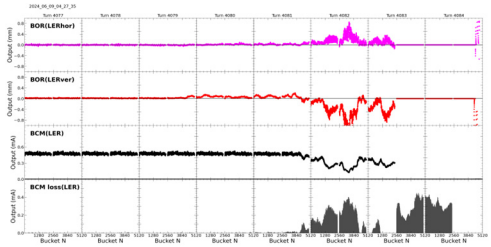



Figure 1: From top to bottom: horizontal orbit, vertical orbit, bunch current, and beam loss compared to the previous turn at the SBL abort.

## BEAM SIZE MEASUREMENT

We decided to measure the beam size when the SBL-induced abort occurred. The setup of SuperKEKB visible light monitor consists of an extraction mirror, optical window, transfer mirrors and optical system. An extraction mirror of visible light is made of thick polycrystalline diamond [10, 11]. It is possible to obtain a sufficient amount of light for beam profile measurement for each bunch. Extraction chamber is set up to downstream 23 m of the source bending magnet. At the downstream of the chamber, five mirrors are used to relay light to the above ground SRM hat about 30 m downstream. An optical system for beam measurement, a gated camera, streak camera etc. are installed in the SRM hat on the ground.

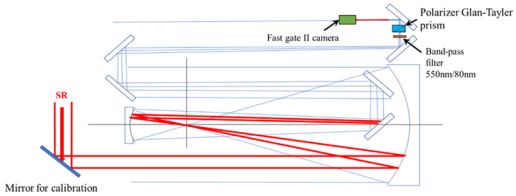



Figure 2: Gregorian objective for observation of injection beam f = 7028 mm.

Content from this work may be used under the terms of the CC BY 4.0 licence (© 2025). Any distribution of this work must maintain attribution to the author(s), title of the work, publisher, and DOI.

ISBN: 978-3-95450-262-2 ISSN: 2673-5350 doi: 10.18429/JACoW-IBIC2025-TUPMO08

# PROGRESS ON GAS-SHEET BEAM PROFILE MONITOR

I. Yamada*, J-PARC Center, Japan Atomic Energy Agency, Ibaraki, Japan.

*Abstract*

A non-invasive beam profile monitor using a gas sheet detecting produced photons was developed and tested at a 400 MeV beam line in J-PARC Linac, which accelerates 50 mA, 500 μs pulse length $H^-$ beam. Around such energy, since the emission cross section takes a minimum and high intensity radiation noise is induced by the beam, a very low signal-to-noise ratio was anticipated. In this study, the primary noise source was investigated to reduce them. The most dominant one was the background light, such as induced by a B-A gauge filament, but it can be negligible with gating function of an image intensifier composing the photon detector system. A beam-induced radiation directly acting on the image intensifier follows. Even though these radiation noises existed, the high-intensity J-PARC Linac beam could be observed.

## INTRODUCTION

A non-invasive beam profile monitor using an extra gas injection is developed and tested in many institutes [1–3]. The extra injected gas, particularly of sheet shape, enables a two-dimensional transverse beam profile measurement as well as efficient monitoring due to enhancement of local gas density. We developed and quantitatively demonstrated a photon-detection-type beam profile monitor using a sheet-shaped gas formed based on a rarefied-gas dynamics [4–6]. At first, we evaluated it with 3 MeV $H^-$ high intensity beam at J-PARC RFQ test stand, which is composed of spares of the J-PARC Linac front-end components for commissioning the RFQ. The developed monitor gave a beam profile well consistent with the one measured with a wire-scanner monitor by applying a reconstruction analysis based on a measured response function of the monitor [6]. In addition, it was found that, for a beam below medium energy (MEBT), the monitor has a potential to reduce a beam emittance through a space-charge neutralization, which is caused by plasma produced in the beam-gas interaction process [7].

For the next step, we are attempting to detect a high-energy beam, which is 400 MeV at J-PARC Linac end. At this energy, the cross-section of the beam-gas interaction takes a minimum, and a radiation noise level is very high as compared with the 3 MeV case. These conditions lead a very low signal-to-noise ratio (S/N) and make the measurement difficult. In this paper, we report the recent effort on measurement of a high-energy beam.

## EXPERIMENTALS

### *Gas-Sheet Beam Profile Monitor System*

The gas sheet monitor shown in Fig. 1 comprises a sheet generator, which is a pair of two facing rectangle conduits,

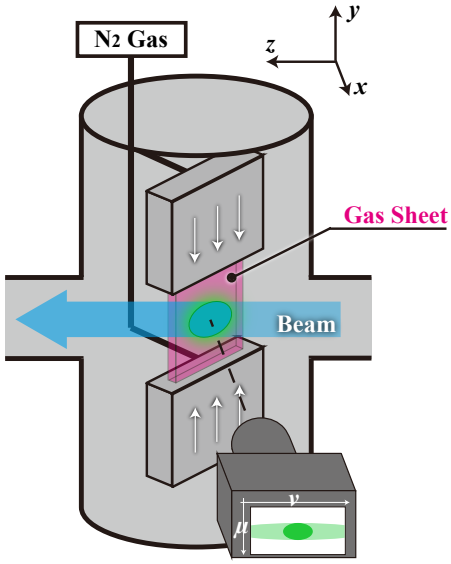



Figure 1: Schematic diagram of the gas-sheet beam profile monitor. The X and Y profile informations are reflected in $\mu$, $\nu$ directions in the captured image.

some vacuum pumps, and a photon detector system. The details of the gas sheet generator and the vacuum system were reported in reference [8]. The maximum gas injection pressure at the generator inlet was 1 kPa to prevent a discharge of nearby cavities, where the gas pressure of the cavity increased from $2\times10^{-7}$ Pa (base pressure) to $4\times10^{-6}$ Pa. The photon detector system consists of a set of optical lenses, an image intensifier which can amplify photon intensity up to $10^4$ times with a built-in multi-channel plate (MCP), and a CCD camera of 16-bit full HD, where a sensor pixel is 5.5 μm square each. The solid angle of photon detection is about 0.012 sr (0.1% of $4\pi$). The image intensifier has a gating function more than 25 ns. The CCD camera can take an image at over 1 ms of shutter speed.

### *Beam Line*

The developed monitor was installed in J-PARC Linac end section. There are three beam dumps near the monitor position: 0-deg. dump at 30 m away, 30-deg. dump at 47 m away, and 100-deg. dump at 150 m away. Radiation from these dumps is one of the noise source of the beam profile measurement, and should be evaluated. The beam parameter is 400 MeV, 50 mA peak current, and 50-500 μs beam pulse length, where the nominal one for user operation is 500 μs.

### *Measurement Method*

To measure a high-energy-beam profile accurately, there are two issues reducing S/N: low photon emission cross

* ippei.yamada@j-parc.jp

Content from this work may be used under the terms of the CC BY 4.0 licence (© 2025). Any distribution of this work must maintain attribution to the author(s), title of the work, publisher, and DOI.

ISBN: 978-3-95450-262-2 ISSN: 2673-5350 doi: 10.18429/JACoW-IBIC2025-TUPMO09

# EXPLOITING NON REDUNDANT APERTURE INTERFEROMETRY AS A DIAGNOSTICS TOOL FOR SYNCHROTRON LIGHT CHARACTERIZATION

L. Torino*, U. Iriso, ALBA CELLS, Cerdanyola del Vallés, Spain
C. Carilli, National Radio Astronomy Observatory (NRAO), Socorro - NM, USA
B. Nikolic, University of Cambridge, Cambridge, UK
N. Thyagarajan, CSIRO, Bentley WA, Australia

*Abstract*

We recently introduced a novel interferometric method inspired by radio astronomy, utilizing a Non-Redundant Aperture (NRA) mask with self-calibration to fully characterize the two dimensional transverse shape of electron beams from a single-shot interferogram. This paper reports the latest advancements in this technique, in particular, the potential of this method for resolving beam halos superimposed on a well-defined Gaussian beam core. We also summarize a new data analysis approach based on closure amplitudes, which removes the need for self-calibration, and we demonstrate the method's applicability to wavefront sensing.

## INTRODUCTION

In recent publications [1–3], we introduced a new technique to fully characterize the electron beam in a single interferogram produced by the synchrotron radiation and a Non-Redundant Aperture (NRA) mask with several holes. This interferogram is analyzed in Fourier space with the so-called "self-calibration" method, which leverages the information from numerous aperture combinations to reconstruct the electron beam shape and corrects for non-uniform mask illumination using gain fitting. Widely used in radio astronomy, this technique has been applied for the first time with visible light to characterize the ALBA electron beam.

The experimental setup is a modified form of two-aperture Synchrotron Radiation Interferometry (SRI) [4]. It uses a lens, filters, and a CCD camera [5] but replaces the typical two-aperture mask with an NRA mask, allowing for simultaneous interference measurements from multiple pairs of apertures, or "baselines" [6, 7].

Figure 1 shows an example of the 5-hole mask (left), its interference pattern (middle), and the amplitude of the 2D-FFT image of the interferogram (right): this process reveals a series of spots, or samples, in the complex Fourier $(u, v)$ plane. Note that he total number of independent samples is determined by the number of apertures ($N$) in the mask using the formula $N(N-1)/2 + 1$.

In the Fourier space, each sample provides specific information. In particular, the central sample (u,v = 0,0), represents the autocorrelation and is proportional to the total light intensity from all the holes. The other samples are generated by every possible baseline (pair of holes). A samples's location in the Fourier space corresponds to the physical

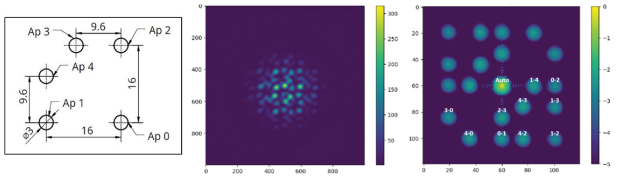



Figure 1: Example of a 5-hole NRA mask (left), its interference pattern (middle) and the 2D FFT (right).

distance and orientation of its generating baseline. The intensity of each sample directly corresponds to the visibility amplitude, of the interference pattern for that particular baseline. This method allows for a comprehensive reconstruction of the beam profile by measuring the complex visibilities for multiple orientations and distances at the same time.

A key advantage of this technique is its ability to account for variations in the illumination of each aperture. What we in fact measure is the visibility $V_{ij}$, that is generated by the interference between light passing the apertures $i$ and $j$, while the information we need to reconstruct the beam shape is the spatial coherence $\gamma_{ij}$. The relation between this two quantity depends on the gain $G_i$ which is the proportional to the square root of the illumination of the aperture $i$:

$$\|V_{ij}\| = \gamma_{\mathrm{ij}} \|G_i\| \|G_j\|. \tag{1}$$

The electron beam is assumed to be an ellipse (or a 2D Gaussian), defined by its major and minor axes and its tilt angle. By adding the autocorrelation information

$$\|V_{\mathrm{auto}}\| = \sum_i \|G_i\|^2 \,, \tag{2}$$

the gains $G_i$ can be treated as fitting parameters. This correction for illumination variations is necessary to obtain an accurate and complete reconstruction of the beam profile in the Fourier space:

$$\gamma(u, v) = V \exp[-(au^2 + bv^2 + 2cuv)], \tag{3}$$

where $u$ and $v$ are the coordinates of the Fourier space and $a$, $b$, $c$ are the standard parameter of a 2D Gaussian. The $\sigma_{\mathrm{u,v}}$s and the angle of the 2D Gaussian can be obtained following [8] and $\sigma$s in the real space are calculated using the following conversion:

$$\sigma_{\mathrm{x,y}} = \frac{\lambda L}{2\pi \sigma_{\mathrm{u,v}}} \,, \tag{4}$$

* ltorino@cells.es

Content from this work may be used under the terms of the CC BY 4.0 licence (© 2025). Any distribution of this work must maintain attribution to the author(s), title of the work, publisher, and DOI.

ISBN: 978-3-95450-262-2 ISSN: 2673-5350 doi: 10.18429/JACoW-IBIC2025-TUPMO10

# PASSIVE TRANSVERSE BEAM PROFILER FOR REAL-TIME MONITORING FOR FLASH RADIOTHERAPY

M. Patel*,[1,2], N. Kumar[1,2], T. Price[3], C. P. Welsch[1,2]
[1] Department of Physics, University of Liverpool, Liverpool, United Kingdom
[2] Cockcroft Institute, Sci-Tech Daresbury, Warrington, United Kingdom
[3] School of Physics and Astronomy, University of Birmingham, Birmingham, United Kingdom

*Abstract*

Beam monitoring has always been crucial in radiotherapy to ensure precise dose delivery and reliable treatment. Passive real-time beam monitors are particularly advantageous because they provide beam information without influencing the beam itself. Such monitors are especially relevant under extreme beam conditions in newly explored modalities that use ultrahigh dose rates (> 40 Gy/s), such as FLASH radiotherapy, where conventional approaches struggle to measure/monitor beam effectively. The study presents a technique to measure the transverse beam size after exit window/nozzle of an accelerator using an all optical monitor. As the therapeutic beam must inherently traverse the ambient air path from the nozzle to the patient, the monitor passively captures beam-induced fluorescence along its path without affecting the beam. This contribution discusses the device in detail and presents one of the measurements taken on a 10.8 – 28 MeV proton beam at MC40 Cyclotron at University of Birmingham for 1 to 25 nA beam current. The measured beam sizes are consistent with those obtained using EBT-3 radiochromic film. A temporal resolution of 100 ms was achieved at 25 nA, demonstrating the feasibility of real-time beam monitoring.

## INTRODUCTION

Beam monitoring in radiotherapy is essential for accelerator control and provides clinicians with feedback to verify that the prescribed dose is being delivered to the correct location. Online beam monitoring devices are typically calibrated against radiochromic films during pre-treatment setup [1], and during treatment they are the only devices providing information on the beam's position, shape, and size. The commonly preferred device, the ionization chamber is often installed at the exit window and exhibit nonlinear responses under extreme conditions, such as those encountered at FLASH dose rates [2]. Thus, although research has contributed to significant advances in beam instrumentation and dosimetry, beam monitoring at FLASH dose rates remains less developed compared to conventional dose rates across electron, proton, and hadron therapies.

Passive monitors measures the beam using the event inherently associated with the beam itself. A charged-particle beam excites neutral atoms or molecules along its trajectory. These excited species release energy through radiative de-excitation (Fluorescence), typically occurring on picosecond to nanosecond timescales, which are much shorter than their thermal transit times. As a result, the emitted photons originate locally along the beam path, allowing the beam position and size to be reconstructed from the fluorescence signal. Since the source of these photons is the neutral medium along the beam trajectory, often absent or intentionally removed in accelerator environments to create high vacuum, fluorescence monitors are not widely adopted in accelerator physics. However, in medical accelerators the therapeutic beam must necessarily travel through ambient air after exiting the window and before reaching the patient. This interaction inevitably generates fluorescence, which can in principle be exploited to passively monitor the beam. Previous attempts have used dark gas-filled tubes with Avalanche Photodiodes (APDs) scanned across the beam to reconstruct profiles [3] and have shown promising results, which can be developed further to improve temporal and spatial resolution.

In this study we demonstrate an all-optical setup capable of capturing the full transverse beam profile in real time, termed the Air Fluorescence Monitor (AFM). We describe the construction of the device and present beam profile measurements for proton beams from the MC40 cyclotron at the University of Birmingham, UK. Results are shown for beam currents ranging from 5 – 25 nA at 20 MeV, with AFM profiles compared against dose distributions obtained from EBT-3 film. The two methods show reasonable agreement within experimental constrains, demonstrating the feasibility of AFM for passive, real-time beam monitoring.

## OPTICAL SETUP

Figure 1 shows the optical setup of the AFM: an imaging assembly consisting of a lens system to create an image of the beam traveling through air, a microchannel-based image intensifier, and a digital camera. The lens system is an apochromatic triplet with a 40 mm aperture having 80 % transmission across the 300 to 700 nm spectral range. This range covers the dominant fluorescence emission lines expected from air [4]. With a design focal length of 160 mm, the objective lens is positioned 320 mm from the beam axis achieve a magnification of –1 on the photocathode of the image intensifier. The beam image is projected onto the input of a Proxikit PKS 2581 TZ-V image intensifier. The image intensifier has a 25 mm diameter UV-enhanced S20 photocathode at the input that provides relatively high quantum efficiency up to 650 nm while maintaining a low dark count rate. The signal is then amplified by a double-stacked

* milaan.patel@liverpool.ac.uk

Content from this work may be used under the terms of the CC BY 4.0 licence (© 2025). Any distribution of this work must maintain attribution to the author(s), title of the work, publisher, and DOI.

ISBN: 978-3-95450-262-2 ISSN: 2673-5350 doi: 10.18429/JACoW-IBIC2025-TUPMO11

# CONCEPTUAL DESIGN OF COLLISION FEEDBACK SYSTEM FOR THE SUPER TAU-CHARM FACILITY*

Q. Chen, Q. Luo†, SNST, University of Science and Technology of China, Hefei, China

*Abstract*

The Super Tau-Charm Facility (STCF), a third-generation electron-positron collider operating in the tau-charm energy region, will be subject to mechanical disturbances and ground vibrations, which can lead to beam-beam misalignments at the interaction point (IP). Such misalignments degrade luminosity and shorten beam lifetime. To maintain an optimum beam collision condition, the development of a high-performance collision feedback system is therefore essential for suppressing orbit offsets at the IP. This study first analyzes the primary sources of orbit perturbations and evaluates the feasibility of three candidate feedback signals for monitoring IP beam offsets in the STCF collision system from the perspective of detection principles. Finally, a preliminary design of the collision feedback system is proposed based on the STCF's performance requirements.

## INTRODUCTION

The STCF is a next-generation high-energy physics experiment currently under construction, designed to cover a center-of-mass energy range of 2-7 GeV with a target peak luminosity of no less than $5\times10^{34}$ $cm^{-2}s^{-1}$[1]. To achieve this luminosity, STCF incorporates several advanced beam dynamics schemes, including emittance compression, the use of a large crossing angle to mitigate the hourglass effect [2], and the application of the crab-waist scheme to suppress coupling resonances induced by large-angle collisions [3]. With these designs, the final focusing (FF) quadrupoles can compress the beam size at IP to the sub-micrometer scale in the vertical direction, while effectively avoiding hourglass limitations and significantly enhancing luminosity. However, such ultra-small beam sizes make the collider highly sensitive to ground motion and mechanical vibrations, where even minute orbit perturbations can cause substantial displacements and crossing angle variations at the IP [4]. These effects severely degrade luminosity and shorten beam lifetime. Therefore, a high-performance collision feedback system with fast response and high-precision orbit control is indispensable for maintaining optimal collision conditions and realizing stable high-luminosity operation.

## ORBIT DISTURBANCES

Orbit deviations at IP can lead to significant luminosity loss and therefore require correction. Such deviations may arise, for example, from vertical displacements of the FF quadrupoles induced by ground vibrations transmitted through components such as cryostats. These displacements result in closed-orbit distortions at the IP, with differing orbit drifts between the two colliding beams that cannot be fully compensated [5]. As illustrated in Fig. 1, the orbit offset at IP can be expressed as:

$$\Delta y_{IP} = \frac{\sqrt{\beta_Q \beta_{IP}}}{2\sin\pi\nu_y} = cos\left(\pi\nu_y - \left|\Delta\psi_y\right|\right) K \Delta y_Q \,, \quad (1)$$

where $\beta_Q$ and $\beta_{IP}$ denote the transverse beta functions at the FF quadrupoles and at the IP, respectively, $\nu_y$ is the vertical tune, $\Delta\psi_y$ is the phase advance between the IP and the FF quadrupoles, K is the quadrupole focusing strength, and $\Delta y_Q$ represents the vertical displacement of the FF quadrupoles.

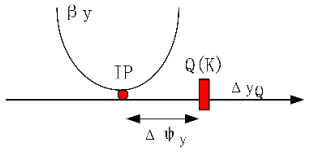



Figure 1: Change of orbit at IP by vertical displacement of the final focus magnets.

## FEEDBACK SIGNALS

### *BPM Signal*

Orbit variations induced by beam-beam interactions at IP can be measured using BPM, enabling the determination of the relative beam displacement at the IP and the implementation of orbit feedback correction [6]. Specifically, when the two beams meet each other with a small offset at the IP, the electromagnetic interaction between the beams generates a beam-beam kick proportional to the offset, which in turn causes a large-angle orbit deflection along the beam propagation direction, as illustrated in Fig. 2.

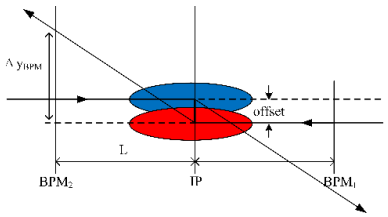



Figure 2: BPM-based principle for orbit offset detection.

The orbit variations of positrons and electrons detected by the BPM can be expressed as:

$$\begin{aligned} \Delta y_{BPM,e} &= L \cdot \Delta y_e'^* = -L\frac{2\pi}{\beta_y^*}\xi_y\left(y_e^* - y_p^*\right), \\ \Delta y_{BPM,p} &= L \cdot \Delta y_p'^* = L\frac{2\pi}{\beta_y^*}\xi_y\left(y_e^* - y_p^*\right). \end{aligned} \quad (2)$$

$\Delta y_{e,p}^*$ represents the beam-beam kick experienced by the electron and positron beams, and $y_{e,p}^*$ denotes their vertical positions at the IP. According to Eq. (2), by monitoring BPM signals upstream and downstream of the IP,

* Work supported by National Key R&D Program of China (2022YFA1602201).

† luoqing@ustc.edu.cn

Content from this work may be used under the terms of the CC BY 4.0 licence (© 2025). Any distribution of this work must maintain attribution to the author(s), title of the work, publisher, and DOI.

ISBN: 978-3-95450-262-2 ISSN: 2673-5350 doi: 10.18429/JACoW-IBIC2025-TUPMO12

# TRANSVERSE EMITTANCE MEASUREMENTS OF ELECTRON BEAMS FROM THE SUPERCONDUCTING RF GUN FOR HIGH-CURRENT OPERATION AT HELMHOLTZ-ZENTRUM DRESDEN-ROSSENDORF

R. Niemczyk*, A. Arnold, A. Ryzhov, J. Teichert, R. Xiang
Helmholtz-Zentrum Dresden-Rossendorf, Dresden, Germany

*Abstract*

High-brightness, megahertz-rate electron sources are a crucial component of future light sources, including the Linac Coherent Light Source II High Energy project, or the high-duty-cycle upgrade of the European X-ray Free-Electron Laser. The Helmholtz-Zentrum Dresden-Rossendorf has employed a superconducting radio-frequency (SRF) gun as one of its CW electron sources for user operation at ELBE since 2010. The SRF gun is used to drive the superradiant THz source TELBE, typically at repetition rates of 50 kHz and bunch charges of 200 pC. To determine the operating envelope of the SRF gun injector, a slit-scan setup was installed in the diagnostics beamline after the SRF gun, enabling characterization of the vertical phase space. In this proceeding, we describe the slit-scan setup at the diagnostics beamline of the SRF gun. Measurements of the vertical emittance at 200 pC bunch charge and beam energies of 3.5 MeV will be presented.

## CENTER FOR HIGH-POWER RADIATION SOURCES ELBE

The Helmholtz-Zentrum Dresden-Rossendorf (HZDR) operates the Center for High-Power Radiation Sources ELBE [1]. It is based on a superconducting radio-frequency (SRF) linear accelerator, which provides continuous-wave (CW) beams. Based on this accelerator, ELBE hosts multiple secondary radiation sources: the infrared free-electron laser (FEL) FELBE, the superradiant THz source TELBE, the positron source pELBE, the $\gamma$-radiation source gELBE, the neutron source nELBE, and the electron irradiation beamline eELBE. In 2024, ELBE achieved 4279 user-confirmed operation hours out of 4524 scheduled hours, corresponding to a reliability of 95 %. The facility employs two electron injectors: a thermionic injector positioned in line with the linear accelerator, and an SRF gun located in parallel. The SRF photoinjector delivers electron beams to the accelerator through a transfer dogleg.

## SRF PHOTOINJECTOR

The photoinjector is based on a 3.5-cell superconducting cavity with a resonance frequency of 1.3 GHz. A normal-conducting photocathode is located in the half-cell, electrically insulated from the cavity and cooled to liquid-nitrogen temperature. Copper and magnesium have been used as photocathode materials in the past, while $Cs_2Te$ has most recently been employed [2,3]. The $Cs_2Te$ photocathodes had quantum efficiencies as high as 5 % inside the SRF gun and showed no significant degradation during user operation. A cross-sectional drawing of the SRF gun at HZDR is shown in Fig. 1. A DC bias voltage of −5 kV is applied to the cathode, which corresponds to 1 MV m$^{-1}$ of accelerating DC field. The radio-frequency field has a peak electric field strength of $E_{\mathrm{peak}} = 17.9\,\mathrm{MV\,m^{-1}}$, which corresponds to a maximum electric cathode field of $E_{\mathrm{cathode}} = 11.3\,\mathrm{MV\,m^{-1}}$, allowing acceleration of electrons to $E_{\mathrm{kin}} = 3.5$ MeV. A dark current of 40 nA is present when operating the gun with this settings. The electrons are emitted from the cathode after illumination with laser pulses in the ultraviolet. When emitting 77 pC per bunch at the maximum laser repetition rate of 13 MHz, the resulting photocurrent is 1 mA. At lower repetition rate a maximal bunch charge of 300 pC can be extracted in a single bunch. More information on the SRF gun can be found in Ref. [4].

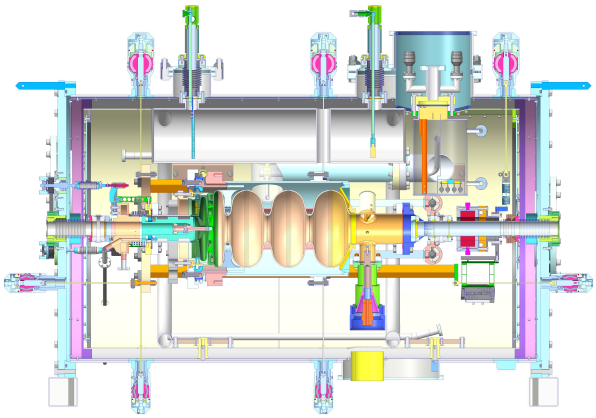


Figure 1: Cut drawing of the SRF gun-II at HZDR.

## PHASE SPACE DIAGNOSTICS

For the characterization of the transverse phase space, the slit-scan technique is employed at a screen station located 2.76 m downstream of the cathode in the diagnostics beamline. The layout of the SRF gun diagnostics beamline, featuring the transfer dogleg, is depicted in Fig. 2. A 1 mm-thick mask with a 100 µm-wide slit enables the measurement of the vertical projected emittance. The cut-out beamlets are detected on a 500 µm-thick YAG scintillating screen located 0.75 m downstream of the slit position, and the generated light is imaged via an in-vacuum 45° mirror and an in-air 45° mirror onto a CCD camera (Basler). The imaging optics result in a screen-to-camera calibration factor

* r.niemczyk@hzdr.de

Content from this work may be used under the terms of the CC BY 4.0 licence (© 2025). Any distribution of this work must maintain attribution to the author(s), title of the work, publisher, and DOI.

ISBN: 978-3-95450-262-2 ISSN: 2673-5350 doi: 10.18429/JACoW-IBIC2025-TUPMO13

# DEVELOPMENT OF LOW DENSITY MATERIALS FOR BEAM INTERCEPTING INSTRUMENTS

R. Veness†, S. Burger, G. Aliana-Cervera, C. Pasquino
CERN, Geneva, Switzerland.

*Abstract*

Materials with a minimal interaction with particle beams are widely used in accelerators in interceptive instruments such as screens, secondary emission grids and wire scanners. Material damage limits are already exceeded in energy frontier and high brightness machines. A new generation of 'low density' materials with nano-structures are becoming available at scales of interest for use in beam instrumentation. Specifications are increasingly of use but still with fundamental issues that limit their application. This paper will demonstrate the potential for this class of materials for beam intercepting materials. It will outline the current limitations and ongoing research to overcome them both in the short and long-term.

## INTRODUCTION

Beam instruments can be divided into two categories: those that do not intercept the beam (non-interceptive), using properties such as emission of light (synchrotron light emission or electro-magnetic coupling; others where the beam physically intercepts some material, either gas or solid, causing an effect which is measured such as particle scattering, emission of light (scintillation, fluorescence, OTR) or emission of secondary particles.

Interceptive instruments have limitations in their field of use due to the nature of their interactions. Intercepting the beam with too much material (mainly an issue for solid interceptors) results in excessive beam-loss, causing irradiation of components, potentially magnet quench in superconducting machines or rendering the instrument 'destructive' of the beam, so only useable in set-up conditions such as in the observation screens 'BTV' in the CERN proton LINAC [1]. Beam-material interactions can also damage or destroy the interacting material in energy frontier machines such as the wire scanner (BWS) in the LHC [2].

Gaseous detectors (either using background or injected gas) can overcome many of these limitations. However, residual beam-gas signals tend to be too low without some amplification such as in the new beam-gas ionisation (BGI) in the CERN PS [3] and injected gas detectors can lead to beam loss such as the Beam-Gas Vertex (BGV) [4] and Beam-Gas Curtain (BGC) [5] in the CERN LHC due to the diffusion of gas along the beam axis.

It is interesting at this point to compare the quantity of material actually intercepted by the beam for commonly used instruments. The number of matter particles intercepted, n is defined in (1):

$$n = \rho L \, [mol.m^{-2}], \tag{1}$$

where ρ is the mass density of the intercepting material and L is the detected length of the intercepting material (the diameter for a wire). For gaseous detectors, the mass density is calculated at the pressure of operation.

This value n allows us to compare the number of matter atoms intercepted by the beam for both solid and gaseous detectors and is plotted in Fig. 1 for some common instruments with typical design characteristics in use at CERN. As the interactions measured are often elastic collisions, the atomic mass is also plotted.

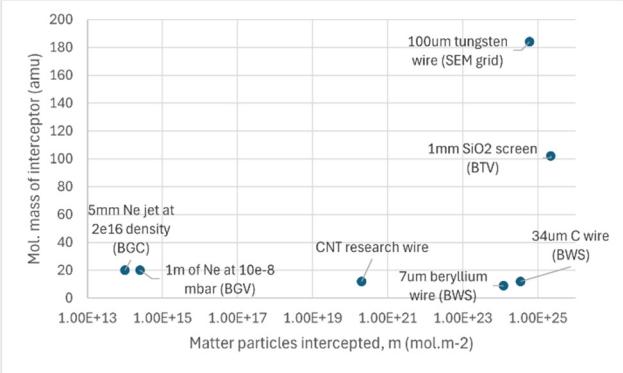



Figure 1: Matter particles intercepted by the beam and atomic mass for common interceptive instruments.

Ignoring for the moment the 'CNT (Carbon Nano-Tube) Research Wire' it is clear by inspection that the intercepting mass groups divide into solids and gases, with a difference of some 10 orders of magnitude in the number of particles intercepted by the detector materials. This expansive 'valley' explains much of the inherent limitations in the two types of interceptors: The solids tend to intercept too much beam and the gases not enough. Even the most highly optimised solid interceptors such as a 7 µm beryllium wire used in the CERN PS wire scanner in the 1980s [6] shows little variation from other solids on this log scale just as with the focussed gas jet in the BGC detector.

## WHAT MATERIAL WOULD MAKE AN IDEAL INTERCEPTOR?

### *Solid or Gas?*

Gases have the advantage of being inherently indestructible by the beam. However, they will diffuse into the accelerator vacuum system so the pressure that can be achieved is limited. Detectors such as the BGI [3] use beam-gas ionisation with focussing and amplification of

† veness@cern.ch

Content from this work may be used under the terms of the CC BY 4.0 licence (© 2025). Any distribution of this work must maintain attribution to the author(s), title of the work, publisher, and DOI.

ISBN: 978-3-95450-262-2 ISSN: 2673-5350 doi: 10.18429/JACoW-IBIC2025-TUPMO14

# NOVEL HOLLOW CORE OPTICAL FIBRE-BASED RADIATION SENSING TECHNIQUE FOR MEDICAL APPLICATIONS AND EXTREME ENVIRONMENTS

R. G. Larsen*[1], A. Gerbershagen, J. M. Schippers
PARTREC, UMCG, University of Groningen, Groningen, Netherlands
A. Gilardi, I. Ortega, CERN, Geneva, Switzerland
E. Buchanan, University of Edinburgh, Edinburgh, Scotland
M. Dosanjh[1], University of Oxford, Oxford, England
I. A. Davidson, G. Jackson, G. Jasion, T.W. Kelly, H. C. Mulvad, F. Poletti, S. Pradhan,
A. Taranta, N. Wheeler, University of Southampton, Southampton, England
[1]also at CERN, Geneva, Switzerland

*Abstract*

As part of our search for radiation-hard techniques for beam profile monitoring, we tested a novel method based on hollow-core optical fibres. These fibres, filled with scintillating gases, combine exceptional radiation tolerance with the inherent radiation hardness of the gases. We tested this new technique at the CLEAR accelerator at CERN, demonstrating its potential for beam diagnostics. The standard deviation of the CLEAR electron beam transverse profile was successfully measured to be 1.15 mm ± 0.02 mm, close to the width of 1.30 mm ± 0.07 mm obtained from a YAG screen. No loss of signal was observed after the fibre received a dose of 0.915 MGy. The technique shows particular promise for FLASH therapy, where it could offer significant improvements in reliability and functionality compared to current instrumentation.

## INTRODUCTION

Future needs for beam instrumentation to measure intense beams, with up to $10^{11}$ particles per second, have motivated a search for suitable techniques, for both research and medical purposes in radiation-hard environments. An overview of this research is presented at IBIC 2025 [1]. Previous work has studied the possibilities of using solid silica glass rods [2, 3] or glass capillary tubes filled with a liquid scintillator [4] coupled to a camera or other photo-sensor. Both of these techniques give a good signal, but suffer from degraded performance at high absorbed doses. The development of hollow core fibres (HCF), capable of guiding light in the visible spectrum [5, 6], presents new opportunities for radiation sensing techniques. HCFs do not suffer from the same radiation-induced attenuation that limits the lifetime of conventional optical fibres in environments with high radiation levels [7]. In this paper, we present work that combines the radiation-hard characteristics of the HCF with an intrinsically radiation-hard noble gas scintillator to obtain a novel radiation-hard beam-sensing technique.

## METHODS

A 200 MeV electron beam from the CLEAR accelerator [8] was used for the experiment. The intensity of the beam was varied in the range from 0 nC to 41.2 nC per bunch train, both by changing the charge per bunch and the total number of bunches in one shot from the accelerator. The irradiation was carried out with a repetition frequency of 0.833 Hz. The bunch length was 10 ps and the bunch spacing was 666 ps.

The key elements of the setup are sketched in Fig. 1. The HCF was placed horizontally in the plane perpendicular to the beam. On one end, the HCF was spliced to a Thorlabs SM450 fibre. The opposite end of the HCF was connected to a compression-based gas feed-through assembly, which interfaced it with a gas distribution pipe. Both the gas pipe and the SM450 fibre were routed to a barrack outside the beam area. The length of HCF between the beam impact point and the splice was 60 cm. The HCF was placed on a support structure holding it steady in the beam. This support was placed on top of a vertical motion stage, allowing the HCF to be scanned through the beam in the direction perpendicular to the beam and the HCF. Immediately upstream of the HCF, the electron beam passed through a beam charge monitor. A scintillating screen was placed downstream of the HCF at an angle of 45° to the beam, and a camera was pointed at the screen perpendicularly to the beam. The HCF used was a 7-tube single-cladding ring fibre, with 170 nm thick capillary membranes, capable of continuous guidance from 360-1100 nm, fabricated from fused silica glass [5, 6]. In the barrack, the SM optical fibre was routed to a black box and placed such that the light exiting the fibre impacted a Hamamatsu S13360-1350PE silicon photomultiplier (SiPM) sensitive to photons in the wavelength range of 300-900 nm. The output of the SiPM was connected to an oscilloscope, acting as a digitiser of the analogue signal from the SiPM. The oscilloscope was triggered by a signal from the accelerator. The digitised pulses from the SiPM were then sent via Ethernet to a PC and timestamped and saved for offline analysis. The gas transport pipe was connected to a custom gas panel, which was used to measure the pressure, $p$, of the gas in the system, as well as switch the connection between

* robert.garbrecht.larsen@cern.ch

Content from this work may be used under the terms of the CC BY 4.0 licence (© 2025). Any distribution of this work must maintain attribution to the author(s), title of the work, publisher, and DOI.

ISBN: 978-3-95450-262-2 ISSN: 2673-5350 doi: 10.18429/JACoW-IBIC2025-TUPMO16

# UPGRADED BEAM PROFILE MONITORING USING CHROMOX AND FIBER OPTIC IMAGING FOR HIGH-RADIATION ENVIRONMENTS

A. Gottstein*, S. Braccini, L. Eggimann, E. Kasanda, I. Mateu
AEC, LHEP, University of Bern, Bern, Switzerland

*Abstract*

We present an upgraded beam monitoring system designed for use in high-radiation environments where conventional imaging solutions rapidly degrade. In the presented device, the radiation-sensitive P47 phosphor screen of the previous system is replaced with a radiation-hard Chromox ceramic scintillator, and the CMOS camera is relocated outside the irradiation zone by transmitting the optical signal through a 20-meter radiation-tolerant fiber optic bundle. To enhance operational flexibility, a pneumatic actuator enables remote insertion and retraction of the scintillating screen into the beam path. The radiation hardness of the Chromox ceramic and the fiber bundle was evaluated, and the optical system's resolution and fidelity were characterized. The new setup demonstrated stable imaging performance under irradiation, solving the frequent maintenance issues of the previous system. These improvements offer a robust and low-maintenance solution for beam profile monitoring in high-radiation accelerator environments.

## INTRODUCTION

At the Bern Medical Cyclotron (BMC) laboratory, an 18 MeV proton beam is available for both routine radioisotope production and multidisciplinary research through a dedicated Beam Transfer Line (BTL) [1]. To support these activities, our group has developed a series of devices for beam diagnostics, such as the now commercialised UniBEaM detector [2], and, in collaboration with TRIUMF, an array of scintillators for non-destructive beam monitoring through the detection of secondary radiation surrounding the beamline [3]. More recently, the two-dimensional beam profiler $\pi^2$ [4] was implemented as a standard diagnostic tool, providing reliable information on beam profiles and intensities with minimal perturbation of the beam.

A new upgraded system has been realised, aimed at extending the operational range of the $\pi^2$ detector and improving its robustness under demanding irradiation conditions. We present the design and performance of the upgraded device, with a focus on the characterization of the response of its components under high proton fluxes and its long-term stability. The results confirm the suitability of this instrument for routine use in radioisotope production research and in dedicated irradiation studies, while also highlighting its potential for broader applications in beam diagnostics.

* alexander.gottstein@unibe.ch

## THE $\pi^2$ UPGRADE

The first iteration of the $\pi^2$ beam monitoring device [4] proved effective for beam imaging but presented several limitations for routine operation. The P47 scintillator layer lacked mechanical stability, showing adhesion issues and progressive degradation over time. In addition, the camera positioned close to the scintillating screen suffered radiation damage from secondary radiation, leading to frequent replacements due to the accumulation of dead pixels.

To overcome these drawbacks, an upgraded design was developed (see Fig. 1). The P47 layer was replaced by a 500 µm-thick Chromox ceramic ($Al_2O_3$ doped with chromium oxide, manufactured by Advatech), offering superior mechanical robustness and long-term stability under irradiation. To mitigate camera damage, the readout was relocated outside the irradiation zone by coupling the scintillator to a 20 m ESKA™ FF-VK80 optical fiber bundle, which guides the image to a radiation-protected area.

Since the Chromox ceramic and its aluminium holder fully stop the 18 MeV proton beam, a pneumatic actuator was integrated to enable remote insertion and retraction of the scintillator, making the system a destructive monitor. Dedicated lens systems are employed to focus the scintillation image onto the fiber input and to project the fiber output onto a commercial CMOS camera (*CS165CU1/M Zelux®*).

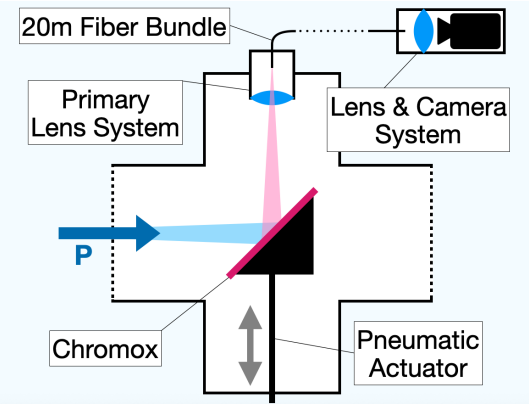



Figure 1: Schematic of the upgraded $\pi^2$ beam monitoring device. The Chromox scintillator is mounted on a pneumatic actuator and read out via a primary lens system, a 20 m optical fiber bundle, and a remote lens–camera system.

Prior to installation on the beam line, the device was assembled and tested in the laboratory using an LCD screen placed at the position of the Chromox scintillator. This procedure enabled a precise calibration of the optical system, which requires a geometric correction due to the inclination

Content from this work may be used under the terms of the CC BY 4.0 licence (© 2025). Any distribution of this work must maintain attribution to the author(s), title of the work, publisher, and DOI.

ISBN: 978-3-95450-262-2 ISSN: 2673-5350 doi: 10.18429/JACoW-IBIC2025-TUPMO17

# PHASE CONTRAST ISSUES OPERATING PINHOLE CAMERAS WITH LOW-EMITTANCE BEAMS

M. Labat*, A. Bence, P. Mercère, P. Dasilva, D. Pédeau, N. Hubert
Synchrotron SOLEIL, Gif-sur-Yvette, France

*Abstract*

In the framework of SOLEIL-II, the project of SOLEIL's storage ring upgrade towards lower emittances, preliminary studies were performed to pinpoint the resolution limits of the exisiting pinhole cameras. However, while reducing the vertical emittance from the SOLEIL's nominal 50 pm·rad value to 9 pm·rad, unexpected filaments were observed in the image plane of the pinhole cameras, severely spoiling the reliability of the emittance measurement. Investigations, on the existing pinhole cameras as well as on the Metrology beamline of SOLEIL, revealed that those filaments correspond to a phase contrast imaging of the UHV Aluminium window, located before the pinhole. In this work, we first report on experimental measurements performed to identify the origin of this issue and on our attempts of mitigation using a phase blurrer and testing different types of window.

## INTRODUCTION

SOLEIL storage ring presently enables to store electron beams with an horizontal emittance of 3.9 nm·rad and a vertical emittance that can be varied from ≈ 7 up to 200 pm·rad. These emittances are measured by two pinhole cameras (PHC) [1, 2], one being used in a feedback loop to maintain the vertical emittance at 50 pm·rad ± 5 % during users' operation. However, on the forthcoming SOLEIL-II storage ring, these emittances will be significantly reduced. Relying on a multibend achromat lattice, the targetted emittances in operation are 85 pm·rad in the horizontal and 53 pm·rad in the vertical plane, with a vertical emittance at minimum coupling expected below 1 pm·rad. The existing PHCs can not resolve such low–emittances. This is why preliminary experiments were launched to anticipate a resolution improvment of our emittance diagnostics.

## EXPERIMENTAL SETUP

The experimental setup of the PHCs [2] is shown in Fig 1. The X-ray content of the Synchrotron Radiation (SR) emitted by one of the ring dipoles (ANS-C02.D1 for PHC1 and ANS-C16.D2 for PHC3) is first extracted from the dipole vacuum chamber through a metallic UHV window. This window is made of Aluminium 6061 T6, an alloy widely used for vacuum components. The two main metals in addition to Aluminium (Z = 13) are Magnesium (Z = 12) about 1 % and Silicium (Z = 14) about 0.8 %. Relying on a parabolic shape, it is only 1 mm thick on the SR path while exhibiting a scratched exit surface (see Fig. 2). The SR then passes through a Copper filter of variable thickness (from 0 up to 2 mm) which enables to block the low energy photons. For emittance measurements (see Fig. 1a), a pinhole is inserted on the X-ray path. This pinhole is made of Tungsten blades defining a rectangular aperture of 15 × 10 µm. The SR finally hits a CdW04 scintillator of 0.5 mm thickness converting the X–rays into visible light. The intensity distribution of this visible light at the rear of the scintillator is then simply imaged on a CMOS camera with a pair of lenses. The ratio between the distance *D* from pinhole to scintillator, and the distance *d* from source point to pinhole sets the magnification of the pinhole. The pinhole can be removed from the X-ray path (see Fig. 1b). This configuration enables to observe the intensity distribution of the SR layer on the scintillator.

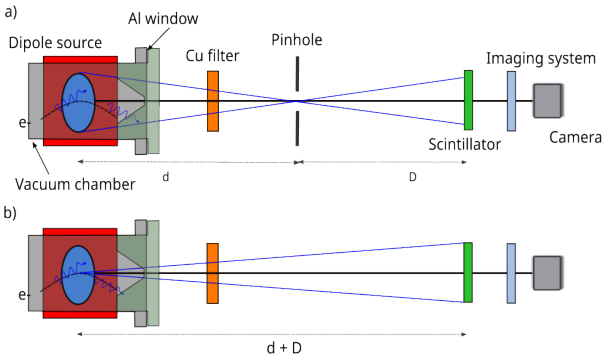



Figure 1: Experimental setup of the pinhole cameras installed at SOLEIL: a) with the pinhole imaging for emittance measurement, b) without pinhole for SR layer measurement.

## PHASE–CONTRAST IMAGING ISSUE

Preliminary experiments on SOLEIL's PHCs aimed at finely compare measurements with SRW [3] simulations with low vertical emittances, for further extrapolation on improved resolutions. SOLEIL storage ring was therefore operated with a dedicated optics allowing to reach the minimum coupling, i.e. the minimum vertical emittance (≈ 7 pm·rad). In these conditions, it rapidly appeared that the emittance measurement was suffering from a strong dependency to the beam orbit. To understand this unexpected dependency, the pinhole was removed, revealing a high–contrast filamented pattern (see Fig. 3). These structures were observed simultaneously on the two PHCs. A scan of the pinhole transverse position confirmed that the emittance value was strongly correlated to the local intensity of the filamented SR, a correlation responsible for the beam orbit dependency previously observed.

* marie.labat@synchrotron-soleil.fr

Content from this work may be used under the terms of the CC BY 4.0 licence (© 2025). Any distribution of this work must maintain attribution to the author(s), title of the work, publisher, and DOI.

ISBN: 978-3-95450-262-2 ISSN: 2673-5350 doi: 10.18429/JACoW-IBIC2025-TUPMO19

# CURRENT STATUS OF DEVELOPING PEPPER-POT EMITTANCE MONITOR FOR HIGH-INTENSITY ION BEAM*

Y. Kotaka†,1, K. Kamakura[1], Y. Sakemi[1], J. Ohnishi[2], H. Matsuzaki[3]
[1]Center for Nuclear Study, The University of Tokyo, Wako, Japan
[2]Riken Nishina Center, Wako, Japan
[3]Micro Analysis Laboratory, Tandem accelerator, The University of Tokyo, Tokyo, Japan

*Abstract*

The experiment to measure the Electric Dipole Moment (EDM) of Francium (Fr) is in progress by Center for Nuclear Study (CNS), UTokyo. Fr is produced via a nuclear fusion reaction by bombarding a gold target with $^{18}$O beam, requiring a beam intensity of 18 $e$μA or higher. However, the transport efficiency of the current beam line decreases to 66 % when the beam intensity exceeds 10 $e$μA. To address this issue, we are developing a pepper-pot emittance monitor (PEM) optimized for high-intensity beams. The improvements include locating the camera far from the beam line to minimize radiation damage, achieving a distance 4.1 m while maintaining the position error of 0.13 mm. Additionally, we conducted beam tests to verify measurement errors and found the results were consistent with the measurement errors estimated from the PEM structure. Furthermore, the beam shutter time 0.27 s was estimated to be acceptable up to the beam power 1000 W to prevent PEM overheating.

## INTRODUCTION

The experiment to measure Fr-EDM with the highest measurement accuracy is in progress by CNS [1]. Fr is produced by a nuclear fusion reaction by bombarding a gold target with $^{18}$O beam accelerated to 7 MeV/u by AVF Cyclotron. To achieve that accuracy, a beam intensity of 18 $e$μA (400 W) or higher is required. However, the beam transport efficiency is 66 % when the beam intensity exceeds 10 $e$μA [2]. To improve the beam transport efficiency, we are developing the PEM [3,4] optimized for high-intensity beams and calculate the optimized beam trajectory.

Based on the PEM developed for beams of ECR ion source (ECRIS) [5], we are developing three additional features. The first is the camera optical system locating the camera far from the beam line to minimize radiation damage. The second is the improvement of measurement error. Since the emittance of AVF cyclotron beam is typically 20$\pi$ mm·mrad, about one-tenth emittance of ECRIS beams, an angular measurement error of 0.3 mrad or less is required to calculate the beam trajectory [2]. To verify the measurement errors, beam tests were conducted at the Micro Analysis Laboratory, Tandem accelerator, UTokyo (MALT) [6]. The third is a beam shutter mechanism aimed at short-time measurements to prevent PEM overheating due to beam irradiation, and the time reached 0.27 s [2].

* This work was supported by JSPS KAKENHI Grant Number JP20K12481.
† kotaka@cns.s.u-tokyo.ac.jp

## ESTIMATING MEASUREMENT ERROR

The measurement errors estimated from the PEM structure are described. To obtain emittances, the beam positions and angles are measured. Our PEM is shown in Fig. 1. The mask is 1 mm thick copper plate having holes whose diameter is 0.3 mm set at 2 mm interval. The image of beam passing through each hole and glowing on the fluorescent plate tilted 45 degrees is taken with digital camera through the window. The true beam position $r_m$ costituting an emittance is any position within a mask hole, and the true beam angles $r'_t$ are calculated by Eq. (1) and shown in the left view of Fig. 2.

$$r'_t = (r_f - r_m)/(z_f - z_m) \ (r = x \ or \ y) \quad (1)$$

$$r'_e = (r_f + r_e - r_c)/(z_f - z_m) \ (r = x \ or \ y) \quad (2)$$

where $z$ is beam axis. The beam position ($x$, $y$) are horizontal and vertical axes perpendicular to $z$-axis, respectively. The scripts $m$ and $f$ mean the true beam positions on the mask and fluorescent plate, respectively.

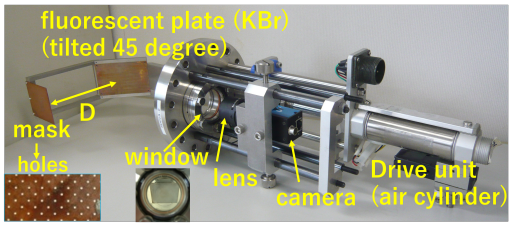



Figure 1: The developed PEM and the constituting pieces. Though this camera is close to the window in this photo, it is located far from the window to minimize radiation damage.

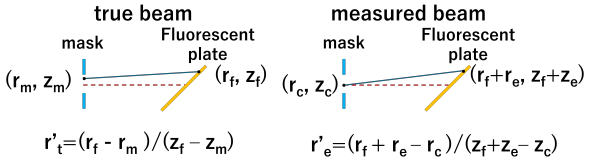



Figure 2: Definition of beam angle and the error of PEM.

However, since we know only center position $r_c$ of the hole instead of $r_m$, the position error of the mask occurs in proportion to the hole radius. For the fluorescent plate, the displacement $r_e$ from the true position $r_f$ is added to $r_f$

Content from this work may be used under the terms of the CC BY 4.0 licence (© 2025). Any distribution of this work must maintain attribution to the author(s), title of the work, publisher, and DOI.

ISBN: 978-3-95450-262-2 ISSN: 2673-5350 doi: 10.18429/JACoW-IBIC2025-TUPMO20

# EVALUATION OF ACCURACY AND RESOLUTION OF THE ELECTRON BEAM PROFILE SCANNER AT THE FERMILAB MAIN INJECTOR*

M. W. Mwaniki†,1, P. Snopok, Illinois Institute of Technology, Chicago, USA
R. Thurman-Keup, R. Ainsworth, Fermi National Accelerator laboratory, Batavia, USA
[1]also at Fermi National Accelerator laboratory, Batavia, USA

*Abstract*

The objective of this work is to assess the accuracy of measurements made by the Electron Beam Profile Scanner (EBPS), which captures the trajectory of an electron beam with and without a proton beam present. The proton beam induces deflection in the electron beam, which is influenced by proton charges. For high-resolution images, the probe beam needs to be of high intensity, small diameter, and small divergence, evaluated using a phosphor screen and an optical transition radiation (OTR) screen. The capabilities of the Kimball Physics electron gun (eGun) will be considered for accuracy. Additionally, the Zemax software will be utilized to characterize the optical elements.

## INTRODUCTION

Understanding the accuracy and resolution of measurement devices is important in order to obtain useful data during measurements. This work focuses on the Electron Beam Profile Scanner (EBPS), a non-invasive measurement tool that determines the transverse beam size of a proton beam using an electron probe beam [1].

### *Electron Beam Profile Scanner*

The EBPS consists of a triode electron gun (eGun) [2], electrostatic deflectors, an intersection space with the proton beam pipe, an optical transition radiation (OTR) mirror that is only inserted in the absence of the proton beam for measuring the size of the electron beam, a $Y_2SiO_5:Ce^{3+}$ $Y_2SiO_5:Ce^{3+}$ phosphor screen [3] that records the electron beam trajectory endpoints and an imaging system consisting of mirrors, lenses, an image intensifier, and a charge injection device (CID) camera that records images of the phosphor and OTR screen during measurements. An exhaustive composition of the EBPS system has been presented before [4], and its measurement techniques have also been discussed [5].

An evaluation of the accuracy and resolution of the EBPS will be conducted by characterizing eGun and the optical components of the EBPS imaging system. The ultimate goal is to achieve EBPS measurements with a resolution of ±0.2 mm, leading to the capability of single bunch measurements.

* Work supported by Fermi Forward Discovery Group, LLC manages and operates the Fermi National Accelerator Laboratory pursuant to Contract number 89243024CSC000002 with the USAs Department of Energy.
† mmwaniki@hawk.illinoistech.edu

## eGUN CHARACTERIZATION

The eGun is the source for the electron probe beam. In order to have improved precision and accuracy, the probe beam is required to be intense with a small divergence and a small diameter relative to the proton beam [6]. Characterizing the eGun is essential to ensure the probe beam has these qualities.

### *Beam Intensity of the eGun*

Beam intensity refers to the amount of electrons emitted from the eGun. Low intensities may allow the protons to interfere with the trajectories of the electrons, while excessively high intensities can damage to the measurement screens. The electron beam intensity is currently regulated by the eGun's cathode and grid voltages and it is measured by collecting the electrons emitted with a Faraday cup that surrounds the phosphor screen as the two voltages are scanned.

The goal was to achieve an electron beam intensity of about 500 µA during measurements. The results are summarized in Fig. 1. The results indicated that 53.9 µA was

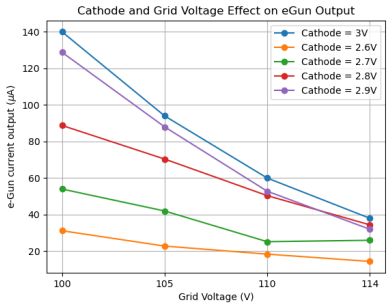



Figure 1: Cathode and grid voltage scan effect on beam intensity from the eGun.

sufficient and higher intensities were unnecessary. Consequently, the ideal setpoint for the cathode voltage was found to be 2.7 V and 100 V for the grid voltage.

### *Diameter of the Electron Beam from the eGun*

The diameter of the electron beam refers to the spot size of the beam, which directly influences the resolution of measurements, much like how wire size and spacing affect precision in a multi-wire. The spot size of the electron beam is controlled by adjusting the eGun's solenoid current and is measured in two ways: 1) using the OTR screen at the proton interaction region (PIR) and 2) using a phosphor screen located below the PIR.

Content from this work may be used under the terms of the CC BY 4.0 licence (© 2025). Any distribution of this work must maintain attribution to the author(s), title of the work, publisher, and DOI.

ISBN: 978-3-95450-262-2 ISSN: 2673-5350 doi: 10.18429/JACoW-IBIC2025-TUPMO21

# PRE-COMMISSIONING OF THE WIDE-DYNAMIC RANGE HALO MONITOR TO BE INSTALLED IN THE FERMILAB MI-8 LINE*

B. Babacan†,1,2, R. Ainsworth[2], Y. Hashimoto[3], T. Mitsuhasi[3], C. Ohmori[3], T. Sasaki[3], Y. Sato[3], A. P. Schreckenberger[2], P. Snopok[1], M. Tejima[3], T. Toyama[3], M. Uota [3]
[1]Illinois Institute of Technology, IL, USA
[2]Fermi National Accelerator Laboratory , IL, USA
[3]KEK/J-PARC, Japan

*Abstract*

The beam halo can contribute to beam losses in accelerators and is very difficult to measure. With an increase in beam intensity following the PIP-II upgrade at Fermilab, the beam losses are expected to be higher with some coming from the beam halo. Therefore, it is important to measure the sources of beam halo to minimize the beam losses. A modified Halo Monitor developed by J-PARC will be installed in Fermilab MI-8 transfer line to measure the beam halo. In this paper, an update on the beam profile monitor fabrication is covered. The updates include the location selection for the Halo Monitor in the MI-8 transfer line, shielding options for instrumentation, and the next steps in commissioning.

## INTRODUCTION

The MI-8 line transfers 8 GeV proton beam with intensity of $5 \times 10^{12}$ from the Booster Ring to the Recycler Ring, the Main Injector, and the Booster Neutrino Beamline at Fermi National Accelerator Laboratory (Fermilab).

Following the PIP-II upgrade at Fermilab, the beam intensity will increase along with beam losses [1]. Therefore, measuring the beam halo will help us determine the sources of halo to minimize the beam losses. The beam halo is defined as the outer layer of the 95 % beam emittance, where these particles will get lost and irradiate the machine.

A Halo Monitor was first installed at J-PARC Main Ring in 2012 to measure the beam halo of a 3 GeV proton beam after collimation to study the effects of collimators [2]. As a part of the US-Japan Science and Technology Cooperation Program in High Energy Physics, a modified design of the Halo Monitor is built by J-PARC to be installed in the Fermilab MI-8 transfer line where it will have the capability to measure the beam halo of an 8 GeV proton beam with intensity of $5 \times 10^{12}$ up to magnitude of $10^{-6}$ [3].

In this paper, the overall design of the wide-range beam profile monitor, location selection using lattice and shielding options are discussed, along with a timeline of completion and further ongoing analysis.

## HALO MONITOR DESIGN

### *Target System*

The Halo Monitor utilizes a three-target system. The first target is a titanium foil to measure the profile of the beam core through optical transition radiation (OTR). The second target is an aluminum foil with a hole at the center to measure the profile of the outer section of the beam core and inner section of the beam tails. The third target is chromium doped alumina screen to measure the beam halo through fluorescence (FL). There are four alumina screens that move in horizontal and vertical directions and this is a separate system than the rest of the targets. This will allow to measure the beam core and the halo at the same time. The similar target system of the Halo Monitor Unit-1 at J-PARC is discussed in more depth in Ref. [4].

### *Optical System*

The Offner optics are installed inside the Halo Monitor and this configuration is shown in Fig. 1 where Zemax was used for ray tracing. There is a 100mm diameter hole in the upper right concave mirror for the path of the proton beam from the right, where the beam interacts with the desired target. The reflected OTR/FL light from the target travels through the Offner optics system, and arrives at the diffuser screen and the rest of the secondary optics system.

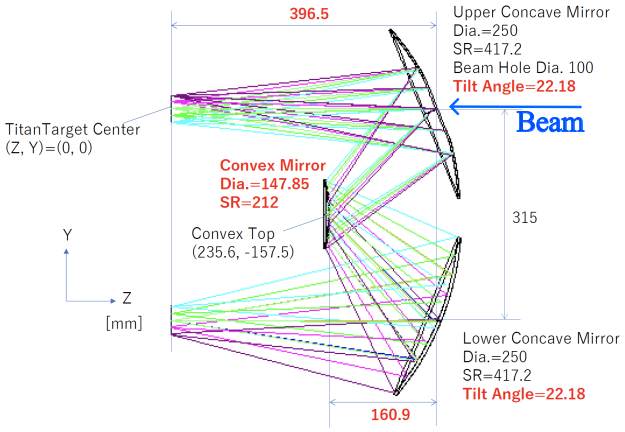



Figure 1: Ray tracing through the Offner optics where the length measurements are given in mm.

* Fermi Forward Discovery Group, LLC manages and operates the Fermi National Accelerator Laboratory pursuant to Contract number 89243024CSC000002 with the United States Department of Energy.
† bbabacan@hawk.illinoistech.edu

Content from this work may be used under the terms of the CC BY 4.0 licence (© 2025). Any distribution of this work must maintain attribution to the author(s), title of the work, publisher, and DOI.

ISBN: 978-3-95450-262-2 ISSN: 2673-5350 doi: 10.18429/JACoW-IBIC2025-TUPMO22

# LOW DENSITY WIRES FOR BEAM HALO MONITORING

G. Aliana-Cervera*,[1,2], C. Pasquino[1], R. Veness[1], D. Mattia[2], A. J. G. Lunt[2]
[1]CERN, Geneva, Switzerland
[2]IMPS, University of Bath, Bath, United Kingdom

*Abstract*

Beam halo monitoring is crucial for high-intensity machines such as the HL-LHC. Carbon Nanotube (CNT) wires offer a promising alternative to conventional carbon fibre scanners due to their lower density, improved thermal properties, and reduced beam interaction. This work evaluates their thermal performance and survivability through simulations at SPS and HL-LHC beam conditions.

Results indicate that CNT wires can tolerate HL-LHC beam-induced heating in dynamic scanning mode for halo measurements in the 3.5–6.5 $\sigma$ range, remaining below the 1600 K sublimation threshold. In contrast, stationary operation closer to the core produces sustained heating and higher thermal risk. While challenges remain in manufacturing, post-processing, and property variability, CNT wires show strong potential for non-destructive halo diagnostics, provided long-term performance can be optimised.

## INTRODUCTION

The HL-LHC will operate at unprecedented beam intensities, increasing the importance of precise and reliable beam-halo diagnostics. The halo, defined as particles beyond 3.5 $\sigma$ from the beam core, must be characterised with better than 1 % precision in its relative fraction and contrast sensitivity down to $10^{-3}$ in a Gaussian beam [1].

Existing diagnostics such as the Beam Wire Scanners (BWS) and Synchrotron Radiation Telescopes (BSRT) are limited by excessive invasiveness, speed, or resolution. Wire-based beam scan methods, while offering good transverse resolution, are typically destructive or limited in terms of operational conditions. Current Carbon Fibers (CF) wires cannot withstand the maximum integrated intensity at the Super Proton Synchrotron (SPS). This limitation is primarily due to the sublimation of the carbon wire when exposed to high energy deposition [2].

Carbon nanotube (CNT) wires are emerging as promising candidates for more resilient beam wire scanners (BWS), owing to their combination of low density, high thermal conductivity, and reduced diameters, which together minimise beam interaction and enhance heat dissipation. Whereas conventional carbon fibre wires exhibit densities around 1.8 g/cm$^3$ with diameters near 7 µm, CNT yarns typically show densities close to 1 g/cm$^3$ and can be manufactured with diameters as small as 2 µm [3]. These properties significantly reduce energy deposition. Nonetheless, their performance under HL-LHC beam halo conditions requires thorough investigation before they can be adopted operationally.

* gerard.aliana.cervera@cern.ch

Despite the lower (about 30 % when compared to CF) signal-to-noise ratio exhibited by CNT wire scanners, they were able to successfully record beam profiles of 450 GeV proton beam at the SPS. They were tested up to SPS intensity of $3.4 \times 10^{13}$ protons, where they failed due to metallic inclusions inherent to the manufacturing procedure [4, 5].

This article focuses on thermal simulations of CNT wires beyond SPS energies, extending to the HL-LHC, where temperature rises are expected to scale by a factor of ~150. It assesses their survivability, feasibility, and potential for use in non-destructive beam halo monitors.

## SIMULATION SETUP

Carbon nanotubes (CNTs) are broadly divided into single-walled (SWCNTs) and multi-walled (MWCNTs) types. SWCNTs are a single rolled graphene sheet, typically 1–10 nm in diameter (see Fig. 1), whereas MWCNTs are formed from several concentric tubes, which enhances their structural robustness. Individual CNTs exhibit exceptional intrinsic properties, including Young's moduli approaching 1 TPa or tensile strengths exceeding 50 GPa. These combined characteristics underpin their promise as materials for demanding high-performance applications [3].

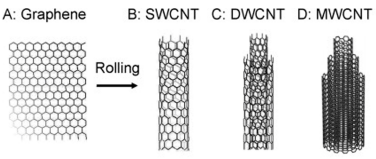



Figure 1: Different CNT structures [6].

To transition from the nanoscale to macroscopic scale, CNTs must be processed into aligned and continuous forms such as wires. This typically involves wet-spinning or other fibre-forming techniques where dispersed CNTs are assembled into bundles and then drawn into cohesive, conductive strands [3, 7]. The wires used in this study, produced by Dexmat, represent such a transformation, combining individual CNTs into low-density wires. Initial microscopy and density measurements of these samples revealed substantial batch-to-batch variability. Average values were therefore adopted for all analyses in this study, as they are the most representative. The wires exhibited diameters of about 10 µm (±1 µm) and densities close to 1.0 g/cm$^3$ (±0.2 g/cm³).

### *Beam Parameters*

The simulations were set up for beam profiles and parameters of the SPS and HL-LHC. Thermal simulations were performed assuming a Gaussian beam profile at 450 GeV and 7 TeV, with intensities up to $5.7 \times 10^{14}$ protons. For

Content from this work may be used under the terms of the CC BY 4.0 licence (© 2025). Any distribution of this work must maintain attribution to the author(s), title of the work, publisher, and DOI.

ISBN: 978-3-95450-262-2 ISSN: 2673-5350 doi: 10.18429/JACoW-IBIC2025-TUPMO24

# PEPITES: AN ULTRA-THIN BEAM PROFILER WITH WIDE DYNAMIC RANGE FOR CHARGED PARTICLE BEAMS *

M. Verderi†, L. Bernardi, R. Duhamel, A. Esper, F. Gastaldi, R. Guillaumat, F. Joubert, C. Larran, A. Mahjoub, C. Thiebaux
Laboratoire Leprince-Ringuet, Institut Polytechnique de Paris, Palaiseau, France
C. Koumeir, GIP ARRONAX, Saint-Herblain, France
M. Donetti, A. Mereghetti, M. Pullia, C. Viviani
CNAO National Center for Oncological Hadrontherapy, Pavia, Italy
F. Gebreyohannes, O. Gevin, CEA-IRFU, Université Paris-Saclay, Saclay, France
A. Flacco
Laboratoire d'Optique Appliquée, Institut Polytechnique de Paris, Palaiseau, France

*Abstract*

PEPITES is an ultra-thin profiler with wide dynamics range for charged particle beams. Secondary Electron Emission (SEE) is used for its signal, which provides these assets. A first, 10 µm Water Equivalent Thickness (WET), monitor has been permanently installed at ARRONAX, Saint-Herblain, France, in May 2022. It is used in routine operations with continuous and "FLASH" beams, the latter referring to a promising radiotherapy modality based on short and intense pulses. A second profiler is developed with CNAO, Pavia, Italy, in view of being integrated in the beam control protocol for conventional patient irradiation. The monitor is foreseen 6.5 m upstream the patient, contraining its material budget to a few µm WET, to maintain the beam dispersion at a tolerable level.

Researches on the FLASH modality explore irradiation durations from O(100 ms) down to O(10 fs), for a same delivered dose. The intense beams used challenge the beam instrumentation, calling for innovation in the domain.

This contribution presents results on PEPITES at ARRONAX, the development for the CNAO version, and a series of measurements to assess the viability of the SEE signal for µs down to 10 fs long beams.

## PEPITES DETECTOR PRINCIPLE

SEE occurs near the surface of materials when a charged particle generates ionisation electrons that escape from the volume. If emitted in vacuum, these low energy electrons can travel away, which, in a metal, generates an electrical signal. Only the O(10 nm) closest to the surface contribute to SEE, which, augmented to at least 30 nm for a metal to make it conductive, allows for ultra-thin electrode design. SEE is in addition a very linear phenomenon.

Figure 1 a) illustrates the PEPITES detection principle. Gold is chosen for the strips as it is a good electron emitter and is easy to handle. Thin films techniques are used to construct the sensitive area electrodes. Their versatility allows for many monitor variants, beyond the simple strip pattern used here. As the monitor operates in vacuum, the membranes are free from mechanical stress, which is favorable to the detector lifetime. In addition, the membranes are made of CP1™, which, as a polyimide, has a good resistance to radiation [1]. These plans have shown to withstand up to $10^9$ Gy with electron irradiation [2].

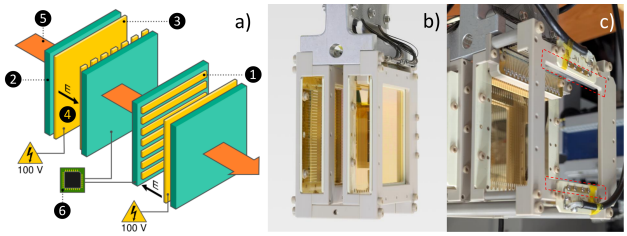



Figure 1: a) Schematic representation of the sensitive area: ❶ 50 nm thick gold strips are deposited on a ❷ 1.5 µm polyimide membrane; the beam profile along X and Y axes by plans with vertical and horizontal strips, respectively; ❸ an anode is made of a fully golden membrane facing the trip plane, ❹ a positive bias voltage is applied to collect the emitted electrons. When the ❺ beam crosses the monitor, secondary electrons leave the crossed strips, the related generated currents are read individually by ❻ a dedicated low noise electronic. Picture b) shows the sensitive area as built for ARRONAX. There are 32 strips, 1.9 mm wide, with a 0.35 mm inter-strip gap. The sensitive area is about $7 \times 7$ cm$^2$ large and has a 10 µm WET. Picture c) shows one anode of the modified sensitive area as tested at CNAO to reduce to 5 µm WET the amount of material crossed by the beam: the "in-axis" anodes of a) are replaced by metallic bars (indicated by the dashed red lines) that are put "off-axis". The collection electric field is hence not parallel and not uniform anymore, the effect of which is discussed in the text.

## PEPITES AT ARRONAX

The sensitive area built for the monitor installed at ARRONAX is shown on Fig. 1 b). The beam is sampled along the X(Y) direction by one plan with vertical(horizontal)

* Work supported by Agence Nationale de la Recherche ANR-17-CE31-0015 and ANR-11-EQPX-0004 CNRS, Mission pour les Initiatives Transverses et Interdisciplinaires, PIB2023
† marc.verderi@llr.in2p3.fr

Content from this work may be used under the terms of the CC BY 4.0 licence (© 2025). Any distribution of this work must maintain attribution to the author(s), title of the work, publisher, and DOI.

ISBN: 978-3-95450-262-2 ISSN: 2673-5350 doi: 10.18429/JACoW-IBIC2025-TUPMO25

# INITIAL IMPLEMENTATION OF A NEW ORBIT FEEDBACK SYSTEM USING MicroTCA.4 FOR THE PF USER OPERATIONS

R. Takai*,[1], T. Obina[1], M. Tadano, H. Sagehashi, M. Shiozawa
High Energy Accelerator Research Organization (KEK), Tsukuba, Ibaraki, Japan
[1]also at SOKENDAI (The Graduate University for Advanced Studies), Tsukuba, Ibaraki, Japan

Content from this work may be used under the terms of the CC BY 4.0 licence (© 2025). Any distribution of this work must maintain attribution to the author(s), title of the work, publisher, and DOI.

*Abstract*

A new fast orbit feedback system has been introduced to the PF-ring since the third user operation in FY2024. The new system incorporates digital signal processing circuits based on the MicroTCA.4 standard. The transition from the legacy VME-based system, which had been in service for nearly 30 years, was conducted meticulously and incrementally during the start-up of the third user operation. The reference orbit was successfully transferred to the new system. At present, the effective bandwidth of the orbit feedback has reached 200 times that of the legacy system. This paper presents the transition process from the legacy system, initial performance results of the new system, and plans for future upgrades.

## FOFB SYSTEM FOR THE PF-RING

In storage ring-based synchrotron light sources, a fast orbit feedback (FOFB) system that continuously corrects the stored beam orbit relative to the reference orbit is essential for stable photon beam delivery. At the Photon Factory storage ring (PF-ring) of KEK, an FOFB system using VME-based digital signal processors had been in service since FY1997 [1]. The system used up to 65 beam-position monitors (BPMs) and 28 fast steering magnets (FSs) for vertical orbit correction[1]. However, because only 12 analog detection circuits were available, semiconductor switches were installed before each circuit to sequentially process the signals from the four button electrodes and from 5–6 BPMs. This switching process limited the closed-orbit distortion (COD) measurement frequency to 80 Hz and reduced the effective feedback bandwidth to approximately 0.3 Hz. Furthermore, the aging of components had increasingly resulted in system malfunctions and more frequent interruptions in user operations over time.

An upgrade project was launched in FY2020 to modernize the system [2]. In the new system, each BPM unit is equipped with its own signal processing channel, obviating the need for switching. The design is based on the MicroTCA.4 standard, which provides high availability and a high-speed data bus [3]. The COD measurement frequency was increased to 10 kHz, thereby enabling a feedback bandwidth exceeding 100 Hz. Circuit fabrication was completed in FY2021, despite difficulties caused by the global semiconductor shortage, followed by extensive hardware and software modifications carried out in parallel with the operation of the legacy FOFB system [4]. During the start-up of the third user operation in FY2024, the transition to the new system was successfully completed; the upgraded FOFB has since maintained stable beam delivery to users.

This paper presents an overview of the FOFB system replacement, completed in February 2025, along with its initial performance and planned future upgrades.

## SYSTEM REPLACEMENT

The legacy FOFB system was replaced with the new system during the start-up of the third user operation in FY2024. The first step was to close the feedback loop with the new system, using 17 BPMs that had not been employed in the legacy system and 8 FSs selected at appropriate intervals. Starting from this configuration, groups of approximately 10 BPMs were gradually transferred from the legacy system to the new system, while confirming that the closed orbit could be stably maintained utilizing orbit feedback. This process was implemented carefully at a low stored current of 30 mA, considering the reproducibility of the beam orbit before and after reconnecting the BPMs, which required dumping the stored beam, as well as the risk of sudden orbit divergence due to feedback failure. Another important issue in such a replacement concerns the transfer of the reference orbit measured with the legacy system to the new system. Our approach was to perform a COD correction[2] each time several BPMs units were reconnected by using the closed orbit measured immediately before the reconnection as the reference. Thus, the orbit drifts at each step were minimized, and the original reference orbit defined by the legacy system could be reliably inherited by the new system.

After four reconnection steps, the number of BPMs incorporated into the new system was successfully increased to 63. The number of FSs was also increased to 16 during this process. The distributions of BPMs and FSs resulting from this staged replacement are shown in Fig. 1. Although 15 BPMs were intentionally retained on the legacy circuits for comparison, those integrated into the new system were distributed almost uniformly around the storage ring.

Subsequently, with the FOFB turned on, the beam was gradually accumulated up to the nominal current of 450 mA for the PF-ring, confirming that the feedback operated correctly even at high current. Tests were conducted at 100 mA and full 450 mA by closing the gaps of the in-vacuum undulators (IVUs) so as to verify that the reference orbit had been correctly transferred to the new system. In this procedure,

* ryota.takai@kek.jp

[1] The horizontal orbit is stabilized solely by a slow orbit feedback (SOFB), running every few tens of seconds.

[2] This correction was performed manually with the SOFB system, independent of the FOFB.

ISBN: 978-3-95450-262-2 ISSN: 2673-5350 doi: 10.18429/JACoW-IBIC2025-TUPMO26

# ELECTRON BEAM ENERGY MEASUREMENT IN THE SLRI 6 MeV LINAC USING X-RAY SCINTILLATOR IMAGING

P. Boonpornprasert, J. Nadeedanklang, N. Yachum, D. Khampiranon,
K. Manasatitpong, S. Kokkrathoke, T. Chanwattana, S. Chunjarean *
Synchrotron Light Research Institute, Muang District, Nakhon Ratchasima, Thailand

*Abstract*

The Synchrotron Light Research Institute (SLRI) in Thailand aims to operate a 6 MeV electron linear accelerator for irradiation, supporting various agricultural and industrial applications. This study presents a method for measuring the electron beam energy using the existing dipole magnet in the beamline, originally designed to scan X-rays on samples through a scan horn. An aluminum sheet coated with terbium-doped gadolinium oxysulfide ($Gd_2O_2S$) was used as a scintillation screen for X-ray imaging and placed downstream of the scan horn. X-ray scintillator images were captured with a CCD camera. By analyzing shifts in the X-ray image centroid as the dipole magnet current varied, the electron beam energy was determined.

## INTRODUCTION

Electron linear accelerators (linacs) with energies from a few to tens of MeV are used for applications such as medical sterilization and agricultural irradiation [1]. The Synchrotron Light Research Institute (SLRI) has developed a 6 MeV linac for irradiating fresh fruit [2], an application where the beam energy is an important parameter for effective sterilization.

Figure 1 shows the layout of the linac. Its main components are a thermionic cathode DC gun, a side-coupling S-band linac, a beam current monitor (ACCT), a vacuum chamber and bellow for beam transport, a scanning magnet, a scan horn, and finally, a tungsten target. The electrons produce X-rays upon hitting the target, and these X-rays are used to irradiate samples. The distances from the linac exit to the tungsten target and the sample irradiation area are approximately 1.0 m and 1.3 m, respectively. Table 1 summarizes the operational parameters of the system. Further details on the control and timing systems are described elsewhere in [3, 4].

A measurement of the beam energy is necessary for proper operation. Typically, this measurement requires a dipole magnet and a screen to observe the electron beam directly. Since the linac beamline lacks a dedicated screen, this study introduces an indirect measurement method. The existing scanning magnet shifts the position of the electron beam on the tungsten target, which consequently shifts the location of the X-ray source. By imaging the X-rays with a scintillator, we can determine the beam energy from the relationship between the magnet current and the position of the X-ray spot. This method avoids installing additional in-vacuum hardware. This paper presents the configuration, simulation, and results of this measurement.

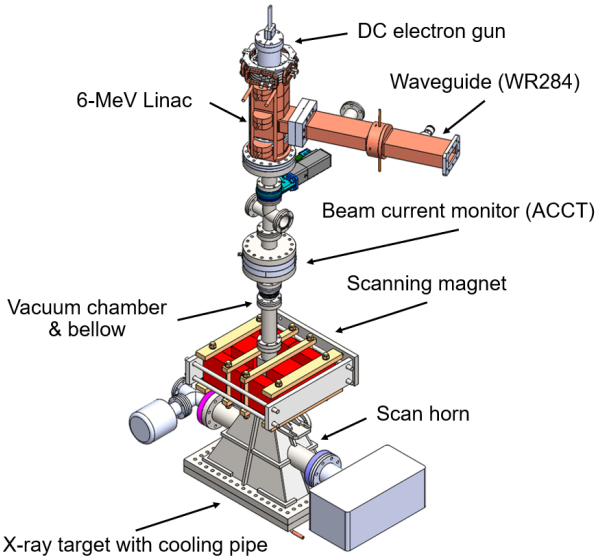



Figure 1: Layout of the 6 MeV linac at SLRI.

Table 1: Operational Parameters of the 6-MeV Linac System

| Parameters | Details |
|---|---|
| Gun cathode filament voltage | 4.4-4.6 V |
| Gun modulator voltage | 950 V |
| Gun modulator pulse width | 5 µs |
| RF modulator voltage | 1043 V |
| RF peak power | 3.2 MW |
| RF pulse repetition rate | 100-200 Hz |
| RF macropulse width | 5-10 µs |
| Linac resonance frequency | 2.998 GHz |
| Beam average current | 130 mA |

## CONFIGURATION FOR BEAM ENERGY MEASUREMENT

The principle used for beam energy measurement is illustrated in Fig. 2. The electron beam, after passing through the linac and scanning magnet, strikes a composite X-ray target located at the end of the scan horn. The target is designed for both efficient Bremsstrahlung conversion and thermal stability. It consists of a 0.8 mm thick tungsten sheet brazed to an Oxygen-Free High-Conductivity (OFHC) copper substrate. Tungsten was selected for its high atomic number (Z), which

* somjai@slri.or.th

Content from this work may be used under the terms of the CC BY 4.0 licence (© 2025). Any distribution of this work must maintain attribution to the author(s), title of the work, publisher, and DOI.

ISBN: 978-3-95450-262-2 ISSN: 2673-5350 doi: 10.18429/JACoW-IBIC2025-TUPMO27

# MODEL-BASED OPTIMAL CONTROL DESIGN FOR THE ORBIT FEEDBACK SYSTEM AT SIAM PHOTON SOURCE*

S. Klinkhieo†, N. Suradet, N. Yachum, S. Kokkrathoke, S. Chunjarean, T. Chanwattana, T. Pulampong, Synchrotron Light Research Institute, Nakhorn Ratchasima, Thailand

Content from this work may be used under the terms of the CC BY 4.0 licence (© 2025). Any distribution of this work must maintain attribution to the author(s), title of the work, publisher, and DOI.

*Abstract*

A model-based optimal control approach has been developed for the slow orbit feedback (SOFB) system to enhance orbit stability in the Siam Photon Source (SPS) storage ring. The control strategy utilizes a Linear Quadratic Regulator (LQR) based on a multi-input, multi-output (MIMO) state-space model of the linear SPS storage ring, derived through system identification using MATLAB and SIMULINK. The necessary and sufficient conditions for controllability and boundedness of the dynamic system are established. Experimental simulations were conducted to assess the performance of the LQR controller in a practical SPS storage ring. The results demonstrate that the proposed control method effectively minimizes the quadratic cost function and error signals between setpoints and process variables for both horizontal and vertical orbit positions while ensuring system stability and robustness. The study also outlines the fundamental principles of optimal control theory, system identification, and future development directions.

## INTRODUCTION

The Siam Photon Source (SPS), Thailand's first synchrotron light source, has played a crucial role in advancing scientific research and technology development in the region. The history of SPS dates back over two decades when a dedicated group of Thai scientists and educators successfully secured a second-generation synchrotron machine from Japan. Originally designed for X-ray lithography in integrated circuit manufacturing, the machine was repurposed to serve the growing demand for synchrotron radiation research in Thailand and beyond. Today, the Synchrotron Light Research Institute (SLRI) operates SPS as a national facility, supporting over 4,000 hours of user experiments annually with a high availabil-ity rate of 95% [1, 2].

Over the past 20 years, continuous upgrades and improvements have enhanced the performance of SPS. These developments include extending photon energy into the hard X-ray region, improving beam positional stability, and increasing machine reliability. The SPS complex consists of a 40 MeV linear accelerator (LINAC), a 1 GeV booster synchrotron (SYN), and a 1.2 GeV electron storage ring (STR). As part of ongoing efforts to further upgrade its capabilities, the booster synchrotron energy is being increased to 1.2 GeV, necessitating enhancements in the RF cavity and magnet systems. These upgrades aim to support the increasing demand for higher energy X-ray applications and ensure the long term sustainability of synchrotron operations in Thailand. A critical aspect of maintaining high quality synchrotron radiation is beam stability, particularly in terms of orbit correction.

To address beam stability challenges, a model-based optimal control approach was developed for the SOFB system at the SPS. This approach utilizes a Linear Quadratic Regulator (LQR) based on a MIMO state-space model of the SPS storage ring, derived using MATLAB and SIMULINK system identification techniques. By ensuring system controllability and stability, this strategy enhances the precision and robustness of beam position correction [3].

This paper outlines the LQR-based SOFB system's implementation, covering its theoretical framework, system identification, and simulation-based validation. Results confirm the control methodology's effectiveness in minimizing orbit deviations while maintaining stability. Future development directions for SPS and orbit correction enhancements are also discussed.

## SYNTEM IDENTIFICATION

System identification involves creating a mathematical model of a dynamic system using observed input-output data, analyzing system responses to various inputs to construct an accurate representation of its behavior. The primary objective is to develop a model that supports effective controller design, ensuring optimal system performance and stability.

An ideal model is of the lowest possible order while accurately capturing the system's dynamics. Low-order models simplify analysis, reduce computational demands, and improve control implementation efficiency. However, they must encompass critical dynamic characteristics, such as time delays, oscillations, and nonlinearities, to ensure reliable predictions and robust control performance.

A well-crafted model forms the basis for designing control strategies, including PID controllers, state-space controllers, or adaptive systems, tailored to specific performance needs. Thus, striking a balance between model simplicity and accuracy is essential for successful system identification [4, 5].

### *System Identification Using MATLAB*

The MATLAB System Identification Toolbox offers powerful tools for building dynamic system models from experimental data. It supports pre-processing, model selection, and parameter estimation to ensure accurate representation of system behavior. Its strength lies in generating simplified yet precise models, even from noisy time-series data, making it ideal for control design, signal processing, and forecasting. The toolbox supports various model structures, providing flexibility in system modeling. (Fig. 1).

* Work supported by SLRI

† supat@slri.or.th

ISBN: 978-3-95450-262-2 ISSN: 2673-5350 doi: 10.18429/JACoW-IBIC2025-TUPMO28

# OVERVIEW AND STATUS OF BEAM DIAGNOSTICS FOR THE INJECTOR LINAC OF THE SIAM PHOTON SOURCE

P. Boonpornprasert, T. Chanwattana*, S. Bootiew, S. Chunjarean,
C. Dhammatong, N. Juntong, T. Pulampong, S. Klinkhieo
Synchrotron Light Research Institute, Nakhon Ratchasima, Thailand

Content from this work may be used under the terms of the CC BY 4.0 licence (© 2025). Any distribution of this work must maintain attribution to the author(s), title of the work, publisher, and DOI.

*Abstract*

The Synchrotron Light Research Institute (SLRI) operates the Siam Photon Source (SPS) in Nakhon Ratchasima, Thailand. The primary injector for this facility is a linear accelerator (linac) that accelerates electron bunches to 40 MeV. The beam is then guided to a booster ring via the Low-Energy Beam Transport (LBT) line. To ensure the delivery of a high-quality beam for injection, a set of diagnostic instruments is used to monitor the beam properties. This paper presents the current status of the beam instrumentation for the SPS injector linac, providing an overview of the systems used to measure the beam current, transverse profiles, and energy. The latest measurement results show an overall transmission efficiency of 25.6 % and indicate that the beam energy is approximately 10 % lower than the nominal value. These findings provide a new baseline for the future optimization of the injector system.

## INTRODUCTION

The Synchrotron Light Research Institute (SLRI), located in Nakhon Ratchasima, Thailand, operates the 1.2 GeV Siam Photon Source (SPS). For many years, the facility has provided synchrotron light to a community of academic and industrial users [1]. In parallel with the design and planning phase for a new 3 GeV, 4th generation light source, the Siam Photon Source II (SPS-II) [2], the continued improvement and the maintenance of a high-performance operation for the existing SPS facility remain a high priority.

The SPS consists of a injector linac, a booster synchrotron, and a storage ring. The facility was established with components from the former SORTEC facility in Japan [3]. During the reassembly in Thailand, the original designs of the linac and the booster remained unchanged, while the High-Energy Beam Transport line (HBT) and the storage ring were modified [4]. The design and performance of the linac, which can generate and accelerate an electron beam to 40 MeV, are reported in [5]. The beam is then transported to the booster ring through the Low-Energy Beam Transport line (LBT). The properties of this electron beam determine the injection efficiency into the booster. Consequently, diagnostic instruments are installed in the beamline to monitor and optimize the beam, ensuring its high quality and efficient transport.

To ensure reliable monitoring and optimization, the beam diagnostics of the SPS injector linac have recently been upgraded [6]. This paper provides an overview of the current instrumentation for the linac and the LBT. Furthermore, recent measurement results are presented, which provide an updated performance baseline for the ongoing improvement of the SPS injector system.

## LINAC SYSTEM DESCRIPTION

A schematic layout of the SPS injector linac and LBT is shown in Fig. 1. The electron beam is generated and accelerated to 40 MeV by a series of components. The main subsystems are described below, with operational parameters listed in Table 1.

### *Electron Source*

The electron beam is generated from a triode-type thermionic DC gun, which uses a cathode manufactured by EIMAC (Y646B), a control grid, and an anode to generate the initial beam. The gun operates with an accelerating high voltage of 100 kV. A grid pulser supplies a voltage pulse with a duration of 3 µs at a repetition rate of 0.3 Hz to produce the electron beam.

### *Bunching System*

Following the gun, the beam enters a bunching system designed to longitudinally compress the beam. The system consists of two single-gap pre-buncher cavities (PB1 and PB2) and a main buncher, all operating at a resonant frequency of 2856 MHz. The main buncher is a 8.5-cell standing-wave side-coupling structure.

### *Accelerating Structures*

The main acceleration is provided by two S-band (2856 MHz) traveling-wave structures. Each structure is 2.3 m long and operates in the $2\pi/3$ mode with a constant-gradient design. The two structures, operating in series, accelerate the electron beam to its final energy of 40 MeV.

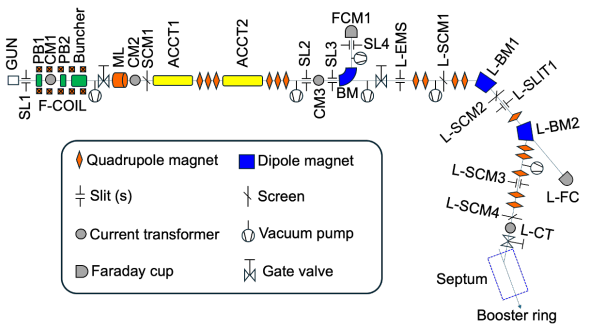



Figure 1: Layout of the SPS injector linac injector and LBT.

* Corresponding Author, thakonwat@slri.or.th

ISBN: 978-3-95450-262-2 ISSN: 2673-5350 doi: 10.18429/JACoW-IBIC2025-TUPMO29

# DESIGN OF AN UPGRADED SCREEN MONITOR SYSTEM FOR THE SIAM PHOTON SOURCE INJECTOR LINAC

T. Chanwattana*, P. Boonpornprasert, S. Bootiew, S. Chunjarean, C. Dhammatong, N. Juntong, W. Promdee, T. Pulampong, S. Klinkhieo
Synchrotron Light Research Institute, Nakhon Ratchasima, Thailand

Content from this work may be used under the terms of the CC BY 4.0 licence (© 2025). Any distribution of this work must maintain attribution to the author(s), title of the work, publisher, and DOI.

*Abstract*

The Siam Photon Source (SPS) is a 1.2 GeV synchrotron facility in Thailand, operated by the Synchrotron Light Research Institute (SLRI), providing synchrotron radiation for various applications to the user community. The SPS injector linac generates 40 MeV electron bunches, which are then transported to the booster synchrotron via the Low-Energy Beam Transport line (LBT). To ensure effective beam monitoring along the injector linac and LBT, key beam diagnostics—including beam current, transverse profile, and energy profile monitoring—have been installed in the injector linac. In order to maintain full diagnostic performance, the screen monitor system is planned to be upgraded to enhance transverse beam profile monitoring, improve radiation resistance, and support injector linac optimization for higher machine performance. This paper presents the current status of the screen monitor system for the SPS injector linac and discusses the design and implementation plan for its upgrade.

## INTRODUCTION

The Synchrotron Light Research Institute (SLRI) has operated the 1.2 GeV Siam Photon Source (SPS) for over two decades, providing synchrotron radiation to a broad community of academic and industrial users, both domestic and international [1]. As the Siam Photon Source II (SPS-II) project [2] is still in the design and development stage, SPS continues to serve as a key synchrotron facility in Thailand and the ASEAN region, necessitating ongoing machine maintenance and upgrades.

The SPS accelerator complex comprises an injector linac, a booster synchrotron, and a storage ring. The facility was constructed using components transferred from the former SORTEC facility in Japan [3]. The High-Energy Beam Transport line (HBT) and the storage ring were modified during reassembly in Thailand [4]. The linac, capable of generating and accelerating electrons up to 40 MeV, is described in detail in Ref. [5]. Electrons are subsequently transported to the booster synchrotron through the Low-Energy Beam Transport line (LBT). The quality of the beam transported through the LBT strongly influences booster injection efficiency. Therefore, diagnostic devices are installed along the transport line to ensure reliable beam delivery. Earlier diagnostic upgrades included the installation of an AC Current Transformer (ACCT) from Bergoz Instrumentation to replace a wall current monitor (WCM) at the linac exit, as well as modified optics and support for the screen monitors [6].

* thakonwat@slri.or.th

The current status of beam instrumentation at the SPS injector linac and LBT, along with recent measurement results, is reported in Ref. [7]. The overall beam transmission efficiency from the injector linac to the end of LBT was measured to be 25.6 %, with significant beam loss observed in the LBT section. To provide more reliable beam diagnostics and support injector linac and LBT optimization, an upgraded screen monitor system is being developed to overcome limitations from radiation damage and maintenance issues, enabling more precise beam measurements.

## SPS INJECTOR LINAC AND LBT

A schematic layout of the SPS injector linac and the LBT line together with beam diagnostic devices is shown in Fig. 1. The details of both parts of the SPS accelerator are as follows:

### *Injector Linac*

The injector consists of a triode-type thermionic DC gun with an EIMAC Y646B cathode, operating at 100 kV, with a grid pulser providing 3 µs pulses at 0.3 Hz. The beam is then longitudinally compressed by a bunching system with two single-gap pre-buncher cavities (PB1 and PB2) and a 8.5-cell standing-wave side-coupling structure, operating at 2856 MHz. Final acceleration to 40 MeV is achieved with two S-band (2856 MHz), 2.3 m-long traveling-wave structures operating in the $2\pi/3$ constant-gradient mode. The operational parameters of the injector linac are listed in Ref. [7]. The injector linac was designed to produce beams with a current of about 30 mA and a normalized emittance of 3.8 mm·mrad [5].

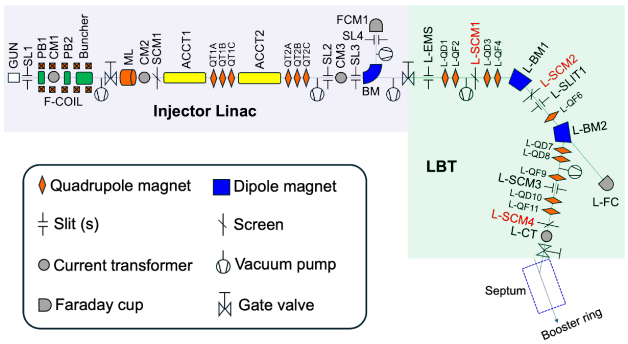



Figure 1: Layout of the SPS injector linac injector and LBT.

### *Low-Energy Beam Transport Line (LBT)*

The LBT line transports the 40 MeV beam from the linac to the booster synchrotron and was originally designed to

ISBN: 978-3-95450-262-2 ISSN: 2673-5350 doi: 10.18429/JACoW-IBIC2025-TUPMO31

# DESIGN OF A NON-INVASIVE LASER-BASED BEAM PROFILE MONITOR SYSTEM FOR THE NEW FERMILAB PIP-II SUPERCONDUCTING H- LINAC*

V. Scarpine†,[1], R. Thurman-Keup[1], T. Johnson[1], D. Krokosz[1], P. Landon[2], J. Ruan[1], A. Saewert[1], R. Steinberg[1], J. Thangaraj[1]
[1]Fermi National Accelerator Laboratory, Batavia, IL, USA
[2]Boston University, Boston, MA, USA

*Abstract*

As part of the new Proton Improvement Plan (PIP-II), Fermilab is undertaking the development of a new 800 MeV, 2 mA H- superconducting RF linac to replace its present normal conducting 400 MeV linac. The PIP-II linac consists of a series of superconducting RF cryomodules from 2.1 MeV to 800 MeV. To limit the potential damage to the superconducting RF cavities, PIP-II will utilize non-invasive laser-based monitors (laserwires) to obtain beam profiles via photoionization. This paper will present the design of this PIP-II laserwire system including the picosecond pulsed laser, optical transport line, 13 individual laserwire stations, laser feedback and timing controls.

## OVERVIEW

The PIP-II project at Fermilab is in the late stages of building a 2 mA, 800 MeV H- superconducting (SC) Linac to fuel the next generation of intensity frontier experiments [1].

Non-invasive laser-based profile monitors (laserwire) are being developed as the primary SC Linac beam profiling instruments using photoionization ($H^- + \gamma \rightarrow H^0 + e^-$) [2, 3]. PIP-II will have 13 laserwire stations from 2.1 MeV up to 800 MeV. Figure 1 shows the functional layout of the PIP-II laserwire system.

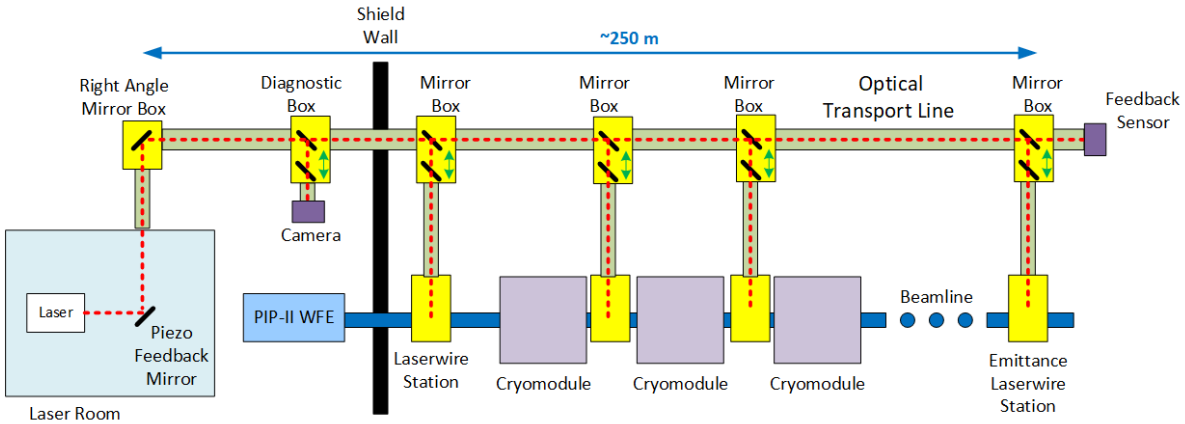



Figure 1: Functional layout of PIP-II laserwire system.

A prototype version of a laserwire profiling system based on optical fiber laser transport was tested at the PIP- II Injection Test facility (PIP2IT) [4]. This system successful measured core beam profiles but was limited by several systematic effects and proved to be impractical for a 13 station laserwire system for PIP-II. Therefore, a fiber-based laser transport system was abandoned in favor of a free-space laser transport system. A free-space transport design allows for more freedom in the choice of laser but entails the design a free-space transport system.

## LASER TRANSPORT OPTICAL DESIGN AND FEEDBACK SYSTEM

The laser path from the laser room to the selected laserwire station will be via an evacuated free-space transport system (Fig. 1). The vacuum transport prevents air currents from distorting the laser and also serves as a safety interlock system. The laserwire system will be comprised of two lasers: a low power 532 nm CW alignment and feedback laser, and the main high power 1064 nm pulsed photoionizing laser. The low power CW laser serves two purposes. One is to aid in the alignment of the transport line, and the second is to provide a feedback signal to a piezo-controlled mirror in the laser room to adjust

* This manuscript has been authored by FermiForward Discovery Group, LLC under Contract No. 89243024CSC000002 with the U.S. Department of Energy, Office of Science, Office of High Energy Physics.
† scarpine@fnal.gov

Content from this work may be used under the terms of the CC BY 4.0 licence (© 2025). Any distribution of this work must maintain attribution to the author(s), title of the work, publisher, and DOI.

ISBN: 978-3-95450-262-2 ISSN: 2673-5350 doi: 10.18429/JACoW-IBIC2025-TUPMO32

# WIDE RANGE LOW COST DIGITAL RF PHASE SHIFTER

K. Zenker*, U. Lehnert, A. E. Rivera Osorio, R. Steinbrück, M. Kuntzsch
Institute of Radiation Physics, Helmholtz-Zentrum Dresden-Rossendorf, Dresden, Germany

Content from this work may be used under the terms of the CC BY 4.0 licence (© 2025). Any distribution of this work must maintain attribution to the author(s), title of the work, publisher, and DOI.

*Abstract*

Shifting RF phases is a common task in particular at particle accelerators. At the ELBE Center for High-Power Radiation Sources we use the phase shifter to shift the phase of the superconducting RF gun laser with respect to the accelerator cavity RF field and for delay compensation in general. The phase shifter presented in this contribution consists of a custom board, that includes a high-performance quadrature modulator, voltage regulators and an 16-bit digital-to-analogue converter that offers an I2C interface. The quadrature modulator is specified to work in the frequency range between 50 MHz and a 6 GHz. The board is combined with commercial off-the-shelf products to provide a software interface, which in our case is implemented as OPC UA interface. All components are integrated to a compact RF tight housing. We present amplitude and phase noise measurements and amplitude stability measurements at selected frequencies in the range between 78 MHz and 1.3 GHz.

## INTRODUCTION

At particle accelerators the ability to shift the phase of a radio frequency (RF) signal is a common task. Different commercially available phase shifters exist. They make use of different approaches of shifting the RF phase, e.g. in case of mechanical phase shifters the length of an RF guide is manipulated, they cover different frequency ranges and they provide different interfaces, such as knobs (mechanical), input voltage (analog) or digital interfaces. In addition, not all phase shifter are able to shift the RF phase by full 360°. However, none of the commercial available solutions covered our requirements at ELBE Center for High-Power Radiation Sources [1] listed in Table 1.

Table 1: Phase Shifter Requirements at ELBE

| | |
|---|---|
| Frequency range | 78 MHz to 3900 MHz |
| Input level | −5 dBm to 12 dBm |
| Phase noise jitter at 1.3 GHz | ≤ 10 fs |
| Phase stability (24h) | 0.1° |
| Amplitude stability (24h) | ≤ 0.1 dB |
| Phase range | 360° |
| Supply voltage | 12 V |
| Interface | digital |

The phase shifter presented here was designed to fulfill these requirements. It is based on a quadrature modulator introduced in the following.

* k.zenker@hzdr.de

## PHASE SHIFTER BOARD

The main component of the phase shifter board (PSB) is the low-noise direct quadrature modulator TRF370417 from Texas Instruments [2]. It is implemented as a double balanced mixer. Figure 1 shows an overview of the phase shifter including a picture of the 7 cm × 5.5 cm 2-layer printed circuit board that uses a ground plane in the RF section and ground vias surrounding the RF lines. The in-phase positive

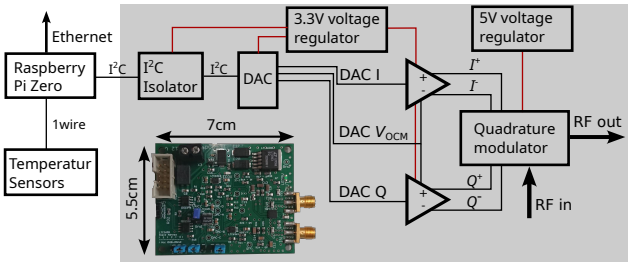



Figure 1: Phase shifter block diagram. The gray box indicates components that are part of the printed circuit board. In the addition a picture of the fully equipped printed circuit board is shown.

and negative inputs ($I^+$, $I^-$) as well as the quadrature-phase positive and negative input signals ($Q^+$, $Q^-$) are generated using a differential operational amplifier (LTC6363 [3]). A digital-to-analog converter [4] (DAC) is used to generate the differential operational amplifier input signals. It is also used to generate the output common mode voltage of the differential operational amplifier that is defined as

$$V_{\mathrm{OCM}} = \frac{V_{\mathrm{out}}^{+} + V_{\mathrm{out}}^{-}}{2}.$$

For best linearity of the quadrature modulator $V_{\mathrm{OCM}}$ is set to 1.7 V [3] for all measurements presented below. The DAC has 16-bit resolution and provides an I$^2$C interface. For ground isolation, high voltage protection and to prevent noise currents from entering the local ground a bidirectional I$^2$C isolator ISO1541 [5] is added to the board. The board is configured such that the maximum baseband voltage - i.e. for the in-phase voltage $V_{\mathrm{BB},I} = |I^+ - I^-|$ - is 1 V for the maximum DAC setting. The quadrature modulator output power level in dependence of the baseband voltage is shown in Fig. 2a. Figure 2b shows the measured output power $P_{\mathrm{out}}$ as a function of the RF frequency at maximum $V_{\mathrm{BB}}$ in the range of 50 MHz to 5 GHz.

The quadrature modulator is powered by a 12 V low noise voltage regulator LT1761 [6], whereas the DAC, I$^2$C isolator and the differential operational operators are power by a 3.3 V low noise voltage regulator LT1963 [7].

ISBN: 978-3-95450-262-2 ISSN: 2673-5350 doi: 10.18429/JACoW-IBIC2025-TUPMO34

# DEVELOPMENT OF WHITE BEAM PROFILE MONITOR FOR KOREA-4GSR

W. Song, M. Chung,* Pohang University of Science and Technology, Pohang, Korea
S. Kim, H. Hyun, S. Hwang, S. Lee, M. Kim, Y. Park, J. Lim, G. Hahn
Pohang Accelerator Laboratory, POSTECH, Pohang, Korea

Content from this work may be used under the terms of the CC BY 4.0 licence (© 2025). Any distribution of this work must maintain attribution to the author(s), title of the work, publisher, and DOI.

*Abstract*

Accurate measurement of photon beam position and profile is crucial for beamline users to achieve precise alignment and efficient utilization of the desired photon beam. In low-emittance storage rings, however, the power density of the photon beam has increased, making it challenging for conventional profile monitors such as wire scanners and scintillating screens to withstand the high power without damage. Here, we present the development of a White Beam Profile Monitor (WBPM) capable of robustly measuring the photon beam position and enabling non-destructive beam profile measurement. The WBPM, consisting of two chambers, was designed to enable simultaneous measurements of horizontal and vertical beam profiles. Its performance was evaluated at the PLS-II wiggler beamline, where results were compared against those from a screen monitor. The photon beam profile, sharply defined by a slit, was successfully measured in both directions, and the point spread function was estimated to be approximately 120 µm. Furthermore, vertical position measurements demonstrated a position resolution of 30 µm at an exposure time of 0.3 ms, confirming the feasibility of the WBPM for photon beam diagnostics.

## INTRODUCTION

In diffraction-limited storage rings (DLSRs), the electron beam emittance is reduced by nearly two orders of magnitude compared to third-generation facilities. This reduction leads to a smaller photon beam size and divergence approaching the diffraction limit. At Korea-4GSR, the concentrated beam reaches power densities up to ten times higher than those of existing sources. For beamline operation, photon beam profile measurements are required to identify the central cone of undulator radiation. However, conventional diagnostics such as wire scanners and fluorescent screens face severe thermal challenges under high-power white beam conditions. This necessitates the development of alternative non-invasive methods.

An ionization profile monitor (IPM) is a non-destructive diagnostic device, unlike conventional monitors. Because the IPM does not directly intercept the beam, it avoids damage and enables continuous, real-time monitoring. The principle relies on the ionization of residual gas within the vacuum chamber by charged particles or photon beams. The resulting ion–electron pairs are extracted before recombination and accelerated in opposite directions under an applied electric field. As the ions reach the readout, their spatial distribution is converted into an electrical signal or image. In this way, regions of higher beam density produce stronger signals, allowing the transverse intensity distribution of the beam to be reconstructed.

IPMs are already widely used in synchrotrons [1–3], and more recently have been developed for photon beam diagnostics [4–6]. To measure the white-beam profile in insertion device (ID) beamlines, we are developing a White Beam Profile Monitor (WBPM). Particular emphasis has been placed on analyzing the Point Spread Function (PSF) to ensure sufficient spatial resolution. In this paper, we present the results from installing the WBPM at the PLS-II beamline, where synchrotron radiation was directly measured to evaluate the beam profile and position.

## WHITE PHOTON BEAM PROFILE MONITOR

As shown in Fig. 1, the WBPM consists of guiding electrodes for ion extraction, and a readout assembly composed of a Microchannel Plate (MCP) and a shield plate [7]. Each electrode and the MCP are biased individually through dedicated high-voltage feedthroughs. The MCP used was Hamamatsu's F2223-21P model. It consists of a 2-stage chevron-type channel and features a phosphor screen at the exit. The overall configuration of the WBPM is shown in Fig. 2. It consists of a horizontal chamber on the left, a central chamber for gas injection and pumping, and a vertical chamber on the right. The beam distribution obtained from the MCP is measured as an image through a window using an externally mounted CMOS camera (Manta G-235b). Xenon gas is injected into the central chamber using a mass flow controller to maintain a constant pressure, and a residual gas analyzer is installed to measure the residual gas and xenon gas composition environment.

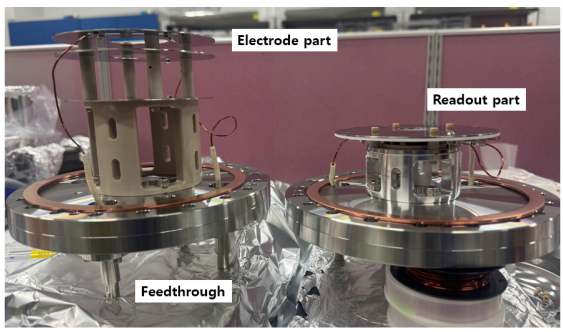



Figure 1: Assembly of the WBPM readout and electrodes.

* moses@postech.ac.kr

ISBN: 978-3-95450-262-2 ISSN: 2673-5350 doi: 10.18429/JACoW-IBIC2025-TUPMO35

# IMPROVED DESIGN OF THE EMITTANCEMETER FOR THE C-BAND PHOTOINJECTOR AT IHEP*

W. Chen[1,2], F. Li[1,2], R. Yang†[,1,2], B. Zhang[1,2]
[1]Institute of High Energy Physics, Beijing, China
[2]China Spallation Neutron Source, Dongguan, China

*Abstract*

To enhance the performance of next-generation X-ray Free Electron Lasers (XFELs), the high-quality driven beam with a low emittance, particularly for attaining emittances below 0.2 mm·mrad for 100 pC bunch charges, is of great importance. The use of a C-band photocathode RF gun is one of the promising routines to deliver such low-emittance beam. Prior to the commissioning of beams from such an injector, a precise and efficient measurement tool must be established. In this report, we introduce an emittance measurement method using an orthogonal dual-slit technique, aimed at enhancing measurement efficiency and achieving the necessary measurement accuracy for such small emittances. The primary parameters, for instance, the slit width, the beamlet drift distance, the sub-beamlet drift distance, are optimized through numerical simulations.

## INTRODUCTION

The X-ray free electron laser driven by high-brightness electron beams is a cutting-edge tool for studying atoms and molecules with unprecedented temporal and spatial resolutions. Most current XFELs operate with normalized transverse emittances below 1 mm·mrad [1]. To make XFELs more affordable and accessible, compact designs with lower linac energies have been proposed [2], which requires an high-brightness electron source [3, 4].

Among the feasible high-bright electron sources, the high-gradient RF gun with a low-intrinsic-emittance photocathode is promising. For photocathode RF guns, emittance minimizes at gradients about 140-150 MV/m [5, 6]. However, the L-band and S-band RF guns can only reach a stable acceleration gradient of about 120 MV/m [7, 8].To achieve a higher acceleration gradient, the RF gun operating at an elevated resonant frequency like C-band or X-band has been developed in recent years [9–11]. Among them, the C-band photocathode RF gun features a maximum gradient about 150 MV/m and can provide a normalized emittance of below 0.2 mm·mrad with a bunch charge of 100 pC.

As a starting element of linear injector for the future Southern Advanced Light Source (SAPS), a C-band photoinjector test platform has been proposed and is under construction at Institute of High Energy Physics (IHEP). This test platform employs a 3.6-cell normal conducting RF gun operating at 5.712 GHz. With a designed acceleration gradient of about 150 MV/m, the expected normalized emittance is lower than 0.2 mm·mrad for a bunch charge of 100 pC [12]. The primary parameters are summarized in Table. 1. Towards the successful commissioning and operation of this C-band RF gun, a short diagnostic beamline has been designed. It consists of an emittancemeter (EM), an integrating current transformer (ICT), an energy measuring instrument consisting of two slits and a screen, and a Faraday cup (FC), as shown in Fig. 1.

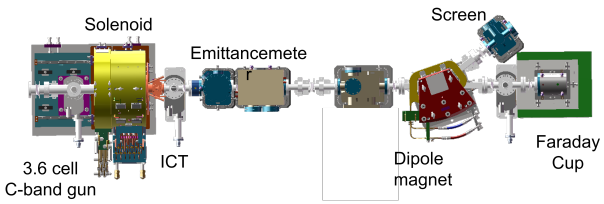



Figure 1: Schematic diagram of the C-band photocathode RF gun test platform at IHEP.

Table 1: The Major Beam Parameters at the Gun Exit for a Bunch Charge of 100 pC

| Parameter | Unit | Value |
|---|---|---|
| RF frequency | GHz | 5.712 |
| Accelerating gradient | MV/m | 150 |
| Beam energy | MeV | 7.3 |
| 95 % emittance | mm·mrad | 0.11 |
| RMS beam size | μm | 42.5 |
| RMS beam divergence | mrad | 0.37 |
| RMS bunch length | ps | 5 |

In the previous studies, a new emittance diagnostic scheme based upon parallel-slit scan was proposed and optimized [13, 14]. To further improve the accuracy of the emittance measurement at the exit of the RF gun, an orthogonal-slit scan scheme has been recently proposed and evaluated through numerical simulations. For a target 95 % emittance of 0.1–0.2 mm·mrad, a measurement error of 5–10 % is achieved employing this orthogonal-slit scan method.

## FROM PARALLEL-SLIT SCAN TO ORTHOGONAL-SLIT SCAN

The parallel dual-slit scan method operates on the similar principle as the single-slit method, but offers a key advantage: it significantly reduces space charge effects, leading to higher measurement precision, with a measurement error less than 10 % for measuring 100 pC beam emittance

* Work supported by National Natural Science Foundation of China (No. 12305166) and the Natural Science Foundation of Guangdong Province, China (No. 2024A1515010016).
† yangrenjun@ihep.ac.cn

Content from this work may be used under the terms of the CC BY 4.0 licence (© 2025). Any distribution of this work must maintain attribution to the author(s), title of the work, publisher, and DOI.

ISBN: 978-3-95450-262-2 ISSN: 2673-5350 doi: 10.18429/JACoW-IBIC2025-TUPMO37

# DEVELOPMENT OF AN OPTICAL SIMULATION TOOLKIT FOR TRANSVERSE BEAM PROFILE CHARACTERIZATION

Xin-ru Gao*, Yong-bin Leng
National Synchrotron Radiation Laboratory (NSRL),
University of Science and Technology of China, Hefei, China

Content from this work may be used under the terms of the CC BY 4.0 licence (© 2025). Any distribution of this work must maintain attribution to the author(s), title of the work, publisher, and DOI.

*Abstract*

The increasing demands for high-resolution beam diagnostics necessitate advanced simulation tools capable of modeling complex wave-optics phenomena. We present an optical simulation toolkit based on the angular spectrum propagation method, validated through comparisons with SRW. For synchrotron radiation interferometer simulations,the toolkit demonstrates excellent agreement with SRW results.The toolkit's unique capabilities are further demonstrated through three key application case studies. Through its physics-based modeling and wave-optics simulation capabilities, the simulation toolkit provides support for both optimized hardware design and methodology research to enhance the accuracy of beam profile characterization.

## INTRODUCTION

High-precision diagnostics of particle beams are critical for improving accelerator performance. As beam quality requirements continue to rise, advanced optical simulation tools are required for high-precision beam diagnostics. Geometric optics models fail to capture key wave-optics phenomena (e.g., diffraction, coherence, and wavefront distortion), leading to deviations in beam profile characterization. Current wave-optics simulation frameworks (SRW [1], SHADOW3 [2]) provide robust capabilities for modeling radiation fields according to key parameters and wavefront propagation for synchrotron radiation. However, they exihibit a few limitations in simulating complex optical systems, which include:

- Restricted wavefront propagation capabilities for complex optical elements (e.g. X-ray pinhole camera with more precise 3-D pinhole structure)
- Limited capabilities of modeling multiphysics coupling phenomena (e.g., thermal/mechanical-induced wavefront distortions)

To bridge these gaps, we develop a versatile optical simulation toolkit based on angular spectrum propagation theory. Its design prioritizes both high-precision propagation through arbitrary optical paths (lenses, drift spaces, apertures or other complex optical elements) and extensibility, which allows for modulations of multiphysics coupling effects.

* gaoxinru@mail.ustc.edu.cn

## METHODOLOGY

### *Angular Spectrum Propagation*

Angular spectrum method models optical wavefront propagation by decomposing an input electric field $E(x, y, 0)$ at plane $z = 0$ into a superposition of plane waves via Fourier transform [3]:

$$A(f_x,f_y,z) = \mathscr{F}\{E(x,y,0)\}, \tag{1}$$

where $A(f_x,f_y,0)$ is the angular spectrum, and $f_x, f_y$ denote spatial frequencies. The propagated spectrum to plane $z$ is calculated by

$$A(f_x,f_y,z) = A(f_x,f_y,0) \cdot H(f_x,f_y,z), \tag{2}$$

with the transfer function $H$ defined as

$$H(f_x,f_y,z) = \exp\left(i\frac{2\pi z}{\lambda}\sqrt{1-(\lambda f_x)^2-(\lambda f_y)^2}\right). \tag{3}$$

The output field $E(x, y, z)$ is then reconstructed by inverse Fourier transform:

$$E(x,y,z) = \mathscr{F}^{-1}\{A(f_x,f_y,z)\}. \tag{4}$$

This method was selected as the computational core of our toolkit due to its unique capabilities as follows:

- The transfer function of ASM strictly satisfies the Helmholtz equation without Fresnel or Fraunhofer approximations, enabling precise simulations regardless of distance and non-paraxial effects.
- Propagation through multi-element systems is simulated by cascading transfer functions of each element(e.g., drift space → lenses → masks) :

  $$H_{total} = H_{drift} \cdot H_{lens} \cdot H_{masks}, \tag{5}$$

  which allows for flexibility in compound optical system.
- Thermal/mechanical distortions are incorporated as phase modulators $\phi(x, y)$ in the spatial domain:

  $$E_{pertubed}(x,y) = E(x,y) \cdot exp(i\phi(x,y)), \tag{6}$$

  which enables direct analysis of multiphysics coupling impacts on beam profile diagnostics.

### *Toolkit Framework*

The toolkit employs a modular three-layer architecture (Fig. 1) designed for optical simulation and extensibility.

ISBN: 978-3-95450-262-2 ISSN: 2673-5350 doi: 10.18429/JACoW-IBIC2025-TUPMO39

# NANOSTRUCTURED TARGETS FOR ADVANCED BEAM DIAGNOSTICS

M. Siano*,[1], B. Paroli[1], C. Piazzoni, M. A. C. Potenza[1], Università degli Studi di Milano, Milan, Italy
U. Iriso, A. Nosych, E. Solano, L. Torino, ALBA-CELLS Synchrotron, Cerdanyola del Valles, Spain
D. Butti, T. Lefevre, S. Mazzoni, F. Roncarolo, G. Trad, CERN, Geneva, Switzerland
[1]also at Istituto Nazionale di Fisica Nucleare, Milan, Italy

*Abstract*

Transverse beam diagnostics with standard imaging techniques represent a challenge for next-generation accelerators and colliders due to the extremely small beam sizes, and X-ray interferometry offers an interesting method to overcome this challenge. In this regard, the X-ray Heterodyne Near Field Speckles (X-HNFS) technique has successfully been used to resolve few-micrometer beam sizes and at the same time attain a full 2D beam reconstruction. The method relies on diffracting the emitted X-ray radiation off a water suspension of spherical nanoparticles, which however pose several limitations for the full exploitation of the technique during normal operations. In this contribution we report on recent advances in the development of solid targets based on nanostructured materials with characteristics compatible with accelerator requirements. We present numerical and experimental results on the target design, prototyping and testing. Emphasis is given to the application as a transverse beam size monitor in the framework of the Feasibility Study of the Future Circular Collider (FCC) at CERN.

## INTRODUCTION

Transverse beam profile monitors are fundamental tools in synchrotron light sources and particle colliders to infer the beam emittance, a key parameter that quantifies the performance of any accelerator. Direct imaging with an X-ray pinhole camera is routinely employed in storage rings to monitor the two-dimensional (2D) beam profiles [1]. However, diffraction effects limit its spatial resolution, thereby posing challenges for next-generation accelerators and colliders due to the extremely small beam sizes. In this context, X-ray interferometry is extensively being investigated as a possible approach to high-resolution transverse beam diagnostics [2].

Within the FCC collaboration among ALBA, CERN and Unimi, we are pursuing R&D activities on a Speckle-based Beam Size Monitor (SpBSM) to achieve few-µm beam size measurements [3]. The SpBSM is based on the interference patterns generated by a water suspension of spherical nanoparticles [4]. Such samples however undergo Brownian motions and sedimentation that limit the full exploitation of the technique during normal operations. In addition, the contrast of the interference patterns is low, especially at the high X-ray energies envisioned at FCC-ee [5]. Therefore, as part of these R&D activities, solid nanostructured targets are being investigated with characteristics compatible with long-term operations inside accelerator rings and specifically tailored to the FCC-ee requirements.

* mirko.siano@unimi.it

In this paper we report on recent advances in the development of solid nanostructured targets for advanced beam diagnostics with the SpBSM at FCC-ee, showing numerical and experimental results on the target design, prototyping and testing.

## SPECKLE-BASED BEAM SIZE MONITOR

Figure 1 (top) shows the basic required components of the SpBSM: a magnetic structure to produce the X-ray synchrotron radiation, a monochromator ($\lambda$), a nanostructured sample and a camera. The SpBSM principle is based on the interference between the light diffracted by the nanostructured sample and the transmitted X-ray beam. Such interference generates random intensity modulations known as speckles (Fig. 1, bottom-left). Fourier analysis of these speckles (Fig. 1, bottom-center) provides direct access to the full 2D transverse coherence of the X-ray beam, hence the full 2D beam profile can be reconstructed [4,6]. The method has been validated at the NCD-SWEET undulator beamline at the ALBA synchrotron light source, proving micron-size resolution [4,6] as shown in Fig. 1 (bottom-right).

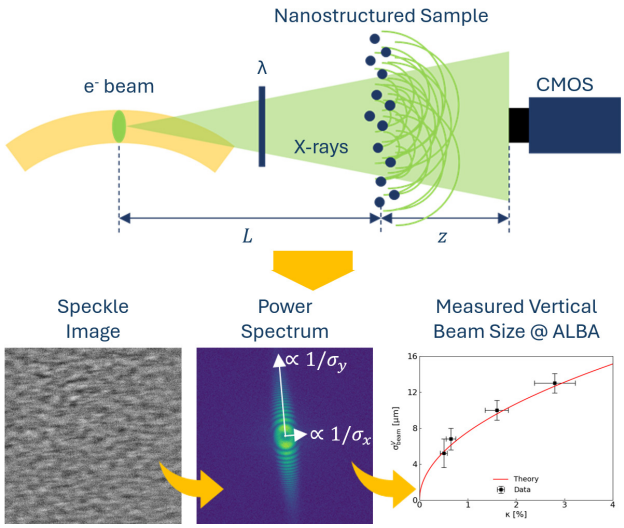



Figure 1: (Top) Basic required components of the SpBSM: a radiation source, a monochromator ($\lambda$), a nanostructured sample, a camera. $L$ = 33 m in [4], $L$ = 100 m in a typical FCC-ee extraction line [3]. In the current SpBSM, $z$ = 1 m. (Bottom) Operating principles of the SpBSM: Fourier analysis of the speckle images allows retrieving the 2D beam profile. The current SpBSM enables resolving beam sizes as small as 4 µm at ALBA, corresponding to 12 µm at FCC-ee due to the different $L$.

Content from this work may be used under the terms of the CC BY 4.0 licence (© 2025). Any distribution of this work must maintain attribution to the author(s), title of the work, publisher, and DOI.

ISBN: 978-3-95450-262-2 ISSN: 2673-5350 doi: 10.18429/JACoW-IBIC2025-TUPMO40

# OTR BEAM PROFILE MONITOR AT ALS/ALS-U*

C. Sun†, J. De Chant and C. Steier, Lawrence Berkeley National Laboratory, Berkeley, USA

Content from this work may be used under the terms of the CC BY 4.0 licence (© 2025). Any distribution of this work must maintain attribution to the author(s), title of the work, publisher, and DOI.

*Abstract*

Optical Transition Radiation (OTR) is a well-established diagnostic technique for high-resolution beam profile measurements in accelerator facilities. This work reports on the development and testing of OTR-based beam profile monitors for the transfer lines at the Advanced Light Source (ALS) and its upgrade (ALS-U). The objective is to minimize radiation generated by diagnostic screens while enabling online, high-resolution beam characterization. We present key design considerations for OTR screens, including material selection, optical properties, and mechanical integration, along with experimental results from tests at ALS. Performance is evaluated in terms of spatial resolution, signal-to-noise ratio, and linearity with beam current. The results demonstrate that OTR profile monitor can be a promising and easy-to-implement alternative to existing scintilator-based ones and their implementation could provide improved, real-time beam quality control at the ALS and ALS-U.

## INTRODUCTION

Beam Profile Monitors are essential diagnostic tools for accelerator commissioning, tuning, and routine operation. In single-pass transfer lines it most commonly employ scintillator screens, which interact with the charged particle beam, converting its energy into visible light that can be imaged with a camera. At the Advanced Light Source (ALS), Chromox-6 scintillator-based beam profile monitors have been in operation since commissioning nearly 30 years ago [1]. This system has provided invaluable information for injector and transfer line tuning, and its applicability has been evaluated for the ALS Upgrade (ALS-U).

Despite their utility, the scintillator-based beam profile monitors are destructive to the beam, generate significant background radiation while in operation, and offer limited spatial resolution. Optical Transition Radiation (OTR) provides a promising alternative and a simple replacement for existing Beam Profile Monitors at the ALS [2]. With appropriate design, OTR-based profile monitors offer higher spatial resolution, reduced background radiation, and the potential for quasi-online measurements.

We are implementing OTR screens for ALS and ALS-U. Key design considerations include screen material, optical properties, and integration with existing designs. Experimental results from ALS tests are presented, evaluating spatial resolution, signal-to-noise ratio, and linearity with bunch charge. These developments are expected to significantly improve beam quality control at the ALS and ALS-U.

* Work supported by the Director Office of Science of the U.S. Department of Energy under Contract No. DE-AC02-05CH11231

† ccsun@lbl.gov

## OPTICAL TRANSITION RADIATION

When a relativistic charged particle beam crosses the interface between two media with different dielectric constants—typically from vacuum to a metallic foil—it emits radiation. A portion of this radiation falls in the visible range, allowing capture by standard optical systems. The resulting image provides a measurement of the beam's transverse spatial distribution. The intensity distribution at the image plane can be expressed as [3]:

$$I(x,y) \propto \left[ \int_0^{\theta_{\max}} \frac{\theta^2}{\theta^2 + \gamma^{-2}} J_1 \left( \frac{k\theta\sqrt{x^2+y^2}}{M} \right) d\theta \right]^2, \quad (1)$$

where $k = 2\pi/\lambda$ is the wave number with $\lambda$ the radiation wavelength, $x$ and $y$ are the transverse coordinates at the imaging plane, $M$ is the magnification of the imaging system, $\theta$ is the OTR emission angle, $\gamma$ is the Lorentz factor of the particle beam, $\theta_{\max}$ is the collection angle defined by the lens aperture, and $J_1$ is the first-order Bessel function.

### *Point Spread Function*

Equation (1) incorporates angular distribution, optical aperture, and diffraction, and is widely used to model the point-spread function (PSF) of an OTR-based beam profile monitor. The $1/\gamma$ dependence reflects the relativistic narrowing of the OTR emission cone, while the Bessel function captures the Fourier transform relationship between angular distribution and image-plane intensity.

For a 1.9 GeV electron beam, the calculated intensity distribution at the imaging plane exhibits an RMS width of approximately 2 μm as shown in Fig. 1. For beams with sizes of a few tens to hundreds of micrometers, this result indicates that the intrinsic resolution of the OTR screen is not constrained by the emission itself, but instead by the optical performance of the imaging system, which plays a dominant role.

### *Sensitivity*

The main limitation of OTR is its relatively weak emission intensity compared to scintillators, requiring higher-sensitivity cameras and carefully designed imaging system. In addition, because the foil must intercept the beam, the measurement is inherently invasive and can introduce scattering. However, the perturbation to the beam can be minimized with the use of very thin foils, allowing OTR monitors to provide online measurements during beam operation

The weak emission challenge can be mitigated by modern camera technology. Advanced CCD and CMOS cameras provide sufficient sensitivity for OTR detection. To evaluate the sensitivity requirements, one can estimate the number of photons collected by the imaging system. Since the photons are distributed across many pixels on the image plane, the

ISBN: 978-3-95450-262-2 ISSN: 2673-5350 doi: 10.18429/JACoW-IBIC2025-TUPMO41

# PRELIMINARY DATA ANALYSIS OF AN IPM PROTOTYPE AT CSNS RCS*

M. A. Rehman[1,2], Y. Guo[1,2], Z. Xu[1,2], X. Nie[1,2], M. Liu[1,2], B. Zhang[1,2], R. Yang†[,1,2]
[1]Institute of High Energy Physics, Beijing, China
[2]China Spallation Neutron Source, Dongguan, China

*Abstract*

To improve the performance of the China Spallation Neutron Source (CSNS) accelerator complex, a non-invasive beam profile monitor is essential for tuning and operating the CSNS 1.6 GeV Rapid Cycling Synchrotron (RCS). A residual gas Ionization Profile Monitor (IPM) prototype has been constructed to address challenges associated with high-intensity beam profile measurement and to enable real-time monitoring. The RCS IPM prototype was improved through troubleshooting and is now capable to measure the bunch by bunch beam profiles. This paper presents the preliminary analysis of the IPM signals, emphasizing on the temporal resolution and the observations of beam profile during the beam injection.

## INTRODUCTION

The China Spallation Neutron Source (CSNS) is one of the major scientific facilities in China, constructed to deliver intense pulsed neutron beams for diverse scientific research and industrial applications [1, 2]. Its accelerator complex consists of an 80 MeV linac, a 1.6 GeV rapid cycling synchrotron, a beam transport line, and a solid tungsten target station. Through a multi-turn charge exchange injection process, the 80 MeV $H^-$ beam from the linac is converted into proton and injected in the RCS. Subsequently, the RCS accelerates the proton beam to 1.6 GeV with a beam intensity of $1.56 \times 10^{13}$ ppb, delivering a beam power of 100 kW to the neutron target. The CSNS power upgrade project (CSNS-II) has been launched aiming to increase the beam power to 500 kW [3]. The major upgrade of the accelerator complex includes the superconducting accelerator downstream of the DTL section, the update of the injection area, and the implementation of the dual-harmonic RF cavities. The primary parameters of both CSNS and CSNS-II are summarized in Table 1. The beam transverse profile information is of great importance for the successful commissioning and operation of a circular accelerator at intensity frontier, such as CSNS RCS. A prototype IPM has been designed and installed in the RCS. This paper presents the preliminary analysis of the IPM signals to extract the temporal resolution and beam profile under the ion-collection mode.

## IONIZATION PROFILE MONITOR

The IPM was first proposed and developed in the 1960s [4, 5]. However, due to the complexity of the instrument, experience and debugging are required to ensure its effective operation and accurate results.The IPM system of the CSNS Rapid Cycling Synchrotron (RCS) comprises two primary components: the IPM detector, located in the beam tunnel, and the signal readout system [6]. The IPM field cage consists of 28 electrodes with an aperture of 220 mm × 231 mm, as shown in Fig. 1. To enhance electric field uniformity, adjacent electrodes are interconnected via 100 MΩ resistors. The collection electrodes are gold-coated to suppress secondary electron emission from their surfaces. Additionally, a grounded top electrode features a central rectangular opening of 30 mm × 80 mm, allowing secondary ions and electrons, generated from beam-residual gas interactions, to pass to the Micro Channel Plate (MCP). Following chamber venting and installation, high-voltage conditioning was performed to mitigate potential arcing during IPM operation.

Table 1: CSNS and CSNS–II RCS Parameters

| Parameters | CSNS | CSNS–II | Units |
|---|---|---|---|
| Beam Power | 100 | 500 | kW |
| Injection Energy | 80 | 300 | MeV |
| Ring Circumference | 227.92 | 227.92 | m |
| Extraction Energy | 1.6 | 1.6 | GeV |
| Repetition Rate | 25 | 25 | Hz |
| $f_{RF}$ | 1.02-2.44 | 1.02-2.44 | MHz |
| Number of Bunches | 2 | 2 | |
| Beam Intensity | $1.56\times10^{13}$ | $7.8\times10^{13}$ | ppb |

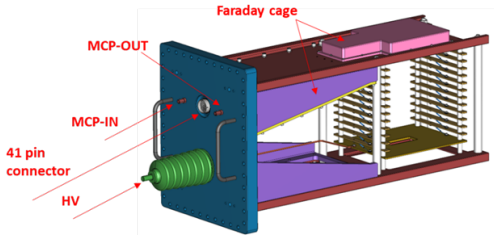



Figure 1: The schematic of the IPM prototype at the CSNS RCS.

A maximum bias voltage of 30 kV has been applied to the field cage after iterative conditioning. To suppress beam-induced electromagnetic interference (EMI), a honeycomb-shaped RF shield is mounted on the center opening, forming a Faraday cage together with the frame and top cover. The honeycomb structure features a hexagonal shape with a width of 3.2 mm and a depth of 6 mm. On the opposite side, an ion trap structure is incorporated to suppress secondary electrons during electron-mode operation. For detecting the

* Work supported by National Natural Science Foundation of China (No. 12305166) and the Natural Science Foundation of Guangdong Province, China (No. 2024A1515010016)
† yangrenjun@ihep.ac.cn

Content from this work may be used under the terms of the CC BY 4.0 licence (© 2025). Any distribution of this work must maintain attribution to the author(s), title of the work, publisher, and DOI.

ISBN: 978-3-95450-262-2 ISSN: 2673-5350 doi: 10.18429/JACoW-IBIC2025-TUPMO42

# RESULTS FROM THE NEW TITANIUM WIRED HARP AT THE SPALLATION NEUTRON SOURCE*

W. Blokland†, A. Aleksandrov, B. Cathey, W. Willis
Oak Ridge National Laboratory, Oak Ridge, TN, USA

Content from this work may be used under the terms of the CC BY 4.0 licence (© 2025). Any distribution of this work must maintain attribution to the author(s), title of the work, publisher, and DOI.

*Abstract*

A new harp has been installed in the Ring To Target Beam line (RTBT) section of Spallation Neutron Source. The harp is made of two planes with 32 titanium 50-micron wide wires each plane. The narrow, low-Z wires versus the 100-micron tungsten wires of the original harp, are to minimize the beam scattering. This harp will be both a backup and a complement to the existing harp further downstream. The newly created data-acquisition system is also suitable to replace the existing's harp data-acquisition system, now over 20 years old. We show the use of a cRIO platform as a cost-effective way to process many channels and sample the beam profile at the full 60 Hz beam repetition rate. We also describe the performance of the titanium wires. A passive analog board is used to lengthen the signals to allow sampling at ≤10 kS/s/ch. The data is acquired by the FPGA, passed on to the real-time OS, LabVIEW RT, and through the SNS EPICS Channel Access server presented to the control room.

## INTRODUCTION

The original RTBT Harp is used to qualify the beam on the target and has been in operation for over 20 years. It was meant to be retractable but because of an early actuator failure it has remained in the beam, operating without major problems. It is in a location that is hard to access and highly radioactive. A failure would require downtime. To handle this failure, we have implemented a backup Harp. This new harp, further upstream, is accessible and replaceable. It is called Harp25 for its location relative to a quadrupole, while the old harp is called Harp30.

The Harp25 differs from the Harp30 in its unshielded location; therefore, the primary design consideration was to reduce proton scattering in the harp wire material. This was achieved by minimizing the amount of material in the beam path and by using materials with as low a Z (atomic number) as possible. The Harp30 consists of 5 parallel frames sandwiched together: horizontal signal wires, diagonal signal wires, vertical signal wires and two bias planes in between made of the same 100 µm tungsten wire. To reduce the amount of material, we eliminated the diagonal signal wires and the two bias planes. The bias is provided using a solid plate below the signal wires frames as shown in Fig. 1.

The signal wire frames are arranged in triangular configuration to allow the bias field to reach both planes' wires. The angle between the planes is determined by the ID of the vacuum chamber vertical leg as shown in Fig. 1. Our experience with the Harp30 has shown that tungsten wires are durable. However, since we aimed to reduce activation due to scattering, we sought a material with a lower Z. Although carbon or SiC monofilament would be ideal, their maximum available size is 30 µm, and the wire fragility makes assembling a multiwire harp challenging. Therefore, based on our prior positive experience with the SNS laser emittance harp, we decided to use 50 µm titanium wire for the prototype.

## MECHANICAL DESIGN

The harp was designed to have two identical planes, with one mounted so that the wires are horizontal and the other with the wires mounted vertical. The two planes are mounted to a frame that sets them at a 15-degree angle from vertical. The 32 wires in each plane are 50 µm diameter titanium (99.8 % pure) and are spaced 4 mm apart. The wires are tensioned individually using spring-loaded copper collets in a Macor block on one end. The wires are clamped to a Garolite block using copper leads that are held in place by swivel head set screws. The copper leads extend from the block to make it easy to solder on signal wires. There is an electrically isolated bias plate under the two planes that can have up to 250 V bias voltage. The entire Harp head is mounted to a repurposed wire scanner actuator with an eight-inch stroke. This allows the Harp to be retracted completely out of the beam pipe and to be fully inserted for making measurements. The harp head and vacuum chamber are shown in Fig. 1.

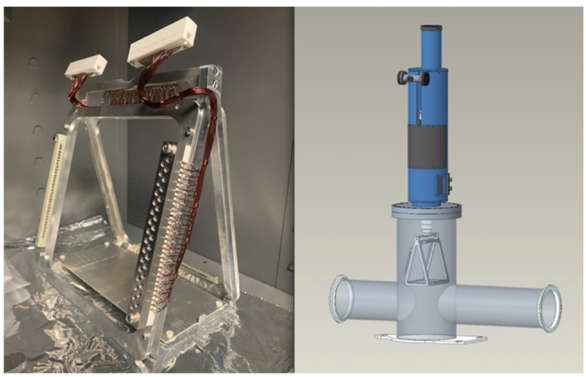


Figure 1: The harp head and vacuum chamber.

## DATA ACQUISITION

The harp has custom analog boards, see [1], to reshape the short pulse coming from the wires to a longer pulse to match the bandwidth of the digitizers. The system is implemented in cRIO hardware. It has:

* SNS is managed by UT-Battelle, LLC, under contract DE-AC05-00OR22725 for the U.S. Department of Energy.
† blokland@ornl.gov

ISBN: 978-3-95450-262-2 ISSN: 2673-5350 doi: 10.18429/JACoW-IBIC2025-TUPMO43

# TIME-RESOLVED MEASUREMENTS OF TRANSVERSE BEAM EXCITATION IN AN ELECTRON STORAGE RING

M. Noll*, E. Bründermann, M. Caselle, E. Huttel, J. L. Steinmann, A.-S. Müller
Karlsruhe Institute of Technology, Karlsruhe, Germany

*Abstract*

In the Karlsruhe Research Accelerator (KARA), electron beams of up to 200 mA are stored with an energy of 2.5 GeV, while injection is performed at 500 MeV. At the injection energy, the beam life time and the injection efficiency depend largely on Touschek scattering. As a counter-measure, the beam size can be enlarged transversally by an exciting modulation, e.g. applied via a strip-line. In an existing setup, the vertical beam size is measured with a double-slit interferometer. Here, we examine different detectors for this setup. A different choice from the conventional CMOS camera is the ultra-fast line camera KALYPSO, which can not only measure on a turn-by-turn basis, but can also stream frames to a computer and thus can capture larger time frames than, for example, a fast-gated camera.

## INTRODUCTION

To improve the injection efficiency and life-time of the electron beam in the KARA storage ring, one area of research is artificially blowing up the beam size by transversal modulation with a strip-line. Since the vertical beam size is smaller than the diffraction limit, techniques such as double-slit interferometry are employed to measure the vertical beam size. Conventionally, the interferogram is digitized with an industrial CMOS camera [1]. Its integration time in the order of microseconds to milliseconds prevents the system from discriminating fast modulations of merely the beam position from the desired beam size increase.

## BEAM SIZE MEASUREMENT

In a double-slit interferometer, the interference pattern at the detector has a $\mathrm{sinc}^2$ shape [2] (see Fig. 1) with a global intensity maximum $I_{\max}$ and the first intensity minimum $I_{\min}$ adjacent to the peak. The visibility, or contrast ratio, $V$ is related to the intensities $I_1$ and $I_2$ at the slits by the magnitude of the complex coherence $\gamma$ and is given by

$$V = \frac{I_{\max} - I_{\min}}{I_{\max} + I_{\min}} = \frac{2\sqrt{I_1 I_2}}{I_1 + I_2} |\gamma| . \tag{1}$$

Hence, without an intensity imbalance at the slits, $V$ and $|\gamma|$ are identical.

With the distance $L$ from source to the double-slit, the slit separation $d$ and the source wavelength $\lambda$, the van Cittert-Zernike theorem states the complex coherence is given by the Fourier transform of the light source's spatial profile $f(x)$ as

$$\gamma = \int f(x) \exp\left[-j\frac{2\pi d}{\lambda L}x\right] \mathrm{d}x. \tag{2}$$

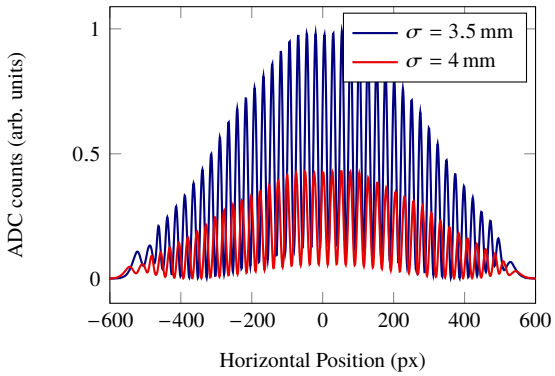



Figure 1: Ray optics simulation showing the interference pattern for a Gaussian beam at the detector plane. The inverse relation between beam size $\sigma$ and visibility $V$ is apparent.

The profile $f(x)$ can be assumed as a Gaussian beam [3] with width $\sigma$. The visibility then becomes

$$V = |\gamma| = \exp\left[-2\left(\frac{\pi\sigma d}{\lambda L}\right)^2\right], \tag{3}$$

and can be rearranged to

$$\sigma = \frac{\lambda L}{\pi d}\sqrt{0.5 \ln \frac{1}{V}}. \tag{4}$$

By measuring the intensities $I_{\max}$ and $I_{\min}$, the beam size $\sigma$ can be computed [4, 5].

The conventional CMOS camera setup has a limited time resolution in the order of microseconds to milliseconds set by the integration time and the lack of hardware trigger. A fast-gated camera can be used, but commercial devices are limited to one acquisition every few hundred turns [1,6]. The frame-buffer of commercial cameras is also often limited. Furthermore, to measure the visibility $V$ of a double-slit setup in one orientation, the second dimension of conventional and fast-gated cameras is not necessary. To measure coupling between the $x$ and the $y$ planes, the CMOS setup will still be used.

Therefore, the fast line camera KALYPSO is employed to get turn-by-turn profiles of the interferogram and thus turn-resolved beam sizes. With its streaming mode, the beam size evolution can be measured for several seconds.

## EXPERIMENTAL SETUP

The experimental setup is located approximately 4 m after a dipole magnet of the KARA storage ring. The synchrotron radiation is guided upwards with an aluminum-coated copper mirror and leaves the vacuum through a sapphire window. A

* marvin.noll@kit.edu

Content from this work may be used under the terms of the CC BY 4.0 licence (© 2025). Any distribution of this work must maintain attribution to the author(s), title of the work, publisher, and DOI.

ISBN: 978-3-95450-262-2 ISSN: 2673-5350 doi: 10.18429/JACoW-IBIC2025-WEAC01

# ANALYSIS OF A PHASE MODULATED INTERFEROMETRIC ELECTRO-OPTIC BPM AT THE CERN SPS

M. Z. C. Bosman*, S. M. Gibson, D. M. Harryman, A. Arteche
John Adams Institute at Royal Holloway, University of London, UK
T. Lefèvre, T. E. Levens, CERN, Geneva, Switzerland

*Abstract*

The Electro-Optic Beam Position Monitor (EO-BPM) is a new diagnostic tool being developed to enhance the intra-bunch transverse beam position monitoring in the High Luminosity LHC at CERN. This EO-BPM has been installed in the Super Proton Synchrotron (SPS) since 2024. The Pockels effect in lithium niobate crystals is exploited to detect the propagating electric field from passing proton bunches, enabling measurement of beam position and intra-bunch instabilities. Light is conveyed from a remote laser via optical fibres to a Mach-Zehnder interferometer formed between two waveguide pick-ups. The rapid response of the EO-BPM enables intra-bunch turn-by-turn measurements. Data recorded over a range of beam conditions have been studied to characterise its performance, stability, and sensitivity. This paper presents the latest data collected from the SPS and discusses the analysis and future development of the EO-BPM.

## INTRODUCTION

The High-Luminosity Large Hadron Collider (HL-LHC) at CERN will increase the luminosity of the LHC by installing crab cavities to improve bunch overlap at the interaction point which require high-bandwidth diagnostics [1]. Electro-optical systems offer fast response and strong resistance to electrical noise, making them attractive for high-bandwidth beam position measurements in accelerator environments [2].

### *Working Principle*

Lithium niobate (LN) is a birefringent electro-optic crystal [3], meaning that one of its three principal refractive indices differs from the others. Through the Pockels effect, this birefringence can be modulated by applying an external electric field. When linearly polarised laser light passes through the crystal, interferometric techniques can detect the resulting change in refractive index. This enables measurement of the external field, which in this context corresponds to the bunch shape [4].

The Electro-Optic Beam Position Monitor (EO-BPM) employs a fibre-coupled 780 nm laser, which is split, passing through two opposing LN crystals on either side of the beampipe (see Fig. 1). The laser then recombines to act as an Mach-Zehnder (MZ) interferometer. Since the refractive index of each crystal changes linearly with the applied electric field from the proton bunch, the response of this interferometer is of the form:

$$V = A + B\cos\left(\phi_0 + \pi\frac{E}{E_\pi}\right), \tag{1}$$

where $\phi_0$ is defined as the phase offset, $E_\pi$ the electric field required for a phase advance of $\pi$ and $E$ is given by:

$$E = \begin{cases} E_l, & \text{for the left side mode interferometer} \\ E_r, & \text{for the right side mode interferometer} \\ E_l - E_r, & \text{for the difference interferometer} \end{cases}$$

with $E_l$ and $E_r$ being the fields in the left and right crystals, respectively [5].

### *Previous Iterations*

The EO-BPM design has evolved since the initial installation in the SPS in 2016. From free space optics and low signal strength, to a fibre-coupled laser interferometer with several techniques to increase electric field modulation [5–8].

The main challenge cited in the 2024 proceedings was a mismatch of the pick-ups leading to a combination of sum and difference signals [5]. To address this, the new pick-up is adjustable and can be calibrated in situ. Additionally, a new phase control mechanism allows for three separate interferometric read-outs.

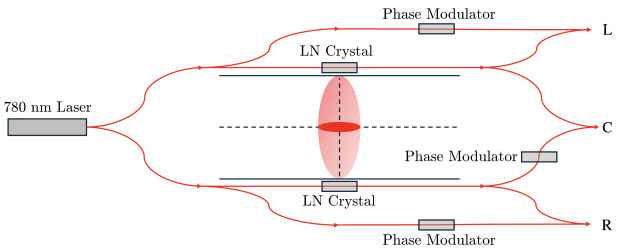



Figure 1: New EO-BPM splitter tree comprising of three Mach-Zehnder interferometers.

## DESIGN OF ADJUSTABLE PICK-UP

### *Button Design*

The new button changes several components. The conical design has been replaced by a cylindrical structure surrounded by ceramic, with a characteristic impedance of 20 Ω, matching that of the bottom electrode.

* max.bosman@rhul.ac.uk

Content from this work may be used under the terms of the CC BY 4.0 licence (© 2025). Any distribution of this work must maintain attribution to the author(s), title of the work, publisher, and DOI.

ISBN: 978-3-95450-262-2 ISSN: 2673-5350 doi: 10.18429/JACoW-IBIC2025-WEBC01

# BLM SIGNAL THRESHOLDS FOR ION OPERATION DURING THE LHC RUN 3

S. Morales Vigo*, B. Salvachua, R. Bruce, F. Carra, A. Lechner, D. Mirarchi, L. Puddu, S. Redaelli, V. Rodin, N. Triantafyllou, C. Zamantzas, CERN, Geneva, Switzerland

*Abstract*

In 2024, the Large Hadron Collider (LHC) delivered Pb-Pb ion collisions at a beam energy of 6.8 Z TeV with a stored beam energy of more than 20 MJ. In order to clean beam halo particles and avoid quenching the LHC superconducting magnets, the novel crystal collimation method employing 4 mm-long crystals was introduced for ion operation in the LHC Run 3. The LHC Beam Loss Monitoring (BLM) system triggers the beam dump in case the measured losses are above certain predetermined thresholds. Important adjustments were needed in order to optimize these thresholds in accordance with the peculiar loss pattern produced by crystal collimation. This contribution explains the newly observed beam loss patterns during Pb ion operation with crystal collimation in place, as well as the study that was carried out to update the BLM thresholds at the betatron collimation region for Pb ion operation in the LHC Run 3.

## INTRODUCTION

Most of the operation of the LHC at CERN is aimed at accelerating and colliding proton beams. However, there are also scheduled periods for ion collisions, normally with Pb, typically of around one month every operational year [1].

The next major upgrade for CERN's flagship collider and its experiments, called High Luminosity LHC (HL-LHC), has the goal of increasing the LHC instantaneous luminosity beyond its design values [2]. For proton beams, HL-LHC operation is expected to begin in 2030, at the start of Run 4.

On the other hand, the HL-LHC upgrades for Pb ion operation were already implemented for Run 3, the present LHC operation period. These upgrades have resulted in more than a factor 6 higher instantaneous luminosity at the ALICE experiment, specialized in heavy-ion collisions [3]. This comes together with a stored beam energy reaching more than 20 MJ [4].

One of the main hardware upgrades concerned the LHC betatron collimation system, that was initially designed primarily for proton operation. This same system had been used for heavy-ion operation despite its cleaning being around 100 times less efficient in this case [5].

During Run 3 Pb ion operation, due to the increased stored beam energy, the particles escaping from the standard betatron collimation system would risk to quench the superconducting magnets located downstream. In order to mitigate this issue, it was decided to introduce a novel collimation method called "crystal collimation" that has been proven to reduce significantly the leakage to the aforementioned magnets down to acceptable levels for operation [6–8].

This new setup includes four crystal collimators, two per beam and plane; horizontal and vertical. If correctly aligned, halo particles are trapped in the potential well between crystalline planes and follow their bending. They hence exit the crystal with an angular kick and are "channelled" onto four different dedicated absorbers, creating completely different loss patterns compared to operation with the standard collimation system. However, if the alignment between the crystal and the beam changes such that the incoming particles are no longer trapped between the planes, the channelling conditions are lost, which increases the leakage to the downstream superconducting magnets.

In addition to the collimation system, the LHC BLM system actively protects the machine elements to avoid high energy deposition from beam losses by triggering the beam extraction when its recorded signals exceed certain predetermined thresholds [9]. For proton operation, the thresholds of the BLM detectors that are placed in the collimation areas are based on the specifications of maximum loss rates at the collimators and the expected loss patterns resulting from regular cleaning.

Run 3 Pb ion operation requires an adjustment of these thresholds not only due to the different loss patterns produced by crystal collimation, but also because the leakage to the downstream superconducting magnets is more critical. In this case, the BLM thresholds at the collimators must constitute an extra layer of protection for the magnets. This means that the allowed beam power loss at the collimators must adapt to the mode of interaction of the halo particles with the crystals at all times, posing a challenge to the management of the BLM signal thresholds.

This contribution describes the main differences between the beam loss patterns recorded at the LHC betatron collimation system in Run 3 for protons and Pb ions. The necessary updates and BLM signal thresholds strategy for Pb ion operation are explained.

## LHC COLLIMATION SYSTEM

In order to clean the beam halo particles and prevent them from hitting the vacuum chamber at the superconducting regions, the LHC has a betatron collimation system that intercepts the beam losses with very high efficiency, minimizing the leakage to the superconducting magnets.

### *Standard Betatron Collimation System*

The standard betatron collimation system comprises an arrangement of so-called Target Collimator Primary (TCP) and Target Collimator Secondary (TCS) collimators. Each collimator is composed of two parallel blocks, typically

* sara.morales.vigo@cern.ch

Content from this work may be used under the terms of the CC BY 4.0 licence (© 2025). Any distribution of this work must maintain attribution to the author(s), title of the work, publisher, and DOI.

ISBN: 978-3-95450-262-2 ISSN: 2673-5350 doi: 10.18429/JACoW-IBIC2025-WEBC02

# LESSONS LEARNED IN COMMISSIONING THE NEW BEAM-LOSS MONITORS FOR THE SUPERCONDUCTING UPGRADE TO LCLS*

A. S. Fisher†, G. W. Brown, E. P. Chin, S. Chowdhury, W. G. Cobau, J. E. Dusatko, B. T. Jacobson, T. Kabana, K. Kruchinin, R. S. M. Martinez, J. Pigula, Evan Rodriguez
SLAC National Accelerator Laboratory, Menlo Park, California, USA

*Abstract*

The superconducting upgrade to the LCLS x-ray free-electron laser at SLAC is now in commissioning, as we gradually raise the repetition rate of the 4 GeV beam toward 1 MHz and the beam power toward 120 kW. A further upgrade in 2026 will double the energy and power. Machine protection at this extremely high power required a novel system of fast beam-loss monitors (BLMs). Points of concern, such as collimators or kickers, are covered by diamond detectors (PBLMs). Long optical fibres (LBLMs) of up to 200 m span the entire 4 km facility, generating and capturing Cherenkov emission from beam-loss showers. Previous papers have reported on the design and early commissioning of this safety system, and on plans to use the loss signals for wire scanners and loss localisation. Subsequent experience in commissioning and operating the full system has demonstrated that the concept is sound and sensitive, but several aspects of the implementation have proven troublesome. Extensive testing and debugging uncovered issues with both hardware and firmware. We will detail these problems, their remedies, and the improvements in performance.

## INTRODUCTION

Over the past decade, SLAC installed and has been commissioning the new 700 m superconducting (SC) linac that replaced the first 1 km of its original 3 km normal-conducting (NC) copper linac. Using continuous-wave 1.3 GHz radio-frequency (RF) power, the new 4 GeV accelerator is gradually being ramped up to a beam power of 120 kW with a pulse rate of up to 929 kHz. In 2026, the High-Energy (HE) upgrade will install additional cryomodules to double the beam's energy and power. With a high risk of damage from this beam power, we replaced our previous beam-loss monitors (BLMs) based on ionization chambers, which are limited by the slow transport of ions [1], with new, faster BLMs. Expected loss points are now protected by point BLMs (PBLMs) using 4-mm-square diamond detectors from Cividec (type B1-HV). The entire 4 km beam path is monitored by long BLMs (LBLMs) using radiation-hard optical fibres from the Polymicro division of Molex (FBP600660710). The new BLMs and the signal processing were described in [2-7].

Initial commissioning [4, 5] showed good sensitivity and fast response, with the linac still at low rate. Further experience at higher loss power uncovered several performance problems, especially with the LBLMs—not with the fibres themselves but with the associated photomultiplier tubes (PMTs), electronics, and processor software. Some issues are common to the PBLMs. This paper presents these problems and their resolutions, to update those who might want to replicate our approach.

* SLAC is supported by the U.S. Department of Energy, Office of Science, under contract DE-AC02-76SF00515.
† afisher@slac.stanford.edu

## LONG BEAM-LOSS MONITORS

### Layout

When a beam-loss shower passes through the optical fibre of an LBLM, some of the emitted Cherenkov radiation is captured in the fibre and carried to the ends. The fibres are typically 200 m long, but shorter lengths span specific segments of the machine, such as the L2 section of the SC linac (between bunch compressors 1 and 2) or a warm section for compression, collimation, or diagnostics. Each fibre runs between two chassis in electronics racks outside the tunnel. In each chassis, which is both the end of one fibre and the start of the next, a PMT measures light arriving at one fibre's downstream end, and a modulated LED sends weak light into the upstream end of the next, as a continuous self-check. A motherboard both processes the PMT signal and drives the LED.

After outlining the signal processing [6], we examine the problems with the PMTs, the self-check, and the electronics, as well as control of the PMT and LED temperatures.

### Integrated Loss Signal

A passive filter (Fig. 1) splits the PMT signal into low and high frequencies, $V_L$ and $V_H$. For $V_L$, charge from the PMT accumulates immediately on capacitor $C_1$ and discharges through $R_1$ with a time constant $R_1C_1$ = 500 ms. This integrated signal measures the beam's loss rate independently of its repetition rate.

A buffer op amp multiplies $V_L$ by a gain $G$ ($1 \le G \le 74$) that matches the sensitivity needed for each fibre. In the warm regions separating linac sections, $G = 6$. In cold sections, where losses must pass through the thick steel of the cryostat housing, $G = 50$. Along the 2 km bypass beamline over the NC linac, where the fibre is only 40 cm above the SC beam, $G = 1$. Most other locations use $G = 20$.

An analogue comparator stops the beam if $GV_L$ exceeds the threshold selected for the Beam Containment System (BCS). The same $GV_L$ is buffered and sent outside the chassis to a node of the Machine Protection System (MPS) in an ATCA crate, where it is digitised and compared to a separate threshold [2]. Depending on the location, the MPS can block the photocathode laser, lower the beam rate, or stop a kicker from sending beam into a specific beamline. The BCS shuts off RF power to the electron gun. Because recovery is slow from a BCS trip, the MPS threshold is set

Content from this work may be used under the terms of the CC BY 4.0 licence (© 2025). Any distribution of this work must maintain attribution to the author(s), title of the work, publisher, and DOI.

ISBN: 978-3-95450-262-2 ISSN: 2673-5350 doi: 10.18429/JACoW-IBIC2025-WEBI01

# SIMULTANEOUS MEASUREMENTS WITH FAST BEAM SIZE AND POSITION MONITORS DISENTANGLE THE SUDDEN BEAM LOSS EVOLUTION MECHANISM

G. Mitsuka*,[1], KEK, Tsukuba, Ibaraki, Japan
R. Nomaru, University of Tokyo, Bunkyo, Japan
T. Ishida, S. Iwabuchi, H. Ikeda[1], T. Mitsuhashi[1], KEK, Tsukuba, Ibaraki, Japan
[1]also at Sokendai, the Graduate University for Advanced Studies, Hayama, Kanagawa, Japan

*Abstract*

At the SuperKEKB electron-positron collider, which aims to achieve the world's highest luminosity, "Sudden Beam Loss (SBL) events" have prevented its stable operation, in which several tens of percent of the beam current is lost and aborted within several turns (20 µs–50 µs). Elucidating SBLs, which can cause extensive damage to accelerator components and the Belle II experiment detectors, is a pressing issue for SuperKEKB. To measure the beam size and position variation, key information for disentangling SBLs, over dozens of turns just before the SBL-induced beam aborts, we have developed new turn-by-turn beam size monitors in two different wavelength regions, X-ray and visible light, and bunch-by-bunch beam position monitors where one has utilized a novel architecture AMD/Xilinx RFSoC. Simultaneous measurements of turn-by-turn beam size and bunch-by-bunch beam position enable elucidation of the cause and time evolution mechanism of the SBL events. We will introduce recently developed fast beam size and beam position monitors, then show their simultaneous measurements of SBL events. We will also discuss the possible causes and time evolution mechanisms of the SBL events.

## INTRODUCTION

The SuperKEKB accelerator is a collider consisting of a 7 GeV electron ring (the high-energy ring, HER) and a 4 GeV positron ring (the low energy ring, LER). As indicated in Fig. 1, the highest luminosity recorded by SuperKEKB in 2024 December was $5.1 \times 10^{34}$ cm$^{-2}$ s$^{-1}$, which is the world record as of 2025 August. On the other hand, to achieve SuperKEKB's target $6 \times 10^{35}$ cm$^{-2}$ s$^{-1}$, it is clear that further beam current enhancement and beam operation stabilization are needed.

The biggest obstacle to the current enhancement and long-term stability of beam operation is Sudden Beam Loss (SBL) events [1,2]. SBL events occur when the beam (bunch) orbit suddenly begins to oscillate without any obvious precursor, and more than 10 % of the beam current is lost in just a few turns (tens of microseconds), leading to beam abort. Figure 2 indicates an example of a SBL event in LER. The top two panels show the bunch positions measured by Bunch Oscillation Recorders (BORs, monitors that can record the orbit of each bunch for more than 100 turns). The topmost panel shows the horizontal orbit, and the second panel shows

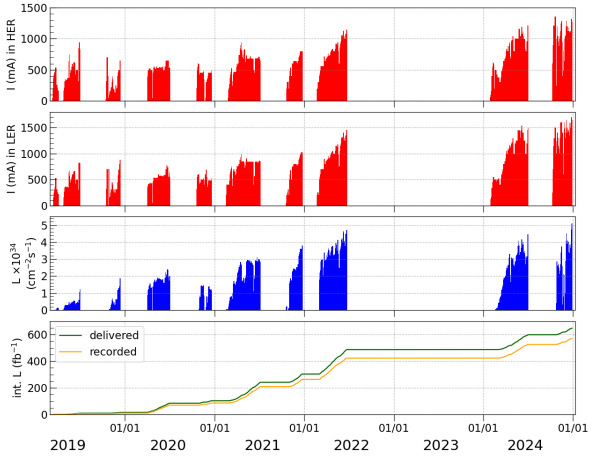



Figure 1: Luminosity record of the SuperKEKB collider in 2019–2024.

the vertical orbit. The horizontal axis represents the bunch train, and the vertical grid indicates divisions per turn. The leftmost division corresponds to 6 turns before beam abort. The third row shows the bunch current, normalized to 1 at the left edge of the plot. A beam loss occurred two turns before the abort, causing the current to drop. The bottom row expresses the beam loss in current (mA), showing a large loss immediately before the abort.

The SBL events can cause significant damage to the Belle II detectors and accelerator components in proportion to the beam current, so it is an urgent issue to elucidate the mechanism of the occurrence of such events and to take measures to suppress them. Analysis of data acquired by loss monitors and BORs installed at various locations in the ring [3] indicates that the occurrence of sudden beam loss events is caused by a change in bunch position or an increase in bunch size due to some reason, which leads to a collision with the collimator system. There are three possible patterns of bunch position and size changes, as shown in Fig. 3. *Pattern A* is a usual bunch, *Pattern B* is a bunch position variation, *Pattern C* is an increase in size, and *Pattern D* is a variation in position and size.

As discussed in Ref. [4], we developed a high-speed profile monitor that measures the beam size at each turn. In this study, by comparing the beam size measurement results with the bunch position measured by BOR and the bunch

* gaku.mitsuka@kek.jp

Content from this work may be used under the terms of the CC BY 4.0 licence (© 2025). Any distribution of this work must maintain attribution to the author(s), title of the work, publisher, and DOI.

ISBN: 978-3-95450-262-2 ISSN: 2673-5350 doi: 10.18429/JACoW-IBIC2025-WEDC02

# SUB-MICRON ULTRA THIN SiC FREE STANDING MEMBRANES FOR SOFT X-RAYS BEAM MONITORING

G. Trovato[1,2,3,4], M. Camarda[2,3,5], N. La Rosa[2,6], M. Andrä[7], K. Desjardins[7], S. Finizio[8]
[1]Dipartimento di Fisica e Astronomia "E. Majorana", Università degli studi di Catania, Catania, Italy
[2]STLab s.r.l., Catania, Italy
[3]CNR-IMM, Catania, Italy
[4]Istituto Nazionale di Fisica Nucleare, Sezione di Catania, Catania, Italy
[5]SenSiC GmbH, Villigen, Switzerland
[6]DIEEI, Via Santa Sofia, Catania, Italy
[7]Synchrotron SOLEIL, L'Orme des Merisiers, Saint-Aubin, Gif-sur-Yvette, France
[8]Swiss Light Source, Paul Scherrer Institute, Villigen, Switzerland

Content from this work may be used under the terms of the CC BY 4.0 licence (© 2025). Any distribution of this work must maintain attribution to the author(s), title of the work, publisher, and DOI.

## ABSTRACT

X-ray beam position monitors (XBPMs) are essential diagnostics in modern synchrotron light sources, where they must operate with minimal beam disturbance, excellent linearity and stability under intense photon fluxes. For soft X-ray beamlines, the limited photon penetration depth demands highly transparent detectors. Single-crystal CVD diamond devices, the current standard for many XBPM applications, have been thinned down to a few micrometres to improve transmission, but fabrication challenges and residual absorption below 2 keV remain.

In this work, we characterize a submicrometric free-standing 4H-SiC membrane for the first time using a soft X-ray source, proving such a device to be effective as a beam monitoring element. The membrane, fabricated using a doping-selective electrochemical etching process, has a nominal thickness of 220 nm and a 2 mm × 2 mm active area, with Al electrodes deposited on both sides. Measurements were carried out at the Pollux beamline (SLS) and the Metrologie beamline (SOLEIL) using photon energies of 900 eV and 1000 eV, respectively. Raster-scan transmission mapping demonstrated good and uniform transparency, while current–voltage and beam-induced current measurements yielded the charge collection efficiency across the device.

These results demonstrate that ultra-thin 4H-SiC membranes combine exceptional transparency, mechanical integrity, and electrical performance, making them a promising alternative to diamond for non-invasive beam diagnostics in soft X-ray synchrotron beamlines.

## INTRODUCTION

X-ray beam intensity monitors (XBIMs) and X-ray beam position monitors (XBPMs) are essential diagnostics in synchrotron light sources, where they provide continuous, high-precision measurements of beam position and number of photons. XBIMs and XBPMs must operate with minimal disturbance to the beam, maintain excellent linearity, and remain stable under intense photon fluxes. Solid-state detectors are now a consolidated reality as in-line elements for beam diagnostic, and it is especially true for hard and tender X-rays. For soft X-ray applications, an additional challenge arises from the limited photon penetration depth, making high transmission through the detector a key requirement. This capability is particularly critical for soft X-ray beamlines, where advanced spectroscopic and microscopic techniques require beam stability over extended time scales.

Over the past years, single-crystal chemical vapour deposition (scCVD) diamond has become the material of choice for XBPMs in many synchrotron facilities. Diamond offers a unique combination of low atomic number (Z), excellent thermal conductivity, high carrier mobility, and exceptional radiation hardness. These properties enable reliable operation under high heat loads and intense radiation while maintaining a linear response over a wide dynamic range. Diamond detectors with thickness of 20 µm and 50 µm are now standardized products [1, 2]. Although offering good performance, such devices are still too thick to be used below 2 keV in energies. An attempt to obtain even thinner beam monitors was made by Desjardins et al. [3]. Starting from a 60 µm thick scCVD chip, a 3.3 µm thick membrane was realised using an argon-oxygen plasma etching. This device operates in the low keV range, having high transparency, but showing a 50 % intensity variation in the beam-induced current.

In recent years, 4H-SiC has emerged as a promising alternative material for radiation detectors, including XBIMs and XBPMs [4–6]. 4H-SiC is a wide-bandgap semiconductor with high radiation resistance, good carrier transport properties, and the ability to operate at elevated temperatures. Furthermore, it benefits from mature wafer-scale growth and Silicon-like manufacturing techniques. SiC free standing membranes are produced by SenSiC GmbH with an innovative doping selective electrochemical etching technique. This wet-etching process is favorable to produce membranes given the improved membrane uniformity compared to dry etching techniques. SenSiC's membranes are already a standard in beamline instrumentation technology, offering commercially available devices with thickness >2 µm for tender and hard X-rays applications.

To the same extent of the works on scCVD diamond, submicrometric SiC free-standing membranes would drastically

ISBN: 978-3-95450-262-2 ISSN: 2673-5350 doi: 10.18429/JACoW-IBIC2025-WEPCO01

# SINGLE-SHOT ELECTRON BUNCH PROFILE MONITOR BASED ON COHERENT TRANSITION RADIATION IMAGING

A. Guisao-Betancur*,[1], C. P. Welsch[1], J. Wolfenden[1], University of Liverpool, Liverpool, UK
O. Grimm, E. Mansten, S. Thorin, MAX IV, Lund University, Lund, Sweden
J. Lundquist, Department of Physics, Lund University, Lund, Sweden
[1]also at the Cockcroft Institute, Daresbury, UK

Content from this work may be used under the terms of the CC BY 4.0 licence (© 2025). Any distribution of this work must maintain attribution to the author(s), title of the work, publisher, and DOI.

*Abstract*

The development of longitudinal diagnostics for short-pulse electron accelerators is challenging but necessary to provide high-brightness electron bunches. This is equally true in novel plasma accelerators and for free electron lasers. The gold standard for such measurements is the transverse deflecting cavity (TDC); however, these devices are typically invasive and costly to produce and operate. As an alternative, a THz-based reflective imaging system has been designed and installed at the MAX IV short pulse facility (SPF) for imaging coherent transition radiation (CTR) for bunch profile reconstruction. This contribution presents the progress towards applying transfer learning to deep learning models for evaluating the reconstruction of bunch profiles from experimentally acquired CTR images, building on previous successes in profile prediction using simulated data. Practical resolution limits and the next steps in the development of the monitor are also discussed, where the reconstructions of the longitudinal profile will be achieved using single-shot CTR images and benchmarked against the TDC bunch profiles.

## INTRODUCTION

Ultra-short bunch length measurements are crucial in novel facilities such as high-gradient plasma-based accelerators and light sources like free electron lasers (FELs), where high-quality electron bunches on the femtosecond (fs) range are required. This range poses significant challenges for the development of beam instrumentation and diagnostics [1].

Although transverse deflecting cavities (TDCs) are the gold standard for longitudinal phase space characterization, including bunch profile and length measurements [2–5], minimally or non-invasive setups often rely on radiative techniques instead. In such cases, polarization radiation [6] is produced when the bunch charge is made to emit broadband radiation, which is then studied. Some examples of polarization radiation include Cherenkov (ChR) [7], Smith-Purcell (SPR) [8, 9], and transition radiation (TR) [10]. In all cases, radiation will be coherent for all the wavelengths that are equal to or longer than the bunch length itself, and the analysis can be done using either spectral [10, 11] or time domain methods.

For spectral analysis, the spectral distribution is analyzed using iterative phase retrieval algorithms, knowing that the spectrum of the coherent radiation $S(\rho(z), \omega)$ is given by:

$$S(\rho(z), \omega) = S_p(\omega)[N + N(N-1)F_z(\rho(z), \omega)] ,$$

where $S_p(\omega)$ is the single particle spectrum, $N$ the number of particles in the bunch, and $F_z(\rho(z), \omega)$ the longitudinal form factor [12]. The longitudinal form factor carries information about the bunch profile since it is defined as the modulus squared of the Fourier transform of the longitudinal particle distribution $\rho(z)$:

$$F_z(\rho(z), \omega) = \left| \int_{-\infty}^{\infty} \rho(z) e^{-i\frac{\omega}{c}z} dz \right|^2 .$$

However, the spatial distribution of the image in coherent transition radiation (CTR) has also been proven to contain information about the bunch profile [13]. The image distribution for an electron bunch $I^i_{\text{bunch}}$ for a specific bandwidth is given by:

$$\frac{dI^i_{\text{bunch}}}{dr} \approx N_e^2 \int_{\Delta\omega} \frac{d^2 I^i_e}{d\omega dr} F_z(\rho(z), \omega) d\omega ,$$

where $I^i_e$ is the image distribution for a single electron and $\Delta\omega$ is the bandwidth [13, 14]. With the imaging approach, other sources of radiation, such as synchrotron radiation, become defocused and flattened in the background since they originate outside the TR source plane.

The analysis of the resulting CTR images is not straightforward, as the information about the bunch profile is encoded in the spatial distribution alongside external effects from the optics and detector used, for example. This motivates the use of deep learning to reconstruct the bunch profiles by learning these complex patterns from large amounts of simulated data and transferring the knowledge (transfer learning) to perform reconstructions from the more limited amount of experimental data.

## SETUP AND CTR IMAGING SYSTEM

The CTR imaging system was designed for installation at the MAX IV short pulse facility (SPF) (see Fig. 1), where it is possible to test with 3 GeV e-beams. SP01 and SP02 are located within the SPF, where the former is the diagnostic beamline containing the high-energy TDC, and the latter is the beamline connecting to FemtoMAX (i.e., to the users) and where the CTR target actuator and imaging system are located.

In the setup (schematic shown in Fig. 2) the production of CTR is achieved by placing with an actuator a 25 mm diameter, 5 mm thick aluminum substrate with a 200 nm gold

* A.M.Guisao-Betancur@liverpool.ac.uk

ISBN: 978-3-95450-262-2 ISSN: 2673-5350 doi: 10.18429/JACoW-IBIC2025-WEPCO02

# STUDY OF XBPM DIAGNOSTIC PARAMETERS IN THE TPS FRONTEND*

C. M. Cheng†, Y. C. Yang, Y. T. Cheng, Y. M. Hsiao, B. Y. Chen, C. Shueh, C. K. Chan
National Synchrotron Radiation Research Center, Hsinchu, Taiwan

*Abstract*

The XBPM installed in the TPS frontend determines the center position of the photon beam using four CVD diamond blades. The combination of XBPM and upstream/downstream EBPM readings of the insertion device enables verification of the photon beam's alignment along the correct trajectory. Significant changes in the beam position or profile, as well as prolonged periods without recalibration, may cause the XBPM measurement data to lose its reliability. Therefore, evaluating the reliability of the XBPM measurement data is of critical importance. By analyzing the deviation between the theoretical and measured blade intensities and calculating the standard deviation of the similarity percentage among the four blades, a reliability indicator is established. The variation of this indicator is analyzed under different conditions and compared with the corresponding Q values.

## INTRODUCTION

The X-ray Beam Position Monitor (XBPM) is mounted within the frontend vacuum chamber of the accelerator and serves to monitor the spatial position of the transmitted synchrotron radiation beam, thereby enabling accurate beamline alignment and diagnostics. In the frontend of the Taiwan Photon Source (TPS), a blade-type XBPM is employed. The main structure of the XBPM is based on the design developed by the Advanced Photon Source (APS) in the United States [1, 2]. Four gold-coated chemical vapor deposition (CVD) diamond blades are mounted on an oxygen-free copper base equipped with internal cooling water channels. The distances between the blade tips are 5 mm in the horizontal direction and 3 mm in the vertical direction. Schematic diagrams showing the side and front views of the XBPM are presented in Fig. 1.

Signal acquisition and processing are performed using a LIBERA PHOTON, which captures the micro-current generated by CVD diamond blades and calculates the center position of photon beam in real time. Most of XBPM1 units installed in the TPS insertion device frontend have completed calibration procedures. These units now provide real-time measurements of the synchrotron radiation beam center position at the frontend, serving as a reference for the control room and beamlines.

### *XBPM Diagnostic Parameters*

The XBPM center position is computed using dedicated calibration parameters. Nevertheless, its positional accuracy is subject to fluctuations arising from multiple factors, including variations in electron beam current, insertion device gap widths, and the dynamic properties of the synchrotron radiation source. Therefore, diagnostic parameters are required to determine whether the position values provided by the XBPM still maintain the same level of accuracy as achieved during the initial calibration.

The Q-value in a four-signal position detector is commonly employed as an indicator of signal stability, particularly in electron position monitor. It is defined by comparing the diagonal signal pairs of the detector. Specifically, the signals from two opposite blades are summed, and the difference between the two diagonal sums is calculated. This difference is then normalized by the total signal amplitude and scaled by a calibration constant $K$, where $A$, $B$, $C$ and $D$ denote the signal intensities collected by the four blades. The corresponding expression is given by Eq. (1):

$$Q = K \frac{(A+C)-(B+D)}{(A+B+C+D)}. \quad (1)$$

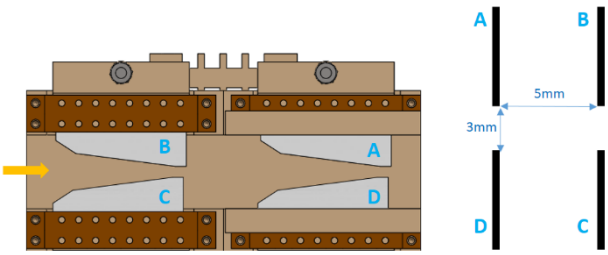



Figure 1: Schematic diagrams of the side and front views of the XBPM in TPS.

The principle of XBPM calibration is based on the correlation between the beam position and the signal intensities collected by four diamond blades. As the synchrotron radiation source shifts position, the photocurrents induced on each blade exhibit corresponding changes in intensity. Within a range of several hundred micrometers, these variations demonstrate an approximately linear relationship, defining what is referred to as the effective linear region. Within this linear region, a stable and reproducible correspondence exists between the beam center position and the blade signal values. Consequently, the beam center can be reliably calculated using a predefined formula [3]. Accordingly, the theoretical blade signal values corresponding to a given beam center position can be calculated using a proportional formula. By comparing these theoretical values with the actual measured blade signals, one can assess whether the current beam position remains accurate relative to the original calibration.

The proportional formula used to compute the theoretical blade signal values is given below. As an example, the calculation for Blade A is shown; the same principle is applied to Blades B, C, and D accordingly. The parameters involved in calculating are defined as Eq. (2):

* Work supported by vacuum group NSRRC.
† chiamucheng@nsrrc.org.tw

Content from this work may be used under the terms of the CC BY 4.0 licence (© 2025). Any distribution of this work must maintain attribution to the author(s), title of the work, publisher, and DOI.

ISBN: 978-3-95450-262-2 ISSN: 2673-5350 doi: 10.18429/JACoW-IBIC2025-WEPCO03

# RESULTS OF HESR BPM TESTING

C. Böhme, Forschungszentrum Jülich, Germany
A. Halama, V. Kamerdzhiev, G. Koch
GSI Helmholtzzentrum für Schwerionenforschung, Darmstadt, Germany

*Abstract*

For the High Energy Storage Ring (HESR) diagonally cut BPMs were designed, with 63 manufactured and tested with a purpose-built BPM test stand. This test stand had to host BPMs of various lengths, the overall length of the vacuum chamber varies from 450 mm to 158 mm. For all BPMs the geometric factors or the electrical center in relation to the geometric center were measured utilizing the test stand. The results of these measurements are presented together with the challenges resulting from the design choices made for the layout of the test stand.

## INTRODUCTION

The HESR, part of the Facility of Antiproton and Ion Research in Europe (FAIR) in Darmstadt, Germany, is dedicated to the field of antiproton and heavy ion physics. The envisaged energy range is 0.8 GeV to 14 GeV for antiprotons and 0.17 GeV/a to 5 GeV/a for heavy ions [1]. The ring will be a racetrack shape with a length of 574 m. The beam instrumentation consists of 64 Beam Position Monitors (BPM), 118 Beam Loss Monitors (BLM), 2 Beam Current Transformers (BCT), 2 Ionization Beam Profile Monitors (IPM), 1 In-Gap Particle Measurement, 1 Schottky Pick-up, 1 Phase Pick-up, 1 Dynamical Tune-meter, 5 Viewer, 2 Scraper, as well as 73 Ion Clearing Chambers and a fast orbit feedback based on the LIBERA beam processors.

## BPM SYSTEM

The pick-up design is based upon the diagonally cut shoebox design of the COSY BPMs [2]. The design is shown in Fig. 1, with more details presented in [3]. While 63 BPMs will have the inner diameter of 89 mm, one is designated to be located downstream of the injection septum, where the beam pipe has a diameter of 150 mm. Therefore, this BPM has to have a larger diameter to not limit the aperture at this place.

In the arcs of the synchrotron, between the dipole magnets, different configurations of quadrupole, sextupole and steering magnets are foreseen, with at least one quadrupole magnet per slot, but a different secondary magnet being in place. Due to the space limitations of the very dense magnet placement, beam pipes of different lengths are directly welded to the BPM vacuum enclosure. This approach results in BPM assemblies of different lengths, 1585 mm, 1249 mm, or 1180 mm. In the straight sections, these restrictions do not apply, therefore a 450 mm long vacuum chamber is used there. The pick-ups themself are identical in each configuration.

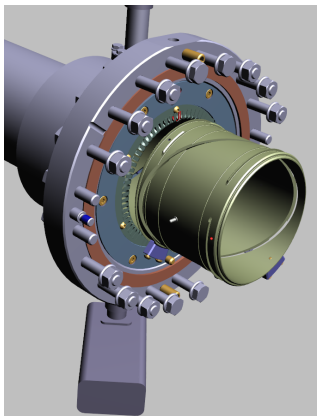


Figure 1: Design of the 89 mm BPM Pick-up.

### *BPM Signal Chain*

Within the FAIR project, the standard BPM signal chain consists of the A110 pre-amplifier [4], which features an amplification range of +60 dB to -60 dB. For the readout and calculation of the beam position the LIBERA Hadron [5] was chosen.

As an addition to the FAIR standard, taking the low expected signal for the HESR into account, an additional 20 dB low-noise head amplifier will be installed directly on the vacuum feedthroughs boosting the input signal of the A110 pre-amplifiers.

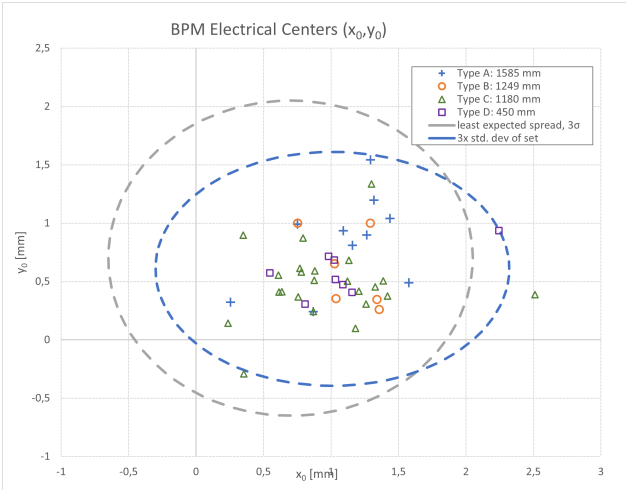



Figure 2: Overview of the measured offsets between the mechanical and the electrical center of the HESR BPMs. The standard deviations of the offsets are $x_0$ = 0.44 mm and $y_0$ = 0.33 mm.

Content from this work may be used under the terms of the CC BY 4.0 licence (© 2025). Any distribution of this work must maintain attribution to the author(s), title of the work, publisher, and DOI.

ISBN: 978-3-95450-262-2 ISSN: 2673-5350 doi: 10.18429/JACoW-IBIC2025-WEPCO04

# $H^-$ BUNCH SHAPE MEASUREMENTS AT LANSCE*

M. J. Kay†, C. E. Taylor, P. M. Anisimov
Los Alamos National Laboratory, Los Alamos, New Mexico, USA

*Abstract*

A Feschenko-style Bunch Shape Monitor (BSM) was used to measure the longitudinal profile of $H^-$ bunches at the Los Alamos Neutron Science Center (LANSCE) accelerator. The measurements were taken in the 201.25 MHz drift tube linac (DTL), where the design beam energy is 72.72 MeV. The results of the measurements are presented, and several unexpected features of the measurements are discussed.

## INTRODUCTION

Ion beams with three different beam structures are accelerated in the 201.25 MHz DTL at LANSCE. These include a 4 mA $H^+$ beam and two $H^-$ beams, distinguished by different chopping patterns and peak currents of 10 mA and 25 mA [1]. To better understand the longitudinal dynamics of each beam type, a BSM system was acquired from the Institute for Nuclear Research (INR) at the Russian Academy of Sciences and installed between the 3rd and 4th accelerating modules in the DTL, where the design beam energy is 72.72 MeV. The BSM measures the longitudinal profile of individual bunches with comparatively high resolution and is independent of the charge of the incident beam particles. These devices were originally developed for the $H^+$ linac at INR in the 1980s [2, 3] and have since become common diagnostic tools in hadron accelerators around the world [4]. The authors report the results of a study done at the end of the 2024 run cycle to measure longitudinal bunch profiles of the $H^-$ beam and discuss several unanticipated features of the measurements.

## BSM WORKING PRINCIPLE

The operation at the core of the BSM is a coherent transformation of the longitudinal bunch distribution in the temporal domain into a spatial distribution of secondary electrons emitted from a wire target. All variations of the original design put forth by Feschenko perform this core operation [5,6]. The working principle of the BSM at LANSCE is illustrated in Fig. 1. Following from left to right, the bunched ion beam crosses a thin tungsten wire, which is 100 µm in diameter and biased at −10 kV. The interaction liberates low-energy secondary electrons from the surface of the wire at a rate correlated with the incident beam current. The electrons are accelerated away from the wire by the high negative potential, and a fraction pass through an input slit with narrow angular acceptance into the RF deflector. The field inside the RF deflector is a superposition of an electrostatic focusing field and a 402.5 MHz RF field, which imparts a time-dependent transverse kick along the electron beam. The deflecting field maps the phase coordinate of the electrons to a transverse position downstream, coherently transforming the longitudinal distribution into a transverse distribution. The transverse distribution is sampled by the output slit, which transmits electrons corresponding to a "slice" of the longitudinal distribution. The transmitted electrons are then collected in a secondary electron multiplier (SEM) to generate a measurable signal. The steering magnet between the RF deflector and output slit is used to correct static offsets, and the bending magnet and registration collimator provide energy discrimination before the SEM.

The intensity of the SEM signal is proportional to the charge density within a phase slice of the original bunch. The BSM has a phase resolution of 0.5°, which is equivalent to 3.45 ps. The entire longitudinal profile is measured by scanning the phase offset of the deflecting RF field over a sufficient range, which has the effect of translating the spatial distribution of secondary electrons across the output slit. Each phase slice is measured in a separate macropulse, under the assumption that all macropulses are identical. The phase sampling rate is limited to the repetition rate of the macropulses, while the SEM signal is digitized at 1 MHz, allowing observation of the bunch profile evolution within the macropulse. The BSM produces a 2-D measurement of SEM signal strength versus time and phase offset of the deflecting field, which is, in general, not equal to the phase of the linac RF. The BSM wire can also be translated over a 6 mm range to take measurements at different points along the horizontal profile of the beam.

## BUNCH SHAPE MEASUREMENTS

The ion beam parameters used during the study differed from the normal production settings. The macropulse length and repetition rate were lowered from the operational duty factor of 625 µs at 120 Hz to 150 µs at 4 Hz, and the $H^-$ beam current was reduced. This change of configuration was necessary to avoid destroying the BSM wire. A phase step size of 0.2° was used throughout the study, and bunches were sampled within the macropulse every 1 µs. A total of 13 measurements were taken at different horizontal positions separated by 0.5 mm. Figure 2 shows 5 scans, taken at the approximate center of the beam and $\pm$1.0 mm and $\pm$2.5 mm from the center. The top row shows the 2-D scan results. The colormaps are scaled to the maximum signal recorded at each location to maximize contrast with the background. The bottom row shows the longitudinal bunch profiles averaged over the region between 110 µs and 140 µs. The shaded area around the lines represents the $\pm 2\sigma$ uncertainty. The measurements in Fig. 2 exhibit three unexpected features: an intra-macropulse temporal instability; asymmetric bunch

* Work supported by the U.S. Department of Energy and the National Nuclear Security Agency under contract no. DE-AC52-06NA25396.
† mkay@lanl.gov

Content from this work may be used under the terms of the CC BY 4.0 licence (© 2025). Any distribution of this work must maintain attribution to the author(s), title of the work, publisher, and DOI.

ISBN: 978-3-95450-262-2 ISSN: 2673-5350 doi: 10.18429/JACoW-IBIC2025-WEPCO05

# DESIGN OF SPECTROMETER ENERGY MEASUREMENT SETUPS FOR THE FUTURE EUPRAXIA@SPARC_LAB AND SSRIP LINACS

D. Quartullo*, D. Alesini, F. Demurtas, L. Faillace, G. Franzini, A. Ghigo, A. Giribono, R. Pompili, L. Sabbatini, A. Stella, C. Vaccarezza, A. Vannozzi, L. Verra, INFN-LNF, Frascati, Italy
A. Cianchi, Università Tor Vergata, Rome, Italy

*Abstract*

EuPRAXIA@SPARC_LAB is a FEL user-facility currently under construction at INFN-LNF in the framework of the EuPRAXIA collaboration. The electron beam will be accelerated to 1 GeV by an X-band RF linac followed by a plasma wakefield acceleration stage. This high-brightness linac requires diagnostic tools able to measure the beam parameters with high accuracy and resolution. To monitor the beam energy and its spread, magnetic dipoles and quadrupoles will be installed along the linac, together with viewing screens and CCD cameras. Macroparticle beam dynamics simulations were performed to determine the optimal energy measurement setup in terms of accuracy and resolution. Similar diagnostics evaluations were carried out for the spectrometer installed at the 100 MeV RF linac of the beam facility SSRIP (IFIN-HH, Romania), whose commissioning planned for 2026 will be performed by INFN-LNF in collaboration with IFIN-HH. Optics measurements were performed to characterize the resolution and magnification of the optical system foreseen to be used at EuPRAXIA@SPARC_LAB and SSRIP for beam energy monitoring.

## INTRODUCTION

EuPRAXIA@SPARC_LAB is a multi-disciplinary user-facility under construction at INFN-LNF [1, 2]. It is composed of an X-band photoinjector and linac, a discharge plasma capillary and a FEL undulator. The high-brightness linac requires diagnostics tools able to measure with high accuracy and resolution the electron beam parameters along the machine. The beam energy monitoring is important for instance at the exit of the plasma module to quantify the energy jitter, which is the dominant source of the FEL performance instability. Beam energy measurements will be also needed at the beam facility SSRIP (IFIN-HH), based on an RF linac accelerating electron bunches to 100 MeV.

Spectrometers are commonly used in linacs to measure the beam energy and its rms [3–8]. Each spectrometer is a dipole magnet which disperses the beam by energy in the horizontal plane. Quadrupole magnets installed before the dipole focus the beam onto a viewing screen placed after the dipole. From the beam spot at the screen, the energy profile is estimated. The magnets and the screen should be designed to have the desired energy resolution and accuracy. Macroparticle simulations can help significantly for this task.

In this paper, the energy-measurement design is presented for EuPRAXIA@SPARC_LAB and SSRIP. The last section describes the characterization of the optics system which will be used at these accelerators to acquire the beam spots.

## DESIGN OF ENERGY MEASUREMENTS FOR EUPRAXIA@SPARC_LAB

Three spectrometers will be installed along the beamline (Fig. 1, top): downstream of the photoinjector and before the first linac (120 MeV), after the bunch compressor and before the second linac (400 MeV), after the plasma module and before the undulator (1 GeV). For each spectrometer,

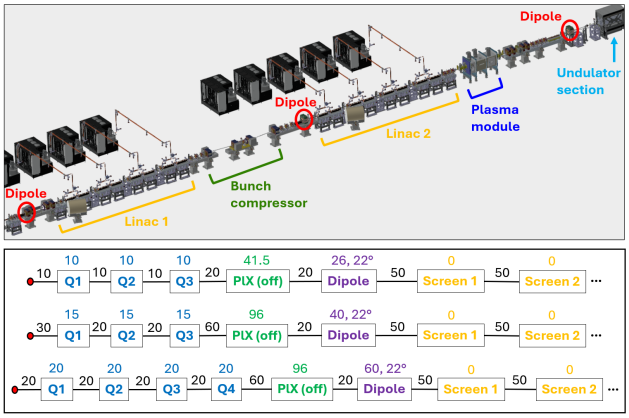



Figure 1: Top: part of the CAD layout of the accelerator EuPRAXIA@SPARC_LAB. The first spectrometer is rectangular (first magnet of the laser-heater chicane), the other two are sector dipoles. Bottom: lattice schemes assumed in the simulations, at 120 MeV (top), 400 MeV (middle) and 1 GeV (bottom). The numbers are lengths in centimeters. The red dots indicate where simulations start. The quadrupoles are in blue. The PolariX RF structures (green) are switched off during the energy measurements. Dipole arc length and bending angle are in purple. After each dipole, the beam spot is analyzed at six evenly-spaced positions ('screens').

macroparticle simulations were performed with the Elegant code [9] to determine where to position the screen (Fig. 1, bottom). The initial beam distributions were obtained from separate macroparticle simulations [2]. The quadrupole strengths found with the MAD-X code [10] minimized the beta function $\beta_x$ at the screen. The quadrupole strengths were below the limits set by the maximum quadrupole gradients. The macroparticle transverse displacements up to the dipole were lower than the smallest half aperture of the lattice. The magnification was chosen as low as possible to maximize the energy resolution at the screen, while avoiding

* danilo.quartullo@lnf.infn.it

Content from this work may be used under the terms of the CC BY 4.0 licence (© 2025). Any distribution of this work must maintain attribution to the author(s), title of the work, publisher, and DOI.

ISBN: 978-3-95450-262-2 ISSN: 2673-5350 doi: 10.18429/JACoW-IBIC2025-WEPCO06

# PERFORMANCE ANALYSIS OF RF ANALOG FRONTEND FOR DIAMOND–II ELECTRON BEAM POSITION MONITORS

H. I. Malik*, M. G. Abbott, L. Bobb, M. Zeeshan
Diamond Light Source, Oxfordshire, United Kingdom

*Abstract*

Diamond-II is a major upgrade to the current synchrotron facility, Diamond Light Source. The low emittance electron beam requires more stable, low drift beam position monitor electronics which are also essential for the Fast Orbit FeedBack system. This paper presents simulated results of the analog frontend for the electron beam position monitors. This work aims to deliver an analog frontend with stable gain and high linearity that meets the dynamic range and noise figure requirements effectively to capture beam positions for single and multi-bunch operation. Performance evaluations have been conducted using the SystemVue simulation suite.

## INTRODUCTION

Diamond Light Source currently operates using a 3 GeV electron beam for the generation of high power X-rays for beamline experiments. A major upgrade is on the way to upgrade the current machine to a fourth generation synchrotron where the electron beam energy will be increased from 3.0 to 3.5 GeV. This will provide scientists with increased brightness and coherence for enhanced experimentation and analytic capabilities. Table 1 summarizes the system requirements for the Electron Beam Position Monitors (EBPM) for Diamond–II (D-II) [1–3].

Table 1: Diamond-II EBPM Requirements

| Parameter | Diamond-II |
|---|---|
| Number of EBPMs | 252 (11/12 per cell) |
| Geometric factor $k$ | 7.3 mm |
| Short-term motion (<1 s) | |
| Commissioning (0.3 mA) | <130 nm/$\sqrt{\text{Hz}}$ |
| User beam (300 mA) | <2 nm/$\sqrt{\text{Hz}}$ |
| Long-term motion (<1wk) | <1 µm pk-pk |

Figure 1 presents the system level diagram for the complete EBPM electronics. In the storage ring the longitudinal placement of the analog frontend (AFE) on the girder is determined by the position of the button assemblies, and vertically they will be placed at the base of the girder to receive minimal radiation. Each girder has 6-8 analog frontends as shown in Fig. 1. A latest inclusion in the design architecture is the Pilot Tone Distributor module (PTD). A PTD module is responsible for receiving the pilot tone from the Control and Instrumentation Area (CIA) and distributing it to Pilot Tone Injectors (PTI), where the power out of the pilot tone distributor is remotely configurable depending on operational mode requirements.

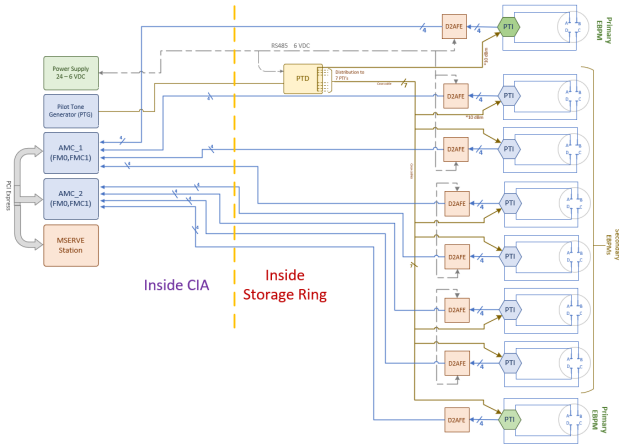



Figure 1: System level diagram of the EBPM architecture.

## D-II ANALOG FRONTEND

The initial work on the D-II analog frontend (D2AFE) is described in [2]. Figure 2 presents the proposed RF chain. The input signal is fed from to the low pass filter (LPF) at 500 MHz, followed by an LC bandpass filter and a digital tunable step attenuator. The first amplifier is a Low Noise amplifier (LNA) with a noise figure of 0.45 name and gain of 24 name, where it contributes mainly towards defining the overall noise figure of the RF chain. The amplifier is followed by a LPF for harmonic suppression and a step attenuator for amplitude control.

The second stage amplifier is a gain block amplifier with higher linearity and a linear gain of 20 dB. A second LC bandpass filter is used for extra filtering and signal conditioning before providing the signal to a 0.5 dB directional coupler. The coupler couples the signal to a log detector for power estimation of the RF signal. An onboard micro controller based analog to digital converter is then used to digitize the detected RF power.

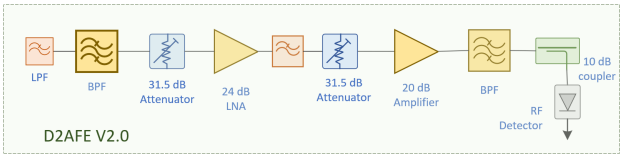



Figure 2: Proposed analog frontend RF chain.

* hasan.malik@diamond.ac.uk

Content from this work may be used under the terms of the CC BY 4.0 licence (© 2025). Any distribution of this work must maintain attribution to the author(s), title of the work, publisher, and DOI.

ISBN: 978-3-95450-262-2 ISSN: 2673-5350 doi: 10.18429/JACoW-IBIC2025-WEPCO07

# FAST BEAM-BASED ALIGNMENT OF BPMS AND QUADRUPOLE MAGNETS FOR SPring-8-II

H. Maesaka*, [1], RIKEN SPring-8 Center, Sayo, Hyogo, Japan
M. Masaki, H. Dewa, S. Takano[2], JASRI Accelerator Division, Sayo, Hyogo, Japan
[1]also at JASRI Accelerator Division, Sayo, Hyogo, Japan
[2]also at RIKEN SPring-8 Center, Sayo, Hyogo, Japan

Content from this work may be used under the terms of the CC BY 4.0 licence (© 2025). Any distribution of this work must maintain attribution to the author(s), title of the work, publisher, and DOI.

*Abstract*

For the SPring-8-II project, a low-emittance upgrade of the SPring-8 light source, an alignment accuracy of 10 µm or better between each BPM and the center of its neighboring quadrupole magnet is required to achieve the design performance. With 340 BPMs in SPring-8-II, a fast beam-based alignment (BBA) method is essential for efficient commissioning. We will install fast power supplies on some steering magnets to rapidly scan the beam orbit, and use auxiliary power supplies or remote-controlled shunt resistors to vary the strength of the target quadrupoles. To assess the feasibility of this method, we conducted a fast BBA experiment at the current SPring-8 storage ring using new MicroTCA.4-based BPM readout electronics, which enable a 10 kHz data acquisition rate. We modulated the strength of a quadrupole magnet adjacent to a BPM with the new readout and scanned the electron beam across the center of the quadrupole by sweeping the strength of a steering magnet. The BPM offset relative to the quadrupole center was determined by analyzing data from all BPMs connected to the fast readout. The BBA precision was estimated to be approximately 10 µm, which satisfies the requirement for SPring-8-II.

## INTRODUCTION

To achieve the design performance of modern low-emittance electron storage rings for high-brightness light sources, precise beam orbit control is essential. The SPring-8-II project [1], a major upgrade of the SPring-8 storage ring aiming for a natural emittance of below 100 pm rad, requires an orbit accuracy of 10 µm. Beam-based alignment (BBA) is a powerful technique for aligning the electrical center of a BPM with the magnetic center of an adjacent quadrupole magnet. Since SPring-8-II will have 340 BPMs [2], performing BBA for all of them would be time-consuming. Therefore, a fast BBA procedure is necessary for efficient beam commissioning.

A fast BBA method has been proposed and demonstrated at the Spanish light source, ALBA [3]. In this approach, specific orbit corrector magnets are sinusoidally excited at several Hz, and beam position data from each BPM is collected with a high sampling rate of 10 kHz. The magnetic center of a target quadrupole is identified by modulating its strength and finding the beam position that remains invariant. This technique allows the BBA for all BPMs to be completed in approximately 10 minutes at ALBA.

* maesaka@spring8.or.jp

At SPring-8, we have replaced the readout electronics of single-pass BPMs with new ones based on MicroTCA.4 (MTCA.4) [4], prior to the complete replacement of the main BPMs for Closed Orbit Distortion (COD) measurement. The new electronics have both single-pass and COD BPM readout capabilities and provides three data rates of the COD, 209 kHz turn-by-turn (TbT), 10 kHz fast acquisition (FA), and 10 Hz slow acquisition (SA). Since the 10 kHz FA data is suitable for the fast BBA procedure, we considered possible setup for the fast BBA at SPring-8-II and tested a similar method at the current SPring-8 storage ring.

## FAST BBA FOR SPring-8-II

The fast BBA method requires dedicated steering magnets capable of rapidly scanning the beam orbit. In the SPring-8-II lattice, there are ten steering magnets per unit cell for both horizontal and vertical planes: two are independent magnets, six are integrated into sextupoles, and two are integrated into octupoles. However, these magnets are used for COD correction during normal operation and are driven by conventional DC power supplies. Since these power supplies cannot generate sinusoidal patterns at several Hz, these magnets are unsuitable for the fast BBA method.

Each unit cell contains four octupoles, all of which have additional coil windings to generate either of a steering dipole field or a skew quadrupole field. While two of them are already allocated as standard steering magnets, the remaining two are available for other purposes. The number of required skew quadrupoles is estimated to be one per two cells, leaving three octupoles every two cells. These can be utilized for fast BBA by equipping them with pattern-capable fast power supplies. The number of fast steering magnets required is estimate to be about four.

The maximum kick angle of the steering magnet integrated with the octupole is 0.2 mrad. Based on the magnet response, a beam position variation of ±0.5 mm is expected at the BPMs when a suitable steering magnet is chosen. This scanning range is considered to be sufficient, since the initial error of the BPM electrical centers is anticipated to be 0.1 mm std. level before BBA.

To determine the magnetic center of a quadrupole, it is necessary to slightly vary its strength and compare the resulting orbits. However, since quadrupoles at the same location in each cell are powered in series by a single large power supply, an additional method is required to individually change the excitation current for BBA. As shown in Fig. 1, there are seven BPMs in each cell, but targeting five quadrupoles is

ISBN: 978-3-95450-262-2 ISSN: 2673-5350 doi: 10.18429/JACoW-IBIC2025-WEPCO08

# DETERMINATION OF DETECTOR FREQUENCY RANGES FOR AN ELECTRON BUNCH LENGTH MONITOR FOR AWAKE RUN 2C

J. McGunigal*,[1,2], G. Xia[1], The University of Manchester, Manchester, UK
C. Davut, TENMAK, Ankara, Turkey
P. Karataev, John Adams Institute at Royal Holloway, University of London, London, UK
T. Lefevre, S. Mazzoni, CERN, Geneva, Switzerland
[1]also at Cockcroft Institute, Warrington, UK
[2]also at CERN, Geneva, Switzerland

*Abstract*

The AWAKE 150 MeV electron beamline at CERN is used to provide a witness bunch for plasma wakefield acceleration, with a bunch length shorter than the plasma wavelength to ensure efficient capture and acceleration. To accomplish this, a real-time, non-invasive bunch length monitor is essential. A monitor is being studied to calculate the RMS bunch length by measuring coherent Cherenkov diffraction radiation with 3 Schottky diodes across different frequency ranges. In this paper, we present theoretical bunch length calculations based on the polarization current approach (PCA) to determine the appropriate frequency ranges for the Schottky diodes. Results show that while higher frequencies are more sensitive to variations in bunch length, they are also influenced by the skewness of a Gaussian longitudinal bunch profile.

## INTRODUCTION

The goal of the Advanced Wakefield Experiment (AWAKE) is to accelerate externally injected electrons using a plasma wakefield driven by a 400 GeV proton bunch [1]. AWAKE Run 2 started in 2021 with the aim to accelerate injected witness electron bunches while preserving the quality of the beam with short bunch lengths of around 200 fs [2]. An electron bunch length monitor based on coherent Cherenkov diffraction radiation (ChDR) is being developed for AWAKE which has been manufactured and experimentally verified to measure shot-by-shot RMS bunch lengths between 100 – 1200 fs demonstrating coherent ChDR as a suitable technique for non-invasive bunch length measurements [3].

Cherenkov radiation (ChR) occurs when a relativistic charged particle passes through a medium faster than the phase velocity of light of that medium. The emitted radiation forms coherent wavefronts that interfere constructively, producing a cone of radiation at a well-defined angle

$$n\beta\cos(\theta_{ChR}) = 1, \tag{1}$$

where $n$ is the refractive index of the medium and $\beta = v/c$. Cherenkov diffraction radiation (ChDR) is produced when the charged particle travels close to a dielectric medium, by inducing polarization currents within the dielectric. ChDR has become a popular mechanism for non-invasive diagnostic tools and its advantages have been studied over the recent years [4, 5].

## PCA THEORY

The spectral angular distribution of ChDR from a point charge traveling in close vicinity to a finite size dielectric prism, as illustrated in Fig.1, can be described using the polarization current approach (PCA). The radiation arises from the polarization current induced at the interface between the dielectric and a medium. This occurs when the effective field radius of the electron, $r_e = \beta\gamma\lambda/2\pi$, where $\gamma$ is the Lorentz factor and $\lambda$ is the wavelength of the emitted polarization radiation, is greater than the impact parameter, $b$ [6].

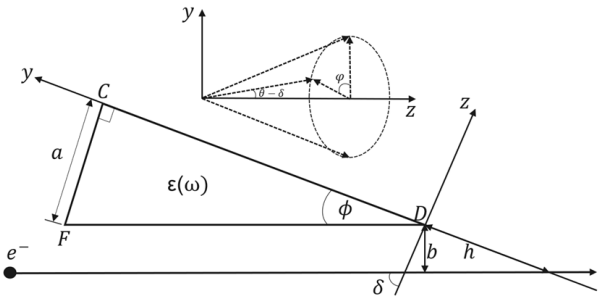



Figure 1: A point-charge electron traversing in close vicinity to a dielectric prism with a cone representing the direction of emitted polarization radiation.

The spectral angular distribution is obtained from Maxwell's equations and Fresnel coefficients. The derivation and more details can be found in Ref. [7] for this particular geometry.

The prism size along the x-axis is assumed to be infinite. This approximation is appropriate when the condition $a/\tan(\phi) >> \lambda$ is satisfied.

## METHODOLOGY

The setup of the monitor for the single-shot RMS bunch length measurements, as shown in Fig. 2, consists of zero-bias Schottky diode detectors with horn antennas 10 cm away from the exit of three alumina radiators. The radiator

* jack.mcgunigal@postgrad.manchester.ac.uk

Content from this work may be used under the terms of the CC BY 4.0 licence (© 2025). Any distribution of this work must maintain attribution to the author(s), title of the work, publisher, and DOI.

ISBN: 978-3-95450-262-2 ISSN: 2673-5350 doi: 10.18429/JACoW-IBIC2025-WEPCO09

# BUNCH BY BUNCH MEASUREMENT AT THE HEPS BY OSCILLOSCOPE

J. He†,1, F. Q. Huang[1], D. C. Zhu[1], Y. Zhao[1], T. G. Xu[1], Y. F. Sui[1,2], J.H. Yue[1], J.S. Cao[1,2]
[1] Institute of High Energy Physics Chinese Academy of Sciences, Beijing, China
[2] University of Chinese Academy of Sciences, Beijing, China

*Abstract*

By directly sampling beam position monitor (BPM) signals using a high-speed oscilloscope, individual bunches' transverse positions and longitudinal phases are resolved with unprecedented precision. A novel technique for extracting longitudinal phase information from oscilloscope data is detailed, achieving a resolution of 0.1 ps. Triggered by the injection timing signal, the oscilloscope captures transient dynamics during beam injection, enabling the derivation of critical parameters such as the longitudinal tune and residual oscillation amplitude, which are essential for optimizing injection efficiency. The injection processes of the High Energy Photon Source (HEPS) — spanning from the linear accelerator to the booster, from the booster to the storage ring, and subsequently from the storage ring back to the booster before re-entering the storage ring — have been thoroughly analysed and optimized using this method, demonstrating substantial potential for practical applications.

## INTRODUCTION

The High Energy Photon Source (HEPS), China's first fourth-generation synchrotron radiation facility, commenced construction in July 2019 and is scheduled for completion in December 2025. During the first beam commissioning phase in the second half of 2024, the stored beam current in the storage ring exceeded 40 mA [1,2]. A critical milestone in beam store was fine-tuning the RF frequency, underscoring the interdependence of three key parameters: the RF frequency, beam energy from the booster, and beam energy set of the storage ring.

Most storage ring diagnostics—including orbit, betatron tune, and dispersion measurements—rely on turn-by-turn or multi-turn beam position data. However, bunch-by-bunch diagnostics provide far richer information. Acquiring transverse positions, longitudinal phases, and charge quantities for individual bunches is essential for understanding accelerator performance, particularly during initial commissioning.

Existing Bunch-by-bunch measurement systems fall into three categories: commercial bunch-by-bunch feedback systems [3], high-speed acquisition boards [4-5], and digital oscilloscopes [6-7]. Among these, the longitudinal phase reconstruction method developed by Prof. Leng's group at the Shanghai Synchrotron Radiation Facility (SSRF) has significantly expanded the applicability of oscilloscope data [8-9].

Commercial oscilloscopes are the most accessible hardware. With tailored algorithms, they can extract extensive accelerator parameters, including the equilibrium phase of bunches, the Phase oscillation amplitudes of injected bunches, the Synchrotron radiation damping coefficients, the Longitudinal tune, and others.

A distinctive feature of the HEPS, setting it apart from typical third- or fourth-generation light sources, is its beam reinjection system. In addition to on-axis injection from the booster to the storage ring, HEPS can kick low-charge bunches back to the booster, merge them with linac-supplied bunches to form higher-charge bunches, and then reinject them into the storage ring [10]. This process demands precise matching of RF systems (energy and phase) between the booster and storage ring.

## DATA PROCESSING METHOD FOR BUNCH-BY-BUNCH LONGITUDINAL PHASE CALCULATING

In this study, BPM signals were acquired using two high-speed oscilloscopes: a Tektronix MSO64BW-6000 (6 GHz bandwidth, 25 GS/s maximum sampling rate) and a LeCroy 760Zi-A (20 GS/s maximum sampling rate). As illustrated in Fig. 1, signals from the BPMs are transmitted via 30-meter LMR-240 coaxial cables to the 6 GHz oscilloscope, synchronized with beam injection triggers. The HEPS employs dual radiofrequency systems operating at 166.6 MHz and 499.8 MHz, though only the 499.8 MHz system is presently operational. The bunch spacing is approximately two ns, and the harmonic number is 2268, with typical bunch charges around 1 nC.

The longitudinal phase of bunches could theoretically be resolved by sampling BPM signals at ultrahigh sampling rates. However, achieving a phase resolution of 0.1 ps would require a sampling rate of 10 THz—a currently unfeasible target due to hardware limitations and prohibitive data storage demands. The amplitude of the longitudinal oscillation of the newly filled bunch is several tens of picoseconds. The difference in equilibrium phases between different bunches is a few picoseconds. To study such issues, a resolution of 0.1 ps is mandatory. The non-integer ratio between the oscilloscope sampling rate and the RF frequency results in non-integer values for both $N_{\mathrm{turn}}$ and $N_{\mathrm{rf}}$. During data concatenation, all sampled points $t_{\mathrm{sampling}}/(T_{\mathrm{rf}} \cdot t_0)$ are rounded to integers and assigned to their respective buckets and turns. For Steady-state studies where the BPM signal self-triggered acquisitions, bunch-filling verification is required only for the first turn. The first and last turns must be checked for injection-triggered acquisitions to identify newly injected bunches and their bucket numbers. Fig. 2(b) demonstrates the concatenated data of one bunch over 550 turns, yielding 27,500 points per RF period. This corresponds to an effective sampling rate of 13.75 THz (25 GHz × 550). Although these points are non-uniformly distributed, interpolation generates a standard

† hejun@ihep.ac.cn

Content from this work may be used under the terms of the CC BY 4.0 licence (© 2025). Any distribution of this work must maintain attribution to the author(s), title of the work, publisher, and DOI.

ISBN: 978-3-95450-262-2 ISSN: 2673-5350 doi: 10.18429/JACoW-IBIC2025-WEPCO10

# BUTTON BPM DEVELOPMENT AND PROTOTYPING FOR ALBA II

L. Torino*, J. M. Alvarez, U. Iriso, O. Traver Ramos, ALBA CELLS, Cerdanyola del Vallés, Spain

*Abstract*

As part of the ongoing ALBA II upgrade, which aims to significantly enhance the performance of the ALBA Synchrotron Light Source, a new design for button Beam Position Monitors (BPMs) is under investigation. In this contribution, we present the results of a characterization study conducted on button prototypes supplied by two different manufacturers.

## INTRODUCTION

In the framework of the upgrade of the ALBA machine [1], 20 buttons have been produced as prototypes by two different manufacturers [2]. The buttons were designed at ALBA [3]: It has a straight design, the button diameter is 4 mm, the gap is anticipated to be 200 µm, no sleeve is expected, the insulator material is borosilicate glass, and the selected connector is a Reverse Polarity SMA. The dimensions, tolerances, and material used are listed in Fig. 1. Each button is labeled with a Serial Number (SN) from 1 to 20.

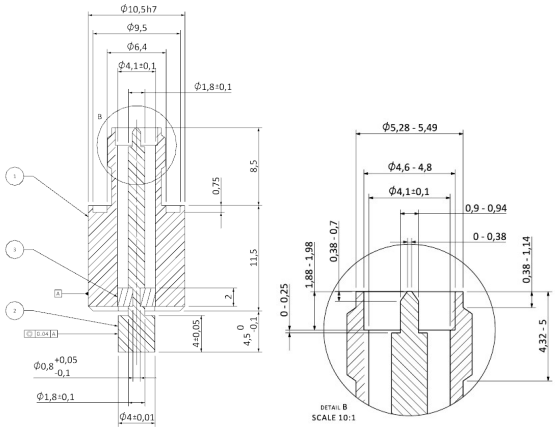



Figure 1: ALBA Button BPM mechanical design.

Materials for each part of the button are listed in the Table 1.

Table 1: BPM button material, the button material differs depending on the manufacturer.

| | | |
|---|---|---|
| 1 | Housing | SS316L |
| 2 | Button | M1: 2.4602 Alloy C22 + Au coating<br>M2: Molybdenum |
| 3 | Insulator | Borosilicate glass |

Extensive mechanical and electromagnetic characterization has been performed to verify that the prototypes were in tolerance. The buttons were then grouped and welded in 4 different blocks, produced by two different companies. Labertson method has been applied to measure the electromagnetic center of each block, and verify the grouping effectiveness. Results are presented in this proceeding.

## ELECTROMAGNETIC CHARACTERIZATION

Time Domain Reflectometry (TDR) measurements were performed using a 9 GHz Vector Network Analyzer (VNA) to assess the electronic properties of the feed-through [4]. Each button was inserted into the aperture of the BPM block for measurement. A complete VNA calibration was performed before each measurement, using the same cable throughout, to minimize the influence of cables and adapters. The obtained TDR rise time result agrees well with the one expected from the CST simulation.

To compare different BPMs we decided to use extract from the TDR the capacitance using the 10 % to 90 % rise time ($\tau_{10-90}$) of the curve and considering the VNA load of 50 Ohm ($Z_0$):

$$C = \frac{Z_0}{\tau}.$$

Each button was measured 10 times after repeated extraction and insertion into the BPM block. Figure 2 shows the results for the two different manufacturers, with dots representing the mean and error bars indicating the standard deviation of the 10 measurements. Measurements were repeated two separate days to assess repeatability.

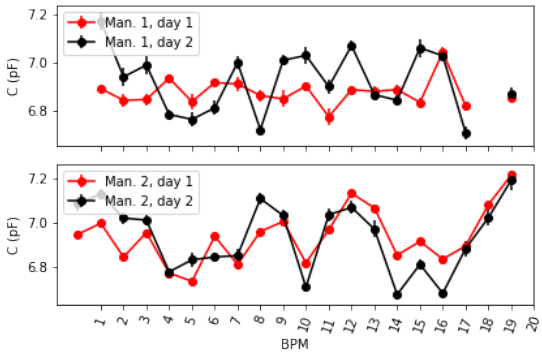



Figure 2: Capacitance measurement of the 20 buttons in two different days. Manufacturer 1: top, Manufacturer 2, bottom.

In case of Manufacturer 1, two of 20 buttons did not fit in the BPM block. The measured capacitance is close to the simulated value (7.5 pF), but measurements taken on different days showed poor repeatability, which is instead present in the case of Manufacturer 2.

* ltorino@cells.es

Content from this work may be used under the terms of the CC BY 4.0 licence (© 2025). Any distribution of this work must maintain attribution to the author(s), title of the work, publisher, and DOI.

ISBN: 978-3-95450-262-2 ISSN: 2673-5350 doi: 10.18429/JACoW-IBIC2025-WEPCO12

# DEVELOPMENT OF A RECTANGULAR DIAGONAL CUT–PLANE BPM FOR THE CSNS-II INJECTION UPGRADE *

M. A. Rehman, X. Nie, Z. Xu, R. Liu, M. Liu, F. Li, B. Zhang, R. Yang, R. J. Yang†
Institute of High Energy Physics, Chinese Academy of Sciences (CAS), Beijing, China
also at China Neutron Spallation Source, Dongguan, China

*Abstract*

As a part of the CSNS-II upgrade, an improved injection scheme will be implemented to mitigate the space charge effect. To precisely measure the transverse beam position during injection, painting, and storage in the Rapid Cycling Synchrotron (RCS), a large-aperture (260 mm × 180 mm) Beam Position Monitor (BPM) is essential. The rectangular cut-plane BPM was selected for its excellent linearity over a large area and high signal-to-noise ratio (SNR). Due to limited space in the injection section, the BPM must be integrated into the AC steering magnet. To prevent thermal heating from eddy current flow, a rib structure has been incorporated into the BPM's outer body. The BPM was designed using numerical simulation codes. This paper details the simulation, design, and experimental results of the diagonal cut-plane BPM.

## INTRODUCTION

The China Spallation Neutron Source (CSNS) [1, 2] is a major facility designed to generate intense pulsed neutron beams, supporting diverse scientific and industrial applications. Its accelerator system comprises three key components: an 80 MeV linear accelerator (linac), a 1.6 GeV Rapid Cycling Synchrotron (RCS), and a solid tungsten target station. The linac produces an 80 MeV $H^-$ beam, which is injected into the RCS via a multi-turn charge exchange mechanism. The RCS accelerates the beam to 1.6 GeV, achieving a beam intensity of $1.56 \times 10^{13}$ protons per pulse and a power output of 100 kW. Recent upgrades, including the integration of harmonic cavities, have increased the beam power to 170 kW [3].

As part of the CSNS-II upgrade, significant hardware improvements are planned to increase the beam power to 500 kW. A critical component of this upgrade involves boosting the beam energy in the linac from 80 MeV to 300 MeV, achieved through the implementation of superconducting cavities. To ensure precise measurement of the transverse beam position, phase, and energy in the new superconducting section of the linac, shorted stripline Beam Position Monitors (BPM) [5, 6] will be utilized. The parameters of CSNS and CSNS-II are summarized in Table 1.

A new injection painting scheme has been proposed [4] for CSNS-II to mitigate injection beam losses and space charge effects. To ensure accurate and precise transverse beam position measurements during injection, painting, and storage in the RCS, a large-aperture BPM is essential. The rectangular cut-plane BPM has been selected due to its excellent linearity over a large area, high signal-to-noise ratio (SNR), and compact mechanical structure, which also allows for integration into the corrector magnet. Since the BPM must be installed within the AC corrector magnet, eddy currents induced by the magnet can cause thermal heating. To address this, a special discontinuous structure has been incorporated into the BPM's outer body to minimize eddy current-induced heating.

Table 1: CSNS and CSNS–II RCS Parameters

| Parameters | CSNS | CSNS–II | Units |
|---|---|---|---|
| Beam Power | 100 | 500 | kW |
| Injection Energy | 80 | 300 | MeV |
| Ring Circumference | 227.92 | 227.92 | m |
| Extraction Energy | 1.6 | 1.6 | GeV |
| Repetition Rate | 25 | 25 | Hz |
| $f_{RF}$ | 1.02-2.44 | 1.02-2.44 | MHz |
| Number of Bunches | 2 | 2 | |
| Beam Intensity | $1.56\times10^{13}$ | $7.8\times10^{13}$ | ppb |

Table 2: Diagonal Cut-plane BPM Parameters

| Parameters | Values |
|---|---|
| Aperture | 260 mm × 180 mm |
| Position Accuracy | 1 % half of Aperture |
| Position Resolution | 200 µm |

## DESIGN AND SIMULATIONS OF DIAGONAL CUT–PLANE BPM

The BPM in the injection region must provide transverse position measurements for the injection, painting, and circulating beam, which has a horizontal offset of approximately ±30.25 mm and a vertical offset of up to ±15 mm. Therefore, the horizontal and vertical apertures of the BPM were set to 260 mm and 180 mm, respectively, allowing for a larger acceptance during beam orbit tuning. The required position measurement accuracy is 1% of the half-aperture of the BPM. Due to stringent space requirements in the injection area, the BPM must also be installed inside the AC corrector magnet. To satisfy all the above requirements, a rectangular-shaped diagonal cut-plane BPM was chosen. The design parameters of the BPM are listed in Table 2.

* Work supported by National Science Foundation for Young Scientists of China (12305166).
† yangrenjun@ihep.ac.cn

Content from this work may be used under the terms of the CC BY 4.0 licence (© 2025). Any distribution of this work must maintain attribution to the author(s), title of the work, publisher, and DOI.

ISBN: 978-3-95450-262-2 ISSN: 2673-5350 doi: 10.18429/JACoW-IBIC2025-WEPCO14

# SPIRAL BEAM POSITION MONITOR FOR HEAVY ION BEAMS

T. Adachi†, T. Nishi, T. Watanabe, O. Kamigaito
RIKEN Nishina Center, Wako, Japan

*Abstract*

For slow, short, and thick beams, spiral shaped beam position monitors (BPMs) are expected to provide good linearity and multiple information readouts despite their small size. At the RIKEN Nishina Center, ion beams are accelerated using linacs and cyclotrons. However, some beams are slow enough compared to relativistic speeds, the bunch length is about the same as the electrode size, and the beam diameter may be close to the electrode spacing. For such beams, conventional "diagonal cut" or "cosine two-theta cut" (for quadratic moments) BPMs produce deviations in signal heights. To solve this problem, it is expected that the signal height deviation can be eliminated by cutting the electrode in a spiral shape. Furthermore, by cutting in a spiral shape, multiple cuts can be placed in one BPM, and it is expected that beam intensity, horizontal position, vertical position, and second moment can be read out at a single location. The simulation results show small error within a few percent.

## INTRODUCTION

At RIKEN's RI Beam Factory (RIBF) at the Nishina Center, a combination of multiple accelerators is used to accelerate various ions—from hydrogen to uranium—for experimental applications. Ion beams, due to their large mass, often remain non-relativistic even after acceleration. Such slow beams are susceptible to space-charge effects, necessitating beam transport at large diameters to mitigate these effects. Under these conditions, conventional assumptions for BPM responses, such as the beam traveling at near light speed ($\beta \sim 1$) or having a width $\sigma$ much smaller than electrode gap $D$ ($\sigma << D$), do not hold, requiring special design considerations. For large width beam, high-linearity BPM types, such as diagonal-cut or cosine-two-theta-cut (for second-order moment measurement), exist. However, under our beam conditions, these BPMs yield measurement inaccuracies unless corrected [1].

For instance, a simulation of a diagonal-cut BPM is shown in Fig. 1. It has electrode length of 50 mm, duct inner diameter 40 mm, beam length 0.3 ns, $\beta = 0.1$, and output impedance of 95 Ω reveal differing signal amplitudes between the upper and lower electrodes even when the beam passes through the duct centre. This offset phenomenon can be qualitatively attributed to variations in the axial structure of each electrode.

Notably, this offset becomes negligible when the beam length $\sigma_z$ is much longer than the electrode length $L$ ($\sigma_z >>$ L).

† taihei.adachi@riken.jp

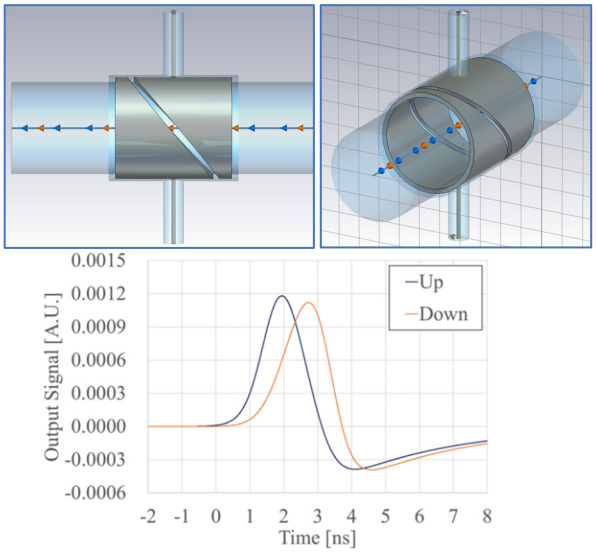



Figure 1: Side view and perspective view of a BPM Model (Top) and simulated signals of the BPM (Bottom).

## SPIRAL CUT BPM

A spiral cut type BPM [2] is shown in Fig. 2. It has 8 electrodes. Each electrode is separated by cosine $\theta$, sine $\theta$, or cosine $2\theta$ curve. The spiral BPM is axisymmetric. So, no deviation in signal height occurs.

By selecting electrode combinations, one can extract four kinds of information: beam intensity, horizontal position, vertical position, and quadratic moments.

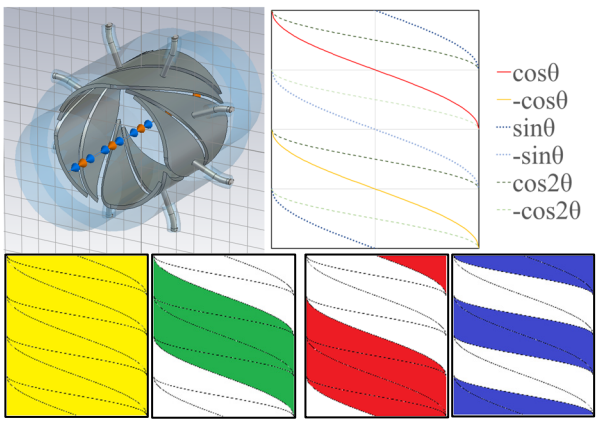



Figure 2: (Top Left) A perspective view of the 8 electrodes spiral BMP model, (Top Right) developed view of electrodes, (Bottom, left to right) the combinations of electrodes to measure intensity, $x$, $y$, and $x^2$-$y^2$.

## DOUBLE INTEGRAL

Even spiral cut type BPM shows non-linearity at non-relativistic velocities. The electric field spreads out along

Content from this work may be used under the terms of the CC BY 4.0 licence (© 2025). Any distribution of this work must maintain attribution to the author(s), title of the work, publisher, and DOI.

ISBN: 978-3-95450-262-2 ISSN: 2673-5350 doi: 10.18429/JACoW-IBIC2025-WEPCO15

# INFLUENCE ANALYSIS OF DIPOLE MAGNET DESIGN AND BEAM COLLIMATION IN THE HIGH-PRECISION ENERGY SPECTROMETRY SYSTEM*

Y. Zeng†, D. Xiao†, D. Lu, Y. Wang, H. Hu
Huazhong University of Science and Technology, Wuhan, China
W. Han‡, The Institute of High Energy Physics of the Chinese Academy of Sciences, Beijing, China
K. Liu, T. Hu‡, Huazhong University of Science and Technology, Wuhan, China

*Abstract*

The high-precision energy spectrometry system, as a key electron beam diagnostic, enables accurate measurement of beam energy distribution and supports injector performance optimization. Beam collimation prior to the system affects measurement accuracy. For electron injectors operating at a few MeV, a high-precision spectrometry system based on the magnetic deflection method is developed, and an energy spectrum model is established to study the design and magnetic field optimization of the key dipole magnet (D-magnet) as well as the influence of upstream beam collimation on beam trajectory accuracy. Simulation results indicate that the optimized D-magnet enhances performance, and beam collimation analysis verifies effective trajectory control, improving system precision and providing technical support for high-precision energy measurements.

## INTRODUCTION

The high-precision energy spectrometry system is employed to measure core electron beam parameters, including energy and energy spread, and to support injector performance optimization in facilities such as free-electron lasers [1, 2], colliders [3, 4], synchrotron light sources [5], and ultrafast electron diffraction systems [6]. For linear accelerators below 20 MeV, used in industrial and medical applications [7–11], accurate beam energy measurement is essential for ensuring both injector output quality and downstream system performance.

Among common beam energy diagnostic methods [12–17], compared with the time-of-flight method, which is characterized by strong energy dependence, the Compton backscattering and synchrotron radiation measurement methods, which are constrained by the need for modification of the original beamline, and the range measurement method, which is limited by slow measurement speed, the D-magnet-based energy analysis method is favored due to its simplicity, ease of implementation, and high resolution. However, this method is dependent on the design quality of the D-magnet and the theoretical description of beam transport, and it is also influenced by deviations in beam alignment during transport.

Based on the compact low-energy injector experimental platform under development at Huazhong University of Science and Technology [18], which is designed for the measurement of key parameters of 3–15 MeV electron beams, the D-magnet has been subjected to an optimized design, and the upstream beam collimation system has been analyzed.

## PRINCIPLE AND DESIGN OF THE ENERGY SPECTROMETRY SYSTEM

The energy spectrometry system, based on magnetic deflection, consists of a D-magnet, drift sections, and a measurement screen. In Fig. 1, the spectrometry system with beam collimation is shown, where the electron bunch is corrected and introduced into the system.

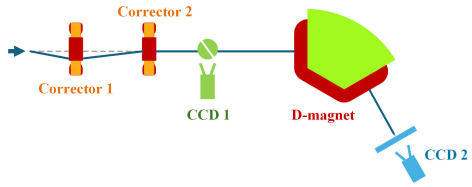



Figure 1: The spectrometry system with beam collimation.

Due to the Lorentz force, electron beams with different energies $E$ and longitudinal distributions are deflected along distinct trajectories when subjected to the magnetic field $B$ of the D-magnet:

$$E = \sqrt{(B\rho ec)^2 + m_0^2 c^4}, \tag{1}$$

where $\rho$ is the radius of curvature, $c$, $e$, and $m_0$ are the speed of light, electron charge, and electron mass, respectively.

On this platform, the energy spectrometry system is designed for point-to-point imaging, with a slit at the entrance to ensure the target distribution reflects the electron bunch energy spread $ES$.

$$ES = \frac{\left(1+\gamma^{-1}\right)}{m_{13}} \sqrt{\langle x_1^2\rangle - m_{11}^2 \langle x_0^2\rangle}, \tag{2}$$

where $\gamma = \frac{E}{E_0}$ denotes the Lorentz factor, $E_0$ is the electron rest energy. The variable $x$ represents the horizontal position, with the subscripts 0 and 1 referring to the entrance and exit parameters of the system, respectively. The quantities

* Work supported by the National Key R & D Program of China (No.2024YFA1612200) and the National Natural Science Foundation of China (No.12341501).
† Equal contribution
‡ hanwj@ihep.ac.cn, TongningHu@hust.edu.cn

Content from this work may be used under the terms of the CC BY 4.0 licence (© 2025). Any distribution of this work must maintain attribution to the author(s), title of the work, publisher, and DOI.

ISBN: 978-3-95450-262-2 ISSN: 2673-5350 doi: 10.18429/JACoW-IBIC2025-WEPCO16

# THE FERMI FEL2 ELECTRO OPTICAL SAMPLING DESIGN AND OPERATIONAL EXPERIENCE

M. Veronese*, A. Abrami, E. Allaria, M. Bossi, P. Cinquegrana, M. Danailov, A. Demidovich, G. Gaio, S. Grulja, G. Pangon, G. Penco, P. Sigalotti, C. Spezzani, M. Trovò, M. Tudor
Elettra Sincrotrone Trieste, Basovizza, Italy

*Abstract*

This paper reports on the design and operational experience of an electro optical sampling (EOS) diagnostics based on the same femtosecond laser used for the seeding process of the FERMI FEL2. This design allows operating in parallel with the FEL2, minimizing time jitter with respect to the seed laser which is the main time marker of the FEL process by removing the time jitter contributions related to the use of an external laser. In our setup a fraction of the energy from the seed laser amplifier is extracted and delivered via a dedicated low vacuum transport system to the EOS setup in the tunnel with beam pointing stabilization actively obtained by piezo actuators. The laser beam size, pulse compression management, polarization cleaning and selection are performed in the tunnel prior to injecting the laser beam in the vacuum chamber. The spatial decoding scheme is employed, with a 100 micron thick GaP crystal and a detection performed in cross polarizers setup using a CMOS camera. The EOS has been characterized in terms of temporal resolution, jitter and drift. Finally, its capability to operate as longitudinal feedback system is also reported.

## INTRODUCTION

The FERMI FEL has the peculiar characteristics to be a seeded FEL [1]. This means that the bunching at the origin of the FEL amplification process is generated by a UV fs laser overlapped in time and space with the electron beam. The energy modulation that is imposed on the electron beam is converted in longitudinal charge modulation by a dispersive section. The temporal properties of the FERMI FEL are hence phase locked with the seed laser. Using a fraction of the seed laser beam for an Electro Optical Sampling (EOS) it is possible to achieve electron beam profile measurements locked with the seed laser timing. In this way one aims at obtaining better performances in terms of temporal jitter and drift compared to using an external laser.

## FEL LAYOUT

FERMI is a seeded FEL based on the high gain harmonic generation (HGHG) scheme [2]. Two FEL lines, FEL-1 and FEL-2, are presently installed at the facility. FEL-1 is a single stage seeded FEL generating coherent light in the 65-20 nm wavelength range. FEL-2 is a double stage seeded FEL based on the fresh bunch injection technique [3], where the additional stage extends the spectral range to 20-4 nm. At FERMI the electron bunch is generated at 10 Hz by a photo-injector GUN with energy of 5 MeV. The electrons are accelerated by an S-band linac. The bunch length can be manipulated by means of a magnetic bunch compressor chicane (BC1). The microbunching present in the bunch can be mitigated before BC1 by a laser heater (LH) system. The final energy is up to 1.5 GeV in FEL operative conditions. After the acceleration, the electrons are injected into one of the two FEL lines (either FEL-1 or FEL-2).

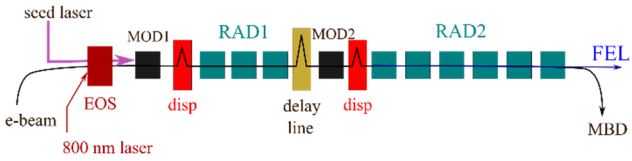



Figure 1: Layout of the FERMI FEL-2.

The EOS diagnostics, as shown in Fig. 1, has been installed in the FEL-2 line, close to the interaction point of the seed laser with the electrons, just before the first modulator of the first stage of FEL-2.

## EOS DESIGN

### *Concept*

The EOS beam instrumentation described in this paper is based on the spatial decoding scheme [4]. In such a design the laser passes the EO crystal at an angle and the position of the beam induced birefringence on the crystal maps the relative timing of the electron beam with respect to the laser.

### *Source*

The laser pulses for the EOS are extracted just outside the IR amplifier (800 nm) in the seed laser optical table locate in the SLR room. The main beam travels to the OPA and is converted to UV in the range 238–267 nm [5] and transported in low vacuum from the SLR room to the undulator hall injection point. The EOS beam is instead directed to another low vacuum transport that brings it to the EOS optical table located in the undulator room just before the first modulator undulator, as depicted in Fig. 2. The IR beam used for EOS has an initial energy of about 100 µJ, a pulse duration of about 350 fs and a diameter of 8 mm.

### *Transport*

The transport consists of a low vacuum line equipped with low GDD mirrors. There are two remotely controllable beam steering points. The first in the SLR optical table

* email address: marco.veronese@elettra.eu

Content from this work may be used under the terms of the CC BY 4.0 licence (© 2025). Any distribution of this work must maintain attribution to the author(s), title of the work, publisher, and DOI.

ISBN: 978-3-95450-262-2 ISSN: 2673-5350 doi: 10.18429/JACoW-IBIC2025-WEPCO20

# DEVELOPMENT OF NOVEL, RADIATION-HARD, ULTRA-COMPACT ACTIVE BEAMSTOPS WITH INTEGRATED 4-QUADRANT X-RAY SENSORS FOR SCATTERING EXPERIMENTS ON HIGH-BRILLIANCE UNDULATOR BEAMLINES

G. Trovato[1,2,3,4], K. Nygard[5], M. Birri[6], D. F. Sanchez[6],
D. Grolimund[6], N. La Rosa[2,7], S. Moscato[2,7], M. Camarda[2,3,7]
[1]Dipartimento di Fisica e Astronomia "E. Majorana", Università degli studi di Catania, Catania, Italy
[2]STLab s.r.l., Catania, Italy
[3]CNR-IMM, Catania, Italy
[4]Istituto Nazionale di Fisica Nucleare, Sezione di Catania, Catania, Italy
[5]MAX IV Laboratory, Lund University, Lund, Sweden
[6]Swiss Light Source, Paul Scherrer Institute, Villigen, Switzerland
[7]DIEEI, Via Santa Sofia, Catania Italy
[8]SenSiC GmbH, Villigen, Switzerland

## ABSTRACT

Beamstopper-Integrated Sensors (BIS) based on silicon carbide (SiC) represent a novel class of compact, radiation hard devices that combine beam interception with real-time diagnostics. We present the first characterization of four-quadrant BIS designed for simultaneous intensity and position monitoring on synchrotron beamlines. Based on the established reliability of single-pixel BIS as intensity monitors at SLS, we demonstrate quadrant-resolved response and linearity with photon flux, despite minor contacting issues in one channel. These results establish SiC BIS as robust, visible-blind diagnostics, leading the way for deployment of position-sensitive BIS in high-brilliance undulator experiments.

## INTRODUCTION

Previous generations of so-called 'active beamstops' attempted to integrate sensing functionality by embedding silicon diodes either directly exposed to the beam [1] or indirectly detecting backscattered photons [2]. Although these pioneering devices provided the first proof-of-concept of beamstop-integrated diagnostics, they were limited by radiation damage, energy-dependent sensitivity, and challenges in miniaturization. The Beamstopper-Integrated Sensor (BIS) represents a new approach, based on silicon carbide (SiC) as the sensing material (Fig. 1). SiC offers a wide bandgap, intrinsic insensitivity to visible light, high thermal conductivity, and extraordinary radiation hardness [3], enabling stable long-term operation even under the most intense synchrotron and XFEL beams. These properties allow BIS devices to provide both intensity monitoring and beam position sensing in ultra-compact footprints (<1 mm), while maintaining robustness and reliability. SiC-based BIS are no longer at the prototype stage: they have been extensively deployed as intensity monitors ($I_0$) at the microXAS beamline of the Swiss Light Source (SLS-PSI), where they have been permanently used for several years across a broad spectrum of scientific experiments.



Figure 1: Left) BiS as intensity monitor, packaging. Right) BiS in operation.

Publications using SiC BIS as flux monitors include environmental and life science applications, such as studies of cyanobacterial microfossils [4], arsenic detoxification in microbial mats [5], and toxicokinetics of uranium nanoparticles in aquatic organisms [6–8]. In parallel, SiC BIS have supported biomedical and materials research, including bone fracture healing [9], zirconium hydride phase mapping in Zircaloy-2 [10], and electrochemical studies of solid oxide cell electrodes and coatings [11, 12]. In the field of additive manufacturing, BIS-enabled operando X-ray diffraction and scattering experiments have been reported in studies of titanium alloys [13–15], steels [16], and programmable alloys [17]. Furthermore, BIS have been instrumental in energy research, including operando studies of Li–air batteries [18]. These results on BIS for intensity monitoring demonstrate that the sensors are reliable and radiation hard, providing robust support for scattering experiments on high-brilliance undulator beamlines. Based on this extensive validation, we now present the first dedicated characterization of BIS devices as position sensors, with the goal of extending their functionalities and enabling novel experiments that exploit post-sample beam position information as an additional diagnostic, complementing the measurements already available.

Content from this work may be used under the terms of the CC BY 4.0 licence (© 2025). Any distribution of this work must maintain attribution to the author(s), title of the work, publisher, and DOI.

ISBN: 978-3-95450-262-2 ISSN: 2673-5350 doi: 10.18429/JACoW-IBIC2025-WEPCO21

# EXPERIMENTS ON A BSM TEST BENCH FOR CSNS-II LINAC UPGRADE*

X. Yang¶, University of Electronic Science and Technology of China, Chengdu, China
W. L. Huang†, L. Zeng, Q. R. Liu, X. Y. Liu, X. J. Nie, Y. G. Wang, B. Tan, J. Liang, J. H. Wei, F. Li, Z. H. Xu, R. Y. Qiu, M. A. Rehman, R. Yang, Y. F. Sui, Institute of High Energy Physics, CAS, Beijing, China, also at China Spallation Neutron Source, Dongguan, China

Content from this work may be used under the terms of the CC BY 4.0 licence (© 2025). Any distribution of this work must maintain attribution to the author(s), title of the work, publisher, and DOI.

## Abstract

A test bench for commissioning the 324 MHz RF deflectors used in BSMs has been in use for the upgrade project CSNS-II linac. The pulsed 10 keV electron beam produced by a Kimball focusable electron gun has been captured by a YAG:Ce screen and imaged by an industrial camera installed vertically right above the view port of the screen after passing through the body of the RF deflector undertest. This paper introduces the verification experiments of static electric lens, RF deflections and bending magnet, also with the postprocessing of the beam spot images. Results of theoretical analysis and the tests were compared and agreed very well. The experiments verified the feasibility of the BSM test bench, playing a critical role in shortening the future commissioning time of BSM equipment in the tunnel.

## INTRODUCTION

The China Spallation Neutron Source (CSNS) comprises an 80 MeV negative hydrogen ion linear accelerator, a 1.6 GeV rapid cycling synchrotron, and a target station [1]. It achieved its design specifications in February 2020, reaching a beam power of 100 kW. In March 2024, the second-phase upgrade project, CSNS-II, was initiated. Table 1 provides a comparative analysis of the parameters between CSNS and CSNS-II [2].

## BSM TEST BENCH SETUP

To meet the requirements for measuring the longitudinal density distribution of beam bunches following the upgrade of the linear accelerator in the second phase of the spallation neutron source project, the independent development of the Bunch Shape Monitor (BSM) was initiated [2]. Prior to the installation of the new BSM in the CSNS linear accelerator tunnel, extensive preparatory and testing work in the laboratory was essential. The 324 MHz radiofrequency deflection cavity and the bending magnet used for deflecting the particle beam was designed, fabricated and commissioned [3].

Currently, a complete BSM verification setup has been established in the laboratory. The full optical path has been constructed, and preliminary verification of the BSM principle has been achieved. A wealth of beam spot observation images has been obtained, and extensive analysis has been conducted. These efforts have laid a solid foundation for the practical application of the BSM in the upgraded accelerator system.

Table 1: Main Parameters of CSNS and CSNSII

| **Project Phase** | I | II |
|---|---|---|
| Beam Power on target [kW] | 100 | 500 |
| Proton energy [GeV] | 1.6 | 1.6 |
| Average beam current [μA] | 62.5 | 312.5 |
| Pulse repetition rate [Hz] | 25 | 25(+25) |
| Linac energy [MeV] | 80 | 300 |
| Linac type | DTL | +Spoke+ELL |
| Linac RF frequency [MHz] | 324 | 324 |
| Macropulse. ave current [mA] | 15 | 50 |
| Macropulse duty factor | 1.0 | 1.7 |
| RCS circumference [m] | 228 | 228 |
| harmonic number | 2 | 2 |
| RCS Acceptance [πmm-mrad] | 540 | 540 |
| Target Material | Tungsten | Tungsten |

## OPTICAL PATH CALIBRATION AND PREPARATORY WORK

The experimental verification setup for the BSM includes a Kimball EGS4212 electron gun, a 324 MHz radiofrequency deflection cavity prototype, an ion pump system, a six-way vacuum chamber, a dipole magnet, a straight-through optical path fluorescence screen, and an imaging assembly consisting of a Microchannel Plate (MCP), a fluorescence screen, and a Basler camera. During the debugging of the electron beam straight-through optical path, the dipole magnet and the MCP+fluorescence screen+Basler camera imaging assembly are not required, as illustrated in Fig. 1.

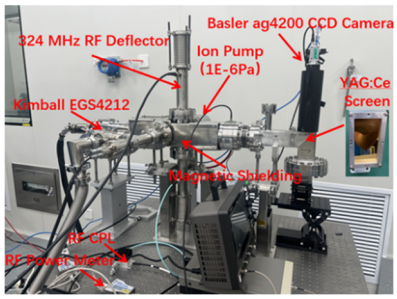



Figure 1: Direct beam optics of the BSM test bench.

During the operation of the electron gun, the parameters are set as follows: $V_{source}$ = 1.2 V, $I_{source}$ = 1.433 A, $I_{emission}$

* Work supported by National Natural Science Foundation, 12275294, Doctoral and Master's Joint Training program of Dongguan Songshan Lake High-Teck Industrial Development Zone, and Mega Science Project Operation Fund of CSNS.
¶ xyang@ihep.ac.cn
† Corresponding author: huangwei@ihep.ac.cn

ISBN: 978-3-95450-262-2 ISSN: 2673-5350 doi: 10.18429/JACoW-IBIC2025-WEPCO22

# HIGH-RESOLUTION LONGITUDINAL BEAM DIAGNOSTICS WITH A FAST FARADAY CUP AT THE UNILAC ACCELERATOR

N. Schmidt*,[1,2], W. Barth[1,3,4], S. Klaproth[1,2,5], M. Miski-Oglu[1], P. Forck[1], R. Singh[1], T. Sieber[1]
[1]GSI Helmholtz Centre for Heavy Ion Research, Darmstadt, Germany
[2]Technical University of Darmstadt, Darmstadt, Germany
[3]Johannes Gutenberg University Mainz, Mainz, Germany
[4]Helmholtz Institute Mainz, Mainz, Germany
[5]Technische Hochschule Mittelhessen, Friedberg, Germany

Content from this work may be used under the terms of the CC BY 4.0 licence (© 2025). Any distribution of this work must maintain attribution to the author(s), title of the work, publisher, and DOI.

*Abstract*

At the heavy ion accelerator UNILAC at GSI Helmholtz Centre for Heavy Ion Research in Darmstadt, measurements were carried out with a FFC in order to precisely measure the time structure of the particle beam. The FFC offers a highly accurate time-resolved recording of the charge distribution along the longitudinal beam profile. The data obtained in combination with a dipole magnet is used to determine the longitudinal phase space and emittance of the beam. After analysing the measurement results, the method will be integrated into the regular beam diagnostics to ensure continuous monitoring and control of the particle beam during operation. Measurement procedure and results are presented.

## INTRODUCTION

The longitudinal charge distribution of a particle bunch is a key property of a beam in ion LINear ACcelerators (LINACs). Due to varying cavity frequencies and acceptance along the accelerator, it is necessary to adjust the longitudinal phase space. This includes knowledge of spread in particle time of arrival with respect to the RF and energy spread.

Typically, one determines the full longitudinal phase space ellipse by measuring one of the projections of the phase space under controlled longitudinal optics settings [1]. This reduces the complexity of longitudinal emittance determination to precise measurement of the longitudinal charge distribution, also referred to as "phase/time of arrival spread" or often just "bunch shape/length".

For this purpose, the UNIversal Linear ACcelerator (UNILAC) has recently been equipped with many Fast Faraday Cups (FFCs) and Bunch Shape Monitors (BSMs). FFCs are variants of the regular Faraday cups optimized for measuring fast time varying charge distributions in the ns regime. This work focuses on a more direct approach to measuring longitudinal emittances using FFCs in dispersive regions. The data presented here has been recorded in July 2025 in a target location called X2 at the UNILAC at GSI with a Radially Coupled Fast Faraday Cup (RCFFC).

This paper provides a brief introduction to the functionality of the FFC, the experimental setup and methods. The focus lies on the ion beam measurement results of the longitudinal phase space distribution performed with the RCFFC.

* nim.schmidt@gsi.de

## FAST FARADAY CUP

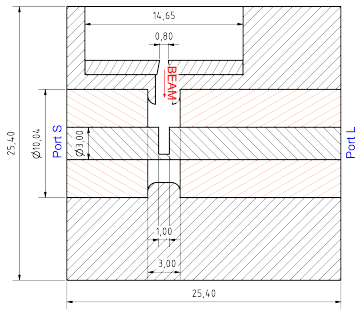



Figure 1: Cross section view of the RCFFC. The beam incidence and port for signal coupling are indicated [2].

The RCFFC has a bandwidth of 5 GHz and a time resolution of 30 ps at $\beta = 0.15$ limited by field dilation effects [3,4] although the RF bandwidth of the FFC structure is higher [5]. It is capable of measuring the longitudinal charge distribution of each bunch along the macro pulse. The beam couples through a blind hole from the side of a coaxial cable through the dielectric medium into the central conductor. In order to minimize the leakage of Secondary Electrons (SEs) , the hole is designed with a width of 1 mm and depth of 2.5 mm, see Fig. 1. Additionally, positive biasing is applied on the collector of the RCFFC to further suppress SEs. The blind hole in the outer conductor of the co-axial is covered with a Titanium-Zirconium-Molybdenum alloy (TZM) disk with a small 0.8 mm hole with the dual purpose of tolerating the heat deposited by the beam and reducing field dilution effects [6].

## MEASUREMENTS

The measurements presented in this work were conducted using $Ar^{8+}$ with an ion beam energy of 11.4 MeV/u and an average beam current of 35 µA. The purpose of this measurement is the determination of the longitudinal emittance using dispersion. When charged particle beams pass through a dispersive section, particles with different kinetic energies are deflected on different trajectories. Hence, in circumstances where the dispersion is sufficiently large, the energy spread can be translated into transverse deflection.

The determination of the dispersion in the X2 beamline at the exit of UNILAC (see Fig. 2) is shown in Fig. 3. For this

ISBN: 978-3-95450-262-2 ISSN: 2673-5350 doi: 10.18429/JACoW-IBIC2025-WEPCO23

# RECENT UPGRADES OF LONGITUDINAL DIAGNOSTICS AT FLASH

M. K.Czwalinna*, J. Kral, J Roever, B. Steffen
Deutsches Elektronen-Synchrotron DESY, Hamburg, Germany

*Abstract*

In the framework of the recent FLASH2020+ upgrade program, the longitudinal electron beam diagnostics of the FLASH accelerator had been modernized and extended by additional devices, including an electro-optical bunch length detector (EOD), as well as an additional bunch compression monitor (BCM) and a bunch arrival-time monitor (BAM) in the new direct seeding beamline FLASH1. Also, the THz intensity spectrometer (CRISP) received a modernized control interface that will allow non-experts to perform bunch profile measurements. The paper presents an overview on the current status of the longitudinal electron beam diagnostics at FLASH and the ongoing (re-)commissioning.

## OVERVIEW

FLASH, the Soft X-Ray and Extreme-UV Free Electron Laser at DESY, has undergone a substantial upgrade and refurbishment within the framework of the FLASH2020+ project. In a previous phase the focus of upgrade had been on renewal of injector lasers for the photo-cathode and an energy upgrade of the linac section to reach 1.35 GeV total beam energy [1]. Within the recent shutdown phase, from June 2024 to August 2025, the FLASH1 beamline has been completely rebuild to allow externally seeded FEL operation [2]. A post-compression arc had been added in front of the IR undulator to further allow for superradiant THz pulse generation.

The remodeling of the FLASH1 electron beamline required, in addition to the primary objective of enabling seeding, the redesign of the electron beam diagnostics or their relocation inside the beamline. This placed significant demands on the beam dynamics engineers, the mechanical designers, and the technical staff who implemented the work. In this paper, we give a short overview of changes and upgrades applied to the following longitudinal diagnostic devices:

- BAM : Bunch Arrivaltime Monitor,
- BCM : Bunch Compression Monitor,
- EOD : Electro-optical Diagnostics,
- CRISP: Coherent Radiation Intensity Spectrometer.

These devices have in common the single-shot capability, mostly non-invasive measurement techniques and their suitability for implementation in beam-based feedback systems. Not covered in this work are destructive detection methods incorporating transverse deflecting structures (TDS) to measure the longitudinal phase space, such as the *LOLA* [3] in FLASH 1 beamline, and the *PolariX*-TDS [4] in FLASH2 as well as in FLASH3 (FLASH Forward) beamline.

* marie.kristin.czwalinna@desy.de

## REQUIREMENTS ON BUNCH DIAGNOSTICS FOR FLASH

The stability level achieved with the previously established beam-based feedback systems is planned to be enhanced by additional beam diagnostics and more advanced algorithms [5]. The additional bunch compression chicanes in FLASH 1 beamline (in the seeding section and in the post-compression arc for THz generation) requires additional diagnostic devices to monitor the bunch compression rate and their timing, e.g. relative to the external seeding lasers. The adjustable current of magnetic bunch compressor chicanes in both, FLASH1 and FLASH2 beamlines, are leading to an arrival time variation from few fs to multiple 10 ps: any timing sensitive equipment thus needs to automatically follow or readjust to these changes. FLASH is operated in a 10 Hz burst mode, with up to 800 µs long bunch trains of 1 MHz intra-burst repetition rate. Comparable to European XFEL, also at FLASH the beam region concept had been implemented already before this shutdown, to allow for individual tunability of beam energy and compression for bunches with different beam destinations within the burst. This poses certain constraints for operation of bunch diagnostics and beam-based feedbacks which act on different bunches within the burst [6].

For the physical requirement reports of the FLASH2020+ project, the demands on beam diagnostics and feedbacks were reconsidered (also based on the optics design for the new FLASH beamline [7]); an extract is given in the Table 1.

Table 1: Operation Parameters, Measurement Accuracy and Stability Demands within Beam-Based Feedback (BBF) Operation at FLASH

| Parameter | Value |
|---|---|
| burst rate | 10 Hz |
| intra-burst rep. rate | 0.05 MHz to 1 MHz |
| bunch charges | 0.01 nC to 1 nC |
| beam regions (BR) | typ. 2 (up to 3) |
| time diff. between BR | ±20 ps (max. ±200 ps) |
| arrival time stability | < 10 fs rms |
| arrival time accuracy | < 5 fs |
| compression accuracy | < 0.1 mrad (RF phase) |

## LONGITUDINAL DIAGNOSTICS DEVICES

This section briefly summarizes the changes applied to the mentioned beam diagnostic devices. Details can be found in the referenced articles. Figure 1 provides a schematic overview of the FLASH facility with its new FLASH1 beamline; highlighted are the locations of the longitudinal beam

Content from this work may be used under the terms of the CC BY 4.0 licence (© 2025). Any distribution of this work must maintain attribution to the author(s), title of the work, publisher, and DOI.

ISBN: 978-3-95450-262-2 ISSN: 2673-5350 doi: 10.18429/JACoW-IBIC2025-WEPCO24

# COMPACT ELECTRO-OPTICAL BUNCH LENGTH DETECTOR: FROM AN EXPERT DEVICE TO AN OPERATOR TOOL

B. Steffen*, M. K. Czwalinna, T. Kozak, D. Rothe
Deutsches Elektronen-Synchrotron DESY, Hamburg, Germany

*Abstract*

Laser-based electro-optic detection (EOD) has been a valuable tool to measure the longitudinal electron bunch shape with sub-ps resolution for more than a decade, but it has always been a tool for expert use. Recently, the server and the user interface have been updated, allowing automated laser locking, time calibration, and measurements to prepare for general operator use at the EuXFEL. It is currently prepared for EO Spectral Decoding measurements, but the implementation of advanced reconstruction algorithms (Diversity Enhanced EO Spectral Decoding) is ongoing. The paper presents details of the setup and user interface, as well as recent measurements.

## INTRODUCTION

Short electron bunches with a high peak current are needed to drive the SASE process in free electron lasers (FELs) like FLASH or the European-XFEL [1, 2]. To reach these short bunches, the initially long electron bunches created at the photocathode guns are compressed in several magnetic bunch compressor chicanes at different electron bunch energies of hundreds of MeV in between accelerating sections.

Electro-optical bunch length detection (EOD) [3] offers the possibility of measuring the longitudinal bunch profile and arrival time in a non-destructive manner with single bunch resolution for every bunch in the bunch train.

The compact EOD setup at Eu-XFEL is in operation since 2016 and at FLASH a copy of the system has been installed in 2024 as part of the enhancement of longitudinal diagnostic capabilities within the recent FLASH2020+ upgrade [4]. However, until recently, the EOD measurements required expert knowledge, python or Matlab programs and a significant amount of manual interaction to the accelerator control system.

## EOD SETUP

Electro-optically active crystals like gallium phosphide (GaP) become birefringent in the presence of an electric field. The electro-optical detection techniques use this effect to transfer the temporal profile of fast changing electric fields by sampling the change in birefringence with laser pulses. Afterwards, the modulated temporal profile of the laser pulse can be analysed with classical laser techniques. A schematic drawing of the setup for spectrally encoded electro-optical detection (EOSD) can be found in Fig. 1.

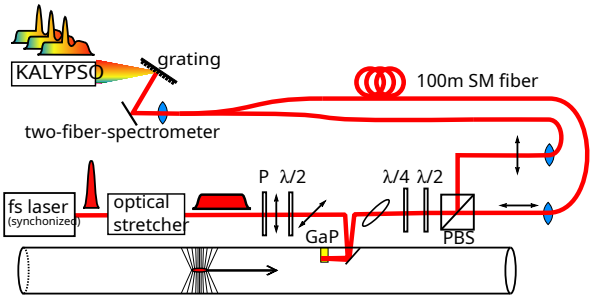



Figure 1: Schematic drawing of a spectrally encoded electro-optical detection setup. P: polariser; PBS: polarizing beam splitter.

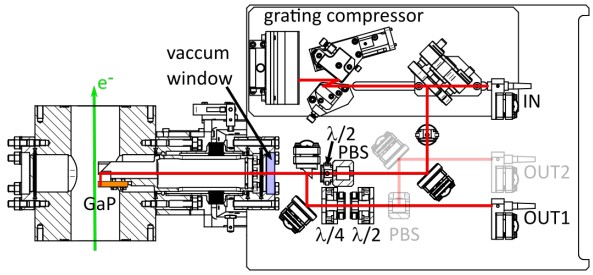



Figure 2: Assembly drawing of the optics set-up at the electron beam line including the vacuum chamber (left). PBS: polarizing beam splitter.

The EOD setup at the European-XFEL is installed at the exit of the 2nd bunch compressor, where the electron bunches have an energy of 700 MeV and usually a bunch length of 250 fs to 1 ps. The crystal is inserted from the side to avoid it being hit by the synchrotron radiation from the bunch compressor magnets (vertical dispersion). The edge of the crystal in the normal measuring position has a distance of about 5 mm from the electron beam path, which is sufficient to avoid particles from the beam halo in normal operation.

The required laser optics (see Fig. 2) are placed above the electron beamline, directly connected to the crystal holder for best alignment stability, while the laser and all electronics are placed in a radiation shielded rack underneath the beamline. For an extensive description of the setup, see Ref. [5].

The setup at FLASH is placed at the entrance of the 2nd bunch compressor at 550 MeV with similar electron bunch conditions, but the laser and electronics can be placed outside the accelerator shielding and can be accessed during accelerator operation and it is equipped with a two-channel

* bernd.steffen@desy.de

Content from this work may be used under the terms of the CC BY 4.0 licence (© 2025). Any distribution of this work must maintain attribution to the author(s), title of the work, publisher, and DOI.

ISBN: 978-3-95450-262-2 ISSN: 2673-5350 doi: 10.18429/JACoW-IBIC2025-WEPCO25

# SOLEIL II BPMS DEVELOPMENT PROGRESS

M. El Ajjouri*, N. Hubert, F. Alves, Z. Fan, A. Gamelin
Synchrotron SOLEIL, Gif sur Yvette, France

*Abstract*

SOLEIL II is the low emittance upgrade project for Synchrotron SOLEIL, targeting a natural emittance of ~ 80 pm · rad. The new lattice includes 196 Beam Position Monitors (BPMs), distributed in three different types depending on the vacuum chamber diameter. To optimize the BPM impedance, the button shape is conical. Electromagnetic and thermal simulations have been performed to validate the proposed designs. In parallel, button prototypes have been installed and tested on the existing machine to confirm the simulation results.

## INTRODUCTION

The upgrade of the SOLEIL synchrotron aims at transforming the facility into a high-performance, fourth-generation light source. This upgrade is driven by significant photon beam properties improvement particularly in terms of brightness, coherence and stability. At the core of the SOLEIL II design is a non-standard MBA lattice: 7BA/4BA, enabling a substantial reduction in horizontal emittance from the current 3.9 nm · rad to 80 pm · rad. As a result of extensive miniaturization of the equipments. The vacuum chamber aperture is only 12 mm in diameter. This reduction demands high precision alignment and the use of advanced materials and mechanical design to minimize impedance and maintain beam stability [1].

## SOLEIL II BPM SPECIFICATION

The BPM system for SOLEIL II is designed to meet stringent performance requirements in terms of resolution, stability and signal-to-noise ratio. Under nominal operating conditions, it will provide a fast acquisition resolution of 100 nm · rms within a bandwidth extending from DC up to approximately 2 kHz, as well as a turn-by-turn (TbT) resolution of 1 µm · rms. During commissioning, with beam currents as low as 0.1 mA. The system will still deliver a TbT resolution of 100 µm · rms. Across the full operating range from 0.1 mA to nominal current, the beam current dependence will be limited to 10 µm. In terms of absolute accuracy, performance will reach better than 500 µm before and 5 µm after beam-based alignment (BBA). Long-term stability will also be a critical feature, with drifts of measurement constrained to 500 nm over one day and 1 µm over one week.

## BPM DESIGN

SOLEIL II baseline lattice includes 196 BPMs distributed along the storage ring. All BPMs are in the shadow of the synchrotron radiation with enlarged tapered section with respect to the vacuum chamber diameter. Depending on their location, BPM will have a different design (Fig. 1):

- BPM16-6 (144 units): achromat BPM with an inner diameter of 16 mm and button diameter of 6 mm including 16 BPMs welded onto dipole vacuum chamber.
- BPM20-7 (40 units): Nominal straight section (SS), or nearby long SS adaptative section BPM with an inner diameter of 20 mm and button diameter of 7 mm.
- BPM24-7 (12 units) : Long SS BPM with an inner diameter of 24 mm and button diameter of 7 mm.

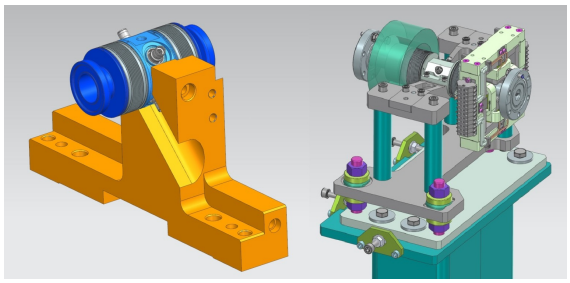


Figure 1: BPM16 for the arcs (left). Including bellows and flanges. The BPM length is only 74.2 mm. BPM20 for the nominal straight sections with Invar stand (right).In addition to the bellows, the block also includes a dedicated thin section to host a fast corrector.

Each BPM acts as a mechanically fixed reference within the vacuum chamber, mounted on dedicated supports attached either to the girder (in arc sections) or to the floor (in straight sections). To minimize thermal expansion, Invar is selected for supports in the straight sections, whereas water cooled steel structures are foreseen for the arcs, pending validation through thermal and vibration analysis. To reduce mechanical stress induced by the vacuum chamber, nearly all BPMs are positioned between two bellows. BPM chambers are fabricated from stainless steel and coated with a 10 µm copper layer to optimize beam impedance.

### *Bunch Length and Profile*

SOLEIL II main operating mode is uniform filling with 416 bunches and a total beam current of 500 mA. 3rd harmonic cavity (HC) will be used to lengthen the bunches to approximately 50 ps · rms, resulting in a non-Gaussian longitudinal profile. This profile will produce a broader frequency spectrum than in the Gaussian case. In the case of a broad band resistive wall type impedance, simulations show that the total beam power loss will be equivalent to the one of a Gaussian bunch 15 % shorter (Fig. 2).

In the case of resonator-like impedances, such as those associated with trapped modes, the broader beam

* moussa.elajjouri@synchrotron-soleil.fr

Content from this work may be used under the terms of the CC BY 4.0 licence (© 2025). Any distribution of this work must maintain attribution to the author(s), title of the work, publisher, and DOI.

ISBN: 978-3-95450-262-2 ISSN: 2673-5350 doi: 10.18429/JACoW-IBIC2025-WEPCO26

# FIRST MEASUREMENTS OF A PROTOTYPE STRIPLINE BPM FOR PETRA IV COMPARISON WITH SIMULATION

S. Strokov†, G. Kube, M. Lantschner, D. Lipka
Deutsches Elektronen-Synchrotron DESY, Hamburg, Germany

*Abstract*

We present signal and thermal measurements from the first prototype of a stripline Beam Position Monitor (BPM) intended for the PETRA IV synchrotron ring. The monitor was installed at the PETRA III testbed for evaluation and compared against CST Studio Suite simulation results. Initial measurements revealed unexpected signal oscillations and significant heating (up to 135 °C) which were not reproduced in ideal models. For a smooth beam pipe, the expected power loss based on the wake-loss factor would only be 5 W. Including mechanical details such as flanges and copper gaskets in the simulation revealed cavity-induced resonances which increased the power loss up to 96 W. The updated model showed good agreement with the measured signals in both time (TD) and frequency domains (FD) as well as with thermal data. Replacing the gasket with a RF-sealing variant lowered the measured temperature to 65 °C. This study highlights that multiple mechanical and electromagnetic factors must be understood and included in simulations to predict beam-induced effects in high-frequency diagnostics accurately.

## INTRODUCTION

The PETRA IV synchrotron [1] requires all vacuum components to have a very low electromagnetic impedance to ensure a stable, high-quality electron beam. Designing diagnostic devices like stripline BPMs is therefore challenging, as they must be sensitive without disturbing the beam.

This paper describes the testing of a stripline BPM prototype for PETRA IV. While simulations of an ideal model predicted successful operation, initial beam tests at the PETRA III facility revealed unexpected problems: the device severely overheated and its signal was distorted.

We demonstrate that these issues were caused by resonant electromagnetic modes trapped in small cavities created by vacuum flanges and gaskets. By identifying this root cause, we developed and successfully tested a modified gasket that solved the problem. Similar challenges with parasitic resonances arising from small geometric discontinuities have recently been reported at the ESRF [2].

This work highlights that for modern accelerators, accurate performance prediction requires simulation of the complete mechanical structure of a component, not just its core elements.

## ELECTROMAGNETIC SIMULATION

The BPM geometry was optimized using High Frequency and Wakefield solvers of CST Studio Suite [3]. The resulting signal from the simulation shows good coupling between the strips and feedthroughs without oscillations behind the main signal peaks (Fig. 1). From the wakefield simulation, a loss factor of approximately 2.7e-03 V/pC was obtained. For the nominal PETRA III beam parameters (100 mA, 40 bunches) this corresponds to a power loss of 5 W.

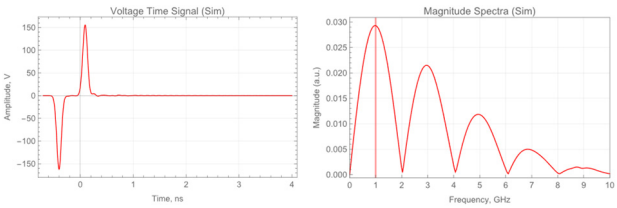



Figure 1: Signal in TD (left) and FD (right). Simulation was performed for bunch length $\sigma_z$ = 13.2 mm (44 ps), bunch charge = 19.2 nC (100 mA, 40 bunches mode). Working frequency of 1 GHz indicated by the red line.

## FABRICATION OF PROTOTYPE

For experimental validation with beam, a prototype was fabricated for installation in the PETRA III test section. While the BPM housing was designed for the 60 mm beam pipe, the core electrode geometry was kept identical to the final 34 mm design intended for PETRA IV (Fig. 2).

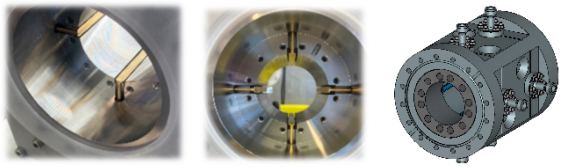


Figure 2: Prototype for PETRA III test section.

## RF MEASUREMENTS

Prior to installation, the prototype's RF characteristics were measured using a Vector Network Analyzer. The S11 values for all eight ports were below the -20 dB requirement across the DC 2 GHz frequency range (Fig. 3).

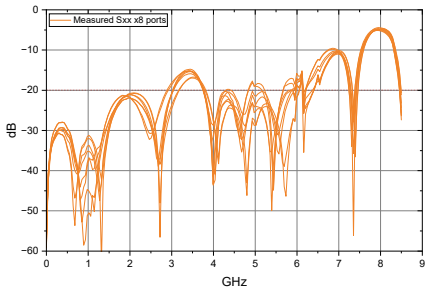



Figure 3: Measured reflection coefficients (S11) of 8 ports.

† sergey.strokov@desy.de

Content from this work may be used under the terms of the CC BY 4.0 licence (© 2025). Any distribution of this work must maintain attribution to the author(s), title of the work, publisher, and DOI.

ISBN: 978-3-95450-262-2 ISSN: 2673-5350 doi: 10.18429/JACoW-IBIC2025-WEPCO27

# MEASUREMENT OF CRABBING ANGLE WITH PHASE INFORMATION FROM BPM*

I. Pinayev†, Brookhaven National Laboratory, Upton, NY, USA

Content from this work may be used under the terms of the CC BY 4.0 licence (© 2025). Any distribution of this work must maintain attribution to the author(s), title of the work, publisher, and DOI.

*Abstract*

The Electron-Ion Collider is being constructed at the Brookhaven National Laboratory. The crab cavities will be utilized for the increase of the luminosity. While the initial set-up of crab cavities can be based on the orbit measurements during dedicated development time, we need to utilize a less invasive approach for monitoring the longitudinal beam tilt during operations. We propose to measure a phase shift between two beam position monitor channels for this purpose. The signal can be easily incorporated into the RF system feedback to suppress noise in the system. Theoretical considerations as well as tests with the electron beams are presented.

## INTRODUCTION

Electron-ion collider will employ multiple transverse deflecting (crabbing) cavities to increase luminosity [1].

For proper compensation of the crossing angle each crab cavity should individually calibrated and phased. At KEK the crabbing angle was measured with the beam displacement [2] depending on the crab-cavity phase. The amplitude of orbit deviation is used for the kick calibration, and the two settings for zero crossings separated by 180 degrees provide information for the phase shift.

During regular operations the scanning of the crab cavities is not possible, and we need to develop alternative method.

## THEORETICAL CONSIDERATIONS

In [3-6] it was proposed to measure the longitudinal tilt using phase information from BPM signals. Following the calculations in [6] we can find the phase shift between two electrodes. Charged induced by relativistic beam with gaussian profile on the buttons A (top) and B (bottom) can be described by formulas [7]:

$$\begin{aligned} Q_A(t) &= \frac{qQ_{bunch}}{\sqrt{2\pi}c\sigma}\left(1+S(y+\alpha ct)\right)exp\left(-\frac{t^2}{2\sigma^2}\right), \\ Q_B(t) &= \frac{qQ_{bunch}}{\sqrt{2\pi}c\sigma}\left(1-S(y+\alpha ct)\right)exp\left(-\frac{t^2}{2\sigma^2}\right), \end{aligned} \quad (1)$$

where $Q_{bunch}$ is bunch charge, $q$ characterizes pick-up geometry (like the ratio of button area to pipe diameter), $\sigma$ is bunch length, $S$ is a BPM scaling factor, $y$ is the position of the bunch center (deflection is in the vertical plane), $\alpha$ is a crabbing angle, $c$ is the speed of light. Here we assume that the induced charge is proportional to the bunch linear charge density ($r/\gamma c \ll \sigma$, where r is vacuum chamber radius and $\gamma$ is a relativistic factor).

The varying button charge will induce a voltage on the cable with impedance Z (neglecting button capacitance). The cosine and sine components can be found using Fourier transformation at the observation angular frequency $\omega$, which might be harmonic of the repetition frequency.

$$\begin{aligned} U_{cosA,B} &= \frac{2}{T}\int_{-T/2}^{T/2} U_{A,B}(t)\cos\omega t\, dt\,, \\ U_{sinA,B} &= \frac{2}{T}\int_{-T/2}^{T/2} U_{A,B}(t)\sin\omega t\, dt\,. \end{aligned} \quad (2)$$

For the short bunches ($\omega \ll T$) the integral limits can be extended to infinity, and the integral can be calculated analytically.

$$\begin{aligned} U_{cosA,B} &\approx \pm\frac{2}{T}ZqQ_{bunch}S\alpha\sigma^2\omega^2 e^{-\frac{\omega^2\sigma^2}{2}}, \\ U_{sinA,B} &\approx -\frac{2}{T}\frac{ZqQ_{bunch}}{c}(1\pm Sy)\omega e^{-\frac{\omega^2\sigma^2}{2}}. \end{aligned} \quad (3)$$

In case of small beam displacements ($Sy \ll 1$) the phases of the signals will be

$$\varphi_{A,B} = \pm\cot^{-1} cS\alpha\sigma^2\omega\,. \quad (4)$$

For small crabbing angles the phase shift between two channels will be

$$\varphi_B - \varphi_A = 2S\alpha c\sigma^2\omega_{BPM}\,. \quad (5)$$

## EXPERIMENTAL SET-UP

Experimental measurement of the longitudinal beam tilt in [6] showed factor two difference between theoretical and observed values of the phase shift. Such large discrepancy required additional investigation to find a source of error. This is also essential since the vertical tilt was developed using fast kicker installed in the region with non-zero dispersion [8].

There are two transverse deflecting cavities available at the C-AD complex for the test of the proposed method. The first one is installed in the Coherent electron Cooling (CeC) experiment, and the second cavity is used by Low-energy RHIC electron Cooling (LEReC). Both cavities are intended for measurement of the longitudinal profile. We can monitor beam size (current profile and bunch length) for both setups during measurements. The longitudinal tilt can be estimated from the vertical r.m.s. beam size (assuming that the emittance contribution is small) and r.m.s. bunch length. It can be also calculated from deflecting cavity

* Work supported by Brookhaven Science Associates, LLC under Contract No. DE-SC0012704 with the U.S. Department of Energy.

† pinayev@bnl.gov

ISBN: 978-3-95450-262-2 ISSN: 2673-5350 doi: 10.18429/JACoW-IBIC2025-WEPCO28

# MEASUREMENT OF TWO BEAMS POSITIONS WITH BUTTON BPM*

I. Pinayev†, Brookhaven National Laboratory, Upton, NY, USA

*Abstract*

Modern BPM processors utilize digital processing of the beam induced signals. The information on the signal amplitudes is used for the delta over sum calculation of the beam position, while the readily available phase information is usually discarded. We have experimentally tested measurement of the individual positions of two beams propagating in the common beampipe utilizing both phase and amplitude data. The proposed method can be used for the energy recovery linacs and colliders.

## INTRODUCTION

Energy recovery linacs (ERL) are considered as next step in development of accelerators with record parameters such as luminosity for the colliders and brightness for the synchrotron radiation light sources.

The essence of the ERL operation implies that at least two beams (accelerated and decelerated) are co-propagating in the same vacuum vessel, and each beam has its own trajectory with more beams co-propagating in the common accelerator section. The conventional beam position monitors (BPM) will measure only "average" trajectory but not that of an individual beam, unless the time separation between bunches is so large that one can resolve individual bunches [1]. Unfortunately, it is not always possible. To overcome the problem, we proposed to utilize phase information of the signal induced on the pick-up electrodes by the circulating beams [2, 3]. Calculations show that the phase difference is directly proportional to the relative displacement of two beams.

The average position of two beams can be found using conventional delta over sum calculations

$$\frac{\delta_1+\delta_2}{2} = \frac{1}{S}\frac{A_{up}-A_{down}}{A_{up}+A_{down}}, \quad (1)$$

where $\delta_{1,2}$ are beams displacement, $A_{up,down}$ are amplitudes of the signal on the electrodes, $S$ is BPM sensitivity coefficient.

The phase shift between two channels is proportional to the positions difference

$$\Delta\varphi = S(\delta_1 - \delta_2)tan(\omega\Delta t_{12}/2). \quad (2)$$

This approach requires measurement of the initial phase shift between channels and suppression of the phase drifts.

## EXPERIMENTAL TESTS

The tests were performed on the Relativistic Heavy Ion Collider (RHIC) at Brookhaven National Laboratory during Run24 utilizing protons at injection energy. RHIC has 120 buckets with 110 filled during regular operations. The arrival time to the common section can be adjusted using phasing of the RF cavities. Wall current monitor is utilized to monitor the charge in the individual bunches. The relativistic parameter β was calculated from the revolution frequency and ring circumference.

RHIC has two rings called blue and yellow for counter-propagating beam. Three Libera Electron Single Pass E BPM receivers [4] are placed in the common section where two beams are separated vertically to avoid collision. The vacuum chamber is round with 50 mm diameter. The button configuration is straight: top-bottom and inside-outside. The positions of the BPMs relative to the center of the straight section are -6.5, 1.1 and 6.5 meters. The BPMs are identified as modulator (mod), amplifier (amp), and kicker (kck) according to the accelerator section names. Since the beams in the collider propagate in opposite direction, the phase shift between them depends on the location of the BPM. For collision point coinciding with the canter the phase shifts are 2.58, -0.39, and -2.53 radians. The measured phase shifts were 2.45, -0.49, and -2.67 radians.

The blue ring has buckets 1-56 filled and yellow ring has buckets 29-84 filled. This way we have three regions of equal duration: a) only blue ring beam, b) both yellow and blue ring beams, c) only yellow ring beam. Regions a and c were used for conventional beam position measurement and for the measurement of the phase offset between channels in BPM. Region b was used for calculation of the beam position using the proposed method. The characteristic fill pattern is shown in Fig. 1. Variation of charge per bucket is few percent.

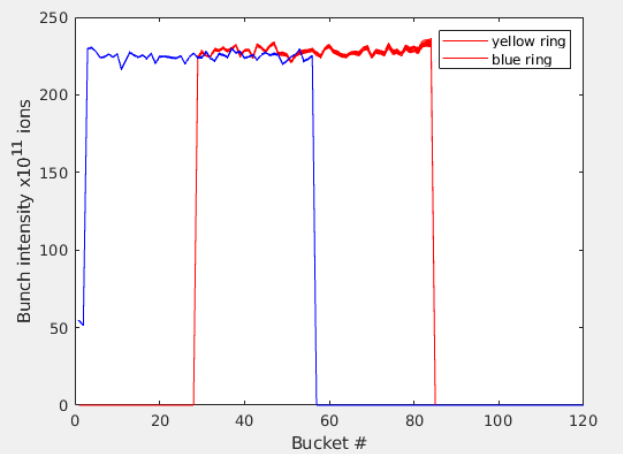



Figure 1: Fill pattern of two rings during experiment.

The observed signals from the pick-up electrodes of on of the kicker BPM are shown in Fig. 2. The ADC readings are fitted with sine wave with known phase advance per

* Work supported by Brookhaven Science Associates, LLC under Contract No. DE-SC0012704 with the U.S. Department of Energy.

† pinayev@bnl.gov

Content from this work may be used under the terms of the CC BY 4.0 licence (© 2025). Any distribution of this work must maintain attribution to the author(s), title of the work, publisher, and DOI.

ISBN: 978-3-95450-262-2 ISSN: 2673-5350 doi: 10.18429/JACoW-IBIC2025-WEPCO29

# DEVELOPMENT OF ANALOG FRONT-END MODULE FOR THE BPM SIGNAL PROCESSOR AT SSRF*

H. Jiang[1,2], L. W. Lai[†,1], Y. K. Xu[3], S. L. Wang[1,2], Q. R. Yan[†,2], Z. Xu[1,2], Z. J. Tang[3]
[1]Shanghai Advanced Research Institute, Chinese Academy of Sciences, Shanghai, China
[2]School of Information Engineering, Nanchang University, Nanchang, China
[3]Shanghai Institute of Applied Physics, Chinese Academy of Sciences, Shanghai, China

*Abstract*

A new BPM processor is being developed to address the ageing of BPM signal processors and the new demand for synchronised data acquisition at the storage ring of Shanghai Synchrotron Radiation Facility (SSRF). The BPM processor consists primarily of a digital carrier board and an analog front-end (AFE) module. The AFE is responsible for the conditioning of the BPM output RF signal and for the compensation of long-term drift. This paper presents the design of the AFE module and gives an evaluation of its performance. The experimental results show that the AFE module under development fully satisfies the high resolution and high stability requirements of the upgraded SSRF BPM processor.

## INTRODUCTION

The Shanghai Synchrotron Radiation Facility (SSRF) is a third-generation synchrotron radiation sources that has been open to users since 2009. The main parameters of SSRF storage ring are given in Table 1.

Table 1: Parameters of SSRF Storage Ring

| Parameter | Value |
|---|---|
| Energy | 3.5 GeV |
| RF frequency | 499.654 MHz |
| Harmonic number | 720 |
| Revolution frequency | 693.964 kHz |
| Current (single bunch) | 5 mA |
| Current (multi bunch) | 200-300 mA |

The storage ring of the SSRF consists of 20 cells and 140 BPM probes. Currently, SSRF employs the Libera Electron and Brilliance series processors for beam position measurements. However, these devices are facing ageing-related issues. To address this, an intelligent upgrade of the storage ring is planned within the next two years, requiring high-speed synchronized acquisition of beam position data across the entire ring. Consequently, the BPM processors must be upgraded to support synchronized timing information from White Rabbit timing system.

In the early stage, we developed an in-house prototype processor using which can no longer meet the present requirements[1-2]. Therefore, a new processor development has been initiated. The new processor will be based on a system-on-chip FPGA, not only reproducing the functionalities of the existing BPM processors, but also integrating White Rabbit timing information.

The RF front end plays a critical role in determining the performance of the BPM processor. By filtering, amplifying, and applying gain control to the four electrode signals from the BPM pickup, the RF front end converts them into RF signals compatible with various beam intensities, facilitating subsequent digitization and processing. In the clock subsystem, phase locking to the accelerator's 694 kHz revolution clock is achieved, followed by generation of a synchronous clock with a 169× frequency multiplication, thereby producing the pilot signal.

## ELECTRONICS DESIGN

Table 2 lists the specification requirements for the AFE module at SSRF.

Table 2: Goals of AFE Module

| Parameter | Value |
|---|---|
| Dynamic range | 60 dB |
| Noise figure | <10 dB |
| Input power | -50 to 0 dBm |
| Center frequency | 499.654 MHz |
| Crosstalk | < -50 dB |
| 3 dB bandwidth | < 30 MHz |
| 1 dB compression point | > 20 dBm |
| RMS Phase Jitter(12K-20M) | < 300 fs |

### *Analog Module*

To meet these requirements, the analog module has been carefully designed. Figure 1 presents the block diagram of the RF chain, while Fig. 2 shows a photograph of the implemented hardware.

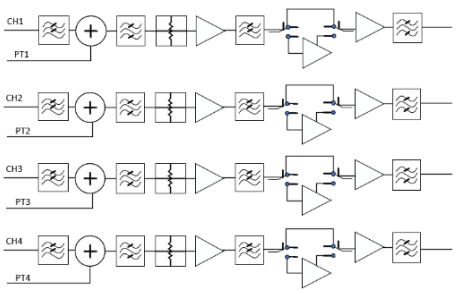



Figure 1: Analog front end block diagram.

* Work supported by The National Science Foundation of China (Grant No.12175239). Youth Innovation Promotion Association, CAS (Gant No.2019290). Outstanding member of the Youth Innovation Promotion Association, CAS(Gant No.Y2023079).
† Corresponding author: lailw@sari.ac.cn, yanqiurong@ncu.edu.cn

Content from this work may be used under the terms of the CC BY 4.0 licence (© 2025). Any distribution of this work must maintain attribution to the author(s), title of the work, publisher, and DOI.

ISBN: 978-3-95450-262-2 ISSN: 2673-5350 doi: 10.18429/JACoW-IBIC2025-WEPCO31

# DEVELOPMENT AND EVALUATION OF AN RFSoC BASED STRIPLINE BPM READOUT HARDWARE PROTOTYPE

B. Urbschat*, Nagoya University, Nagoya, Japan
G. Mitsuka, High Energy Accelerator Research Organization, Oho, Tsukuba, Japan
L. Ruckman, SLAC National Accelerator Laboratory, Menlo Park, California, USA

*Abstract*

We have developed a Stripline BPM readout device based on an AMD/Xilinx RFSoC chip which integrates multiple ADCs, DACs, a large scale FPGA, and an ARM processor in a single package. The developed device is intended for use at the beam transport line connecting the KEK injector Linac to the SuperKEKB collider rings. SuperKEKB will operate at unprecedented luminosities requiring very high beam currents. To reach and maintain such currents, high injection efficiency is essential which in turn requires precise tuning of the injection process. The RFSoC based BPM will provide a highly flexible platform for beam orbit measurements near the injection point required for the tuning. One objective is to enable the separate resolution of the orbit of both bunches in the two-bunch injection mode, where two bunches are accelerated and injected with 96 ns spacing. Additionally, we plan to utilize resulting measurements as inputs for real-time automated injection tuning and feedback to the upstream steering in the beam transport line. Here, we present the status of the development including results from prototype tests conducted at the KEK injector Linac.

## INTRODUCTION

The SuperKEKB collider, while already holding the current luminosity world record of $5.1 \times 10^{34}$ cm$^{-2}$ s$^{-1}$, is still aiming for luminosities much beyond this value. To achieve such high luminosities, beam currents on the order of Ampere must be sustained, which due to the short beam life requires high performance (top-up) injection.

While the injection rate is limited at 25 Hz, a *two-bunch injection* mode is available where charge is injected into two 96 ns spaced buckets within the same injection cycle. However, present instrumentation near the injection point is not able to measure the trajectory of both injected bunches separately, complicating injection tuning.

Specifically the readout electronics of the last last Beam Position Monitor (BPM) before the injection point are not able to process signals from both bunches separately. Thus we develop a new readout device based on the highly flexible Radio Frequency System on a Chip (RFSoC) platform [1].

## HARDWARE

One main advantage of the RFSoC platform is the simplification of hardware development as high performance ADCs and DACs, an FPGA as well as ARM CPU are contained all in the same package. Further, the ADCs of the 3rd generation RFSoCs are known to be highly performant, providing 9.3 effective bits at 4 GS per second [2].

Thus, for the purpose of our development effort a readily available 3rd generation RFSoC evaluation board (RFSoC4x2 by RealDigital, shown in Fig. 1) already provides most of the required functionality, including clock and trigger inputs.

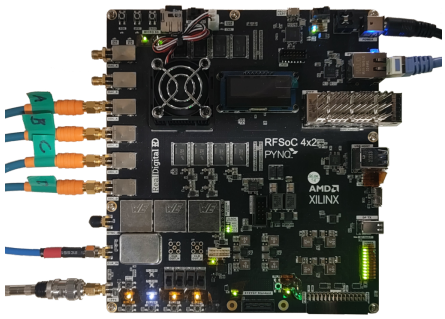



Figure 1: RFSoC4x2 evaluation board used for development.

## SuperKEKB INJECTION POINT BPM

The injection point BPMs for the positron and electron rings of SuperKEKB are each located just after the last septum magnet, slighly upstream of the injection point. A simplified model of the injection point BPM chamber (electron ring) is shown in Fig. 2. The injection beam traverses the small chamber attached to the side of the larger storage beam chamber. Four electrodes of stripline type are located on the top and bottom of the small rectangular chamber.

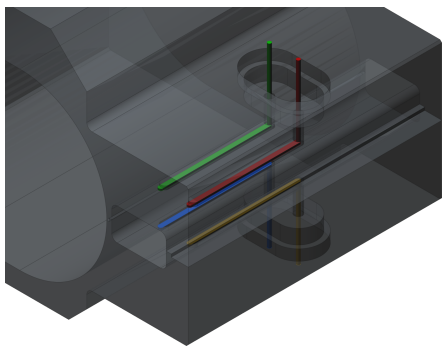


Figure 2: Simplified model of the SuperKEKB injection point BPM chamber (electron ring). The four pickups located on the top and bottom of the chamber are shown in different colors.

* urbsch@hepl.phys.nagoya-u.ac.jp

Content from this work may be used under the terms of the CC BY 4.0 licence (© 2025). Any distribution of this work must maintain attribution to the author(s), title of the work, publisher, and DOI.

ISBN: 978-3-95450-262-2 ISSN: 2673-5350 doi: 10.18429/JACoW-IBIC2025-WEPCO32

# Upgrade of Beam Position Diagnostics System at FELiChEM *

Y.M. Deng[1], Y.B. Leng[†,1], X. Yang[1], D.Y. Wang[1]
[1]University of Science and Technology of China, Hefei, China

*Abstract*

FELiChEM is a user facility dedicated to energy chemistry research, developed at University of Science and Technology of China in Hefei. The beam position diagnostics system at FELiChEM has recently been upgraded. The facility typically operates in a special mode: macro-pulses at 1 Hz repetition rate with microsecond duration, each containing micro-pluses at a 59.5 MHz repetition rate. Both repetition rates are adjustable. The key advancement of beam position diagnostics system lies in the upgraded which now achieves the measurement of micro-pulse position. This enhancement enables real-time measurement of transverse position deviations for individual micro-pluses, providing essential diagnostics for investigating intra-macro-pulse instabilities. Post-upgrade characterization demonstrates a transverse position resolution better than 20 μm, satisfying design specifications. The upgraded system has been successfully integrated into routine operations. This paper will give a brief introduce of the machine, the hardware and software structure of the new micro-pulse position measurement system, and its performance in machine commissioning and operation.

## INTRODUCTION

Free Electron Laser for Innovation Center of Energy Chemistry (FELiChEM) is a user-dedicated facility for energy chemistry research, capable of delivering infrared laser beams in both mid-infrared and far-infrared spectral ranges. The facility's electron gun can generate electron macro-pulses with a maximum duration of approximately 10 μs, each consisting of a train of micro-pulses with a pulse width of about 1 ns and selectable repetition rates of 238, 119, 59.5, or 29.75 MHz [1, 2]. Within the same pulse train, micro-pulses may exhibit positional, phase, and energy discrepancies due to various factors. If the micro-pulse discrepancies are not actively compensated, they will directly degrade the optimal lasing efficiency. However, the previous beam diagnostics system cannot provide micro-pulse-level measurement results, failing to provide effective data support for beam operators during operation. Therefore, during the upgrade, the upgrade of the beam position diagnostics system incorporated micro-pulse-level diagnostic capabilities, with a position measurement resolution better than 20 μm.

## HARDWARE

The hardware of the new beam position diagnostics system consists of a signal processor, a front-end signal processing module, and a frequency synthesizer. The block diagram is shown in Fig. 1.

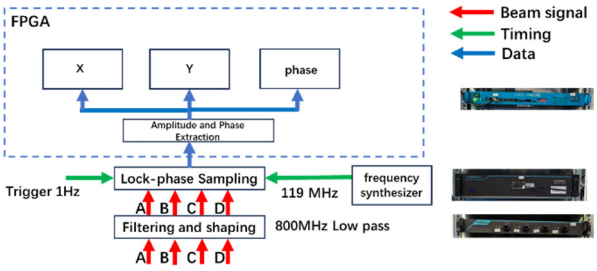



Figure 1: Block diagram of beam position diagnostics system.

The electronics parameters of the new beam position diagnostics system are listed in Table 1.

Table 1: The Electronics Parameters

| Parameter | Value |
|---|---|
| Bandwidth | DC~800MHz |
| ADC bits | 14 |
| MAX ADC rate | 1 GSPS |
| FPGA | xczu15eg |
| Clock | Ext.@119 MHz |
| Trigger | Ext. |

The frequency synthesizer provides a 119 MHz reference clock to the system, which is phase-locked with the beam signal. Additionally, the frequency synthesizer can programmatically adjust the clock phase, ensuring that the sampling points of the measurement system align precisely with the designated positions. The front-end signal processing module is responsible for filtering and shaping, optimizing the beam signal waveform for accurate measurement. The signal processor consists of an ADC module and an FPGA. The ADC module receives the reference clock from the frequency synthesizer and generates a 952 MHz sampling clock using its internal clock chip. The ADC then digitizes the analog signal at a 952 MSPS rate and inputs the digital signal into the FPGA. The FPGA processes the sampled signals to calculate the micro-pulse position data.

The layout of the beam diagnostic system for the FELiChEM is shown in the left panel of Fig. 2. The entire setup employs 10 sets of button probes for beam position measurement. The right panel of Fig. 2 shows the actual hardware configuration, including the signal processor, frequency synthesizer, and the front-end signal processing module.

* Work supported by Large-Scale Scientific Facility Renovation and Upgrade Project of the Chinese Academy of Sciences -"Universal SignalProcessing Platform for Accelerator Beam Measurement and Control"
† email address: lengyb@ustc.edu.cn

Content from this work may be used under the terms of the CC BY 4.0 licence (© 2025). Any distribution of this work must maintain attribution to the author(s), title of the work, publisher, and DOI.

ISBN: 978-3-95450-262-2 ISSN: 2673-5350 doi: 10.18429/JACoW-IBIC2025-WEPCO37

# STUDY OF BEAM POSITION MONITORS FOR PERLE

M. B. Abdillah†, IJCLab, University Paris Saclay, Orsay, France
on behalf of PERLE project team

Content from this work may be used under the terms of the CC BY 4.0 licence (© 2025). Any distribution of this work must maintain attribution to the author(s), title of the work, publisher, and DOI.

*Abstract*

PERLE is an Energy-Recovery Linac (ERL) to be constructed at the IJCLab in Orsay. It will be the First multi-turn ERL with superconducting RF (SRF) with the ambition to reach 5 MW beam operation (20 mA beam current and 250 MeV beam energy). Diagnostics are a key element for PERLE operation and among diagnostics, the salient feature for Beam position monitors (BPMs) is the presence of multiple beams which need to be individually diagnosed and controlled. This document describes the study of PERLE BPMs with particular attention given to how these BPMs will handle multiple beams during commissioning and under normal operation of PERLE.

## INTRODUCTION

PERLE facility is a new generation energy recovery machine covering the 10 MW power regime with 20 mA beam current and 500 MeV beam energy [1]. It is a compact multiple pass ERL based on SRF technology, to serve as testbed for validation and testing a broad range of accelerator phenomena and technical choices for future projects.

An overview of PERLE is sketched in Fig. 1. The photocathode gun is on the far right with the injector section immediately following. In this configuration, the peak beam energy is 250 MeV. This is achieved by passing three times through a SRF cryomodule.

Starting from a 7 MeV injector, the beam gains 82.2 MeV per turn, reaching successively 89 MeV, 171 MeV and a final energy of 250 MeV after 3 recirculation passes. After a path length shift of exactly half of RF period, it is then decelerated through the same linac structure to recover the beam energy up to the final dump at 7 MeV, thereby demonstrating full multi-pass energy recovery at high current.

Looking further ahead, an additional phase of the project is being considered. This upgrade would involve the installation of a second cryomodule in the second straight section, as originally foreseen in the conceptual design report.

## PERLE CONSTRUCTION PHASES

PERLE is currently under construction in the IGLOO building at the IJCLab in Orsay, France. The project is progressing in successive phases, each designed to validate a key step toward the full ERL operation.

The first phase, scheduled for late 2028, focuses on commissioning the injector. This includes testing the high current electron gun, aiming to deliver up to 20 mA of 350 keV electron bunches at a repetition rate of 40 MHz, as well as the superconducting RF booster that accelerates these bunches to 7 MeV. During this phase, the merger section and a diagnostic mirror line will also be constructed and tested to ensure that the beam properties meet the design specifications.

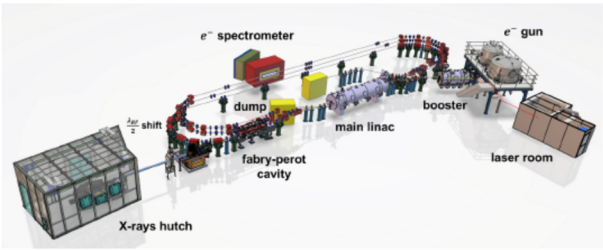



Figure 1: An overview of PERLE.

The second phase, expected to begin in 2029‑2030, will establish and test the one-turn ERL loop. Key objectives of this phase include:

- Calibration of the linac.
- Fine tuning of the beam path length to ensure a maximum energy recovery efficiency.
- A first energy recovery with 89 MeV, 20 mA beam.

The third phase will implement the full three-turn, 250 MeV ERL configuration. Key objectives of this phase include:

- Achievement of 5 MW of energy recovery with 250 MeV, 20 mA beams.
- Demonstration of multi-pass high power energy recovery.

Beam Positions Monitors (BPMs) are a major diagnostic that would ensure a proper operation of PERLE along its construction phases, also for PERLE key components commission and PERLE operation.

The scope of this document is to detail BPMs specifications and operations at different stages of PERLE.

## BPM FOR PERLE INJECTOR

Based on beam dynamics studies, BPM locations are mentioned in Fig. 2.

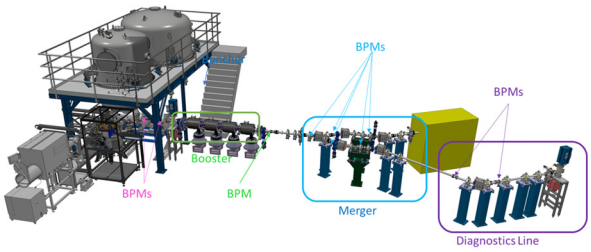



Figure 2: Injector BPMs locations.

As mentioned above, the injector aims to deliver up to 500 pC beam charge with a repetition rate of 40 MHz; the bunch length is about dozens of ps. However, for injector

† sidi-mohammed.ben-abdillah@ijclab.in2p3.fr

ISBN: 978-3-95450-262-2 ISSN: 2673-5350 doi: 10.18429/JACoW-IBIC2025-WEPCO39

# DEVELOPMENT OF BUNCH SELECTOR MODULES FOR DOUBLE BUNCH OPERATION IN PAL-XFEL BPM SYSTEM*

D.C. Shin†, G.J. Kim, C. Kim, H. Yang, S.-W. Jang, H. Heo
Pohang Accelerator Laboratory, Pohang, South Korea

*Abstract*

PAL-XFEL plans to begin double-bunch operation in 2027, with two electron bunches separated by 25 ns. The existing beam position monitor (BPM) electronics were designed for single-bunch operation, so the two signals overlap and bias the position measurement. To support this mode without modifying the electronics, we developed an external radio-frequency (RF) switch-based bunch selector that routes only the selected bunch to the BPM input. We built a prototype and conducted laboratory and on-site tests. This paper presents the hardware and experimental results.

## INTRODUCTION

PAL-XFEL began user service in June 2017 [1]. Initially, only one of the two beamlines could be served at a time. In 2021, time-sharing enabled simultaneous operation of the hard X-ray (HX) and soft X-ray (SX) lines, but it divided the 60 Hz free-electron laser (FEL) repetition rate.

To address this limitation, PAL-XFEL plans to begin double-bunch operation in 2027. Two electron bunches separated by 25 ns are generated in the injector, accelerated together, and then separated by a kicker into the HX and SX beamlines for FEL lasing (Fig. 1). This delivers 60 Hz electron beams to both lines concurrently, effectively doubling facility utilization.

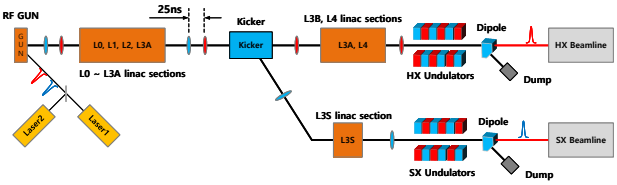



Figure 1: Double-bunch operation at PAL-XFEL.

To realize this mode, several systems are being built or upgraded. This paper reports on the development and initial tests of an external RF switch-based bunch selector that supports double-bunch operation without changes to the existing BPM electronics.

## MOTIVATION AND CONCEPT

Because the BPM electronics include a narrow band-pass filter centered at 300 MHz, two bunches separated by 25 ns overlap at the BPM input and are sampled together. This degrades the accuracy of the X/Y position measurement and perturbs the machine feedback, hindering stable operation.

To improve this, we widened the filter bandwidth and synchronized the sampling clock to the RF timing, then modified the program to conduct multi-bunch processing experiments. However, the increased noise due to the wider bandwidth degraded the measurement resolution, and the risk of RF card damage from high temperature during filter replacement led us to exclude this option.

As a second option, we considered digital down-conversion (DDC) with a low-$Q$ cavity pickup as implemented at SwissFEL [2], but the required hardware changes were prohibitively costly; therefore, this option was also excluded.

Discussions with the beam-physics group led to the conclusion that measuring both bunch positions is not necessary. The trailing-bunch trajectory can be inferred from the leading-bunch position, and after the branch section the remaining controls can satisfy the FEL conditions for each bunch. Consequently, as shown in Fig. 2, an external RF switch-based bunch selection was proposed as the alternative.

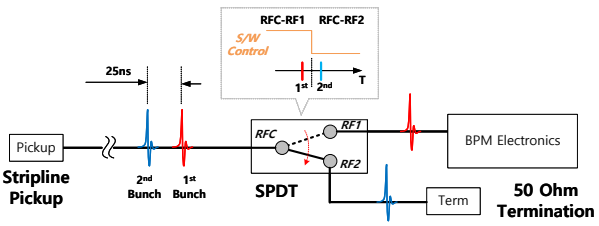



Figure 2: Operating principle of the bunch selector.

By using the switch to pass only one of the two bunches, a single bunch is delivered to the existing BPM electronics. This concept meets the beam-physics requirements while leaving the BPM electronics and operational systems unchanged, and it has the advantage of being realizable within the existing facility operating budget.

## SPECIFICATIONS AND TEST RESULTS

### *Specification*

**System Specifications**

- Operating mode: Select either 1st or 2nd bunch (separated by 25 ns) and route only the selected bunch to the BPM input.
- Resolution: The target position resolution of the selected bunch shall match the single-bunch resolution; the acceptance limit is within 150 % of the single-bunch resolution and shall not exceed 10 µm, as per the initial PAL-XFEL BPM specification [3].

* Work supported by Ministry of Science and ICT of Korea
† dcshin@postech.ac.kr

Content from this work may be used under the terms of the CC BY 4.0 licence (© 2025). Any distribution of this work must maintain attribution to the author(s), title of the work, publisher, and DOI.

ISBN: 978-3-95450-262-2 ISSN: 2673-5350 doi: 10.18429/JACoW-IBIC2025-WEPCO40

# FIBRE-COUPLED OSCILLATOR-DRIVEN ELECTRO-OPTIC SPECTRAL INTERFEROMETRY AS A LONGITUDINAL BUNCH PROFILE MONITOR

S. N. O. Norman*,[1,2], C. Pakuza[3], D. M. Graham[1,2], T. Lefevre[3], D. A. Walsh[1,4], M. T. Hibberd[1,2]
[1]Cockcroft Institute, Sci-Tech Daresbury, Keckwick Lane, Daresbury, UK
[2]University of Manchester, Oxford Road, Manchester, UK
[3]CERN, Meyrin, Geneva, Switzerland
[4]ASTeC, STFC Daresbury Laboratory, Sci-Tech Daresbury, Keckwick Lane, Daresbury, UK

*Abstract*

Electro-optic (EO) diagnostics offer non-destructive methods to resolve the longitudinal charge profile of highly relativistic bunches without the need for complex calibrations or ambiguous phase recovery techniques. The most common technique, EO spectral decoding (EOSD), is favoured for its simplicity, reliability, and straightforward output interpretation, however its resolution is constrained to the geometric mean of the transform-limited and chirped probe laser durations. We have introduced a new technique utilising spectral interferometry (EOSI), which overcomes this limitation by adding a single optical element to an EOSD setup, with successful measurements shown previously on the CLARA accelerator at Daresbury Laboratory. To further explore this technique, we have performed EOSI on the CLEAR accelerator at CERN (160 MeV, 40-70 pC and 0.7-3.5 ps FWHM) utilising a 3 nJ oscillator and optical fibre-coupled transport. Our results highlight the potential for low power, turn-key operation and flexible integration of EOSI systems for single-shot ultrashort bunch length and arrival time monitoring, with the laser and spectral characterisation occurring away from the accelerator.

## INTRODUCTION

With improvements in RF technology, as well as potential novel terahertz (THz) or plasma-based acceleration mechanisms, particle bunches have the potential to be compressed to the 10 fs regime [1–3]. To complement these advances, more precise longitudinal beam diagnostics are required.

Electro-optical (EO) methods detect the Coulomb field of electron bunches, offering direct and non-destructive measurements of the profile of each bunch. A common method is Electro-Optic Spectral Decoding (EOSD) [4, 5], where a chirped laser pulse samples the field and reconstruction is achieved using time-wavelength mapping. This offers some substantial benefits - most notably for its simplicity in implementation and interpretation - but it has a temporal resolution limit of

$$T_{\text{min}} \approx \sqrt{T_{\text{trans-limited}} \cdot T_{\text{chirped}}}, \tag{1}$$

where $T_{\text{trans-limited}}$ and $T_{\text{chirped}}$ are the transform limited and stretched probe laser widths [4]. This leads to a trade off between the sampling window size and the achievable resolution.

Several methods exist that overcome this resolution limitation, but they often require high laser power due to various non-linear processes (*e.g.* temporal encoding [6] or spectral upconversion [7]) or face additional limitations such as in their geometry (*e.g.* spatial encoding [8]). A recent approach has utilised phase diversity to overcome this limit, and is being actively developed [9]. We investigated an alternative technique: Electro-Optic Spectral Interferometry (EOSI) [10]. This adds only one optic to an existing EOSD setup to overcome the limits, with previous work at the CLARA accelerator at Daresbury laboratory measuring bunches as short as 190 fs RMS and showing potential to measure shorter. Here we show that this performance is sustained whilst using a low energy oscillator (3 nJ) with transport to the accelerator hall through long (∼ 70 m) optical fibres, therefore demonstrating the ease of implementation and robustness of this diagnostic tool.

## ELECTRO-OPTIC SPECTRAL INTERFEROMETRY

In all these methods, a laser probe pulse is passed through a zincblende crystal simultaneous to the electric field that is to be detected. Most of the probe passes through unchanged, but a small modulation is created with a polarisation orthogonal to the probe and with a magnitude [11]

$$E_{\text{mod}}(t) = B\frac{d}{dt}\left[E^{\text{eff}}_{\text{clmb}}(t)E_{\text{probe}}(t)\right], \tag{2}$$

where $B$ is a constant accounting for crystal thickness and absorption, and $E^{\text{eff}}_{\text{clmb}}$ is the effective Coulomb field after accounting for the second-order non-linear susceptibility and phase-matching effects. This modulation has the same frequency as the probe, but the temporal envelope is now the same as the Coulomb field and therefore also proportional to the longitudinal charge density profile of the electron bunch.

EOSI measures this modulation by applying a small time delay between the modulation and the probe (in this setup $\tau \sim 1$ ps) using a birefringent crystal, before combining the two pulses with a polariser to create interference in the measured spectrum

$$S_{\text{SI}}(\omega) = S_{\text{probe}}(\omega) + S_{\text{mod}}(\omega) + 2\sqrt{S_{\text{probe}}(\omega)}\sqrt{S_{\text{mod}}(\omega)} \times \cos(\phi_{\text{mod}}(\omega) - \phi_{\text{probe}}(\omega) + \omega\tau), \tag{3}$$

* E-mail: samuel.norman-2@postgrad.manchester.ac.uk

Content from this work may be used under the terms of the CC BY 4.0 licence (© 2025). Any distribution of this work must maintain attribution to the author(s), title of the work, publisher, and DOI.

ISBN: 978-3-95450-262-2 ISSN: 2673-5350 doi: 10.18429/JACoW-IBIC2025-WEPMO02

# PREPARING THE NEXT PHASE OF THE STEADY-STATE MICROBUNCHING PROOF-OF-PRINCIPLE EXPERIMENT AT THE METROLOGY LIGHT SOURCE

A. Kruschinski*, C. Mai, M. Marongiu, M. Ries, Helmholtz-Zentrum Berlin, Berlin, Germany
A. Hoehl, R. Klein, Physikalisch-Technische Bundesanstalt, Berlin, Germany
A. Chao, X. Deng, X. Liu, X. Lu, C. Tang, L. Yan, Z. Yang†, Tsinghua University, Beijing, China

*Abstract*

Steady-state microbunching (SSMB) is a proposed scheme to generate coherent radiation at short wavelengths from a microbunched electron beam in a storage ring. The feasibility of the idea is investigated in an ongoing proof-of-principle (PoP) experiment conducted at the Metrology Light Source (MLS). Phase I of the SSMB PoP experiment has been using an experimental setup employing a single-shot modulation laser to show the general viability of the idea, and has explored the underlying complex storage ring dynamics. The next step in the SSMB PoP campaign is to progress from the single-shot setup of phase I towards quasi-steady state. To this end, a new laser system is installed at the MLS that can provide turn-by-turn modulation of the electron beam for 1000 revolutions or more. The main goal of this phase II of the SSMB PoP experiment will be to show bounded motion of electrons within individual laser-induced microbunches. In this paper, we show the progress of preparation for PoP phase II, with emphasis on the setup and integration of the new laser system and diagnostics challenges.

## INTRODUCTION

The feasibility of SSMB [1–4] has been explored in a proof-of-principle experiment at the MLS since 2018. The first phase of this experimental campaign has recently been completed after showing the feasibility of generating microbunches using the full circumference of an electron storage ring and exploring the necessary conditions on the accelerator to enable this [5–9]. The next phase of the PoP experiment is currently in preparation. The main goal of PoP phase II is to go towards quasi-steady state and show that electrons can be confined within microbunches by providing a turn-by-turn laser modulation. To this end, a new 6.25 MHz repetition rate laser system was designed and set up at Tsinghua University [10], matching the revolution frequency of the MLS. It is currently being installed into the MLS storage ring bunker. Preparations are also being made to make the accelerator setup and radiation detection scheme ready for the next phase of the SSMB PoP campaign.

## PREPARING THE NEW LASER SYSTEM

The main work in preparation of SSMB PoP phase II at the MLS has been the preparation and installation of the new laser system. After shipment of the laser to Berlin, it was commissioned in a separate laser lab at the MLS, its beam properties verified and a telescope set up and characterized to ensure the proper focusing of the beam in the center of the MLS undulator.

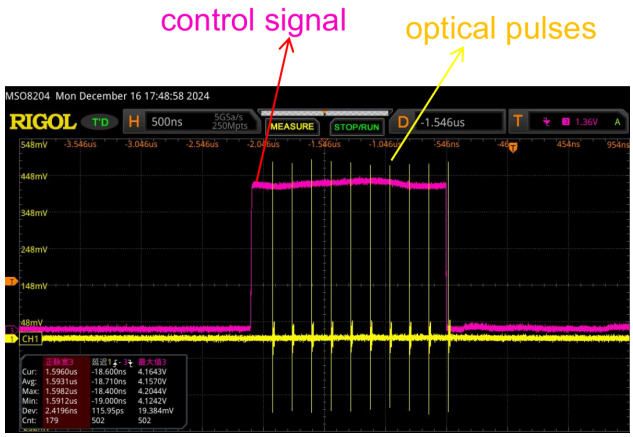



Figure 1: Output of the PoP II laser: Macropulses emitted at a repetition rate on the order of 1 Hz consist of a variable number of micropulses emitted at 6.25 MHz (yellow). The laser supplies a control signal outlining the macropulse to trigger the detection setup (pink).

### *Laser Pulse Properties*

A phase-stabilized seed laser (wavelength 1064 nm), locked to an Iodine absorption line [11], provides the frequency reference for the laser. On the basis of this seeder, a laser amplifier provides a stream of pulses (width: 0.5 ns, peak radiation power: 25 kW) at a repetition rate of 6.25 MHz. An external trigger derived from the MLS revolution clock can be input to synchronize this repetition rate with the accelerator.

From this stream of micropulses, macropulses are formed consisting of a variable number of micropulses (see Fig. 1 for an example macropulse consisting of 10 micropulses). The laser provides a control signal marking the beginning and end of each macropulse, in order to synchronize the radiation detection setup of the SSMB PoP experiment. In this way, the microbunching properties can be studied for an arbitrary number of consecutive modulation events.

### *Installation in the Storage Ring Bunker*

The PoP II laser has been moved into the MLS storage ring bunker in August 2025 (see Fig. 2), and installation of the

* arnold.kruschinski@helmholtz-berlin.de
† yang-z23@mails.tsinghua.edu.cn

Content from this work may be used under the terms of the CC BY 4.0 licence (© 2025). Any distribution of this work must maintain attribution to the author(s), title of the work, publisher, and DOI.

ISBN: 978-3-95450-262-2 ISSN: 2673-5350 doi: 10.18429/JACoW-IBIC2025-WEPMO03

# SMITH-PURCELL AND TRANSITION RADIATION BASED CHARGED PARTICLE BEAM DIAGNOSTICS FOR THE FEMTOSECOND-RANGE

B. Stacey*,[1], W. Kuropka, T. Vinatier, Deutsches Elektronen-Synchrotron DESY, Hamburg, Germany
W. Hillert, Universität Hamburg, Hamburg, Germany
[1]also at Universität Hamburg, Hamburg, Germany

*Abstract*

We will give an overview of the Smith-Purcell and Transition Radiation based longitudinal diagnostic methods employed at the ARES (Accelerator Research Experiment at SINBAD) linear accelerator to characterize femtosecond long electron bunches. The Smith-Purcell radiation mechanism has been studied for the case of metallic gratings, but not much experimental data has been published yet with respect to dielectric gratings as charged particle beam diagnostic devices. We expect a number of advantages in the detection of the radiation at the substrate side and the spectral properties of the radiation tailored by the geometric shape of the grating structures. Due to the advances in lithographic techniques dielectric gratings can be produced with optical wavelength periodicities and the shapes can be controlled with nanometre precision. For femtosecond bunch lengths the coherence of transition radiation starts to reach the near-infrared to optical regime. This opens up the possibility of characterizing the spectrum with readily available high sensitivity semi-conductor based detectors to draw conclusions on the form factor and measure bunch lengths.

## INTRODUCTION

The length of a particle bunch is an important parameter for the accurate operation of accelerators and a crucial requirement in the development of novel acceleration techniques, such a Dielectric Laser Acceleration (DLA) and Plasma Wake Field Acceleration (PWFA). ARES (Accelerator Research Experiment at SINBAD) is a dedicated R&D linac for the production and subsequent diagnosis of single-digit femtosecond bunches and shorter, complete with a movable bunch compressor [1] and PolariX TDS [2] which is capable of single-digit femtosecond resolution through streaking the bunch at numerous angles. This diagnostic method is destructive to the bunch and there is much interest in the development of passive longitudinal bunch diagnostics.

Smith-Purcell Radiation (SPR) has been extensively studied from charged particle bunches passing metallic gratings [3–6], however the case of dielectric gratings has been neglected. A significant advantage of using dielectric gratings is the opportunity to observe the radiation on the substrate side, allowing for simpler geometries [7]. Dielectric gratings can be produced with nanometre precision and properties of the radiation's spectral power distribution can be tailored through careful consideration of the structure's geometry.

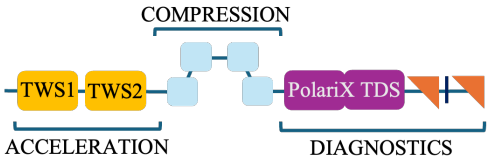



Figure 1: Schematic layout of ARES linac. The acceleration section consists of an electron gun (not pictured) and two Travelling Wave Structures (TWS) and is followed by a magnetic chicane. The diagnostics section has a PolariX TDS and two 45° silver mirrors, one in-vacuum and one in-air after a 50 µm Ti foil.

The radiation factors of SPR scale roughly inversely proportional to $\gamma^2$ [4], which means that, from ultra-relativistic beams, incoherent SPR is extremely challenging to detect. For the use of SPR in beam diagnostics, it is necessary that there is coherent enhancement of the radiation. This means that the bunch should already be shorter than the period of the gratings used. In order to obtain this information "online", Transition Radiation (TR) at optical frequencies can be used as an uncalibrated bunch compression monitor. For single-digit femtosecond bunch lengths, TR at optical frequencies is coherently enhanced and easily detectable.

The spectra of TR and the SPR contains information about the bunch form factor, which can be used to calculate the longitudinal current profile, $S(z)$,

$$F(\omega) = \left| \int_0^\infty dz S(z) \exp^{i(\omega/c)z} \right|^2 . \quad (1)$$

In order to accurately calculate the longitudinal bunch shape, the relative phases of the spectrum are also required. A number of techniques have already been utilised for this purpose, including Kramers-Kronig pairs [8–10] and Frequency Resolved Optical Gating (FROG) [11, 12].

## TRANSITION RADIATION DIAGNOSTICS

The TR produced by the beam incident upon the first 45° silver mirror in Fig. 1 has been used as a bunch compression monitor. The radiation was first imaged by a Basler camera outside of the vacuum chamber sensitive from 400 to 1000 nm. The camera was then replaced by an Ocean HDX spectrometer sensitive to wavelengths between 200 and 1100 nm. The responsivity of the spectrometer has not yet been considered in the following analysis.

Evident in Fig. 2 is the strong dependence of the TR signal on the phase of TWS2. Altering the phase of TWS2 will

* blae.stacey@desy.de

Content from this work may be used under the terms of the CC BY 4.0 licence (© 2025). Any distribution of this work must maintain attribution to the author(s), title of the work, publisher, and DOI.

ISBN: 978-3-95450-262-2 ISSN: 2673-5350 doi: 10.18429/JACoW-IBIC2025-WEPMO04

# DIAMOND DOSIMETER FOR THE MEASUREMENT OF THE PROTON BEAM IMPACT POSITION ON A NEUTRON SPALLATION TARGET

C. Weiss*,[1], M. Bacak, E. Griesmayer[1], E. Jericha, J. Melbinger[1]
TU Wien, Atominstitut, Wien, Austria
M. Diakaki, K. Kaperoni, M. Kokkoris, National Technical University of Athens, Athens, Greece
H. Frais-Kölbl, University of Applied Sciences, Wiener Neustadt, Austria
[1]also at CIVIDEC Instrumentation GmbH, Wien, Austria
and the n_TOF Collaboration

*Abstract*

In close proximity to the spallation neutron source of the neutron time-of-flight facility n_TOF at CERN, diamond dosimeters were installed to characterise the fast neutron beam. The intensity of the 20 GeV/c proton beam from CERNs Proton Synchrotron (PS) is monitored with a beam current transformer (BCT) installed in the PS extraction line to n_TOF. The proton beam position is measured using a SEM grid 3 m before the spallation target. A linear correlation between the horizontal proton beam impact position on the Pb-target and the measured dose of the secondary radiation at the measurement station for each pulse is observed. While the proton beam impact position varies by 22 mm, the normalised dose varies by 17 %. The linearity of the diamond dosimeter and the correlation of proton beam position and detector response are presented.

## INTRODUCTION

Close to the n_TOF Pb-spallation target at CERN [1, 2], as shown in Fig. 1, the high-flux irradiation station NEAR is in operation since 2021 [3]. The measurement station for neutron activation measurements a-NEAR is located 2.3 m from the center of the spallation target at 100° with respect to the impinging proton beam. The measurement station is installed behind a shielding wall with embedded neutron collimator. At this measurement station two diamond dosimeters were installed to measure the neutron flux as function of time-of-flight (TOF).

The PS accelerator [4] delivers 20 GeV/c proton bunches with a maximum repetition rate of 0.8 Hz on the spallation target. The proton beam intensity can be varied, with a nominal value of 8.5e12 protons/bunch in 16 ns FWHM for dedicated bunches to n_TOF. The beam size on target is $\sigma$ = 34 mm horizontally and $\sigma$ = 16 mm vertically for dedicated bunches [5, 6].

The simulated neutron fluence spectrum [7] of the neutron beam at a-NEAR as a function of TOF is shown in Fig. 2. The integrated neutron flux at the center of the collimator at a-NEAR is ≈1.51e9 n/cm$^2$/7e12 protons/bunch. Neutrons arriving within the first 100 ns have an energy of 3 MeV < $E_n$ < 300 MeV and can be measured with a diamond detector without additional neutron converter [8, 9]. The neutron rate in this TOF window is 100-1000 n/ns/cm$^2$. This very high neutron rate allows a direct dosimetric measurement of the neutron beam, without the need of amplification.

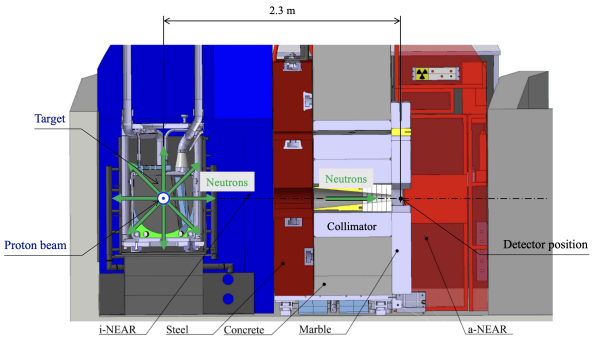



Figure 1: Model of the n_TOF spallation target with the neighboring measurement station for neutron activation measurements, the so-called "a-NEAR", where diamond dosimeters were installed to measure the fast neutron beam.

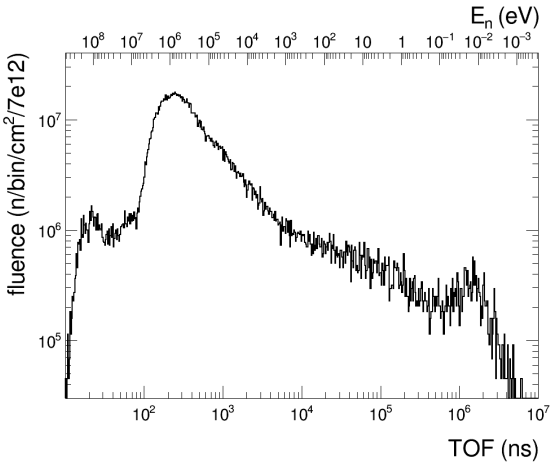



Figure 2: Neutron fluence at a-NEAR as function of time-of-flight. Neutrons with $E_n$ > 3 MeV arrive in the first 100 ns at the detector position.

## EXPERIMENTAL SETUP

Two diamond dosimeters equipped with single-crystal chemical vapour deposition (sCVD) diamond sensors with 50 µm thickness and 4 mm × 4 mm active area were used for fast-neutron beam monitoring at a-NEAR. The detectors

* christina.weiss@cividec.at

Content from this work may be used under the terms of the CC BY 4.0 licence (© 2025). Any distribution of this work must maintain attribution to the author(s), title of the work, publisher, and DOI.

ISBN: 978-3-95450-262-2 ISSN: 2673-5350 doi: 10.18429/JACoW-IBIC2025-WEPMO05

# TESTING OF SiC BLADE X-RAY BEAM POSITION MONITORS FOR SYNCHROTRON FRONT-ENDS

C. Houghton *, L. Bobb, Diamond Light Source, Oxfordshire, UK

*Abstract*

X-ray beam position monitors (XBPMs) play a crucial role in accurately measuring the position of the white beam in synchrotron front ends. Traditional XBPM designs typically feature four tungsten blades arranged at the full width at half maximum (FWHM) of the white beam. However, the high absorption and lower thermal resistance of tungsten limit the proximity of the blades to the X-ray source, which may negatively impact measurement precision. This study investigates the performance of an innovative XBPM design that utilises silicon carbide (SiC) blades, which provide enhanced thermal stability and reduced absorption of bending magnet radiation. This advancement may allow for closer placement of the blades to the beam, potentially improving measurement accuracy. This experimental setup aims to assess the impact of SiC blades on measurement accuracy, signal-to-noise ratio, and linearity compared to conventional tungsten XBPMs. The results will offer valuable insights into the benefits and limitations of SiC-based XBPMs compared to their tungsten counterparts.

## INTRODUCTION

Diamond is upgrading its front-end tungsten vane XBPMs [1, 2] to handle the higher brilliance and power anticipated for Diamond-II [3]. This provided an opportunity to evaluate a prototype silicon-carbide XBPM as a potential alternative. SiC blades are understood to offer several potential advantages over traditional materials, such as reduced absorption of bending-magnet background radiation and improved thermal stability of the signal. Monochromatic XBPMs utilising SiC have previously been successfully benchmarked against conventional single-crystal diamond XBPMs [4], demonstrating comparable performance under operating conditions.

For simplicity and consistency, the prototype was installed using the existing blade holder design, see Fig. 1. Each beamline front-end contains two XBPMs spaced approximately 4 m apart, enabling angular measurements of the photon beam. In this study, the prototype SiC vane XBPM [5] replaced the downstream XBPM-02 located 16.53 m from the insertion device sourcepoint. The upstream XBPM-01 is a tungsten vane XBPM installed in 2007 at a distance of 12.25 m from the sourcepoint. Simultaneous measurements from both devices allowed for direct comparison.

The SiC blades used in this prototype consist of doped epitaxial layers forming a p-n junction: a 15 µm thick n- nitrogen-doped inactive layer and a 1.5 µm thick p+ phosphorous-doped active layer grown on an n+ substrate, see Fig. 2. At the chips edge the p+ layer is selectively removed, creating an inactive border region, this will act as a photon filter limiting low photon energy (UV and soft X-rays) contributions [6]. The blades are mounted between a cathode and an anode, allowing for bias application and photo-current measurement. Unless stated otherwise throughout this experiment, a bias of −20 V was applied to the anode of each SiC blade.

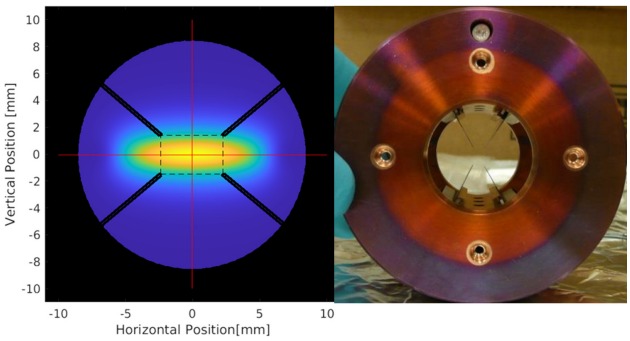



Figure 1: Left: Schematic of a vane XBPM, showing the blades interacting with the photon beam. Right: Image of a tungsten vane XBPM.

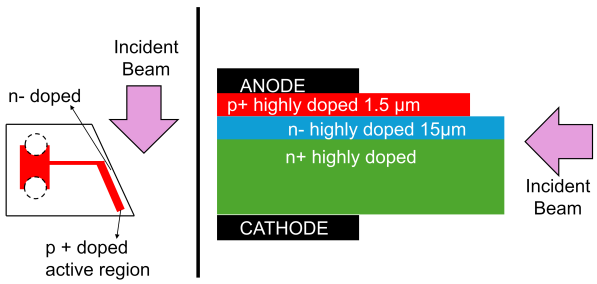



Figure 2: Diagram of the SiC blade setup. Left: top view focusing on the active SiC area with a built-in photon filter to reduce UV light. Right: side view showing doped SiC layers, the anode and cathode [6].

## ELECTRICAL TESTING

Without beam incident to the XBPM a ±10 V input voltage was sequentially applied to the anode of each blade. The current response was measured of the input blade and the voltage output of the remaining three blades was recorded, see Fig. 3. The results for the tungsten vane XBPM demonstrated an output current within µA range and showed no significant response to the applied voltage, indicating effective electrical isolation between the blades. Conversely, the silicon carbide vane XBPM saw a markedly higher current output, reaching the mA range, along with a significant positive correlation to the input voltage. Notably, the application

* claire.houghton@diamond.ac.uk

Content from this work may be used under the terms of the CC BY 4.0 licence (© 2025). Any distribution of this work must maintain attribution to the author(s), title of the work, publisher, and DOI.

ISBN: 978-3-95450-262-2 ISSN: 2673-5350 doi: 10.18429/JACoW-IBIC2025-WEPMO06

# GEOMETRICAL STUDIES FOR THE ARC BEAM POSITION MONITORS OF THE FCC-ee

E. Howling*[1], M. Gasior, N. Chambers, R.Kieffer, M. Krupa, T. Lefevre, B. Moser, H. Sullivan, C. Zannini, CERN, Geneva, Switzerland
P. N. Burrows, University of Oxford, UK

*Abstract*

The electron-positron Future Circular Collider (FCC-ee) has challenging requirements for beam instrumentation, including the need for thousands of high-resolution beam position monitors (BPMs) presenting low impedance to the circulating beam. This paper details the requirements for the FCC-ee arc BPMs and investigates button-type pickups with various geometries through electromagnetic simulations using FCC-ee design parameters. The simulation results are used to estimate key BPM characteristics, including impedance and heating.

## INTRODUCTION

The FCC-ee is a 90.7 km circumference $e^+$-$e^-$ collider proposed to be built at CERN [1]. It would operate at four key centre of mass energies and provide a Higgs factory at the precision frontier of high energy physics. This paper focuses on the BPM design for the arc sections of the collider ring.

The arc BPM system must deliver bunch by bunch, turn by turn and beam orbit measurements. The requirements for the arc BPMs are given in Table 1.

The impedance of the BPM shall also be low enough to prevent excessive heating of the button electrodes and to ensure beam stability. From the conceptual design report, 4000 BPMs in the collider, based on a design used at DANE, led to a total loss of 40.1 V/pC. This value was taken as an initial impedance budget for the BPMs [2]. However, due to heating concerns, the actual impedance may need to be significantly lower. The BPMs must also be reliable and have a suitable cost for mass production.

Table 1: Current Arc BPM Requirements

| Parameter | Requirement |
|---|---|
| orbit resolution | 0.1 µm |
| turn by turn resolution | 1 µm |
| accuracy | 20 µm |
| minimum bunch spacing | 25 ns |

These high resolution and low impedance requirements must be met across the four different running modes of the FCC-ee, as summarised in Table 2. They must also have sufficient resolution during commissioning, when the bunches would have a tenth of the nominal charge. The limits of heating must be met at the most extreme conditions foreseen. Simulations using CST Studio Suite show up to a factor 30 difference between the peak-to-peak voltage expected at the different extreme beam parameters.

Table 2: Beam Parameters of the FCC-ee at the Four Modes of Operation, the First Value for the Bunch Length is Before Collisions, and the Second, During Collisions [1]

| Mode | Z | W | ZH | $t\bar{t}$ |
|---|---|---|---|---|
| E [GeV] | 45.6 | 80 | 120 | 182.5 |
| $Q_{bunch}$ [nC] | 34.3 | 23.2 | 18.4 | 24.8 |
| $l_{RMS}$ [mm] | 5.6/15.5 | 3.5/5.4 | 3.4/4.7 | 1.8/2.2 |
| No. bunches | 11200 | 1780 | 440 | 60 |
| Bunch spacing [ns] | 25 | | | |
| $I_{beam}$ [mA] | 1270 | 137 | 26.7 | 4.9 |

This range of beam conditions makes it challenging to provide the required resolution at the lowest beam intensities, whilst maintaining acceptably low levels of impedance and heating at the highest beam intensities. Therefore, the geometry of the pickups must be optimised and suitable materials chosen.

## BUTTON GEOMETRIES

Initially, a simplified BPM button was simulated with CST and the four dimensions highlighted in Fig. 1a were varied. A greater electrode peak-to-peak voltage corresponds to better resolution, while a smaller wake loss factor indicates a smaller impedance. The wake impedance as a function of frequency was also studied with the objective of mitigating resonances, either by reducing their amplitudes or by shifting them to higher frequencies, where the beam spectral content is smaller. The impact of each geometrical dimension on these figures of merit was explored to optimise the design.

In summary,

- **Peak-to-peak voltage**: increases significantly with the electrode radius, increases slightly with gap size, and decreases slightly with back gap size, whilst height has a negligible effect.
- **Wake loss factor**: increases with both radius and gap size, whilst back gap and height have negligible effect.
- **Resonant peak amplitudes in the wake impedance spectrum**: increase with radius and gap. Increasing the back gap slightly decreases the amplitude of the largest peak.

* emily.rose.howling@cern.ch
[1] also at University of Oxford, UK

Content from this work may be used under the terms of the CC BY 4.0 licence (© 2025). Any distribution of this work must maintain attribution to the author(s), title of the work, publisher, and DOI.

ISBN: 978-3-95450-262-2 ISSN: 2673-5350 doi: 10.18429/JACoW-IBIC2025-WEPMO07

# GAIN CALIBRATION FOR ELIMINATING X-Y COUPLING IN X-RAY BEAM POSITION MONITORS AT SPring-8 PHOTON BEAMLINES

Hideki Aoyagi†
Japan Synchrotron Radiation Research Institute (JASRI/SPring-8), Hyogo, Japan

*Abstract*

Although synchrotron radiation originates from charged particle beams, monitoring its positional stability requires distinct technical approaches. To enhance the accuracy of position and angle measurements of the synchrotron radiation beam at SPring-8 BL15XU, both a quadrant-type XBPM and a fixed-blade XBPM were installed on the same beamline. In the quadrant-type XBPM, widening the detector spacing led to noticeable X-Y coupling. To address this, a 2×2 correction matrix was introduced to perform linear transformation of the measured signals. The proposed method successfully eliminated X-Y coupling while maintaining resolution, enabling simultaneous operation of both XBPMs.

## INTRODUCTION

At the synchrotron radiation facility SPring-8, X-ray Beam Position Monitors (XBPMs) based on photoelectron emission are installed at the front end of each beamline to measure angular fluctuations of the synchrotron radiation beam emitted from the light source [1]. The horizontal and vertical position sensitivity coefficients (correction factors) are determined by shifting the monitor body from its reference position in each direction and analyzing the output signals from four detectors.

However, synchrotron radiation beam generated by the fringe field of the bending magnet can generally induce slight horizontal–vertical coupling (hereafter referred to as X-Y coupling). This effect tends to become more pronounced as the distance to the tip of blade-shaped detectors increases.

To enhance the accuracy of both position and angle measurements, a second XBPM was added. Therefore, at BL15XU, a quadrant-type XBPM with independently adjustable detector spacing was installed approximately 20 m upstream from the source, while a conventional fixed-blade XBPM was installed approximately 25 m downstream. This configuration was designed to prevent the upstream XBPM's detectors from obstructing the synchrotron beam. However, increasing the detector spacing in the quadrant-type XBPM resulted in noticeable X-Y coupling in the correction factors, limitating on simultaneous operation of both XBPMs.

Several methods have been reported for correcting relative gain deviations between electrodes in electron beam position monitors of storage rings, such as beam-based gain calibration [2–4] and fast determination of BPM offsets from quadrupole magnet centers [5]. We propose a simple calibration method that effectively eliminates X-Y coupling in the correction factors. This method introduces a new formula to calculate the components of a 2×2 transformation matrix using only four measurement points—up, down, left, and right—enabling accurate mapping through linear transformation.

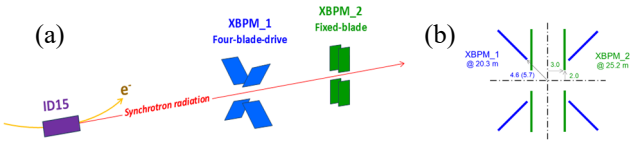



Figure 1: (a) XBPM_1 is positioned to avoid interference with XBPM_2. (b) Blade tips of XBPM_1 are set 4.6 mm from the center, corresponding to a projected distance of 5.7 mm at the XBPM_2 location.

This report presents a quantitative evaluation of X-Y coupling in the quadrant-type XBPM, the procedure of the proposed calibration method, and experimental results obtained by intentionally modifying the electron beam orbit to verify the XBPM response characteristics.

## X-Y COUPLING IN XBPM

This section presents a quantitative evaluation of X-Y coupling and discusses relevant design constraints. At BL15XU, a quadrant-type XBPM and a fixed-blade XBPM were installed at the upstream (20.3 m from the light source) and downstream (25.2 m), respectively, of the photon beamline frontend (Fig. 1(a)). The upstream XBPM_1 features independently adjustable blade detectors, allowing it to avoid interference with the downstream XBPM_2. The XBPM_2 is the standard model used in SPring-8 insertion device beamlines, with blade tips are fixed at ±3.0 mm horizontally and ±2.0 mm vertically from the center. To prevent obstruction, the blade tips of the XBPM_1 must be positioned at least 3.8 mm from the center. In practice, a safety margin was added, resulting in a tip position of 4.6 mm (Fig. 1 (b)).

To evaluate the degree of X-Y coupling in the output of the quadrant-type XBPM (calculated as the difference-over-sum of the four signals), the blade tip positions were varied to scan across the X-Y plane. The resulting plots of the difference-over-sum values are shown in Fig. 2. Ideally, the measured points should align with the vertices of a square lattice. However, the actual measurements revealed distortions, indicating that even when the beam is displaced purely in the horizontal or vertical direction, the XBPM output erroneously includes components from the orthogonal axis. This distortion—i.e., the increase in X-Y coupling—was found to intensify as the blade tips moved farther from the center.

To mitigate X-Y coupling, it is necessary to optimize the blade tip positions while maintaining sufficient detector current for resolution. Furthermore, applying a new correc-

† aoyagi@spring8.or.jp

Content from this work may be used under the terms of the CC BY 4.0 licence (© 2025). Any distribution of this work must maintain attribution to the author(s), title of the work, publisher, and DOI.

ISBN: 978-3-95450-262-2 ISSN: 2673-5350 doi: 10.18429/JACoW-IBIC2025-WEPMO08

# DEVELOPMENT OF BPM ELECTRONICS FOR TRIUMF'S BL4N*

H. Jones†, TRIUMF, Vancouver, Canada

*Abstract*

The BL4N beamline at TRIUMF, currently under development within the scope of the ARIEL expansion, will transport a proton beam from the 500 MeV cyclotron to a new ISOL target station. The peak beam current will be varied from 1 to 100 microamps, and the beam position is expected to be accurately measured over a 10 mm range. The beam position is measured using inductive type pickups and new narrowband front-end electronics. The electronics consist of a crossbar-switched front-end, FPGA-based down-conversion and position calculation, and an SoC module for nonlinear corrections and device readout. This report presents the design and testing of the BPM electronics, including benchtop validation and beam test results. Measurements of position sensitivity, beam current dependence, and non-linearity are included.

## INTRODUCTION

The TRIUMF BL4N [1] will deliver protons from the 500 MeV cyclotron to a new ARIEL ISOL target station. Routine operation is expected at peak currents below 10 µA for certain RIB production targets. The principal beam parameters are listed in Table 1.

Existing inductive BPMs [2] cannot operate reliably at such low currents due to the electronics' limited dynamic range and transfer impedance of the pickups. To address this, a new inductive BPM has been developed with a ferrite core for improved sensitivity, as well as electronics with extended dynamic range.

Table 1: Basic Beam Parameters of BL4N

| Parameter | Value | Unit |
|---|---|---|
| Beam species | H+ | |
| Beam energy | 500 | MeV |
| Peak current | 1-100 | µA |
| Pulse duty cycle | 1-99 | % |
| Pulse frequency | 375-1126 | Hz |
| Bunch frequency | 23.06 | MHz |

## MONITOR DESIGN

The BPM is based on the design presented in [2], with a ferrite core added to increase the magnetic flux through each loop pickup, thus increasing the transfer impedance of the monitor. The ferrite core is made from M2 material from National Magnetics Group and is supported by an aluminium support (Fig. 1).

Operation is at the second harmonic of the bunch frequency (46.1 MHz), chosen for its stronger coupling and reduced background noise. The coupling between the beam and pickups was simulated in HFSS, with and without the ferrite, as shown in Fig. 2. The ferrite increases the transfer impedance by 12 dB at 46 MHz. A drawback is a stronger crosstalk between the pickup electrodes, which reduces the transverse sensitivity of the monitor. HFSS simulations show the sensitivity to decrease from 0.42 dB/mm to 0.2 dB/mm, increasing the demand on the front-end electronics.

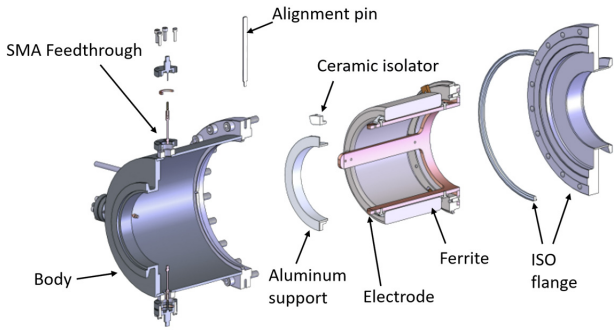



Figure 1: Exploded view of monitor.

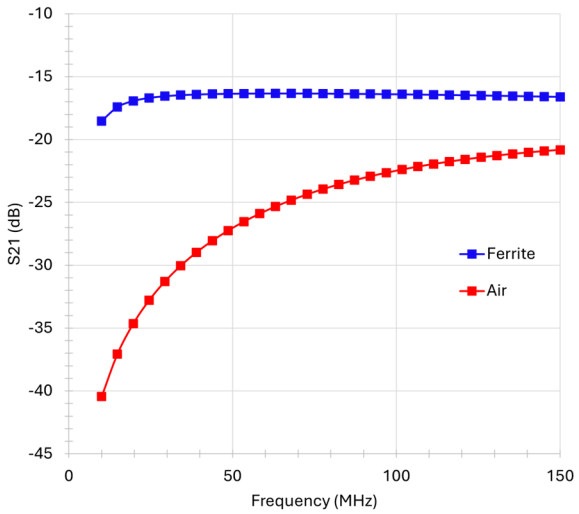



Figure 2: HFSS results for S21 coupling between beam and individual pickup, with and without ferrite core.

## FRONT-END DESIGN

The BPM electronics consist of an RF front-end, an under-sampling analog-to-digital converter (ADC) and a FPGA-based digital down-conversion and position calculation (Fig. 3).

### *RF Front-End*

The RF front-end (RFFE) was designed for 46.1 MHz operation. Each front-end (horizontal and vertical) consists of 2 wideband low-noise amplifiers (LNAs), matched to 46.1 MHz, separated by SAW bandpass filters centred at 46.1 MHz and variable 18 dB attenuators (Fig. 4). To reduce drift and gain mismatch, a crossbar switching scheme [3] was implemented using a DPDT switch placed after the

* Funded under a contribution agreement with National Research Council Canada

† hjones@triumf.ca

Content from this work may be used under the terms of the CC BY 4.0 licence (© 2025). Any distribution of this work must maintain attribution to the author(s), title of the work, publisher, and DOI.

ISBN: 978-3-95450-262-2 ISSN: 2673-5350 doi: 10.18429/JACoW-IBIC2025-WEPMO09

# ONLINE POSITION CONVERSION FACTOR CALIBRATION STUDY FOR BPM SYSTEM*

J. Chen†, L.W. Lai, R.X. Yuan
Shanghai Advanced Research Institute, CAS, Shanghai, China

*Abstract*

Transverse beam position is one of the most critical parameters in accelerator commission and operation. As non-invasive diagnostic devices, beam position monitors (BPMs) are the main "workhorse" in accelerators, providing beam center of mass position information. The position conversion factor (K-factor) of BPM systems constitutes a fundamental determinate of measurement accuracy. While precision calibration traditionally relies on moveable calibrate platforms, the prohibitive cost of equipping each BPM with a dedicated two-dimensional calibration platform remains a widespread practical constraint. In this paper, an innovative online calibration method that synergizes machine learning with beam response matrix analysis to achieve per-BPM K-factor determination is introduced. The preliminary beam experiments have been carried out at Shanghai Soft X-ray Free-Electron Laser (SXFEL) facility. The proposed method offers a robust and resource-efficient calibration solution, particularly advantageous for cavity BPM systems where conventional approaches such as theoretical calculation and offline wire scanning, fail to provide reliable results.

## INTRODUCTION

Beam Position Monitors (BPMs) are indispensable and critical diagnostic devices in particle accelerators, whose performance is directly related to the precise measurement of beam trajectory, the stability of feedback controls, and the optimization of accelerator performance. Transverse beam position is one of the most critical parameters during accelerator commissioning and operation. As non-invasive devices, BPM systems continuously provide beam center-of-mass position information, serving as the main "workhorse" for ensuring high-quality beam transmission and efficient experimentation.

For stripline or button-type BPMs, the position conversion factor (K-factor) is primarily determined by the vacuum chamber aperture and electrode geometry, and can often be approximated by a simplified theoretical formula:

$$K_x = \frac{a \cdot s}{4\sin(\phi_s/2)}\ , \qquad (1)$$

where $K_x$ is a conversion coefficient related to the electrode shape and size, $a$ is the beam pipe radius and $\phi_s$ is the angle of the electrode. This model provides a reasonable estimation of the K-factor under ideal conditions. In practical engineering, besides theoretical calculation, electromagnetic simulation software such as CST Studio Suite or ANSYS HFSS can be used for precise modeling of BPM probes to obtain the K-factor for both stripline and button BPMs. Numerous studies have shown that simulation results are generally in good agreement with theoretical values [1]. Furthermore, establishing a high-precision wire-scanning test platform is a widely adopted offline calibration method. By simulating the beam with a moving wire in a laboratory environment and measuring the electrode response, integrated K-factor calibration for the probe, front-end electronics, and data acquisition system can be performed [2]. These methods are relatively mature and reliable for SBPMs.

However, for cavity BPMs (CBPMs) based on the resonant cavity principle, their working mechanism and calibration challenges are fundamentally different from those of SBPMs. CBPMs utilize the wake-field excited by the beam in the resonant cavity to couple out signals, aiming to accurately characterize the original information of the bunch (e.g., position, charge). The sensitivity of a CBPM probe (i.e., the system K-factor) is a more complex systemic issue: it depends not only on the electromagnetic design of the cavity (e.g., operating mode, R/Q value) but is also significantly influenced by a combination of factors including probe manufacturing precision (e.g., dimensional tolerances, surface finish), signal conditioning circuitry (e.g., bandwidth, gain flatness), and channel characteristics of the digital acquisition system (e.g., amplitude/phase consistency, impedance matching). This implies that even two perfectly identical CBPM probes may exhibit significantly different final system K-factors if connected to different electronics systems. More critically, the traditional offline wire-scanning calibration method has limited applicability for CBPMs. When a metal wire is inserted through the CBPM resonant cavity, it severely perturbs the cavity's electromagnetic field distribution, altering its resonant frequency and quality factor (Q-value). Furthermore, the excitation signal propagates along the wire, causing mode leakage and introducing systematic deviations between the measured signal response and the actual response under real beam excitation. Consequently, the K-factor obtained offline can hardly reflect the true system performance during online beam operation and fails to provide reliable results.

For large-scale accelerator projects like the Shanghai High repetition rate XFEL and Extreme light facility (SHINE), which deploy a vast number of CBPM probes, a comprehensive strategy is essential. To ensure the consistency of all BPM measurement data and obtain accurate K-factors, we must implement strict quality control at the source (probe manufacturing) to ensure the performance consistency of individual probes. On the other hand, there is a pressing need to develop a novel online calibration method that does not rely on offline platforms and can

*Work supported by The National Science Foundation of China (Grant No.12175239). Youth Innovation Promotion Association, CAS (Gant No.2019290). Outstanding member of the Youth Innovation Promotion Association, CAS(Gant No.Y2023079).
† chenjian@sari.ac.cn

Content from this work may be used under the terms of the CC BY 4.0 licence (© 2025). Any distribution of this work must maintain attribution to the author(s), title of the work, publisher, and DOI.

ISBN: 978-3-95450-262-2 ISSN: 2673-5350 doi: 10.18429/JACoW-IBIC2025-WEPMO11

# DESIGN AND EXPECTED PERFORMANCE OF THE NEW BPM SYSTEMS FOR AWAKE RUN 2c

L. T. Stant*, A. Boccardi, T. Bogey, I. Degl'Innocenti,
A. Jevtic, M. Krupa, S. Mazzoni, C. Pakuza, CERN, Geneva, Switzerland

*Abstract*

The AWAKE facility at CERN uses novel proton beam-driven plasma wakefields to accelerate electron bunches over a 10 m plasma source. The facility will soon be rebuilt to study methods to improve the quality of the accelerated electron beam, requiring better resolution from the proton beam position monitors (BPMs). In addition, it is desirable to replace the existing bespoke electron BPMs with an in-house solution. Both upgrades will reuse the existing BPM pickups (electrostatic buttons and striplines, respectively) but replace the electronic front-ends and control system interfaces. An RFSoC-based BPM front-end is concurrently being developed for the HL-LHC upgrade, which, if appropriate for AWAKE, would reduce production and maintenance efforts. For the proton BPMs, distributed along an 800 m transfer line, time-multiplexing of both pickups per plane has been chosen both to reduce cabling and channel count and improve systematic errors in the measurements. We present the expected performance of both the AWAKE proton and electron BPMs using the prototype HL-LHC BPM front-end, based on measurements from the existing facility.

## INTRODUCTION

The Advanced Wakefield Experiment (AWAKE) facility at CERN has now entered a long shutdown to rebuild the beamline ahead of the Run 2c phase of the project [1]. As part of the beam instrumentation upgrades to measure the lower emittance beams, the acquisition electronics for the beam position monitors (BPMs) of both the proton beamline and the electron beamline will be upgraded. Additional complete BPMs will be provided for a second electron beamline to deliver dedicated witness bunches for acceleration. The Run 2c layout is shown in Fig. 1.

The existing proton BPMs reuse 60 mm button pickups (see Fig. 2a) from the LEP collider that feed local digitisers based on narrowband filtering and demodulating logarithmic amplifiers. The acquisition electronics were a prototype for the ALPS system, later installed in the SPS [2, 3]. This system achieves an average 70 µm of noise-limited resolution, which the project would like to reduce to 20 µm with the upgrade.

For the electron BPMs, stripline pickups and custom acquisition electronics were contributed by TRIUMF who were then a member of the AWAKE collaboration. The striplines are of two apertures: 40 mm for the electron beamline, shown in Fig. 2b, and 60 mm after the merging point with the protons. Similar to the proton BPMs, the acquisition electronics also use narrowband filtering, but downconvert and sample the signal instead of demodulating it [4, 5]. Although the existing best-case noise-limited resolution of 10 µm meets the requirements for Run 2c, it is no longer feasible to acquire further BPMs from TRIUMF and so both the new units and replacements for existing BPMs will be produced at CERN. This will provide a single in-house source and reduce future maintenance effort.

Concurrently with the AWAKE Run 2c design work, the HL-LHC BPM project began designing wideband direct-sampling acquisition electronics based around the Zynq Ul-

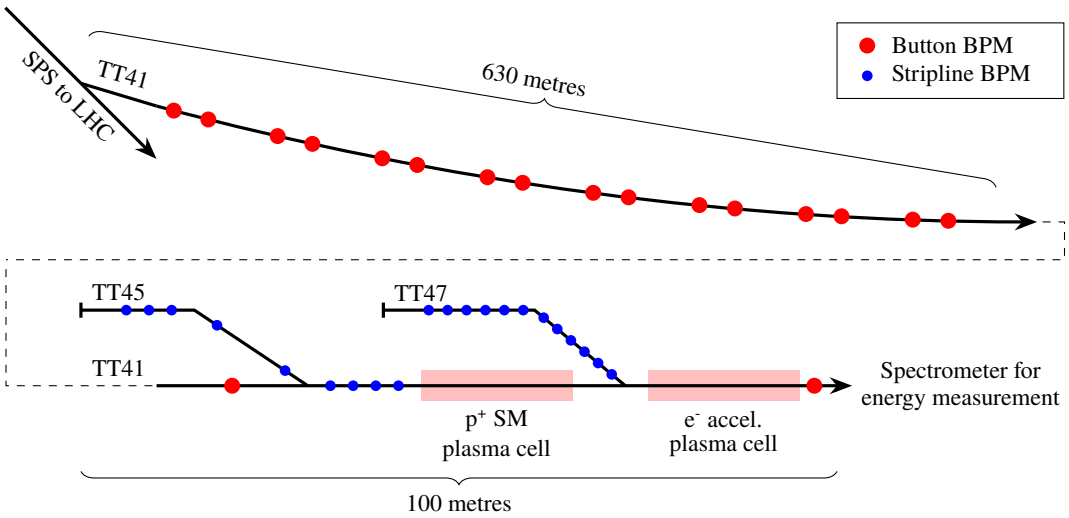



Figure 1: The AWAKE layout for Run 2c. TT47 and the plasma chamber downstream will be added for this run.

* l.stant@cern.ch

Content from this work may be used under the terms of the CC BY 4.0 licence (© 2025). Any distribution of this work must maintain attribution to the author(s), title of the work, publisher, and DOI.

ISBN: 978-3-95450-262-2 ISSN: 2673-5350 doi: 10.18429/JACoW-IBIC2025-WEPMO12

# DIGITAL SIGNAL PROCESSING IMPROVEMENTS OF THE SPIRAL2 BEAM POSITION MONITORS AT LOW INTENSITY

P. Salou*, C. Jamet, S. Rueff, C. Potier de Courcy, C. Tréangle, C. Houarner, O. Delahaye
Grand Accelerateur National d'Ions Lourds, Caen, France

*Abstract*

The SPIRAL2 accelerator, designed for high intensity beams (up to 5 mA), needs to evolve for low intensities in order to reach the requirements of the S3 (Super Separator Spectrometer) experimental room. This means increasing the operating range of diagnostic monitors including the Beam Position Monitors (BPM). Twenty BPM are installed in the warm sections of the linac to measure positions, ellipticities and phases. The digital processing of the BPM acquisition has been modified to operate at low intensity. This was done by improving the signal-to-noise ratio with an increase of the averaging resolution, an improvement of the channel equalisation system and with a deduction of parasitic signals induced by the surrounding equipment. The process was also modified to operate with chopper frequencies above 1 kHz. A new BPM interface, with tables and graphical displays in order to control beam phases and energies in the linac, is now available. These new developments and measurement results in laboratory and with SPIRAL2 beams are presented, which show good results with a low intensity down to 1 µA.

## INTRODUCTION

The Beam Position Monitors (BPM) are beam diagnostics installed in the quadrupoles of the warm sections of the SPIRAL2 LINAC. Twenty BPMs and their instrumentation chain measure the following characteristics: beam position, ellipticity (a characteristic of the transverse size) [1], beam phases and energy.

The four electrodes of a BPM pick up the electric field induced by the ion bunches from the beam. The generated signal is periodic and can be decomposed in harmonics, mainly at the accelerator frequency ($h_1$=88.0525 MHz) and at its double frequency ($h_2$=176.105 MHz). The level of the signal is mainly due to the beam intensity, its energy and the considered harmonic. Table 1 shows the expected signal level. The red values are below the detection threshold of the BPM device before modifications.

The BPM acquisition system was designed by the Bhabha Atomic Research Centre (BARC) to measure characteristics from high intensity beam. To meet the future demand of low intensity beam, an improvement of the instrumentation chain was previously done [1], making possible to measure beam characteristics with an intensity down to 50 µA, namely signal power down to -90 dBm. Below this intensity, the measurement precisions deteriorate quickly. Future beams of S3, including those of NEWGAIN [2], could have an intensity below this value. We should then increase the dynamic of measure for the low levels of signal. This improvement was achieved by modifying the digital signal processing.

Table 1: Signal Level as a Function of the Beam Intensity

| | $h_1$ (dBm) | | $h_2$ (dBm) | |
|---|---|---|---|---|
| Beam intensity | min | max | min | max |
| 5000 µA | -32.9 | -22.4 | -27.5 | -22.6 |
| 500 µA | -52.9 | -42.4 | -47.5 | -42.6 |
| 50 µA | -72.9 | -62.4 | -67.5 | -62.6 |
| 5 µA | -92.9 | -82.4 | -87.5 | -82.6 |
| 1 µA | -106.9 | -96.4 | -101.5 | -96.6 |

## DIGITAL SIGNAL PROCESSING IMPROVEMENTS

The signal coming from the four capacitive pickups are measured with an acquisition system developed by BARC. It consists of an analog section that filters and amplifies the signal which is digitized in the digital section. In this section, the data are processed by a Field-Programmable Gate Array (FPGA). A VME CPU board collects the data from several BPM for further digital processing and publication to the network. The signal processing modifications were made to the FPGA code in the digital section and to the C driver in the VME-CPU.

### *Architecture Modifications*

In order to correct amplitude and phase differences between channels for all gains and ensure a stable measurements over time, the acquisition system is equipped with an equalization system [3]. A known sinusoidal signal, called "*Offset Tone*", is injected at the four inputs of the analog section. The frequency of this signal is close enough to the frequency of measured BPM signals so that the gain and phase shift of the acquisition channels are considered identical between the signal to be measured and the *Offset Tone*.

The measure of the *Offset Tone* allows the calculation of correction factors (in phase and gain) which are applied to the measurement of signals coming from the BPM. This correction was previously performed on the digital board. The gain and phase correction factors required to be calculated from IQ measurements by a CORDIC which introduced calculation errors.

To increase the precision of low amplitude signal measurement, the way to process the stabilization was changed. It is now achieved by the VME-CPU with a new driver. The *Offset Tone* generation is produced by a feed back loop in the FPGA. The new equalizations (in amplitude and phase)

* salou@ganil.fr

Content from this work may be used under the terms of the CC BY 4.0 licence (© 2025). Any distribution of this work must maintain attribution to the author(s), title of the work, publisher, and DOI.

ISBN: 978-3-95450-262-2 ISSN: 2673-5350 doi: 10.18429/JACoW-IBIC2025-WEPMO13

# SINGLE-SHOT DETECTION OF SHORT ELECTRON BUNCH SHAPES AT MHz REPETITION RATES USING DIVERSITY ELECTRO-OPTIC SCHEME WITH ADVANCED RECONSTRUCTION ALGORITHMS AT EuXFEL AND FLASH

Q. Demazeux[1], C. Szwaj[1], E. Roussel[1], B. Steffen[2], M.-K. Czwalinna[2], S. Bielawski[1]
[1] PhLAM, CNRS/Lille University, Lille, France
[2] Deutsches Elektronen-Synchrotron DESY, Hamburg, Germany

Content from this work may be used under the terms of the CC BY 4.0 licence (© 2025). Any distribution of this work must maintain attribution to the author(s), title of the work, publisher, and DOI.

*Abstract*

Real-time diagnostic of sub-picosecond relativistic electron bunches remains a significant challenge for accelerator facilities. While single-shot spectral decoding techniques are well-suited for high-repetition-rate operations, they introduce inherent limitations, compromising both temporal resolution and signal fidelity, especially for sub-ps signals. To overcome this fundamental trade-off, we propose a multi-channel measurement approach based on the diversity concept. By utilizing a multi-output electro-optic setup combined with a novel self-adaptive reconstruction algorithm, we enable the accurate retrieval of electron bunch shapes from distorted measurements. This new algorithm compensates for imperfections in the laser chirp, such as higher-order dispersion, enabling high-fidelity bunch shapes measurements over an extended temporal window. This paper details the underlying principles of our method, presents numerical results, and provides an update on the ongoing experimental implementations at the European XFEL and FLASH facilities. These advancements represent a significant step toward a robust, high-resolution, real-time bunch shape monitor.

## INTRODUCTION

Accurate, real-time diagnostics of ultra-short electron bunches is a critical requirement for accelerators and Free-Electron Lasers (FELs) [1]. These facilities generate highly relativistic electron bunches with sub-picosecond durations at MHz repetition rate. The precise measurement of their time-domain profile is indispensable for optimizing machine performance, as it provides crucial information on key parameters such as bunch length, arrival time jitter, and bunch shapes. A common method for single-shot characterization of these profiles is spectral decoding [2, 3]. This technique uses the THz electric field from the electron bunch to modulate a chirped laser probe pulse, and the resulting spectral changes are captured in a single shot using an optical spectrum analyzer.

However, this method has long been considered fundamentally limited in its temporal resolution. This intrinsic constraint has been defined by the minimum resolvable duration, $\tau_R$, which is expressed by the relationship [3]:

$$\tau_R = \sqrt{\tau_W \tau_L}\,, \qquad (1)$$

where $\tau_W$ is the compressed laser pulse duration, and $\tau_L$ is the stretched pulse duration. This limitation leads to significant distortions in the measured waveforms, which often fail to faithfully represent the actual bunch profile (see Fig. 1). This work addresses the key challenge of accurately recovering the true bunch shape from these distorted measurements.

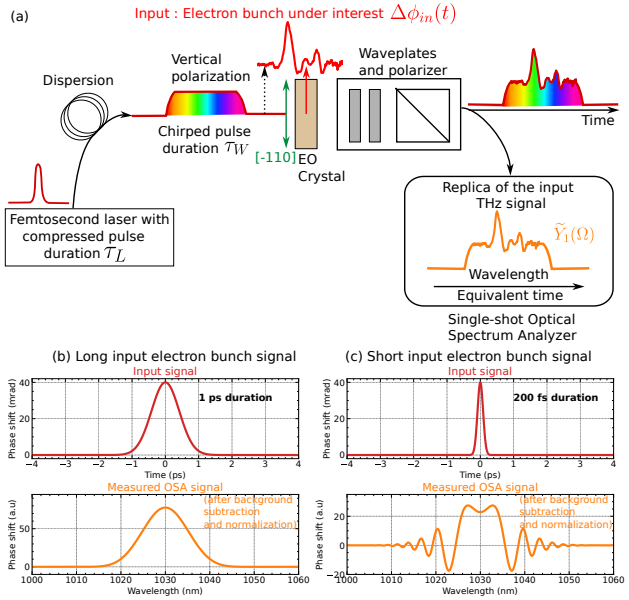



Figure 1: Inherent limitations of conventional electro-optic bunch diagnostics.

Figure 1(a) details the operating principle and shortcomings of a classical electro-optic beam diagnostic. A chirped laser pulse acts as a probe, getting modulated by the Coulomb electric field from an electron bunch, with the resulting spectrum recorded in a single shot. "Long Bunch Durations" (Fig. 1(b)): This method provides a reasonably accurate diagnostic of the bunch profile, but this only works for relatively low-bandwidth THz pulses from long electron bunches. "Short Bunch Durations" (Fig. 1(c)): For the sub-picosecond electron bunches required by modern facilities, the method fundamentally fails. The recorded spectrum shows significant distortions that do not accurately represent the true bunch shape, leading to a loss of critical diagnostic information and underscoring the urgent need for more advanced techniques.

ISBN: 978-3-95450-262-2 ISSN: 2673-5350 doi: 10.18429/JACoW-IBIC2025-WEPMO15

# TIMING SYSTEM AT THE CANADIAN LIGHT SOURCE

T. D. Batten*, Canadian Light Source, Saskatoon, Canada

*Abstract*

The Canadian Light Source (CLS) is a third generation 2.9 GeV synchrotron comprised of a 250 MeV linear accelerator (LINAC), a full energy booster, and a storage ring with 13 insertion devices and 22 operational beamlines. The synchronization required to produce, transport, accelerate and inject electrons into the storage ring is achieved using a timing system that was designed and built by the CLS. This paper provides a detailed overview of the history of this system and its operational performance.

## OVERVIEW

The timing system, shown in Fig. 1 [1], is crucial as it supplies the trigger signals necessary to synchronize operation of all components required to inject current into the storage ring. These operations include firing the electron source, accelerating the electrons, injecting into the booster, ramping the booster, extraction from the booster and injection into the storage ring. Signals from the timing system are also used to synchronize data collection from diagnostic and experimental equipment.

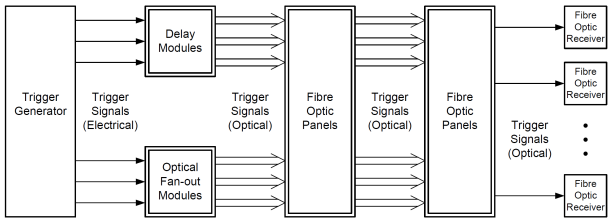



Figure 1: Simplified timing system block diagram.

## HARDWARE

### *Trigger Generator*

At the core of the timing system is the trigger generator which produces all of the trigger signals necessary to support operation and monitors the 500 MHz master oscillator and the timing system for interlock conditions.

The first trigger generator was called the Trigger Generator Module (TGM). The TGM, described in Fig. 2 [2] was a double width VXI module that was controlled using an on-board 8051 microprocessor via RS-232 which went into operation in 2001.

The second version of the trigger generator, called the Trigger Generator Unit (TGU), was introduced to deal with component obsolescence. The TGU, described in Fig. 3 [3], went into operation in 2012, and is currently being controlled using a GE Fanuc VMIVME2536 digital I/O VME module [4].

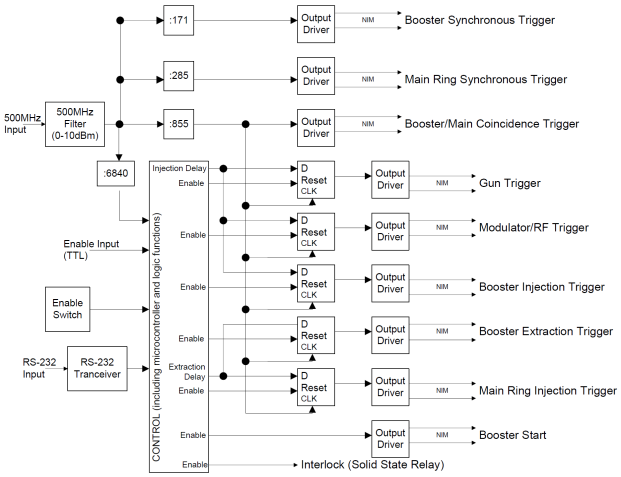



Figure 2: Trigger Generator Module schematic.

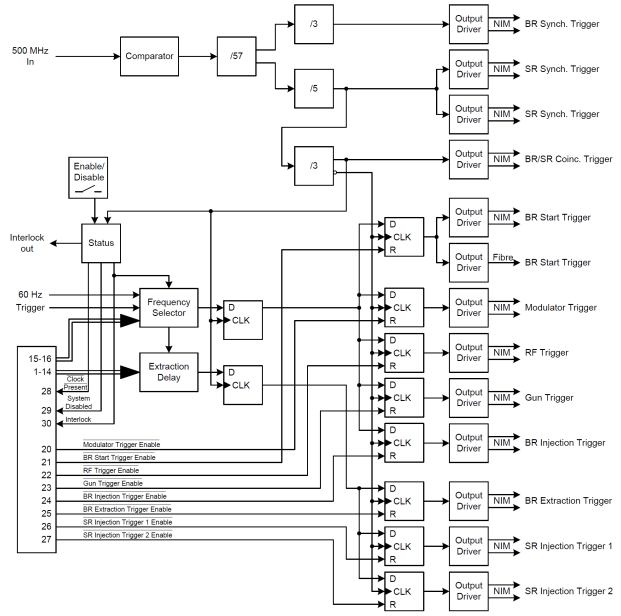



Figure 3: Trigger Generator Unit schematic.

The control architecture and a number of components were changed between the TGM and the TGU. The operational theory and the supported functionality remains the same, with the exception of some minor improvements that were derived from operational experience. The trigger generator produces three different subsets of signals; clock signals and injection and extraction triggers.

* tonia.batten@lightsource.ca

Content from this work may be used under the terms of the CC BY 4.0 licence (© 2025). Any distribution of this work must maintain attribution to the author(s), title of the work, publisher, and DOI.

ISBN: 978-3-95450-262-2 ISSN: 2673-5350 doi: 10.18429/JACoW-IBIC2025-WEPMO16

# A COMPACT DEVICE FOR MEASURING AND MONITORING THE ENERGY OF ACCELERATED PARTICLE BEAMS

Z. Kormány, HUN-REN Institute for Nuclear Research, Debrecen, Hungary

Content from this work may be used under the terms of the CC BY 4.0 licence (© 2025). Any distribution of this work must maintain attribution to the author(s), title of the work, publisher, and DOI.

*Abstract*

A Beam Energy Monitor (BEM) using time-of-flight (TOF) measurements on a short flight path was developed for the cyclotron of the HUN-REN Institute for Nuclear Research. The sensor unit comprises two capacitive probes 20 cm apart; the entire geometry is approximately 40 cm long. Its compact size enables the unit to be installed in the main beamline, allowing the beam energy to be measured and monitored independently of the beamline in use.

Probe signals are acquired by a digital oscilloscope, and digital signal processing algorithms determine the time difference between pulses generated by a beam bunch on the probes. The unique design of the sensor unit, together with the signal processing hardware and software, provides accurate beam energy measurement despite the short flight path.

The accuracy of the monitor in practical operation was investigated using neutron threshold reactions. These reactions showed that the measurement accuracy is at least one order of magnitude better than the accuracy of the energy value calculated from the cyclotron settings. The accuracy of the signal processing indicates that the beam energy can be scaled up to several hundred MeV while maintaining measurement accuracy at the tenth of a percent level.

## INTRODUCTION

The MGC-20 cyclotron at the HUN-REN Institute for Nuclear Research is a multi-particle, variable-energy machine that accelerates the four lightest ions within a broad energy range, up to 18 MeV for protons and 20 MeV for alpha particles. The cyclotron's beam transport system has nine target locations. The system also contains an analysing magnet (AM), which, in addition to its primary function of reducing the energy spread of the beam, can be used for beam energy measurements. However, this function is only available for dedicated beamlines and targets located behind the magnet. Furthermore, an AM measures beam energy indirectly, meaning the measured quantity (magnetic field strength) is not directly proportional to the kinetic energy of the accelerated particles. Instead, the connection is made with another parameter: the bending radius in the given magnetic field. The accuracy of the measured beam energy value therefore depends on how close the actual bending radius is to the nominal one, which is largely determined by the quality of the beam transport.

From this perspective, TOF measurements are superior to AM energy measurements. They determine quantities, such as flight time and particle velocity, that are directly related to the beam energy. However, they can only be used in dedicated beamlines due to the geometric requirements of the beam path. Conventional TOF systems require a flight path of several metres or even more than 10 metres, which prevents them from being installed in the typically short main beamline of the accelerator. Consequently, when the beam is transported to another beamline, the energy value can only be calculated with limited accuracy from the accelerator settings. For example, the accuracy of such calculations is typically several percent for cyclotrons [1, 2].

## DESIGN ASPECTS OF THE BEM

The Beam Energy Monitor was developed to overcome the drawbacks of the above systems. It uses time-of-flight measurement; therefore, the measured value is directly proportional to the kinetic energy of the beam. At the same time, its novel sensor construction makes it possible to achieve high accuracy over a short flight path. To achieve this, the two sensors are arranged within a vacuum chamber in a common geometric construction. In conventional TOF systems, the two (or three) probes are built into the beam transport system independently of each other, which leads to relatively large values of the absolute error in the flight path length and the measured flight time due to the existing differences in the signal paths. That is why the flight length and time cannot be short in these systems. The novel construction of the BEM enables highly accurate distance measurement between the probes, as well as determining the exact delay time difference in the signal paths from the probes. Knowing the existing delay time difference, the measured time difference between the pulses can be corrected to provide an accurate flight time value.

Figure 1 shows the conceptual structure of the sensor unit with the main components inside the vacuum chamber. It has two cylindrical capacitive probes, each 5 cm long, which allow the time of flight of the beam bunches between them to be measured. The inner diameter of the probes is larger than that of the beam pipe preventing beam particles from directly hitting them. The probe-to-probe distance (the flight path length) is defined by 3 spacers with an azimuthal separation of 120 deg. A grounded electrode is placed between the probes. The inner diameter of this cylindrical electrode is equal to that of the beam pipe and its length and position provide longitudinal geometrical and electrical symmetry on both sides of the probes. This special and unique construction [3] makes it possible to measure the time-of-flight value and thus the beam energy with high accuracy despite the applied short probe-to-probe distance of 20 cm and the longer beam bunches (typically around 30 cm at this cyclotron). The length of the vacuum chamber is only 26.4 cm and with connecting flanges and beam pipe sections the entire mechanics occupies less than 40 cm longitudinal space in the beamline. With such a compact size it could be easily installed into the main beamline of the cyclotron. Installation at that location not only enables to measure the beam energy on

ISBN: 978-3-95450-262-2 ISSN: 2673-5350 doi: 10.18429/JACoW-IBIC2025-WEPMO17

# NEW PHOTON BPM SETUP USING SiC DEVICES IN PHOTOCONDUCTIVE MODE

M. Colja*, G. Brajnik, G. Cautero, D. Giuressi, S. Krecic, R. Sergo
Elettra Sincrotrone Trieste, Trieste, Italy
M. Cautero, V. Di Trapani, Dipartimento di Fisica, Università degli Studi di Trieste, Trieste, Italy
G. Bonano, Università di Modena e Reggio Emilia, FIM, Modena, Italy
M. Coreno, CNR-ISM, Istituto di Struttura della Materia Trieste branch, Trieste, Italy
M. Alagia, M. de Simone, CNR-IOM, Istituto Officina dei Materiali, Trieste, Italy
E. Lagosh, M. Montagnese, W. Mühleisen, J. Pribošek, Silicon Austria Labs GmbH, Villach, Austria

*Abstract*

Photon beam position monitors (pBPMs) are essential diagnostic tools in synchrotron light sources, providing real-time information on photon beam stability and trajectory. Conventional designs, including photoemission blades and diamond detectors, face limitations at fourth-generation facilities, where beams exhibit sub-micron dimensions, high brilliance, and impose severe thermal loads. We present a novel pBPM concept based on intrinsic silicon carbide (SiC) sensors operated in photoconductive mode. A sensor matrix, integrated near the beamline collimator, enables distinct detection of bending-magnet (BM) and insertion-device (ID) radiation. Initial tests at Elettra demonstrate micron sensitivity, effective BM/ID separation, and real-time discrimination between positional drifts and intensity fluctuations. These results establish SiC photoconductive devices as promising candidates for next-generation photon diagnostics.

## INTRODUCTION

The development of fourth-generation synchrotron light sources presents significant challenges for pBPMs. These facilities deliver photon beams with high brilliance and sub-micrometer dimensions, requiring diagnostics that combine high spatial resolution, wide dynamic range, and radiation hardness. Effective methods in earlier generations of storage rings often could be inadequate under the demanding conditions of these new machines.

A commonly used pBPM design involves crossed-blade monitors based on photoemission [1, 2]. These systems are non-invasive as they rely on detection of the beam's outer tails, however they become progressively less suitable as beam sizes decrease. In fourth-generation sources, thermal management necessitates the use of upstream apertures or collimators to remove beam tails, transmitting only the central core of the photon beam. This configuration eliminates the signal upon which blade monitors depend.

Alternative approaches, such as diamond detectors with four-quadrant electrodes, offer improved sensitivity for micrometer-sized beams and can provide good sensitivity [3]. However, their performance is strongly photon-energy dependent: at low photon energies, the diamond must be thinned to ensure transmission, compromising mechanical integrity and thermal stability. A more fundamental limitation arises when these detectors are placed downstream of a collimator. If the transmitted beam corresponds only to the flat peak of a Gaussian-like profile, any upstream beam displacement will be invisible to the monitor, regardless of the detection scheme employed.

Additionally, existing pBPMs lack the ability to discriminate between radiation originating from bending magnets (BM) and insertion devices (ID), as both contributions are spatially overlapped along the beamline. This limitation hinders precise diagnostics and beamline tuning.

To overcome these challenges, we propose and demonstrate a novel approach for the forthcoming Elettra 2.0 light source [4]: integrating a matrix of radiation-hard sensors directly onto the upstream surface of the collimator itself. This location preserves access to the full beam profile, including the tails before their clipping. The collimator, being water-cooled and structurally robust, provides a suitable platform for sensor integration in this high-radiation environment. The sensor matrix is strategically arranged such that specific regions are exposed only to BM radiation (characterized by a broad profile), while others intercept both BM and ID radiation, which is more spatially confined. This configuration allows for clear separation of BM and ID contributions and provides comprehensive information about the beam profile at the point of tail suppression.

It is worth emphasizing that pBPMs fulfill two critical roles. First, they provide valuable feedback for accelerator operators, as the electron trajectory in the ring is directly correlated with the photon beam trajectory. Second, they serve the user community by ensuring beam stability at the experimental station, reducing the risk of beam-related artifacts in measurements. Our approach addresses both requirements by providing the necessary diagnostic information without interfering with machine operation or ongoing experiments. We present the first implementation of this concept using SiC sensors operating in photoconductive mode.

## SiC SENSORS

The sensors employed in this study are based on intrinsic SiC operated in photoconductive mode, analogous to the configuration commonly used for chemical vapor deposition (CVD) diamond detectors. Specifically, the 4H SiC polytype

* matija.colja@elettra.eu

Content from this work may be used under the terms of the CC BY 4.0 licence (© 2025). Any distribution of this work must maintain attribution to the author(s), title of the work, publisher, and DOI.

ISBN: 978-3-95450-262-2 ISSN: 2673-5350 doi: 10.18429/JACoW-IBIC2025-WEPMO18

# BEAM MEASUREMENT DURING SWAP-OUT INJECTION OF THE APS-U STORAGE RING*

W. Cheng#, A. Brill, R. Hong, S. Wang, Argonne National Laboratory, Lemont, IL, USA

*Abstract*

The Advanced Photon Source Upgrade (APS-U) implements a novel swap-out injection scheme. To comprehensively characterize the beam dynamics during swap-out injections, approximately 20 beam position monitors (BPMs) in the initial sections of the storage ring have been equipped with high-precision single-bunch electronics. These systems measure the turn-by-turn (TBT) positions of the injecting bunch. Using similar techniques, the longitudinal phase and energy of the injecting bunch can also be accurately assessed. This paper presents results of beam measurements during swap-out injections using these advanced systems.

## INTRODUCTION

APS-U is an ultimate low emittance storage ring [1] that has been constructed and commissioned at Argonne National Laboratory. To accommodate the small dynamic aperture of the storage ring, swap-out injection [2] scheme is used.

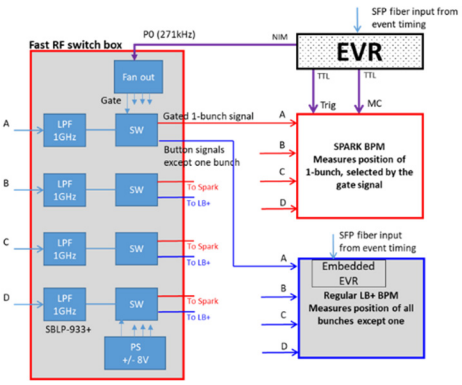



Figure 1: Schematic of the single-bunch BPM.

A single-bunch BPM system, with fast RF switches and high precision electronics, has been designed, implemented, and commissioned. The fast RF switches are capable of selecting any bucket in the storage ring, with a focus on the swap-out injection target bucket. The principle of the system and earlier test results on the original APS machine were introduced in [3]. As shown in Fig. 1, the button BPM signals pass through the fast RF switches. A 1-bunch signal is gated to the Libera Spark electronics, while the signals from the remaining bunches are routed to regular electronics of Libera Brilliance+ (LB+). The Micro Research Finland (MRF) timing system provides the related clocks for the RF switches and electronics. The system can measure a selected bunch (e.g., the swap-out bunch) during machine studies and operation. Precise single-bunch TBT measurement of the x/y positions and the sum signals help characterize the injection.

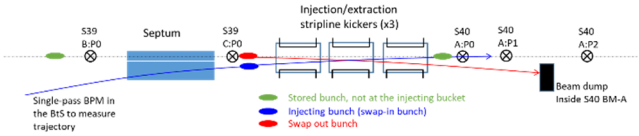



Figure 2: Swap-out injection scheme and nearby BPMs equipped with single-bunch BPM electronics.

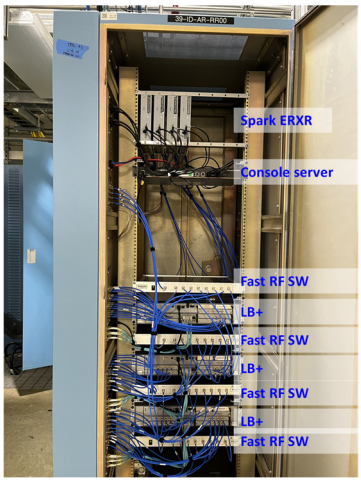



Figure 3: Installed BPM electronics in one section of the ring with RF switches and Libera Sparks.

A total of 18 BPMs from the first three sectors are equipped with single-bunch, single-pass electronics [4, 5] to measure the trajectory of the newly injected bunch and the betatron motions of the swap-out bunches (for both the old bunch to be kicked out and the new bunch being injected). Additionally, two BPMs near the injection area (S39CP0 and S40AP0) have single-bunch electronics for various diagnostics. See Fig. 2 the BPMs near the injection straight and Fig. 3 for the installed electronics in one of the mezzanine racks. The rack shown has four BPMs equipped with single-bunch electronics.

We report commissioning and beam measurements in the APS-U storage ring, most of which are related to swap-out injection.

## TIMING ALIGNMENT

The P0 clock at 271 kHz is used to select a single bunch for the Spark electronics; its width and precise delay are controlled in the MRF EVR modules. Similarly, the EVR provides P0 fiducial and trigger signals to the Spark electronics. Figure 4 shows a typical ADC waveform of the gated single bunch. There are 398 ADC samples per turn for APS-U BPM electronics, and for the 1-bunch signal, it

*Work supported by DOE contract No: DE-AC02-06CH11357
# wcheng@anl.gov

Content from this work may be used under the terms of the CC BY 4.0 licence (© 2025). Any distribution of this work must maintain attribution to the author(s), title of the work, publisher, and DOI.

ISBN: 978-3-95450-262-2 ISSN: 2673-5350 doi: 10.18429/JACoW-IBIC2025-WEPMO19

# LONGITUDINAL PROFILE MEASUREMENTS OF PARTICLE BEAMS WITH DECONVOLUTION IN THE APS-U STORAGE-RING*

X. Sun†, W. Cheng, A. Brill
Advanced Photon Source, Argonne National Laboratory, Argonne, IL, USA

*Abstract*

Accurate measurement of the longitudinal profile (bunch length) of particle beams is essential for evaluating and optimizing beam quality in the Advanced Photon Source Upgrade (APS-U) storage ring. Although Beam Position Monitor (BPM) are designed for position measurements, their signals also contain information about the longitudinal bunch distribution convolved with the BPM system transfer function. To recover the true bunch profile, we compute the BPM transfer function with CST Studio by driving the BPM model with a short Gaussian pulse that approximates a Dirac delta function, then combine measured transfer functions of accessories to form an end-to-end system response. This composite response is used as the deconvolution kernel to reconstruct time-domain bunch profile from measured BPM signals. BPM signals from the tuned Bunch Lengthening System (BLS) are analyzed in both time and frequency domains. Deconvolution yields longitudinal profiles and bunch lengths that will be compared with streak camera measurements for validation.

## INSTRUCTION

Measuring bunch length or longitudinal profile of particle beam is essential for assessing and controlling beam quality in APS-U and helps interpret the measured beam lifetime. A near-term goal is to demonstrate bunch lengthening produced by the BLS [1, 2]. A streak camera provides direct profiles [3], but the optical transport line at APS-U was not fully ready.

The APS-U storage ring has 560 RF BPMs in 40 sectors (14 per sector) for position measurements. Raw broadband BPM button signals are available at selected locations which can be used for various developments. The broadband button signals, as measured at the end of long-haul cable on the mezzanine, contain beam longitudinal profile information filtered by the feedthrough, the cables and other components in the signal path. The transfer function of those components can be measured and simulated. By deconvolving measured BPM signals with this transfer function, the time-domain bunch profile can be reconstructed, and the bunch lengths can be evaluated.

Direct measurement of the APS-U RF BPM short-pulse response is difficult, so we obtain the BPM transfer function from CST Studio simulations and combine it with measured accessory responses to form the end-to-end system response [4].

* Work supported by the U.S. Department of Energy, Office of Science, under Contract No. DE-AC02-06CH11357.
† xiang@anl.gov

## LONGITUDINAL PROFILE FROM DECONVOLUTION

By the convolution theorem, r(t) = h(t) * g(t) implies R(f) = H(f) G(f), so H(f) = R(f) / G(f), where g(t) is a short Gaussian bunch and r(t) is the simulated BPM response; h(t) is the end-to-end impulse response and H(f) = FFT[h(t)] is the transfer function. Figure 1 summarizes the workflow: simulation of the APS-U BPM transfer function (top), and deconvolution of measured BPM signals using that transfer function (bottom).

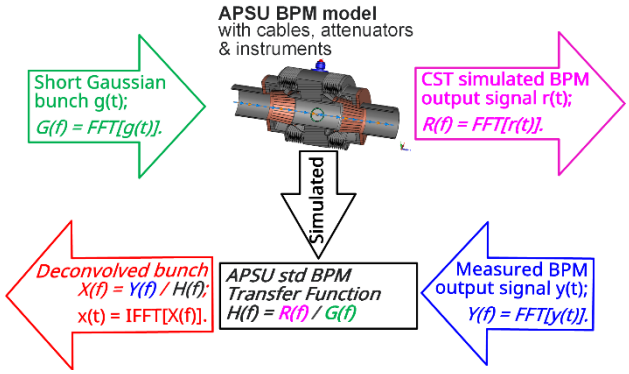



Figure 1: Workflow: simulate the APS-U BPM transfer function and deconvolve measured BPM signals to recover the input bunch profile.

Given a measured BPM waveform y(t) with Y(f) = FFT[y(t)] and known H(f), the input spectrum is X(f) = Y(f) / H(f), and the time-domain bunch profile follows from x(t) = IFFT[X(f)].

## APS-U BPM SIMULATION AND END-TO-END TRANSFER FUNCTIONS

The APS-U transfer function was simulated with different wake lengths, e.g., s = 300 mm and s = 600 mm. Finite wake length introduces spectral ripple. A longer wake window reduces ripple at the cost of runtime. We use s = 600 mm as a tradeoff. Figure 2 shows the simulated transfer functions for a $\sigma_z$ = 2 mm Gaussian bunch.

Composite end-to-end transfer functions were built for specific locations by combining the simulated BPM response with measured responses of cables, connectors, attenuators, and the instrument. Figure 3 compares S37CP1:BO [standard (std) BPM, 11.5 m SPF250 cable, 15 dB attenuator, oscilloscope, connectors] and S39AP0:TO (P0 BPM, 26 m SPF250 cable connectors), capturing location-dependent differences.

Content from this work may be used under the terms of the CC BY 4.0 licence (© 2025). Any distribution of this work must maintain attribution to the author(s), title of the work, publisher, and DOI.

ISBN: 978-3-95450-262-2 ISSN: 2673-5350 doi: 10.18429/JACoW-IBIC2025-WEPMO20

# STUDY OF A NOVEL EIGHT ELECTRODES RF PICKUP*

J. Herranz, A. Ortega, I. Podadera, IFMIF-DONES España, Granada, Spain
J. F. Valenzuela-Valdés, UGR, Granada, Spain
C. Oliver, CIEMAT, Madrid, Spain

Content from this work may be used under the terms of the CC BY 4.0 licence (© 2025). Any distribution of this work must maintain attribution to the author(s), title of the work, publisher, and DOI.

*Abstract*

The IFMIF-DONES facility located at Escúzar in Spain will consist of an accelerator delivering 125 mA of 40 MeV deuterons onto a Lithium target. At the last part of the accelerator, when the beam footprint is almost shaped, different beam diagnostics are considered. In order to protect the machine against changes of the beam and give a safe interlock, a novel RF pickup made of eight electrodes is designed. This RF pickup is designed with the objective to sense displacements of the beam centroid as changes of the beam profile. In this paper a preliminary study is presented based on an analytical and CST simulation approaches. Both are compared considering pencil and real beams from TraceWin simulations. A sensitivity study of how different parameters affect the response is performed in CST simulations.

## INTRODUCTION

The IFMIF-DONES facility will be built on Escúzar site at Granada in Spain [1]. The objective of the facility is testing materials for the future nuclear fusion reactors as DEMO. For that, the facility will consist of a superconducting linear accelerator that accelerates a deuteron beam of 125 mA up to 40 MeV. These deuterons will impact onto a lithium target, producing a neutron flux of $10^{15}$ n/cm$^2$·s. The damage produced by this neutron spectrum will simulate the irradiation conditions in fusion reactors.

In this study, we are concerned about measuring the beam properties at the target, when the beam impacts on the lithium target. The shape and the temporal distribution of a single bunch obtained in TraceWin simulations are shown in Fig. 1. The beam has a rectangular shape to meet the requirements at the lithium target [2].

Several diagnostics are considered at this point. First, an optical method capable of measuring the light produced when the deuteron beam moves into the liquid lithium surface (OTR and Fluorescence). While this method is useful to have a direct measurement of the beam profile, it has a slow response time (less than ms), due to the necessity of integrating the low signal. A second diagnostic is proposed, based on the RF pickup technology, in order to measure deviations of the beam centre and the beam profile. This RF pickup does not provide a direct measurement of the beam profile, but the response velocity is very fast (~10-100 µs), and it could be used to send an interlock signal.

* This work has been carried out partly within the framework of the EUROfusion Consortium (Grant Agreement No 101052200 — EUROfusion), funded by the European Union via the Euratom Research and Training Programme, and also by the Regional Andalousian Government under the project TECHAC (ProyExcel_00989).

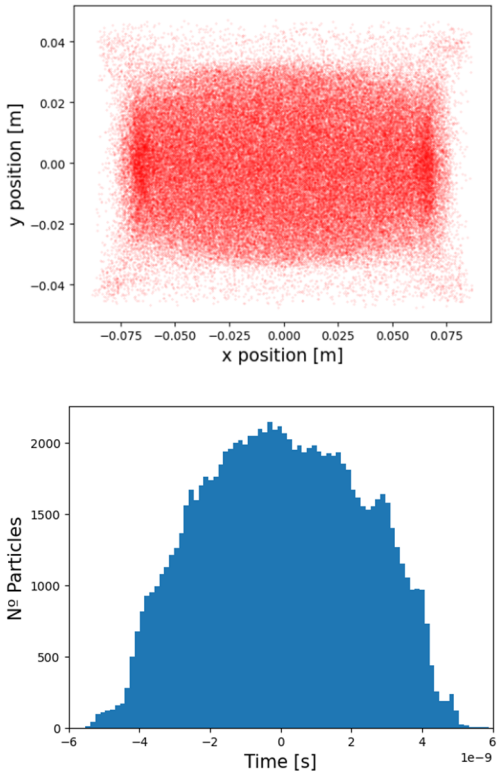



Figure 1: (Top) Beam profile at the end of IFMIF-DONES HEBT simulated with TraceWin [3]. (Bottom) Time evolution of a single bunch at the end of HEBT.

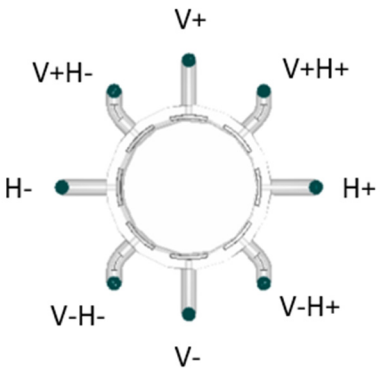



Figure 2: Design of an eight electrodes RF Pickup.

As shown in Fig. 1, the beam shape is not gaussian but rectangular. In order to accommodate the antennas to this shape, an eight electrodes RF pickup is designed to increase the number of symmetry planes (Fig. 2).

ISBN: 978-3-95450-262-2 ISSN: 2673-5350 doi: 10.18429/JACoW-IBIC2025-WEPMO21

# STATUS OF THE EIC HSR COLD BEAM POSITION MONITORS MECHANICAL DESIGN AND INTEGRATION*

F. Micolon†, L. Flader, D. M. Gassner, K. Matsushima, I. Pinayev, M. Wendt
Brookhaven National Laboratory, Upton, New York, USA

Content from this work may be used under the terms of the CC BY 4.0 licence (© 2025). Any distribution of this work must maintain attribution to the author(s), title of the work, publisher, and DOI.

*Abstract*

The Electron Ion Collider (EIC) Hadron Storage Ring (HSR) aims to leverage as much hardware from the Relativistic Heavy Ion Collider (RHIC) storage ring as possible. However, the RHIC stripline beam position monitors (BPM) used in the superconducting magnet (SC) cryostat will not be compatible with the planned EIC hadron beam parameters that include shorter bunches, higher beam current and operation of the beam with a radial offset in the vacuum chamber. A new cryogenic BPM design using button pick-ups, integrated in a new interconnect bellow assembly, will be installed next to the decommissioned and shielded RHIC stripline BPMs. This paper will review some of the challenges faced in the design of the BPM pick-ups ahead of their procurement.

## INTRODUCTION

The EIC HSR is designed to leverage the existing collider infrastructure from the RHIC project including instrumentation [1] and SC magnets [2]. However early studies found that the new beam structure, with shorter bunches and higher beam current, would not allow reusing the RHIC striplines BPM due to integration and heating concerns, especially at large horizontal beam offset [3, 4]. A new BPM pick-up design has been developed in the last years [5, 6]. This paper will cover some aspects driving the mechanical design and its integration in the SC magnets interconnect space.

## SYSTEM REQUIREMENTS

### *HSR Beam Parameters*

The EIC HSR hadron beam parameters will be significantly more challenging than for RHIC (see Table 1).

Table 1: Proton Beam Parameters for High Center of Mass ($E_{cm}$) and High Luminosity ($\mathscr{L}$) Collisions (From [7, 8])

| | RHIC achieved | EIC HSR | |
|---|---|---|---|
| | | $E_{cm}$ | $\mathscr{L}$ |
| **Number of bunches (-)** | 111 | 290 | 1160 |
| **Beam current (A)** | 0.28 | 0.69 | 1.00 |
| **RMS bunch length (cm)** | 60 | 6 | |
| **Bunch spacing (ns)** | 108 | 40.6 | 10.2 |

The short and intense HSR proton bunches will impose a challenging dynamic range for the BPM system. So an important design aspect was the trade-off between signal sensitivity and heating concerns. Accelerator physics requirements for the HSR BPM are summarized in Table 2.

Table 2: BPM System Design Requirements as of 2025

| Requirements | Pilot bunch | Store |
|---|---|---|
| **Bunch charge (nC)** | 5 | 30.6 |
| **Bunch length (mm rms)** | 1500 | 60 |
| **Beam position range H/V (+/- mm)** | 5/5 | 23/2 |
| **Beam position range H (aperture)** | 16 % | 72 % |
| **Resolution turn-by-turn (mm)** | 2 | 0.2 |
| **Resolution integrated 1s (mm)** | 0.2 | 0.02 |

*Note: these are still being finalized at the time of writing.*

As seen on Table 2 the BPM system needs to perform through a large dynamic range, between a long (1500 mm rms) low-intensity 5 nC gold pilot bunch and a ~20x shorter train of 30.6 nC store bunches. To keep the synchronicity between ultra-relativistic electron and only moderately relativistic hadron bunches at all beam energies, the hadron beam pathlength must be adjusted by shifting the beam radially in the beampipe up to ±20 mm close to the focusing quadrupoles [9] which represents 72 % of the beampipe aperture.

### *BPM Center Position Accuracy Requirements*

The EIC HSR BPM system can unfortunately not benefit from Beam-Based Alignment (BBA) in the arcs because the SC circuit does not allow powering of each SC quadrupole magnet separately. While BBA can be done in the interaction regions [10], the arcs BPM will have to rely on a careful fiducialization during installation and the resulting BPM center position will be hard coded in the beam control system.

Table 3: BPM System Position Accuracy Requirement

| Requirement | Positional requirement (mm) |
|---|---|
| **Vertical (mm RMS)** | 0.3 |
| **Horizontal (mm RMS)** | 0.6 |

The EIC HSR physics program puts a special emphasis on the collision of polarized beams. Beam polarization is very sensitive to vertical deflections which must be minimized. Therefore, a careful quadrupole magnet alignment then becomes critical, as well as a precise fiducialization of the BPMs, especially in the vertical plane (see Table 3). The requirement of Table 3 refers to the position accuracy of BPM electrical center relative to the quadrupole magnetic center.

## BPM BUTTON INTEGRATION

The HSR BPM button will be integrated in the new beamline interconnect module between superconducting

* Work supported by Brookhaven Science Associates, LLC under Contract No. DE-SC0012704 with the U.S. Department of Energy.
† fmicolon@bnl.gov

ISBN: 978-3-95450-262-2 ISSN: 2673-5350 doi: 10.18429/JACoW-IBIC2025-WEPMO22

# BUTTON-TYPE BEAM POSITION MONITORS FOR ELETTRA 2.0: FROM DESIGN TO REAL MEASUREMENTS

S. Cleva*, M. Barnaba, S. Bassanese, G. Brajnik, R. De Monte, L. Novinec, G. Pangon, D. Pozzecco, L. Rumiz, R. Sauro, R. Sergo, F. Zudini, Elettra-Sincrotrone Trieste, Trieste, Italy
F. Niccoli, C. Maletta, 2SMArtEST Srl, Rende (CS), Italy
E. Maccallini, SAES Getters S.p.A., Lainate, Italy
C. Schröter, FMB Feinwerk- und Messtechnik GmbH, Berlin, Germany

*Abstract*

This paper describes the main stages of the journey from preliminary ideas on button shapes to actual measurements on prototypes of Beam Position Monitor (BPM) devices for Elettra 2.0. In the first stage, the electromagnetic phenomena involved in BPM sensors were studied taking into account different pick-up geometries, dielectric and conductive materials, and bunch lengths. Critical aspects such as beam coupling impedance, transfer impedance, impedance matching, trapped/propagating mode effects and heating were evaluated through numerical simulations. In the second stage, three families of vacuum-tight pick-up samples were fabricated in-house, and their actual performance was evaluated both on a microwave test bench and in real operating conditions on the Elettra storage ring. To carry out future measurements on alternative BPM designs, the third family was specifically conceived and built to allow quick and easy pick-up replacement using ultra-high vacuum (UHV) shape memory alloy sealing technology. The third stage focused on comparing the signals produced by the Elettra BPMs with those foreseen for Elettra 2.0, and also allowed validation of the in-house developed BPM electronics.

## INTRODUCTION

The Elettra synchrotron light source is currently undergoing a major upgrade toward a new ultra-low-emittance storage ring, known as Elettra 2.0. The redesigned lattice will reduce the horizontal emittance by more than an order of magnitude, enabling the delivery of brighter, more coherent photon beams. Such performance improvements, however, impose stringent requirements on beam diagnostics and orbit control systems. In particular, the reduced beam size and tighter dynamic aperture demand beam position monitors with significantly enhanced sensitivity, linearity, and thermal stability compared to the present generation.

## GENERAL CONSIDERATIONS ABOUT BPM DESIGN

A detailed description about the electromagnetic design criteria involved in pickups (PUs) is reported in [1]. Mechanical tolerances and vacuum constraints add complexity to the electromagnetic design. The main goals the BPMs have to get are:

- low beam coupling impedance, ideally as close as possible to resistive wall behavior. Impedance peaks, if any, should be located away from revolution harmonics and at the highest possible frequency;
- high transfer impedance at the detection frequencies (500 MHz and 1.5 GHz for Elettra 2.0);
- long time reliability;
- bake out compatibility;
- simple manufacturing to get device as close as possible each other, both mechanically and electromagnetically;

According to the reduction of the effect of the first trapped mode in cylindrical pick-ups, the conical shape has been adopted for Elettra 2.0 [2]. Both ceramic and glass have been evaluated by numerical simulations as insulating materials, but not yet tested. The delivery time of the prototypes represents a strong constraint in case redesign is required.

## REAL DEVICES

In order to reduce the delivery time from theoretical design and real testing, three types of home made pickups, in the following indicated as generations, have been in house machined following an incremental manufacturing complexity approach. Once a generation has been proven reliable in real applications, the next generation has been designed and manufactured to overcome the limitations of its predecessor [3].

### *First Generation*

A PU sample of the first generation is shown in Fig. 1. The PU body, made of stainless steel, is split in two parts screwed together. The central pin is made of copper, the insulator is made of steatite. The UHV proof capability is assured by a thin layer of UHV compatible glue deposited on the top of the steatite ring. The glue is also used for sealing and mechanically connect the PUs to the BPM body. This kind of PU is big enough to be easily assembled and glued by hand, without any extra tool. The signal induced by the beam is extracted through a commercial Sub-Miniature version A connector mounted of the top of the PU assembly. The main goal of the first generation PUs and the corresponding BPM device has been the validation of the UHV sealing capability of glued components in real working conditions.

### *Second Generation*

The second generation PU is shown in Fig. 2. The PU body is made of stainless steel, the central pin of aluminum.

* stefano.cleva@elettra.eu

Content from this work may be used under the terms of the CC BY 4.0 licence (© 2025). Any distribution of this work must maintain attribution to the author(s), title of the work, publisher, and DOI.

ISBN: 978-3-95450-262-2 ISSN: 2673-5350 doi: 10.18429/JACoW-IBIC2025-WEPMO23

# PERFORMANCE RESULTS OF NOVEL PHOTOEMISSION MASK X-RAY BEAM POSITION MONITOR FOR 'WHITE' UNDULATOR RADIATION*

P. Ilinski†, MAX IV Laboratory, Lund, Sweden

*Abstract*

A prototype of a novel Photoemission Mask type X-ray Beam Position Monitor (PheM XBPM) for the 'white' undulator radiation which concept was proposed and has been built and tested. The prototype was designed and manufactured at MAX IV. Two PheM XBPMs were in-stalled at MAX IV 3 GeV storage ring at SoftiMAX and CoSAXS beamline frontends. Signal modelling, optimization and performance results of the PheM XBPM are discussed.

## INTRODUCTION

Fixed mask is a component of the Storage ring beamline frontend, which function is to absorb unnecessary to beamline undulator radiation power. Fixed mask is a source of the photoelectrons, which can be used to determine undulator beam position. This kind of XBPM may not substitute the standard Blade type XBPMs, but due to a simple design and luck of heat load issues may be a worth to consider addition to beamline diagnostics.

## DESIGN

The PheM XBPM [1] is utilising photoelectrons generated at upstream and downstream fixed masks under undulator radiation illumination. Fixed mask is a beamline frontend component, which function is to block and absorb most of undulator radiation, reducing transmitted to the beamline power.

The PheM XBPM upstream fixed mask has a rectangular exit aperture of 1.0 mrad x 1.0 mrad, Fig. 1, the downstream fixed mask has a rectangular exit aperture of 0.9 mrad x 0.9 mrad.

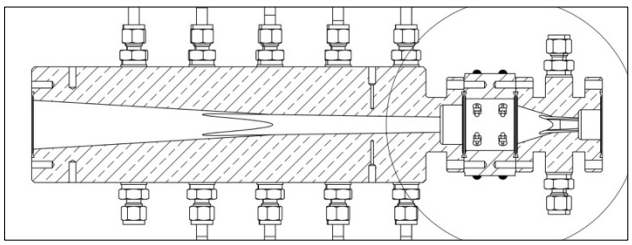


Figure 1: PheM XBPM design: (from left to right) upstream fixed mask, readout, downstream mask.

PheM XBPM has upstream and downstream sets of four electrodes. Each electrode has a SMA feedthrough with push-on connector. Two sets of electrodes were chosen for prototype version to explore various electrostatical and signal readout configurations. Electrodes are positioned at 45 degrees to vertical axis, and 2 mm away from the corners of upstream exit aperture, so they are not exposed to direct undulator radiation (Fig. 2 left).

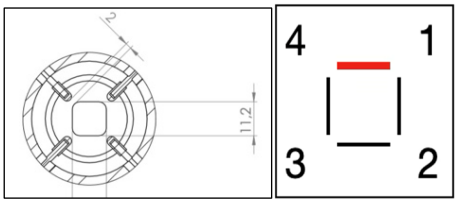



Figure 2: PheM XBPM electrodes locations (right), exit aperture surfaces with electrodes numbering (left).

## SIGNAL MODELING

Undulator spectral calculations were performed using SRW program [2]. Photoelectron signal is the product of undulator spectrum and copper total electron yield (TEY). Undulator radiation flux spectral density for CoSAXS 2-m-long, 19.3-mm-period planar undulator at K=1.25 (gap 7.42 mm) is show at Fig. 3 along with copper TYE and resulting signal on-axis and at 1 mrad. As can be seen, at 1 mrad beam direction, photoelectron signal is dominated by 200 eV energy photons.

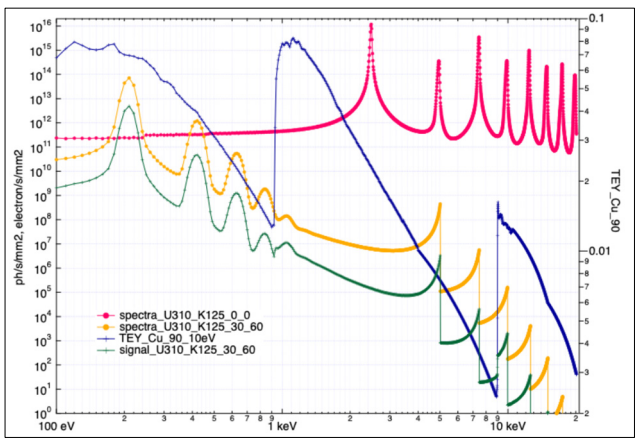



Figure 3: CoSAXS undulator radiation flux spectral density, K=1.25: on-axis (pink), 1 mrad (yellow). Copper TEY (blue). Signal spectral density at 1 mrad (green).

Once the incident photon spectre is known, we can estimate the resulting spectra of primary and secondary electrons. Electron spectra calculations were performed for incident photon energy of 200 eV and different configurations with Sessa program [3]. Total yield electron (TYE) for copper is shown at Fig. 4. Electron signal modelling allows to estimate energy distribution of the produced photo-electrons. As can be seen at Fig. 4, low energies secondary electrons are dominating, making an extended continuum.

* Research conducted at MAX IV is supported by the Swedish Research council (contract 2018-07152), the Swedish Governmental Agency for Innovation Systems (contract 2018-04969), and Formas (contract 2019-02496)

†petr.ilinski@maxiv.lu.se

Content from this work may be used under the terms of the CC BY 4.0 licence (© 2025). Any distribution of this work must maintain attribution to the author(s), title of the work, publisher, and DOI.

ISBN: 978-3-95450-262-2 ISSN: 2673-5350 doi: 10.18429/JACoW-IBIC2025-WEPMO24

# OPTIMIZATION OF PHOTOEMISSION BLADE X-RAY BEAM POSITION MONITOR FOR WIDE RANGE OF UNDULATOR GAP OPERATION*

P. Ilinski†, MAX IV Laboratory, Lund, Sweden

*Abstract*

Optimization of the photoemission blade type XBPM mostly performed to increase its resolution by increasing the readout signal current and by optimizing blades geometry. This requires tailoring of the XBPM for a particular undulator, making almost every XBPM unique at the Synchrotron Radiation facility. In many cases the calibration coefficient is gap dependent. To overcome those drawbacks an alternative optimization strategy is considered which will help to minimize gap dependence and could provide a unified XBPM design for all XBPM at Synchrotron Radiation (SR) facility.

## MAX IV XBPM STATUS

The choice of the undulator parameters dictated by desired beamline operation energy range and current permanent magnets technology. In most cases undulator operates with on-axis magnetic field in the range of 0.7 T to 1.2 T. The required energy range is achieved by a choice of the undulator period, which will define the range (see Fig. 1) of undulator deflection parameter $K = 0.934\ \lambda_u[\mathrm{cm}]\ B[\mathrm{T}]$, where $\lambda_u$ is undulator period and $B$ is on-axis magnetic field.

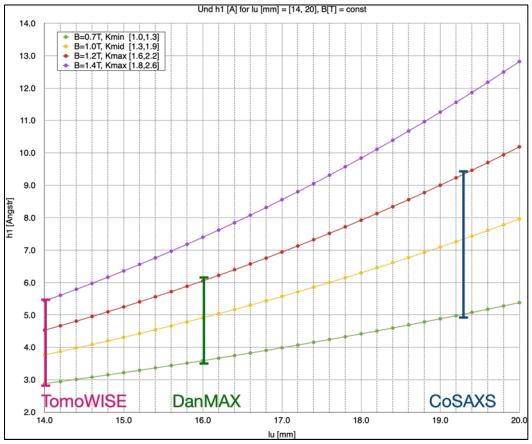



Figure 1: Operation range of the undulator deflection parameter $K$ for the range of on-axis magnetic field $B$ of 0.7-1.2 T.

MAX IV upstream XBPM is located downstream from the frontend first Fixed Mask, which has an exit aperture of 1.0 mrad x 1.0 mrad, second XBPM is located 2.5 m downstream. The XBPMs have a X/Y stage for positioning. Blades geometry is chosen to increase signal and resolution and not to shield second XBPM, Fig. 2.

* Research conducted at MAX IV is supported by the Swedish Research council (contract 2018-07152), the Swedish Governmental Agency for Innovation Systems (contract 2018-04969), and Formas (2019-02496).

†petr.ilinski@maxiv.lu.se

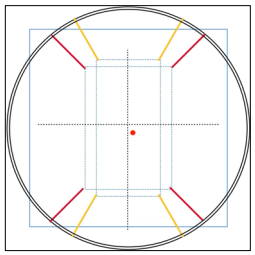


Figure 2: MAX IV NanoMAX XBPMs upstream (red), downstream (yellow) blades orientation relative to the Fixed Mask and XBPM pre-mask.

In most cases, XBPM blades geometry is chosen to maximise spatial resolution [1], which can be achieved by increasing the signal and changing the calibration coefficient. This choice of optimization leads to multiple XBPM configurations with different opening of the blades. Opening of the blades for MAX IV XBPMs is presented at Fig. 3.

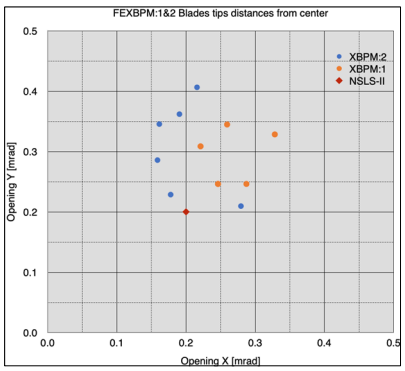



Figure 3: MAX IV XBPM blades opening angle.

MAX IV XBPMs are operated with negative Bias voltage of -120 V applied to the blades. Typical blade current is in the range of 100-300 μA, at which XBPMs are achieving sub-micron spatial resolution. The XBPMs calibration coefficients [mm/au] depend on the undulator gap, this requires XBPM spatial calibration in the gap operation range.

XBPM calibration can be performed by moving the XBPM with X/Y stage or by deviating undulator beam, these approaches may give different results of calibration coefficients. The effect is purely geometrical (Fig. 4), it depends on the blade geometry relative to the upstream aperture. In case of MAX IV NanoMAX XBPM (Fig. 2), calibration in vertical direction using y-stage will be changing exposed by the beam length of the blades, which will lead to a different result compared to the calibration performed with the beam deviation. Since in regular operation the beam is moving relative to the XBPM, it is appropriate to use beam deviation method for XBPM spatial calibration.

Content from this work may be used under the terms of the CC BY 4.0 licence (© 2025). Any distribution of this work must maintain attribution to the author(s), title of the work, publisher, and DOI.

ISBN: 978-3-95450-262-2 ISSN: 2673-5350 doi: 10.18429/JACoW-IBIC2025-WEPMO25

# SUITABILITY OF GHz FREQUENCY BEAM POSITION MONITORS FOR ELECTRON BUNCH POSITION DISCRIMINATION IN THE AWAKE FACILITY

B. Spear*, P. N. Burrows, John Adams Institute, University of Oxford, Oxford, United Kingdom
C. Pakuza, M. Krupa, S. Mazzoni, T. Lefevre, M. Wendt, CERN, Geneva, Switzerland
S. Liu, TRIUMF, Vancouver, Canada

Content from this work may be used under the terms of the CC BY 4.0 licence (© 2025). Any distribution of this work must maintain attribution to the author(s), title of the work, publisher, and DOI.

*Abstract*

The AWAKE facility at CERN utilises proton beam-driven plasma wakefields to accelerate electron bunches in a 10-meter long rubidium plasma cell. Precise monitoring of the electron bunches in the presence of the more intense proton bunches, which have distinct temporal and spatial characteristics, requires a beam position monitor (BPM) operating in the tens of GHz frequency range, assuming Gaussian longitudinal particle distributions. Two types of BPMs, one based on Cherenkov diffraction radiation (ChDR), and the other utilising high frequency (HF) conical shaped pickups, have been explored as a method to distinguish the electromagnetic signals of the shorter electron bunches (a few ps) from those of the longer proton bunches (a couple of hundred ps) co-propagating in the AWAKE beam line. Recent tests of both BPMs in the AWAKE common beam line have been conducted at frequencies above 20 GHz. The sensitivity of the HF and ChDR BPMs to the electron beam position was determined under various beam conditions, with and without proton bunches present. The read-out, utilising an RF front-end developed by TRIUMF, is additionally discussed.

## INTRODUCTION

The Advanced Proton-Driven Plasma Wakefield Experiment (AWAKE) at CERN employs a 400 GeV/c proton bunch from the SPS to excite wakefields in a 10 m rubidium plasma, with the aim of accelerating externally injected witness electron bunches to multi-GeV energies. For Run 2, stable and reproducible injection of the electron beam into the plasma cell requires sub-millimetre knowledge of its transverse position along the common beam line [1]. This measurement must be performed in the presence of the drive proton bunch, which carries between $1 \times 10^{11}$ and $3 \times 10^{11}$ protons with an RMS bunch length of 6–12 cm, corresponding to frequency content concentrated below a few GHz. In contrast, the electron bunch is typically between 50 and 150 pC with an RMS length of a few ps, yielding spectral components extending well into the tens of GHz regime.

Conventional electron stripline beam position monitors in the AWAKE transfer line operate at 404 MHz and are therefore dominated by the proton signal when both beams are present. For Gaussian bunch profiles, the spectral amplitude of the proton and electron beam are equal at 1.9 GHz; above this frequency, the shorter electron bunch becomes increasingly dominant. This motivates the development of BPM systems with an operational frequency band in the tens-of-GHz range to achieve electron-only sensitivity by exploiting the difference in bunch length.

Two novel high-frequency BPM concepts are investigated: a conical button-based BPM with a cut-off frequency around 40 GHz, and a Cherenkov diffraction radiation (ChDR) BPM utilizing dielectric radiators to couple to the high-frequency components of the electron bunch. Both designs target frequency bands above 10 GHz, where the spectral power of the electron bunch dominates, enabling spectral discrimination from the proton signal.

## A HIGH FREQUENCY BUTTON BPM

Electrostatic, or capacitive, pickups are the most common type of non-invasive BPMs. A typical configuration employs four metallic electrodes mounted symmetrically around the beam pipe in the horizontal ($x$) and vertical ($y$) planes. As a charged particle bunch traverses the vacuum chamber, image charges are induced on the electrodes. The relative signal amplitudes provide information on the beam's transverse displacement with respect to the electric centre of the BPM.



Figure 1: (Left) Bottom view of the HF pickup with conical electrode and curved lower surface. (Right) Side view of the HF pickup.

For a button-type pickup, the induced voltage is proportional to the beam current and inversely proportional to the distance between the beam and the electrode surface, with polarity equal to that of the beam charge. By comparing the signals from opposing electrodes, the beam position can be reconstructed using the standard difference-over-sum method:

$$x = k_x \frac{(V_R - V_L)}{(V_R + V_L)}, \quad y = k_y \frac{(V_T - V_B)}{(V_T + V_B)}, \tag{1}$$

where $V_R$, $V_L$, $V_T$, $V_B$ are the voltages from the right, left, top, and bottom electrodes, and $k_x$, $k_y$ are calibration factors that

* bethany.spear@physics.ox.ac.uk

ISBN: 978-3-95450-262-2 ISSN: 2673-5350 doi: 10.18429/JACoW-IBIC2025-WEPMO26

# INVESTIGATION OF READOUT METHODS FOR ELECTRO-OPTICAL BEAM POSITION MONITOR PICKUPS

D. M. Harryman*,[1], M. Z. C. Bosman[1], S. M. Gibson[1]
T. Lefèvre[2], T. E. Levens[2], A. Schlögelhofer[2], G. Tangari[2,3]
[1]John Adams Institute, Royal Holloway, University of London, Egham, UK
[2]CERN, Geneva, Switzerland
[3]Sapienza University of Rome, Rome, Italy

*Abstract*

Electro-optical pickups are being explored at CERN for the development of a high-bandwidth ($\geq 5$ GHz) beam position monitor capable of measuring intra-bunch beam position. To support this effort, a prototype electro-optical beam position monitor has been installed in the Super Proton Synchrotron. The installation utilises a fibre-coupled laser directed into lithium niobate crystals. As the beam passes a crystal, its electromagnetic field induces a proportional phase shift in the laser light by altering the refractive index of the crystal. Signal readout is typically performed using multiple Mach-Zehnder interferometers, with crystals placed on either side of the beam. This configuration currently faces challenges, including baseline instability and limited dynamic range. This paper examines and evaluates methods and techniques for reading out the beam position from the phase-shifted laser to mitigate these limitations.

## INTRODUCTION

An Electro-Optical Beam Position Monitor (EO-BPM) system has been installed in the Super Proton Synchrotron (SPS) accelerator since 2024 [1]. This Beam Position Monitor (BPM) uses two fibre-coupled Lithium Niobate (LNB) crystals integrated into button pickup assemblies where a 780 nm Continuous Wave (CW) laser is injected into the crystals. As the particle beam passes by, its electric field modulates the phase of the laser light by changing the refractive index of each crystal proportionally. A signal of varying optical amplitude is produced and measured from these phase shifts by placing the LNB crystals into a Mach-Zehnder (MZ) interferometer configuration. Detailed descriptions of pickup development and EO-BPM operating principles appear in [1–5].

The SPS system employs three MZ interferometers, shown in Fig. 1, to generate signals for the difference channel ($\Delta$), the left side-mode ($L$), and the right side-mode ($R$). Optical detectors and an oscilloscope are used to digitise the signals [6, 7]. The beam position is then calculated using

$$x = K_x \frac{\Delta}{L + R}, \tag{1}$$

where $x$ is the beam position, and $K_x$ is a geometric scaling factor [8].

* daniel.harryman@cern.ch

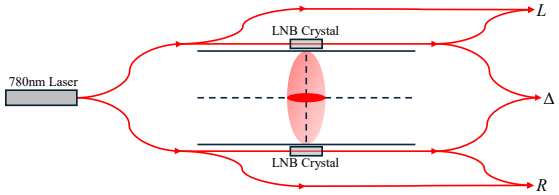



Figure 1: EO-BPM MZ interferometer configuration used in the SPS [1].

## LIMITATIONS

Electro-Optical (EO) systems are well-suited for accelerator environments due to their resistance to electrical noise and their rapid response time [9]. However, employing EO-BPM pickups in an interferometric configuration, as shown in Fig. 1, presents challenges related to dynamic range and baseline stability.

### *Dynamic Range*

The output of each MZ interferometer is given by

$$V = A + B\cos\left(\phi_0 + \pi\frac{E}{E_\pi}\right), \tag{2}$$

where $A$ is the offset, $B$ the fringe amplitude, $\phi_0$ the initial phase, $E_\pi$ the electric field strength in a crystal required for a phase shift of $\pi$, and $E$ is given by:

$$E = \begin{cases} E_l, & \text{for the left side-mode interferometer} \\ E_r, & \text{for the right side-mode interferometer} \\ E_l - E_r, & \text{for the difference interferometer} \end{cases}$$

with $E_l$ and $E_r$ being the fields in the left and right crystals, respectively.

An initial phase of 90° gives a sine response with maximum pseudo-linear range. As $E$ increases, the response becomes non-linear and can invert (over-rotate), leading to ambiguity due to the system's periodic nature and hence limiting the dynamic range.

### *Stability*

The initial phase of each EO-BPM interferometer in the SPS drifts independently at rates in the order of 1 rad/s [1], making it difficult to compare side-mode and difference channels without active stabilisation. While [1] describes a feedback system that stabilises one interferometer by tuning the laser wavelength, this method cannot be applied to all

Content from this work may be used under the terms of the CC BY 4.0 licence (© 2025). Any distribution of this work must maintain attribution to the author(s), title of the work, publisher, and DOI.

ISBN: 978-3-95450-262-2 ISSN: 2673-5350 doi: 10.18429/JACoW-IBIC2025-WEPMO27

# TRANSVERSE AND LONGITUDINAL BEAM DIAGNOSTICS AND CHARACTERIZATIONS AT IUAC-HIGH CURRENT INJECTOR

R. V. Hariwal†, S. Kumar, P. S. Lakshmi, K. Mal, S. Kumar,
T. Varughese, G. O. Rodrigues, C. P. Safvan, R. Mehta
Inter-University Accelerator Centre, New Delhi, India

Content from this work may be used under the terms of the CC BY 4.0 licence (© 2025). Any distribution of this work must maintain attribution to the author(s), title of the work, publisher, and DOI.

*Abstract*

The High Current Injector features normal-conducting Radio Frequency Linac structures intended to accelerate various ion species with a mass-to-charge ratio of up to 6, achieving a maximum output energy of 1.8 MeV/u. It can deliver an intense analyzed beam up to 100 enA/q at the target. In order to maintain beam transmission and quality from the ion source to the target, as well as to enhance the performance of RF cavities, both destructive and non-destructive, fast and precise transverse and longitudinal beam diagnostics are deployed at various locations. Recently, during 20 $Ne^{9+}$ beam test, the beam energy was confirmed to be 1.8 MeV/amu using the existing Surface Barrier Detector. We also observed a notable energy spread of approximately 1 %, which led to the pronounced debunching and a complete loss of signal in the downstream Beam Profile Monitors. To reduce the energy spread, slits have been installed at the image plane of the fourth achromatic bending magnets. It was found that optimally adjusting these slits can reduce the spread by more than 50 % while maintaining satisfactory current intensity. This paper will discuss the most recent measurements, challenges encountered and future plans.

## INTRODUCTION

The High Current Injector (HCI) is a forthcoming Heavy Ion Beam Accelerator Facility at Inter-University Accelerator Centre (IUAC) in New Delhi. It has been specifically designed to produce the beam currents in the dynamic range of tens of enA to tens of eμA. This will overcome the beam current limitation of the existing Pelletron -an electrostatic accelerator. This will also act as an alternative beam injector to the existing superconducting linear accelerator (SC-Linac) at IUAC (Fig.1). The increased current intensity and higher charge state will enable the exploration of previously unexplored areas in the experimental and research fields of high energy physics. The higher current intensity will also enable the nuclear physics researchers to investigate and perform the low cross-section reactions. HCI comprises of an 18 GHz High Temperature Superconducting Electron Cyclotron Resonance ion source referred to as PKDELIS, a 48.5 MHz four rod structure Radio Frequency Quadrupole (RFQ), and six Inter-digital H-type structure Drift Tube Linacs (DTL) functioning at 97 MHz [1,2].

† dr.hariwal@gmail.com, hariwal@iuac.res.in

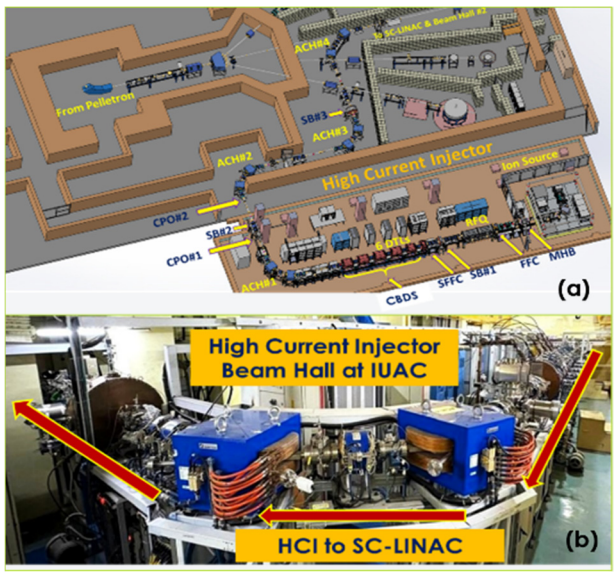



Figure 1: (a) Schematic layout of HCI to SC-LINAC with various transverse and longitudinal beam diagnostic devices. (b) Actual beam hall showing the beam direction from HCI Ion source to SC-Linac beam line via Achromatic Bending Magnet#1.

To ensure synchronization with the master clock, the RF structures within the HCI are engineered to function at frequencies that are harmonics and subharmonics of the operating frequency of the existing SC-Linac, which is 97 MHz. The RFQ receives an ion beam of 8 keV/amu from the ion source and boosts it to 180 keV/amu. Subsequently, the downstream accelerators, referred to as DTLs, further accelerate the ions from 180 keV/amu to 1.8 MeV/amu. This accelerated beam then advances to the SC-LINAC for an additional increase in energy. In order to diagnose the various beam parameters, HCI primarily includes Faraday Cups (FC), Beam Profile Monitors (BPMs), Compact Beam Diagnostic System (CBDS), Coaxial Fast Faraday Cup (FFC), Strip-line FFC (SFFC), Capacitive pick-offs (CPOs), and Surface Barrier Detectors (SBD). They are employed to measure the transverse and longitudinal beam parameters such as beam current, profiles, phase, bunch length, Time of Flight (ToF), beam energy, and the associated energy spread.

To achieve the initial longitudinal bunching of the beam originating from the ion source, a compact Multi-Harmonic Buncher (MHB) is utilized in the LEBT Section. The Coaxial Fast Faraday Cup (FFC) located upstream of the RFQ will measure the bunch length and supply the

ISBN: 978-3-95450-262-2 ISSN: 2673-5350 doi: 10.18429/JACoW-IBIC2025-WEPMO28

# OPTIMISATION OF A FIBRE-BASED TWO-COLOUR BALANCED OPTICAL CROSS-CORRELATOR*

J. Christie† [1], L. Corner[1], The University of Liverpool, Liverpool, U.K.
E. W. Snedden, ASTeC, STFC Daresbury Laboratory, UK
J. R. Henderson, Coherent Scotland Ltd, Glasgow, UK
[1]also at The Cockcroft Institute, Daresbury, UK

*Abstract*

As part of the ongoing Full Energy Beam Exploitation (FEBE) upgrade to the Compact Linear Accelerator for Research and Applications (CLARA) at the Daresbury Laboratory, UK, few-femtosecond optical synchronisation between the new Ti:Sapphire terawatt FEBE laser and the Er:Yb optical master oscillator (OMO) is required for user experiments. To achieve this, a fibre-based two-colour balanced optical cross-correlator (BOXC) using waveguided periodically-poled lithium niobate (PPLN) crystals is being developed. A fibre-based BOXC could have greater sensitivity to timing jitter between two lasers than traditional free-space devices. In this manuscript, the design of the fibre-based two-colour BOXC is presented. The effect of pulse chirp on the sensitivity of the BOXC is investigated, and plans for optimising the design of the BOXC are discussed along with plans for integrating the fibre-based BOXC into the optical synchronisation network at Daresbury.

## INTRODUCTION

The Compact Linear Accelerator for Research and Applications (CLARA) is an electron accelerator based in Daresbury Laboratory, UK, that serves as a user facility for academia and industry. At the time of writing, CLARA is undergoing commissioning of its Phase 2 upgrade, with the goal of generating 250 MeV electron bunches with a maximum bunch charge of 250 pC at 100 Hz [1]. Part of the Phase 2 upgrade is the Full Energy Beam Exploitation (FEBE) beamline, a dedicated user experimental area where 100 TW pulses from the new Ti:Sapphire FEBE laser can co-propagate and interact with the 250 MeV electron bunches from CLARA. Having access to high-power laser pulses and mid-energy electron bunches in the same experimental area will enable further research into novel acceleration techniques such as laser and plasma wakefield acceleration. However, such experiments will require femtosecond-level synchronisation of the FEBE laser to the Er:Yb optical master oscillator (OMO) for sufficient temporal resolution [2].

To achieve the required synchronisation performance between the FEBE laser and the OMO, a fibre-based two-colour balanced optical cross-correlator (BOXC) is being developed at Daresbury. A BOXC determines the timing delay between two laser pulses via sum-frequency generation (SFG) in a nonlinear crystal. However, many existing two-colour BOXCs utilise bulk free-space nonlinear crystals [3], limiting their long-term stability due to environmental factors affecting the alignment of the free-space optics. A fibre-based two-colour BOXC would remove the need for most free-space optics, potentially improving the stability of the BOXC. However, dispersion from the fibre components in the BOXC will cause the laser pulses to broaden in time, which could affect the BOXC performance due to reduced sum-frequency conversion.

In our previous work, a proof-of-concept fibre-based two-colour BOXC with a sensitivity of 0.971 mV/fs was demonstrated [4]. Here, we are looking to optimise the performance of the fibre-based BOXC by investigating the effect of fibre dispersion on sum-frequency generation. This will allow for the generation of more intense sum-frequency radiation for the same input laser power, thus making the BOXC more sensitive to laser pulse arrival time fluctuations.

## FIBRE-BASED TWO-COLOUR BOXC

The layout of the fibre-based two-colour BOXC is shown in Fig. 1; a detailed description of the layout is provided in [5]. The BOXC uses two 5 mm-long, type-0 phase-matched, periodically poled $LiNbO_3$ (PPLN) crystal waveguides, chosen for its large effective nonlinear coefficient of $d_{\text{eff}}$ = 16.1 pm/V [6]. The implemented ridge waveguide also increases the interaction length by reducing laser pulse diffraction within the crystal, leading to increased conversion efficiency compared to bulk-optic crystals.

The Origami-15 OMO, which operates at 249.875 MHz, supplies 1560 nm pulses to the BOXC via a stabilised fibre link. The pulses from the link, which have a full width half maximum (FWHM) spectral width of 10.9 nm and a FWHM pulse duration of 250 fs, are amplified by an erbium-doped fibre amplifier (EDFA) before distribution to the BOXC.

For testing the BOXC, 800 nm pulses are supplied by a Coherent Micra-5 laser system. The Micra-5 operates at 83.292 MHz and produces pulses with a FWHM spectral width of 27.4 nm and a measured FWHM pulse duration of 970 fs, much greater the bandwidth-limited duration of 24.5 fs due to dispersive optical elements within the beam transport to the BOXC.

After coupling and polarisation adjustment, the input pulses are split 50:50 and sent to the PPLN waveguides. The fibre delay stage imparts an additional time delay to one of the 1560 nm components, resulting in the sets of input pulses having different pulse delays. The two waveguides then generate 528.8 nm sum-frequency pulses with different

* Work supported by STFC grant no. ST/V001612/1
† J.S.Christie@liverpool.ac.uk

Content from this work may be used under the terms of the CC BY 4.0 licence (© 2025). Any distribution of this work must maintain attribution to the author(s), title of the work, publisher, and DOI.

ISBN: 978-3-95450-262-2 ISSN: 2673-5350 doi: 10.18429/JACoW-IBIC2025-WEPMO29

# APPLICATION OF PHASE DETECTORS AT THE TAIWAN PHOTON SOURCE

C. H. Huang*, K. T. Hsu, S.-H. Lee, P. C. Chiu, K. H. Hu, C. Y. Wu
National Synchrotron Radiation Research Center (NSRRC), Hsinchu, Taiwan

*Abstract*

A phase detection system has been implemented at the Taiwan Photon Source, employing beam position monitor electronics integrated with a digital in-phase/quadrature (I/Q) demodulation scheme. This system enables high-resolution analysis of beam phase stability, radio-frequency (RF) cavity field phase, and synchronization integrity of the RF clock distribution. It also facilitates the investigation of beam phase variations under dynamic operational conditions, including changes in insertion device gaps and booster ramping cycles. This paper presents the operational principles, implementation architecture, and representative experimental results of the developed detector system.

## INTRODUCTION

The Taiwan Photon Source (TPS), located at the National Synchrotron Radiation Research Center, is a third-generation synchrotron light source operating at an electron energy of 3 GeV with a nominal stored beam current of 500 mA [1]. The storage ring is equipped with two superconducting radio-frequency (SRF) cavities, designated SRF2 and SRF3, to support high-current beam operation [2]. The radio-frequency (RF) system operates at a frequency of approximately 499.654 MHz with a harmonic number of 864. The booster ring (BR) is equipped with a single normal-conducting RF cavity, designated as BRF, and operates with a harmonic number of 828.

Synchronization of the RF systems requires precise distribution of a master clock signal. The master clock is located in the 22nd control instrumentation area (CIA) and is distributed to the SRF2 and SRF3 systems located in the 15th and 17th CIAs, respectively, via Libera Sync modules. For the BRF system, a phase-stabilized coaxial cable (PSCC) is employed to deliver the master clock signal with minimal phase drift.

To monitor the phase stability of signals delivered to the RF systems, a phase monitoring system was implemented using the Libera Brilliance+ (LB+) platform [3]. In addition to RF reference monitoring, the system is also capable of tracking the phase of the cavity field in the SRF cavities, as well as the beam phase in both the storage ring and booster ring.

## PHASE MONITORING SYSTEM FOR DIAGNOSTICS

To measure the RF phase, two beam position monitoring (BPM) modules and one timing module are installed on the LB+ platform located in the 17th CIA, as illustrated in Fig. 1. The revolution clock and a 3 Hz trigger signal are delivered from the TPS timing system to the timing module. The RF reference signal is provided by the master clock located in the 22nd CIA and transmitted via a PSCC.

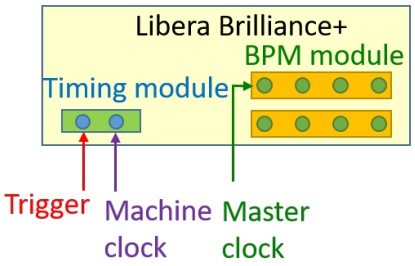



Figure 1: Setup of the beam phase detector, consisting of two beam position monitoring (BPM) modules and one timing module installed on the platform.

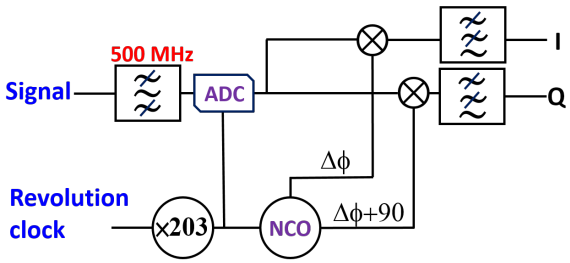



Figure 2: Infrastructure of the beam phase detector. The analog-to-digital converter (ADC) clock is generated by multiplying the revolution clock, while a numerically controlled oscillator (NCO) produces digital signals with a 90-degree phase difference.

Monitor signals—including the RF reference, cavity field signals, and beam signals—are also routed to the BPM modules in the 17th CIA through coaxial cables. As shown in Fig. 2, only the revolution clock is sent to the timing module. Consequently, the analog-to-digital converter (ADC) sampling frequency is derived by multiplying the revolution frequency by a factor of 203, and is therefore not phase-locked to the master clock.

To compensate for this, the RF reference signal from the master clock is directly injected into the first channel of the first BPM module. The in-phase ($I$) and quadrature ($Q$) components of the input signals are extracted digitally and the relative phase $\phi_0$ with respect to the ADC clock is calculated using:

$$\phi_0 = tain^{-1}(Q/I). \quad (1)$$

* huang.james@nsrrc.org.tw

Content from this work may be used under the terms of the CC BY 4.0 licence (© 2025). Any distribution of this work must maintain attribution to the author(s), title of the work, publisher, and DOI.

ISBN: 978-3-95450-262-2 ISSN: 2673-5350 doi: 10.18429/JACoW-IBIC2025-WEPMO30

# DESIGN STUDY OF THE BEAM POSITION MONITOR FOR THE HADRON CENTER AT KUTAISI INTERNATIONAL UNIVERSITY*

Revaz Shanidze†
Kutaisi International University, Kutaisi Hadron Center, Kutaisi, Georgia

*Abstract*

Cyclotron-based proton beams are widely used in research and medical applications due to their capability to deliver bunched beams with a broad range of bunch charges. One of the most critical components in beam diagnostics is the beam position monitor (BPM), which must accurately measure the beam's position while minimizing disturbance to the beam.

At Kutaisi International University (KIU), a superconducting synchro-cyclotron (S2C2) provided by Ion Beam Applications (IBA) will be dedicated exclusively to research, supporting diverse experiments that benefit from proton bunched beams of different intensities. To accommodate these experiments, construction of compact beamline is planned.

In this work, we present the electromagnetic design study of an electrostatic BPM that can operate effectively and meet to the physical and operational constraints of the new beamline.

## INTRODUCTION

The Beam Position Monitors (BPMs) are crucial diagnostic tools to effectively manipulate particle beams, by providing precise beam position. However, achieving sufficient signal levels from low-intensity bunched beams can be challenging. The minimum beam current for which a BPM yields usable position information (the detection threshold) is fundamentally limited by read-out electronic noise and manufacturing errors.

In the case of the IBA superconducting synchro cyclotron (S2C2) [1,2] at Kutaisi International University (KIU), the extracted proton beam consists of short pulses $\sim\mu s$ at a repetition rate of ∼1 kHz, main parameters of cyclotron are presented in the Table 1. The average extracted beam current is of the order of only a few tens of nano amperes. These parameters correspond to low bunch charges of the order of $10^{-11}$ to $10^{-10}$ C per pulse. Capacitive pickups (button-style BPMs) are a convenient choice for this application due to their simplicity, compactness, and ultrahigh vacuum compatibility. As a charged bunch passes, image charges are induced on the buttons, generating a voltage signal proportional to a fraction of the displacement and intensity of the beam. The fraction of the image current of the beam intercepted by a given button (and therefore the signal amplitude) depends on the electrode size, the position of the beam relative to it, and the transfer impedance [3].

This work, presents a simulation-based design study of a capacitive BPM for the S2C2 beamline at KIU. The goal is to determine the optimal button electrode size that yields the sufficient sensitivity to beam position across the expected range of bunch charges and offsets.

Table 1: General Parameters for IBA S2C2 [2]

| Parameter | Description | Value |
|---|---|---|
| Size | yoke/pole radius | 1.25 m/0.5 m |
| | weight | 50 tons |
| Magnetic field | central/extraction | 5.7 T/5.0 T |
| Beam pulse | rate/length | 1000 Hz/7 μs |
| RF system | frequency | 93-63 MHz |
| | voltage | 10 kV |
| Maximum energy | | 250 MeV |

## General Considerations

An electrostatic monitor can typically be represented by an equivalent circuit that includes a current generator with the same value as the fraction of intercepted image current, which is then shunted by the electrode capacitance to ground. To connect the button to the detector circuit, a short length of modified coaxial cable with a characteristic impedance of $R_0$ is used, and an $R_0$ resistor terminates it.

It is worth noting that the circuit model delivers satisfying results with only minor corrections necessary for a circular button geometry and relativistic beam velocities, i.e., TEM-like (transverse electromagnetic) field pattern. If the beam is accelerated to a non-relativistic velocity, $\beta \ll 1$, as for cyclotrons, the electric field cannot be described by a TEM wave anymore. Instead, the field pattern has a significantly longitudinal extension because the electric field propagation is faster than the beam velocity [4]. However, for higher beam velocities, i.e., for $\beta \geq 0.3$, the electric charge distribution squeezes approaching a layer TEM wave, so the circuit model should provide good approximation in our case [5,6].

When the beam is centered, the transfer impedance, which is the complex ratio of the voltage induced by the beam at the external termination to the beam current, can be expressed as:

$$Z_b(\omega) = \phi R_0 \left(\frac{\omega_1}{\omega_2}\right) \frac{j\omega/\omega_1}{1+j\omega/\omega_1}\,, \qquad (1)$$

here, by the frequencies $\omega_1$ and $\omega_2$ represent: $\omega_1 = 1/R_0C_b$ and $\omega_2 = c/2r$, where $C_b$ is the button capacitance to ground, $r$ is the radius of the button, $c$ is the speed of light, and $b$ is the radius of the beam pipe. The coverage factor, $\phi$, is also defined in terms of $r$ and $b$, as $\phi = r/4b$ [7].

* The work has been supported by the Shota Rustaveli National Science Foundation of Georgia: SRNSFG grant No. FR-22-8306.
† revaz.shanidze@kiu.edu.ge

Content from this work may be used under the terms of the CC BY 4.0 licence (© 2025). Any distribution of this work must maintain attribution to the author(s), title of the work, publisher, and DOI.

ISBN: 978-3-95450-262-2 ISSN: 2673-5350 doi: 10.18429/JACoW-IBIC2025-WEPMO31

# NONINTERCEPTIVE BEAM ENERGY MEASUREMENT OF HIGH-FREQUENCY FREE ELECTRON LASERS*

X. Yang, Y. B. Leng†, Y. M. Deng, A. Wang
University of Science and Technology of China, Hefei, Anhui, China

Content from this work may be used under the terms of the CC BY 4.0 licence (© 2025). Any distribution of this work must maintain attribution to the author(s), title of the work, publisher, and DOI.

*Abstract*

Free electron lasers (FEL), which can generate ultra-high brightness radiation are working horses for radiation science research over the world. For FEL, the higher the repetition frequency of the beam in the device, the higher the user's experimental efficiency, and more experimental stations can conduct experiments simultaneously. Therefore, there is a trend to increase the repetition frequency in its development process. Therefore, it is necessary to develop relevant technologies for high repetition frequency FEL. Beam energy is one of the most fundamental and critical parameters in FEL. This paper developed a fusion algorithm based on beam position monitor (BPM) in the dispersion structure of a FEL, which extracts the transverse position of the beam using both the arrival time and amplitude information of the beam, to achieve high-precision and non-interceptive measurement of beam energy. Provide powerful diagnostic, operational, and maintenance tools for high-frequency free electron laser devices.

## INTRODUCTION

For FEL devices, the higher the repetition frequency of the beam in the device, the higher the user's experimental efficiency, and the more experimental stations can be used for simultaneous experiments. Therefore, there is a trend for FEL to develop towards higher frequencies. Correspondingly, high repetition frequency also poses higher requirements for beam diagnosis systems.

Beam energy is one of the most fundamental and critical parameters in FEL. The energy of the beam entering the luminescent structure directly affects the final quality of the laser. Therefore, maintaining long-term stability of beam energy is crucial for the stability of radiation wavelength and laser pulse arrival time. High precision measurement and control of beam energy is a prerequisite for achieving wavelength control of radiation.

There are three commonly used methods for measuring beam energy in FEL. The most commonly used method is based on beam energy profile, and the vast majority of free electron laser devices are equipped with this approach [1]. But this method is interception based, and will affect the device's light supply. The second method is based on the beam arrival time measured by the cavity probe, which can obtain beam energy without interception. SXFEL and SHINE have adopted this scheme [2]. However, the beam signal detected by the cavity probe is relatively long, reaching μs level. As the beam repetition frequency gradually exceeds MHz, this method is no longer applicable. The traditional measurement scheme based on button type beam position detector (BPM) [3] has disadvantages such as low dynamic range and the need for initial beam position calibration.

Based on the above research status, this paper uses a BPM based measurement method in the dispersion structure of FEL, such as a bending magnet (BM) structure. It introduces a method of extracting beam energy using beam arrival time information, which is integrated with the original method of calculating transverse position using amplitude information to further obtain beam energy. This solves the problem of low dynamic range and greatly optimizing the shortcomings of the BPM based method to achieving high-precision and non-destructive beam energy measurement.

This paper achieves non-interceptive energy measurement of high repetition frequency FEL, solving the problem of difficulty in obtaining beam energy in real time without affecting the quality of laser supply.

## MESUREMENT PRINCIPLE

We use HOTCAP to achieve high-precision extraction of BPM signal amplitude and phase. HOTCAP was previously used to extract the bunch-by-bunch 3D position in the electron accelerator storage ring [4]. We have proven that it works well in FEL and conduct a detailed diagnosis of the device [5].

A dipole magnet is a common structure in a linear electron accelerator, which can bend the orbit of the beam. For bunches with energy distribution, after passing through a dipole magnet, the original distribution will change in both the horizontal direction (bending direction) and the forward direction due to the different deflection radii. Therefore, the energy distribution information of the beam can be obtained by the distribution changes at this two-dimensional position.

As shown in the Fig. 1, when the bunch passes through the dipole magnet, the bunch with higher energy has a bigger bending radius and is farther away from the deflection centre. Therefore, in the horizontal direction, there will be significant dispersion due to the difference in energy.

There is a formula:

$$B\rho = \frac{\sqrt{W(W+2\varepsilon_0)}}{zc}, \quad (1)$$

where $B$ is the magnetic field strength, $\rho$ is the bending radius, $W$ is the beam energy, $\varepsilon_0$ is the electron static energy, and zc is a constant. If the horizontal position of the beam can be measured at this time, the energy information of the beam can be obtained.

* Work supported by Large-Scale Scientific Facility Renovation and Upgrade Project of the Chinese Academy of Sciences -"Universal Signal Processing Platform for Accelerator Beam Measurement and Control"
† lengyb@ustc.edu.cn

ISBN: 978-3-95450-262-2 ISSN: 2673-5350 doi: 10.18429/JACoW-IBIC2025-WEPMO32

# BEAM POSITION MONITORING AND POLARIMETRY WITH A TIMEPIX3 PIXEL DETECTOR AT A COMPTON BACKSCATTERING POLARIMETER

M. Switka*, K. Desch, D. Proft, T. Schiffer, Physics Institute, University of Bonn, Bonn, Germany

*Abstract*

The ELSA facility at the University of Bonn uses a storage ring to accelerate polarized electrons up to 3.2 GeV. To monitor the polarization degree of the stored beam a Compton polarimeter is used to analyze the profile of the backscattered beam of gamma rays. In addition to a silicon microstrip detector with vertical resolution, a Timepix3 pixel detector is tested as alternative detector for the usage in beam polarimetry and beam position monitoring. The current status of the alternative detector setup is presented.

## INTRODUCTION

A Compton backscattering polarimeter is used for measuring the degree of polarisation of the electrons in the storage ring at the ELSA facility [1], as shown in Fig. 1. The storage ring applies a 6 GeV/s energy ramp from 1.2 GeV to 3.2 GeV, making polarimetry essential to fine tune those machine settings which prevent the impact of depolarizing resonances in the highly repetitive synchrotron lattice. The Compton polarimeter has shown advantegous performance [2,3] compared to a Møller polarimeter located at one of the extraction beamlines. We investigate the feasibility of using the Timepix3 pixel detector as alternative device for upcoming user experiments [4], where photoproduction experiments with polarized electrons are favored. The polarisation measurment cycle includes backs-cattered photons from electron and laser light interaction with alternating right- and left-handed circular photon polarization as well as background measurements in-between. While the electron polarisation dependent scattering cross section results in a vertical displacement of the photon profile, the background from Bremsstrahlung radiation from residual gas allows for electron beam position and angle monitoring.

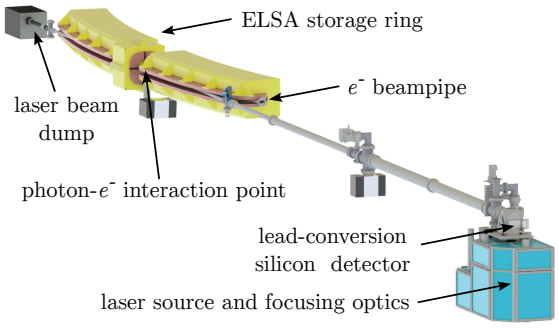



Figure 1: Drawing of the Compton polarimeter at ELSA.

## THE COMPTON POLARIMETER AT ELSA

A 20 W continuous-wave photon beam at 532 nm is circularly polarized and brought to head-on collision with the stored electron beam (see Fig. 2). The Klein-Nishina scattering cross section yields a dependency on photon and electron polarization, $\vec{S}$ and $\vec{P}$ resp., [5]

$$\frac{d\sigma_c}{d\Omega}(\vec{S},\vec{P}) = \Phi_0 + \Phi_1(S_1) + \Phi_2(S_3,\vec{P}), \quad (1)$$

resulting in a vertically shifting scattering profile for alternating photon helicities (Stokes parameter $S_3 = \pm 1$) and vertical electron polarisation $P_z$:

$$\Delta z = z_R - z_L = \mathcal{D} \cdot P_z \cdot S_3. \quad (2)$$

$z_{R,L}$ are the helicity specific profile means and $\mathcal{D}$ is the device specific analyzing power which amounts approximately 70 µm for the conditions at ELSA [2,3]. To maximize the detector signal, lead converter targets of $2X_0$ width (radiation length $X_{0,\mathrm{Pb}} = 5.6$ mm) are used in front of the silicon-based detectors 15 m downstream from the interaction point.

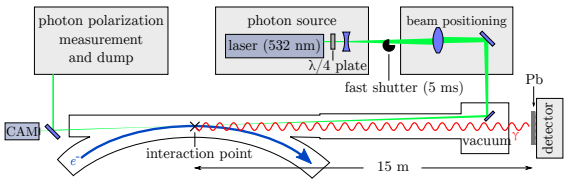



Figure 2: Sketch of the laser, electron and $\gamma$ photon beamlines.

### *Measurement Characteristics*

Figure 3 shows backscattering profiles measured by the 38.4 mm × 38.4 mm microstrip detector with 768 vertically orientated channels at 50 µm pitch [6]. The relevant contribution of $\Phi_2$ from Eq. (1) is retrieved by subtracting the background from $\Phi_0$, $\Phi_1$ and Bremsstrahlung from electrons and residual gas in the vacuum chamber.

The alternating photon beam helicity $S_{3,\pm} = \pm 1$ is achieved by rotating a $\lambda/4$ wave plate with a pneumatically driven motor. During the switching times of some 100 ms fast shutters block the laser beam, allowing for individual background measurements for each pair of $S_3$ measurements. Each bin $(S_{3,+}|0|S_{3,-})$ is typically ~1,000 ms long yielding a full measurement cycle of ~3 s length, which is to be multiply repeated to minimize the statistical error of the measurement. Detector hit rates up to some MHz are obtained and statistical measurand accuracies $\delta(\Delta z)$ of 2 % were achieved within 5 minutes and 1.4 % within 15 minutes of measurement time [2, 3].

* switka@physik.uni-bonn.de

Content from this work may be used under the terms of the CC BY 4.0 licence (© 2025). Any distribution of this work must maintain attribution to the author(s), title of the work, publisher, and DOI.

ISBN: 978-3-95450-262-2 ISSN: 2673-5350 doi: 10.18429/JACoW-IBIC2025-WEPMO33

# STUDIES OF LONGITUDINAL PHASE SPACE TOMOGRAPHY USING BOOSTER CAVITY AND DIPOLE SPECTROMETER

G. Kim, M. Chung*, Pohang University of Science and Technology, Pohang, South Korea
D. Kwak, Korea Atomic Energy Research Institute, Jeonbuk, South Korea

*Abstract*

Information on the longitudinal phase space (LPS) is essential for tuning injectors that deliver 0.1-1 ps electron bunches to beam-plasma interaction experiments and ultrafast diffraction facilities. Instead of relying on specialized diagnostics, we demonstrate that LPS characterization can be achieved using only standard accelerator components, namely a booster cavity and a downstream spectrometer. A phase scan of the booster cavity adjusts the longitudinal chirp, while the spectrometer converts the energy spread into a transverse distribution. In particular, particle tracking simulations show that by applying the simultaneous algebraic reconstruction technique (SART). We obtained the reconstruction image less than 5 % error. Next, we are planning to discuss the potential application of LPS tomography developed to non-relativistic ion beams, using a re-bunching cavity and a bunch shape monitor.

## MOTIVATION

Precise LPS characterization is critical for optimizing ultrafast electron bunch injectors in beam-plasma interaction experiments and ultrafast diffraction facilities. These applications demand a 0.1-1 ps electron bunches with precisely tailored temporal profiles, making LPS diagnostics an essential component of injector tuning protocols [1, 2].

The core idea lies in applying reconstruction algorithms to indirectly measure LPS through phase scan data. By varying the booster cavity phase, we generate different longitudinal chirp conditions that, when combined with dipole spectrometer measurements, provide required information for complete LPS reconstruction using the SART.

## TOMOGRAPHY DATA PREPARATION, AND MODELLING

### *Workflow Overview*

We follow a four-step workflow for LPS tomography: (1) acquire 1D projections by scanning the booster cavity phase; (2) map each phase to an rotation angle in the $(\varphi,\ \delta p)$ plane; (3) pre-process each profile (background subtraction, and normalization); and (4) reconstruct the LPS using an iterative algorithm. Accurate 1D projections and sufficiently uniform angle coverage are the two key factors of high-accuracy reconstruction.

### *Simulation Setup*

The reconstruction validation was performed using comprehensive particle tracking simulations implemented in ASTRA (A Space Charge Tracking Algorithm) [3]. The simulation was configured to represent our beamline (see Fig. 1), called the electron Linear Accelerator for Basic science (eLABs) (see Table 1).

Table 1: The Beamline Parameters

| Parameters | Specifications |
|---|---|
| Energy | 70 MeV |
| Charge | 200 pC |
| The number of particles | 100,000 |
| Space charge | OFF |
| Bunch length | 1.2739 ps |
| Phase increment | 0.1 deg |

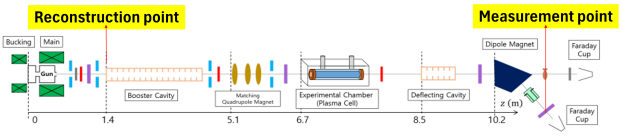



Figure 1: Our beamline can accelerate the beam up to 70 MeV. To reconstruct gun LPS image, reconstruction point is upstream of booster cavity, whereas the measurement point is after the spectrometer.

### *Physical Model*

We neglect space charge in the initial validation because the analytical relations used for angle mapping do not include space charge. For the ultra-relativistic, bunch length is sufficiently conserved through the booster and transport to the spectrometer [4]. So, we assume the bunch length is constant between reconstruction point and measurement point.

Under these assumptions, the longitudinal dynamics across the booster can be written as [5]

$$p_z^{\mathrm{boo}} = p_z^{\mathrm{gun}} + S\,\delta\varphi + \delta p + V\cos(\varphi + \delta\varphi). \qquad (1)$$

Eq. (1) decomposes the $p_z^{\mathrm{boo}}$, into the upstream momentum $p_z^{\mathrm{gun}}$, a linear transport term $S\,\delta\varphi$ capturing longitudinal chirp according to bunch length, an uncorrelated energy jitter $\delta p$, and the RF acceleration term $V\cos(\varphi + \delta\varphi)$.

$$\langle p_z^{\mathrm{boo}} \rangle \approx p_z^{\mathrm{gun}} + V\cos\varphi\left(1 - \frac{\sigma_\varphi^2}{2}\right). \qquad (2)$$

Eq. (2) is a second-order expansion of the mean momentum. In practice, we fit the measured mean momentum versus booster phase to extract an effective gain $V$ and to confirm the on-crest phase $\varphi_0$.

* moses@postech.ac.kr

Content from this work may be used under the terms of the CC BY 4.0 licence (© 2025). Any distribution of this work must maintain attribution to the author(s), title of the work, publisher, and DOI.

ISBN: 978-3-95450-262-2 ISSN: 2673-5350 doi: 10.18429/JACoW-IBIC2025-WEPMO34

# LONGITUDINAL BUNCH PROFILE RECONSTRUCTION VIA CHERENKOV RADIATION IN OPTICAL FIBERS

P. Pushkarna*, P. J. Giansiracusa[1], R. P. Rassool, S. L. Sheehy[2], G. N. Taylor, J. Valerian, M. Volpi
University of Melbourne, Melbourne, Australia
P. Bennetto, R. Dowd, Y-R. E. Tan
Australian Synchrotron - ANSTO, Clayton, Australia
[1]Also at Australian Synchrotron - ANSTO, Clayton, Australia
[2]Also at ANSTO, Lucas Heights, Australia

*Abstract*

Optical beam diagnostics, such as OTR (Optical Transition Radiation) screens and streak cameras, can overcome bandwidth limitations of electronic diagnostics. However, efficient light collection and transport is challenging. At the PEER (Pulsed Energetic Electrons for Research) facility at the AS (Australian Synchrotron), we use Cherenkov radiation (ChR) generated in optical fibers to reconstruct longitudinal bunch profiles at ps timescales, using a streak camera. This is enabled by proportionality of emitted ChR intensity to incident charge, when electrons directly impact the fiber. Streak cameras have been used to image ChR, but generating and transporting ChR in the same fiber is novel, and simplifies diagnostic design. We present bunch profile measurements using this technique, and assess its feasibility. We quantify distortion of ChR due to modal and chromatic dispersion in the fiber, survey methods to reduce distortion, and improve signal-to-noise ratio. Bunch profile measurements at ps resolution could allow bunch purity optimisation and detection of microbunching, previously not possible at PEER. This will greatly benefit PEER users, as well as beam quality in the booster and storage rings of the AS.

## LONGITUDINAL DIAGNOSTICS AT PEER

The PEER (Pulsed Energetic Electrons for Research) beamline at the AS (Australian Synchrotron) is a 100 MeV linear electron accelerator, providing electron beams for radiotherapy and dosimetry studies [1, 2], particle and detector physics [3], and fundamental accelerator science [4]. PEER seeks a sub-ns longitudinal bunch profile diagnostic to improve bunch purity. This is challenging with existing diagnostics, since Fast Current Transformers, (FCTs) and Wall Current Monitors, (WCMs) with 1 GHz bandwidth are not able to resolve previously simulated 3 GHz satellite bunches imposed upon the main 500 MHz RF bucket by S-band accelerating structures [5]. The distribution of S-band microbunches within the main RF bucket has not yet been measured.

This contribution details a picosecond longitudinal bunch profile diagnostic developed for PEER by exploiting the Cherenkov effect in optical fibers. It details direct irradiation of multimode optical fibers with 100 MeV electron bunches to produce Cherenkov radiation (ChR), which is propagated in the same fibers toward a streak camera for detection at few-picosecond resolution. Bunch profiles are reconstructed by visualising ChR intensity with time, and the impacts of pulse broadening in the fiber due to modal and chromatic dispersion are considered.

Existing tunnel layout and engineering constraints at PEER hinder retrofitting in-air optical transport lines for OTR (Optical Transition Radiation) or ChR. Direct bunch streaking with a deflecting cavity is unfeasible due to the lack of additional RF power. Involved in-vacuum optical setups and demanding laser requirements disqualified EO techniques (Electro-Optical techniques). While bandwidths of available in-flange FCTs and Faraday Cups increase, an upgradeable photodetector located outside the accelerator tunnel was desired, to enable future bandwidth increases without disturbance to vacuum and beamline components.

Inspired by ChR fiber beam loss monitors [6, 7], optical fibers are considered a flexible solution to transport light outside the accelerator tunnel from previously inaccessible locations, and this has been demonstrated previously with Synchrotron Radiation (SR) [8]. Several works detail longitudinal phase space measurements using ChR generated in thin dielectric radiators [9], or non-invasively via Cherenkov diffraction radiation (ChDR) [10, 11]. This contribution is novel in combining generation and transport of ChR, simplifying and improving light coupling and easing transport.

## DETECTOR CONFIGURATION

A brief overview of PEER is presented in Fig. 1. A dc 90 kV thermionic gun accelerates electrons toward the Subharmonic pre-buncher (SPB), a 50 mm 500 MHz standing-wave RF cavity operated in $\pi/2$ mode. Bunches are then captured by the Primary Bunching Unit (PBU), with four 3 GHz 20 mm cells, and accelerated from 90 keV to roughly 300 keV. The 3 GHz Final Bunching Unit (FBU), consisting of 16 42.22 mm cells, $\beta$-matches bunches with two travelling wave 3 GHz S-band accelerating structures, which increase energy to the nominal 100 MeV [12]. The linac is operated in "single-bunch" mode, which means that one 500 MHz RF bucket is filled, but may contain more complex 3 GHz microstructure whose observation is desired.

At the PEER in-air endstation, electron bunches directly impinge 15 m 105 µm 0.10 NA multimode silica optical fiber, angled at 47 degrees (the ChR emission angle in silica) to the beam with a Zaber X-RSW-E remotely controlled ro-

* pushkarnap@student.unimelb.edu.au

Content from this work may be used under the terms of the CC BY 4.0 licence (© 2025). Any distribution of this work must maintain attribution to the author(s), title of the work, publisher, and DOI.

ISBN: 978-3-95450-262-2 ISSN: 2673-5350 doi: 10.18429/JACoW-IBIC2025-WEPMO36

# CONCEPTS FOR BEAM DIAGNOSTICS BASED ON PLANAR PICKUPS ON A PRINTED CIRCUIT BOARD*

B. E. J. Scheible†,[1], A. Penirschke, Technische Hochschule Mittelhessen, Friedberg, Germany
M. Czwalinna, H. Schlarb, Deutsches Elektronen-Synchrotron DESY, Hamburg, Germany
W. Ackermann, H. De Gersem, Technische Universität Darmstadt, Darmstadt, Germany
M. Kuntzsch, Helmholtz-Zentrum Dresden Rossendorf HZDR, Dresden, Germany
[1]also at Technische Universität Darmstadt, Darmstadt, Germany

*Abstract*

For the upgrade of the electro-optical bunch arrival-time monitors (EO-BAMs) employed at several free-electron laser (FEL) facilities, a novel pickup structure has been proposed. Its feasibility was successfully tested at the ELBE accelerator. The design comprises planar pickups on a printed circuit board (PCB) with an integrated combination network. It delivers a significantly stronger signal compared to established pickups. Applying the upgrade to existing machines enables two key capabilities: Reliable operation at 1 pC charge levels for FELs and ultrafast electron diffraction facilities, and enhanced arrival-time resolution for standard operational modes. Furthermore, the PCB implementation enables unprecedented flexibility in planar pickup design, facilitating multi-functional diagnostic capabilities. This work presents a compact implementation strategy for integrating high- and low-resolution channels for EO-BAMs on a single substrate through a dual-functionality layout, and conceptual advancements in beam diagnostics using a PCB architecture for measuring other beam properties.

## INTRODUCTION

The electro-optical bunch arrival-time monitor (BAM) implemented in the all-optical synchronization of several free-electron laser (FEL) facilities [1–4] typically uses cone-shape pickups developed for 20 pC bunch charges [5, 6]. The transient bipolar voltage signals induced in two opposite pickups are combined and applied to the electrical input of an electro-optical modulator (EOM) of Mach-Zehnder type [6]. A laser oscillator in a phase-locked loop with the accelerator's main RF oscillator provides short laser pulses as a timing reference [7]. These pulses overlap with the voltage signal in the EOM, leading to an amplitude modulation, which imprints the arrival-time information on the pulse intensity [7]. The intensity modulation is measured and digitized to determine the arrival time [8, 9].

A redesign was proposed to improve the arrival-time resolution and to allow reliable operation with 1 pC bunches [10]. The new design comprises 4 planar pickups in a printed circuit board (PCB) with an integrated combination network [10, 11]. A first demonstrator showed the viability of this approach in beam-based measurements at ELBE [12, 13].

* This work is supported by the German Federal Ministry of Research, Technology and Space (BMFTR) under contract No. 05K22RO2.
† bernhard.scheible@iem.thm.de

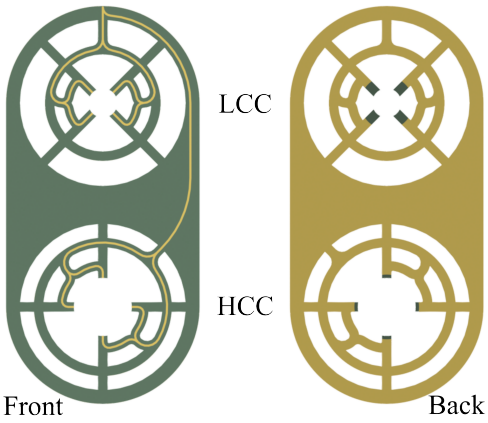



Figure 1: Heuristic PCB layout for a 2-channel BAM. Green indicates the dielectric, yellow shows the conducting layer.

## ARRIVAL-TIME MONITORING WITH DUAL-CHANNEL LAYOUT

FELs can facilitate a wide range of bunch charges, e.g. 20 pC to 1 nC at the European XFEL [14]. Since the signal generated by the EO-BAM pickups scales linearly with the bunch charge, a design optimized for 1 pC experiencing a 1 nC bunch might damage the subsequent components. A multi-channel design may mitigate this problem and provide a robust system capable of operating with a wide range of beam properties. This design has a low-charge channel (LCC) and a high-charge channel (HCC) implemented on a single PCB. To save the investment in a second evaluation chain, it may use a single connector fed with both signals.

This idea can be tested with a simulation model based on some heuristic assumptions. Many design parameters influence the shape and scale of the RF signal induced in planar pickups, but an implementation on a single PCB reduces the number of individually configurable parameters. Both channels will share the same laminate, thus substrate thickness, permittivity, loss tangent and cladding are identical. The sensitivity must be adjusted by the PCB layout. In simulations, we found that a shorter pickup has a decreased signal level and slew rate, reducing the EO-BAM's sensitivity and the voltage experienced by subsequent components. The effect can be increased by a larger aperture and therefore distance from the pickup to the bunch. The first concept is shown in Fig. 1. The pickups were set to lengths of 2.5 mm (LCC) and 0.75 mm (HCC) with a distance to the beam of 3 mm, respectively 6 mm.

Content from this work may be used under the terms of the CC BY 4.0 licence (© 2025). Any distribution of this work must maintain attribution to the author(s), title of the work, publisher, and DOI.

ISBN: 978-3-95450-262-2 ISSN: 2673-5350 doi: 10.18429/JACoW-IBIC2025-WEPMO37

# PRELIMINARY RADIATION HARDNESS CHARACTERIZATION OF ULTRA-BROADBAND DIRECT THz DETECTORS BASED ON SCHOTTKY DIODES AND GaAs TeraFETs*

R. Yadav†,1, F. R. Faridi, F. Bek, S. Preu, TU Darmstadt, Darmstadt, Germany
B. Scheible, A. Penirschke, Mittelhessen Univ. of Applied Sciences, Friedberg, Germany
M. Salman[1], M. Kuntzsch, J. M. Klopf, Helmholtz-Zentrum Dresden-Rossendorf, Dresden, Germany
[1]also at Mittelhessen Univ. of Applied Sciences, Friedberg, Germany

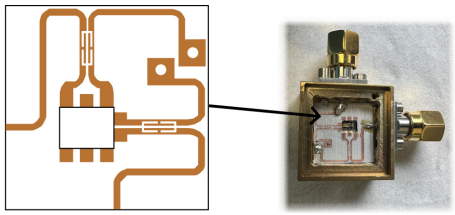
*Abstract*

Many currently operating and future FELs can generate radiation at megahertz repetition rates, requiring an ultra-broadband, compact, robust & fast (response time at least on a single-digit nanosecond scale) diagnostic tool. We develop ultrafast-operating terahertz detectors based on Schottky diodes and GaAs field-effect transistors (TeraFETs) that operate at room temperature. Here, we present the preliminary radiation hardness characterization of these detectors. Promising results demonstrate the ability of these detectors to be commissioned at accelerator facilities for longitudinal beam diagnostics.

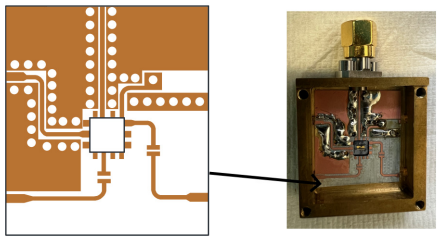
## INTRODUCTION

Modern third- or fourth-generation electron-based accelerator facilities [1] require the accurate and fast characterization of THz pulses, which is crucial for optimizing FEL performance and, consequently, the beam parameters. Therefore, beam diagnostics [2] plays a vital role in machine operations, which requires the use of several instruments [3]. For longitudinal beam diagnostics at THz-generating particle accelerator facilities, conventional detectors [4] often suffer from limitations such as bandwidth restrictions, slow response times, and vulnerability to radiation damage, among others. As the majority of operating FEL facilities are capable of generating a broad THz spectrum [5], it is necessary to have a detector that can meet this ultra-broad bandwidth, along with other parameters such as fast speed, compactness, robustness, and ease of use. Also, the employed electronics are prone to various ionizing radiations [6], which can damage these electronic instruments [7]. This work presents the development of room-temperature operable terahertz (THz) detectors utilizing Schottky diodes and field-effect transistors (TeraFETs), designed to meet the stringent requirements for such applications.

This paper is divided into five sections. Section I gives the introduction to the presented work. Section II highlights the developed THz detectors, explaining their ultra-broadband THz frequency responses. The experimental setup employed for radiation hardness tests of the detectors is described in detail in section III, followed by the results & discussion presented in section IV. The conclusions and outlook of the paper are given in section V.



(a) Specimen of TeraFET packaged detector



(b) Specimen of Schottky diode packaged detector

Figure 1: Illustration of a developed (a) TeraFET and (b) Schottky-based THz detector in the packaged form.

Table 1: List of THz Detector Results Shown in this Paper

| S.No | Device | Technology | Dose [Gy] |
|---|---|---|---|
| 1 | FET-A4 | TeraFET | 15.17 |
| 2 | ZBSD-R4K | Schottky diode | 9.09 |
| 3 | HDD-K48 | Schottky diode | 17.95 |
| 4 | PCTUD121-A1 | Photoconductor | 4.78 |

## DEVELOPED THz DETECTORS

The developed THz detectors are characterized over time with respect to aging when exposed to radiation using a free-electron laser (FEL) source. This work presents only selected results. Figure 1 illustrates exemplary packaged versions of the THz detectors based on (a) TeraFET and (b) Schottky diode. The employed intermediate frequency (IF) circuit used for packaging the respective detector is shown on the left side, while the right side shows an interior view of a fully packaged detector. Similar types of packaged detectors are used for the radiation hardness characterization

* The work is supported by the German Federal Ministry of Education and Research (BMBF) under contract no. 05K22RO1 and 05K22RD1.
† yadav@imp.tu-darmstadt.de

Content from this work may be used under the terms of the CC BY 4.0 licence (© 2025). Any distribution of this work must maintain attribution to the author(s), title of the work, publisher, and DOI.

ISBN: 978-3-95450-262-2 ISSN: 2673-5350 doi: 10.18429/JACoW-IBIC2025-WEPMO40

# OPTIMIZATION AND UPGRADE OF THE BPM ELECTRONICS SYSTEM FOR CSNS-II RCS

R. Y. Qiu, R. J. Yang, M. A. Rehman, Z. H. Xu, W. L. Huang, F. Li, L. Zeng, W. W. Chen
Institute of High Energy Physics, Chinese Academy of Sciences, Beijing, China
also at Spallation Neutron Source Science Center, Dongguan, China

*Abstract*

The China Spallation Neutron Source (CSNS) Phase II project aims to increase the Rapid Cycling Synchrotron (RCS) beam power to 500 kW, resulting in a tenfold increase in Beam Position Monitor (BPM) signal amplitude from 10-20 V to 100 V, necessitating an electronics upgrade for precise position measurements. Inspired by the J-PARC Main Ring 1.3 MW upgrade, we propose a preliminary design featuring a MicroTCA.4-based Rear Transition Module (RTM) equipped with high-power attenuators for stable signal attenuation and impedance matching tailored to CSNS RCS cables (52.88 Ω, 80.6 m). Digital processing utilizes a domestically developed MicroTCA.4 AMC board based on the Xilinx Zynq-7045 SoC, supporting 8-channel 16-bit ADC at 125 MSPS and EPICS integration. Position calculations adopt the GSI least-squares fit algorithm to reduce offset-induced errors and enhance robustness. Using CSNS Phase I BPM offline data, Python simulations based on windowed least-squares fitting compared traditional Δ/Σ methods with the least-squares approach, indicating support for a target resolution of <1 mm and providing a foundation for the BPM electronics upgrade.

## INTRODUCTION

The China Spallation Neutron Source (CSNS) Phase I has successfully operated its Rapid Cycling Synchrotron (RCS) at beam powers of 100 to 140 kW. The Beam Position Monitor (BPM) electronics system, validated through preliminary upgrades, handles dual-bunch frequencies between 1 and 2.44 MHz, with bunch lengths compressed from 500 ns to 100 ns, using a 250 MSPS 14-bit ADC with a dynamic range of 10^4. However, as CSNS Phase II targets an RCS beam power of 500 kW, the BPM signal amplitude is expected to increase tenfold from 10-20 V to 100 V, posing challenges for the existing electronics. The primary attenuation through resistive dividers is prone to temperature-induced drift and impedance mismatch, compromising position accuracy.

To address these challenges, our preliminary design draws inspiration from the J-PARC Main Ring 1.3 MW upgrade, which utilized high-power attenuators (e.g., RF2033 power divider) and nitrogen-sealed reed relays to achieve attenuation from -12 dB to -30 dB [1]. For CSNS II, we optimize the analog front-end while leveraging a domestically developed MicroTCA.4 AMC board based on the Xilinx Zynq-7045 SoC, supporting EPICS IOC integration [2]. Figure 1 shows the BPM electronics architecture based on the MicroTCA architecture, including RTM cards and AMC cards, connected via Zone 3.Algorithmically, we adopt the GSI time-domain least-squares fit method for Δ/Σ tuples to mitigate baseline offsets, enhancing position accuracy [3].

This study outlines the preliminary design, focusing on hardware architecture, algorithmic innovations, and simulation results.

## SYSTEM DESIGN

### *Analog Front-End Design*

The analog front-end is designed around a MicroTCA.4-based Rear Transition Module (RTM) board, adapting the attenuator unit architecture from the J-PARC Main Ring (MR) system, as illustrated in its block diagram

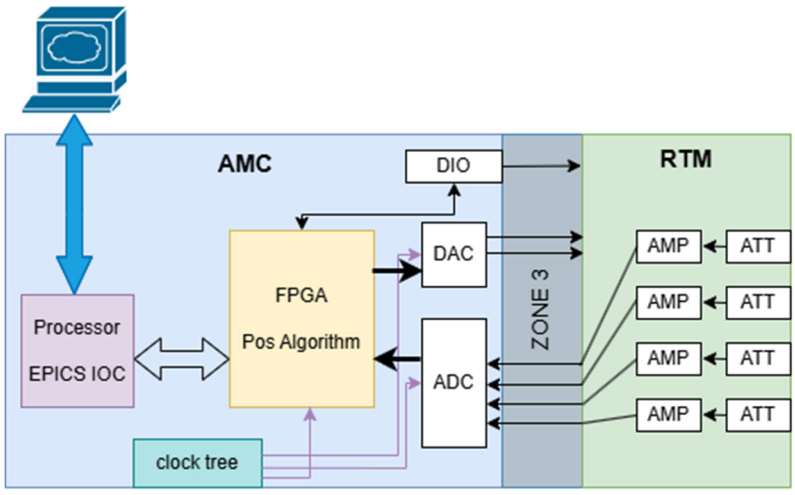



Figure 1: RCS-BPM system architecture diagram.

Content from this work may be used under the terms of the CC BY 4.0 licence (© 2025). Any distribution of this work must maintain attribution to the author(s), title of the work, publisher, and DOI.

ISBN: 978-3-95450-262-2 ISSN: 2673-5350 doi: 10.18429/JACoW-IBIC2025-THBC01

# HIGH-PERFORMANCE BUNCH ARRIVAL TIME MONITORS WITH fs PRECISION AT DESY

J. Kral*, M. Buechler, J. Georg, J. Roever, M. K. Czwalinna
Deutsches Elektronen-Synchrotron DESY, Germany

*Abstract*

Pump-probe experiments at Free-Electron Laser facilities depend heavily on the relative timing precision of the pump and the probe, which determines the resolution of the observed ultrafast phenomena. The DESY's Bunch Arrival Time Monitors (BAM) are state-of-the-art sensors based on an electro-optical detection principle, that delivers information on the bunch timing with unprecedented femtosecond-level precision. Timing synchronization at machine level is achieved through a complex system of arrival time sensors, stabilized optical distribution, and feedback controls. Major advances in the performance, construction, and operation of the BAMs are discussed in detail. Integration of the sensor into the synchronization system, and important global optimization and interplay are mentioned as well. These improvements enabled a synchronization of the electron beam with a world-leading precision of less than 3 fs at European XFEL.

## BAM SYSTEM OVERVIEW

The BAMs are electro-optical sensors that measure arrival time of electron bunches relative to a timing signal [1]. The Coulomb field of an electron beam is sensed by two or four 40 GHz pick-ups, combined to produce a single voltage signal. A laser based synchronization system [2] delivers precise laser pulses over stabilized, polarity-maintaining links. A lithium niobate Mach-Zehnder amplitude modulator front-end, located as close to the beam line as possible, receives the RF voltage signal and modulates the amplitude of the passing laser pulses with it [3]. The amplitude-modulated laser pulses are transferred to the back-end via fiber optics and read out with dedicated back-end MicroTCA electronics. The front-end (Fig. 1) is enclosed in a custom-built box (Fig. 2) that provides power, monitoring, biasing voltage, and a temperature-controlled environment for a compartment in which the modulator with an optical laser chain is located. The back-end electronics processes the digital signal and provides the result over an optical link to a low-level RF station upstream.

## ACHIEVING OPERATION STABILITY

The BAM system underwent a significant improvement in operability and stability. Previously, an expert would spend ≈ 20 minutes after each system reset, and up to an hour after HW interaction, setting up a station, yielding partially non-reproducible configurations. Machine setup changes that produced offsets in arrival time had to be adjusted manually by an expert. A periodic adjustment of system drifts during longer-term operation was required to prevent drifting away from the configured operation point or degradation of res-

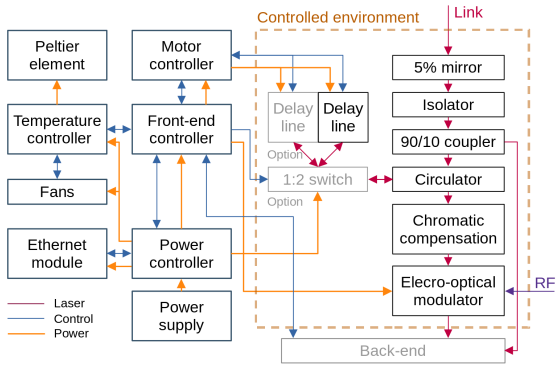



Figure 1: The block diagram shows the main building blocks of the BAM front-end electronics.

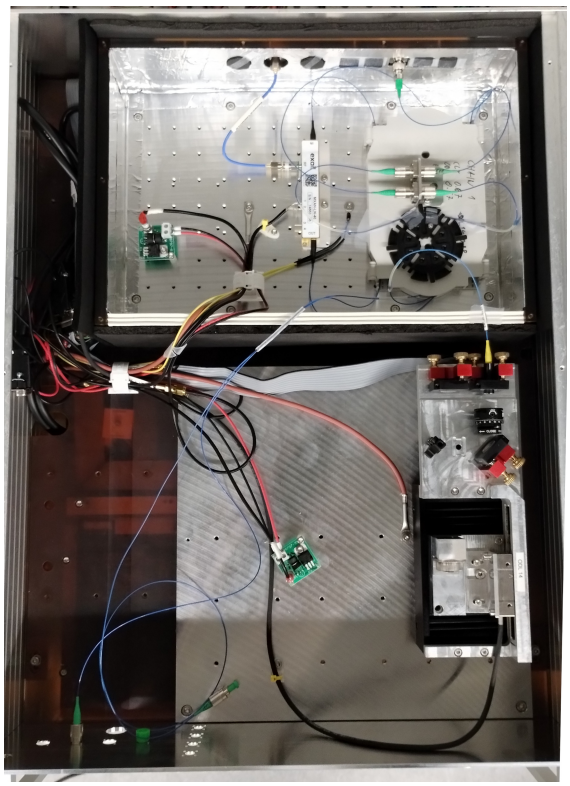


Figure 2: Photo of the top level of the BAM front-end electronics. The controlled environment compartment is located at the top, and houses the optical chain, with an optical delay line being placed outside of it in this version (right bottom). Humidity and temperature sensors are seen as well.

* jiri.kral@desy.de

Content from this work may be used under the terms of the CC BY 4.0 licence (© 2025). Any distribution of this work must maintain attribution to the author(s), title of the work, publisher, and DOI.